



ADVANCES IN CHEMICAL ENGINEERING

Volume 4

Thomas B. Drew

ADVANCES IN CHEMICAL ENGINEERING

Volume 4

This Page Intentionally Left Blank

Advances in

CHEMICAL ENGINEERING

Edited by

THOMAS B. DREW

*Department of Chemical Engineering
Columbia University
New York, New York*

JOHN W. HOOPES, JR.

*Atlas Chemical Industries, Inc.
Wilmington, Delaware*

THEODORE VERMEULEN

*Department of Chemical Engineering
University of California
Berkeley, California*

VOLUME 4

AN
ACADEMIC PRESS
REPLICA REPRINT



1963

ACADEMIC PRESS

A Subsidiary of Harcourt Brace Jovanovich, Publishers

New York London Toronto Sydney San Francisco

COPYRIGHT 1963 BY ACADEMIC PRESS INC.

ALL RIGHTS RESERVED

NO PART OF THIS BOOK MAY BE REPRODUCED IN ANY FORM
BY PHOTOSTAT, MICROFILM, OR ANY OTHER MEANS,
WITHOUT WRITTEN PERMISSION FROM THE PUBLISHERS

ACADEMIC PRESS INC.
111 Fifth Avenue, New York, New York 10003

United Kingdom Edition published by
ACADEMIC PRESS, INC. (LONDON) LTD.
24/28 Oval Road, London NW1 7DX

Library of Congress Catalog Card Number: 56-6600

This is an Academic Press Replica Reprint reproduced directly from the pages of a title for which type, plates, or film no longer exist. Although not up to the standards of the original, this method of reproduction makes it possible to provide copies of books which otherwise would be out of print.

PRINTED IN THE UNITED STATES OF AMERICA

CONTRIBUTORS TO VOLUME 4

KENNETH B. BISCHOFF, *University of Texas, Austin, Texas*

J. T. DAVIES, *The University, Birmingham, England*

D. N. HANSON, *University of California, Berkeley, California*

ROBERT C. KINTNER, *Illinois Institute of Technology, Chicago, Illinois*

OCTAVE LEVENSPIEL, *Illinois Institute of Technology, Chicago, Illinois*

DONALD S. SCOTT, *University of British Columbia, Vancouver, British
Columbia*

G. F. SOMERVILLE, *University of California, Berkeley, California*

This Page Intentionally Left Blank

PREFACE

This year's group of review articles selected for their interest and importance to chemical engineers is devoted in large part to the "engineering science" aspects of our professional field. The papers presented are all applicable to more than one unit operation, and give theories, facts, and techniques from which the design methods in any one operation are constructed.

In a sense, all the present papers treat problems in interphase contacting. On the theoretical and observational sides, respectively, Davies and Kintner explore the properties of two-phase systems undergoing mass transfer. In a third study, both the descriptive and the theoretical properties of cocurrent two-phase flow systems are presented by Scott. Longitudinal dispersion (or axial mixing), which has only recently been identified and analyzed as a substantial factor in equipment performance, is reviewed by Levenspiel and Bischoff.

Finally, an article by Hanson and Somerville takes note of the current impact of high-speed computers upon design, and shows how computers allow very simple calculation steps to be applied repetitively in solving complex arrangements of process operations. These authors provide a very widely applicable computation program for vapor-liquid separation processes. The program typifies present-day computation procedures and should be of direct use to a large number of readers.

The editors express their thanks to the publishers and particularly to Dr. Stanley F. Kudzin, associate editor at Academic Press, for their effective attention to the administrative and production aspects of publication of this volume.

*New York, New York
Wilmington, Delaware
Berkeley, California
August, 1963*

THOMAS BRADFORD DREW
JOHN WALKER HOOPES, JR.
THEODORE VERMEULEN

ERRATA TO VOLUME 2

- p. 155 Below ¶1: in *Type 2*, (if $K_B > 1$) should read (if $K_B > 2$); in *Type 3*, (if $K_B < 1$) should read (if $K_B < 2$).
- p. 157 In Eq. (16), change x_A and x_B to N_A and N_B .
- p. 166 In Eq. (40), change $e^{-2\bar{r}u/3D_t}$ to $e^{-4\bar{r}u/3D_t}$.
- p. 175 Eq. (78) should read $dx/d\tau = k_{fp}x/D$.
- p. 175 Eq. (79), first line, should read
- $$1 + \ln x = k_{fp}(V - v\epsilon - V_{\text{stoic}})/FD.$$
- p. 176 Eq. (81) in the exponent, replace 0.97 by 0.64.
- p. 176 In Eq. (82), omit D .
- p. 183 Eq. (113b) should read $n \approx Uv/SE$
Below, read: $n \approx v/2d_p\epsilon S \dots H_D \approx 2d_p\epsilon$.
- p. 189 Eq. (139), replace x by x^* .
- p. 190 Eq. (145), replace y by y^* .
- p. 199 In Eq. (162), insert a coefficient 1/2 before the right-hand "erf" term.
- p. 199 In the second line of Eq. (165), change π to $\sqrt{\pi}$.
- p. 203 k also may indicate a mass-transfer coefficient (ft./hr., or cm./sec.); $k\epsilon$ here corresponds to the usual k_G or k_L .
- p. 288 Credit: Fig. 32 was *originally* published in an article by W. C. Peck, *Chem. & Ind. (London)* pp. 159–163 (1956).

CONTENTS

CONTRIBUTORS TO VOLUME 4	v
PREFACE	vii
ERRATA TO VOLUME 2	viii

Mass-Transfer and Interfacial Phenomena

J. T. DAVIES

I. Evaporation	3
II. Transfer between Gas and Liquid Solvent	5
III. Transfer between Two Liquid Solvents	20
IV. Drops and Bubbles	33
V. Practical Extraction	42
VI. Distillation	44
References	46
Nomenclature	49

Drop Phenomena Affecting Liquid Extraction

R. C. KINTNER

I. Introduction	52
II. Dispersion into Drop Form	54
III. Shape of Forming Drops	57
IV. Velocities of Moving Drops	59
V. Internal Circulation	67
VI. Shapes of Moving Drops	71
VII. Oscillations of Drops	74
VIII. Boundary Layers	78
IX. Effects of Surfactants	80
X. Field-Fluid Currents	84
XI. Flocculation and Coalescence	85
XII. Summary	90
Nomenclature	91
References	92

Patterns of Flow in Chemical Process Vessels

OCTAVE LEVENSPIEL AND KENNETH B. BISCHOFF

I. Introduction	95
II. Dispersion Models	105
III. Tanks-in-Series or Mixing-Cell Models	150
IV. Combined Models	158
V. Application of Nonideal Patterns of Flow to Chemical Reactions	171
VI. Other Applications	187
VII. Recent References	189
Nomenclature	190
Text References	192

Properties of Cocurrent Gas-Liquid Flow

DONALD S. SCOTT

I.	Introduction to Two-Phase Gas-Liquid Flow Processes	200
II.	Description of Two-Phase Gas-Liquid Cocurrent Flow	204
III.	Pressure Drop and Holdup	214
IV.	Correlating Methods for Two-Phase Pressure Drops and Void Fractions	220
V.	Mechanics of Specific Flow Patterns	233
VI.	Heat Transfer to Two-Phase Mixtures	254
VII.	Mass Transfer in Cocurrent Gas-Liquid Flow	265
VIII.	Miscellaneous Considerations	270
	Nomenclature	272
	References	273

A General Program for Computing Multistage Vapor-Liquid Processes

D. N. HANSON AND G. F. SOMERVILLE

I.	Introduction	279
II.	Calculation Methods	281
III.	Description of the Program	291
IV.	Program GENVL	316
	References	356
	AUTHOR INDEX	357
	SUBJECT INDEX	367

MASS-TRANSFER AND INTERFACIAL PHENOMENA*

J. T. Davies

Department of Chemical Engineering
The University of Birmingham, England

I. Evaporation	3
II. Transfer between Gas and Liquid Solvent	5
A. Surface Instability	6
B. Theoretical Values of R_1	8
C. Theoretical Values of R_2	8
D. Experiments on Gas-Liquid Systems with a Plane Interface	13
III. Transfer between Two Liquid Solvents	20
A. Spontaneous Emulsification and Interfacial Instability	22
B. Theoretical Values of R_1 and R_2 in Liquids	22
C. Experiments on Liquid-Liquid Systems with a Plane Interface	23
IV. Drops and Bubbles	33
V. Practical Extraction	42
VI. Distillation	44
References	47
Nomenclature	49

When a molecule passes across an interface without chemical reaction, it encounters a total resistance R which is the sum of three separate diffusional resistances. These originate in phase 1, in the interfacial region (perhaps 10A thick) and in phase 2 (see Fig. 1). This additivity of resistances is expressed by:

$$R = R_1 + R_I + R_2 \quad (1)$$

Of these resistances, R_1 and R_2 are usually (but not always) much larger than R_I , and liquid-phase resistances are usually much larger than gas-phase resistances. Typical values (1) for R_1 (if phase 1 is a gas other than of the material diffusing) are 1-100 sec. cm.⁻¹. Values for R_2 (phase 2 being a solvent for the material diffusing) often lie in the range 100-1000 sec. cm.⁻¹. For a clean interface R_I is very small, of the order 0.002 sec. cm.⁻¹; but for an interface covered with a monolayer of some sur-

* In this chapter, references will be cited by italic numbers in parentheses.

face-active material R_I reaches values of up to 100 sec. cm.⁻¹. Here we shall discuss the simultaneous effects of surface-active agents on R_1 , R_I ,

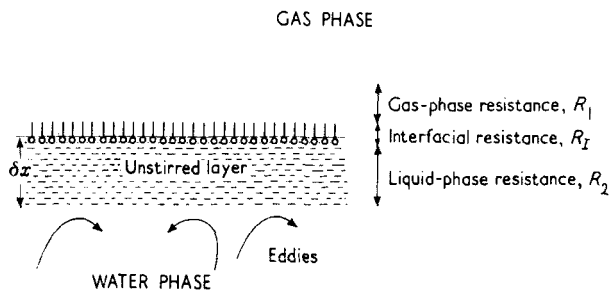


FIG. 1. Total resistance $R = R_1 + R_I + R_2$. The unstirred layer is shown as a simplified approximation.

and R_2 , for both plane interfaces and drops. For transfer processes, under a concentration gradient Δc , the basic equation is:

$$\frac{dq}{dt} = Ak \Delta c \quad (2)$$

where q is in moles of material transferring, the time t is expressed in seconds, and A is the area across which transfer occurs. The permeability constant k (cm. sec.⁻¹) is measured over a region where the concentration difference is Δc (moles cm.⁻³). The reciprocal of k is the resistance R (sec. cm.⁻¹). Equation (2) may be alternatively written (2) in terms of the diffusion coefficient D for the region of thickness Δx under consideration:

i.e.,

$$k = \frac{1}{R} = \frac{D}{\Delta x} \quad (3)$$

and

$$\frac{dq}{dt} = AD \frac{\Delta c}{\Delta x} \quad (4)$$

where $\Delta c/\Delta x$ is the concentration gradient.

For a pure gas or liquid, R_1 or R_2 is extremely small, and is dependent only on the rate at which molecules strike the interface. This rate is given by the kinetic theory, and is extremely high; and R_1 or R_2 is of the order 0.1 sec. cm.⁻¹. However, for a solute such as CO₂ diffusing from the surface of water, the concentration gradient of this solute below the surface may extend over an appreciable thickness Δx , so reducing k_2 [see Eq. (3)]. Thus k_2 will depend on D and on the thickness Δx of the unstirred

region below the surface: Δx will depend markedly on the hydrodynamics of the surface, as is discussed in more detail below.

1. Evaporation

Here R_2 is extremely low, since phase 2 consists of pure water. The total resistance, therefore, is given to a very close approximation by

$$R = R_1 + R_I$$

Above a *plane surface*, the resistance R_1 of the gas phase may be quite large, of the order 100 sec. cm.⁻¹, if there is a stagnant film (e.g., of air) overlying the water. Compared with such a value of R_1 , the resistance R_I is rather small, even if a monolayer of a long-chain alcohol or acid is present. But if the air pressure is reduced below atmospheric, or if the air is stirred (e.g., by wind or by a fan), R_1 can be reduced to only a few sec. cm.⁻¹, and the resistance R_I (up to 20 sec. cm.⁻¹ with suitable films) may become controlling.

Under natural conditions, R_1 may be reduced by wind, so that spread monolayers of hexadecanol or similar materials may significantly retard evaporation. In the last few years they have found commercial application in reducing evaporation from lakes and reservoirs in hot, arid regions where the amount of water lost by evaporation may be so great as to exceed the amount usefully used. Another application is to reduce the evaporation from heated swimming-pools: here it is important to save the latent heat of evaporation rather than the water.

Reducing the evaporation by using only a monolayer of a polar oil (3, 4) has not only the advantage that quite small amounts are required, but also that the oxygen necessary to support life can still diffuse into the water, and stagnation of the lake is thereby avoided. The reason that enough oxygen penetrates a quiescent surface covered with a monolayer lies in the high diffusional resistance R_2 encountered in the aqueous solution subjacent to the surface: compared with this resistance, the monolayer has a smaller effect (5). If, however, a thick film of oil were used to retard evaporation, its enormous resistance would become dominant in retarding the entry of oxygen. Under natural conditions, the uptake of oxygen into a lake or reservoir is aided by the wind and by convection currents, which stir the liquid near the surface: the surface viscosity and the resistance to local compression of a monolayer will reduce this stirring and so decrease the uptake of oxygen towards the rate for a quiescent surface. The effect of this in practice is that the monolayer doubles R_2 , and this in turn doubles the oxygen deficit (5); consequently, the effect of placing a monolayer of hexadecanol on a reservoir contain-

ing water which is 90% saturated is to reduce the oxygen content to 80% of saturation. This has little effect on the living organisms in the water. In practice, hexadecanol is very suitable, spreading spontaneously and sufficiently rapidly from solid beads in small gauze-covered "rafts" in the surface to give a monolayer with a value of Π^* of 40 dynes cm.^{-1} ; this retards evaporation into the atmosphere by about 50%. Spreading from solution in kerosene is also feasible (4), and is preferable if the reservoir is dirty. Trials reported in America describe the pumping of stearyl alcohol suspensions through a perforated plastic hose to give a spray application at the windward end of the reservoir (4). Longer hydrocarbon chains in the monolayer improve the efficiency, though the spreading properties of the alcohols become less favorable. To overcome this difficulty, one may add an ethylene-oxide group at the polar end of the molecule.

Evaporation from drops of liquid is generally much faster than from a plane surface, on account of the geometry of the system aiding the concentration to fall steeply away from the surface, and so making the concentration gradient steep.

The complete equation for such evaporation is:

$$\frac{1}{A} \frac{dw}{dt} = \frac{Mp}{RT(a/D + R_I)} \quad (5)$$

where w represents weight, M is the molecular weight, a the drop radius, D the diffusion coefficient and p the saturation vapor pressure of the material evaporating under the given circumstances. R is the gas constant and T the absolute temperature. This equation is based on the assumption that the air around the drop is completely unsaturated. For clean surfaces, one calculates that while a drop of water of initial radius 0.1 cm. would take 11 min. to evaporate completely into dry, still air at 18°C., the time would be only 0.06 sec. for a drop of initial radius 10 μ .

From Eq. (5) it is clear that for very small droplets (a small) the rate of evaporation will become extremely great unless R_I is appreciable. Conversely, a small amount of surface impurity may have a large effect on the rate of evaporation of very small drops. Thus, a monolayer of a long-chain alcohol or acid, which at room temperature can increase R_I (from 0.002 sec. cm.^{-1} for the clean water surface) to 10 sec. cm.^{-1} , should be able to reduce the rate of evaporation of a very small drop by 5000 times. The life-times in dry air of water drops of 1 μ radius are correspondingly increased from a few milliseconds to about a minute by

* Π is the lowering of surface tension due to the adsorbed film. It is known as the surface pressure (1).

such a monolayer; in air of 80% relative humidity the life of a $10\ \mu$ drop is increased from 2.5 sec. to 1300 sec. (6). Even oleic acid monolayers (making R_I about $0.1\ \text{sec. cm.}^{-1}$) considerably reduce the rate of evaporation of water droplets, as Whytlaw-Gray showed (7). Besides monolayers, traces of dust, nonvolatile impurities and oxidation or decomposition products may similarly reduce the evaporation rate, particularly if the droplets are small. The tarry material in town fogs is thus responsible for delaying dispersal of the fog by "isothermal distillation." Mercury droplets, if a skin of oxidized products is allowed to form, may evaporate 1000 times more slowly than calculated.

If the drop is exposed to a turbulent stream of air the diffusion coefficient in Eq. (5) must be modified by multiplication by the calculated correction factor $[1 + b (Re)^{1/2}]$, where the second term in the bracket allows for eddy diffusion of the vapor away from the surface in the air-flow of Reynolds number Re . The constant b is related to the diffusion coefficient of the solute and the kinematic viscosity of the gas. This correction factor is in good accord with experiment. Self-cooling may become more important under these conditions: a full discussion of the experimental findings for droplets moving relative to the gas is given by Green and Lane (8).

An interesting application of small water drops is in the binding of dust in coal mines. It is, however, necessary to prevent the evaporation of the aerosol of water by previously dispersing in the water a little cetyl alcohol. The spray of water drops, each about 12 microns in radius, is then relatively stable, though without the cetyl alcohol complete evaporation occurs in a few seconds (6). A fuller account of evaporation may be found in Chapter 7 of reference 1.

II. Transfer between Gas and Liquid Solvent

If a gas such as ammonia or CO_2 (phase 1) is absorbing into a liquid solvent (phase 2), the resistance R_2 is relatively important in controlling the rate of adsorption. This is also true of the desorption of a gas from solution into the gas phase. Usually R_2 is of the order 10^2 or $10^3\ \text{sec. cm.}^{-1}$, though the exact value is a function of the hydrodynamics of the system: consequently various hydrodynamic conditions give a variety of equations relating R_2 to the Reynolds number and other physical variables in the system. For the simplest system where the liquid is infinite in extent and completely stagnant, one can solve the diffusion equation

$$\frac{\partial c}{\partial t} = D \left(\frac{\partial^2 c}{\partial x^2} \right) \quad (6)$$

in which x is the distance from the interface and D the diffusion coefficient.

Hence, for absorption controlled by R_2 in a stagnant liquid

$$\frac{dq}{dt} = A(c_s - c_\infty) \left(\frac{D}{\pi t} \right)^{1/2} \quad (7)$$

where t is the time for which the surface has been exposed to the gas, and c refers to concentration. Subscript s refers to the constant (saturation) concentration of the gas at the surface, and subscript ∞ refers to the concentration of dissolved gas in the liquid far from the surface: c_∞ is usually made zero. By comparison with Eqs. (2) and (3) we see that

$$k_2 = \frac{1}{R_2} = \left(\frac{D}{\pi t} \right)^{1/2} \quad (8)$$

so that R_2 is a function of the time of exposure. If, for example, $D = 10^{-5}$ cm.² sec.⁻¹, R_2 is about 500 sec. cm.⁻¹ when $t = 1$ sec., increasing to 5000 sec. cm.⁻¹ after 100 sec. of exposure. For the desorption of a gas the same equations apply, c_s usually being zero if the desorbing gas is rapidly removed, for example, by a stream of inert gas or by evacuation of the vessel.

The total number of moles that have transferred in a time t is found by integrating Eq. (7):

$$q = 2A(c_s - c_\infty) \left(\frac{Dt}{\pi} \right)^{1/2} \quad (9)$$

and it is this quantity q which is often conveniently measured and compared with theory. If the liquid phase is not infinite in extent, the relations become more complicated (9).

In general, when the system is subject to stirring by mechanical means or by density or temperature variations during absorption, R_2 is difficult to calculate from fundamental principles, and each system has to be considered separately. Among the complicating factors is spontaneous "surface instability" which may reduce R_2 by as much as five times; and, before discussing the relation of R_2 to the external hydrodynamics, we shall outline the conditions under which spontaneous surface turbulence may occur during mass transfer.

A. SURFACE INSTABILITY

During the transfer of a surface-active solute across the surface, unstable surface-tension gradients may occur in the plane of the surface. A good example is furnished by Langmuir's experiment (10) on the evaporation of ether from a saturated (5.5%) solution in water: talc

sprinkled on the surface shows abrupt local movements, caused by differences in surface tension in different regions. The mechanism is that convection currents, either in the air or in the water, cause more ether to be present at some point in the surface than in neighboring regions. Consequently, at this point the pressure Π of the adsorbed monolayer of ether is higher, and so this ether film will therefore spread further over the surface, as shown in Fig. 2. In doing so it will necessarily drag some of the subjacent liquid with it (1), so that an eddy of solution as yet undepleted in ether is brought to the point in question. The consequent local increase in concentration of ether rapidly amplifies the interfacial movement to visible dimensions. Such "surface turbulence" greatly reduces R_2 , and we should therefore expect the ether to evaporate very rapidly from water, since R_t and R_1 are small. This is confirmed by experiment: the ether escapes sufficiently rapidly to burn actively when

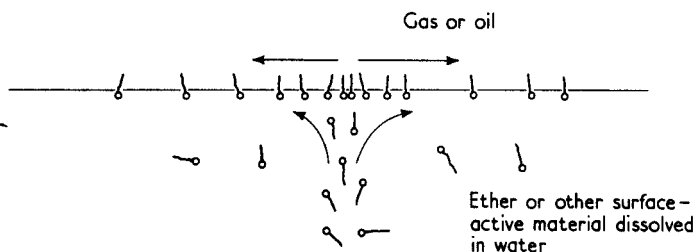


FIG. 2. Ether molecules (symbolically shown as \circ) spreading from a locally high concentration in the surface, carry some of the underlying water with them, bringing up more ether and so amplifying the disturbance.

ignited. A monolayer of oleic acid (or other material—the effect is non-specific) on the surface is sufficiently viscous in the plane of the surface and sufficiently resistant to local compression to reduce considerably the "surface turbulence"; a thicker, unstirred layer of solution immediately subjacent to the surface is set up as a result of the presence of the monolayer. Because of the necessity for the ether to diffuse through this layer, R_2 and hence R are increased [cf. Eq. (1)], and the ether no longer escapes from the surface rapidly enough to burn (10). Stirring with a glass rod will temporarily offset the effect of the monolayer. A similar effect was found by Groothuis and Kramers (11) for the absorption of SO_2 into *n*-heptane. The surface of the liquid becomes violently agitated, and R_2 is thereby reduced.

Turbulence of this kind depends on the solute transferring across the surface: if eddies of fluid rich in solute coming to the surface increase the surface pressure locally, they can cause redistribution by spreading in the surface before the solute is removed into the other phase. The effect

must therefore depend (12) both on the distribution coefficient of the solute and on the sign and magnitude of $(d\gamma/dc)$. This is discussed more fully below.

In a mathematical treatment of the hydrodynamics of surface and interfacial turbulence, Sternling and Scriven (13) have discussed the conditions under which a molecular fluctuation in surface tension during mass-transfer can build up into a macroscopic eddy. They point out that their equations predict that surface eddying will be promoted if the solute transfers from the phase of higher viscosity and lower diffusivity, if there are large differences in D and also in kinematic viscosity $\nu(=\eta/\rho)$ between the two phases, if there are steep concentration differences near the interface, if $d\gamma/dc$ is large negatively, if surface-active agents are absent, and if the interface is large in extent. The heat of transfer can produce interfacial forces only about 0.1% of those due to concentration fluctuations. That there is no mention here (13) of the critical concentration of solute required just to produce surface turbulence, nor of the distribution coefficient of the solute between the phases, distinguishes this theory from that of Haydon (12), and shows that neither treatment is comprehensive in explaining the causative and hydrodynamic behavior of systems showing spontaneous surface turbulence.

B. THEORETICAL VALUES OF R_1

In the passage of (say) CO_2 from water to air, the simple diffusion theory [Eqs. (7) and (8)] will apply if the air is completely unstirred: D for a gas is of the order of $0.2 \text{ cm.}^2 \text{ sec.}^{-1}$ at 1 atm. pressure, so R_1 is only about 1% of R_2 , having values of about 4 sec. cm.^{-1} when $t = 1 \text{ sec.}$ or 40 sec. cm.^{-1} when $t = 100 \text{ sec.}$ Usually, however, the air will be in turbulent motion, and then R_G will depend on the resistance of a layer of air near the surface; typical values of R_G are $5\text{--}80 \text{ sec. cm.}^{-1}$. If pure gas is absorbing into liquid, and if the gas is not highly soluble in the liquid, then usually diffusion through the liquid is rate-determining.

C. THEORETICAL VALUES OF R_2

In a plane static system, Eq. (8) above gives exactly the value of R_2 . In general, however, thermal convection currents or stirring can reduce R_2 much below the value calculated from Eq. (8). Lewis and Whitman (2) proposed that *turbulent stirring* maintains the composition of the solute constant within the liquid, up to a distance Δx below the surface, though within this distance the liquid flow is laminar and parallel to the surface (see Fig. 1). Through this "laminar sublayer" transfer occurs at a steady rate as if the layer were stagnant, and is therefore given by Eqs. (2) and (3). For this mechanism R_2 is thus constant for a given

value of Δx or, if the rate of stirring is varied, Re_2 can be calculated from the variation of Δx near a solid surface with the Reynolds number characterizing the turbulence in the bulk of the liquid:

$$\Delta x = \text{constant} \times (Re)^{-0.67} \quad (10)$$

where $Re = NL^2/\nu$ with N the speed of stirring, L the tip-to-tip length of the stirrer blades, and ν the kinematic viscosity.

Further, if the concentration difference across the laminar sublayer does not vary appreciably with time, Eqs. (2) to (4) may be integrated directly to give linear relations between q and $kt\Delta c$, between k and D , and between q and $Dt(\Delta c/\Delta x)$.

In the limit of *extreme turbulence*, when eddies of fresh solution are rapidly swept into the immediate vicinity of the interface, neither the laminar sublayer nor a stationary surface can exist: the diffusion path may, according to Kishinevskii, become so short that diffusion is no longer rate-controlling, and consequently for such liquid-phase transfer (14)

$$\frac{dq}{dt} = A \cdot \Delta c \cdot \bar{v}_n \quad (11)$$

where \bar{v}_n is the mean velocity of the liquid normal to the interface. By Eq. (2), \bar{v}_n is equal to k_2 , and the latter is now independent of D ; this limit of extreme turbulence is seldom reached in practice.

The steady-state theory of Lewis and Whitman cannot be valid, however, at short times of contact of the gas with a turbulent liquid, when diffusion according to Eq. (8) must be important. This condition may be of practical importance in the *flow of a liquid over packing* in a gas-absorption column, when the flow may be laminar for short times as the liquid runs over each piece of packing, though complete mixing may occur momentarily as the liquid passes from one piece of packing to the next. For the absorption of a gas in such a column, Higbie (15) proposed that moderate liquid movements would have no effect on the diffusion rate for a very short time of exposure of the liquid surface, and that accordingly one should use Eqs. (7) and (9). This is confirmed by experimental studies on the absorption of CO_2 into water with times of exposure t up to 0.12 sec.; k_2 and q vary closely with $t^{1/2}$. Further, k_2 should vary with $D^{1/2}$: this is indeed confirmed by experiments on packed towers (16). The Higbie theory can, however, be valid only for times of exposure so short and for turbulence so low that the diffusing gas does not penetrate into those parts of the liquid which have a velocity appreciably different from that at the surface.

For clean interfaces, it is now generally agreed that turbulence will sweep fresh liquid from the bulk right into the interface, thus displacing

the liquid which had previously formed the interface. There is thus no stagnant layer near a clean interface according to this view. There is, however, disagreement as to the quantitative interpretation of "surface renewal," and to discuss this it is convenient to distinguish by the subscripts D and E the diffusional and eddy-diffusional resistances expressed by Eqs. (8) and (11), so that

$$R_{2D} = (\pi t/D)^{1/2}$$

and

$$R_{2E} = 1/\bar{v}_n$$

If these two resistances act *in series*, i.e., if the physical mechanism corresponds to an eddy coming right into the surface, then residing there for a short time t during which the mass transfer occurs, then the total effective resistance R_2 is given by

$$R_2 = R_{2D} + R_{2E} = \frac{(\pi t)^{1/2} \bar{v}_n + D^{1/2}}{D^{1/2} \bar{v}_n}$$

Now the time t that an element of liquid spends in the interface is related to the fractional rate s of turbulent replacement of elements of liquid in the surface by $t = 1/s$; and s must also be related to \bar{v}_n by dividing the latter by a characteristic projected eddy length l_e in the plane of the surface, as may be understood from Fig. 1, where some eddies are shown as being deflected along the interface. With these substitutions, and putting $k_2 = 1/R_2$, one obtains:

$$k_2 = \frac{D^{1/2} s^{1/2}}{\pi^{1/2} + (D/s l_e^2)^{1/2}}$$

In practice $l_e \sim 0.1$ cm., $D \sim 10^{-5}$ cm.² sec.⁻¹, $s \sim 1$ sec.⁻¹, and so the term $(D/s l_e^2)^{1/2}$ is of the order 0.03, and may be neglected in comparison with $\pi^{1/2}$. The expression for k_2 thus simplifies to

$$k_2 = 0.56(Ds)^{1/2} \quad (12)$$

Because the eddy transport and the diffusional process always act in series, the coefficient k_2 varies with $D^{1/2}$. Danckwerts (17) derived an equation even simpler in form:

$$k_2 = (Ds)^{1/2} \quad (13)$$

where the numerical factor is different from that in our simple treatment [Eq. (12)] above, Danckwerts having made allowance for the different times of residence of the elements of liquid in the surface. Toor and Marchello (18) consider that at very low stirring rates the Lewis and Whitman model should be valid, though at moderate turbulence the rate-

controlling step should become the replacement of elements of liquid according to Eq. (13).

Supposing, on the other hand, that the physical mechanism is that *some* elements of fresh liquid are swept into the surface at a velocity \bar{v}_n which is so rapid that the diffusion path remains negligibly short, then the mass-transfer coefficient of such elements of liquid is given by Eq. (11). At moderate turbulence, other elements of liquid may, however, approach the surface obliquely, so that the fresh liquid resides for appreciable times in the surface, and to such elements Eq. (7) applies. The total resistance to mass transfer is then the sum of the two resistances acting in parallel, i.e.,

$$1/R_2 = 1/R_{2D} + 1/R_{2E}$$

or

$$k_2 = (Ds/\pi)^{1/2} + \bar{v}_n \quad (14)$$

From this relation (24) it is clear that the apparent over-all variation of k_2 with D will depend on the relative importance of $s^{1/2}$ and \bar{v}_n ; as the turbulence is increased, \bar{v}_n will increase faster than $s^{1/2}$, and k_2 will depend less on D , becoming independent of D (i.e., varying as D^0) in the limit of very high turbulence. At very low turbulence, however, k_2 will vary with $D^{1/2}$, and for any narrow range of moderate turbulence the dependence on D will be to some power between 0 and 0.5. Experiments to test the mechanism of the surface renewal in a turbulent liquid are described below.

Whether one would expect the mechanism of mass transfer to be the same across the plane surface between a gas and a stirred liquid in a beaker as across the surface of a liquid flowing over packing is still not clear. Kafarov (19) criticizes Kishinevskii for not distinguishing the two types of surface, pointing out that the turbulence caused by the stirrers in a large mass of liquid may be different from that due to wall friction in a liquid flowing over packing: in particular, the formation of vortices and the entrainment of drops or bubbles of one phase in the other may well be important. It therefore seems possible, though the point has not yet been tested, that the Danckwerts mechanism may apply to absorption during flow over packing, while the Kishinevskii mechanism may apply to transfer between stirred liquids in a vessel.

In a hydrodynamic theory of the *free, clean, surface of a turbulent liquid*, Levich (19a) postulates that there exists an upper zone of liquid, of thickness λ , in which the turbulent regime is so altered by the surface tension (which opposes local deformations) that within this zone the turbulence is severely damped. Right in the plane of the surface (at

$x = 0$) the mean eddy length becomes zero, according to Levich. For mass-transfer, this thickness λ is of great importance, and, according to Levich's equations (136.24) and (136.25),

$$k_2 = D^{1/2} v_e^{1/2} \lambda^{-1/2}$$

where v_e is the characteristic eddy velocity (cm. sec.⁻¹) in the bulk of the turbulent liquid. According to this theory, k_2 should always vary with $D^{1/2}$, as in the theory of Danckwerts. One can take the theory a stage further by estimating the magnitude of λ in terms of experimental quantities. Levich says that if the surface tension γ is the cause of the damping of turbulence at the free surface, λ must be directly proportional to γ . In addition, since λ can be a function of only eddy velocity v_e and of liquid density ρ , dimensional analysis gives Levich's equation (135.7):

$$\lambda = \gamma \rho^{-1} v_e^{-2}$$

Alternatively, one may consider that the capillary pressure γ/λ arising from the deformation compensates for the dynamic thrust ρv_e^2 , preventing the eddies from splashing out of the liquid surface.

Hence, on this analysis,

$$k_2 = D^{3/2} v_e^{1.5} \rho^{1/2} \gamma^{-1/2} \quad (15)$$

For *film-covered surfaces*, the fluctuations in surface pressure Π severely damp out any liquid movement in the plane of the surface. Talc particles sprinkled on the surface become virtually immobile if the surface is even slightly contaminated, indicating that the surface film sets up a considerable resistance to the "clearing" of the surface by eddies of liquid approaching obliquely (see Fig. 12). For such systems one may extend the above theory as follows (24).

The resistance r which an eddy encounters as it approaches the surface will determine the thickness λ of the surface zone of damped turbulence. For clean surfaces, r and λ vary directly with γ ; the eddies, approaching either normally to the clean surface or obliquely, "dent" the surface and so lose energy. But in addition to denting the surface, the oblique eddies sweep out a certain region of the surface, "renewing" the liquid thereon (cf. the term s in the Danckwerts theory). It is therefore these oblique eddies which will encounter an *extra* resistance to movement near the surface if Π is nonzero. Quantitatively one may write that the resistances of the (more or less) normal and oblique eddies are respectively proportional to γ [Levich (19a)] and to $\gamma + \beta \Pi$ [Davies (24)]. If Π is not zero, the "surface clearing" stress $\beta \Pi / \lambda$ will generally be more important than the "deformation" stress represented by γ / λ . For example, the numerical coefficient β may be of the order (24) of 100, from comparison

with the data of Fig. 11. The present writer is attempting to calculate β from hydrodynamic theory. Using now the concept that the different regions of the surface in intermediate conditions (with eddies approaching at various angles of incidence) may be described by resistances in parallel (see also above), one obtains for r , the effective resistance of the film-covered surface to eddies, assuming that the two horizontal and one vertical velocity components are additive:

$$1/r = 0.5/\gamma + 0.5/(\gamma + \beta\Pi)$$

On a more complete theory, one would have to insert other numerical coefficients. For the present, however, we follow Levich in omitting them, except that here it is assumed quite arbitrarily that half the eddies are more or less normal to the surface and that half approach obliquely. This is done to make Eq. (16) below tend to Eq. (15) (as it must) in the limit of $\Pi \rightarrow 0$. From the above equation r is found to be given by:

$$r = \frac{\gamma(\gamma + \beta\Pi)}{\gamma + 0.5 \beta\Pi}$$

Hence, since r determines λ , we can extend Levich's equation (135.7) to:

$$\lambda = \left\{ \frac{\gamma(\gamma + \beta\Pi)}{\gamma + 0.5 \beta\Pi} \right\} \rho^{-1} v_e^{-2}$$

The expression for $k_2 (= D^{1/2} v_e^{1/2} \lambda^{-1/2})$ now becomes (24):

$$k_2 = D^{1/2} v_e^{3/2} \rho^{1/2} \left\{ \frac{\gamma + 0.5 \beta\Pi}{\gamma(\gamma + \beta\Pi)} \right\}^{1/2} \quad (16)$$

When $\Pi \rightarrow 0$ (clean surface), Eq. (16) reduces to Eq. (15). In the limit of $\beta\Pi$ being large compared with γ , k_2 tends to 0.7 times k_2 for a clean surface. In one series of experiments (Fig. 3) the ratio in the limit of large Π is found to be 0.5 and Eq. (16) does correctly give the form of the curves of k_2 against Π (as in Figs. 3, 9, and 11). In particular, the curves have the same, nearly hyperbolic shape, not strongly dependent on the value of the Reynolds number, as is predicted by Eq. (16) if β is a constant. A more detailed analysis (24) shows that β should depend on $v_e^{-1/2}$ if Π is small, and v_e^{-1} if Π is large. The experimental procedures and the results of the dependence of k_2 on D and v_e (i.e., on Re) are discussed below.

D. EXPERIMENTS ON GAS-LIQUID SYSTEMS WITH A PLANE INTERFACE

1. Static Systems

In the rapid absorption of O_2 and CO_2 into unstirred, chemically reactive solutions (20), monolayers of stearyl alcohol may decrease the

uptake of gas by 30%. In such studies, R_1 can be made negligibly low by using pure gases, and R_2 is fairly small because of the simultaneous reaction and diffusion, at least in the terms of the few minutes required for measurements. Hence R_1 may readily be determined. As in evaporation studies, proteins and cholesterol are ineffective, but the values of R_1 for oxygen diffusing through films of the C_{16} and C_{18} alcohols are much higher than found in evaporation studies, being respectively about 80 and 290 sec. cm.⁻¹; the values for CO_2 are similar to these figures (20).

Another technique for studying the absorption of CO_2 into water uses an interferometer to obtain the concentration gradients as close as 0.01 cm. to the surface (21): a ciné-camera permits results to be obtained within 5 sec. of the admission of the CO_2 . Though various corrections are required, it is claimed that this method eliminates convection difficulties and that resistances as low as 0.25 sec. cm.⁻¹ can be detected. Experimental results for CO_2 into distilled water show no detectable interfacial resistance, though, when surface-active agents (Lissapol, Teepol) are dissolved in the water, the values of R_1 are about 35 sec. cm.⁻¹.

That these figures are higher than the evaporation studies would indicate for such expanded films, suggests that though the blocking effect of the "head-groups" is again important, a layer of molecules of bound liquid water is always present around these "head-groups" (which themselves oppose evaporation moderately), and this bound water (otherwise known as "soft ice") can appreciably retard the transfer of solute molecules. More precise studies of the effects of chain length and of the density of packing of the "head-groups" would be of great interest. A discussion on the subject of "soft-ice" will be found on p. 369 of reference 1.

The layer of "soft-ice" adjacent to an interface may be "melted" or disoriented by adding LiCl. By this means Blank (22) has shown that the value of R_1 of a monolayer of octadecanol to the passage of CO_2 could be reduced from about 300 sec. cm.⁻¹ for pure water to only about 30 sec. cm.⁻¹ for 8M LiCl solution. Under the latter conditions we believe that the "soft-ice" is apparently almost completely melted. A small amount of methanol in the water penetrates and somewhat disrupts the film of octadecanol, and R_1 again drops from 300 sec. cm.⁻¹ to about 30 sec. cm.⁻¹, though with further increase in the methanol concentration the resistance increases again to about 500 sec. cm.⁻¹, presumably due to the methanol molecules held in or near the surface increasing the viscosity of the "soft-ice" layer. These interpretations of the experimental data are not those proposed by Blank, and further studies with a "viscous-traction" surface-viscometer (1) should certainly be carried out to test this "soft-ice" theory.

Some recent results of Hawke and Alexander (23) indicate that monomolecular films have considerable influence on the rate of mass-transfer of CO_2 and H_2S gases from aqueous solution into nitrogen. However, the bulk phase resistances are high and unspecified in these experiments, and may well depend on the damping of convection or vibrational ripples by the monolayers. It is also significant that if one plots the resistances quoted by Hawke and Alexander for the diffusion of H_2S against the reciprocal of the concentration of H_2S gas originally in the water, one obtains (24) a curve which, if extrapolated, passes through or below the origin. This dependence is indicative of the importance of concentration gradients, and suggests that if the concentration of solute is so high as to render these gradients no longer rate-controlling, the additional resistance arising from the presence of the monolayer is zero (or apparently negative). We believe, therefore, that the monolayers act in general by reducing convection in the apparatus of Hawke and Alexander, and that the high resistance they obtain ($\sim 10^4$ sec. cm^{-1}) can be attributed to this cause. That monolayers of protein and other polymers affect the rate of mass-transport is in accord with this interpretation.

2. Dynamic Systems

In the steady-state absorption of oxygen into water in stirred vessels, R_2 may vary between 120 sec. cm^{-1} and 12,000 sec. cm^{-1} , the lower figure corresponding to the most rapid mechanical stirring, and the latter to stirring by convection only (25). Application of Eq. (3) to the experimental data shows that, since D is of the order 10^{-5} cm^2 sec^{-1} , Δx would be 0.1 cm. in water stirred by convection only, 26.6×10^{-3} cm. in water stirred at 50 r.p.m., and 5.8×10^{-3} cm. for stirring at 270 r.p.m. Comparison of the ratio of these thicknesses with the ratio of the stirring speeds, gives a power of -0.9 instead of the -0.67 required by Eq. (10): this may well be due to the interface being able to move, instead of being static as in the data on which Eq. (10) is based. At the lower stirring speeds, and with no wind, a monolayer of hexadecanol (effective in reducing evaporation by 25%—see above) does not alter significantly the rate of oxygen absorption, since R_1 is relatively low (about 1 sec. cm^{-1}), and since also R_2 is unaffected by the presence of the film. At high stirring rates, however, the monolayer may increase R_2 fivefold, by partially damping the eddies of liquid approaching the surface. This hydrodynamic effect of the viscosity and incompressibility of a monolayer is discussed in more detail below. At the lower stirring speeds the monolayer is effective only if the hexadecanol monolayer is compressed on part of the surface by a stream of air; in this way R_2 may be approximately doubled. The effect of a monolayer of hexadecanol on the oxygen

level of a wind-blown reservoir may be found from Eq. (2). Thus, for a given oxygen demand dq/dt by the living material in the reservoir, halving k must double Δc , where Δc is the difference between the oxygen concentrations at the surface ($c_{\text{sat.}}$) and in the bulk of the water (c), i.e., it is the oxygen deficit ($c_{\text{sat.}} - c$). In practice c is about 90% of $c_{\text{sat.}}$, so that Δc is 10% of $c_{\text{sat.}}$; consequently doubling the deficit c will now increase ($c_{\text{sat.}} - c$) to 20% of $c_{\text{sat.}}$; or halving k will reduce c from 90% to 80% of $c_{\text{sat.}}$. This change in oxygen level is not important to the life in the reservoir.

Quantitative measurements (26) show that at moderate stirring speeds k varies as $D^{0.25}$. With high turbulence, however, Kishinevskii's experiments (27) with H_2 , N_2 , and O_2 absorbing into water show no influence of the diffusion coefficient, though at lower stirring rates molecular diffusion becomes significant.

In all the above experiments it was difficult or impossible to clean the interface. Since as little as 0.1 mg. of contaminant per square metre of surface can drastically affect the mass-transfer rate, it is essential to carry out studies using a thoroughly cleaned liquid surface. Davies and Kilner (28) have studied the absorption of pure O_2 , CO_2 , and H_2 into a vessel containing two contra-rotating stirrers, these being run at rates such that the liquid surface was stationary on a time average. A little talc powder dusted on to such a clean surface showed, however, random movements, evidently related to localized turbulent eddies entering the surface. Under such conditions k varies approximately as $D^{0.5}$, in agreement with Eqs. (13) or (15). The dependence of k_2 on Re is approximately as $Re^{0.6}$, this rather low power being presumably related to the fact that most of the turbulence is localized between the contrarotating stirrers in the water. When a film is spread on the surface, however, these random movements in the surface are eliminated, mass transfer then being slower by a factor of about 2 (Fig. 3). No eddies are now entering the surface, and the rather incompressible surface film produces a stagnant layer in the underlying liquid. The mass-transfer coefficient now varies approximately as $D^{0.6}$, according to preliminary measurements (28), in reasonable accord with Eq. (16). The dependence of k_2 on Re is again as $Re^{0.6}$, and the form of the curve of k_2 against C_s^{-1} in Fig. 3 is in accord with Eq. (16).

Gas adsorption into the liquid falling down a wetted wall column is of considerable interest. The flow of liquid down the surface of such a tube is essentially laminar if $Re < 1200$, where Re is defined as $4u/\nu l$, u being the volume flow rate of liquid, l the perimeter of the tube, and ν the kinematic viscosity of the solvent. Under these conditions, if there are no surface forces acting, the velocity of the air-water surface of the

falling film is $1.5u/l\delta$, where δ is the thickness of the falling liquid sheet. The residence time t_r of an element of surface in contact with gas is therefore given by $t_r = hl\delta/1.5u$, if it is in contact with the gas while it falls through a height h . If absorption may be regarded as occurring into

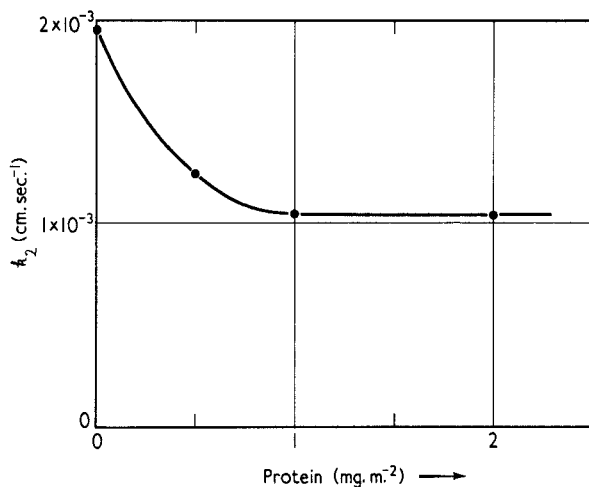


FIG. 3. A spread monolayer of protein decreases k_2 for the absorption of CO_2 (from the gas phase at 1 atm. partial pressure) into water (28). The surface is cleaned thoroughly before the experiment, and the contra-rotating stirrers in the liquid are running at 437 r.p.m. The surface is nonrotating in all the experiments described here, and when k_L is reduced to 1.1×10^{-3} cm. sec.⁻¹, all random surface movements are also eliminated.

a semi-infinite mass of liquid, this calculated value of t_r may be substituted into Eq. (7), or, more strictly, this is valid provided that $hD\nu/g\delta^4 < 0.1$, where g is the acceleration due to gravity (17). If, however, this inequality is not satisfied, the liquid cannot be treated as semi-infinite, nor can the effect of the velocity gradient in the liquid be neglected. To test the applicability of the use of this value of t_r in Eq. (8), i.e., of the expression

$$k_2 = \frac{1}{R_2} = \left(\frac{D}{\pi t_r} \right)^{1/2}$$

Kramers (29) *et al.* studied the absorption of SO_2 into water. This is a comparatively simple process, R_1 being negligibly small and any hydrolysis reactions between CO_2 or SO_2 and water occurring very rapidly relative to the times of contact involved. At low flow rates agreement with theory is satisfactory only if a surface-active agent is present in the system, though without such an agent the experimental results can be as

much as 100% too high (29). At high flow rates, the absorption of SO_2 is independent of the presence of a surface-active agent. These effects are due to rippling of the water sheet which occurs in the absence of surface-active agents: a ripple causes a small velocity component normal to the surface, so facilitating absorption. Such ripples may disappear when a surface-active agent is added (1, 30) and the rate of absorption then agrees with theory. A complicating factor in wetted-wall columns, especially if these are short, is the immobilization of the surface layer: the spreading back-pressure of the monolayer, acting up the falling liquid surface from the pool of liquid below, may reduce its velocity from $1.5u/l\delta$ (quoted above) to practically zero. This effect, clearly visible with a little talc on the surface, causes gas absorption to be much slower than otherwise.

If the times of contact are relatively long (i.e., $hDv/g\delta^4 > 0.1$) the above theory of wetted-wall columns is no longer valid. Instead, one must use Pigford's theoretical equation (16), again valid for laminar flow:

$$k_2 = 3.41D/\delta$$

This assumes that the depth of penetration of the diffusing solute molecules is at least equal to δ , i.e., that $3.6(Dt)^{1/2} > \delta$. Equation (16) is based on normal diffusion theory, and is of the general form of Eq. (3). Again, the ripples formed on the liquid surface may cause results to be several times greater than calculated by diffusion theory if no surface-active agent is present. Now R_2 is at least several hundred sec. cm.^{-1} in typical wetted-wall experiments, and since the surface-active agents used would not increase R_1 beyond 30 sec. cm.^{-1} at the most, the effect of the surface-active agents is entirely hydrodynamic: the ripples when present decrease R_2 below the calculated values.

Absorption of a gaseous solute into a moving liquid at short times can also be conveniently measured using a *falling vertical jet* of liquid, formed in such a way that the liquid velocity is uniform across every section of the jet. Results for CO_2 absorbing into water and dekaline are in close agreement with an equation of the form of Eq. (9), modified to allow for the form of the jet during absorption. This accord shows that R_2 is dominant, R_1 being negligible (31, 32). If surface-active agents are added, the same effects are found as for short wetted-wall columns, an immobile monolayer forming on the lower part of the jet. This monolayer retains powder sprinkled on the surface, and extends to such a distance up the jet that the spreading tendency (forcing it further up the jet) is balanced by the shear stress between the monolayer and the moving liquid of the jet, i.e., $\Delta\Pi = h\tau$, where h is the height the monolayer ex-

tends up the jet, and τ is the calculated mean shear stress. Typical values (32) for 0.2% Teepol are $\tau = 20$ dynes cm.^{-2} and $h = 1.4$ cm., whence $\Delta\Pi = 28$ dynes cm.^{-1} , a quite reasonable value.

Liquid flowing slowly over the surface of a solid sphere is in essentially laminar flow, except that there must be a radial component due to the increase of the amount of surface at the "equator" relative to that at the "poles." This system, useful as a model of packing in an absorption column, has been studied mathematically (33, 34). Further, if a vertical "string" of touching spheres is studied, one finds that this laminar flow is interrupted at each meniscus between the spheres: complete

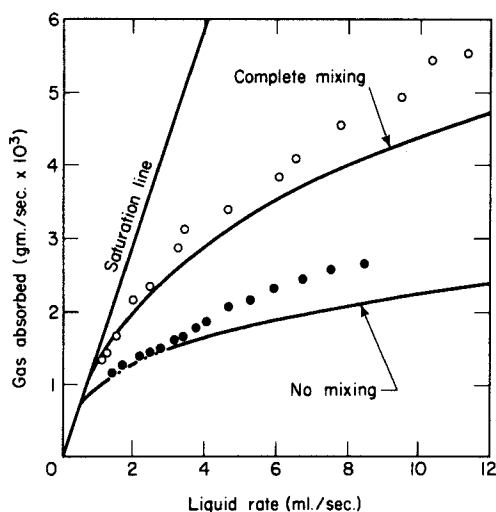


FIG. 4. Carbon dioxide absorption rate for 5 spheres at 25°C: o, experimental results for pure water; ●, Lissapol solution (34).

mixing of the liquid occurs at these points. This is confirmed by measurements and calculations of R_2 for the absorption of CO_2 (Fig. 4). If now a surface-active agent is added to the water flowing over the spheres, the uptake of gas is reduced by about 40%, because the adsorbed monolayer reduces k_2 (by reducing both the eddy mixing at the menisci and the rippling over the spheres (34). This rippling of the clean surface occurs in the system of Fig. 4 at flow rates greater than 3 $\text{cm.}^3 \text{ sec.}^{-1}$, and deviations from the calculated curves at high flow rates are ascribed to ripples and to inertial effects in the liquid flow, not allowed for in the calculations (34). There is no evidence that R_1 is important in any of these studies.

III. Transfer between Two Liquid Solvents

When a solute such as acetic acid is diffusing from water to benzene, the sum of the two R terms for the liquid phases is usually much greater than the interfacial resistance R_I . In the simplest, unstirred system, with both liquids taken as infinite in extent, one must solve the diffusion equations (35)

$$\frac{\partial c}{\partial t} = D_1 \left(\frac{\partial^2 c}{\partial x^2} \right) \quad \text{for } x > 0 \quad (17)$$

$$\frac{\partial c}{\partial t} = D_2 \left(\frac{\partial^2 c}{\partial x^2} \right) \quad \text{for } x < 0 \quad (18)$$

referring respectively to the upper and lower phase (Fig. 5a). The initial conditions are typically that, at $t = 0$, $c = c_0$ for $x < 0$, and $c = 0$ for $x > 0$. If there is a negligible interfacial resistance R_I , then $c_{1I}/c_{2I} = B$

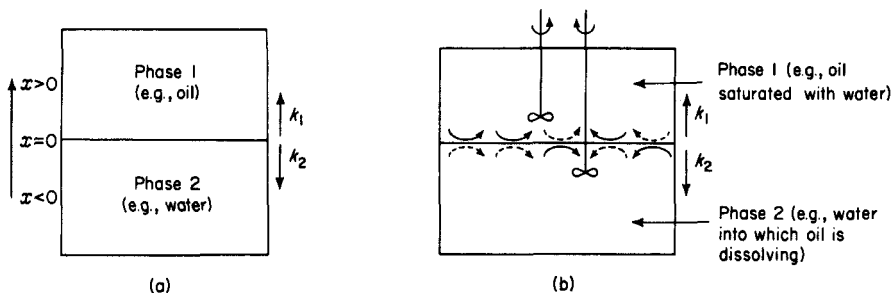


FIG. 5. (a) Unstirred cell. (b) Stirred cell. Full arrows show eddies produced directly by stirrer, broken arrows show eddies induced by momentum transfer across the turbulent liquid interface.

for all $t > 0$, where c_{1I} and c_{2I} are the respective concentrations of the solute immediately on each side of the interface, and B is the distribution coefficient. The continuity of mass transfer across the interface requires that at $x = 0$ the condition $D_1 (dc_1/dx) = D_2 (dc_2/dx)$ is always satisfied, and with these boundary conditions the solutions to the diffusion equations above (if $x = 0$ and $t > 0$) are:

$$c_{1I} = \frac{Bc_0}{1 + B(D_1/D_2)^{1/2}}$$

and

$$c_{2I} = \frac{c_0}{1 + B(D_1/D_2)^{1/2}}$$

These equations imply that the interfacial concentrations must remain

constant as long as the diffusing material has not reached the ends of the cell: for cells which cannot be considered infinite the treatment is more difficult (9).

The total number of moles q of solute which has diffused across the interface after any time t is given by $\int_0^\infty c_1 dx$, which may be integrated (36) to

$$q = \left(\frac{2ABc_o}{1 + B(D_1/D_2)^{1/2}} \right) \left(\frac{D_1 t}{\pi} \right)^{1/2} \quad (19)$$

from which

$$q = 2Ac_{1I} \left(\frac{D_1 t}{\pi} \right)^{1/2} \quad (20)$$

whence the value of k_1 is given with respect to c_{1I} with these initial conditions by

$$k_1 = \frac{1}{R_1} = \left(\frac{D_1}{\pi t} \right)^{1/2} \quad (21)$$

If there is an interfacial resistance, the equations become much more complicated (36, 37), and both q and the ratio c_{1I}/c_{2I} are altered.

These equations, referring to completely unstirred systems, are not usually valid in practice; complications such as spontaneous interfacial turbulence and spontaneous emulsification often arise during transfer, while, if external stirring or agitation is applied to decrease R_1 and R_2 , the hydrodynamics become complicated and each system must be considered separately. The testing of the above equations will be discussed below, after a consideration of overall coefficients and of interfacial turbulence.

In practice, whether the cell is stirred or not, transfer is conveniently referred to "over-all" rather than interfacial concentrations. The over-all transfer coefficient K is related to the individual liquid coefficients by the relations

$$\frac{1}{A} \frac{dq}{dt} = k_1(c_{1I} - c_1) = k_2(c_2 - c_{2I}) \quad (22)$$

and

$$\frac{1}{A} \frac{dq}{dt} = K(c_2 - c_1/B) \quad (23)$$

implying that the material diffusing into the interface must also diffuse away from it. They are applicable at any time t . The factor B must be introduced in the latter equation since the transfer rate will be zero at equilibrium, i.e., when c_1 finally reaches $c_2 B$. Elimination of the rates from Eqs. (22) and (23) gives

$$\frac{1}{K} = \frac{1}{k_2} + \frac{1}{Bk_1} \quad (24)$$

or

$$R_{(\text{over-all})} = R_2 + R_1/B \quad (25)$$

If there is also an interfacial resistance, it will be given by the measured resistance less the $R_{(\text{over-all})}$ value calculated by Eq. (25).

A. SPONTANEOUS EMULSIFICATION AND INTERFACIAL INSTABILITY

If the system contains only two components, such as ethyl acetate and water, the rates of mutual saturation are generally uncomplicated. If, however, a third component is diffusing across the oil-water interface, two complicating effects may occur. The first, spontaneous emulsification (1), is seen when, for example, 1.9 *N* acetic acid, initially dissolved in water, is allowed to diffuse into benzene: fine droplets of benzene appear on the aqueous side of the interface. The mechanism of this spontaneous emulsification is that of "diffusion and stranding"; some benzene initially crosses the interface to dissolve in the water, in which it is slightly soluble due to the presence of the acetic acid. But, as more acetic acid leaves the water to enter the benzene phase, this benzene dissolved in the water phase can no longer remain in solution: it is precipitated as a fine emulsion. No system has yet been found where, under close observation, spontaneous emulsion did not form during the transfer of the third component (1). Although surface-active agents, including protein monolayers, may reduce the amount of emulsion by reducing the interfacial turbulence, as discussed below, they never eliminate it completely.

The second complicating factor is interfacial turbulence (1, 12), very similar to the surface turbulence discussed above. It is readily seen when a solution of 4% acetone dissolved in toluene is quietly placed in contact with water: talc particles sprinkled on to the plane oil surface fall to the interface, where they undergo rapid, jerky movements. This effect is related to changes in interfacial tension during mass transfer, and depends quantitatively on the distribution coefficient of the solute (here acetone) between the oil and the water, on the concentration of the solute, and on the variation of the interfacial tension with this concentration. Such spontaneous interfacial turbulence can increase the mass-transfer rate by 10 times (38).

B. THEORETICAL VALUES OF R_1 AND R_2 IN LIQUIDS

For plane, unstirred cells, the theoretical equations are (21) and (25); and for plane stirred cells there are the theories of Lewis and Whitman, Kishinevskii, Danckwerts, and Levich, and Eqs. (14) and (16) of the present writer. In particular, if Eqs. (7) and (11) represent processes

occurring in parallel, q should depend on some power of D between 0.5 and 0 [Eq. (14)], whereas if they apply in series, Eqs. (2) and (13) should apply.

C. EXPERIMENTS ON LIQUID-LIQUID SYSTEMS WITH A PLANE INTERFACE

1. *Static Systems*

For completely unstirred systems, one may test whether results agree with theory (assuming no interfacial resistance) in one of two ways. Firstly, one may find experimentally c_{1I} and c_{2I} and test whether their ratio is B . Secondly, one may find q at different times and compare the result with Eq. (20). If equilibrium does not prevail across the interface (i.e., if interfacial concentrations are not in the ratio of B), or if the experimental q is less than calculated, then an interfacial resistance must be operative. In systems which are completely unstirred, the amount of material diffusing across the interface may be followed optically, either using the Lamm scale method (36, 37, 39, 40) or following the absorption bands (41). The meniscus at the sides of the cell can be eliminated by using a silane derivative to make the contact angle very close to 90° . Measurements can then be made to within 0.1 mm. of the interface. Radioactive tracers can also be used (42, 43). To minimize convection currents, accurate control of the temperature to $\pm 0.001^\circ\text{C}$. is required; one is also limited to studying systems which maintain at all times an increasing density towards the bottom of the cell. While unstirred cells have the advantage of giving results easily comparable with diffusion theory, they suffer from the disadvantage that the liquid resistances on each side of the interface are so high that an interfacial resistance R_I is experimentally detectable with the most accurate apparatus (36, 37) only if it exceeds $1000 \text{ sec. cm.}^{-1}$ (about $3000 \text{ cal. mole}^{-1}$). Barriers of this magnitude at the interface might arise either from changes in solvation of the diffusing species in passing between the phases, or from a polymolecular adsorbed film.

When acetic acid is diffusing from a 1.9 N solution in water into benzene, spontaneous emulsion forms on the aqueous side of the interface, accompanied by a little interfacial turbulence. Results can be obtained with this system, however, if in analysing the refractive index gradient near the surface a correction is made for the spontaneous emulsion: the rate of transfer is then in excellent agreement (37) with Eq. (20) (Fig. 6). Consequently there is no appreciable energy barrier due to re-solvation of the acetic acid molecules at the interface, nor does the spontaneous emulsion affect the transfer. With a monolayer of sodium lauryl

sulfate or protein at the interface, spontaneous emulsification is virtually eliminated, but the monolayer has no effect on the rate of transfer of the acetic acid (Fig. 6). If, however, a polymolecular "skin" of sorbitan tetrastearate is allowed to form in the interface by dissolving this agent in the benzene, the rate of transfer is considerably reduced (37), the value of R_i being 3000–6000 sec. cm.⁻¹. If acetic acid transfers from water to toluene, spontaneous emulsion and turbulence are again visible (37), and the amount transferred is slightly faster than calculated, presumably on account of the latter factor. Propionic acid transfers from

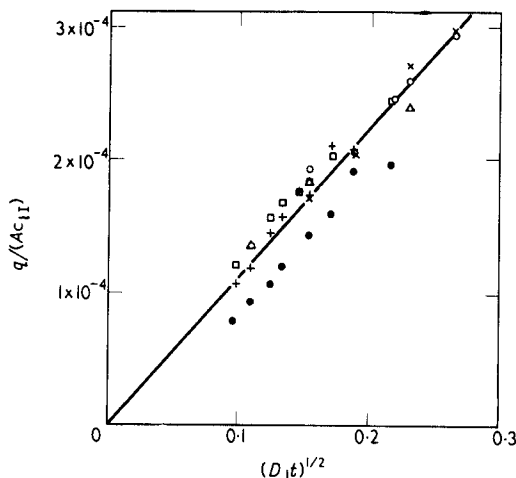


FIG. 6. Experimental data for system of Fig. 5(a), plotted and compared with calculation [Eq. (20)] on the basis of no interfacial resistance to the diffusion of acetic acid from water to benzene (37). Points are: +, clean interface; o, 0.00125 *M* pure sodium dodecylsulfate; Δ, 0.00250 *M* pure sodium dodecylsulfate; □, 0.00250 *M* pure sodium dodecylsulfate + 2.4% lauryl alcohol; +, spread protein; ●, 5000 p.p.m. of sorbitan tetrastearate in the benzene. Units are: q in moles; c in moles liter⁻¹ and $(Dt)^{1/2}$ in cm.

water to toluene in accord with diffusion theory (40, 44), as determined both by comparing the concentrations on each side of the interface with the partition coefficient and by considering the total amount transferred. Butyric and valeric acids, too, give concentration ratios close to the interface in accord with the normal bulk partition coefficients, showing that there is no measurable interfacial barrier: the amounts transferring cannot be determined because of the interfacial turbulence (40).

Diethylamine, transferring from 0.16 *M* solution in toluene to water, shows such strong spontaneous emulsification and turbulence that quantitative results are precluded (36). If, however, 1.25 *mM* sodium lauryl

sulfate is present in the water, the interfacial turbulence is completely eliminated, and transfer then is calculable, if allowance is made for some spontaneous emulsion which is still formed, though less heavily than before. This transfer is in accord with diffusion theory.

The amount of sulfuric acid transferring between water and phenol shows no interfacial resistance for the first 100 min. (42, 43), though subsequently the amount transferring is lower than calculated, suggesting an interfacial resistance of about 4×10^5 sec. cm.⁻¹. Sulfur transferring between certain organic liquids also seems abnormally slow. In view of the long times involved and the possible impurities forming in the system, further experiments would be desirable. In the binary system of *n*-heptane and liquid SO₂, interfacial resistances of 25,000–100,000 sec. cm.⁻¹ are reported (42, 43), though the difficulty of keeping the interface clean in the cells containing rubber gaskets may have been responsible for these extraordinarily high figures.

The extraction of uranyl nitrate from 1 *M* aqueous solution into 30% tributylphosphate in oil is accompanied by an initial interfacial turbulence (41), with more transfer than calculated, even though re-solvation of each uranyl ion at the interface must be a relatively complex process. If the turbulence is suppressed with sorbitan mono-oleate, transfer proceeds at a rate in excellent agreement with theory.

The conclusions we may draw from these results are that, in general, interfacial turbulence will occur, and that it will increase the rate of mass transfer in these otherwise unstirred systems. Monolayers will prevent this turbulence, and theory and experiment are then in good agreement, in spite of spontaneously formed emulsion. There are no interfacial barriers greater than 1000 sec. cm.⁻¹ due to the presence of a monolayer, though polymolecular films can set up quite considerable barriers. Usually there are no appreciable barriers due to re-solvation: however, in the passage of Hg from the liquid metal into water, the change between the metallic state and the Hg₂⁺⁺ (aq) ion reduces the transfer rate by a factor of the order 1000.

Completely unstirred oil-water systems have been only occasionally studied, however, on account of the high experimental accuracy required to obtain reliable results. Much early work concerned slightly stirred systems, studied by direct analysis of samples; again, however, monolayers of protein and other material at the interface do not affect the diffusion rates of solutes which are inappreciably absorbed. These include various inorganic electrolytes and benzoic acid (45). If the solute is surface-active, however, the strong spontaneous interfacial turbulence accompanying transfer greatly increases the rate of transfer relative to that calculated from diffusion coefficients, especially in the early stages

of the diffusion. Since this turbulence can be completely eliminated by surface films, it is not surprising that these reduce the observed high rate of transfer by as much as four times; typical examples of this are found in the transfer of propanol or butanol from water to benzene (46), of phenol from sulfuric acid to water (44), and of acetic acid from CCl_4 to water (47).

2. Dynamic Systems

Vigorously stirred cells have liquid-phase resistances much lower than for unstirred cells, and are therefore useful in investigating interfacial resistances. In practice, R_1 and R_2 can be made quite small; typical values are $10,000 \text{ sec. cm.}^{-1}$ to $100 \text{ sec. cm.}^{-1}$, depending on the rate of stirring. Against this advantage must be set the complications of the turbulent flow: the eddies near the interface are likely to be affected by the proximity of a monolayer.

As an empirical correlation for *clean surfaces*, J. B. Lewis (48) found that his results on systems of the type shown in Fig. 5b obeyed the relation

$$k_2 = 1.13 \times 10^{-7} \nu_2 (Re_2 + Re_1 \eta_1 / \eta_2)^{1.65} + 0.0167 \nu_2 \quad (26)$$

where subscripts 1 and 2 refer to the two liquid phases, where η refers to viscosity, ν to kinematic viscosity ($= \eta/\rho$, in $\text{cm.}^2 \text{ sec.}^{-1}$), and where Re is the Reynolds number of either phase (defined by $L^2 N / \nu$, L being the tip-to-tip length of the stirrer blades and N the number of revolutions of the stirrer per second). A similar equation applies to k_1 by interchanging the subscripts. Various objections have been raised to Eq. (26): though numerically satisfactory to $\pm 40\%$ as written, it requires a further length term on the left side for dimensional uniformity. This could easily be effected using the constant term L . A more piquant criticism (49) is that, since there are no terms in D_2 , this is a form of Eq. (11). It is, however, difficult to see how the eddy diffusion could be completely dominant at the moderate stirring speeds used in the experimental work. Further, the implied proportionality of k_2 and η_2 at low stirring speeds is physically unrealistic, as is the complete cancellation of the term in η_1 in Eq. (26). The dependence of k_2 on $Re_2^{1.65}$ (if ρ_1 is low) is in accord with Eq. (15), which predicts a 1.5 power.

A different empirical correlation of the transfer across a clean interface in a stirred cell comes from the author's laboratory (Mayers (50)):

$$k_2 = 0.00316 (D_2/L) (Re_2 Re_1)^{0.5} (\eta_1/\eta_2)^{1.9} (0.6 + \eta_1/\eta_2)^{-2.4} (Sc_2)^{5/6} \quad (27)$$

where D_2 is the diffusion coefficient of the diffusing species in phase 2 and Sc is the Schmidt number, defined as ν/D . Consequently k_2 varies with $D_2^{1/6}$, this dependence lying between that of the Danckwerts equa-

tion (13) and that of Eq. (26) of J. B. Lewis. This correlation, which is accurate in predicting k_2 to $\pm 40\%$ for different systems, suggests that, when the interface is uncontaminated, the replacement by turbulent flow of elements of liquid in the surface is indeed very important, and that molecular diffusion from these elements has then to occur over a very short distance. Equation (14) can evidently explain the one-sixth power of D_2 .

This continual replacement of liquid is readily visible with talc particles sprinkled on to the interface: though stationary on the average (if the stirrers in phases 1 and 2 are contra-rotated at appropriate relative speeds), they make occasional sudden, apparently random, local movements, which indicate that considerable replacement of the interface is occurring by liquid impelled into the interface from the bulk. Spontaneous interfacial turbulence, associated with such processes as the transfer of acetone from solvent to water, may further increase the rate of transfer by a factor of two or three times (44, 48, 51). Other systems (48), such as benzoic acid transferring (in either direction) between water and toluene, give transfer rates only about 50% of those calculated by Eq. (26), suggesting either that this equation is not valid or that there is an interfacial resistance. This point is discussed in detail below.

Another empirical correlation for clean interfaces is that proposed by McManamey (52):

$$k_2 = 6.4 \times 10^{-4} \nu_2 (Sc_2)^{-0.3} (Re_2)^{0.9} \left[1 + \frac{\eta_1 Re_1}{\eta_2 Re_2} \right] \quad (28)$$

where the numerical factor has the dimensions of cm^{-1} . This equation correlates k_2 with $D^{0.3}$, and the fit to the data of Lewis is somewhat better than that of Eq. (26). The correlation (28) has the advantage that it holds down to low turbulence, when, for example, $Re_1 = 0$. Fig. 7 shows

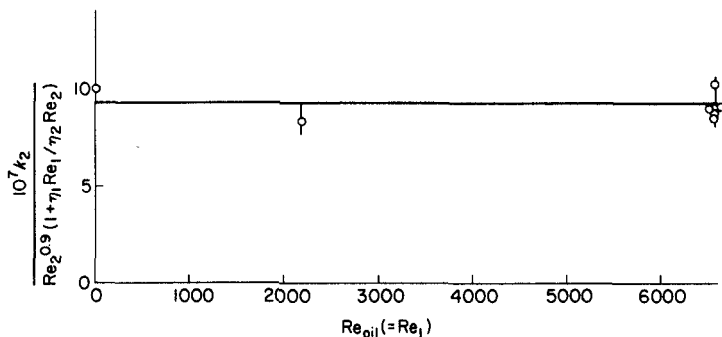


FIG. 7. Experimental data (50) for the solution of ethylacetate into water are platted according to the correlation of Eq. (28). The correlation holds to zero mechanical stirring rate in the oil phase.

that the data of Davies and Mayers (50) are successfully interpreted by Eq. (28): the system is stirred ethylacetate (1) overlying stirred water (2), the latter dissolving some of the ethylacetate at a rate determined by k_2 . In the plot the range of Re_2 is from 1120 to 4480.

Figure 8 shows that for the same system over a range of Re_1 from 0 to 6570, the correlation of k_2 with Re_2 is in accord with Eq. (28).

Study in a stirred cell of the transfer of uranyl ions from water to organic solvents confirms the result for unstirred cells that transfer is faster than theoretical when interfacial turbulence is visible (53). After long times, in systems showing no visible turbulence, the transfer coefficients decrease, becoming less than those calculated from Eqs. (25) and

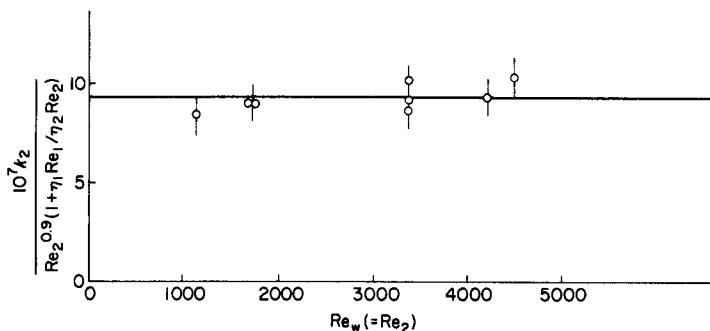
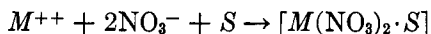


FIG. 8. As for Fig. 7 showing that Eq. (28) is valid down to low rates of mechanical stirring in the water phase.

(26); this retardation is a function of time only and is not due to contamination of the interface. The explanation may lie either in there being some slight spontaneous interfacial turbulence which initially offsets a small error in Eq. (26), or in the slow re-solvation of the uranyl ions at the interface. For the extraction of various metal nitrates from water into *n*-butanol in a stirred cell, there is an interfacial resistance of the order 400 sec. cm.⁻¹, independent of time (54), but dependent on the concentration of the metal nitrate. Such a resistance, which may amount to 50% of the total resistance, is in accord with the kinetic requirements of the complexing equation:



The interfacial resistance is thus due to the metal ion forming a chemical complex with the solvent *S* (here *n*-butanol) at the interface, before it passes completely into the solvent phase. A similar slow step was postulated earlier by Pratt, as discussed below, in connection with practical extraction columns.

For the reverse process of the extraction of the metal salts from *n*-butanol to water, there is spontaneous interfacial turbulence which raises the mass-transfer coefficient to about twice the value expected from the correlation (54).

A technique for studying extraction after times of 10^{-3} –1 sec. has been developed (55), though the hydrodynamic conditions are not exactly known. The laminar jet also constitutes a means of obtaining low values of the liquid phase resistances, permitting relatively low values of R_I to be detected. The rate of solution of isobutanol into a water jet (over contact times of 0.05–0.5 sec.) indicates a resistance R_I of the order 80 sec. cm.⁻¹, whether or not surface-active agents are present (56).

For *surfaces covered with a monolayer* (e.g., a protein), the value of k_2 is reduced by as much as 80%; the effect of a compressed protein monolayer at different stirring speeds can be expressed (48) by:

$$k_2 = 1.13 \times 10^{-7} \nu_2 Re_2^{1.65} + 0.0167 \nu_2 \quad (29)$$

This is Eq. (26) with the term in Re_1 omitted; physically this means that the momentum of the turbulent eddies of oil near the interface is damped out by the monolayer, so that the stirring in the oil (phase 1) can no longer contribute to increasing k_2 . It is surprising, however, that making the interface immobile (and thus damping out the eddies approaching the interface from the stirrer in phase 2) does not reduce k_2 below the value given by Eq. (29). Possibly this indicates an inherent difficulty in the Lewis correlation.

For film-covered interfaces, the mass-transfer rate of ethylacetate (phase 1) into the water (phase 2) is decreased by a factor of 4.3 to a limit of 23.4% of the rate, at equal Reynolds numbers, for transfer across a clean interface (see Fig. 9). The data reported here are those of Davies

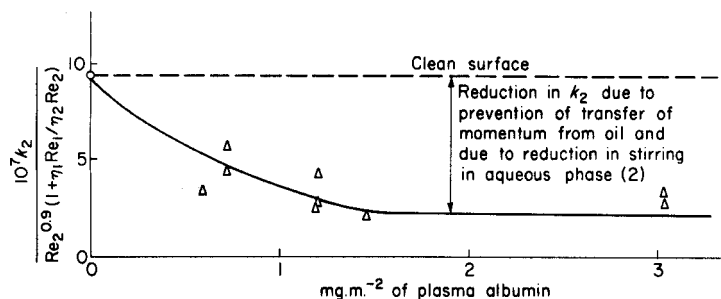


FIG. 9. Reduction in k_2 by spread monolayer of protein, due to prevention of transfer of momentum from ethylacetate, and to reduction in turbulence in the aqueous phase near the interface. Experimental data used here are taken from reference (50).

and Mayers; Re_1 lies between 0 and 6570, and Re_2 lies between 1680 and 4480. The fall in k_2 with increasing amounts of adsorbed material at the interface may be caused by either or both of the effects on k_2 : (i) the interfacial film damps out in phase 2 the turbulent eddies coming from the stirrer in phase 2 (water), and (ii) the interfacial film damps out the momentum transfer across the interface: some of the momentum from the eddies in phase 1 would, for a clean interface, be transferred across into phase 2, stirring the latter near the interface. The second effect can be allowed for by multiplying Re_1 in Eq. (28) by a transfer coefficient α , relating to the transfer of momentum across the interface. For a clean interface $\alpha = 1$, and Re_1 enters the correlation as in Eq. (28), while for an interface appreciably covered with a film, α will tend to zero. Figure 10 shows the effect of α tending to zero: only effect (ii) is then allowed

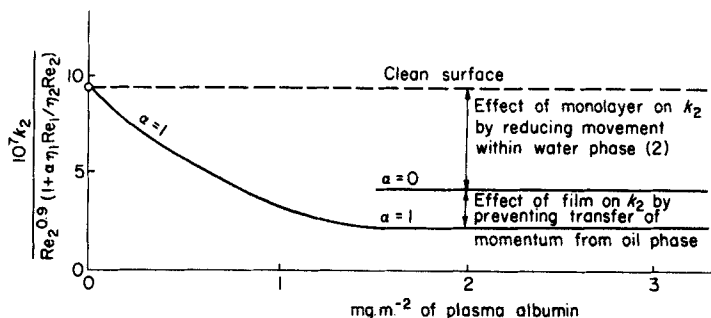


FIG. 10. Quantitative interpretation (24) of plot in Fig. 9.

for, but this reduces k_2 by a factor of 1.9 (i.e., $4.2/2.2$). By difference, factor (i) has reduced k_2 from 9.4 to 4.2, i.e., by a factor of 2.2. These comparisons of k_2 imply fixed values of the Reynolds numbers. The form of the curve for factor (i) is in accord with Eq. (16), though the dependence on $Re_2^{0.9}$ is less than according to theory.

Gas-absorption rates furnish another test of the magnitude of effect (i). If the gas is pure (e.g., CO_2 at a partial pressure of 1 atm.), and is absorbing into stirred liquid, then the momentum-transfer term $\eta_1 Re_1$ is always negligible; thus an interfacial film can reduce k_2 only through effect (i) above. The results of Davies and Kilner (1, 28) show that for the absorption of CO_2 into water, the limiting value of factor (i), by which the film reduces k_2 , is 1.9 (i.e., $1.96/1.04$). This may be compared with the figure of 2.2 quoted above for the ethylacetate-water system.

For a three component system, such as the extraction of isopropanol from benzene to water or vice-versa, one finds the same effects of interfacial films. Fig. 11 shows that in the limit, when the interface becomes

so resistant to local compression as to be immobile, the mass-transfer rate is reduced by a factor of 4.3 (i.e., $15.2/3.5$). This factor is the same within experimental limits as that for the two-component systems of ethylacetate and water described above. That a limit is reached supports the conclusion that the effect of the surface film is purely hydrodynamic, i.e., that it increases R_2 (and, in general, R_1), while any true interfacial resistance R_I is negligibly small (e.g., 30 sec. cm.^{-1} at most for a protein monolayer). Also consistent with this view is the fact that the reduction in the role of mass-transfer (Fig. 11) is a simple function of Re .

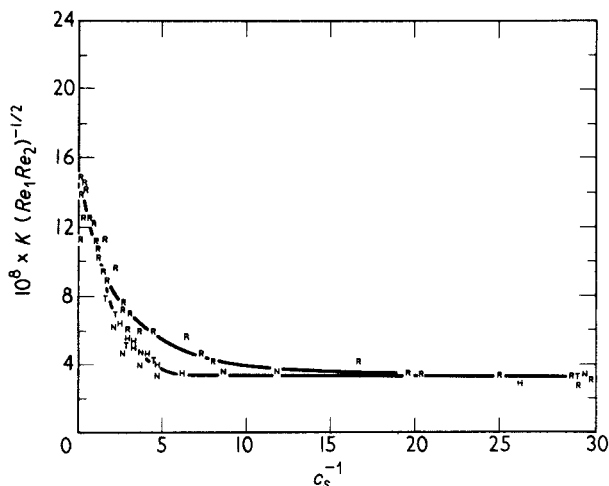


FIG. 11. Plot of $K (Re_1 Re_2)^{-1/2}$ (in cm. sec.^{-1}) against C_s^{-1} (dynes cm.^{-1}) for spread monolayers of bovine plasma albumin. K refers to the over-all mass-transfer coefficient for isopropanol transferring from water to benzene, and various stirring speeds are employed in the apparatus of Fig. 5(b). R refers to the runs using re-distilled water, H to those using $0.01 N \text{ HCl}$, N to those using 0.01 NaOH , and T to those using tap water (50).

The observed rates of transfer are lower than those calculated by the correlation of Eq. 26 for organic molecules which themselves are surface-active, without specifically added long-chain molecules: thus in the transference of $(\text{C}_4\text{H}_9)_4\text{NI}$ from water to nitrobenzene, of benzoic acid from toluene to water and the reverse, of diethylamine between butyl acetate and water, of n -butanol from water to benzene, and of propionic acid between toluene and water, the rates (44, 48) are of the order one-quarter to one-half those calculated by Eqs. (25) and (26). Since with these systems the solute itself is interfacially active, and therefore its monolayers should reduce the transfer of momentum, we interpret these findings as indicative that R_1 and R_2 are increased in this way. This is

confirmed by the experimental rate of transfer of propionic acid from water to toluene in the stirred cell being lower than calculated, while in the unstirred cell there is no interfacial resistance R_I which would explain this. Conversely, sulfuric acid, which is not surface-active, transfers from water to phenol even faster than calculated (although in the unstirred cell a resistance, presumably due to an interfacial skin of impurities, is reported) (42, 44).

The effect of protein and other monolayers on mass-transfer rates depends quantitatively (50) on the surface compressional modulus, C_s^{-1} : this is defined as the reciprocal of the compressibility of the "contaminating" surface film, i.e., $C_s^{-1} = -A d\Pi/dA$. For films at the oil-water interface C_s^{-1} is often close to Π , the surface pressure, which is equal to the lowering of the interfacial tension by the film.

The quantity C_s^{-1} correlates the effects of monolayers, both spread and adsorbed, on K , as in Fig. 11. As one may show quantitatively with talc particles, the eddy velocity at the interface is greatly reduced by the monolayer. The latter restrains fresh liquid from being swept along the surface, i.e., there is less "clearing" of the old surface. If now $\Delta\Pi$ is the surface pressure resisting the eddy due to its partly clearing an area (Fig. 12) in

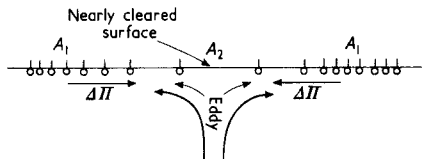


FIG. 12. Eddy brings fresh liquid surface into the interface, but this is opposed by the back pressure $\Delta\Pi$ of the spread film.

the interface (and consequently changing the available area per molecule from A_1 to A_2), then

$$\Delta\Pi = \left(\frac{\partial\Pi}{\partial A}\right)(A_2 - A_1)$$

whence, if A_2/A_1 is defined as j ,

$$\Delta\Pi = C_s^{-1}(j - 1) \quad (30)$$

Since the differential spreading pressure $\Delta\Pi$ will oppose the movement of the eddy at the interface, it will also oppose surface renewal and hence mass transfer. Equation (16) explains the form of the plot of Fig. 11.

Solubility of the film will "short-circuit" the compressional modulus: a minimum in the transfer coefficient is often observed (50, 57, 58) (Fig. 13). From this figure it is also clear that, whereas monolayers affect greatly the stirring near the surface (and so reduce k_2 and the transfer

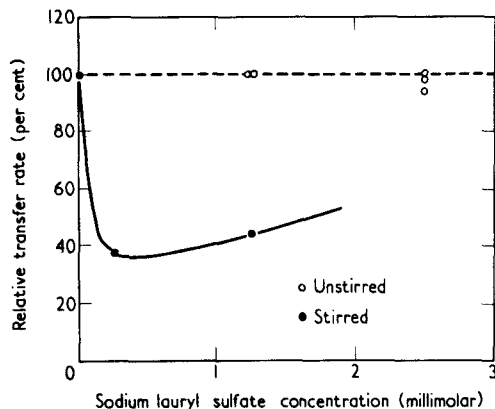


FIG. 13. Comparison of effect of sodium lauryl sulfate on the transfer of acetic acid from water to benzene at 25°C. in an unstirred (36, 37), and in a stirred cell (50).

rates in stirred cells) they have no measurable effect in unstirred liquid-liquid systems.

IV. Drops and Bubbles

The value of R_L^* within a falling drop of liquid is of interest in view of the applications of spray absorbers. A wind-tunnel (59) for the study of individual liquid drops, balanced in a stream of gas, has shown (60) that R_L for a drop depends on its shape, velocity, oscillations, and internal circulation. The drop will remain roughly spherical only if

$$\frac{\Delta\rho a^2 g}{\gamma} < 0.1$$

where $\Delta\rho$ is the density difference between the drop and the continuous phase, γ is the surface tension, and a is the radius of the drop. In general, if this inequality is not satisfied, the shape of the drop is a complicated function of the variables. Because of such distortion, liquid drops over about 2 mm. diameter fall more slowly than would the equivalent solid sphere. Oscillations of the drop are usually about the equilibrium spherical shape, which becomes alternately prolate and oblate with a frequency in accord with the theoretical value of $(8\gamma/3\pi w)^{1/2}$, where w is the weight of the drop. Though oscillation of the drop appears to increase k_L , there is no simple relation between these quantities.

During the first few seconds after the formation of a drop, k_L for gas absorption may be as much as sixty times greater than predicted by diffu-

*Subscript L refers to the liquid phase.

sion into a static sphere (60, 61): this is related to the high initial rate of circulation in the drop, caused by the breakaway of the drop from the nozzle. As this initial rapid circulation dies away, k_L falls to about 2.5 times that predicted for a static sphere: this factor of 2.5 is in accord with calculation (62), assuming that the natural circulation inside the falling drop is in streamline flow (Fig. 14a).

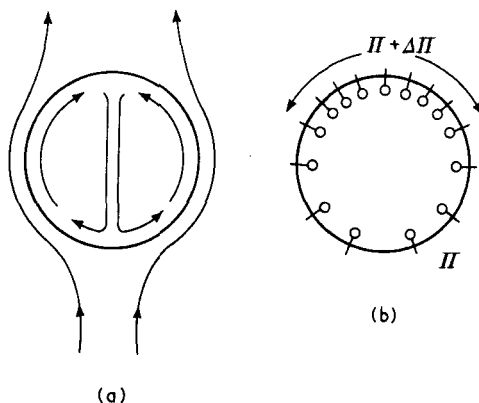


FIG. 14. Circulation within a falling liquid drop, and opposing effect of surface pressure gradient.

This natural circulation occurs by a direct transfer of momentum across the interface, and the presence of a monolayer at the interface will affect it in two ways. Firstly, the surface viscosity of the monolayer may cause a dissipation of energy and momentum at the surface, so that the drop behaves rather more as a solid than as a liquid, i.e., the internal circulation is reduced. Secondly, momentum transfer across the surface is reduced by the incompressibility of the film, which the moving stream of gas will tend to sweep to the rear of the drop (Fig. 14b) whence, by its back-spreading pressure Π , it resists further compression and so damps the movement of the surface and hence the transfer of momentum into the drop. This is discussed quantitatively below, where Eq. (32) should apply equally well to drops of liquid in a gas.

If this natural circulation within the drop is thus reduced by adsorption at the surface, k_L and the rate of gas absorption fall to the values calculated for molecular diffusion into a stagnant sphere (60).

Any surface turbulence will greatly increase k_L : this is found in the absorption of SO_2 into drops of *n*-heptane, which is ten times faster than expected, according to Groothuis and Kramers (11).

Transfer of gas from a rising bubble into a liquid is becoming increasingly important: bubble and foam columns are often more efficient than

are packed towers for gas absorption. *Small bubbles* (<0.2 cm. diameter) behave as rigid spheres, possibly because they are very sensitive to surface films [see Eq. (36) below]: k_L is independent both of the mechanical agitation and of bubble size. However, k_L does vary linearly with $D^{2/3}$: this is all as required by theory (63–65). Surface films reduce the momentum transfer at the bubble surface and hence the rate of rise (64–66). *Large bubbles* no longer behave as rigid spheres, though k_L is still independent of the bubble size and of the liquid agitation; the values of k_L , however, are considerably higher than for small bubbles (63–65, 67), and k_L varies with $D^{0.84}$. The movements of the surface of a large rising bubble are very complex and defy exact hydrodynamic analysis. The rate of absorption of CO_2 into pure water from large (>1.5 cm³.) spherical cap bubbles (67a) is about 50% higher than the rate calculated from the surface renewal theory: this high mass-transfer rate occurs when the rear of the bubble is rippling turbulently. Addition of 0.1% *n*-hexanol to the water, however, eliminates this turbulent rippling, and k_L is reduced to a value close to that calculated. If, instead of the *n*-hexanol, one adds 0.01% “Lissapol” to the water, the mass-transfer rate is lowered to only about 50% of the theoretical: not only are the turbulent ripples at the rear of the bubble suppressed, but the surface-active agent is so strongly adsorbed that the surface renewal over the spherical part of the surface is now eliminated (67a).

Diffusion from single drops is easily measured: the process of formation of a drop of organic liquid, containing a solvent to be extracted into water, induces internal circulation which in turn so promotes transfer that up to 50% of the extraction may occur during the period of formation of the drop (68). Even after release of the drop, as it rises freely through the water, the rate of extraction is often as much as twenty or forty times higher than that calculated from diffusion alone, suggesting that the liquid in the drop must still be circulating rapidly (68, 69). Indeed, this internal circulation, often accompanied by oscillation, may cause removal of each element of liquid at the interface after a residence only 10% of the period required for the drop to rise through one diameter: empirically (57, 58) one finds that K varies as $D^{0.38}$. The reason for this circulation of liquid within the drop lies in the drag exerted along the surface by the relative motion of the continuous phase: the circulation patterns (69–71) are shown in Fig. 14.

The effects of interfacial monolayers on the extraction from drops are particularly striking. Early work showed that traces of either impurity or surface-active additives can drastically reduce extraction rates: even plasticiser, in subanalytical quantities dissolved from plastic tubing by benzene, reduces the mass-transfer rate by about ten times by retarding

the hydrodynamic renewal of elements of liquid at the interface (72). Further, more polar solvents are particularly liable to give the high mass-transfer coefficients associated with circulation (73), presumably because at their surfaces the energy of adsorption of surface-active impurities is relatively low. Thus, while oils such as benzene and hexane are very easily contaminated, drops of butylacetate and isopropylether in water are much less readily affected by surface-active impurities (74).

When an interfacial film has reduced the circulation within a drop, the wake vortex becomes more marked, while the extraction rate falls to that for a stagnant sphere (74). More detailed studies of the hydrodynamics of naturally moving drops have recently been carried out (75). The mass-transfer rate in 2-component systems should correlate (76) with $Re^{1/2} Sc^{1/2}$ if the drops are circulating, but with $Re^{1/2} Sc^{1/3}$ if the drops are stagnant. One practical study (76) gave a dependence on $Re^{1/2} Sc^{0.42}$, indicating partial circulation.

The mechanism by which the surface film inhibits internal circulation is that the fluid flow will drive the adsorbed material towards the rear of the drop: consequently the surface concentration and surface pressure will be higher here, and the monolayer will tend to resist further local compression (Fig. 14b). This resistance to flow in the surface damps down circulation inside the drop by reducing the movement of the interface, and hence reduces the transfer of momentum across it (and also the rate of rise or fall of the drop (72), by perhaps 12%). Again, as for stirred liquids separated by a plane interface, the surface compressional modulus C_s^{-1} of the interfacial film is often the determining quantity, though with a highly viscous monolayer the interfacial viscosity must also play a part. The resistance to the circulation of a drop will depend on the drop radius a , since the smaller the drop the larger will be the surface pressure gradient between the front and the rear, and the smaller will be the tangential frictional stress. In terms of a dimensionless group (1), the circulation will be reduced by some function of $(C_s^{-1}/a^2 \cdot g \cdot |\Delta\rho|)$ where $|\Delta\rho|$ is the difference in density of the liquids in the drop and in the continuous phase, and g is the gravitational acceleration. The ratio of the bulk viscosities of the outer and inner liquids, $(\eta_{\text{outer}}/\eta_{\text{inner}})$ must also have an effect on the circulation. Hence, in general

$$\text{Degree of circulation} = \phi_1 \left[\frac{\eta_{\text{outer}}}{\eta_{\text{inner}}} \right] \times \phi_2 \left[\frac{C_s^{-1}}{a^2 g \cdot |\Delta\rho|} \right] \quad (31)$$

where ϕ_1 and ϕ_2 are functions to be determined. There is an additional proviso that the surface film must not be too highly soluble—formic acid is ineffective, while octyl alcohol reduces circulation greatly. Let us define the “percentage circulation” in a drop by:

% circulation = [% velocity of circulation][fraction of liquid circulating] where the first bracket refers to the viscous drag effect, and is given by $100/[1 + 1.5\eta_{\text{inner}}/\eta_{\text{outer}}]$. The second term corrects for the fact that the interfacial film, compressed to the rear of the drop, prevents circulation there. With slight contamination, only the fluid in the rear of the drop will stop circulating, but with appreciable contamination all the fluid within the drop will be immobilized. The second bracketed term will thus depend on the dimensionless group $C_s^{-1}/a^2g|\Delta\rho|$, and will involve a numerical constant. The expression for drop circulation thus becomes:

$$\% \text{ circulation} = \left[\frac{100}{1 + 1.5 \left(\frac{\eta_{\text{inner}}}{\eta_{\text{outer}}} \right)} \right] \left[1 - \frac{fC_s^{-1}}{a^2 \cdot g|\Delta\rho|} \right] \quad (32)$$

where f is a numerical coefficient. The value of f has been evaluated (24) by comparison with the experiments on rates of rise and fall of Linton and Sutherland (69): for their systems it is about 0.6, i.e., the group $C_s^{-1}/a^2 \cdot g|\Delta\rho|$ must read 1.5.

This semi-empirical approach may be compared with a calculation based on the hydrodynamic stress gradient at the equator of a steadily moving drop with a rigid surface, and for $Re < 1$. The latter condition is easily satisfied for small drops. The tangential stress gradient is given (70, 77) by:

$$P_t = 0.33ga|\Delta\rho| \sin \theta$$

where θ is measured from the forward direction of drop movement. If this stress gradient is just balanced by the surface pressure gradient of an insoluble film (so that the interface is, in the practical case, immobile), then

$$\frac{d\Pi}{d(a\theta)} = P_t = 0.33ga|\Delta\rho| \sin \theta \quad (33)$$

Integration gives

$$\Pi = -0.33ga^2|\Delta\rho| \cos \theta + \Pi_e \quad (34)$$

where Π_e is the surface pressure at the equator. The maximum value of Π will occur at $\theta = 180^\circ$, when [by Eq. (34)],

$$\Pi_{\text{max}} = \Pi_e + 0.33ga^2|\Delta\rho|$$

and the minimum value of Π (at $\theta = 0$) is given by:

$$\Pi_{\text{min}} = \Pi_e - 0.33ga^2|\Delta\rho|$$

When circulation is just prevented all over the drop, Π will be zero at

$\theta = 0$, with the surface pressure over the surface increasing with θ . At this minimum surface coverage, therefore,

$$\Pi_e = 0.33a^2g|\Delta\rho| \quad (35)$$

and so all circulation will be just stopped when:

$$\frac{3\Pi_e}{a^2g \cdot |\Delta\rho|} = 1$$

In practice one cannot measure Π_e on the moving drop, and it is preferable to use the "mean compressional modulus" of the surface film, defined by $C_s^{-1} = -A \, d\Pi/dA$. For the drop as a whole this becomes

$$C_s^{-1}(\text{mean}) = -4\pi a^2 \cdot d\Pi/2\pi a \sin \theta \, d(a\theta)$$

Elimination of $d\Pi$ between this equation and Eq. (33) above gives the "damping group" requirement for the condition of a *totally* immobile interface:

$$\frac{C_s^{-1}(\text{mean})}{a^2g \cdot |\Delta\rho|} \geq 0.7 \quad (36)$$

At Reynolds numbers in the range 10–100, often found in practice, the symmetrical equation (33) will no longer hold strictly: the stress then reaches a maximum at a value of θ which tends towards 57° at high Reynolds numbers (e.g., $Re > 500$). Under such conditions P_t will be given by a more complicated expression (69).

If the interface is completely clean ($C_s^{-1} = 0$), fluid drops will always circulate, according to Eq. (32); but it predicts that if the drop is very small, the circulation should become highly sensitive to small values of C_s^{-1} . Thus, for a drop of benzene of $a = 0.1$ cm., a film of $C_s^{-1} = 1.9$ dynes cm.⁻¹ will completely stop circulation; but a drop of $a = 0.01$ cm. should cease to circulate when $C_s^{-1} = 2 \times 10^{-2}$ dynes cm.⁻¹, corresponding to a surface coverage of about 1 molecule per 10^5 \AA^2 (about 0.02% coverage). Formic acid is not effective in reducing circulation because, even though C_s^{-1} may be of the order 1 dyne cm.⁻¹, the fractional desorption rate is too high: calculation (24) of $(1/n)(-dn/dt)$ suggests that this is as high as 10^4 sec.^{-1} for the weakly adsorbed film of formic acid. If this rate is very much greater than the rate of movement of the bubble or drop through one diameter, one may expect (24) that an effective build-up of surface-active material at the rear of the drop or bubble will not be possible. Often this rate of movement will be of the order 50 sec.^{-1} .

The rates at which drops and bubbles rise and fall are rather more sensitive to traces of surface-active materials than are the mass-transfer coefficients (77a, 77b). Whereas, for example, the rate of fall of CCl_4 drops

reaches a lower limit when $10^{-5} M$ $C_{11}H_{23}SO_4^-$ is present in the water, the mass-transfer rate does not reach its lower limit until the concentration of this surface-active agent reaches about $10^{-4} M$ (77a). The present author interprets these results as follows. Under the conditions of the experiments just mentioned (when the aqueous phase contained $2 \times 10^{-3} M$ citric acid), one may calculate that a 10-fold increase in concentration of the surface-active agent will increase the amount of the adsorbed $C_{11}H_{23}SO_4^-$ by a factor of only $10^{1/3}$, i.e., by a factor of 2.16. The method of calculation is that given on pp. 191 and 195 of reference 1. The surface pressure and C_s^{-1} will be affected by the same factor. Now the rate of fall of the CCl_4 drops at moderate Re depends principally on the characteristics of the turbulent wake. In the absence of surface-active material, the mobile surface of the drop or bubble can behave in such a way that the rear offers somewhat less resistance to motion than does that of a solid sphere; but if the rear of the drop or bubble is covered beyond $\theta > 135^\circ$, the velocity of rise or fall becomes close to that of a solid sphere (77c). Levich (77d) claims that, at $Re = 300$, the turbulent wake of an uncontaminated bubble (mobile interface) occupies the small solid angle of $\theta > 178^\circ$, whereas for a body whose interface is immobile, the turbulent wake occurs at θ greater than about 90° .

Using the value of $\theta = 135^\circ$, one calculates from Eq. (34) that Π_{\max} will be only 15% of the value required for complete coverage. Similarly, by Eq. (36), the value of the group $C_s^{-1}/a^2g|\Delta\rho|$ is reduced to only 0.1 for the limiting retardation of velocity. If, on the other hand, the entire rear hemisphere of the drop or bubble must be covered for the limiting velocity to be reached (77e), the group $C_s^{-1}/a^2g|\Delta\rho|$ would have to reach the value 0.33, one-half that given in Eq. (36). This could explain the factor of 2.16 calculated above from the experimental finding of Boye-Christansen and Terjesen (77a).

It is interesting to note that Π_{\max} , when calculated by the above equations, may exceed the maximum surface or interfacial pressure to which the film can, in practice, be subjected. The absorbed film will then desorb or crumple, or it may rather suddenly be shed to the rear of the drop as a filament or, if the interfacial tension is very close to zero, as emulsion. The drop may thus, on suddenly losing its surface film, accelerate again, as has indeed been noted (without explanation) by Terjesen. For the same reason, drops larger than given by some critical radius, may have a calculated Π_{\max} greater than the adsorbed film can maintain, and hence will rise or fall with virtually no retardation, though drops below this critical size will be retarded to the velocity expected for solid spheres (70).

A detailed analysis by Griffith (77f) of the velocity of fall of a clean fluid drop gives the following equation for the terminal velocity v_t :

$$v_t = \{2a^2g|\Delta\rho|/9\eta_{\text{outer}}\} \{(\eta_{\text{inner}} + \eta_{\text{outer}})/(\eta_{\text{inner}} + 0.67\eta_{\text{outer}})\} \quad (37)$$

For a solid particle, Stokes' Law gives the terminal velocity (v_{ts}) as

$$v_{ts} = 2a^2g|\Delta\rho|/9\eta_{\text{outer}} \quad (38)$$

In the presence of surface-active material, however, the measured terminal velocity v_t for a fluid drop approaches v_{ts} : the ratio v_t/v_{ts} depends again on the group $\Pi/a^2g|\Delta\rho|$. Calculation gives a value of 0.08 for this group if the surface-active material is to cause v_t to be halfway between the values in Eqs. (37) and (38) above. For v_t to approach closely to v_{ts} , the group must be 0.25, though v_t should become appreciably different from that given by Eq. (37) when the group is as low as 0.02. Experiments (77f) show that this theory works quite well in practice: v_t is found to be halfway between the values in Eqs. (37) and (38) when $\Pi/a^2g|\Delta\rho|$ is between 0.05 and 0.10 (cf. 0.08 by theory), for CCl_4 drops in glycerol, in the presence of various surface-active additives. With "Aerosol O.T.," however, the corresponding experimental value of the group is 0.25, i.e., 3 times too high, suggesting that an anomalously high value of Π is required because of the ready solubility of this material in oils.

Small gas bubbles ($a \sim 0.08$ cm.) rising in water are found to circulate less when $4.5 \times 10^{-4}M$ caproic acid is present (65). Here since the desorption rate ($1/n$) ($-dn/dt$) is much lower (~ 70 sec. $^{-1}$, i.e., of the order of the usual reciprocal time for the bubble to rise through one diameter), the caproic acid film adsorbed from the $4.5 \times 10^{-4}M$ solution should be able to reduce circulation within the bubble provided that the damping group $C_s^{-1}/a^2g|\Delta\rho|$ is large enough. Substitution of the calculated C_s^{-1} for the adsorbed film gives a value of about 0.07 for this ratio, in rough accord with the experimental finding that circulation is inhibited under these conditions. A few parts per million of octanol will also prevent bubble circulation: this is consistent with the estimated fractional desorption rate of only 6 sec. $^{-1}$, and the value of about 0.4 dynes cm. $^{-1}$ for C_s^{-1} . The group $C_s^{-1}/a^2g|\Delta\rho|$ then becomes about 0.07. For small bubbles rising in water, trace contamination always prevents circulation if $a < 0.03$ cm., while if $a = 0.07$ cm., $10^{-6}M$ sodium lauryl sulfate slightly reduces circulation (78) (and hence the rate of rise). More appreciable reduction in circulation occurs in solutions of $10^{-5}M$ sodium lauryl sulfate: here one may calculate (24) from the properties of ionized monolayers (1) that Π and C_s^{-1} are about 0.2 dyne cm. $^{-1}$. Though such a small value of Π would be extremely difficult to measure, the group $C_s^{-1}/a^2g|\Delta\rho|$ has a value of about 0.03, which is sufficiently high, we believe, to explain the observed reduction in circulation. Raising the concentration of sodium lauryl sulfate to $10^{-4}M$ reduces still further the rate of rise of the bubbles, the ratio then

being calculated (24) to approach unity. Further addition of sodium lauryl sulfate is found to have little effect. Similar effects are found with iso-amylalcohol as the surface-active agent: a concentration of $2 \times 10^{-3}M$ greatly reduces circulation (78), and the damping group is calculated (24) to be about 0.3.

The rate of mass-transfer, unlike the terminal velocity, may reach its lower limit only when the whole surface of the drop or bubble is covered by the adsorbed film. In the absence of surface-active material, the freshly exposed interface at the front of the moving drop (due to circulation here) could well be responsible for as much mass transfer as occurs in the turbulent wake of the drop. The results of Baird and Davidson (67a) on mass transfer from spherical-cap bubbles are not inconsistent with this idea, and further experiments on smaller drops are in progress in the author's laboratory. In general, if these ideas are correct, while the rear half of the drop is noncirculating (and the terminal velocity has reached the limit of that for a solid sphere), the mass transfer at the front half of the drop may still be much higher, due to the circulation, than for a stagnant drop. Only when sufficient surface-active material is present to cover the *whole* of the surface and eliminate all circulation will the rate of mass-transfer approach its lower limit.

If the concentration of added surface-active agent is varied, one often finds that the extraction rate passes through a shallow minimum (between 30% and 40% of the value with no additive) (72). Where this occurs, the concentration of surface-active agent is usually of the order $10^{-3}mM$ to $1mM$. This may be related to the similar maximum found for wave-damping at a certain concentration of surface-active agent (1, 30).

Many commercial solvents, particularly those which are nonpolar, are very liable to have poor circulation, due to traces of strongly adsorbed impurities: the commercial polar oils form circulating drops because the impurities are less strongly adsorbed, and so C_s^{-1} is low. Further, according to the theory above, the smaller the drop the more sensitive it should become to traces of surface-active impurity, as is confirmed by Linton and Sutherland's experiments (69). These show that 1 mm. benzene drops can be made to circulate only by rigorous attention to the removal of adventitious impurities; even large drops of commercial benzene are always stagnant. Protein in concentrations as low as 0.0005% will reduce the circulation of drops (5 mm. in diameter) of oils of interfacial tension greater than 30 dynes cm^{-1} .

One can displace the film of impurity from the interface by adding a sufficient amount of a short-chain alcohol. The films of short-chain alcohols, are, however, so readily desorbed that they do not greatly in-

hibit the circulation of the liquid, though they may produce other circulation patterns due to the spontaneous interfacial turbulence associated with their redistribution. In this way the reduction (by a surface film) of k_L for any component being extracted can be offset by the addition of a few per cent of short-chain alcohol or acetic acid to the oil drop (71, 72): this increases the extraction efficiency as much as ten times, bringing it back to the value for a circulating drop (71). In the absence of a surface film the spontaneous interfacial turbulence, on the addition of a little alcohol or otherwise, increases k_L still further (51). Since interfacial turbulence is reduced or nullified by strongly adsorbed monolayers, it is likely that only the effects of rather weakly adsorbed surface films can be offset by the addition of a short-chain alcohol.

Mechanically imposed oscillations at frequencies of 5–50 cycles sec.⁻¹ cause increases of up to 4 times in the rates of extraction of acetic acid from drops of CCl₄ into water (79). The increase is due to the periodic deformation of the drops causing fluid circulation inside and outside, particularly at certain "resonant" frequencies.

V. Practical Extraction

In liquid-liquid extraction using wetted-wall columns, analysis is possible only by dimensionless groups (73): for the core fluid, flowing up inside the tube, k_c varies as approximately $D_c^{0.67}$ and for the fluid falling down the inner walls, k_w varies as $D_w^{0.38}$. Systems studied include phenol-kerosene-water, acetic acid-methylisobutylketone-water, and uranyl nitrate between water and organic solvents (73, 80–82); interfacial resistances of the order 100 sec.cm.⁻¹ are observed in the last system. These resistances are interpreted as being caused by a rather slow third-order interfacial exchange of of solvent molecules (S) coordinated about each UO_2^{++} ion:



The square of the uranyl nitrate concentration is required in the kinetic analysis. Mass transfer with chemical reaction (16, 83) is, however, too specialized a subject to be discussed fully here.

Study of the efficiency of packed columns in liquid-liquid extraction has shown that spontaneous interfacial turbulence or emulsification can increase mass-transfer rates by as much as three times when, for example, acetone is extracted from water to an organic solvent (84, 85). Another factor which may be important for flow over packing has been studied by Ratcliff and Reid (86). In the transfer of benzene into water, studied with a laminar spherical film of water flowing over a single sphere immersed in benzene, they found that in experiments where the interface was clean

there was agreement with calculation, assuming that the stresses were freely transmitted across the interface. Under these circumstances, the calculated variation of the mass-transfer rate with the flow-rate u of the benzene and the diffusion coefficient D for benzene in water is as $u^{1/3} D^{1/2}$.

If, however, trace impurities are present to an extent at which there is a stagnant film over the liquid-liquid interface, calculation shows that the mass-transfer rate should vary as $u^{1/9} D^{2/3}$, with a numerical reduction (compared with mobile interfaces) of up to 64% in the rate. Experiments (86) showed reductions of the order of 50%.

Fluctuations of interfacial tension may alter the coalescence rate: if between two adjacent drops of the phase into which extraction is occurring, there arrives an eddy of undepleted continuous phase, the drops must "kick" towards each other (for summary, see reference 1) this process assisting coalescence. This increase in the coalescence rate will occur if (as is usual) the fluid component being extracted causes an appreciable decrease in interfacial tension. An alternative explanation (85) of the more ready coalescence under certain conditions is that, when transfer is occurring from the drops to the continuous phase, the region between the drops is more concentrated in solute than is a region away from the line of approach of the drops, and adsorption of the solute is therefore enhanced between the drops. This adsorption in turn leads to spreading of the surface film away from this region, some of the intervening bulk liquid also being carried away with the surface film: this is termed the Marangoni effect (1). The film of liquid separating the drops is thus thinned, and coalescence of the drops is consequently promoted. However, the "kicking" mechanism leads to the same conclusion, namely that the drops are brought into close proximity if the liquid between them is more concentrated in solute; and so far the two explanations have not been subjected to rigorous experimental tests. The important experimental difference is that in the former explanation a local thinning of the liquid film between the drops is responsible (leading presumably to protuberances on the surfaces of the drops), whereas in the latter it is the excess pressure inside the drops, far from the point of approach, that deforms the whole drops, driving them together. Possibly high-speed ciné-photography or variations in the viscosity of the phases might lead to a clarification of the mechanism. For "kicking" drops approaching a plane interface, the thinning appears to be dependent only on the Marangoni effect, though the "kicking" produces considerable lateral movements of the drop (87).

If, in laminar flow, transfer is occurring into drops, the region between two of the latter becomes preferentially depleted in solute. The lowered adsorption in this region then causes spreading of the surface film and

associated liquid into this region (or possibly the drops "kick" away from each other), and coalescence becomes unlikely. As pointed out above, however, if an eddy of the undepleted solution happens to be swept between the drops, this will favor coalescence.

In practical plants for liquid-liquid extraction the effect of surface-active agents is usually to increase the rate of extraction: presumably the smaller droplet sizes associated with the lower interfacial tension more than compensate for the reduction in the stirring by momentum transfer at the interface. Thus in a column packed with Raschig rings, the rate of extraction increases linearly (to about 50%) with the decrease in interfacial tension (88), though at higher concentrations of surface-active additive the rate passes through a maximum, due either to adsorption of rather impermeable multilayers or to the back-mixing associated with very small drop sizes. In a rotating-disc contractor, addition of 0.01% Teepol similarly increases the extraction efficiency (89). Further, if the column is operated with oil as the continuous phase, the dispersed drops of water coalesce on, and subsequently run down, the glass and metal surfaces. This reduces the efficiency of extraction by a "bypassing" effect, which can be avoided by rendering these surface hydrophobic with silicones.

VI. Distillation

When the diffusion of a component from a vapor bubble to the liquid is measured, one finds that the mass-transfer coefficient is larger when the surface tension is increased by the mass transfer (90-93): this is due to spontaneous interfacial turbulence. Further, when the surface tension of the liquid in a distillation column is higher towards the bottom of the column, the plate efficiencies are relatively high (70-80%) because thin sheets of liquid, such as stabilize slightly the bubbles of vapor, are fairly stable, leading to a longer time of contact of vapor and liquid on each plate. With a surface tension decreasing down the column, however, the bubbles are highly unstable, and the plate efficiency is lowered to perhaps 60%. The appearance of Oldershaw perforated plates (94) with liquid chosen so that the surface tension increases down the column (as with the ethanol-water system) is shown in Fig. 15, in which V_R denotes the vapor velocity relative to the velocity just sufficient to prevent seepage of liquid. For acetic acid-water mixtures, in which the surface tension decreases down the column, the appearance is as shown in Fig. 16.

The foaming ability of a liquid mixture depends on the magnitude of the variation of surface-tension with concentration, but not on its sign (95). In practice, however, the effect of surface tension on plate efficiency

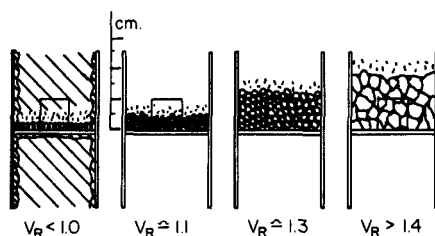


Fig. 15. Interfacial structure for systems in which the surface tension increases towards the bottom of the column (94).

depends on the sign of the surface-tension gradient, but not on its magnitude (96). One explanation (97) of the results is that drops of liquid formed as spray on the plate by the upward vapor flow can sometimes break a lamella by being blown on to its underside: if the surface tension is decreasing down the column, spray blown on to the lamella from below will cause spreading and consequent destabilization (98). But if the surface tension is increasing down the column, the drops would have a higher surface tension than the liquid in the lamella (which is assumed to have reached equilibrium with the vapor above the plate), and so would *not* destabilize the lamella by spreading across it if they impinge. Another explanation (99) involves the mass-transfer process directly: the thin region of any lamella will lose the M.V.C. fastest, so that if the M.V.C. has a lower surface tension, the surface tension will rise locally on the lamella, and fresh liquid will spread in along the surface (Marangoni effect), so stabilizing the lamella. This system again corresponds to an increasing surface tension down the column. Conversely, if the M.V.C. is of higher surface tension, the surface tension on the lamella will be lowered by the relatively rapid local evaporation, and liquid will spread away from the lamella, so destabilizing it.

These effects may be less pronounced in industrial sieve-plate columns, because the higher vapor velocities shorten the life of any froth on the trays; the material on the tray is in the form of a spray of droplets

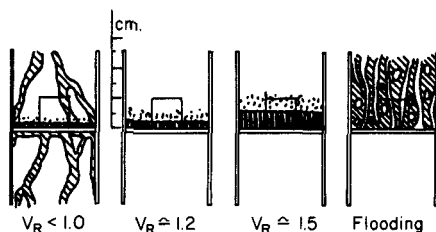


Fig. 16. Interfacial structure for systems in which the surface tension decreases towards the bottom of the column (94).

(100). Because of the operation of up to three factors (interfacial turbulence, impingement of drops on foam and the Marangoni effect on foam) the behavior of columns containing plate-contacting devices should be more sensitive to surface tension effects than packed columns, in which only interfacial turbulence should affect the rate of mass-transfer. Experiments on packed columns should therefore show the relative importance of the effect of interfacial turbulence, but the results available (101, 102) are unfortunately not decisive, and much further work remains to be carried out before the relative importance of the different factors is established. Recent experiments at Birmingham (103), however, support the contention that Vigreux and Kintmesh columns show surface-tension effects very similar to those found in small sieve-tray columns, suggesting that surface turbulence is the dominant factor. The present author believes that some of the discrepancies in the literature arise from varying local vapor velocities, and that the relative importance of turbulence thus mechanically induced to the spontaneous surface turbulence should be investigated.

REFERENCES

1. Davies, J. T., and Rideal, E. K., "Interfacial Phenomena." Academic Press, New York, 2nd ed., 1963.
2. Lewis, W. K., and Whitman, W. G., *Ind. Eng. Chem.* **16**, 1215 (1925).
3. Mansfield, W. W., *Nature* **175**, 246 (1955); *Australian J. Appl. Sci.* **9**, 245 (1958); **10**, 65, 73 (1959).
4. Grundy, F., *Proc. 2nd Intern. Congr. Surface Activity, London* **1**, 270 (1957). Dressler, R. G., and Johanson, A. G., *Chem. Eng. Progr.* **54**, 66 (1958).
5. Linton, M., and Sutherland, K. L., *Australian J. Appl. Sci.* **9**, 18 (1958).
6. Bradley, R. S., *J. Colloid Sci.* **10**, 571 (1955); Eisner, H. S., Brookes, F. R., and Quince, B. W., *Nature* **182**, 1724 (1958); Eisner, H. S., Quince, B. W., and Slack, C., "Experiments on Dust Binding with Aerosols." *Min. Power (Gt. Brit.) Safety Mines Res. Estab. Res. Rept.* **180** (1959).
7. Whytlaw-Gray, R., and Patterson, H. S., "Smoke." Arnold, London, 1932.
8. Green, H. L., and Lane, W. R., "Particulate Clouds, Dusts, Smokes and Mists." Spon, London, 1957.
9. Scott E. J., Tung, L. H., and Drickamer, H. G., *J. Chem. Phys.* **19**, 1075 (1951).
10. Langmuir, I., and Langmuir, D. B., *J. Phys. Chem.* **31**, 1719 (1927).
11. Groothuis, H., and Kramers, H., *Chem. Eng. Sci.* **4**, 17 (1955).
12. Haydon, D. A., *Nature* **176**, 839 (1955); *Proc. Roy. Soc. A* **243**, 483 (1958).
13. Sternling, C. V., and Scriven, L. E., *A.I.Ch.E. Journal* **5**, 514 (1959).
14. Kishinevskii, M. K., and Pamfilov, A. V., *Zh. Prikl. Khim.* **22**, 1173 (1949).
15. Higbie, R., *Trans. Am. Inst. Chem. Engrs.* **31**, 365 (1935).
16. Sherwood, T. K., and Pigford, R. L., "Absorption and Extraction," pp. 20, 22, 265-267. McGraw-Hill, New York, 1952.
17. Danckwerts, P. V., *Ind. Eng. Chem.* **43**, 1460 (1951).
18. Toor, H. L., and Marchello, J. M., *A.I.Ch.E. Journal* **4**, 97 (1958).
19. Kafarov, V. V., *Zh. Prikl. Khim.* **29**, 40 (1956).

- 19a. Levich, V. G., see pp. 135, 136 in ref. 77d below.
20. Blank, M., and Roughton, F. J. W., *Trans. Faraday Soc.* **56**, 1832 (1960).
21. Harvey, G. A., and Smith, W., *Chem. Eng. Sci.* **10**, 274 (1959).
22. Blank, M., *J. Phys. Chem.* **65**, 1698 (1961).
23. Hawke, J. G., and Alexander, A. E., *Proc. 3rd Intern. Congr. Surface Activity Mainz, Germany* Vol. 2, p. 184 (1961).
24. Davies, J. T., unpublished calculations.
25. Downing, A. L., and Truesdale, G. A., *J. Appl. Chem.* **5**, 570 (1955); "Water Pollution Research 1956." H.M.S.O., London; Linton, M., and Sutherland, K. L., *Australian J. Appl. Sci.* **9**, 18 (1958).
26. Hutchinson, M. H., and Sherwood, T. K., *Ind. Eng. Chem.* **29**, 836 (1937).
27. Kishinevskii, M. K., and Serebryansky, V. T., *Zh. Prikl. Khim.* **29**, 27 (1956).
28. Davies, J. T., and Kilner, A. A., to be published; see also ref. 1, p. 315.
29. Lynn, S., Straatemeier, J. R., and Kramers, H., *Chem. Eng. Sci.* **8**, 81 (1958).
30. Davies, J. T., in press.
31. Vielstich, W., *Chem.-Ing.-Tech.* **28**, 543 (1956).
32. Cullen, E. J., and Davidson, J. F., *Trans. Faraday Soc.* **53**, 113 (1957).
33. Lynn, S., Straatemeier, J. R., and Kramers, H., *Chem. Eng. Sci.* **4**, 63 (1955); Davidson, J. F., and Cullen, E. J., *Trans. Inst. Chem. Engrs. (London)* **35**, 51 (1957); Cullen, E. J., and Davidson, J. F., *Chem. Eng. Sci.* **6**, 49 (1956); Davidson, J. F., *Trans. Inst. Chem. Engrs. (London)* **37**, 131 (1959).
34. Davidson, J. F., Cullen, E. J., Hanson, D., and Roberts, D., *Trans. Inst. Chem. Engrs. (London)* **37**, 122 (1959).
35. Crank, J., "The Mathematics of Diffusion." Oxford Univ. Press, London and New York, 1956.
36. Wiggill, J. B., Ph.D. Thesis, University of Cambridge, England, 1958.
37. Davies, J. T., and Wiggill, J. B., *Proc. Roy. Soc.* **A255**, 277 (1960).
38. Maroudas, N. G., and Sawistowski, H., *Nature* **188**, 1186 (1960).
39. Lamm, O., "The Ultracentrifuge" (T. Svedberg, and K. O. Pedersen, eds.). Oxford Univ. Press, London and New York, 1940; Lamm, O., and Polson, A., *Biochem. J.* **30**, 528 (1936).
40. Ward, A. F. H., and Brooks, L. H., *Trans. Faraday Soc.* **48**, 1124 (1952).
41. Hahn, H. T., Report HW-32626 (Richland), U.S. Atomic Energy Commission, Washington, D. C.
42. Tung, L. H., and Drickamer, H. G., *J. Chem. Phys.* **20**, 6, 10 (1952).
43. Sinfelt, J. H., and Drickamer, H. G., *J. Chem. Phys.* **23**, 1095 (1955).
44. Blokker, P. C., *Proc. 2nd Intern. Congr. Surface Activity, London* Vol. 1, p. 503 (1957).
45. Sjölin, S., *Acta Physiol. Scand.* **4**, 365 (1942); Davies, J. T., *J. Phys. Chem.* **54**, 185 (1950).
46. Hutchinson, E., *J. Phys. Chem.* **52**, 897 (1948).
47. Sigwart, K., and Nassenstein, H., *Naturwissenschaften* **42**, 458 (1955).
48. Lewis, J. B., *Chem. Eng. Sci.* **3**, 248, 260 (1954).
49. Sherwood, T. K., *Chem. Eng. Sci.* **4**, 290 (1955).
50. Davies, J. T., and Mayers, G. R. A., *Chem. Eng. Sci.* **16**, 55 (1961); Mayers, G. R. A., *Chem. Eng. Sci.* **16**, 69 (1961); Thesis, University of Cambridge, England, 1959.
51. Sherwood, T. K., and Wei, J. C., *Ind. Eng. Chem.* **49**, 1030 (1957).
52. McManamey, W. J., *Chem. Eng. Sci.* **15**, 251 (1961).
53. Lewis, J. B., *Chem. Eng. Sci.* **8**, 295 (1958).

54. McManamey, W. J., *Chem. Eng. Sci.* **15**, 210 (1961).
55. Martin, T. W., *Nature* **183**, 312 (1959).
56. Quinn, J. A., and Jeannin, P. J., *Chem. Eng. Sci.* **15**, 243 (1961).
57. Holm, A., and Terjesen, S. G., *Chem. Eng. Sci.* **4**, 265 (1955).
58. Boye-Christensen, G., and Terjesen, S. G., *Chem. Eng. Sci.* **7**, 222 (1958).
59. Garner, F. H., and Kendrick, P., *Trans. Inst. Chem. Engrs. (London)* **37**, 155 (1959).
60. Garner, F. H., and Hale, A. R., *Chem. Eng. Sci.* **2**, 157 (1953); Garner, F. H., and Lane, J. J., *Trans. Inst. Chem. Engrs. (London)* **37**, 162 (1959).
61. Groothuis, H., and Kramers, H., *Chem. Eng. Sci.* **4**, 17 (1955); Hatta, S., and Baba, A., *J. Soc. Chem. Ind. (Japan)* **38**, 544B (1935); Calderbank, P. H., and Korchinski, I. J. O., *Chem. Eng. Sci.* **6**, 65 (1956).
62. Kronig, R., and Brink, J. C., *Appl. Sci. Res.* **A2**, 142 (1950).
63. Calderbank, P. H., *Trans. Inst. Chem. Engrs. (London)* **36**, 443 (1958); **37**, 173 (1959).
64. Frossling, N., *Beitr. Geophysik* **32**, 170 (1938).
65. Gorodetskaya, A. V., *Zh. Fiz. Khim.* **23**, 71 (1949); Stuke, B., *Naturwissenschaften* **39**, 325 (1952).
66. Fedosov, A. I., *Russ. J. Phys. Chem. (English Transl.)* **8**, 109 (1959).
67. Hammerton, D., and Garner, F. H., *Trans. Inst. Chem. Engrs. (London)* **32**, S18 (1954).
- 67a. Baird, M. H. I., and Davidson, J. H., *Chem. Eng. Sci.* **17**, 87 (1962).
68. Sherwood, T. K., Evans, J. E., and Longcor, J. V. A., *Am. Inst. Chem. Engrs.* **35**, 597 (1939); Licht, W., and Conway, J. B., *Ind. Eng. Chem.* **42**, 1151 (1950); Licht, W., and Pansing, W. F., *Ind. Eng. Chem.* **45**, 1885 (1953).
69. Linton, M., and Sutherland, K. L., *Proc. 2nd Intern. Congr. Surface Activity, London* Vol. 1, p. 494 (1957).
70. Levich, V. G., *Zh. Eksperim. i Teor. Fiz.* **19**, 18 (1949); Frumkin, A., and Levich, V. G., *Zh. Fiz. Khim.* **21**, 1183 (1947).
71. Garner, F. H., and Skelland, A. H. P., *Chem. Eng. Sci.* **4**, 149 (1955).
72. West, F. B. et al., *Ind. Eng. Chem.* **43**, 234 (1951); **44**, 625 (1952); Garner, F. H., and Hale, A. R., *Chem. Eng. Sci.* **2**, 157 (1953); Lindland, K. P., and Terjesen, S. G., *Chem. Eng. Sci.* **5**, 1 (1956).
73. Pratt, H. R. C., *Ind. Chemist* **31**, 63 (1955).
74. Fujinawa, K., Nakaike, Y., and Kurihara, T., *Kagaku Kogaku* **22**, 429 (1958).
75. Elzinga, E. R., and Banchemo, J. T., *A.I.Ch.E. Journal* **7**, 394 (1961).
76. Garner, F. H., Foord, A., and Tayeban, M., *J. Appl. Chem.* **9**, 315 (1959).
77. Stuke, B., *Chem.-Ing.-Tech.* **33**, 173 (1961).
- 77a. Boye-Christiansen, G. and Terjesen, S. G., *Chem. Eng. Sci.* **9**, 225 (1959).
- 77b. Thorsen, G., and Terjesen, S. G., *Chem. Eng. Sci.* **17**, 137 (1962).
- 77c. Fedosov, A. I., *Russian J. Phys. Chem. (English ed.)* **33**, 109 (1959).
- 77d. Levich, V. G., "Physicochemical Hydrodynamics," Prentice-Hall, Englewood Cliffs, New Jersey, 1962.
- 77e. Elzinga, E. R. and Banchemo, J. T., *A.I.Ch.E. Journal* **7**, 394 (1961).
- 77f. Griffith, R. M., *Chem. Eng. Sci.* **17**, 1057 (1962).
78. Okazaki, S., Miyazaki, Y., and Sasaki, T., *Proc. 3rd Intern. Congr. Surface Activity, Mainz, Germany* Vol. 2, p. 549 (1961).
79. Siemens, W., and Franke, M., *Chem.-Ing.-Tech.* **30**, 165 (1958).
80. Hunter, T. G., and Nash, A. W., *J. Soc. Chem. Ind. (London)* **54**, 49T (1935); **56**, 50T (1937).

81. Brinsmade, D. S., and Bliss, H., *Trans. Am. Inst. Chem. Engrs.* **39**, 679 (1943).
82. Murdoch, R., and Pratt, H. R. C., *Trans. Inst. Chem. Engrs. (London)* **31**, 307 (1953).
83. Kishinevskii, M. K., *Zh. Prikl. Khim.* **27**, 382, 450 (1954).
84. Gayler, R., and Pratt, H. R. C., *Trans. Inst. Chem. Engrs. (London)* **35**, 273 (1957).
85. Groothuis, H., and Zuiderweg, F. J., *Chem. Eng. Sci.* **12**, 288 (1960).
86. Ratcliff, G. A., and Reid, K., *Trans. Inst. Chem. Engrs. (London)* **39**, 423 (1961).
87. MacKay, G. D. M., and Mason, S. G., *Nature* **191**, 488 (1961).
88. Chu, J. C., Taylor, C. C., and Levy, D. J., *Ind. Eng. Chem.* **42**, 1157 (1950).
89. Davies, J. T., Ritchie, I. M., and Southward, D. C., *Trans. Inst. Chem. Engrs. (London)* **38**, 331 (1960).
90. Zuiderweg, F. J., and Harmens, A., *Chem. Eng. Sci.* **9**, 89 (1958).
91. Frank, O., Dissertation Eng. Technische Hochschule No. 2827, Zürich, Switzerland, 1958.
92. Grassmann, P., and Anderès, G., *Chem.-Ing.-Tech.* **31**, 154 (1959).
93. Ellis, S. R. M., and Contractor, R. M., *J. Inst. Petrol.* **45**, 147 (1959).
94. Ellis, S. R. M., and Bennett, R. J., *J. Inst. Petrol.* **46**, 19 (1960).
95. Andrew, S. P. S., *Intern. Symp. Distillation, Inst. Chem. Engrs. (London)* **84** (1960).
96. Ellis, S. R. M., and Legg, R. J., to be published.
97. Davies, J. T., and Rideal, E. K., ref. 1, p. 339.
98. Davies, J. T., and Rideal, E. K., ref. 1, p. 415.
99. Danckwerts, P. V., Smith, W., and Sawistowski, H., *Intern. Symp. Distillation, Int. Chem. Engrs. (London)* (1960).
100. Ellis, S. R. M., Barker, P. E., and Contractor, R. N., *Trans. Inst. Chem. Engrs. (London)* **38**, 21 (1960).
101. Zuiderweg, F. J., *Intern. Symp. Distillation, Inst. Chem. Engrs. (London)* **34** (1960).
102. Danckwerts, P. V., *Intern. Symp. Distillation, Inst. Chem. Engrs. (London)* **38** (1960).
103. Ellis, S. R. M., and co-workers, to be published.

Nomenclature

A	area [cm ²]	Sc	Schmidt number
B	distribution coefficient	T	temperature
C_s^{-1}	surface compressional modulus, defined by $-Ad\Pi/dA$ [dynes cm. ⁻¹]	a	radius of drop [cm.]
D	diffusion coefficient [cm. ² sec. ⁻¹]	c	concentration [moles cm. ⁻³]
K	over-all transfer coefficient	f	numerical factor of Eq. (32)
L	length of stirrer blade [cm.]	g	gravitational acceleration [cm. sec. ⁻²]
M	molecular weight	h	height [cm.]
R	gas constant	k	mass-transfer coefficient [cm. sec. ⁻¹]
R_1	resistance to mass-transfer in phase 1 [sec. cm. ⁻¹]	l	perimeter [cm.]
R_i	resistance to mass-transfer in interface [sec. cm. ⁻¹]	l_e	projected eddy length along surface [cm.]
Re	Reynolds number	n	number of adsorbed molecules per cm. ²

p	saturation vapor pressure [dynes cm. ⁻²]	x	distance normal to interface [cm.]
q	moles of material transferring	λ	thickness of liquid at surface in which eddies are damped
r	resistance to eddy reaching free surface	Π	surface pressure of film, i.e., lowering of surface or interfacial tension by film [dynes cm. ⁻¹]
s	fractional rate of turbulent replacement of elements of liquid in surface [sec. ⁻¹]	Π_0	surface pressure at equator of drop $\pi = 3.14$.
t	time [sec.]	γ	surface or interfacial tension, [dynes cm. ⁻¹]
u	volume flow rate [cm. ³ sec. ⁻¹]	δ	thickness of sheet of liquid [cm.]
v	linear velocity [cm. sec. ⁻¹]	η	viscosity [gm. cm. ⁻¹ sec. ⁻¹]
v_0	characteristic eddy velocity in bulk of liquid	θ	angle measured from forward direction of drop movement
\bar{v}_n	mean velocity normal to the interface [cm. sec. ⁻¹]	ν	kinematic viscosity [cm. ² sec. ⁻¹]
w	weight [gm.]	ρ	density [gm. cm. ⁻³]

DROP PHENOMENA AFFECTING LIQUID EXTRACTION

R. C. Kintner

Department of Chemical Engineering
Illinois Institute of Technology, Chicago, Illinois

I. Introduction	52
A. The Extraction Cycle	52
B. Single-Drop Analysis	53
II. Dispersion into Drop Form	54
A. Slow Formation at Nozzles	54
B. Fast Formation at Nozzles	55
C. Rayleigh Jet	56
D. Turbulent Dispersers	57
III. Shape of Forming Drops	57
A. True Shape	57
B. Other Models for the Shape	58
IV. Velocities of Moving Drops	59
A. Navier-Stokes Equations	59
B. Hadamard-Rybczynski Model	60
C. Boussinesq Model	61
D. Drag	61
E. Wall Effects	66
V. Internal Circulation	67
A. Rigid vs. Fluid Spheres	67
B. Indirect Evidence	68
C. Direct Evidence	68
VI. Shapes of Moving Drops	71
A. Low Reynolds Numbers	71
B. High Reynolds Numbers	72
VII. Oscillations of Drops	74
A. Axially Symmetric Type	74
B. Random Wobbling	74
C. Surface Indentations	75
D. Amplitude and Rupture	75
E. Interfacial Turbulence	77
VIII. Boundary Layers	78
A. Flow Around a Sphere	78
B. Nonoscillating Drops	78
C. Oscillating Drops	80
IX. Effects of Surfactants	80
A. Evaluation of Existing Data	81
B. Damping of Oscillations	82
C. Increased Drag	83

D. Internal Circulation	83
X. Field-Fluid Currents	84
XI. Flocculation and Coalescence	85
A. Flocculation and Liquid-Liquid Foams	85
B. Coalescence of Drops	86
XII. Summary	90
Nomenclature	91
References	92

I. Introduction

The importance of moving fluid phenomena in liquid-liquid contacting operations has been recognized ever since the two-film mass transfer theory was first proposed. If a unidirectional rate of mass transfer through a fluid field from one location to a second one is visualized as being equal to the product of a transfer coefficient, an interfacial area and a concentration gradient

$$\left(\frac{dN}{dt}\right)_{1,2} = KA_i \left(\frac{\Delta c}{\Delta x}\right)_{1,2} \quad (1)$$

any hydrodynamic factor affecting any one of the four right-member variables will be reflected in the transfer rate. Thus K should be affected by temperature, since field viscosity, diffusivity, and density are involved. It is also dependent upon concentration level. The area may be constant and static or it may be in a state of dynamic renewal. As will be shown in a later paragraph, the concentration gradient $(\Delta c/\Delta x)$ may vary enormously over short time increments. It is with the fluid factors influencing these variables that this chapter is concerned.

A. THE EXTRACTION CYCLE

A liquid-liquid mass-transfer operation proceeds in several distinguishable steps, whatever may be the particular type of equipment chosen to carry it out. *Dispersion* of one phase into the other creates a large interfacial area. It may be accomplished by mixing impellers, nozzles, orifices, perforated plates, drip points or edges, tower packings, eductors, centrifugal pumps, or by the turbulence created when the two phases are forced at high speed through a pipeline. Time for dispersion is of the order of fractions of a second.

A *holding time* of several seconds must be maintained for mass transfer to proceed to a satisfactory stage. The dispersed droplets must then undergo a *settling* operation to attain separation and recovery. This usually requires many minutes. The total area remains practically constant, but is being continuously renewed by local creation and destruction. The holding and settling zones are often the same and the time duration of

both may be identical. It is sometimes erroneously designated as the residence time or contact time. The settled droplets will collect in a flocculation zone near the main phase interface.

Under certain conditions drops of phase A, surrounded by a film of phase B, and the whole moving in a field of phase A, can come together to form a layer which can best be described as a liquid-liquid foam.

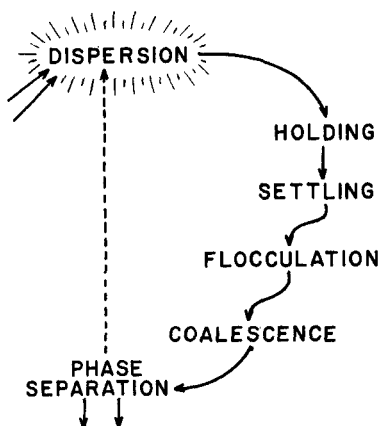


FIG. 1. Extraction cycle.

Drops combine in this flocculation zone, and then join the main drop phase pool by extremely fast *coalescence*. Drops may remain in the flocculation zone for many seconds or minutes, but combine into the main pool phase in a small fraction of a second.

The phases must be finally *separated* and recovered by mechanical devices. The entire cycle of operations is shown in Fig. 1.

B. SINGLE-DROP ANALYSIS

The complex situation involving untold billions of tiny droplets moving in a highly mobile liquid field does not lend itself to fundamental investigation. Simplifications necessary to set up a model upon which to base mathematical analyses are numerous and often unrealistic. To gain knowledge that will lead to better models, many investigators have invested a considerable effort in examining the phenomena pertinent to single moving drops. It is not immediately obvious that knowledge gained from observations on the performance of individual large drops can be directly applied to complex extraction operations. However, if even a little progress can be made by way of this approach, the extensive research devoted to it will have been worth while.

It is in this light that we shall examine the phenomena exhibited by large single moving drops.

II. Dispersion into Drop Form

Two effects are of predominant importance during drop formation. The primary goal of dispersing one phase into the other is to create a large interfacial area available for mass transfer. Subdivision into micron-size droplets will create enormous interfacial area. But one must also be concerned with the recovery of pure phases, and there is therefore an optimum drop size below which dispersion becomes undesirable.

The second important goal is to achieve a very high rate of mass transfer per unit of interfacial area, which has been observed by many experimenters for the drop-formation period. As new area is formed, the concentrations in the main streams are momentarily adjacent to each other. The distance (Δx) can have an extremely small value at the same instant of time. In terms of Eq. (1), the gradient ($\Delta c/\Delta x$) over a small but macroscopic distance is momentarily of a very high order, perhaps approaching infinity. A similar situation arises from the stretching of a surface during oscillation of the drop about a spherical norm. The resulting transfer rates are many times those for unrenewed interfacial area in the same system. Hence, it is quite possible that drop formation is the *major* feature affecting mass transfer in highly turbulent fields which break up the dispersed phase into very small droplets.

Dispersions may be classified into two types, based upon size range of the droplets formed. Turbulence creators (mixing impellers, mixing valves, eductors, orifice plates) will produce fine emulsions of micron-size droplets. Nozzles, perforated plates, bubble caps, tower packings, etc., can form discrete drops of relatively large size which will quickly settle through the continuous phase.

A. SLOW FORMATION AT NOZZLES

The slow formation of a drop at a submerged circular orifice or nozzle will result in a drop size, predicted by equations for determining interfacial tension by the drop-weight method. At the instant a slowly forming drop breaks away from a nozzle, the force balance may be written

$$\pi D_N \sigma = \frac{\pi D_D^3}{6} (\Delta \rho)(g/g_c) \quad (2)$$

A set of correction factors $\psi(D_N/D_D)$ is necessary for exact quantitative results. The model is of course a false one, in that the drop does not break from the nozzle. There is an elongation of a neck of drop fluid connecting the main portion of the drop with that part which is adhering to the nozzle (N1). Rupture is across this neck, often with the formation

of one or more tiny satellite droplets which follow the large one. Called "Plateau's spherules," they may be a source of contamination in many instances. With the correction factors, the method is accurate for drop-size prediction (H6), and is the starting point for analysis of the fast formation of drops at such nozzles (H8).

B. FAST FORMATION AT NOZZLES

For nozzle velocities above the slow-formation range but less than 30 cm./sec., Hayworth and Treybal (H8) accounted for the kinetic energy due to nozzle velocity. Their force balance (written in the form of an equivalent-volume balance) stated that the total volume (V_T) would be equal to the volume (V_σ) necessary to overcome interfacial tension, plus the volume (V_∞) necessary to produce a rising velocity at least equal to the nozzle velocity, plus a negative volume (V_K) equivalent of the kinetic energy supplied by the stream from the nozzle, thus

$$V_T = V_\sigma + V_\infty - V_K \quad (3)$$

From the corrected form of Eq. (2), above

$$V_\sigma = \frac{\pi D_N \sigma}{\Delta \rho g} \left(\psi \frac{D_N}{D_D} \right) \quad (4)$$

Bond's (B5) equation for terminal velocity yielded

$$V_\infty = 0.5236 \left[\frac{18K v_N \mu_c}{\Delta \rho g} \right]^{3/2} \quad (5)$$

in which v_N replaces U_∞ , the terminal velocity of a freely rising (or falling) drop of volume V_∞ .

The volume due to the kinetic energy supplied to the drop was

$$V_K = \frac{V_T \rho_D v_N^2}{2g \Delta \rho D_D} \quad (6)$$

Substitution of these values into Eq. (3) yielded

$$V_T + V_T^{2/3} \left(\frac{0.403 \rho_D v_N}{g \Delta \rho} \right) = \frac{\pi D_N \sigma}{g \Delta \rho} \psi \left(\frac{D_N}{D_D} \right) + 0.5236 \left(\frac{18K v_N \mu_c}{g \Delta \rho} \right)^{3/2} \quad (7)$$

which reduced to Eq. (4) with the correction factor at $v_N = 0$.

This was further simplified by assuming an average value of 0.655 for $\psi(D_N/D_D)$, with the following experimentally established expression for K

$$K = \frac{4.05 D_N^{0.747}}{v_N^{0.635}} \quad (8)$$

the result being

$$V_T + 4.11(10^{-4})V_T^{2/3}\left(\frac{\rho_D v_N^2}{\Delta\rho}\right) = 21(10^{-4})\left(\frac{\sigma D_N}{\Delta\rho}\right) + 1.069(10^{-2})\left[\frac{D_N^{0.747}v_N^{0.365}\mu_C^{0.186}}{\Delta\rho}\right]^{3/2} \quad (9)$$

The equation was considered accurate to within seven per cent for determination of drop volume.

Null and Johnson (N1) suggested that a drop adhering to a nozzle, at the moment of breaking away as shown in Fig. 2, will be composed of a hemisphere A, surmounted by a truncated cone B, which in turn is surmounted by a second truncated cone C. The larger end of the last

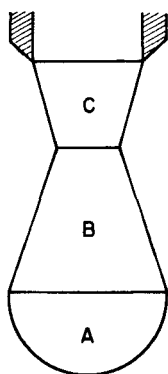


FIG. 2. Drop shape at formation; Null and Johnson model (N1).

section is visualized as adhering either to the edge of the nozzle tip or to the inner surface of the tube leading to the tip. Energy balances, including kinetic energy due to velocity of the liquid in the tube, permit the determination of drop size. A set of experimentally determined correlation factors is necessary.

C. RAYLEIGH JET

If the nozzle velocity is quite high, or if $(\Delta\rho)$ is small enough that the forming drops do not move away from the nozzle sufficiently fast, coalescence of two or more successively formed drops will occur which is not accounted for in any available equation. At still higher nozzle velocities, a Rayleigh jet will form. A node will form in the flowing jet, pass along it and form a drop at the end. This may be several inches from the nozzle. Lamb (L2) derives an expression giving the wavelength for maximum instability, in a cylindrical thread of liquid issuing from a nozzle or orifice at velocities above that for formation of discrete drops. Its direct application to shower-head and multiple-nozzle drop formation in an extraction unit is tenuous. Such jets create turbulence in the sur-

rounding continuous phase, and a cloud of drops with a spectrum of drop diameters will result. A photograph of such action is given by Hayworth and Treybal (H8).

D. TURBULENT DISPERSERS

As this chapter is primarily concerned with single-drop performance, it seems best to omit consideration of drop sizes in highly turbulent liquid fields. The work of Shinnar and Church (S7), utilizing Kolmogoroff's hypothesis of local isotropy, seems to bear excellent promise from a fundamental viewpoint. Correlating equations for predicting drop size in stirred tanks and mixers have been given by Treybal (T3).

III. Shape of Forming Drops

Equations which predict the volume or equivalent spherical diameter of a formed drop are not sufficient for extraction calculations, in the light of the very high rate of mass transfer during drop formation. It is desirable that the equation also lend itself to mathematical manipulation for the calculation of instantaneous interfacial area. To do this, the shape of the drop throughout the formation period must be defined.

A. TRUE SHAPE

The shape of a drop forming slowly at a submerged orifice is the basis for the hanging-drop (pendant-drop) method for determining inter-

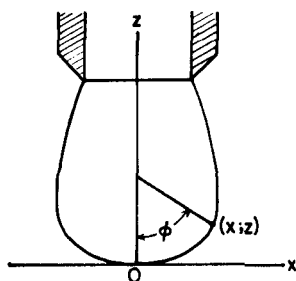


FIG. 3. True shape of hanging drop (B1).

facial tension. The correct equation for the shape, shown in Fig. 3, is (A2, B1, J1, P1)

$$\frac{1}{\rho} + \frac{\sin \phi}{x} = \frac{2}{b} + \frac{\beta z}{b^2} \quad (10)$$

in which ρ and $x/\sin \phi$ are the two principal radii of curvature at $(x:z)$, b is the radius of curvature at 0, and

$$\beta = \frac{b^2 g(\Delta \rho)}{\sigma} \quad (11)$$

This equation does not lend itself to easy mathematical manipulation.

B. OTHER MODELS FOR THE SHAPE

Garner and Hale (G1) assumed hanging drops to be spherical, to facilitate calculation of an average area during formation. The approximate nature of this model was well known to them. During the early stages of formation, the portion of the sphere covered by the orifice is large. During the later stages, the combination of elongation, necking down and abandonment of a portion behind the neck cause deviations of some magnitude. In spite of these shortcomings, the model served rather well.

Poutanen and Johnson (P1) show that the equation of a lituus ($r^2\theta = 1$) resembled the true shape of a gas bubble forming at a submerged nozzle. They varied this geometry by using $r^n\theta = 1$, to describe such shapes quite accurately. Their method for calculating area involves a shape factor similar to that of Andreas *et al.* (A2), with a series of auxiliary graphs. Area becomes

$$A = \int_{\theta_1}^{\pi} \frac{\sin \theta}{\theta^{2/n}} \sqrt{1 + \frac{1}{n^2 \theta^2}} d\theta \quad (12)$$

The volume is

$$V = -\pi \int_{\theta_1}^{\pi} \frac{\sin^2 \theta}{\theta^{2/n}} \left(1 + \frac{1}{n\theta \tan \theta} \right) d\theta \quad (13)$$

Using a digital computer, they established tables of A and V for various values of θ and n . The method should be equally applicable to liquid

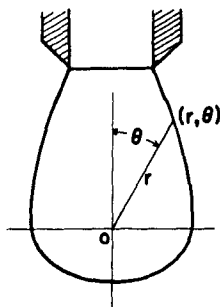


FIG. 4. Shape of hanging drop; lituus model (P1).

drops. With some modification and simplification, it should aid in the calculation of mass-transfer area during formation. The lituus model is illustrated in Fig. 4.

IV. Velocities of Moving Drops

Three kinds of velocities are important for moving drops. True vectorial velocities are necessary when considering point conditions in a field. They can not be measured directly, but may be obtained from streamline plots by a process of graphical differentiation. Semivectorial velocities can be estimated by trace-photography methods (K2). A very useful velocity for determining residence times for drops is called the gross terminal velocity. It is defined as a long vertical distance of travel divided by the corresponding elapsed time. The distance and time must be large enough that all cyclic phenomena such as helical paths or oscillations will have been repeated many times.

A. NAVIER-STOKES EQUATIONS

Any hydrodynamic consideration of a drop moving in a liquid field starts with the Navier-Stokes equations of motion, as given in representative books on fluid mechanics (L2, S11). Using vector notation to conserve space, these equations may be written (B3, B4)

$$\rho \frac{D\mathbf{v}}{Dt} = -\nabla p + \mu \nabla(\nabla \cdot \mathbf{v}) + \mu \nabla^2 \mathbf{v} + \rho \mathbf{g} \quad (14)$$

One can apply these equations and the continuity equations only after some simplification. The divergence term can be dropped for our incompressible liquid-liquid systems, leaving

$$\rho \frac{D\mathbf{v}}{Dt} = -\nabla p + \mu \nabla^2 \mathbf{v} + \rho \mathbf{g} \quad (15)$$

The equations of continuity are

$$\nabla \cdot \mathbf{v} = 0 \quad (16)$$

The velocity of the fluid at the surface of a rigid sphere, held in an infinite expanse of a fluid moving in laminar motion past it, must be zero. Using spherical coordinates, the solutions then become (B4, L2, S11)

$$v_r = U \left[1 - \frac{3}{2} \left(\frac{R}{r} \right) + \frac{1}{2} \left(\frac{R}{r} \right)^3 \right] \cos \theta \quad (17)$$

$$v_\theta = -U \left[1 - \frac{3}{4} \left(\frac{R}{r} \right) - \frac{1}{4} \left(\frac{R}{r} \right)^3 \right] \sin \theta \quad (18)$$

$$p - p_0 = -\frac{3U\mu}{2R} \left(\frac{R}{r} \right)^2 \cos \theta \quad (19)$$

Utilization of Eq. (16) and the sum of the resistance forces over the surface of the sphere (B4) leads to an expression for the form drag

$$F_p = 2\pi\mu RU \quad (20)$$

Addition of the shear forces over the surface of the sphere, with use of Eqs. (17) and (18), leads to an expression for the viscous drag

$$F_\mu = 4\pi\mu RU \quad (21)$$

These two, when added, give the total drag,

$$F_T = 6\pi\mu RU \quad (22)$$

which is Stokes' law of settling, applicable at Reynolds numbers of 0.2 or less. Note that the total drag is composed of two-thirds skin friction and one-third form drag.

B. HADAMARD-RYBCZINSKI MODEL

For a spherical liquid drop moving in a liquid field, the boundary is not rigid. Instead, it moves over the surface of the sphere in axial symmetry from a front stagnation point to a rear stagnation point. New area is being continuously created in the forward regions and an equivalent area is being destroyed in the rear portion of the drop. Utilizing this idealized internal-flow pattern and the resulting boundary conditions (H3), we find that

- (1) $v_\theta = v_s$;
- (2) stresses through the interface are continuous;
- (3) v_θ is continuous through interface;
- (4) there is no movement of fluid across the interface;
- (5) the interfacial tension is zero.

Hadamard (H3), and independently Rybczinski (R5), carried out similar analyses. Carrying the solution only to the first approximation, one arrives at a Stokes-law correction factor

$$F = 6\pi\mu_c RU \left(\frac{3\mu_D + 2\mu_c}{3\mu_D + 3\mu_c} \right) \quad (23)$$

which simply states that

$$U_L = \left(\frac{3\mu_D + 3\mu_c}{3\mu_D + 2\mu_c} \right) U_s \quad (24)$$

For a liquid drop falling in air or for a very viscous drop in a low viscosity field liquid, the correction term reduces to unity, and Eq. (23) becomes equivalent to Stokes' law. For a gas bubble rising through a liquid or a low viscosity drop moving in a very viscous liquid field, the limiting correction factor of 1.5 may be realized for a fully circulating drop. These two limiting values have been confirmed by many experi-

menters. If the viscosities of the two fluids are equal, the correction factor is 1.20.

C. BOUSSINESQ MODEL

Surface-tension forces act in a direction tangent to the interface. Boussinesq (B6) assumed, for a surface undergoing "dilatation," that there must also be another force acting normal to the interface. Utilizing the same assumptions as Hadamard, he arrived at a Stokes-law correction factor of

$$U_L = \left[\frac{\epsilon + r_D(3\mu_D + 3\mu_c)}{\epsilon + r_D(3\mu_D + 2\mu_c)} \right] U_s \quad (25)$$

in which ϵ is "the dynamic increment to the normal surface tension." It is often labelled a "surface viscosity" and used to rationalize data for a partially circulating drop into effective data for an equivalent fully circulating drop. It can only be evaluated from experimental data, and is used to explain a drag curve intermediate between those of rigid and fully circulating fluid spheres.

The derivations of Hadamard and of Boussinesq are based on a model involving laminar flow of both drop and field fluids. Inertial forces are deemed negligible, and viscous forces dominant. The upper limit for the application of such equations is generally thought of as $Re \approx 1$. We are here considering only the gross effect on the terminal velocity of a drop in a medium of infinite extent. The internal circulation will be discussed in a subsequent section.

D. DRAG

Most drop situations in extraction are far above the upper limit of application of the preceding equations. A drop moving through a liquid at a velocity such that the viscous forces could be termed negligible can not exist. It will break up into two or more smaller droplets (H10, K5). Most real situations involve both viscous and inertial terms, and the Navier-Stokes equations can not then be solved.

Consider the velocity vs. drop size curve shown in Fig. 5. Several modern papers (E1, H7, H10, J1, K1, K3, K4, L3, L4, S8, S12, W1) report carefully taken data upon a wide variety of liquid-liquid systems. Small drops in region A will be spherical in shape, will not circulate internally, and act like rigid spheres. Their ultimate velocity will generally be that of a rigid sphere of equal size and density moving in the same continuous phase. In region B the drops will be increasingly distorted into a spheroidal (ellipsoidal) shape with the minor axis oriented along the direction of movement. As drop size is increased the ultimate velocity

passes through a maximum, or peak, velocity. Larger drops will travel at about the same speed, independent of size. Finally at some maximum size, drops can not exist as single entities but will break up into two or more smaller ones.

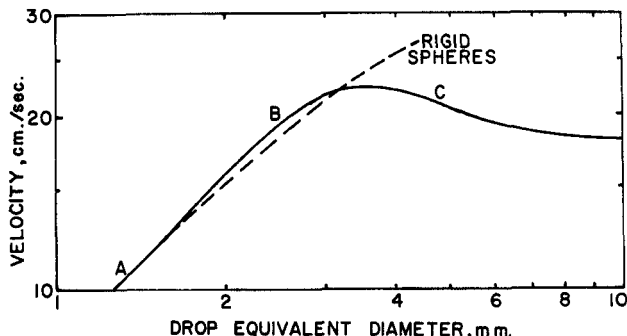


FIG. 5. Generalized terminal-velocity curve.

Correlations have been developed to relate terminal velocity, drop size, peak size, peak velocity, and maximum drop size to the physical properties of the system (E1, H10, K5). Some of the accumulated information in these areas is given below.

1. Force Balance on a Falling Drop

At steady-state terminal velocity, the acceleration term in the force balance (B9) on a moving submerged body is zero, and the balance may be written so that gravity forces are balanced by the sum of buoyancy and resistance forces.

$$Vg\rho_D - Vg\rho_c = C_D A \frac{\rho_c U^2}{2} \quad (26)$$

In this equation the right-hand member is Newton's resistance force, with A equal to the projected frontal area. The equation serves to define the drag coefficient (C_D).

For a sphere the equation becomes

$$\frac{\pi D^3}{6} g(\Delta\rho) = \frac{C_D \pi D^2 \rho_c U^2}{8} \quad (27)$$

and

$$C_D = \frac{4}{3} \cdot \frac{\Delta\rho}{\rho_c} \cdot \frac{gD}{U^2} \quad (28)$$

in which D is the diameter of the sphere.

For an oblate ellipsoidal drop with the major axis D_H in a horizontal

plane and the minor axis D_V in the vertical direction, the equations become

$$\frac{\pi}{6} (D_H^2 \cdot D_V) g(\Delta\rho) = C_D \cdot \frac{\pi}{8} (D_H^2) \rho_c U^2 \quad (29)$$

and

$$C_D = \frac{4}{3} \cdot \frac{\Delta\rho}{\rho_c} \cdot \frac{g D_V}{U^2} \quad (30)$$

from which it may be noted that the minor axis of the ellipsoid is the more reasonable length term to be used in the drag coefficient (G2). A similar treatment for a prolate ellipsoidal drop yields the major axis as the proper length. In either case it is the axis parallel to the line of motion which would be involved in C_D .

The utilization of such a length term requires a knowledge of the eccentricity of the droplet as a function of drop size. This item is reviewed below. The length term usually used is the very convenient equivalent spherical diameter (D_e), defined as the diameter of a sphere having the same volume as that possessed by the drop, regardless of the actual shape of the latter.

Cornish (C4) has discussed seven length terms which may be useful in mass- and heat-transfer correlations.

2. Low-Viscosity Liquid Fields

A plot of the terminal velocity of a drop moving in an infinite medium vs. drop size will show the features shown in Fig. 5. To exhibit all of these features, both drop and field liquids must be of very high purity. Using the pertinent fluid properties, a plot of C_D vs. Re will appear as in Fig. 6. In this plot the length term used is the very convenient D_e , in

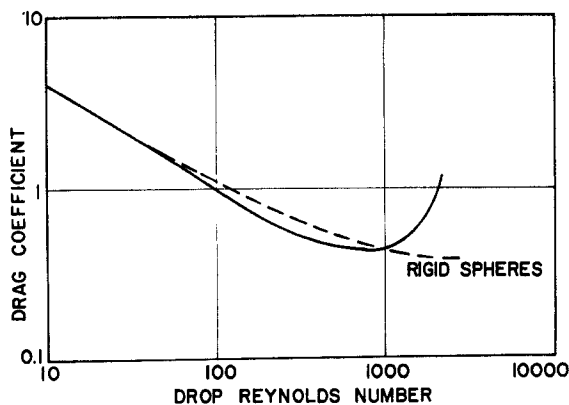


FIG. 6. Drag curve for liquid drops.

both C_D and Re . Many such curves are available in the current literature (K5), but they must be carefully evaluated as to purity of materials and the size of the container in which the work was carried out.

The prediction of such a curve for a specific system has defied mathematical analysis, except in the region of low inertial effects. Recourse must be made to the time-honored method of graphical empirical correlation. Klee and Treybal (K3) arrived at two equations, one for the region below the peak diameter and one for that above the peak. They warn that these are simply good approximations, and that their dimensionless-group equations describe their data and those of other authors fairly accurately. The field liquid in all systems used was one of low viscosity.

Hu and Kintner (H10) observed that a plot of $C_D \cdot We$ as ordinate against Re as abscissa resulted in a uniquely parallel set of curves with a characteristic break point corresponding to peak values of D_e and U_∞ . The use of dimensionless physical-property group

$$P = \left[\frac{\rho_c}{\Delta\rho} \cdot \frac{\rho_c \sigma^3}{g\mu^4} \right] \quad (31)$$

permitted the establishment of the curve shown in Fig. 7, from which the

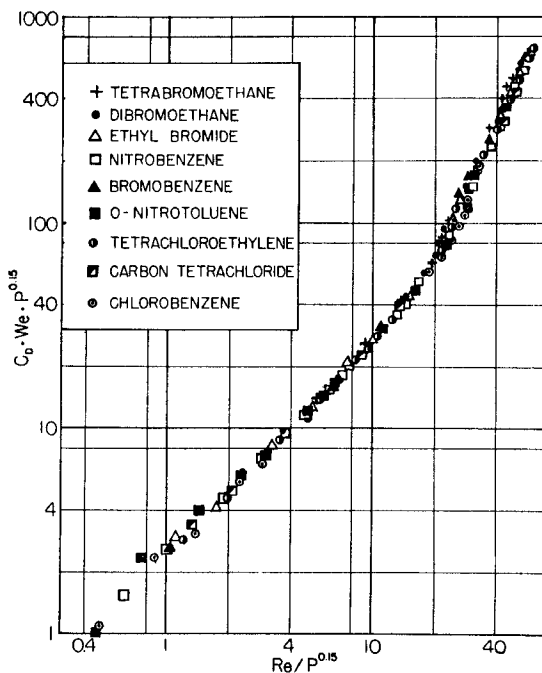


FIG. 7. Generalized correlation for drops falling through low-viscosity liquids (H10) (Courtesy *A.I.Ch.E. Journal*).

entire relationship could be predicted for a liquid drop falling (or rising) through a field liquid of ordinary viscosity (up to 5 cp.). The physical-property group is the cube of the reciprocal of the Sd group of Hughes and Gilliland (H11) and is a more general case of the group $(g\mu^4/\rho_c\sigma^3)$ used by Schmidt (S4), Grimley (G9), Rosenberg (R4) and Haberman and Morton (H1) for gas-bubble correlations. In a more recent paper (K5) containing a very large storehouse of data, a similar correlation but with slightly differing exponents was presented.

3. High-Viscosity Fields

Calderbank and Korchinski (C1) showed that the correlations described above are limited in applicability to systems in which the viscosity of the continuous phase is lower than 5 cp. Johnson and Braida (J1) used an additional parameter in the ordinate of Fig. 7 to extend its range to continuous-phase viscosities of 20 cp. The parameter was $(\mu_c/\mu_{\text{water}})^{-0.15}$. Data on systems involving field viscosities up to 400 cp. (W1) showed that the best correlation would be that of Boussinesq, using an experimental value of ϵ .

Two papers (F1, M3) described the shapes of very large drops moving in non-Newtonian liquid fields of the pseudoplastic variety. The employment of a Reynolds number based on the power-function relationship permitted a good description of the variation of terminal velocity vs. drop size.

Weaver *et al.* (W2) determined the velocities of multidrop systems in a spray tower. By plotting volumetric holdup against slip-velocity ratio, they found that drop size could be used as a third parameter. The average field-phase velocity was obtained by dividing volumetric flow rate by column cross-section (first corrected for dispersed-phase holdup). Average drop velocity was determined from dispersed-phase volumetric flow rate divided by volumetric holdup to get the mean residence time; this was then divided into the fall height to give the velocity. These two were then combined into a slip velocity. The resulting correlations appear excellent.

Such average velocities are useful in estimating residence times. But a knowledge of the velocity distribution of both drop and continuous phases seems desirable in order to obtain their relative velocities. Amberkar (A1) obtained data on large drops falling through stationary water in a 4-in. tower. Although the data points exhibited a very high degree of scatter, the total indicated a parabolic distribution of drop velocities across the tower. Bendre (B2), using a better technique, also found such a distribution. McAvoy (M1), working with small droplets of about 1 mm. diameter falling in a 2-in. tower, found the velocity distribu-

tion to be uniform. This would indicate that an additional parameter (D_D/D_T) is needed to describe the system better. At present, however, the correlations of Weaver *et al.*, are the best available.

E. WALL EFFECTS

Many of the data on the gross terminal velocity of drops have been taken in vertical cylindrical glass tubes of limited size. To interpret such data in terms of a drop moving in an infinite medium, a wall correction factor is necessary.

A number of authors from Ladenburg (L1) to Happel and Byrne (H4) have derived such correction factors for the movement of a fluid past a rigid sphere held on the axis of symmetry of the cylindrical container. In a recent article, Brenner (B8) has generalized the usual method of reflections. The Navier-Stokes equations of motion around a rigid sphere, with use of an added reflection flow, gives an approximate solution for the ratio of sphere velocity in an infinite space to that in a tower of diameter D_T :

$$K_w = \frac{U_\infty}{U} = \frac{1 - 0.759(D_D/D_T)^5}{1 - 2.105(D_D/D_T) + 2.087(D_D/D_T)^3} \quad (32)$$

The stream function satisfying the fourth-order differential equation, used by Haberman and Sayre (H2) is

$$\left[\frac{\partial^2}{\partial r^2} + \frac{1 - \cos^2 \theta}{r^2} \cdot \frac{\partial^2}{\partial (\cos \theta)^2} \right] \psi = 0 \quad (33)$$

Their solution, involving Gegenbauer functions, resulted in a wall correction factor for rigid spheres which is the same as the full expression corresponding to Eq. (32).

Using a similar attack for a fully circulating fluid sphere in a stationary field but using only $n = 2$ due to inconsistency of the equations for higher order functions, their wall correction factor was

$$K_{w1} = \frac{1 - 0.759 \left(\frac{1-r}{1+\frac{2}{3}r} \right) \lambda^5}{\psi} \quad (34)$$

in which

$$\begin{aligned} \psi = 1 - 2.105 \left(\frac{1 - \frac{2}{3}r}{1+r} \right) \lambda + 2.807 \left(\frac{1}{1+r} \right) \lambda^3 \\ - 1.707 \left(\frac{1 - \frac{2}{3}r}{1+r} \right) \lambda^5 + 0.726 \left(\frac{1-r}{1+r} \right) \lambda^6 \end{aligned}$$

$$\begin{aligned} r &= \mu_C/\mu_D \\ \lambda &= D_D/D_T \end{aligned}$$

Haberman and Sayre also derived correction factors for a fluid sphere moving along the axis of a cylinder in which the field fluid was also in axial motion;

$$K_{w2} = \frac{1 - \frac{2}{3} \left(\frac{1}{1 + \frac{2}{3}r} \right) \lambda^2 - 0.202 \left(\frac{1-r}{1 + \frac{2}{3}r} \right) \lambda^5}{\psi} \quad (35)$$

These factors were to be used in the equation

$$F = 6\pi\mu R \left(\frac{1 + \frac{2}{3}r}{1 + r} \right) (UK_{w1} - v_m K_{w2}) \quad (36)$$

in which v_m is the maximum velocity in the parabolic velocity distribution of the moving field phase. The correction was found applicable for λ values of 0.5 or less.

The above equations are limited to the creeping-flow range. For large drops moving under conditions such that inertial terms are not negligible, an empirical equation based on experimental data (S12) is

$$\frac{U}{U_\infty} = \frac{1}{K_w} = \left[1 - \left(\frac{D_s}{D_T} \right)^2 \right]^{1.43} \quad (37)$$

This relation has proved useful for systems in which the field fluid was stationary.

V. Internal Circulation

A. RIGID vs. FLUID SPHERES

The essential differences between a rigid and a fluid sphere are the internal circulation and mobile interface of the latter. Total interfacial area for mass transfer from a rigid sphere to the surrounding fluid phase remains constant except for slight changes due to sublimation or dissolution. But interfacial area is being continuously created on the upstream half of a circulating fluid sphere and continuously destroyed on the downstream hemisphere. It is commonly stated that the area is created *at* the front stagnation point and destroyed *at* the rear stagnation point. In ultra pure systems it should be stated that these things occur *near* the stagnation points. In systems of lesser purity the destruction of area must occur at some distance from the axis of symmetry. It is therefore a stagnation ring. This means that lines of motion must leave the interface and enter the drop at the point of area reduction. Some of them must also come from the drop interior to the interface at a location near the forward center of symmetry.

B. INDIRECT EVIDENCE

Most of the evidence for the existence of internal circulation within drops was, until recent years, circumstantial in character. Hadamard's development for conditions at low Reynolds numbers became the basis for comparison of fluid vs. rigid sphere performance. It predicted, for the limiting case of a low viscosity drop moving in a highly viscous field, an increase of 50% in the terminal velocity as compared to that of an equivalent rigid sphere. Much experimental evidence has confirmed the theory. The resulting calculated drag coefficients, dependent only on velocity for a specific drop size and chemical system, were observed to be low by the proper magnitude. Most observers were able to observe visually that internal circulation existed, and the observed patterns were very much like those predicted for the creeping-flow range even though the observed drop Reynolds numbers were too large for Hadamard's model to be strictly satisfied.

If the equations of motion, the continuity relationship, and the proper stream function are properly combined, equations result which enable one to plot the flow lines for both internal and external motion. The stream function for an infinite extent of continuous phase around a single drop is (B7, H2)

$$\psi_c = \frac{1}{2} \sin^2 \theta \left[\frac{UR^3}{2} \cdot \frac{\mu_D}{\mu_D + \mu_C} \cdot \frac{1}{r} - \frac{3}{2} UrR \left(\frac{3\mu_D + 2\mu_C}{3\mu_D + 3\mu_C} \right) \right] \quad (38)$$

and for the drop phase (H2)

$$\psi_D = \frac{1}{2} \sin^2 \theta \left[-Ur^2 + \frac{Ur^2\mu_C}{2(\mu_D + \mu_C)} \left(\frac{r^2}{R^2} - 1 \right) \right] \quad (39)$$

There is, of course, symmetry about the axis of flight of the sphere.

The streamlines are plotted in the left half of the circle in Fig. 8. It has been noted (H11) that a ring of zero velocity occurs inside the drop on the equatorial plane of symmetry at the distance of $0.707R$ from the center of the sphere. Several articles in the literature erroneously show the stagnation ring to be at some other location. Hughes and Gilliland also defined the amount of circulation as the flow through this ring (and through the annulus between the ring and the surface)

$$Q = \frac{\pi D^2}{32} \frac{\bar{v}}{(1 + \mu_C/\mu_D)} = \frac{\pi D^2 \mu_D \bar{v}}{32(\mu_D + \mu_C)} \quad (40)$$

C. DIRECT EVIDENCE

Equations are based upon simplifying assumptions. Observations reported in words do not always accurately describe a scientific situation.

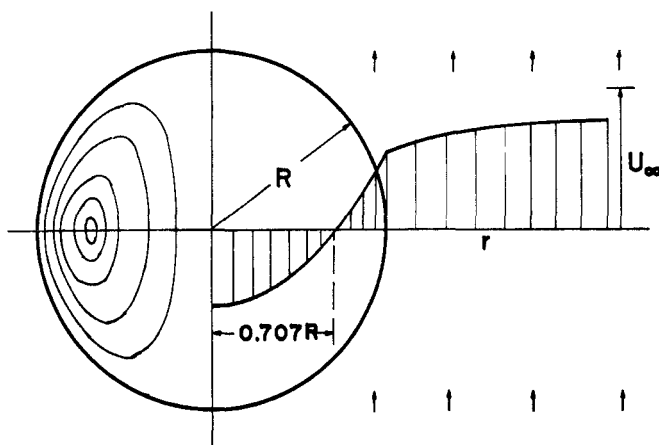


FIG. 8. Equatorial plane velocities and Hadamard streamlines for fluid sphere (H2).

Measurable items should be measured and visual items should be photographed for a convincing report.

1. Qualitative Reports

Photographs of the internal circulation pattern were made by Spells (S9) who took advantage of the photoviscosity effect exhibited by high-concentration glycerine. Savic (S2, K2), using powdered aluminum in water drops falling through castor oil, and employing a flat beam of light, obtained excellent photographs of the internal circulation pattern. Figure 9 shows such a pattern. All such photographs provide a somewhat erroneous impression due to the bending of the light beam as it leaves the drop and enters the surrounding liquid (G6). Only if both drop and continuous phases have the same refractive index (G2) is there no distortion.

In order to cope with this light-distortion problem, the above-mentioned traces must be transposed from their apparent position to a true one. A method (K2) which lends itself to the processing of large amounts of data combines six equations expressing the geometry of the drop, Snell's Law of refractive light bending, and the angles involved, into a single pair of equations. The two equations, though voluminous, can be easily and rapidly processed on a digital computer. They express the true coordinates (x' , y') of a point in terms of the apparent ones (x , y), the vertical half-axis of the assumed ellipse, the index of refraction of the field fluid (η_1), and the index of refraction of the drop fluid (η_2). The horizontal half-axis is assumed to be unity for convenience. The equations are:

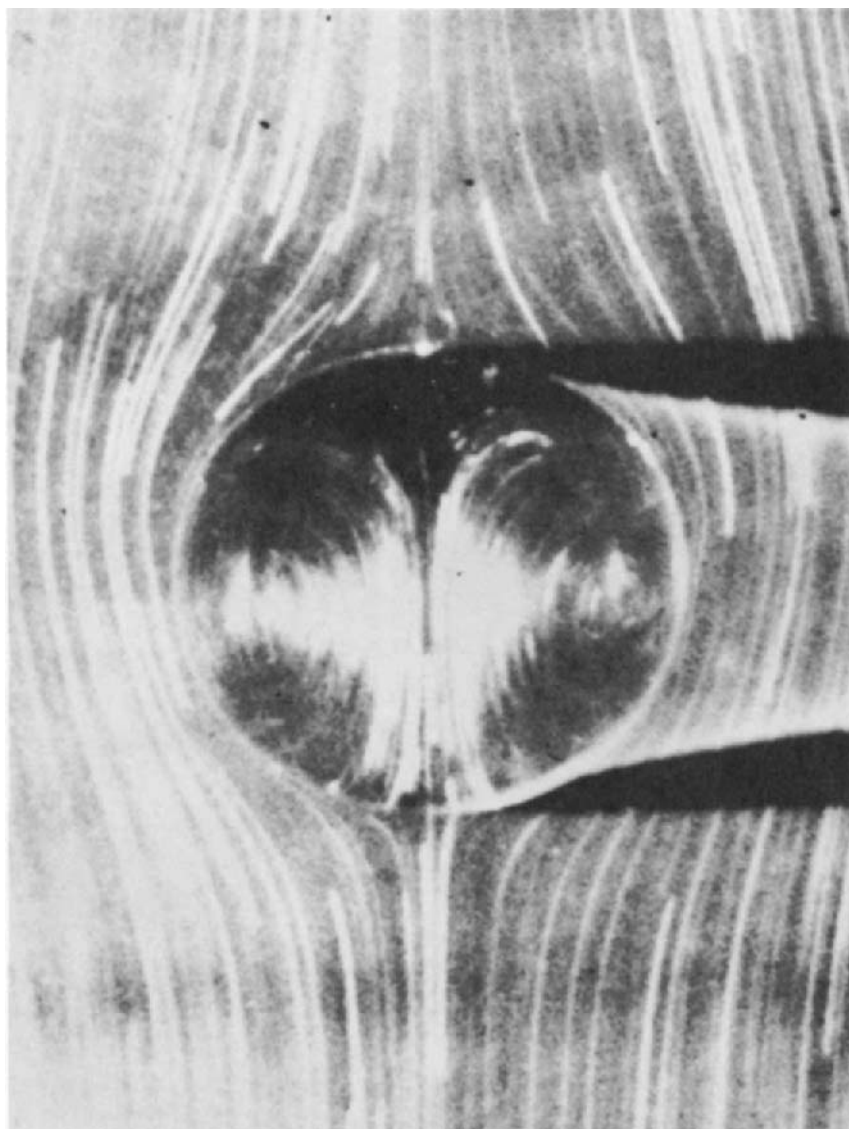


FIG. 9. Flow pattern in drop held in tapered tube (H9).

$$x' = x \left[1 - \zeta \left(\frac{\omega - \kappa \zeta}{\zeta \omega + \kappa \chi^2} \right) \right] \quad (41)$$

$$y' = y \left[1 - \frac{\zeta}{b^2} \left(\frac{\omega - \kappa \zeta}{\zeta \omega + \kappa \chi^2} \right) \right] \quad (42)$$

in which

$$\chi = \left(x^2 + \frac{y^2}{b^4} \right)^{1/2}$$

$$\zeta = \left(1 - x^2 - \frac{y^2}{b^2} \right)^{1/2}$$

$$\omega = \left(1 - \frac{y^2}{b^2} + \frac{y^2}{b^4} - \kappa^2 \chi^2 \right)^{1/2}$$

$$\kappa = \eta c / \eta_D = \eta_1 / \eta_2$$

Although the greatest displacement will be in the outermost regions of the drop due to the high interfacial surface angles, there will be no change in the drop outline since the light beams from the extreme edges do not pass through a bending surface.

2. *Work of Garner and Haycock*

Garner and Haycock (G2) made quantitative measurements of the velocity pattern in drops falling through glycerine solutions, using a motion picture technique in which the camera fell with the drop. The refractive indices of their drop and field fluids were identical. There is no distortion due to bending of light beams in such cases. They found that no circulation was possible until the fall velocity exceeded 0.5 cm./sec.

3. *Tapered-Tube Method*

Horton (H9, K2), using a tapered tube, was able to match the velocity of fall of the drop with the velocity of the rising field and thereby observe the behavior of the system for an hour or more. Using a dark field trace photography technique, the semi-vectorial velocities were recorded. In every case the internal circulation was slowly damped out as the interface changed its character and became more contaminated.

VI. Shapes of Moving Drops

The shape of a liquid drop moving in a liquid field is dependent upon the balance between the hydrodynamic pressure exerted because of the relative velocities of drop and field and the surface forces which tend to make the drop a sphere (H7).

A. LOW REYNOLDS NUMBERS

In region A of Fig. 5, the drops are either perfect spheres or are distorted to such a small degree that their eccentricity is not observable. They travel at such a speed that the Reynolds number ($D_D U \rho_c / \mu_c$) is

quite small. Small Reynolds numbers can be attained in either of two ways. For field liquids of ordinary viscosity ($\mu \approx 1$ cp) the drop must be very small. But if the viscosity of the field liquid is 300 to 2000 cp., the drop can be quite large. In either case the drop shape will be a sphere (F1).

B. HIGH REYNOLDS NUMBERS

At higher Reynolds numbers, the inertial forces become increasingly predominant and the drop will be distorted from the spherical shape.

1. Low-Viscosity Fields

Most of the data in the literature deals with drops of organic chemicals rising or falling in a field of water at room temperature. Economic aspects of filling large tanks with other liquids, as well as health and fire hazards if large glass vessels are filled with organic liquids, have contributed to this situation. As shown in Fig. 10a, drops moving in water

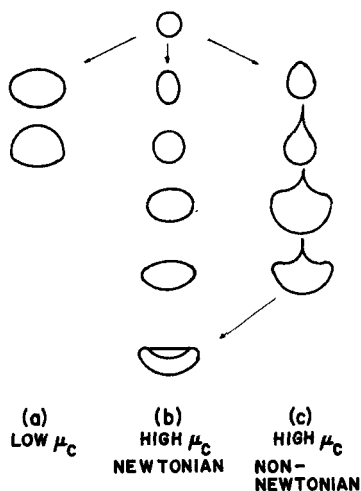


FIG. 10. Shapes of moving drops.

will first be distorted to a generally oblate ellipsoidal shape. This corresponds to region B of Fig. 5. The eccentricity of the nonoscillating ellipsoidal drop will increase with drop size. The area of such nonoscillating drops can be closely estimated from (G7)

$$A = \frac{\pi}{2} \left[D_H^2 + \frac{D_V D_H}{E^2 - 1} \ln (E + \sqrt{E^2 - 1}) \right] \quad (43)$$

The ratio of the area of an ellipsoid to that of a sphere of equal volume is (G7)

$$\frac{A}{A_s} = \frac{1}{2} \left[E^{2/3} + \frac{1}{E^{1/3} \sqrt{E^2 - 1}} \ln (E + \sqrt{E^2 - 1}) \right] \quad (44)$$

The horizontal planar symmetry will be lost as the peak drop diameter is approached. Oscillation will set in and become more and more violent as the drop size is increased (H10, L3). Finally at some large size the drop will rupture (H10, K5).

In order to allow for a variation of interfacial area from that of an equivalent sphere, the eccentricity of the ellipsoidal drop must be taken into account. The area ratio of Eq. (44) does not exceed unity by a serious amount until an eccentricity of 1.5 is attained. An experimental plot of eccentricity as ordinate vs. equivalent spherical drop diameter as abscissa may result in a straight line (G7, K1, K3, S12). A parameter is yet to be developed by which the lines can be predicted without recourse to experiment. Eccentricity is not an accurate shape description of violently oscillating drops and should therefore be used only for drop size below the peak diameter (region B of Fig. 5).

2. High-Viscosity Field

If a drop of low viscosity moves through a field of corn syrup of viscosity of about 300 c.p., the series of shape changes shown in Fig. 10b will occur. The succession is spherical, ovate, spherical, symmetrical oblate ellipsoidal, nonsymmetrical ellipsoidal and, finally, inverted mushroom-like shapes with an indented rear surface (F1).

3. Non-Newtonian Fields

Large drops moving through non-Newtonian liquid fields exhibit the same shape changes as those moving in high viscosity Newtonian liquids (F1, M3). A trailing filament will accompany all shapes except the sphere. The classical teardrop shape has only been reported for drops moving in such liquids.

4. Prolate Shape

Saito (S1) showed that the prolate form is possible if the drop density is very large and the ratio of drop viscosity to field viscosity is so small as to become negligible. His criterion, obtained by considering the second-order velocity terms in Hadamard's model, is

$$E' = \frac{\rho_D}{3} \left(1 + \frac{\mu_D}{\mu_c} \right) - \rho_c \left\{ \frac{10}{3} + \frac{319}{30} \left(\frac{\mu_D}{\mu_c} \right) + \frac{37}{5} \left(\frac{\mu_D}{\mu_c} \right)^2 + \frac{1}{20} \left(\frac{\mu_D}{\mu_c} \right)^3 \right\} \quad (45)$$

If $E' > 0$, the distortion is prolate. If $E' < 0$, the distortion is oblate. It is obvious that, for the first term to be dominant, the drop density

must be at least 3.33, a condition satisfied by liquid metal drops such as mercury. Hughes and Gilliland (H11) relate such an observation by Williams (W4) for mercury drops in air. If the field viscosity is very high, Saito's equation will also predict the prolate shape for mercury drops. This has been confirmed for mercury drops falling through corn syrup ($\mu \approx 2000$ cp), the eccentricity, $E = D_H/D_V$, being 12/13. The equation predicts oblate distortion for all other conditions, but such shapes can occur for the conditions reported above (F1, M3).

Haberman and Sayre (H2) report the prolate shape for drops of a glycerine-water mixture and of Dow-Corning "200" Silicone falling through castor oil in tubes of 1.24-in. and 2.74-in. I.D. Their ratio of D_V/D_H was shown to be dependent on the ratio of drop diameter to tube diameter and the viscosity ratio γ . Values of D_V/D_H as high as 1.6 were observed when drop diameter reached 0.70 tube diameter. It is believed that these prolate shapes were largely due to the effect of a nearby cylindrical boundary, and that some of their drops would have exhibited a spherical or oblate spheroidal shape if falling in larger vessels.

VII. Oscillations of Drops

A. AXIALLY SYMMETRIC TYPE

As the drop size in a given system is increased above the laminar-flow region, a size is reached at which the drop flattens and assumes a generally oblate ellipsoidal shape. Such a shape is unstable in fields of low viscosity, and the drop begins to oscillate. The oscillatory action may be triggered by the shedding of vortices into the wake (E1, H11). The term "oscillation" is used here to denote the axially symmetric periodic change from an oblate ellipsoid to a prolate form and back to oblate again. As may be observed in Fig. 11, the shape descriptions are only approximate and become progressively less accurate as the amplitude of the oscillations approaches the rupture value.

B. RANDOM WOBBLING

Large drops ($D_e = 1$ cm) of chlorobenzene will fall through water with a somewhat erratic oscillatory motion (L3). The drop pitches and rolls. The flight is not vertical but is erratically helical in nature. A series of oscillations, accompanied by waves moving over the interface, can cause the drop to drift several inches in a horizontal direction in a range of a foot or two of fall. Such drops can not oscillate violently as described above, due to the damping action of such movement by the sliding side-wise motion of the wobble. Motion pictures indicate that internal circulation is also considerably damped out by this type of oscillation. Rate of

mass transfer is, however, increased over that of a noncirculating drop due to surface deformation. This type of oscillation is indicated in Fig. 12.

C. SURFACE INDENTATIONS

A third type of surface disturbance is like that envisioned by Bousinesq (B6). Fluttering surface instabilities of a very local nature may be observed. A small area of the drop surface can dilate and recede in a periodic fashion much like that observed on the front of large air bubbles rising through liquids. Interference from other types of oscillations quickly compel a change in frequency and location of these surface instabilities.

With all three types of oscillations superimposed, the final result has a random appearance. Since a sphere has the smallest area per unit volume, all oscillatory movements cause an alternate creation and destruction of interfacial area. The rate of mass transfer is thereby enhanced for oscillating drops. Since surface stretch due to oscillations is not uniformly distributed, all such oscillations produce interfacial turbulence (see Section VII, E).

D. AMPLITUDE AND RUPTURE

Little quantitative work has been published on drop oscillations in liquid-liquid systems. Lamb (L2) reviews two methods for the analysis of a spherical mass of liquid. Elzinga and Banchemo (E1) use the primary mode of oscillation

$$f = \left(\frac{192\sigma g_e}{(3\rho_D + 2\rho_c)D_e^3} \right)^{1/2} \quad (46)$$

in which f is in radians per second. If the natural frequency of the drop matches the frequency of vortex discharge to the wake, it is deemed possible that the amplitude of oscillation could be sufficient to cause drop rupture.

Violent oscillations of the axially symmetric type can be induced in single drops formed at a nozzle. Drops of chlorobenzene ($D_e = 0.985$ cm) were so formed, and allowed to fall in water. At about five inches below the nozzle two types of rupture were observed. A small droplet was formed at the front and hurled ahead of the drop by the next oscillation. A second mode of formation caused a droplet to be formed by inertial pinch at the rear of the oscillating drop. This rear-formed droplet was always larger than the very small one formed in front. There were, on occasion, two successive pinch-formed droplets from the rear. In a few instances both front and rear formation occurred, as shown in Fig. 13 in selected

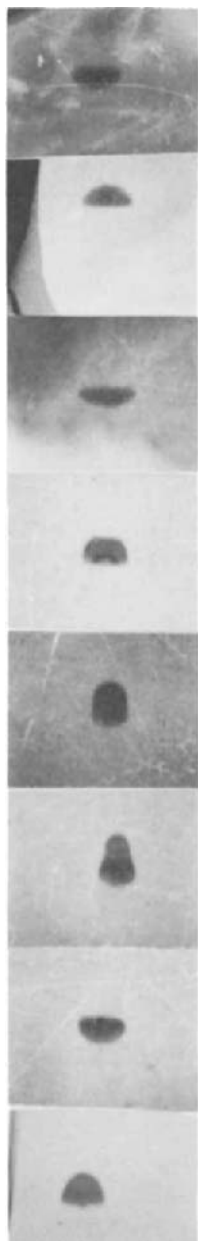


FIG. 11. Axially symmetric oscillation.

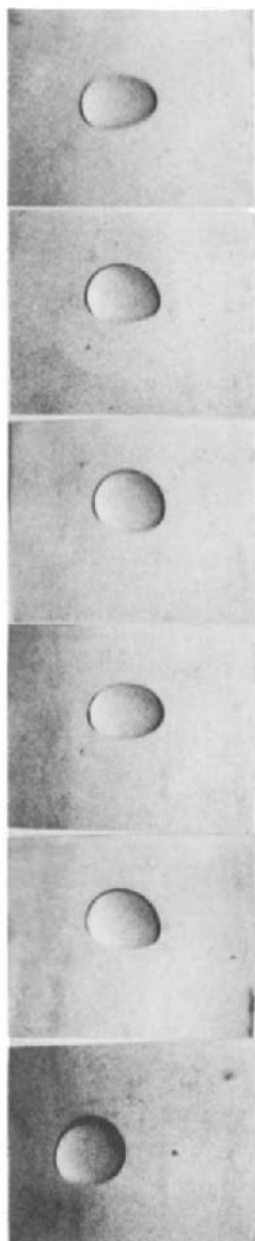


FIG. 12. Random wobble oscillation.

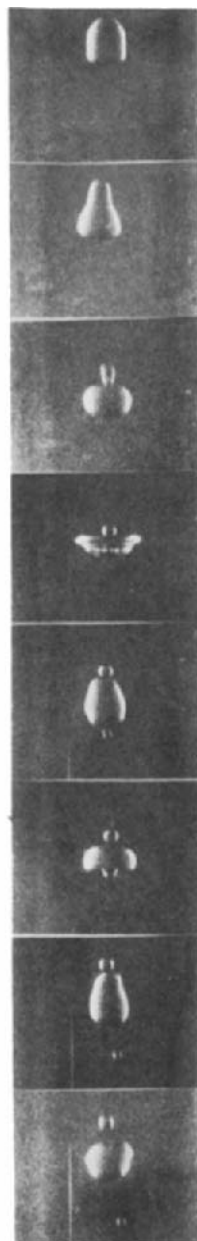


FIG. 13. Rupture by oscillation.

frames from motion pictures. It must be borne in mind that these ruptures are not the same as those treated by Elzinga and Banchero.

E. INTERFACIAL TURBULENCE

The various kinds of small flows generated at the interface and in the immediately adjacent layers are usually grouped together as interfacial turbulence. A description of the various kinds of such disturbances and their amazing effects have been summarized in several recent publications (D2, O1, S6, S10). Spontaneous emulsification, localized stirring with rippling and twitching of the interface, slowly moving streamers of one phase moving into the other, drop formation from the tips of such slowly moving streams, local eruptions at the interface, violent and erratic pulsations in drops and unsteady flow along the interface have all been observed and recorded. The action is three-dimensional and the interface must be regarded as including the immediately adjacent sub-layers on either side of the bulk phase separation plane.

All of these disturbances cause a many-fold increase in the rate of transfer of solute across the interface. If a chemical or thermal difference along an interface causes an interfacial tension gradient, violent flow in the direction of low σ will result. This action is usually termed the Marangoni effect.

Sternling and Scriven (S10) analyzed the hydrodynamic aspects of interfacial turbulence by means of a greatly simplified two-dimensional roll cell model. Their analysis suggests that interfacial tension is usually promoted by solute transfer into the phase of lower viscosity, solute transfer toward the phase of higher diffusivity, large viscosity and diffusivity differences between the phases, large concentration gradients near the interface and low order of viscosities and diffusivities. It is inhibited and damped by the presence of surfactants and by nearly rigid boundaries.

While the model of Sternling and Scriven is a radically simplified one, it serves remarkably well to predict the creation, propagation, and damping of turbulence. Orell and Westwater (O1) used Schlieren photographic methods to produce excellent pictures of three dimensional convection cells, including polygonal cell clusters, stripes, and ripples. Their polygonal cell clusters exhibited a size one order of magnitude larger than the dominant wave length for roll cells as predicted by the Sternling and Scriven development.

An excellent discussion of the phenomenon of spontaneous emulsion has been included in a recent book by Davies and Rideal (D2). Interfacial turbulence has been advanced (D2, O1) as a possible cause but has been eliminated in at least one case (D2). Diffusion and stranding seems

to be a much more plausible mechanism for the ethanol-toluene-water system. Alcohol, diffusing into the water phase, carries some toluene with it. Upon dilution in the aqueous phase, the toluene is left stranded as tiny droplets to form an emulsion. A third mechanism (D2) postulates a locally negative interfacial tension which causes the area to increase spontaneously. More than one of these mechanisms may be operating simultaneously.

VIII. Boundary Layers

Any consideration of mass transfer to or from drops must eventually refer to conditions in the layers (usually thin) of each phase adjacent to the interface. These boundary layers are envisioned as extending away from the interface to a location such that the velocity gradient normal to the general flow direction is substantially zero. In the model shown in Fig. 8, the continuous-phase equatorial boundary layer extends to infinity, but the drop-phase layer stops at the stagnation ring. At drop velocities well above the creeping flow region there is a thin laminar sublayer adjacent to the interface and a thicker turbulent boundary layer between this and the main body of the continuous phase.

A. FLOW AROUND A SPHERE

Many authors (B4, G3, H2, L2, S11) have considered the flow pattern and wakes involved in the flow of a fluid past a rigid sphere. Nearly every book on fluid mechanics contains a chapter on flow around submerged shapes. Flow around fluid shapes is only touched upon by a few advanced treatises such as that by Lamb (L2).

B. NONOSCILLATING DROPS

Very small drops travelling at low speeds in low viscosity liquid fields will exhibit a flow pattern similar to that shown in Fig. 8. Large spherical drops moving in fields of higher viscosity will show the same type of flow pattern. The field fluid will separate on the front portion of the drop, move over the forward surface in accelerating fashion, then over the rear surface under deceleration and finally converge near the down stream line of symmetry. There is a laminar sublayer and a very thick laminar transition layer. The sublayer is created near the front stagnation point and vanishes near the rear one. The laminar sublayer on the drop side will also be created and destroyed in like fashion. If a dye is placed in the drop liquid and allowed to be transferred to the continuous phase, it will stream from the rear of the drop as a thin thread along the axis of sym-

metry. It must be dispersed throughout the main continuous phase by diffusion or slow convection. There is no wake except the thin thread.

As the range of Reynolds numbers ($D_D U \rho_c / \mu_c$) is increased well above the creeping-flow range, a pattern like that shown in Fig. 14 will be seen (G7). A boundary separation will be observed as a ring on the rear surface of the drop. There is a wake enclosed within the boundary layer and this wake travels with the drop. The boundary-layer material converges behind the wake into a thin thread which trails behind the whole. Within the wake there is a ring of rotating liquid which gradually shears off into

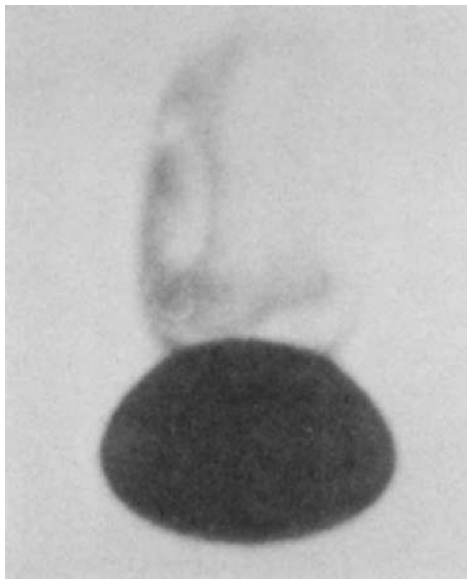


FIG. 14. Wake behind nonoscillating drop.

the threadlike trail. Most of the mass transfer from drop to field occurs into the boundary layer forward of the separation ring and travels in this layer around the wake to the trailing filament. There is some transfer from the rear drop surface into the wake. Only when the solute concentration has increased in this portion to such a level that it is greater than that in the enveloping boundary layer can mass transfer occur from wake to field. When transfer from drop to wake through the surface enclosed in the boundary separation ring equals that from the enclosed wake to the surrounding continuous phase, steady state will have been attained.

Elzinga and Banchero (E1) use Meksyn's boundary layer equation (M2) for flow around a rigid sphere, with the boundary condition that the interfacial velocity is not zero, to calculate a shift in the boundary-separation ring from an equivalent rigid-sphere location. Their calculated positions are slightly less than their observed shifts but confirm the thesis that these shifts are due to internal circulation. Similar quantitative results are reported by Garner and Tayeban (G7).

C. OSCILLATING DROPS

At still higher Reynolds numbers the drop will oscillate. Unsteady-state cyclic conditions are set up in both boundary layer and wake. The general pattern is indicated in Fig. 15; somewhat similar photographs have been published by others (E1, G7). "Still" photographs, however, do not properly present the action. The boundary-separation ring shifts violently as the oscillating drop moves through the liquid field. The liquid within and behind the ring is a highly disturbed region with turbulent conditions predominant. Forward of the ring one observes that smooth mass transfer is occurring into the relatively undisturbed boundary layer. The diffusing material moves within this layer around to the separation ring where it is sent into the main stream of the field liquid by turbulent convection. Comparatively little mass transfer occurs in the wildly gyrating wake, which does not travel with the drop as for a non-oscillating one.

IX. Effects of Surfactants

Much of the experimental data on droplet behavior reported in the literature is of very doubtful value, due to an absence of complete specifications regarding the purity of and correct physical constants for the chemicals used. The effects of the presence of minute traces of solid or liquid impurities on experimental results has been reported by nearly every author. Some of the work was quantitative. Many unsuspected impurities in a system can be surface-active. In recirculating systems (E1, H9) which involve aluminum tanks or piping, or packed pumps and gaskets, the equipment itself can supply enough to change the results. Chemicals of dubious purity such as tap water (H1, S8) must be avoided or carefully labeled for what they are. Much of the data in the literature, and some of the authors' conclusions, must be used with caution because of the suspected presence of a surface-active agent. The curve of Fig. 7 was established with data on drops of somewhat less than the highest purity.

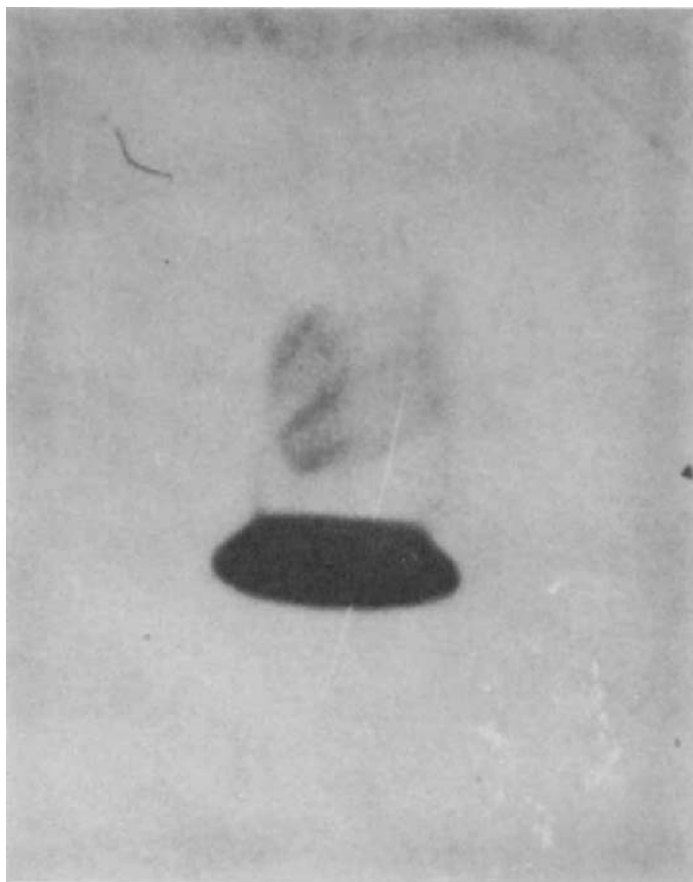


FIG. 15. Wake behind oscillating drop.

A. EVALUATION OF EXISTING DATA

Considerable differences exist among various authors on the terminal velocities of drops for a given system. After due consideration has been given small temperature differences, and degree of accuracy of instruments and methods, the disagreement is still wide. Figure 16 shows the data of several authors for the rate of fall of drops of carbon tetrachloride through water. It will be noted that there is substantial agreement among the data for very small spherical drops and for very large drops. But in

the intermediate region, which includes the sizes of most interest, the disagreement is greatest. The intangible usually blamed is the presence of surface-active agents of a type that can segregate near the interface. In doing so they are said to cause "some sort of surface viscosity" which inhibits circulation and causes the drops to act more like rigid bodies. If one wishes to use data from the literature to make process calculations, he must take this phenomenon into account. The dynamic surface tension factor, ϵ , in the Boussinesq development can be used to more accurately

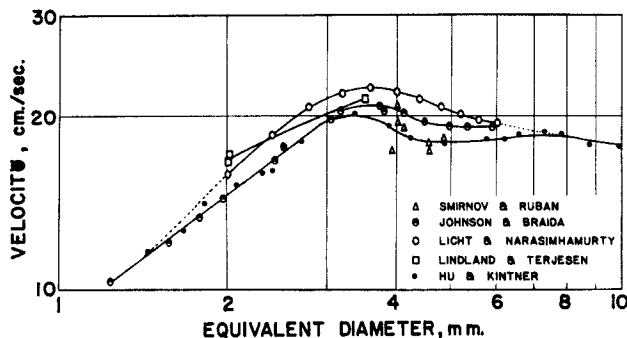


FIG. 16. Gross terminal velocity of carbon tetrachloride drops falling through water.

describe the curve below the peak diameter. It must be evaluated experimentally and is essentially a coefficient of convenience.

The amount of surface-active agent present may be so small that no measurable change in any physical property, including interfacial tension, can be detected. This is particularly true if the agent is a finely divided solid (E1). Lindland and Terjesen (L4) showed that, after a definite but small concentration of surfactant had been used, further additions caused but little change in terminal velocity.

At the same time a definite, radical lowering of the frequency and amplitude of the oscillations was noted. Such reduction in oscillation reduces mass-transfer rates.

B. DAMPING OF OSCILLATIONS

The surface rigidity and lowering of interfacial tension of a drop-soluble surfactant will cause a smaller drop to be formed from a specific size of nozzle. The terminal velocity is lowered in a manner independent of drop size. Figure 17 shows the results of experiments with drops of chlorobenzene in water. Formed from a nozzle made of a piece of $\frac{3}{8}$ -in. brass pipe, the drop of high-purity chlorobenzene fell at 13.1 cm./sec. Ten cm.³ of TMN (trimethyl nonyl ether of polyethylene glycol; supplied by

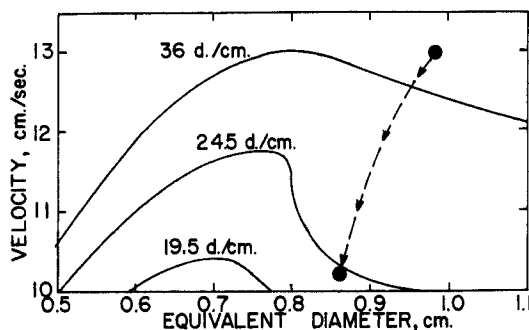


Fig. 17. Reduction of drop size and terminal velocity due to surfactant.

Union Carbide Chemicals Co.) in the 1.5 gal. of distilled water resulted in a smaller drop size (which should have had a higher U_{∞} in pure water) and a 23% lowering of terminal velocity.

C. INCREASED DRAG

The "surface viscosity" effect on terminal velocity results in a calculated drag curve that is closer to the one for rigid spheres (K5). The deep dip exhibited by the drag curve for drops in pure liquid fields is replaced by a smooth transition without a deep valley. The damping of internal circulation reduces the rate of mass transfer. Even a few parts per million of the surfactant are sometimes sufficient to cause a very radical change.

D. INTERNAL CIRCULATION

The effect of slow accumulation of surface-active materials is indicated in Fig. 18, which is a series of photographs of drops suspended in a tapered tube (H9). Tiny amounts of fine solids of colloidal dimensions, as described by Elzinga and Banchero (E1), gradually collected at the interface and were swept around to the rear of the drop. Circulation was progressively hindered until it was nearly stopped. Yet no measurable change could be detected in any physical property, including interfacial tension of the separated phases.

Not until the above effects can be mathematically related can we expect to progress beyond the experimental stage. To predict such items as size of drop formed at a nozzle, terminal velocity, drag curves, changes of oscillations, and speed of internal circulation, one must possess experimental data on the specific agent in the specific system under consideration. Davies (D1, D2) proposes the use of the equation

$$\% \text{ Circulation} = \frac{100}{1 + 1.5 \left(\frac{\mu_D}{\mu_c} \right)} - \frac{32C_s^{-1}}{r_D g \Delta \rho} \quad (47)$$

in which the "surface compressional modulus" C_s^{-1} is a factor expressing the degree of reduction from full Hadamard circulation due to surfactants. For clean surfaces ($C_s^{-1} = 0$) circulation should occur in any drop regardless of size. But small drops would be more sensitive to circulation

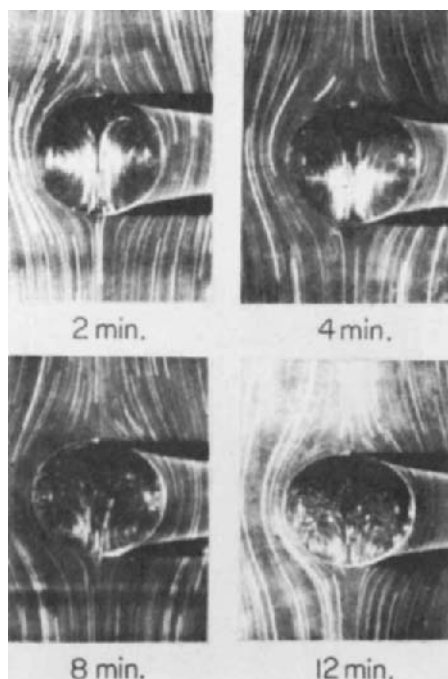


FIG. 18. Damping of circulation due to surfactant (H9).

damping than large. The criterion is experimental, of course, but the equation does satisfy all trends.

A recent paper by Schechter and Farley (S3) presented a modification of the Hadamard approach to relate circulation and mass transfer rates to interfacial tension gradients. Limited to creeping flow regimes, their approach appears to be the best to date.

X. Field-Fluid Currents

As has been previously shown in this chapter, the velocity field around a submerged shape can be mathematically predicted in some cases and experimentally demonstrated in all. Such a field is shown in Fig. 9. But as a large drop moves through a stationary liquid field, it will carry

an envelope of the latter with it. The vortices which are generated behind the large drop will also follow it a short distance before being damped out. There is also a lateral movement in such a case. Since some field fluid is carried downward by a falling drop there must be, in a closed container of finite size, an upward movement of the continuous phase near the container wall. A circulation pattern can be set up in a plate or spray tower by which field liquid will, in a countercurrent flow regime, be carried backward in the vessel. As noted by Treybal (T2) this constitutes a form of backmixing. It is another case in which residence time and valid contact time may not be the same. The vortices behind large drops also produce lateral dispersion. Data taken in tubes of small diameter (less than 4 in.) must account for such backward and lateral dispersions (T2).

XI. Flocculation and Coalescence

After mass transfer in a highly dispersed and intimately mixed system has proceeded to a satisfactory degree, the two phases must be individually recovered. These operations have been described in detail by Treybal (T1). Each phase must carry the smallest possible amount of the other, which now is to be avoided as a containment. If the dispersion operation reduced the droplet size too far, recovery may be expensive. Small amounts of surface active materials can cause a permanent emulsion, i.e., one which cannot be broken by simple settling. Temporary emulsions produced by turbulence creators such as mixing impellers will settle in seconds to a clear line of demarkation between phases. This is the primary break. One or both layers may, at this time, be fogged with an extremely fine dispersion of micron sized droplets of the opposite phase. These are termed secondary emulsions and require a long time (minutes, hours, or days) to clarify by simple settling. Modern practice in the petroleum industry utilizes electrostatic means to aid in the coalescence of these fine droplets into large ones which can settle out.

A. FLOCCULATION AND LIQUID-LIQUID FOAMS

As drops of this dispersed phase collect near the separation interface, they will flocculate into a closely packed mass which can best be described by the term "liquid-liquid foam." Each drop is surrounded by a thin film of the continuous phase. The film between two adjacent drops can rupture and the two combine by coalescence in the foam layer. Only those drops near the general phase boundary can coalesce into the general drop phase layer. The residence time in the flocculation zone can be many minutes, and considerable mass transfer may occur there.

B. COALESCENCE OF DROPS

If a large drop falls (as in a spray tower) to a pool at the bottom of the equipment, it will rest on the interface for a time and then coalesce in an instant with the main body of the heavier phase. If two drops of phase A are pushed together by an externally applied force, they will remain in apparent contact for a short time before combining by coalescence into a single larger drop. In either of these cases, the significant stages of the operation may be listed as approach, film thinning, film rupture, hole expansion, and surface contraction.

1. *Film Thinning and Rest Time*

Consider a large drop of water to be formed at a nozzle submerged in a continuous phase of benzene contained in a beaker. Let there be a layer of water under the benzene. The drop of water will fall through the benzene, rest for a time upon the interface between the layers and coalesce into the main pool of water. If the phases are very pure, the time of residence of the drop at the interface (rest time) before coalescence will be reproducible within a small percentage variation. It is affected by such variables as viscosity (of continuous phase), electrostatic charges, mass transfer (G10), interfacial tension, density difference between phases, drop diameter, and purity of materials. If all other factors are held constant, the rest time is a nearly quantitative measure of the amount of impurities present. The condition of the experiment, including the geometry of the apparatus, must be carefully adhered to if reproducible results are to be attained. Even with these precautions, a Gaussian distribution of the rest time will result.

The rate of film thinning as a sphere approaches a plane surface has been analyzed by assuming a slow squeezing-out process. The reduction of volume of the liquid between the surfaces is equal to that which flows radially outward through the cylindrical surface connecting the two. The resulting equation for the time for approach of the sphere from h_1 to h_2 distance of separation has been presented by a number of authors (C2, G8, H5):

$$t_{1,2} = \frac{6\pi\mu cr^2}{F} \ln \frac{h_1}{h_2} \quad (48)$$

2. *Rupture*

The rest time is measurable evidence of the rate of thinning of the benzene film which separates the drop from the main pool of water. It has been postulated that when this film has been reduced to some definite "critical" film thickness, rupture will occur. But several authors have

reported that the critical film thickness was not a constant value for a given system in a set of carefully controlled experiments (S4).

3. *Partial Coalescence*

When a drop (water) falls to a flat interface (benzene-water) the entire drop does not always join the pool (water). Sometimes a small droplet is left behind and the entire process, called partial coalescence, is repeated. This can happen several times in succession. High-speed motion pictures, taken at about 2000 frames per second, have revealed the details of the action (W3). The film (benzene) ruptures at the critical film thickness and the hole expands rapidly. Surface and gravitational forces then tend to drag the drop into the main pool (water). But the inertia of the high column of incompressible liquid above the drop tends to resist this pull. The result is a horizontal contraction of the drop into a pillar of liquid above the interface. Further pull will cause the column to be pinched through, leaving a small droplet behind. Charles and Mason (C2) have observed that two pinches and two droplets occurred in a few cases. The entire series of events required about 0.20 sec. for aniline drops at an aniline-water interface (C2, W3).

What happens to the drop liquid after coalescence? If the drop is dyed before release, the progress of that particular portion can be followed in the main pool. As the neck of the column is pinched through, surface forces acting along the raised interface cause the drop liquid to be hurled into the main body with sufficient force to form a vortex ring which looks very analogous to a smoke ring in air. Such vortex rings have been observed to penetrate as much as 4 in. from the interface.

4. *Two-Drop Coalescence*

When two large drops are forced together in a liquid field, the same succession of events will occur as for a drop at a flat interface. Selected frames from high-speed (3000 frames per second) motion pictures of the process are shown in Fig. 19. The drops were of *n*-butyl benzoate in a field of distilled water. One of the drops was dyed, and it was observed that no mixing occurred during the one-twelfth-second sequence. Some mixing by slow convection currents did occur after coalescence was complete. Excellent photographs of coalescence of two drops adhering to nozzles were presented by Groothuis and Zuiderweg (G10). They showed that mass transfer from drops to liquid promoted immediate coalescence.

5. *Fibrous-Bed Phenomena*

If two liquids of only slight mutual solubility are dispersed by high-turbulence devices in the absence of a surfactant or emulsifying agent, a

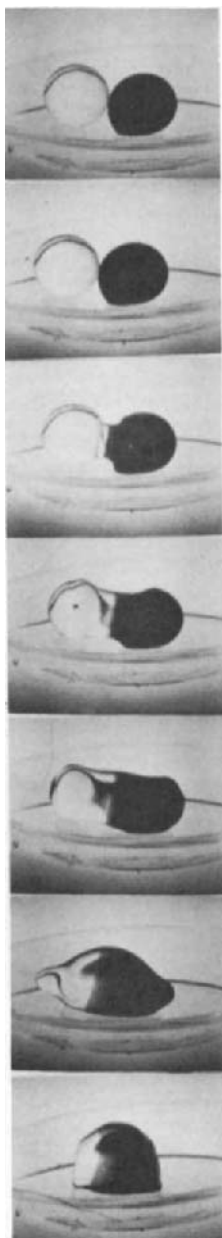


FIG. 19. Stages of coalescence of two equal sized drops.

temporary emulsion will form. The primary settling break will occur in seconds. If one or both of the two liquids involved be of a polar nature, one or both of the two layers which result from the settling operation will be clouded with a fine mist or fog of extremely fine droplets of the opposite layer (B10). Such fogged layers (secondary emulsions) consist of untold billions of droplets of submicron size suspended in a field of the opposite phase. These secondary emulsions can not be settled clear for many minutes or hours. Such an emulsion of benzyl alcohol in water has been observed to persist for weeks. Coalescence of these tiny droplets into big ones is necessary if separation by settling is to be completed in reasonable time.

Passage of an emulsion through a fibrous or porous bed will often cause coalescence and facilitate separation (B10, J2, R2, T1, V2). Such beds are sometimes dependable and sometimes not. The mechanism of their operation is shrouded in vagueness and conjecture. No accepted theory exists on how they accomplish the coalescence of the submicron droplets into large ones of manageable size. Were one available, it would facilitate design and aid in selection of materials of construction of such devices. The following bits of evidence are generally accepted as "facts":

- (a) The fibrous bed must be closely packed and possess a high ratio of surface area to volume (T1, V2).
- (b) The size of the capillary openings must be relatively large (T1).
- (c) The fibers must be preferentially wetted by the dispersed phase (R2, T1).
- (d) The flow rate must be above a certain minimum but below a certain maximum. Superficial velocities between 0.25 and 1.0 ft./min. have been recommended for water dispersed in petroleum fractions (B10, T1, V2). Velocities much higher than these have been successfully used.
- (e) Higher temperatures promote coalescence (B10, T1).
- (f) Thin beds will separate coarse emulsions (50- μ droplets), but a bed of several inches is required to coalesce secondary emulsions of submicron drops (B10). Beds of less than one inch have been successfully used to remove water from petroleum fractions.
- (g) A high-interfacial-tension system is more easily coalesced than one of low interfacial tension (J2).
- (h) Surfactants, dirt, and high viscosity tend to prevent coalescence.
- (i) Large drops form and grow on the leading surface (V2).
- (j) Large drops "wander" through the bed to the downstream edge, grow there by accretion of other drops, and break off by a drip-point formation method.

Several theories have been proposed to explain the action. The fine droplets are crowded together in the capillaries, where pressure and inter-drop scraping facilitate film thinning and coalescence. Drops wet the fiber, stick, and grow by accretion of the other drops, acting as impact targets for the latter. Electrostatic charges in the fibrous bed cause droplets to combine on the fiber surface with greater ease. Brownian movement of submicron particles causes a greater number of collisions between them in the crowded capillaries. London-Van der Waals forces can cause orientation of charged particles and aid in coalescence. It is the present writer's belief that most of these mechanisms are operative at various times in various portions of various types of beds. A bed of Teflon fibers can be made to clarify a secondary emulsion of water in kerosene. The fibers were very fine ($10\ \mu$), and Teflon has a unique property of acquiring and holding electrostatic charges although it is not likely to be wetted by water. A bed of medical cotton will coalesce benzene fog from water if the cotton is first soaked in benzene. Wettability here seems paramount. The impact mechanism seems unlikely, as the drop phase should be heavier than the field phase for successful contact. Submicron particles should follow streamlines around the target. Capillary crowding and rubbing against the benzene film on the fibers seems indicated. Observation through the microscope at about $100\times$ showed fine droplets approaching a $50\text{-}\mu$ drop held on fine fibers ($8\ \mu$ diam.) of glass but not continuing onward. This would tend to confirm the impact theory for this system (water in *n*-butanol).

XII. Summary

Much has been accomplished during the past fifteen years to define and describe quantitatively the action of single drops in a liquid environment. Much has also been done to understand more clearly the complex action present when two liquids are mixed in a highly turbulent field. Let us examine our needs.

(1) The work by Shinnar and Church (S7) on the use of the concept of local isotropy should be pursued and extended.

(2) The applicability of the modified lituus equation suggested by Poutanen and Johnson (P1), to liquid-liquid systems for area during formation looks promising.

(3) Rates of coalescence in pipelines and other turbulent field apparatus should be studied.

(4) A good model is needed for mass transfer during the formation of new area, whether this area be created by circulation, oscillations, formation stretch, interfacial turbulence, or any other mechanism.

(5) Little is known of liquid-liquid foam zones and the mode of mass transfer within such zones.

(6) Action occurring in the continuous phase should be investigated more thoroughly. Both axial and lateral dispersion should be pinpointed more accurately.

(7) The role of normal impurities in liquid-liquid systems in the light of surfactants should be clarified and made quantitative. A goal worth attaining would consist of setting up equations which, with use of experimentally determined constants, would permit accurate prediction of terminal velocity, amplitude and frequency of oscillations, and their combined effect on mass transfer.

(8) Coalescence must occur through the rupture of a separating film at a "critical film thickness." Why can we not predict this thickness more accurately?

(9) What is the mechanism which results in rapid coalescence if mass transfer occurs from the drops but slow or no coalescence if both phases are mutually saturated? Interfacial turbulence caused by local gradients in interfacial tension looks promising.

(10) We have excellent hydrodynamic equations in the creeping-flow region, and some very good relations for very large drops; but nearly all important situations must deal with the intermediate range between these regions. Fundamentally defensible relationships must soon be developed to replace our present multitude of empirical equations.

(11) Ten thousand partially unknown details of the birth, life, and death of liquid droplets in a liquid environment are needed. They may not be dignified with an "analytical" pedigree at once, but they can help the hydrodynamicist go about his business more soundly.

ACKNOWLEDGMENTS

Most of the Illinois Institute of Technology theses referred to report work supported by the National Science Foundation. Illustrative photographs were taken by Messrs. S. Amberkar, R. W. DeCicco, T. J. Horton, J. P. Roth and E. E. Tompkins.

Nomenclature

A	Area, cm^2	g	Gravitational acceleration, cm./sec.^2
a, b	Coefficient	g_c	Units conversion constant (unity in dyne c.g.s. system)
C	Coefficient; C_D is drag coefficient	K	Mass transfer coefficient; also any coefficient
c	Concentration, gm. mols/cm.^3	N	Number of moles
D	Diameter	p	Pressure, dynes/cm.^2
E	Eccentricity of drop; D_H/D_V	Q	Quantity of flow, $\text{cm.}^3/\text{sec.}$
E'	Eccentricity of drop; D_H/D_o	R	Radius of sphere, cm.
F	Force, dynes		
f	Frequency, sec.^{-1}		

r Radius, cm.	$\bar{u}, \bar{v}, \bar{w}$ Average velocities, cm./sec.
t Time, sec.	V Volume, cm. ³
U Gross terminal velocity, cm./sec.	x Distance, cm.
u, v, w Velocities, cm./sec.	x, y, z Coordinate axes

GREEK LETTERS

α, θ, ϕ Angles	π 3.1416
β Function [Eq. (11)]	ρ Density, gm./cm. ³
γ Viscosity ratio, μ_c/μ_d	$\Delta\rho$ Density difference, gm./cm. ³
ϵ Boussinesq's "dynamic surface tension," gm./sec.	σ Interfacial tension, dynes/cm.
ξ Parameter in Eqs. (41)–(42)	χ Parameter in Eqs. (41)–(42)
η Refractive index	ψ Function; if a stream function, cm. ² /sec.
λ Diameter ratio, D_D/D_W	ω Parameter in Eqs. (41)–(42)
μ Viscosity, poise	

SUBSCRIPTS

C Continuous phase	p Pressure
D Drop phase	r Radial
e Equivalent sphere	S Surface; also solid
H Horizontal	T Total; also tank
i Interfacial	V Vertical
L Liquid	W Wall
m Midpoint	μ Viscous
N Nozzle	θ Tangential
O Orifice	∞ In infinite medium

REFERENCES

The present writer's files contain over one thousand references pertinent to these topics, which are considerably less than half of those extant. The omission of any important reference from the following list should not be construed as lack of appreciation of its value.

- A1. Amberkar, S., M.S. Thesis, Illinois Inst. Technol., Chicago, Illinois, 1960.
- A2. Andreas, J. M., Hauser, E. A., and Tucker, W. B., *J. Phys. Chem.* **42**, 1001 (1938).
- B1. Bashforth, F., and Adams, H., "Capillary Action." Cambridge Univ. Press, London and New York, 1883.
- B2. Bendre, A. R., M.S. Thesis, Illinois Inst. Technol., Chicago, Illinois, 1961.
- B3. Bird, R. B., *Advan. Chem. Eng.* **1**, 155–239 (1956).
- B4. Bird, R. B., Stewart, W. E., and Lightfoot, E. N., "Transport Phenomena." Wiley, New York, 1960.
- B5. Bond, W. N., *Phil. Mag.* [7] **4**, 889 (1927).
- B6. Boussinesq, J., *Compt. Rend. Acad. Sci.* **156**, 1124 (1913).
- B7. Bowman, C. W., Ward, D. M., Johnson, A. I., and Trass, O., *Can. J. Eng.* **39**, 9 (1961).
- B8. Brenner, H., *J. Fluid Mech.* **12**, 35 (1962).
- B9. Brown, G. G. and Associates, "Unit Operations." Wiley, New York, 1950.
- B10. Burtis, T. A., and Kirkbride, C. G., *Trans. A.I.Ch.E.* **42**, 413 (1946).
- C1. Calderbank, P. H., and Korchinski, I. J. O., *Chem. Eng. Sci.* **6**, 65 (1956).

- C2. Charles, G. E., and Mason, S. G., *J. Colloid Sci.* **15**, 105 (1960).
C3. Charles, G. E., and Mason, S. G., *J. Colloid Sci.* **15**, 236 (1960).
C4. Cornish, A. R. H., Ph.D. Thesis, Ill. Inst. Technol., Chicago, Illinois, 1962.
D1. Davies, J. T., *Trans. Inst. Chem. Engrs. (London)* **38**, 289 (1960).
D2. Davies, J. T., and Rideal, E. K., "Interfacial Phenomena." Academic Press, New York, 1961.
E1. Elzinga, E. R., and Banchero, J. T., *A.I.Ch.E. Journal* **7**, 394 (1961).
F1. Fararoui, A., and Kintner, R. C., *Trans. Soc. Rheol.* **5**, 369 (1961).
G1. Garner, F. H., and Hale, A. R., *Chem. Eng. Sci.* **2**, 157 (1953).
G2. Garner, F. H., and Haycock, P. J., *Proc. Roy. Soc.* **A252**, 457 (1959).
G3. Garner, F. H., and Keey, R. B., *Chem. Eng. Sci.* **9**, 119 (1958).
G4. Garner, F. H., and Skelland, A. H. P., *Trans. Inst. Chem. Engrs. (London)* **29**, 315 (1951).
G5. Garner, F. H., and Skelland, A. H. P., *Ind. Eng. Chem.* **48**, 51 (1956).
G6. Garner, F. H., Skelland, A. H. P., and Haycock, P. J., *Nature* **173**, 1239 (1954).
G7. Garner, F. H., and Tayeban, M., *Anales Real Soc. Espan. Fis. Quim. (Madrid)* **B56**, 479 (1960).
G8. Green, H., *Ind. Eng. Chem. (Anal. Ed.)* **13**, 632 (1941).
G9. Grimley, S. S., *Trans. Inst. Chem. Engrs. (London)* **23**, 228 (1945).
G10. Groothuis, H., and Zuiderweg, F. J., *Chem. Eng. Sci.* **12**, 288 (1960).
H1. Haberman, W. L., and Morton, R. K., David Taylor Model Basin (Navy Dept., Washington, D.C.), Rept. No. 802 (1953).
H2. Haberman, W. L., and Sayre, R. M., David Taylor Model Basin (Navy Dept., Washington, D.C.), Rept. No. 1143 (1958).
H3. Hadamard, J. S., *Compt. Rend. Acad. Sci.* **152**, 1735 (1911); **154**, 109 (1912).
H4. Happel, J., and Byrne, B. J., *Ind. Eng. Chem.* **46**, 1181 (1954).
H5. Hardy, W. B., and Bircumshaw, I., *Proc. Roy. Soc.* **A108**, 12 (1925).
H6. Harkins, W. D., and Brown, F. E., *J. Am. Chem. Soc.* **41**, 499 (1919).
H7. Harmathy, T. Z., *A.I.Ch.E. Journal* **6**, 281 (1960).
H8. Hayworth, C. B., and Treybal, R. E., *Ind. Eng. Chem.* **42**, 1174 (1950).
H9. Horton, T. J., M.S. Thesis, Illinois Inst. Technol., Chicago, Illinois, 1960.
H10. Hu, S., and Kintner, R. C., *A.I.Ch.E. Journal* **1**, 42 (1955).
H11. Hughes, R. R., and Gilliland, E. R., *Chem. Eng. Progr.* **48**, 497 (1952).
J1. Johnson, A. I., and Braida, L., *Can. J. Chem. Eng.* **35**, 165 (1957).
J2. Jordan, G. V., *Trans. ASME (Am. Soc. Mech. Engrs.)* **77**, 394 (1955).
K1. Keith, F. W., and Hixson, A. N., *Ind. Eng. Chem.* **47**, 258 (1955).
K2. Kintner, R. C., Horton, T. J., Graumann, R. E., and Amberkar, S., *Can. J. Chem. Eng.* **39**, 235 (1961).
K3. Klee, A. J., and Treybal, R. E., *A.I.Ch.E. Journal* **2**, 244 (1956).
K4. Krishna, P. M., Venkateswarlu, D., and Narasimhamurty, G. S. R., *J. Chem. Eng. Data* **4**, 336 (1959).
K5. Krishna, P. M., Venkateswarlu, D., and Narasimhamurty, G. S. R., *J. Chem. Eng. Data* **4**, 340 (1959).
L1. Ladenburg, R., *Ann. Physik* [4] **23**, 447 (1907).
L2. Lamb, H., "Hydrodynamics," 6th ed. Cambridge Univ. Press, London and New York, 1932.
L3. Licht, W., and Narasimhamurty, G. S. R., *A.I.Ch.E. Journal* **1**, 366 (1955).
L4. Lindland, K. P., and Terjesen, S. G., *Chem. Eng. Sci.* **6**, 265 (1956).
M1. McAvoy, R., M.S. Thesis, Illinois Inst. Technol., Chicago, Illinois, 1961.
M2. Meksyn, D., *Proc. Roy. Soc.* **A194**, 218-228 (1948).
M3. Mhatre, M. V., and Kintner, R. C., *Ind. Eng. Chem.* **51**, 865 (1959).

- N1. Null, H. R., and Johnson, H. F., *A.I.Ch.E. Journal* **4**, 273 (1958).
O1. Orell, A., and Westwater, J. W., *A.I.Ch.E. Journal* **8**, 350 (1962).
P1. Poutanen, A. A., and Johnson, A. I., *Can. J. Chem. Eng.* **38**, 93 (1960).
R1. Rayleigh, Lord, *Phil. Mag.* [5] **34**, 177 (1892).
R2. Robinson, J. W., U.S. Patent 2,611,490 (1952).
R3. Rodger, W. A., Trice, V. G., and Rushton, J. H., *Chem. Eng. Progr.* **52**, 535 (1956).
R4. Rosenberg, B., David Taylor Model Basin (Navy Dept., Washington, D.C.), Rept. No. 727 (1950).
R5. Rybezinski, W., *Bull. Acad. Sci. Cracovie, Ser. A* **40** (1911).
S1. Saito, S., *Sci. Rept. Tohoku Univ.* **2**, 179 (1913).
S2. Savic, P., *Natl. Council Can. Mech. Eng. Rept.* **MT22** (1953).
S3. Schechter, R. S., and Farley, R. W., *Can. J. Chem. Eng.* **41**, 103 (1963).
S4. Schmidt, E., *Z. Ver. Deut. Ingr.* p. 77 (1933).
S5. Sheludko, A., *Kolloid-Z.* **155**, 39 (1957).
S6. Sherwood, T. K., and Wei, J. C., *Ind. Eng. Chem.* **49**, 1030 (1957).
S7. Shinnar, R., and Church, J. M., *Ind. Eng. Chem.* **52**, 253 (1960).
S8. Smirnov, N. I., and Ruban, V. L., *Zh. Prikl. Khim.* **22**, 1068 (1949); **22**, 1211 (1949); **24**, 57 (1951).
S9. Spells, K. E., *Proc. Phys. Soc (London)* **B65**, 541 (1952).
S10. Sternling, C. V., and Scriven, L. E., *A.I.Ch.E. Journal* **5**, 514 (1959).
S11. Streeter, V. L., "Fluid Dynamics." McGraw-Hill, New York, 1948.
S12. Strom, J. R., and Kintner, R. C., *A.I.Ch.E. Journal* **4**, 153 (1958).
T1. Treybal, R. E., "Liquid Extraction." McGraw-Hill, New York, 1951.
T2. Treybal, R. E., *I.E.C. Revs. Ind. Eng. Chem.* **52**, 264 (1960).
T3. Treybal, R. E., *Ind. Eng. Chem.* **53**, 597 (1961).
V1. Vermeulen, T., Williams, G. M., and Langlois, G. E., *Chem. Eng. Progr.* **51**, 85F (1955).
V2. Voyutskiy, K. A., Kal'yanova, R. M., Panich, R. M., and Fodiman, N. M., *Dokl. Akad. Nauk. SSSR* **91**, 1155 (1953).
W1. Warshay, M., Bogusz, E., Johnson, M., and Kintner, R. C., *Can. J. Chem. Eng.* **37**, 29 (1959).
W2. Weaver, R. E. C., Lapidus, L., and Elgin, J. C., *A.I.Ch.E. Journal* **5**, 533 (1959).
W3. Westwater, J. W., *Chem. Eng. Progr.* **55**, 49 (1959).
W4. Williams, G. C., Ph.D. Thesis, Massachusetts Inst. Technol., Cambridge, Massachusetts, 1942.

PATTERNS OF FLOW IN CHEMICAL PROCESS VESSELS

Octave Levenspiel

Department of Chemical Engineering

Illinois Institute of Technology, Chicago, Illinois

and

Kenneth B. Bischoff

Department of Chemical Engineering

University of Texas, Austin, Texas

I. Introduction	95
A. Scope	95
B. Types of Flow	96
C. Stimulus-Response Methods of Characterizing Flow	98
D. Ways of Using Tracer Information	104
II. Dispersion Models	105
A. General Description	105
B. Mathematical Description	107
C. Measurement of Dispersion Coefficients	109
D. Relationships Between Dispersion Models	134
E. Theoretical Methods for Predicting Dispersion Coefficients	142
III. Tanks-in-Series or Mixing-Cell Models	150
A. Introduction	150
B. Mathematical Description	151
C. Comparison with the Dispersion Model	156
IV. Combined Models	158
A. Introduction	158
B. Definition of Deadwater Regions	159
C. Matching Combined Models to Experiment	161
D. Application to Real Stirred Tanks	167
E. Application to Fluidized Beds	170
V. Application of Nonideal Patterns of Flow to Chemical Reactors	171
A. Direct Use of Age Distribution Information	173
B. Stirred Tank Reactors	178
C. Tubular and Packed Bed Reactors	179
D. Fluidized Bed Reactors	186
VI. Other Applications	187
A. The Intermixing of Fluids Flowing Successively in Pipelines	187
B. Brief Summary of Applications to Multiphase Flow and Other Heterogeneous Processes	187
VII. Recent References	189
Nomenclature	190
Text References	192

I. Introduction

A. SCOPE

Fluid is passed through process equipment so that it may be modified one way or other. It may be heated or cooled, it may gain or lose material

by mass transfer with an adjoining phase (either solid or fluid), or it may react chemically.

To predict the performance of equipment we must know: (a) the rate at which fluid is modified as a function of the pertinent variables, and (b) the way fluid passes through the equipment.

Of all possible flow patterns two idealized patterns, plug flow and backmix flow, are of particular interest. Plug flow assumes that fluid moves through the vessel "in single file" with no overtaking or mixing with earlier or later entering fluid. Backmix flow assumes that the fluid in the equipment is perfectly mixed and uniform in composition throughout the vessel. Design methods based on these ideal flow patterns are relatively simple and have been developed for heat and mass transfer equipment as well as for chemical reactors.

All patterns of flow other than plug and backmix flow may be called *nonideal flow patterns* because for these the design methods are not nearly as straightforward as those for the two ideal flow patterns. The methods of treating nonideal patterns either have only recently been developed or are yet to be developed.

In real vessels flow is usually approximated by plug or backmix flow; however, for proper design, the departure of actual flow from these idealizations should be accounted for. Here we intend to consider these nonideal flow patterns; to characterize them, to measure them and to use this information in design.

The treatment of these nonideal flow patterns divides naturally into two parts.

(1) *Flow of Single Fluids*. The major application here is the design of chemical reactors (homogeneous and solid-catalyzed fluid systems using tubular, packed bed or fluidized bed reactors). Of relatively minor importance is the application to heat transfer from a single flowing fluid and contamination of fluids flowing successively in pipelines.

(2) *Flow of Two Fluids*. The major applications are in absorption, extraction, and distillation, with and without reaction. Other applications, also quite important, are for shell-and-tube or double-pipe heat exchangers, and noncatalytic fluid-solid reactors (blast furnace and ore-reduction processes).

This paper deals with the nonideal flow of single fluids through process equipment.

B. TYPES OF FLOW

Names have been associated with different types of flow patterns of fluid in vessels. First of all, we have the two previously mentioned ideal flow patterns, plug flow and backmix flow. Flow in tubular vessels ap-

proximates the ideal conditions of plug flow, while flow in agitated or stirred tanks often closely approximates backmix flow.

Descriptive terms, not mutually exclusive, such as channeling, recycling, eddying, existence of stagnant pockets, etc., are used in connection with various forms of nonideal flow. In channeling, large elements of fluid pass through the vessel faster than others do; however, all fluid does move through the vessel. Channeling may be found in flow through poorly packed vessels or through vessels having small length-to-diameter ratios. Stagnant pockets of fluid may occur in headers, at the base of

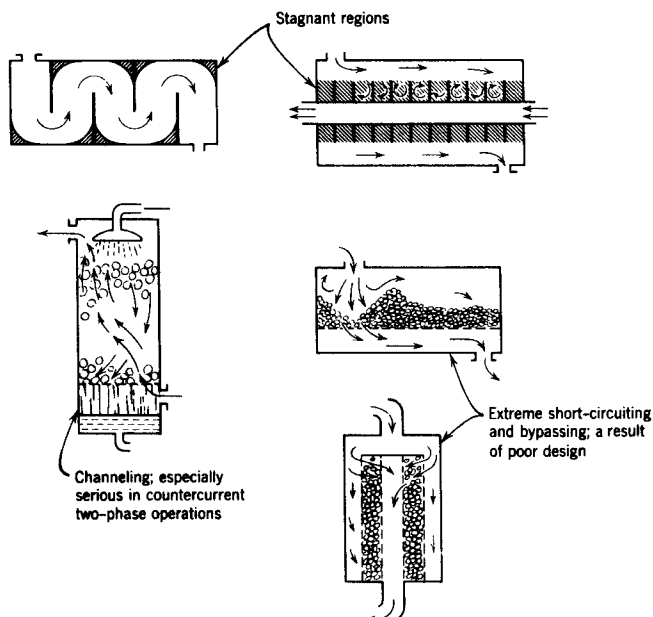


FIG. 1. Nonideal flow patterns which may exist in process equipment (L13).

pressure gages, and in odd-shaped corners, and cause bypassing of these regions. By-passing serves to cut down the effective or useful volume of the equipment, is not desirable, and is an indication of poor design. In recycling, a certain amount of fluid is recirculated or returned to the vessel inlet. This type of flow may be desirable, for example, in autocatalytic or autothermal reactions, and can be promoted by suitable baffling arrangements or by proper vessel design. These various types of nonideal flow are illustrated in Fig. 1.

In most cases nonideal flow is not desired, and by proper design its gross aspects can be eliminated. However, even with proper design, some extent of nonideal flow remains due both to molecular and turbulent

diffusion and to the viscous characteristics of real fluids which result in velocity distributions. Hence nonideal flow must be accounted for, preferably in such a manner that quantitative predictions of performance of real equipment can be made.

C. STIMULUS-RESPONSE METHODS OF CHARACTERIZING FLOW

To be able to account exactly for nonideal flow requires knowledge of the complete flow pattern of the fluid within the vessel. Because of the practical difficulties connected with obtaining and interpreting such information, an alternate approach is used requiring knowledge only of how long different elements of fluid remain in the vessel. This partial information, not sufficient to completely define the nonideal flow within the vessel, is relatively simple to obtain experimentally, can be easily interpreted, and, either with or without the use of flow models, yields information which is sufficient in many cases to allow a satisfactory accounting of the actual existing flow pattern.

The experimental technique used for finding this desired distribution of residence times of fluid in the vessel is a stimulus-response technique using tracer material in the flowing fluid. The stimulus or input signal is simply tracer introduced in a known manner into the fluid stream enter-

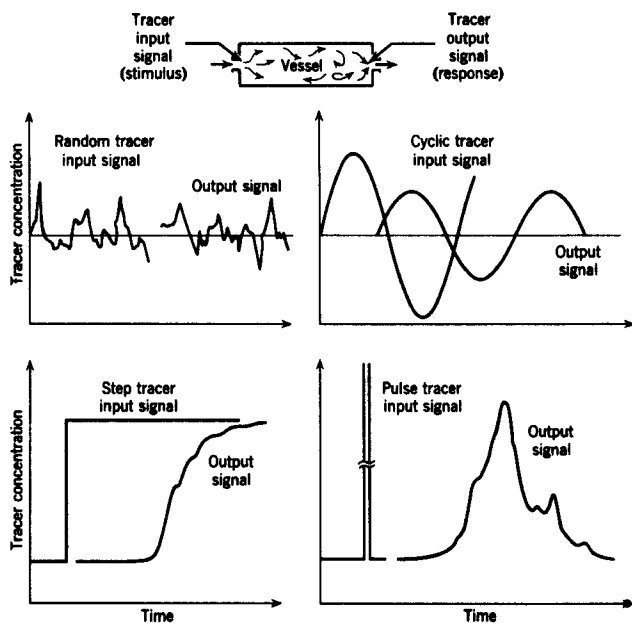


FIG. 2. Stimulus response techniques commonly used in the study of the behavior of flow systems (L13).

ing the vessel. This input signal may be of any type; a random signal, a cyclic signal, a step or jump signal, a pulse or discontinuous signal or any arbitrary input signal. The response or output signal is then the recording of tracer leaving the vessel (see Fig. 2).

We will restrict this treatment to steady-state flow with one entering stream and one leaving stream of a single fluid of constant density. Before proceeding further let us define a number of terms used in connection with the nonideal flow of fluids.

1. *Open and Closed Vessels*

We shall define a *closed vessel* to be one for which fluid moves in and out by bulk flow alone. Plug flow exists in the entering and leaving streams. In a closed vessel diffusion and dispersion are absent at entrance and exit so that we do not, for example, have material moving upstream and out of the vessel entrance by swirls and eddies.

An *open vessel* is one where neither the entering nor leaving fluid streams satisfy the plug flow requirements of the closed vessel. When only the input or only the output fluid stream satisfies the closed vessel requirements we have a *closed-open* or *open-closed vessel*.

2. *Mean Residence Time of Fluid in a Vessel*

The mean residence time of fluid in a vessel is defined as:

$$\bar{t} = \frac{\text{volume of vessel available for flow}}{\text{volumetric flow rate of fluid through vessel}} = \frac{V}{v} \quad (1)$$

3. *Reduced Time*

It is frequently convenient to measure time in terms of the mean residence time of fluid in the vessel. This measure, called the reduced time, is dimensionless and is given by

$$\theta = \frac{t}{\bar{t}} \quad (2)$$

4. *I and I(t)—The Internal Age Distribution of a Fluid in a Closed Vessel*

Taking the age of an element of fluid in a vessel to be the time it has spent in the vessel, it is evident that the vessel contains fluid of varying ages. Let the function *I* be the measure of the distribution of ages of fluid elements in the vessel and let it be defined in such a way that *I dθ* is the fraction of fluid of ages between *θ* and *θ + dθ* in the vessel.

Since the sum of all these fractions of fluid is unity (the total vessel contents) we have

$$\int_0^{\infty} I d\theta = 1 \quad (3)$$

The fraction of vessel contents younger than age θ is

$$\int_0^{\theta} I d\theta'$$

The fraction older than θ is

$$\int_{\theta}^{\infty} I d\theta' = 1 - \int_0^{\theta} I d\theta'$$

Where time rather than reduced time is used let the internal age distribution function be $I(t)$. Then

$$I = \bar{t} I(t) \quad (4)$$

and the relationships corresponding to those using reduced time follow (see Fig. 3).

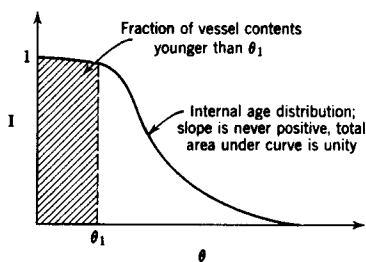


FIG. 3. Typical internal age distribution of vessel contents (L13).

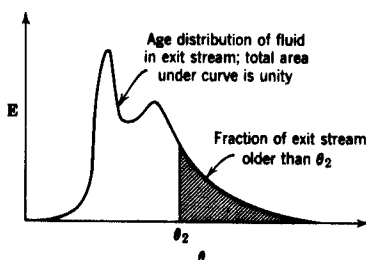


FIG. 4. Typical distribution of residence times of fluid flowing through a vessel (L13).

5. E and $E(t)$ —The Residence-time Distribution of Fluid in a Closed Vessel or the Age Distribution of Exit Stream

In a manner similar to the internal age distribution function, let E be the measure of the distribution of ages of all elements of the fluid stream leaving a vessel. Thus E is a measure of the distribution of residence times of the fluid within the vessel. Again the age is measured from the time that the fluid elements enter the vessel. Let E be defined in such a way that $E d\theta$ is the fraction of material in the exit stream which has an age between θ and $\theta + d\theta$. Referring to Fig. 4, the area under the E vs. θ curve is

$$\int_0^{\infty} E d\theta = 1$$

The fraction of material in the exit stream younger than age θ is

$$\int_0^\theta \mathbf{E} d\theta'$$

while the fraction of material older than θ , the shaded area of Fig. 4, is

$$\int_\theta^\infty \mathbf{E} d\theta' = 1 - \int_0^\theta \mathbf{E} d\theta'$$

Where time rather than reduced time is used let the residence time distribution be designated by $\mathbf{E}(t)$. Then

$$\mathbf{E} = \bar{t}\mathbf{E}(t) \quad (6)$$

and the relationships corresponding to those using reduced time follow.

6. **F** Curve—*The Response to a Step Tracer Input*

With no tracer initially present, let a step function (in time) of tracer be introduced into the fluid entering a vessel. Then the concentration-time curve for tracer in the fluid stream leaving the vessel, measured in terms of tracer concentration in the entering stream C_0 and with time in reduced units, is called the **F** curve. As shown in Fig. 5, the **F** curve rises from 0 to 1.

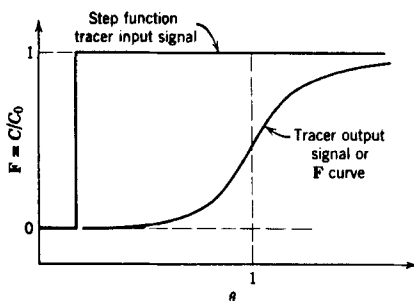


FIG. 5. Typical downstream response to an upstream step input; in the dimensionless form shown here this response is called the **F** curve (L13).

7. **C** Curve—*The Response to an Instantaneous Pulse Tracer Input*

The curve which describes the concentration-time function of tracer in the exit stream of any vessel in response to an idealized instantaneous or pulse tracer injection is called the **C** curve. Such an input is often called a delta-function input. As with the **F** curve, dimensionless coordinates are chosen. Concentrations are measured in terms of the initial concentration of injected tracer if evenly distributed throughout the

vessel, C^0 , while time is measured in reduced units. With this choice the area under the C curve always is unity, or

$$\int_0^\infty C \, d\theta = \int_0^\infty \frac{C}{C^0} \, d\theta = 1 \quad (7)$$

or

$$C^0 = \int_0^\infty C \, d\theta = \frac{1}{t} \int_0^\infty C \, dt$$

A typical C curve is shown in Fig. 6.

The terms F , C , I and E were introduced by Danckwerts (D4, D6).

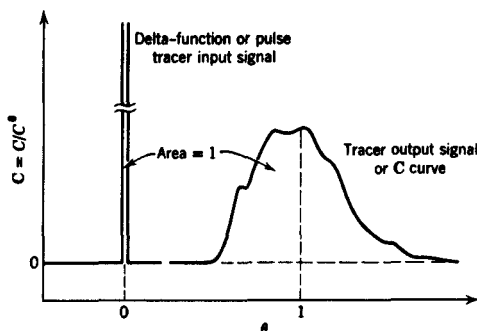


FIG. 6. Typical downstream response to an upstream delta function input; in the dimensionless form shown here this response is called the C curve (L13).

8. Relationship between Tracer Curves, Age Distribution, and Residence-Time Distribution of Fluids Passing through Closed Vessels

By material balance, the experimental response curves F and C can be related to the I and E distributions. Thus, at any time t or θ , we have from Danckwerts (D4) or Levenspiel (L13),

$$F = 1 - I = 1 - \bar{t} I(t) = \int_0^\theta E \, d\theta' = \int_0^t E(t') \, dt' = \int_0^\theta C \, d\theta' \quad (8)$$

or

$$C = E = \bar{t} E(t) = \frac{dF}{d\theta} = -\frac{dI}{d\theta} = -\bar{t}^2 \frac{dI(t)}{dt} \quad (9)$$

Equation (9) is a special case of the easily proven fact that for a linear system, if input 2 is the derivative of input 1, then output 2 is also the derivative of output 1.

These relationships show that the F curve is related in a simple way to the age distribution of material in the vessel, while the C curve gives directly the distribution of residence times of material in the vessel. In addition, the C and E curves represent the slopes of the corresponding

F and **I** curves, while the **F** and **I** curves at a given time represent the area under the corresponding **C** and **E** curves up to that time.

Thus we see that the stimulus-response technique using a step or pulse input function provides a convenient experimental technique for finding the age distribution of the contents and the residence-time distribution of material passing through a closed vessel.

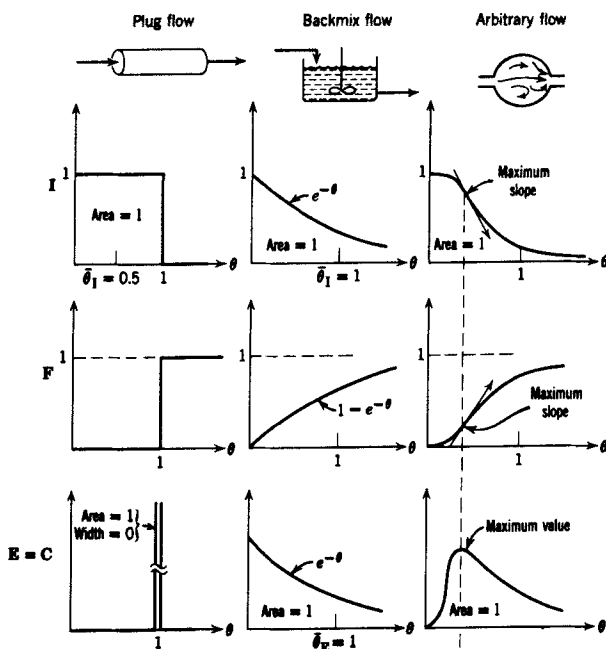


FIG. 7. Properties of the **F**, **C**, **I**, **E** curves for particular patterns of flow (dead-water regions and bypassing flow absent) in closed vessels (L13).

Figure 7 shows the shapes of these curves for various types of flow. It is interesting to relate the mean of the **E** curve

$$\bar{\theta}_E = \frac{\int_0^\infty \theta E d\theta}{\int_0^\infty E d\theta} = \int_0^\infty \theta E d\theta \quad (10)$$

to the mean residence time of fluid in the vessel, $\bar{\theta} = 1$ or \bar{t} . By material balance we find

$$\left. \begin{array}{l} \bar{\theta}_E = \bar{\theta} = 1 \\ \bar{t}_E = \bar{t} \end{array} \right\} \text{only for closed vessels.}$$

For other than closed vessels, this does not hold. This fact, probably

somewhat strange to the intuition, was first shown by Levenspiel and Smith (L16) and was proved in a general manner by Spaulding (S21).

D. WAYS OF USING TRACER INFORMATION

Suppose we are given two separate pieces of information, the residence time distribution for plain unchanging fluid passing through the vessel and the kinetics¹ for a change which is to be effected in the vessel. Can we predict what will be the performance of the vessel when this change is occurring in the vessel? The answer depends on the type of change occurring. If this is simply a linear function of an intensive property of the fluid, then the performance can be predicted, or

tracer information for flowing unchanging fluid	+	rate information for a process with rate linear in an intensive fluid property	→	performance of equipment when this process is occurring
---	---	--	---	---

As illustrations, consider the following three cases. (a) *Isothermal reactor for first order reaction*. Knowledge of the rate constants for the reaction and of response characteristics for the vessel suffices to predict how the vessel will perform as a reactor. (b) *Nonisothermal reactor*. If the temperature, hence, the rate, is a function of position as well as concentration, then tracer plus rate information is insufficient to predict performance. (c) *Heat transfer to a fluid flowing in a heat exchanger*. Since the heat-transfer rate depends not only on the temperature of fluid and of the vessel walls but also on the contacting pattern, the performance of the vessel as a heat exchanger cannot be predicted by having only the tracer information and the heat transfer coefficient. Applications will be treated in more detail later.

If the linear requirements on the kinetics of change are not satisfied, then the performance of equipment cannot be predicted from these separate pieces of information. In this case the actual flow pattern of fluid through the vessel must be known before performance predictions can be made.

As mentioned earlier, obtaining and interpreting the actual experimental flow pattern is usually impractical. Hence, the approach taken is to postulate a flow model which reasonably approximates real flow, and then use this flow model for predictive purposes. Naturally, if a flow model closely reflects a real situation, its predicted response curves will closely match the tracer-response curve of the real vessel; this is one of the requirements in selecting a satisfactory model.

¹ Kinetics is used here to mean any type of rate process.

This is a fruitful approach, and much of what follows concerns the development and use of such flow models. The parameters of these models are correlatable with physical properties of the fluid, vessel geometry, and flow rate; once such correlations are found for all types of fluid processing, performance predictions can be obtained without resort to experimentation.

Many types of models can be used to characterize nonideal flow patterns within vessels. Some draw on the analogy between mixing in actual flow and a diffusional process. These are called *dispersion models*. Others visualize various flow regions connected in series or parallel. When backmix flow occurs in all these flow regions we have the *tanks-in-series*, *mixing-cell*, or *backmix models*. When different types of flow regimes are interconnected, we have *combined models*. Some models are useful in accounting for the deviation of real systems (such as tubular vessels or packed beds) from plug flow, others for describing the deviation of real stirred tanks from the ideal of backmix flow.

Models vary in complexity. One-parameter models seem adequate to represent packed beds or tubular vessels. On the other hand models involving up to six parameters have been proposed to represent fluidized beds.

We shall first discuss the dispersion and backmixing models which adequately characterize flow in tubular and packed-bed systems; then we shall consider combined models which are used for more complex situations. In connection with the various applications, the direct use of the age-distribution function for linear kinetics will also be illustrated.

II. Dispersion Models

A. GENERAL DESCRIPTION

Dispersion models, as just stated, are useful mainly to represent flow in empty tubes and packed beds, which is much closer to the ideal case of plug flow than to the opposite extreme of backmix flow. In empty tubes, the mixing is caused by molecular diffusion and turbulent diffusion, superposed on the velocity-profile effect. In packed beds, mixing is caused both by "splitting" of the fluid streams as they flow around the particles and by the variations in velocity across the bed.

When flow is turbulent the resulting concentration² fluctuations are rapid, numerous, and also small with respect to vessel size. They might be considered to be random, which would lead to a diffusion-type equation.

In actual fact, the fluctuations are not independent, and correlations

² Concentration is used here in a general way. It could also represent temperature, etc.

TABLE I
DISPERSION MODELS*

Name of model	Simplifying assumptions or restrictions in addition to those for the model above	Parameters of model	Defining differential equation
General dispersion: includes chemical reaction and source terms	Constant density	D, u	$\frac{\partial C}{\partial T} + u \cdot \nabla C = \nabla \cdot (D \cdot \nabla C) + S + r_c$ (I-1)
General dispersion in cylindrical co-ordinates	Bulk flow in axial direction only. Radial symmetry	$D_R(R), D_L(R), u(R)$	$\frac{\partial C}{\partial T} + u(R) \frac{\partial C}{\partial X} = \frac{\partial}{\partial X} D_L(R) \frac{\partial C}{\partial X} + \frac{1}{R} \frac{\partial}{\partial R} R D_R(R) \frac{\partial C}{\partial R} + S + r_c$ (I-2)
Uniform dispersion	Dispersion coefficients independent of position hence constant	$D'_{Rm}, D'_{Lm}, u(R)$	$\frac{\partial C}{\partial T} + u(R) \frac{\partial C}{\partial X} = D'_{Lm} \frac{\partial^2 C}{\partial X^2} + \frac{D'_{Rm}}{R} \frac{\partial}{\partial R} R \frac{\partial C}{\partial R} + S + r_c$ (I-3)
Dispersed plug flow	Fluid flowing at mean velocity, hence plug flow	D_R, D_L, u	$\frac{\partial C}{\partial T} + u \frac{\partial C}{\partial X} = D_L \frac{\partial^2 C}{\partial X^2} + \frac{D_R}{R} \frac{\partial}{\partial R} R \frac{\partial C}{\partial R} + S + r_c$ (I-4)
Axial dispersed plug flow	No variation in properties in the radial direction	D'_L, u	$\frac{\partial C}{\partial T} + u \frac{\partial C}{\partial X} = D'_L \frac{\partial^2 C}{\partial X^2} + S + r_c$ (I-5)

* From Bischof and Levenspiel (B14.)

exist between them. Unfortunately, the inclusion of such correlations into the analysis would greatly complicate it; instead of a partial differential equation of the diffusion type, we would obtain an integro-differential equation. Moreover, the detailed theories of turbulence are not yet sufficiently developed to justify their use to describe mixing (especially in such complicated systems as packed beds). Hence, we shall not discuss them deeply; a thorough treatment is given by Hinze (H9).

As the alternative, a phenomenological description of turbulent mixing gives good results for many situations. An apparent diffusivity is defined so that a diffusion-type equation may be used, and the magnitude of this parameter is then found from experiment. The dispersion models lend themselves to relatively simple mathematical formulations, analogous to the classical methods for heat conduction and diffusion.

The only real test of such an assumption is its success in representing real systems. In general such models seems to work well for both empty tubes and packed beds; however, recent work has shown limits on the accuracy with which the mixing may be represented by these models (B4, R3).

The remainder of this section will be devoted to describing the methods for measuring dispersion coefficients and the resulting correlations of the data.

B. MATHEMATICAL DESCRIPTIONS

Table I lists the equations corresponding to the various dispersion models ranging from the most general to the most restricted.

1. *General Dispersion Model*

Equation (I-1) is the general representation of the dispersion model. The dispersion coefficient is a function of both the fluid properties and the flow situation; the former have a major effect at low flow rates, but almost none at high rates. In this general representation, the dispersion coefficient and the fluid velocity are all functions of position. The dispersion coefficient, D , is also in general nonisotropic. In other words, it has different values in different directions. Thus, the coefficient may be represented by a second-order tensor, and if the principal axes are taken to correspond with the coordinate system, the tensor will consist of only diagonal elements.

2. *General Dispersion Model for Symmetrical Pipe Flow*

The first simplification of importance is for the frequently encountered situation of symmetrical axial flow in cylindrical vessels. For this particular geometry, the dispersion coefficient tensor reduces to (H8),

$$D = \begin{bmatrix} D_L(R) & 0 & 0 \\ 0 & D_R(R) & 0 \\ 0 & 0 & D_R(R) \end{bmatrix} \quad (11)$$

and Eq. (I-1) reduces to Eq. (I-2). With the dispersion coefficients in the axial and radial directions, $D_L(R)$ and $D_R(R)$, and the fluid velocity, $u(R)$, all functions of radial position, analytical solutions of this equation are impossible. This makes evaluation of dispersion extremely difficult; hence further simplifications are needed to permit analytical solutions to the differential equation.

3. Uniform Dispersion Model

If the axial and radial dispersion coefficients are each taken to be independent of position, we get Eq. (I-3) for which an analytical solution will sometimes be possible. We shall call the coefficients of this model the uniform dispersion coefficients; thus the parameters of this model are D_{Rm}' , D_{Lm}' and $u(R)$.

4. Dispersed Plug-Flow Model

Even with constant dispersion coefficients, accounting for the velocity profile still creates difficulties in the solution of the partial differential equation. Therefore it is common to take the velocity to be constant at its mean value u . With all the coefficients constant, analytical solution of the partial differential equation is readily obtainable for various situations. This model with flat velocity profile and constant values for the dispersion coefficients is called the dispersed plug-flow model, and is characterized mathematically by Eq. (I-4). The parameters of this model are D_R , D_L and u .

In this model, the effect of the velocity profile is "lumped" into the dispersion coefficients, as will be discussed later. In comparison, the coefficients calculated from the uniform dispersion model, or the general dispersion model, are more basic in the sense that they do not have two effects combined into one coefficient.

5. Axial-Dispersed Plug-Flow Model

When there is no radial variation in composition in the fluid flowing in the cylindrical vessel, the only observable dispersion takes place in the direction of fluid flow. In this situation Eq. (I-4) reduces to Eq. (I-5), and we get the axial-dispersed plug-flow model with parameters D'_L and u .

With this model the mathematical problems are greatly simplified since the radial variable is eliminated completely, decreasing the number

of independent variables by one. Because of this simplification it is convenient to use this form whenever possible. The justification and limitations of this model will be discussed later.

C. MEASUREMENT OF DISPERSION COEFFICIENTS

1. Tracer Injection

As has been discussed, the usual method of finding the dispersion coefficients is to inject a tracer of some sort into the system. The tracer concentration is then measured downstream, and the dispersion coefficients may be found from an analysis of the concentration data. For these tracer experiments there are no chemical reactions, and so $r_c = 0$. Also the source term is given by

$$S = \frac{I}{\pi} \delta(X - X_0) f(R) \quad (12)$$

where

I = injection rate of tracer,
 $\delta(X - X_0)$ = Dirac delta function (S20), simply indicating that tracer is introduced at position x_0 .

$f(R) = 1/E^2, R \leq E,$
 $= 0, E \leq R \leq R_0,$
 E = injector-tube radius.

If Eq. (12) is substituted into Eq. (I-2), it becomes,

$$\frac{\partial C}{\partial t} + u(R) \frac{\partial C}{\partial X} = D_L(R) \frac{\partial^2 C}{\partial X^2} + \frac{1}{R} \frac{\partial}{\partial R} R D_R(R) \frac{\partial C}{\partial R} + \frac{I}{\pi} \delta(X - X_0) f(R) \quad (13)$$

Equation (13) is the starting point for the detailed discussion of measurement techniques to follow.

2. Axial-Dispersed Plug-Flow Model

a. Preliminary. Three methods are commonly used to find the effective axial dispersion coefficient, all involving unsteady injection of a tracer either in the form of a pulse or delta function, a step function, or a periodic function such as a sine wave, over a plane normal to the direction of flow. The tracer concentration is then measured downstream from the injection point. The modification of this input signal by the system can then be related to the dispersion coefficient which characterizes the intensity of axial mixing in the system.

The same information can be found from all methods. The periodic

methods present advantages in situations with extremely rapid response; however, the nonperiodic methods, especially the pulse methods, are often preferable from the point of view of simplicity of experimental equipment and ease of mathematical analysis. For this reason, our discussion will therefore be centered about the pulse methods.

If a pulse of tracer is injected into a flowing stream, this discontinuity spreads out as it moves with the fluid past a downstream measurement point. For a fixed distance between the injection point and measurement point, the amount of spreading depends on the intensity of dispersion in the system, and this spread can be used to characterize quantitatively the dispersion phenomenon. Levenspiel and Smith (L16) first showed that the variance, or second moment, of the tracer curve conveniently relates this spread to the dispersion coefficient.

In general, all moments are needed to characterize any arbitrary tracer curve, the first moment about the origin locating the center of gravity of the tracer curve with respect to the origin, the second moment about this mean measuring the spread of the curve, the third moment measuring "skewness," the fourth measuring "peakedness," etc. However, under the assumptions of the dispersion model, the tracer curve is generated by a random process, so only two moments need be considered independent and the rest are functions of these. For convenience, we choose the first two moments, the mean and variance, as independent.

The next problem is to find the functional relationship between the variance of the tracer curve and the dispersion coefficient. This is done by solving the partial differential equation for the concentration, with the dispersion coefficient as a parameter, and finding the variance of this theoretical expression for the boundary conditions corresponding to any given experimental setup. The dispersion coefficient for the system can then be calculated from the above function and the experimentally found variance.

b. Perfect Pulse Injection. We shall first put Eq. (13) into the form needed for mathematical solution, and then briefly discuss the boundary conditions used by previous workers. In Eq. (13) set the radial terms equal to zero, make the velocity constant, and substitute D_L' for $D_L(R)$. This gives

$$\frac{\partial C}{\partial t} + u \frac{\partial C}{\partial X} = D_L' \frac{\partial^2 C}{\partial X^2} + \frac{I}{\pi} \delta(X - X_0) \frac{1}{R_0^2} \quad (14)$$

The function $f(R)$ becomes $1/R_0^2$, since injection is uniform over the entire plane. The rate of tracer injection, I , is now a function of time. If we define C'_{ave} as the concentration of injected tracer if evenly distributed throughout the vessel, for a perfect pulse input, we have

$$I = C'_{\text{ave}} V \delta(t) \quad (15)$$

It is convenient to change the variables to dimensionless form:

$$\begin{aligned} \theta &= ut/L = vt/V \\ \mathbf{x} &= X/L \\ \mathbf{P} &= uL/D_L' \\ L &= \text{length of test section} \\ c' &= C/C'_{\text{ave}} \end{aligned}$$

Equation (14) then becomes,

$$\frac{\partial c'}{\partial \theta} + \frac{\partial c'}{\partial \mathbf{x}} = \frac{1}{\mathbf{P}} \frac{\partial^2 c}{\partial \mathbf{x}^2} + \delta(\mathbf{x} - \mathbf{x}_0) \delta(\theta) \quad (16)$$

The mean and variance of the tracer curve are defined as

$$\begin{aligned} \mu_1 &= \int_0^\infty \theta c' d\theta = \text{mean about } \theta \text{ origin} \\ &= \text{first moment about } \theta \text{ origin} \end{aligned} \quad (17)$$

$$\sigma^2 = \int_0^\infty (\theta - \mu_1)^2 c' d\theta = \text{second moment about the mean} \quad (18)$$

As shown by van der Laan (V4) and Aris (A7), if Laplace transforms are used to solve Eq. (16), the mean and variance may be easily found from the relations

$$\mu_1 = -\lim_{p \rightarrow 0} \frac{\partial \bar{c}'}{\partial p} \quad (19)$$

$$\sigma^2 + \mu_1^2 = \lim_{p \rightarrow 0} \frac{\partial^2 \bar{c}'}{\partial p^2} \quad (20)$$

and in general,

$$\begin{aligned} \mu_n &= \int_0^\infty \theta^n c' d\theta = n\text{th moment about } \theta \text{ origin} \\ &= (-1)^n \lim_{p \rightarrow 0} \frac{\partial^n \bar{c}'}{\partial p^n} \end{aligned} \quad (21)$$

where

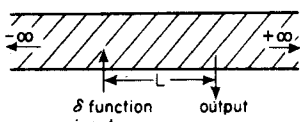
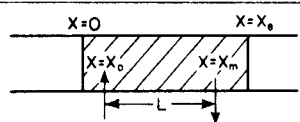
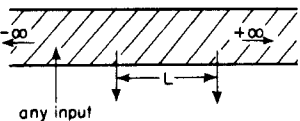
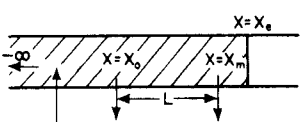
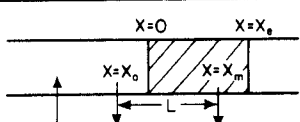
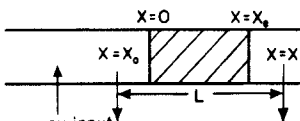
$$\begin{aligned} p &= \text{Laplace transform variable,} \\ \bar{c}' &= \text{Laplace transform of } c'. \end{aligned}$$

The only difference now in various treatments comes from the boundary conditions used to solve Eq. (16).

The simplest type of boundary conditions to use in solving Eq. (16) are the so-called "infinite pipe" conditions. With these conditions, the vessel is assumed to extend from $-\infty$ to $+\infty$. Physically this means that

the changes in flow at the ends of the vessel are neglected. Usually the flowing fluid is led into the vessel in which the dispersion is to be measured through a pipe that has dispersion characteristics different from that of the vessel. Likewise, the exit pipe will generally have different characteristics than the vessel. These end effects will affect the measurement of the dispersion in the main vessel and should be taken into account. It is

TABLE II
EXPERIMENTAL SCHEMES USED IN RELATION TO THE AXIAL-
DISPERSED PLUG-FLOW MODEL

Experimental scheme	Expression for finding the dispersion coefficient	Where first derived
(a) 	$\mu_o = 1 + \frac{2}{P}, \text{Eq. (23)}$ $\sigma_o^2 = \frac{2}{P} + \frac{8}{P^2}, \text{Eq. (24)}$	Levenspiel and Smith [L16]
(b) 	$\mu, \text{Eq. (28)}$ $\sigma^2, \text{Eq. (29)}$	van der Laan [v4]
(c) 	$\Delta\mu_o = \mu_m - \mu_o = 1, \text{Eq. (40)}$ $\Delta\sigma_o^2 = \sigma_m^2 - \sigma_o^2 = \frac{2}{P}, \text{Eq. (41)}$	Aris (A8) Bischoff (B11)
(d) 	$\Delta\mu, \text{Eq. (38)}$ $\Delta\mu^2, \text{Eq. (39)}$	Aris (A8) Bischoff (B11)
(e) 	see reference (B14)	Bischoff and Levenspiel (B14)
(f) 	see reference (B14)	Bischoff and Levenspiel (B14)

found, if tracer is injected and measured far enough from the ends of the vessel, that the end effects are negligible; the distances from the ends that are necessary in order that this be true for various cases will be discussed later.

Levenspiel and Smith (L16) dealt with this simplest of cases which is shown in the first sketch of Table II. Using the open vessel assumption and a perfect delta-function input, they found that the concentration evaluated at $x = 1$ was given by

$$c' = \frac{1}{2} \left(\frac{P}{\pi\theta} \right)^{1/2} \exp \left[-\frac{P(1-\theta)^2}{4\theta} \right] \quad (22)$$

From this equation (or from its Laplace transform) the first and second moments are found to be,

$$\mu_{1\infty} = 1 + \frac{2}{P} \quad (23)$$

$$\sigma_{\infty}^2 = \frac{2}{P} + \frac{8}{P^2} \quad (24)$$

Van der Laan (V4) extended this for much more general boundary conditions that took into account the different dispersion in the entrance and exit sections. These boundary conditions were originally introduced by Wehner and Wilhelm (W4). They assumed that the total system could be divided into three sections: an entrance section from $X = -\infty$ to $X = 0$ (designated by subscript a), the test section from $X = 0$ to $X = X_e$ (having no subscript), and the exit section from $X = X_e$ to $+\infty$ (designated by subscript b), each section having different dispersion characteristics. This is illustrated in the second sketch in Table II.

The boundary-value problem then had the form:

$$\frac{\partial c_a'}{\partial \theta} + \frac{\partial c_a'}{\partial x} - \frac{1}{P_a} \frac{\partial^2 c_a'}{\partial x^2} = 0 \quad x \leq 0 \quad (25a)$$

$$\frac{\partial c'}{\partial \theta} + \frac{\partial c'}{\partial x} - \frac{1}{P} \frac{\partial^2 c'}{\partial x^2} = \delta(x - x_0)\delta(\theta) \quad 0 \leq x \leq x_e \quad (25b)$$

$$\frac{\partial c_b'}{\partial \theta} + \frac{\partial c_b'}{\partial x} - \frac{1}{P_b} \frac{\partial^2 c_b'}{\partial x^2} = 0 \quad x_e \leq x \quad (25c)$$

with boundary conditions,

$$c_a'(x, 0) = c'(x, 0) = c_b(x, 0) = 0 \quad (26a)$$

$$c_a'(-\infty, \theta) = \text{finite} \quad (26b)$$

$$c_a'(0^-, \theta) = c'(0^+, \theta) \quad (26c)$$

$$c_a'(0^-, \theta) - \frac{1}{P_a} \frac{\partial c_a'}{\partial x}(0^-, \theta) = c'(0^+, \theta) - \frac{1}{P} \frac{\partial c'}{\partial x}(0^+, \theta) \quad (26d)$$

$$c'(\mathbf{x}_e^-, \theta) - \frac{1}{P} \frac{\partial c'}{\partial \mathbf{x}}(\mathbf{x}_e^-, \theta) = c_b'(\mathbf{x}_e^+, \theta) - \frac{1}{P_b} \frac{\partial c_b'}{\partial \mathbf{x}}(\mathbf{x}_e^+, \theta) \quad (26e)$$

$$c'(\mathbf{x}_e^-, \theta) = c_b'(\mathbf{x}_e^+, \theta) \quad (26f)$$

$$c_b'(+\infty, \theta) = \text{finite} \quad (26g)$$

The physical significance of these boundary conditions is as follows. Equation (26a) represents the fact that just before the tracer is injected into the system the concentration is everywhere zero. Equations (26b) and (26g) are obvious since a finite amount of tracer is injected. Equations (26d) and (26e) follow from conservation of mass at the boundaries between the sections (W4); the total mass flux entering the boundary must equal that leaving. Equations (26c) and (26f) are based on the physically intuitive argument that concentration should be continuous in the neighborhood of any point. These boundary conditions will be used extensively in the subsequent derivations.

Van der Laan (V4) solved the above system by Laplace transforms, and obtained the following result for the transform of the concentration evaluated at $\mathbf{x} = \mathbf{x}_m$ ($\mathbf{x}_0 < \mathbf{x}_m \leq \mathbf{x}_e$):

$$\bar{c}_m' = \frac{e^{(1/2-q)P}}{2q} \frac{(\mathbf{q} + \mathbf{q}_a)(\mathbf{q} + \mathbf{q}_b) + (\mathbf{q} - \mathbf{q}_a)(\mathbf{q} - \mathbf{q}_b)e^{-2qP(\mathbf{x}_e-1)} + (\mathbf{q} - \mathbf{q}_a)(\mathbf{q} + \mathbf{q}_b)e^{-2qP\mathbf{x}_0} + (\mathbf{q} + \mathbf{q}_a)(\mathbf{q} - \mathbf{q}_b)e^{-2qP(\mathbf{x}_e-\mathbf{x}_0)}}{(\mathbf{q} + \mathbf{q}_a)(\mathbf{q} + \mathbf{q}_b) - (\mathbf{q} - \mathbf{q}_a)(\mathbf{q} - \mathbf{q}_b)e^{-2qP\mathbf{x}_e}} \quad (27)$$

It can be seen, from the complexity of Eq. (27), that to find the inverse Laplace transform in the general case would be exceedingly difficult, if not impossible. Yagi and Miyauchi (Y1) have presented a solution for the special case where $D_a = D_b = 0$. Fortunately, the moments can be found in general from Eq. (27) without evaluating the inverse transform. They are,

$$\mu_1 = 1 + \frac{1}{P} [2 - (1-a)e^{-P\mathbf{x}_0} - (1-b)e^{-P(\mathbf{x}_1-\mathbf{x}_m)}] \quad (28)$$

$$\begin{aligned} \sigma^2 = \frac{2}{P} + \frac{1}{P^2} \{ & 8 + 2(1-a)(1-b)e^{-P\mathbf{x}_1} \\ & - (1-a)e^{-P\mathbf{x}_0}[4\mathbf{x}_0P + 4(1+a) + (1-a)e^{-P\mathbf{x}_0}] \\ & - (1-b)e^{-P(\mathbf{x}_1-\mathbf{x}_m)}[4(\mathbf{x}_1-\mathbf{x}_m)P + 4(1+b) + (1-b)e^{-P(\mathbf{x}_1-\mathbf{x}_m)}] \} \end{aligned} \quad (29)$$

where $a = P/P_a$ and $b = P/P_b$. Van der Laan (V4) shows how these equations reduce to simpler forms for many cases. In particular, they reduce to Eq. (23) and (24) for the open vessel where $a = 1$, $b = 1$.

c. Imperfect Pulse Injection. Both Levenspiel and Smith's and van

der Laan's work depended on being able to represent the tracer injection by a delta function, a mathematical idealization which physically can only be approximated since it requires that a finite amount of tracer be injected in zero time. The closer a physical injection process approximates a perfect delta function, the greater must be the amount of tracer suddenly injected. However, since we are trying to measure the properties of the system, we would like to disturb the system as little as possible with the injection experiment. Thus we should inject slowly from this standpoint. Unfortunately, these two requirements are in opposite directions. To satisfy the mathematical delta function we must inject very rapidly, but in order to not disturb the system we must inject slowly.

Aris (A8), Bischoff (B11), and Bischoff and Levenspiel (B14) have utilized a method that does not require a perfect delta-function input. The method involves taking concentration measurements at two points, both within the test section, rather than at only one as was previously done. The remaining sketches in Table II show the systems considered. The variances of the experimental concentration curves at the two points are calculated, and the difference between them found. This difference can be related to the parameter and thus to the dispersion coefficient. It does not matter where the tracer is injected into the system as long as it is upstream of the two measurement points. The injection may be any type of pulse input, not necessarily a delta function, although this special case is also covered by the method.

Since the injection point is not important, it is convenient to base the dimensionless quantities on the length between measurement points. Therefore, we will here call X_0 the first measurement point rather than the injection point as in Levenspiel and Smith's or van der Laan's work. The position X_m will be taken as the second measurement point. The injection point need only be located upstream from X_0 . Equation (16) is again the basis of the mathematical development. With the test section running from $X = 0$ to $X = X_e$ we shall measure first at $X_0 \leq 0$ and then at $X_m > 0$ where the second measurement point can be either within the test section, $X_m \leq X_e$, or in the exit section, $X_m \geq X_e$. Tracer is injected at $X < X_0$. The boundary-value problem that must be solved is somewhat similar to that of van der Laan:

$$\frac{\partial c_a'}{\partial \theta} + \frac{\partial c_a'}{\partial \mathbf{x}} - \frac{1}{P_a} \frac{\partial^2 c_a'}{\partial \mathbf{x}^2} = 0 \quad \mathbf{x}_0 \leq \mathbf{x} \leq 0 \quad (30)$$

$$\frac{\partial c'}{\partial \theta} + \frac{\partial c'}{\partial \mathbf{x}} - \frac{1}{P} \frac{\partial^2 c'}{\partial \mathbf{x}^2} = 0 \quad 0 \leq \mathbf{x} \leq \mathbf{x}_e \quad (31)$$

$$\frac{\partial c_b'}{\partial \theta} + \frac{\partial c_b'}{\partial \mathbf{x}} - \frac{1}{P_b} \frac{\partial^2 c_b'}{\partial \mathbf{x}^2} = 0 \quad \mathbf{x} \geq \mathbf{x}_e \quad (32)$$

with boundary conditions:

$$c_a'(\mathbf{x}, 0) = c'(\mathbf{x}, 0) = c_b'(\mathbf{x}, 0) = 0 \quad (33a)$$

$$c_a'(\mathbf{x}_0, \theta) = c_0'(\theta) \quad (33b)$$

$$c_a'(0^-, \theta) - \frac{1}{\mathbf{P}_a} \frac{\partial c_a'}{\partial \mathbf{x}}(0^-, \theta) = c'(0^+, \theta) - \frac{1}{\mathbf{P}} \frac{\partial c}{\partial \mathbf{x}}(0^+, \theta) \quad (33c)$$

$$c_a'(0^-, \theta) = c'(0^+, \theta) \quad (33d)$$

$$c'(\mathbf{x}_e^-, \theta) = c_b'(\mathbf{x}_e^+, \theta) \quad (33e)$$

$$c'(\mathbf{x}_e, \theta) - \frac{1}{\mathbf{P}} \frac{\partial c'}{\partial \mathbf{x}}(\mathbf{x}_e, \theta) = c_b'(\mathbf{x}_e^+, \theta) - \frac{1}{\mathbf{P}_b} \frac{\partial c_b'}{\partial \mathbf{x}}(\mathbf{x}_e^+, \theta) \quad (33f)$$

$$c_b'(+\infty, \theta) = \text{finite} \quad (33g)$$

There are no source terms in Eq. (31), since the injection point is upstream from the sections over which the equations are to be used. The boundary conditions are of the same type used by van der Laan (V4), except for Eq. (33b). This merely states that we are going to measure the concentration at $X = X_0$, which we call c_0' . The solution of Eqs. (30), (31), (32), and (33) is again accomplished by the use of Laplace transforms following the same scheme as given in (A8, B11, B14). The Laplace transform of the concentration at $\mathbf{x} = \mathbf{x}_m$ is

$$\begin{aligned} \frac{\bar{c}_m'}{\bar{c}_0'} = \frac{2q_a}{\Delta} \{ & (q - q_b) \exp [(\tfrac{1}{2} + q)\mathbf{P}(\mathbf{x}_m - \mathbf{x}_e)] \\ & + (q + q_b) \exp [(\tfrac{1}{2} - q)\mathbf{P}(\mathbf{x}_m - \mathbf{x}_e)] \}, \quad \mathbf{x}_m \leq \mathbf{x}_e \end{aligned} \quad (34)$$

$$= \frac{4qq_a}{\Delta} \exp [(\tfrac{1}{2} - q_b)\mathbf{P}_b(\mathbf{x}_m - \mathbf{x}_e)], \quad \mathbf{x}_m \geq \mathbf{x}_e \quad (35)$$

where

$$\begin{aligned} \Delta = & (q + q_a) \{ (q - q_b) \exp [(\tfrac{1}{2} + q_a)\mathbf{P}_a\mathbf{x}_0 - (\tfrac{1}{2} + q)\mathbf{P}\mathbf{x}_e] \\ & + (q + q_b) \exp [(\tfrac{1}{2} - q_a)\mathbf{P}_1\mathbf{x}_0 - (\tfrac{1}{2} - q)\mathbf{P}\mathbf{x}_e] \} \\ & - (q - q_a) \{ (q - q_b) \exp [(\tfrac{1}{2} - q_a)\mathbf{P}_a\mathbf{x}_0 - (\tfrac{1}{2} + q)\mathbf{P}\mathbf{x}_e] \\ & + (q + q_b) \exp [(\tfrac{1}{2} + q_a)\mathbf{P}_a\mathbf{x}_0 - (\tfrac{1}{2} - q)\mathbf{P}\mathbf{x}_e] \} \end{aligned}$$

Notice that the right-hand side of Eq. (34) is equal to the ratio of the transformed concentration at the second measurement point to the transformed concentration at the first measurement point. In the terminology of control engineering, this quantity is the transfer function of the system between X_0 and X_m . The Laplace-transform method is possible because the diffusion equation is a linear differential equation. Thus, the right-hand side of Eq. (34) could in principle be used in a control-system analysis of an axial-dispersion process.

The mean and variance can be found from Eqs. (34) and (35) by use of van der Laan's method, Eq. (21). The results are of the form

$$\Delta\mu_1 = \mu_{1m} - \mu_{10} = \psi_1(\mathbf{P}, \mathbf{P}_a, \mathbf{P}_b, \mathbf{x}_0, \mathbf{x}_m, \mathbf{x}_e) \quad (36)$$

$$\Delta\sigma^2 = \sigma_m^2 - \sigma_0^2 = \psi_2(\mathbf{P}, \mathbf{P}_a, \mathbf{P}_b, \mathbf{x}_0, \mathbf{x}_m, \mathbf{x}_e) \quad (37)$$

where ψ_1 and ψ_2 are cumbersome functions given by Bischoff and Levenspiel (B14). In order to use this method, the tracer concentration is measured at two points X_0 and X_m , and the variances calculated. The difference in variances can be found, and this number is then used in Eq. (37) along with the physical dimensions of the experimental apparatus to calculate \mathbf{P} , hence D'_L .

An interesting simplification of these general expressions occurs when we take both measurements within the test section. In this case Eqs. (36) and (37) become

$$\Delta\mu_1 = 1 - \frac{1-b}{\mathbf{P}} (1 - \exp[-\mathbf{P}]) \exp[\mathbf{P}(\mathbf{x}_m - \mathbf{x}_e)] \quad (38)$$

$$\begin{aligned} \Delta\sigma^2 = \frac{2}{\mathbf{P}} + \frac{1-b}{\mathbf{P}^2} \exp[\mathbf{P}(\mathbf{x}_m - \mathbf{x}_e)] \{ & 4(1+b)(\exp[-\mathbf{P}] - 1) \\ & + 4\mathbf{P}(\mathbf{x}_m - \mathbf{x}_e) + (1-b)(\exp[-2\mathbf{P}] - 1) \exp[\mathbf{P}(\mathbf{x}_m - \mathbf{x}_e)] \\ & + 4\mathbf{P}(\mathbf{x}_e - \mathbf{x}_0) \exp[-\mathbf{P}] \} \end{aligned} \quad (39)$$

as found by Aris (A8) and Bischoff (B11).

These expressions reduce even further to particularly simple forms for the case of an infinite tube or where $b = 1$. Thus letting subscript ∞ refer to the infinite tube, or open vessel, case we find as shown in the third sketch of Table II

$$\Delta\mu_{1\infty} = 1 \quad (40)$$

$$\Delta\sigma_{\infty}^2 = \frac{2}{\mathbf{P}} \quad (41)$$

As far as the actual use of these expressions in their most general form, Eqs. (36) and (37), probably the only case which need be considered is that represented by the bottom sketch of Table II. Here measurements are taken only on either side of the test section. This type of measurement could be used to find the dispersion characteristics of a process vessel in a plant where no means are available for inserting a probe inside the vessel. With these equations, measurements need be taken only on either side of the test section.

When the probes can be inserted within the test section, then Eqs. (38) to (41) can be used. Comparing these expressions we see that it is highly

desirable to make measurements far enough away from the ends of the vessels so that end effects become negligible, in which case the extremely simple expressions, Eqs. (40) and (41), can properly be used. Another even more important reason for using the infinite tube expressions is that the end effects cannot be exactly accounted for in real systems because of the complex flow patterns at these locations. Thus Eqs. (38) and (39) at best only give approximate end corrections.

However, there is one important use for Eqs. (38) and (39): to estimate the magnitude of the end effects as represented by the second term in Eq. (39). This will let us know how far in from the ends of the vessel the probes must be placed so that end effects can be neglected and the simpler equation used. Bischoff and Levenspiel (B14) present design charts which allow making such an estimation. As an example in a typical packed bed ($d_t/d_p = 15$) followed by an empty tube these charts show that the measurement points should be placed at least eight particle diameters into the packed section for less than one percent error. For more details see (B14).

d. Perfect Step Injection. For a perfect step input, the injection rate, I , in Eq. (14) will be represented by the unit step function, $U(t)$. The equation in dimensionless form then becomes:

$$\frac{\partial c'}{\partial \theta} + \frac{\partial c'}{\partial \mathbf{x}} = \frac{1}{P} \frac{\partial^2 c'}{\partial \mathbf{x}^2} + \delta(\mathbf{x} - \mathbf{x}_0)U(\theta) \quad (42)$$

As an example of the solution of Eq. (42), Lapidus and Amundson (L3) and Robinson (R4) considered the closed-open (semi-infinite) system and obtained the solution:

$$c' = \mathbf{F} = \frac{1}{2} \left[\operatorname{erfc} \frac{1 - \theta}{2\sqrt{(D_L/uL)\theta}} + e^{uL/D_L} \operatorname{erfc} \frac{1 + \theta}{2\sqrt{(D_L/uL)\theta}} \right] \quad (43)$$

Since the step response (\mathbf{F} curve) is the time integral of the pulse response (\mathbf{C} curve), the Laplace transform of the step response for the general boundary conditions as used by van der Laan will be given by dividing equation (27) by the transform variable, p ,

$$\bar{c}'_{m, \text{step}} = \frac{\bar{c}'_m [\text{Eq. (27)}]}{p} \quad (44)$$

Thus, many other solutions could be generated from Eq. (44) if the inverse transforms could be found. As mentioned previously, however, this would be exceedingly difficult in most cases.

The usual method of relating the dispersion coefficient to the experi-

mental response has been to compare the theoretical and experimental slopes at $\theta = 1$. This immediately leads to some problems, however. In order to have a formula for the slope, the solution in the time domain of Eq. (42) must be available. Since this solution for general boundary conditions is not known, and estimation of end effect error is not possible. Taking the derivative of experimental data is usually very inaccurate, leading to further errors. Also, only a small part of the experimental information, that around $\theta = 1$, is used. It is not an "efficient" method.

A better data analysis method, as yet unused, might be to use the area under the step response curve. It can be shown that the moments are related to the step response by

$$\mu_n = n \int_0^{\infty} \theta^{n-1} \frac{C(\theta)}{C(0)} d\theta$$

for a "down-step" or purge run, and

$$\mu_n = n \int_0^{\infty} \theta^{n-1} \frac{C(\infty) - C(\theta)}{C(\infty)} d\theta$$

for an "up-step" or feed run. Thus the entire range of data could be used, as is done in the pulse method. The general expressions for the moments as given by Eqs. (28) and (29) can again be used for calculating the dispersion coefficients. Hyman and Corson (H17) have devised an on stream analog computer to perform these calculations.

e. Imperfect Step Injection. In principle, by injecting an imperfect step function and then measuring twice, the dispersion coefficient could be calculated. This is so because when solving Eqs. (30), (31), (32), and (33) no assumptions were made about the form of the response at the first measuring point. Thus, $C_0'(\theta)$ could have *any* form, including imperfect pulses and steps. This is also obvious from Eq. (34) which is merely the transfer function, or the ratio of the Laplace transforms of the concentrations at the two measurement points. The method of using slopes could not be used, though, because the time domain rather than the Laplace transformed solution would be necessary.

However, the moment method could again be used to give differences in the moments. This information could then be used with Eqs. (36) and (37) to find the dispersion coefficient.

f. Comparison of Pulse and Step Methods. A brief summary of the advantages of the pulse and step injections methods is given below.

(1) *Experimental Problems.* It is usually easier to approximate a perfect step than a perfect pulse. However, this is not important when two measurements are taken. Also, the imperfect pulse might be prefer-

able for commercial testing since the system would not be disturbed for as long a time as with the step input.

(2) *Characterization of Data.* The use of the moments for either pulse or step data would seem to be best since the data is integrated and, thus, a smoothed "mean square" fit is obtained. Other methods use only the data from a narrow region such as at the pulse maximum or the slope of the step response at a given location.

(3) *Computation Errors in Analyzing the Data.* Probably the most serious drawback in using moments is that the tail end of the recorded curve plays too strong a role and slight errors here are magnified. However, taking the slope of the step response data is usually a rather inaccurate process also.

(4) *Comparison With Model.* Use of moments enables the general expressions with any desired boundary conditions to be utilized. Other methods require time domain solutions to be known which can be found only for limited circumstances.

g. Periodic Injection. The sinusoidal input method has been discussed by Rosen and Winsche (R5), Kramers and Alberda (K14), Deissler and Wilhelm (D13), Ebach and White (E1), and McHenry and Wilhelm (M4).

The output may be found from Eq. (14) by assuming a periodic solution of the form

$$A(\mathbf{x})e^{-i\omega\theta}$$

where ω is a dimensionless frequency, $\omega = \omega L/u$. A simpler and more general method would be to recall from Laplace transform theory that the response to a sinusoidal forcing function for a system can be found by replacing the transform variable, p , by $+i\omega$. (This method is used very widely in automatic-control theory, where the frequency response is found by replacing the transform variable s in the transfer function (impulse response) by $+i\omega$.) With this substitution, the amplitude ratio can be found from the absolute value of the complex transfer function, and the phase lag from the argument of the complex transfer function.

Thus the response to a periodic injection for very general boundary conditions can be found by substituting $p = +i\omega$ into Eq. (34). The results for the general case would be very complicated; so, as an illustration of the form of the periodic response, we will consider only the simplest case: a doubly infinite system. For such a system, $D_{La}' = D_L' = D_{Lb}'$, and Eq. (34) reduces to

$$\frac{\bar{c}_m'}{\bar{c}_0'} = \exp \left[\left(\frac{1}{2} - q \right) \mathbf{P} \right] \quad (45)$$

The transform variable, p , appears only in q ,

$$\begin{aligned}
 q &= \sqrt{\frac{1}{4} + \frac{p}{P}} = \sqrt{\frac{1}{4} + \frac{i\omega}{P}} \\
 &= \frac{1}{2} \sqrt{\sqrt{\frac{1}{4} + \left(\frac{2\omega}{P}\right)^2} + \frac{1}{2}} + \frac{i}{2} \sqrt{\sqrt{\frac{1}{4} + \left(\frac{2\omega}{P}\right)^2} - \frac{1}{2}} \\
 &= \frac{1}{2} \rho_1 + \frac{i}{2} \rho_2
 \end{aligned} \tag{46}$$

Therefore, the response is given by

$$\begin{aligned}
 \frac{\bar{c}_m'}{\bar{c}_0'} &= e^{(P/2)(1-\rho_1-i\rho_2)} \\
 &= e^{(P/2)(1-\rho_1)} \left(\cos \frac{P}{2} \rho_2 - \sin \frac{P}{2} \rho_2 \right)
 \end{aligned} \tag{47}$$

The amplitude ratio is

$$\left| \frac{\bar{c}_m'}{\bar{c}_0'} \right| = e^{(P/2)(1-\rho_1)} \tag{48}$$

and the phase lag is

$$-\angle \left(\frac{\bar{c}_m'}{\bar{c}_0'} \right) = \frac{P}{2} \rho_2 \tag{49}$$

These equations were used, for example, by Ebach and White (E1). The periodic response for more general boundary conditions could be found from Eq. (34) by the same method, but the results would of course be much more complicated.

h. Experimental Findings. Literature data on axial dispersion of numerous investigators are presented in Figs. 8, 9, and 10. One of the problems in bringing the data together in a generalized manner is the choice of a characteristic length which will account for both particle

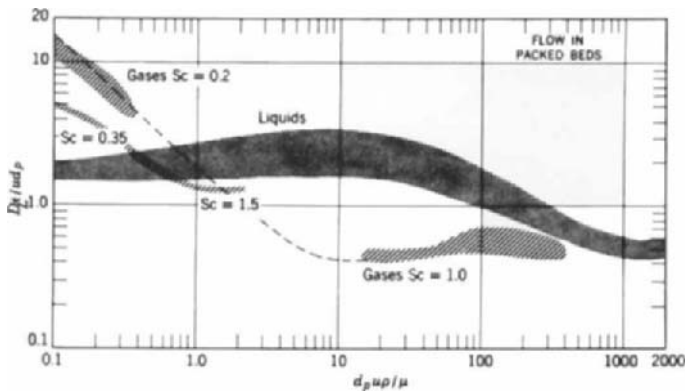


FIG. 8. Axial dispersion in packed beds, dispersed plug flow model (L13).

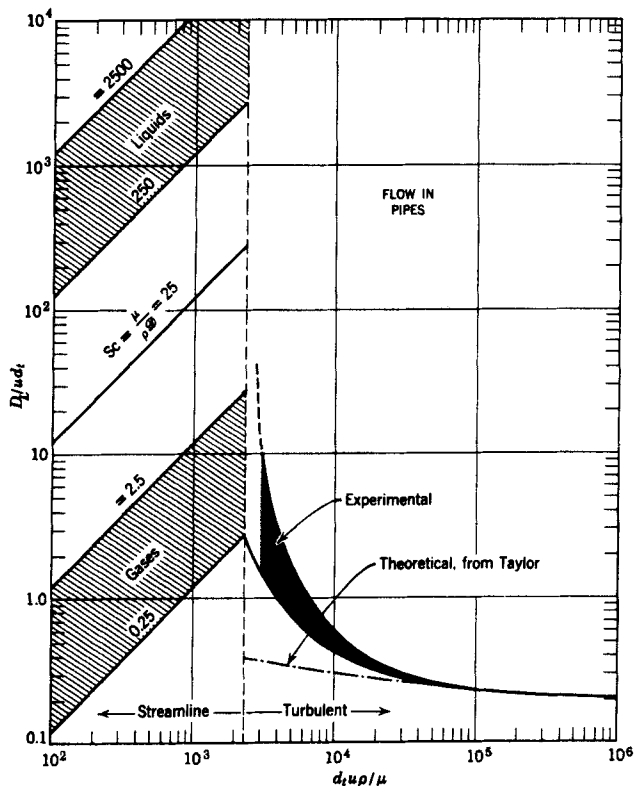


FIG. 9. Axial dispersion in pipes, dispersed plug flow model (L13).

size and tube size, and allow for comparison of packed bed data with empty tube data. For this purpose the hydraulic diameter used by Mott (M12), Wilhelm (W10), and Cairns and Prausnitz (C5) was used. This length is defined similarly to the hydraulic diameter as used for friction factors in pipes (B10):

$$d_e = \frac{4(\text{free volume of fluid})}{\text{wetted area}}$$

or

$$d_e = \frac{4(\pi/4)d_t^2\epsilon}{(6/d_p)(\pi/4)d_t^2(1-\epsilon) + \pi d_t} = \frac{\epsilon d_t}{\frac{3}{2}(d_t/d_p)(1-\epsilon) + 1} \quad (50)$$

We notice that, for empty tubes, $\epsilon = 1$ and $d_e = d_t$. Therefore d_e retains its significance for empty tubes. The results for each type of system will now be discussed.

i. Packed Beds. The use of the effective diameter, Eq. (50), requires the specification of the particle diameter, d_p . It was found that for non-

spherical packing the equivalent spherical diameter as given by Carman (C10), which is the diameter of a sphere with the same volume as the particle, could be used. This gave a simple parameter that correlated all of the data relatively well.

The experimental data was obtained by the investigators through use of several of the above measuring techniques. Data on liquid systems have been obtained using pulse inputs with a single measurement point by Carberry and Bretton (C9) and Ebach and White (E1). No investigators have yet used the method of two measurement points discussed in Section II, C,2,c. Step inputs have been used by Ampilogov, Kharin, and Kurochkina (A4), Cairns and Prausnitz (C5), Danckwerts (D4), Jacques and Vermeulen (J1), Klinkenberg and Sjenitzer (K11) and von Rosen-

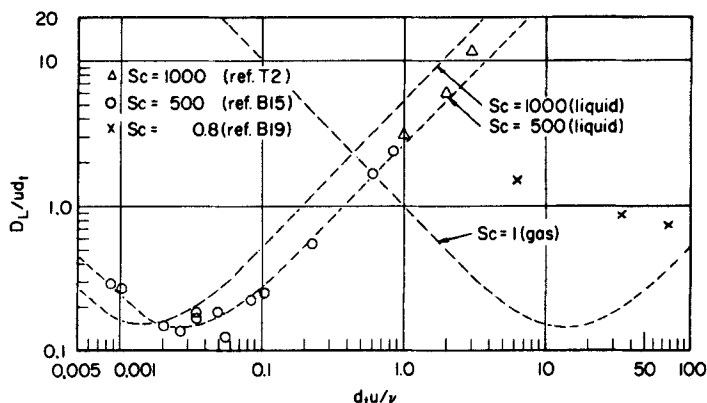


FIG. 10. Axial dispersion in laminar flow in pipes, dispersed plug flow model. Adapted from (B13).

berg (V7). Frequency response methods have been used by Ebach and White (E1), Liles and Geankoplis (L18), Kramers and Alberda (K14), and Strang and Geankoplis (S24).

Gas data have been obtained using pulse inputs by Carberry and Bretton (C9), step inputs by Blackwell *et al.* (B17) and Robinson (R4), and frequency response by McHenry and Wilhelm (M4).

Inspection of Fig. 8 shows that there is considerable scatter in the data. Part of this may be due to the fact that we are attempting to represent a complex phenomenon with a single parameter, the dispersion coefficient. Errors would also be caused by the common practice of taking measurements at or beyond the exit of the packed section. This neglect of end conditions could lead to large errors in the calculated dispersion coefficients, as pointed out by Bischoff and Levenspiel (B14). Also, all the analyses were based on the assumption of having a perfect pulse, step,

or sinusoidal input. These assumptions can now be relaxed with the two-measuring-point method. Thus, even though there is much reported data, it would seem that further experimental work is needed in which all possible experimental errors are minimized.

The length parameter used in this correlation to represent the different types of packing may also contribute to the scatter. The use of the effective diameter may not be the best way to bring the data together, and several of the investigators found that they could correlate their own data quite well by using certain arbitrary functions of the void fraction, ϵ . However, it was found by Bischoff (B13) that the effective diameter was the most satisfactory size parameter when all of the data were considered.

A further problem in plotting the data is that the fluid viscosity has very little effect on the dispersion (E1). Therefore, the Reynolds number might not be appropriate as a plotting variable (C5). However, no other dimensionless group has yet been proposed, and so the Reynolds number was retained in Fig. 8.

Figure 8 shows that the group D_L'/ud_e is roughly constant for all Reynolds numbers. Jacques and Vermeulen (J1) found, however, that their data with regular arrangements of the particles showed a definite break in the values. This seems to be caused by a transition from laminar to turbulent flow.

Rough estimates for axial dispersion coefficients can be made using random walk techniques, and these will be discussed in Section II,E. Also, a theory can be developed for predicting axial dispersion coefficients from radial dispersion coefficients which is the source of the dotted line of Figure 8. This will be discussed in Section II,D. Bischoff (B13), Froment (F9), and Hofmann (H11) have presented summaries of packed-bed data.

j. Turbulent Flow in Empty Tubes. Data for axial dispersion coefficients in turbulent flow in empty tubes has been collected by Levenspiel (L10) and Sjenitzer (S18). Their results are combined in Fig. 9. The liquid data have been obtained using single measurements of a pulse input by Allen and Taylor (A3a), Hull and Kent (H15), Kohl and Newacheck (K13), Lee (L7), Shipley (S15) and Taylor (T4). A step input was used by Fowler and Brown (F7), Smith and Schultz (S19), and no one has used a frequency response method. Gas data was obtained by Davidson *et al.* (D11) using a pulse technique.

Figure 9 shows considerable scatter because much of the data were taken in commercial pipelines with valves, elbows, bends, and other types of flow disturbances. In the transition region of Reynolds numbers below 10,000, the dispersion coefficient rises rapidly. This can be

explained by the build-up of the laminar sublayer at these low Reynolds numbers with its pronounced effect on the velocity distribution. The dashed curves are based on a theory to be discussed in Section II,D.

k. Laminar Flow in Empty Tubes. All of the data have been taken by pulse methods with a single measurement point. The liquid data are by Blackwell (B15) and Taylor (T2), and the gas data by Bournia *et al.* (B19). The dashed lines are again from theory. It is seen that the liquid data agree quite well with the theory. The gas data, however, do not. Bournia *et al.* discussed this and arrived at the conclusion that the axial-dispersed plug-flow model may not be a good representation of the system for this case. Additional experimentation in gases is suggested. Crookewit, Honig, and Kramers (C23) have given results for flow in an annular region.

3. Dispersed Plug-Flow Model

a. Preliminary. The experimental methods for measuring radial dispersion coefficients again involve injecting tracer into the system and measuring its concentration at a point downstream from the injection point. In this case, we do not want to inject over a plane or measure over a plane. Instead we must use an experimental method where the concentration varies with radial position allowing us to study the radial movement of tracer and thereby giving information on the radial mixing occurring in the system. Usually the tracer is injected on the axis of the tube. The axis is chosen so that there will be radial symmetry about the tube axis, which simplifies the mathematics. As the tracer moves down the tube, it will spread radially by dispersion, until a long distance downstream (theoretically infinite) from the injection point the tracer will be completely mixed with the flowing fluid. Therefore, the measurement point must not be too far from the injection point in order to have enough of a concentration profile to get accurate results. The methods for measuring axial dispersion coefficients all required unsteady-state injection methods. Now, however, because we are going to inject at a point rather than over a plane and measure radial concentration profiles, a steady-state method can be used, which simplifies the analysis. Unsteady state methods could also be used, but they would just add unnecessary complications.

The mathematical developments are based on Eq. (13) with all of the coefficients assumed to be constant,

$$\frac{\partial C}{\partial t} + u \frac{\partial C}{\partial X} = D_L \frac{\partial^2 C}{\partial X^2} + \frac{D_R}{R} \frac{\partial}{\partial R} R \frac{\partial C}{\partial R} + \frac{I}{\pi} \delta(X - X_0) f(R) \quad (51)$$

We shall change the variables in Eq. (51) to dimensionless forms which

are different from those used in the previous section on the axial-dispersed plug-flow model. Thus

$$\theta' = \frac{ut}{R_0}$$

$$x = \frac{X}{R_0}$$

$$r = \frac{R}{R_0}$$

$$P_L = \frac{uR_0}{D_L}$$

$$P_R = \frac{uR_0}{D_R}$$

A dimensionless concentration c is defined as follows

$$c = \frac{C}{C_{ave}}$$

where C_{ave} is the mean concentration of tracer far enough downstream from the point of steady-state tracer injection of rate I . By a mass balance, then,

$$(\text{rate of injection}) = (\text{rate of flow out of tube})$$

or

$$I = \pi R_0^2 u C_{ave}$$

With these dimensionless quantities introduced, Eq. (51) becomes

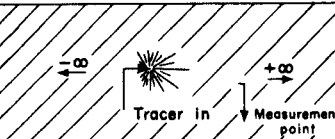
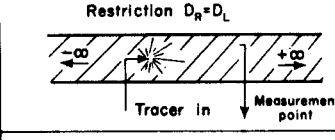
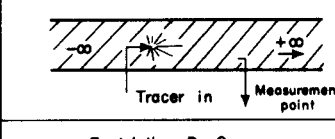
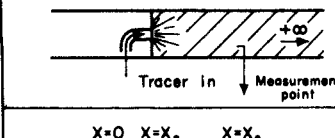
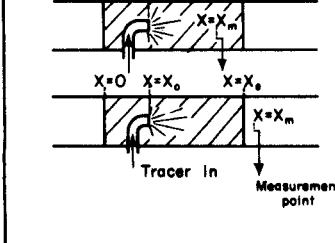
$$\frac{\partial c}{\partial x} - \frac{1}{P_L} \frac{\partial^2 c}{\partial x^2} - \frac{1}{P_R} \frac{1}{r} \frac{\partial}{\partial r} r \frac{\partial c}{\partial r} = \delta(x - x_0) f(r) \quad (52)$$

This equation is used in finding the dispersion coefficients from experimental data.

b. Solutions for Various Measurement Experiments. Most of the measurement techniques have used the same sort of injection: steady flow at the tube axis. Thus the differences in the various contributions were in the exact experimental setup used (which determines the boundary conditions), and in the completeness of the mathematical model used to represent the physical situation. Various simplifying assumptions were usually made in Eq. (52) or in the boundary conditions. These are shown in Table III. Bischoff and Levenspiel (B14) presented a general solution that used no assumptions beyond those inherent in Eq. (52). We will discuss this solution first, since all other cases are special cases of this general solution.

The method of solution is similar to that used for the axial-dispersed

TABLE III
EXPERIMENTAL SCHEME USED IN RELATION TO THE
DISPERSED PLUG-FLOW MODEL

Experimental scheme	Results	Where first used
	$c = \frac{P_R}{4} \exp \left[-\frac{P_R}{2} \left(\sqrt{x^2 + r^2} - x \right) \right] \quad (\text{III-1})$	Towle and Sherwood [79]
<p>Restriction $D_R = D_L$</p> 	$c = 1 + \frac{1}{2} \sum_{a_i > 0} \frac{1}{q_R} \exp \left[\left(\frac{1}{2} - q_R \right) P_R x \right] \frac{J_0(a_i r)}{J_0^2(a_i)} \quad (\text{III-2})$ <p>with $J_1(a_i) = 0$, $q_R = \sqrt{\frac{1}{4} + \frac{a_i^2}{P_R^2}}$</p>	Bernard and Wilhelm [86]
	$c = 1 + \frac{1}{2} \sum_{a_i > 0} \frac{1}{q} \exp \left[\left(\frac{1}{2} - q \right) P_L x \right] \frac{J_0(a_i r)}{J_0^2(a_i)} \quad (\text{III-3})$ <p>with $J_1(a_i) = 0$, $q = \sqrt{\frac{1}{4} + \frac{a_i^2}{P_L^2}}$</p>	Klinkenberg et al. [82]
<p>Restriction $D_L = 0$</p> 	$c = 1 + \frac{2}{\pi} \sum_{a_i > 0} \frac{J_0(a_i r)}{J_0^2(a_i)} \frac{J_1(a_i x)}{a_i} \exp \left[-\frac{a_i^2 x}{P_R} \right] \quad (\text{III-4})$ <p>with $J_1(a_i) = 0$</p>	Fahien and Smith [82]
	<p>Equation (55) and (56)</p> <p>Equation (55) and (57)</p>	Bischoff and Levenspiel [84]

plug-flow model. In the present case, however, the method must be modified in order to keep both axial and radial dispersion in the equations. It will be recalled that the experimental equipment is supposed to consist of three parts: the upstream section $X = -\infty$ to $X = 0$, the test section $X = 0$ to $X = X_e$, and the downstream section $X = X_e$ to $X = +\infty$. The injection takes place at X_0 ($0 \leq X_0 \leq x_e$) and the measurement is at X_m ($X_0 < X_m$); see Table III.

Equation (52) is written for each section, and thus the boundary value problem to be solved is:

$$\frac{1}{P_{L_a}} \frac{\partial^2 c_a}{\partial x^2} + \frac{1}{P_{R_a}} \frac{1}{r} \frac{\partial}{\partial r} r \frac{\partial c_a}{\partial r} - \frac{\partial c_a}{\partial x} = 0 \quad x \leq 0 \quad (53a)$$

$$\frac{1}{P_L} \frac{\partial^2 c}{\partial x^2} + \frac{1}{P_R} \frac{1}{r} \frac{\partial}{\partial r} r \frac{\partial c}{\partial r} - \frac{\partial c}{\partial x} = -\delta(x - x_0)f(r) \quad 0 \leq x \leq x_e \quad (53b)$$

$$\frac{1}{P_{L_b}} \frac{\partial^2 c_b}{\partial x^2} + \frac{1}{P_{R_b}} \frac{1}{r} \frac{\partial}{\partial r} r \frac{\partial c_b}{\partial r} - \frac{\partial c_b}{\partial x} = 0 \quad x \geq x_e \quad (53c)$$

with boundary conditions:

$$\frac{\partial c_a}{\partial r} = \frac{\partial c}{\partial r} = \frac{\partial c_b}{\partial r} = 0 \quad \text{at } r = 1 \quad (54a)$$

$$c_a(-\infty, r) = \text{finite} \quad (54b)$$

$$c_a(0^-, r) = c(0^+, r) \quad (54c)$$

$$c_a(0^-, r) - \frac{1}{P_{L_a}} \frac{\partial c_a}{\partial x}(0^-, r) = c(0^+, r) - \frac{1}{P_L} \frac{\partial c}{\partial x}(0^+, r) \quad (54d)$$

$$c(x_e^-, r) - \frac{1}{P_L} \frac{\partial c}{\partial x}(x_e^-, r) = c_b(x_e^+, r) - \frac{1}{P_{L_b}} \frac{\partial c_b}{\partial x}(x_e^+, r) \quad (54e)$$

$$c(x_e^-, r) = c_b(x_e^+, r) \quad (54f)$$

$$c_b(+\infty, r) = \text{finite} \quad (54g)$$

Equation (54a) means physically that no mass is transferred through the solid pipe wall, and all of the other boundary conditions have been discussed previously. The solution evaluated at the measurement point $X = X_m$ is:

$$c = 1 + \sum_{a_i > 0} \frac{J_0(a_i r)}{J_0^2(a_i)} \frac{J_1(a_i e)}{q a_i e} N_i \quad (55)$$

where

$$J_1(a_i) = 0$$

$$q = \sqrt{\frac{1}{4} + \frac{a_i^2}{P_L P_R}}$$

For measurement within the test section ($x_m \leq x_e$), also

$$N_i = \exp \left[\left(\frac{1}{2} - q \right) P_L (x_m - x_0) \right]$$

$$\left\{ \frac{(q - q_a)(q - q_b) \exp[-2P_L q(x_e - x_m + x_0)] + (q - q_a)(q + q_b) \exp[-2qP_L x_0] + (q + q_a)(q - q_b) \exp[-2qP_L(x_e - x_m)] + (q + q_a)(q + q_b)}{(q + q_a)(q + q_b) - (q - q_a)(q - q_b) \exp[-2P_L q x_e]} \right\} \quad (56)$$

For measurement beyond the test section ($x_m \geq x_e$),

$$N_i = 2q \exp \left[\left(\frac{1}{2} - q \right) P_L (x_e - x_0) + \left(\frac{1}{2} - q_b \right) P_{L_b} (x_m - x_e) \right] \\ \times \left\{ \frac{(q + q_a) + (q - q_a) \exp [-2P_L q x_0]}{(q + q_a)(q + q_b) - (q - q_a)(q - q_b) \exp [-2P_L q x_e]} \right\} \quad (57)$$

The solutions of the various investigators as listed in Table III can be found by suitable simplification of Eq. (55) as shown in (B14).

Eq. (55) is impractical to use. Hence it would be valuable to know under what conditions we are justified in using some of the simpler expressions based on various assumptions. This information can then be used to guide the design of experimental equipment so that the mathematical analysis can be made relatively easily.

Bischoff and Levenspiel (B14) considered this problem, and have presented design charts which allow estimation of errors in the calculated dispersion coefficients for various conditions. It was found that when the ratio of injection to tube diameter is less than 20%, or $e < 0.2$, then the assumption of a point source, or $e \rightarrow 0$, was good to within 5%. Thus for many cases, the neglect of the finite size of injection tube is justified.

It was also found that the end-effect error is smaller than for the measurement of axial dispersion coefficients. Even though the error may be large for measurement right at the end of the vessel, the error decreases very rapidly on moving the probe into the bed. Hence, in most typical packed beds, taking measurements one or two particle diameters into the bed is often sufficient to make the end-effect error negligible.

c. Use of Equations in Interpreting Experimental Data. The experimental setup corresponding to the mathematical model used [Eqs. (53) and (54)] would be as follows. A steady stream of tracer is injected from a tube on the axis of the cylindrical vessel. Then at some point downstream from the injection point the tracer concentration is measured, and Eq. (55) is used to find the dispersion coefficients from the concentration data. A practical problem that arises in the tracer concentration measurement is that the recording instrument usually has to be calibrated to give the proper numerical values of concentration. In most instruments, recalibration is needed from time to time, which is not very convenient. For this reason, many investigators (B6, D20, F2) have measured the experimental average stream concentration, C_A , at a point far downstream, in addition to finding the radial concentration distribution at the measurement point, X_m . Then if the ratio C/C_A is used, any "drifting" in the measuring device will automatically cancel. Therefore, concentration measurements are usually reported as C/C_A (B6).

If our experimental techniques were perfect, the experimental average concentration C_A would be equal to the integral mean concentration C_{ave} .

The extent that they differ from one another can be taken as a "mass balance" for the system. If Eq. (55) is multiplied through by C_{ave}/C_A we get:

$$\frac{C}{C_A} = \frac{C_{ave}}{C_A} + \sum_{a_i > 0} \frac{C_{ave}}{C_A} \frac{J_0(a_i r)}{q J_0^2(a_i)} \frac{J_1(a_i e)}{a_i e} N_i \quad (58)$$

In order to have an estimate of the experimental precision, it is necessary to take several concentration readings. This is most conveniently done at a number of radial positions for a given axial position in the vessel. Suppose we write Eq. (58) as:

$$C/C_A = K_0 + K_1 J_0(a_1 r) + K_2 J_0(a_2 r) + \dots \quad (59)$$

where

$$K_i = \frac{C_{ave}}{C_A} \frac{N_i}{J_0^2(a_i)} \frac{J_1(a_i e)}{q a_i e} \quad (60)$$

Now if we have data of C/C_A as a function of pipe radius, r , we can use standard least-squares techniques to estimate K_0 , K_1 , K_2 , \dots . In addition, we can find the standard deviations of the estimates of K_i by the least-squares procedure, which gives an indication of the precision of the data. The first constant, K_0 , should be unity if we have a perfect mass balance, and the deviation from this value gives an estimate of the reliability of the data. Knowing the injection tube size, we can find the N_i/q from the least squares K_i from Eq. (59).

$$\frac{N_i}{q} = \frac{K_i}{K_0} J_0^2(a_i) \frac{a_i e}{J_1(a_i e)} \quad (61)$$

The dispersion coefficients can now be found from the N_i/q by a nonlinear calculation procedure, such as the Newton-Raphson method, utilizing the expressions for N_i , Eqs. (56) or (57). In the general case, values of P_{L1} , P_{R1} , P_{L2} , P_{R2} , and the physical dimensions of the apparatus are substituted into Eq. (56) or (57), and then P_L and P_R can be found from the simultaneous (nonlinear) solution of the expressions for N_1 and N_2 . The variances of the dispersion coefficients could also be found from the variances of the K_i by standard statistical methods.

Another method has been proposed by Blackwell (B16) and by Hiby and Schümmer (H8) that avoids the necessity of measuring the complete concentration profile. A pipe with a diameter smaller than the system, thus forming an annular region, is used at the sampling point. A mixed mean sample from the annular region is now sufficient to enable one to determine the radial dispersion coefficient. From Eq. (55) this concentration will be, for an annular region of dimensionless radius α ,

$$\begin{aligned}
 c_{\text{ann}} &= \frac{2}{1 - \alpha^2} \int_{\alpha}^1 rc \, dr \\
 &= 1 - \frac{2}{1 - \alpha^2} \sum_{a_i > 0} \frac{J_1(a_i e) J_1(a_i \alpha)}{J_0^2(a_i) q a_i^2} \frac{\alpha}{e} N_i
 \end{aligned} \quad (62)$$

This is the value for general boundary conditions, and it will reduce to the equations given by the above authors for each of their special cases.

d. Experimental Findings. Literature data on radial dispersion of numerous investigators is presented in Figs. 11 and 12. The data of almost

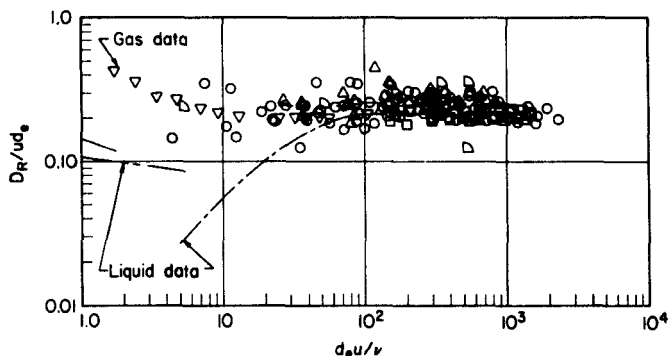


FIG. 11. Radial dispersion in packed beds, dispersed plug flow model. Adapted from (B13).

all the workers were obtained by a steady "point" source injection of tracer on the axis of the tube, with subsequent use of Eq. (59), (61), (56), and (57) to calculate the dispersion coefficients. We will discuss the results for each type of system separately.

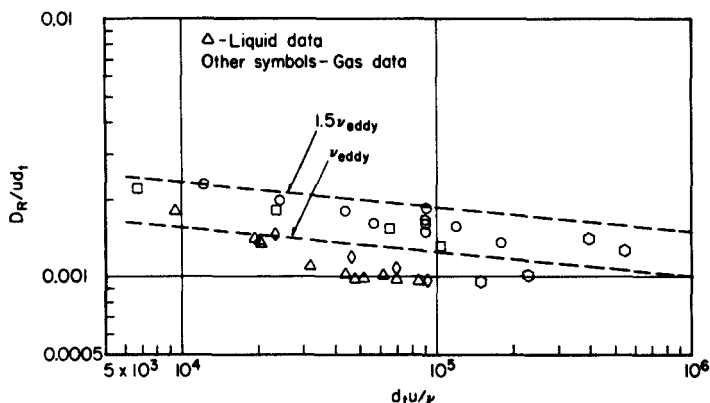


FIG. 12. Radial dispersion in pipes, dispersed plug flow model (B13).

(1) *Packed Beds*. Data on liquid systems using a steady point source of tracer and measurement of a concentration profile have been obtained by Bernard and Wilhelm (B6), Jacques and Vermeulen (J1), Latinen (L4), and Prausnitz (P9). Blackwell (B16) used the method of sampling from an annular region with the use of Eq. (62). Hartman *et al.* (H6) used a bed of ion-exchange resin through which a solution of one kind of ion flowed and another was steadily injected at a point source. After steady state conditions were attained, the flows were stopped and the total amount of injected ion determined. The radial dispersion coefficients can be determined from this information without having to measure detailed concentration profiles.

Data on gas systems, again using a point source, have been obtained by Bernard and Wilhelm (B6), Dorweiler and Fahien (D20), Fahien and Smith (F2), and Plautz and Johnstone (P6). Plautz and Johnstone measured dispersion coefficients under isothermal and nonisothermal conditions and found that there was a difference between the two only for low Reynolds numbers.

The data were plotted, as shown in Fig. 11, using the effective diameter of Eq. (50) as the characteristic length. For fully turbulent flow, the liquid and gas data join, although the two types of systems differ at lower Reynolds numbers. Rough estimates of radial dispersion coefficients from a random-walk theory to be discussed later also agree with the experimental data. There is not as much scatter in the data as there was with the axial data. This is probably partly due to the fact that a steady flow of tracer is quite easy to obtain experimentally, and so there were no gross injection difficulties as were present with the inputs used for axial dispersion coefficient measurement. In addition, end-effect errors are much smaller for radial measurements (B14). Thus, more experimentation needs to be done mainly in the range of low flow rates.

(2) *Turbulent Flow in Empty Tubes*. Figure 12 gives radial dispersion coefficient data for turbulent flow in empty tubes. The liquid data was obtained by Flint *et al.* (F5). Gas data is from Baldwin and Walsh (B1), Flint *et al.* (F5), Longwell and Weiss (L19), Mickelson (M11), Schlenger and Sage (S8), and Towle and Sherwood (T9). All of the above data was obtained by measuring concentration profiles in systems with a steady point source of tracer. Keyes (K4a) used a frequency-response experiment and interpreted his results in terms of a film thickness at the wall. Sherwood and Woertz (S14) and Dhanak (D19) have reported results for flow in rectangular channels.

The radial dispersion coefficient for this case is, of course, the average eddy diffusivity as discussed in works on turbulence (H9). If the various analogies between momentum, heat, and mass transport are used,

estimates of the eddy diffusivity can be obtained. However, we only show the directly measured mass-diffusion data in Fig. 12. There is a fair amount of scatter in the data which is probably caused by two main factors. Some of the investigators used large cumbersome injection systems which might have disturbed the flow, and some of the equipment might not have had an upstream section long enough to insure fully developed flow.

(3) *Laminar Flow in Empty Tubes.* As will be discussed in Section II, D_R , the radial coefficient for the dispersed-plug flow model for laminar flow is merely the molecular diffusivity.

4. General Dispersion Model for Symmetrical Pipe Flow

a. Discussion. As was stated previously, the general dispersion model is much more difficult to use since analytical solutions are not possible. Very little work has been done with these models, and it is entirely possible that the extra accuracy gained with this more complex model does not justify the great increase in the attendant computational difficulties. The only answer to this will be to test whether the simpler dispersion models are sufficient to characterize processing systems.

b. Experimental Findings. For turbulent flow in empty tubes, the problem is one of finding the radial variation of eddy diffusivity, which is discussed, for example, by Hinze (H9). Lynn *et al.* (L20) have presented data for air natural-gas systems. They utilized a relation similar to Eq. (13), but for a compressible fluid. We will illustrate their method with the steady-state form of the simpler Eq. (I-2) with no axial dispersion,

$$Ru(R) \frac{\partial C}{\partial X} = \frac{\partial}{\partial R} R D_R(R) \frac{\partial C}{\partial R} \quad (63)$$

If this equation is integrated once with respect to R and rearranged,

$$\begin{aligned} D_R(R) &= \frac{\int_0^R R' u(R') (\partial C / \partial X) dR'}{R (\partial C / \partial R)} \\ &= \frac{(\partial / \partial X) \int_0^R R' u(R') C dR'}{R (\partial C / \partial R)} \end{aligned} \quad (64)$$

The quantities in the numerator and denominator were directly calculated from the experimental concentration profile data. Some results for $D_R(R)$ are shown in Fig. 13. It is seen that the eddy diffusivity is relatively constant except near the walls. The values seem quite sensitive to the axial position where the concentration profile was measured; in other words, the system is not axially homogeneous. These results have been

discussed in more detail in a previous review by Opfell and Sage (O1).

Carrier (C11) has considered the case of a periodic input for laminar flow in an empty tube.

Fahien and Smith (F2) and Dorweiler and Fahien (D20) have considered the variation of D_R in packed beds, using a separation-of-variables technique to solve Eq. (63). The X -dependent part was solved analytically, and a set of difference equations was used to solve the R -dependent part. Details are given in (F1). The velocity profile data of Schwartz and Smith (S11) was used to calculate values of $D_R(R)$ in the packed column, typical results from Fahien and Smith (F2) being shown in Fig. 14. Dorweiler and Fahien's (D20) data, for a lower Rey-

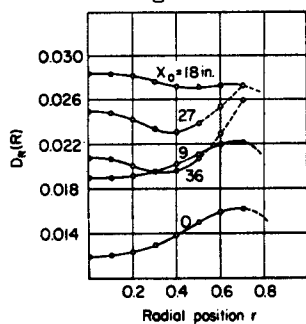


FIG. 13. Radial dispersion in pipes, general dispersion model (O1).

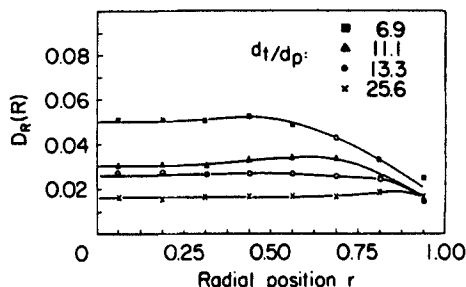


FIG. 14. Radial dispersion in packed beds, general dispersion model. Adapted from (F2).

nolds' number range, was similar. It is seen that for a sufficiently large ratio of tube-to-particle diameter, $D_R(R)$ is approximately constant over the radius. These findings suggest that if the dispersed plug-flow model does not satisfactorily represent the system and a more accurate model with varying velocity profile is needed, then the uniform dispersion model could be used.

D. RELATIONSHIPS BETWEEN DISPERSION MODELS

1. Preliminary

We have discussed methods for experimentally finding dispersion coefficients for the various classes of dispersion models. Although the models were treated completely separately, there are interrelations between them such that the simpler plug-flow models may be derived from the more complicated general models. Naturally, we would like to use the simplest possible model whenever possible. Conditions will be developed here for determining when it is justifiable to use a simpler plug-flow model rather than the more cumbersome general model.

2. Theoretical Deviations

Taylor (T2) and Westhaver (W5, W6, W7) have discussed the relationship between dispersion models. For laminar flow in round empty tubes, they showed that dispersion due to molecular diffusion and radial velocity variations may be represented by flow with a flat velocity profile equal to the actual mean velocity, u , and with an effective axial dispersion coefficient $D_L' = R_0^2 u^2 / 48 \mathfrak{D}$.³ However, in the analysis, Taylor ignored axial diffusion. Aris (A6) later showed that the true axial effect is additive and thus, more correctly, $D_L' = \mathfrak{D} + R_0^2 u^2 / 48 \mathfrak{D}$. Use of D_L' gives the same results as would be obtained from the more rigorous calculation involving radial and axial diffusion and true velocity profile, Eq. (I-2). Aris (A6) generalized the entire treatment to include all types of velocity distribution with any vessel geometry. He showed that the coefficient given as $1/48$ by Taylor is really a function of tube shape and velocity profile.

The mathematical method of Aris assumes a doubly infinite pipe (as does Taylor), with both the velocity distribution and the diffusion coefficients constant in the direction of flow. Hence in any real pipe, the length would have to be long enough so that the buildup of the velocity profile at the entrance would not invalidate the doubly infinite pipe assumption. Thus there are some practical restrictions on the method used by Aris.

Taylor (T4, T6), in two other articles, used the dispersed plug-flow model for turbulent flow, and Aris's treatment also included this case. Taylor and Aris both conclude that an effective axial-dispersion coefficient D_L' can again be used and that this coefficient is now a function of the well known Fanning friction factor. Tichacek *et al.* (T8) also considered turbulent flow, and found that D_L' was quite sensitive to variations in the velocity profile. Aris further used the method for dispersion in a two-phase system with transfer between phases (A11), for dispersion in flow through a tube with stagnant pockets (A10), and for flow with a pulsating velocity (A12). Hawthorn (H7) considered the temperature effect of viscosity on dispersion coefficients; he found that they can be altered by a factor of two in laminar flow, but that there is little effect for fully developed turbulent flow. Elder (E4) has considered open-channel flow and diffusion of discrete particles. Bischoff and Levenspiel (B14) extended Aris's theory to include a linear rate process, and used the results to construct comprehensive correlations of dispersion coefficients.

* Actually, Taylor originally suggested using this formula in reverse for obtaining diffusion coefficients. D_L' could be found simply from experimental data and then the formula could be used to obtain the diffusivity, \mathfrak{D} .

The most straightforward way of comparing the models would be to solve the partial differential equations for each case and compare the solutions. Because we cannot find these solutions in general, we must be satisfied with a comparison of the moments of the concentration distributions given by these models. This method is much used in theoretical statistics, and is useful since most distributions encountered are uniquely determined by their moments.

If we consider the variation of concentration along the axial direction as a "distribution" of concentration, we can calculate the moments for each model in terms of their respective parameters, and then compare the moments to find the relationship between parameters. Since we shall consider the concentration as a distribution function along the axis of the tube, the moments are with respect to axial distance, rather than with respect to time as used previously. Since flow in cylindrical vessels is so common, we will discuss only this case in detail. Aris (A6) gives the more general treatment in vessels of arbitrary cross section.

The moments are defined as:

$$M_k(\theta') = 2 \int_0^1 r dr \int_{-\infty}^{\infty} (x - \theta')^k C(x, r, \theta') d(x - \theta') \quad (65)$$

where subscript k indicates the moment order. Use of the variable $(x - \theta')$ relates the moments to a coordinate system that is moving with the mean speed of the flowing fluid. By using Eq. (65) with the mathematical representations of the various models, Eqs. (I-2), (I-3), (I-4), and (I-5), one obtains the following expressions for the moments. For details see Aris (A6) and Bischoff and Levenspiel (B14).

Axial-Dispersed Plug-Flow Model

$$M_0 = 1 \quad (66a)$$

$$M_1 = 0 \quad (66b)$$

$$M_2 = \frac{2\theta'}{P_L} \quad (66c)$$

Dispersed Plug-Flow Model

$$M_0 = 1 \quad (67a)$$

$$M_1 = 0 \quad (67b)$$

$$M_2 = \frac{2\theta'}{P_L} + O(\exp[-\lambda_1\theta'/P_R]) \quad (67c)$$

For large values of time (the "ultimate" value) M_2 reduces to

$$M_2 = \frac{2\theta'}{P_L} \quad (67d)$$

Uniform Dispersion Model

$$M_0 = 1 \quad (68a)$$

$$M_1 = \text{constant} \quad (68b)$$

$$M_2 = \frac{2\theta'}{P_{Lm}} + 2\theta'hP_{Rm}' + O(\exp[-\lambda_1\theta'/P_R]) \quad (68c)$$

For large values of time M_2 becomes

$$M_2 = \frac{2\theta'}{P_{Lm}} + 2\theta'h P_{Rm}' \quad (68d)$$

General Dispersion Model

$$M_0 = 1 \quad (69a)$$

$$M_1 = \text{constant} \quad (69b)$$

$$M_2 = \frac{2\theta'}{P_{Lm}} + 2\theta'h P_{Rm} + O(\exp[-\lambda_1\theta'/P_{Rm}]) \quad (69c)$$

For large values of time M_2 becomes

$$M_2 = \frac{2\theta'}{P_{Lm}} + 2\theta'h P_{Rm} \quad (69d)$$

In these equations,

$$h = 2 \int_0^1 \frac{dr}{rf_2(r)} \left\{ \int_0^r r' f_1(r') dr' \right\}^2 \quad (70)$$

and f_1 , f_2 , f_3 , D_{Rm} , and D_{Lm} are found from $u(R) = u(1 + f_1(R))$, $D_R(R) = D_{Rm}f_2(R)$, and $D_L(R) = D_{Lm}f_3(R)$. Also, λ_1 is the smallest of eigenvalues that arise during the solution of the partial differential equations for the moments. The various models are now related to each other by comparing the ultimate moments.

Zeroth Moments. The zeroth moment for each of the models is unity. From Eq. (65) the zeroth moment is defined as:

$$M_0 = 2 \int_0^1 r dr \int_{-\infty}^{\infty} C d(x - \theta') \quad (71)$$

This is merely the volume integral of the concentration over the entire vessel. Therefore, the value of unity indicates that the total amount of solute in the system is constant.

First Moments. For both of the dispersed plug-flow cases $M_1 = 0$. This means that the center of gravity of the solute moves with the mean speed of the flowing fluid. For the uniform and the general dispersion models, however, this is not always true. If the solute concentration is initially uniform over a cross-sectional plane, it can be shown (A6) that

the constants in Eqs. (68b) and (69b) are zero; thus, for this special case, the center of gravity of solute does move with the mean speed of flow. If the initial solute concentration is not uniform over a plane, however, the constants in Equations (68b) and (69b) are not zero, and the center of gravity of solute does not move with the mean speed of flow. However, if the initial distribution of solute is fairly uniform over the cross section, as is true in many practical cases, the constants in Eqs. (68b) and (69b) are small, and the first moments of the various models will all be approximately zero.

Second Moment. By equating the second moments of the different models we get the relationships sought between the parameters.

First, comparing Eqs. (66c) and (67d), we see that

$$P' = P_L \quad \text{or} \quad D_L' = D_L \quad (72)$$

Thus we may drop the primed notation on the coefficient for the axial-dispersed plug-flow model and identify this coefficient with the one for the dispersed plug-flow model.

Next we compare the dispersed plug-flow model with the general model by equating Eqs. (67d) and (69d). Thus, as found by Aris (A6),

$$\frac{1}{P_L} = \frac{1}{P_{Lm}} + hP_{Rm} \quad \text{or} \quad D_L = D_{Lm} + \frac{hu^2R_0^2}{D_{Rm}} \quad (73)$$

This equation enables us to calculate the value of P_L from the velocity profile using mean values of the coefficients of the general dispersion model. The constant radial coefficient used in the dispersed plug-flow model is the same as the mean value of the varying radial coefficient in the general dispersion model.

Finally by comparing Eqs. (68d) and (69d), we see that the constant coefficients of the uniform model are the same as the mean values in the general model, or

$$D_{Rm}' = D_{Rm} \quad (74)$$

and

$$D_{Lm}' = D_{Lm} \quad (75)$$

Summary. For all models with either constant or varying velocities we conclude that the constant *radial* coefficients are all alike and equal to the mean value of the varying coefficient, or

$$D_R = D_{Rm}' = D_{Rm} = \frac{2}{R_0^2} \int_0^{R_0} RD_R(R) dR = 2 \int_0^1 rD_R(r) dr \quad (76)$$

In addition, two distinct *axial* coefficients exist: those associated with models using mean velocities (plug-flow models) and those associated with models using a radial velocity profile. The reason for this difference

is that the plug-flow models incorporate in their dispersion coefficients the axial mixing resulting from velocity variations. The general model and the uniform model treat in separate terms the two phenomena responsible for axial dispersion. The equations (72) to (76) summarize the interrelationships between the parameters of the various dispersion models treated in Table I.

The concentration distributions of the dispersed plug-flow models at any time are "normal" (Gaussian), and Aris (A6) has shown that the general model with its larger number of parameters also approaches normality for large time. Hence, matching the first two moments is sufficient to compare distributions and relate parameters as was done above. However, the approach to normality in the general model is slow. Consequently, minor deviations between distributions will persist for some time even though the distributions are essentially similar.

3. *Experimental Verification of the Relationships*

Bischoff and Levenspiel (B14) present some calculations using existing experimental data to check the above predictions about the radial coefficients. For turbulent flow in empty tubes, the data of Lynn *et al.* (L20) were numerically averaged across the tube, and fair agreement found with the data of Fig. 12. The same was done for the packed-bed data of Dorweiler and Fahien (D20) using velocity profile data of Schwartz and Smith (S11), and then comparing with Fig. 11. Unfortunately, the scatter in the data precluded an accurate check of the predictions. In order to prove the relationships conclusively, more precise experimental work would be needed. Probably the best type of system for this would be one in laminar flow, since the radial and axial coefficients for the general dispersion model are definitely known; each is the molecular diffusivity.

Checks on the relationships between the axial coefficients were provided in empty tubes with laminar flow by Taylor (T2), Blackwell (B15), Bournia *et al.* (B19), and van Deemter, Broeder and Lauwerier (V3), and for turbulent flow by Taylor (T4) and Tichacek *et al.* (T8). The agreement of experiment and theory in all of these cases was satisfactory, except for the data of Bournia *et al.*; as discussed previously, their data indicated that the simple axial-dispersed plug-flow treatment may not be valid for laminar flow of gases. Tichacek *et al.* found that the theoretical calculations were extremely sensitive to the velocity profile. Converse (C20), and Bischoff and Levenspiel (B14) showed that rough agreement was also obtained in packed beds. Here, of course, the theoretical calculation was very approximate because of the scatter in packed-bed velocity-profile data.

4. Uses of the Relationships

The most important use of the relationship among models is in showing that the dispersed plug-flow models are good representations of the flow system under certain specified conditions. The relationships can also be used to predict the dispersed plug-flow coefficients from the general coefficients. We have shown how this is done for flow in empty tubes and the predictions are given by the dashed lines on Figs. 8, 10, and 12.

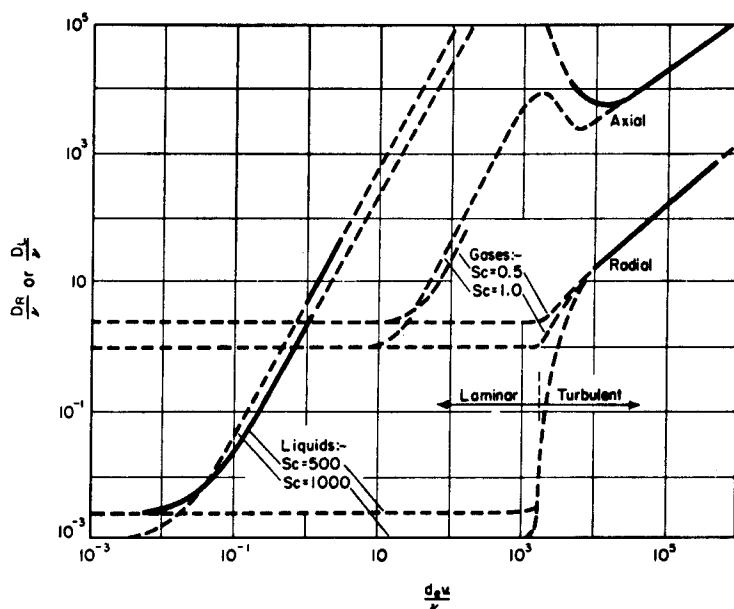


FIG. 15. Comprehensive picture of dispersion—empty tubes (B14).

For packed beds, the use of these equations for predictions is limited by inaccuracy in the velocity-profile data. Therefore, Bischoff and Levenspiel (B14) used the equations in a semiempirical way for interpolating between the existing data. The results are shown in Figs. 15 and 16, for both empty tubes and packed beds. The heavy lines show the regions of experimental data, and the dashed lines, the interpolations. For sufficiently low flow rates, the curves lead into the reciprocal Schmidt number (modified by a "tortuosity factor" in packed beds). The data of Blackwell (B16, B17) at very low flow rates seems to verify this. At high flow rates, liquids and gases show no differences because of the

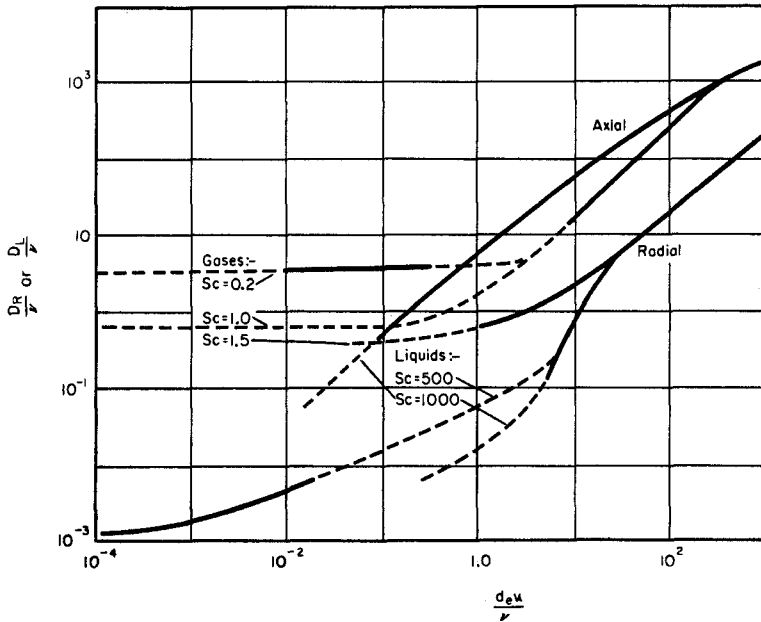


Fig. 16. Comprehensive picture of dispersion—packed beds (B14).

turbulent flow conditions. Figures 15 and 16 give a rather comprehensive picture of dispersion, and point out the areas in which there is a scarcity of experimental data.

5. Limitations of the Theory

When we used the “ultimate” values of the moments in Eqs. (67d), (68d), and (69d), this amounted to assuming that (B14),

$$O(\exp [-\lambda_1 \theta' / P_{Rm}]) < 1 \quad (77)$$

If a ratio of 10:1 is used in the inequality, and if an estimate is used for λ_1 , the limitation is,

$$\frac{t D_{Rm}}{R_0^2} > 0.16 \quad (78)$$

If the mean residence time of the fluid in the system, L/u , is used as a measure of the time, we finally obtain,

$$\frac{L}{d_t} > 0.04 \frac{u d_t}{D_{Rm}} \quad (79)$$

This is approximately the same as the criterion originally used by Taylor (T5) in his treatment of laminar flow. Using the values of D_{Rm} from the

preceeding correlations, the order of magnitude of the necessary length-to-diameter ratio needed for the dispersed plug-flow models to be valid in various types of systems is shown in Fig. 17. This is, of course, only an order of magnitude estimate and should not be relied upon for accurate values. It should be used only to give some sort of idea as to the types of systems where the dispersed plug flow models can be theoretically justified.

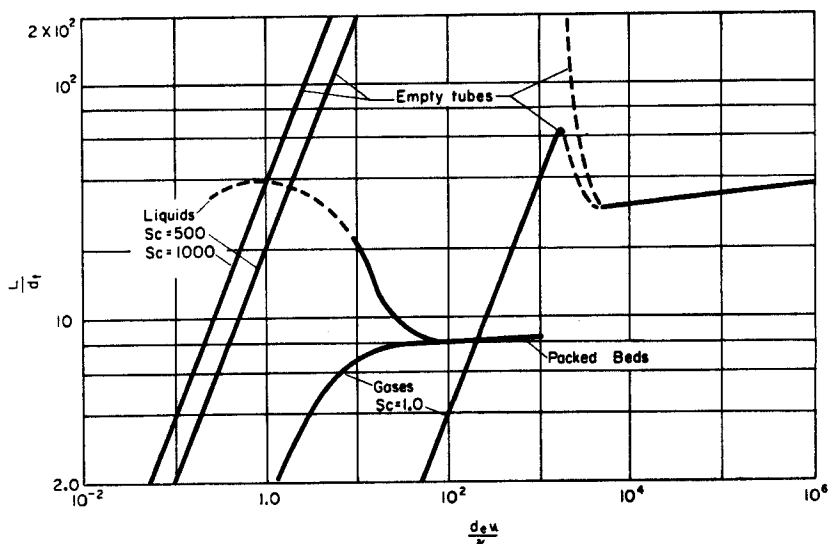


FIG. 17. Restrictions on length to diameter ratio for dispersed plug flow models to be valid (B14).

E. THEORETICAL METHODS FOR PREDICTING DISPERSION COEFFICIENTS

1. Introduction

If the theory of turbulence were complete enough, it would be possible to use it to predict the dispersion coefficients. Unfortunately, even for the simple case of homogeneous isotropic turbulence, this cannot yet be done. For cases of bounded flows in a real pipe and of flow through packed beds, the situation is even more discouraging. Nevertheless, several approximate estimates have given surprisingly good results as to the order of magnitude of the dispersion coefficients. For empty tube turbulence, which is a field in itself, we refer to Hinze (H9) and to a recent article by Roberts (R3). Here we will discuss the models for packed beds, but only very briefly.

2. Random-Walk Models

Since the random-walk approach is successful in molecular diffusion (K5) and Brownian motion studies (C14), it would seem that it might also be useful for the dispersion process. This has been considered by Baron (B2), Ranz (R1), Beran (B5), Scheidegger (S6), Latinen (L4) and more recently by de Josselin de Jong (D14) and Saffman (S1, S2, S3). The latter two did not strictly use random-walk since a completely random process was not assumed. Methods based on statistical mechanics have been proposed by Evans *et al.* (E7), Prager (P8), and Scheidegger (S7).

The sample random-walk analyses postulate that the mixing is caused by "splitting" or side-stepping of the fluid around the particles. Thus, by analogy with the mixing-length theories of turbulence, one might imagine that the mass flux would be proportional to the particle diameter and to the velocity,

$$D \propto u d_p \quad (80)$$

Baron (B2) has given a rather simple treatment for radial dispersion. Let us assume that as a fluid element approaches a particle, it is deflected by an amount $\pm \beta d_p$ where β is a fraction of the order of one-half. As the fluid element flows through the packing, this process keeps occurring. When the fluid element has travelled a distance, L , it has been deflected n times. The fluid element is deflected essentially each time it approaches a particle. Thus, $n = \alpha L/d_p$, where α is of the order of unity. If the deflections are random, the mean-square deviation is the sum of the squares of each deflection,

$$\overline{\Delta X^2} = n \beta^2 d_p^2 \quad (81)$$

If the Einstein equation for diffusion (H9) is used (which again assumes random motion), the dispersion coefficient may be approximated,

$$\overline{\Delta X^2} = 2Dt = n \beta^2 d_p^2 \quad (82)$$

where t is the diffusion time, and may be taken to be $t \simeq L/u$. Thus,

$$\begin{aligned} D &= \frac{n}{2} \beta^2 d_p^2 \frac{u}{L} \\ &= \frac{\alpha \beta^2}{2} d_p u \end{aligned} \quad (83)$$

If Eq. (83) is rearranged and the approximate numerical values of α and β substituted,

$$\frac{D}{u d_p} = \frac{\alpha \beta^2}{2} \simeq 0.1 \quad (84)$$

Comparison of this with the radial dispersion data of Fig. 11 for an average packed bed (using $d_e/d_p \simeq \epsilon = 0.38$) shows good agreement. Notice that Eq. (84) predicts that D/ud_p should be independent of flow rate. From Fig. 11, this is true for the larger Reynolds numbers of fully turbulent flow. At lower Reynolds numbers, the mixing would become less random, and so it would be expected that the theory would break down.

Prausnitz (P10) has devised an approximate mixing length model for estimating the axial dispersion coefficient that allows for the interaction of the velocity profile. He used

$$D_L = \Lambda_L \Lambda_R \frac{\partial u(R)}{\partial R} \quad (85)$$

where Λ_L is an axial and Λ_R is a radial scale of turbulence. From concentration fluctuation studies (to be discussed later), $\Lambda_R \simeq d_p/4$ and $\Lambda_L \simeq 7\Lambda_R$. If the velocity gradient is approximated by u/d_p , the mixing-length theory predicts

$$D_L \simeq \left(\frac{7}{4} d_p\right) \left(\frac{d_p}{4}\right) \frac{u}{d_p} = \frac{7}{16} u d_p$$

or

$$\frac{D_L}{u d_p} \simeq \frac{7}{16} \quad (86)$$

which is of the right order of magnitude (see Fig. 8).

Further details may be found in the above quoted references. In particular, de Josselin de Jong (D14) and Saffman (S1, S2, S3) give relatively rigorous developments that take into account the anisotropy caused by the flow. Thus different estimates are obtained for the dispersion coefficients depending on whether or not the direction considered is perpendicular or parallel to the mean flow.

3. The "Statistical" Models

These models picture the mixing process as consisting of "motion phases" and "rest phases." In a model proposed by Einstein (E3) and discussed by Jacques and Vermeulen (J1) and Cairns and Prausnitz (C5), it is assumed that the time represented by a motion phase is much less than that by a rest phase. For the packed bed, the motion phase might be taken as the period when the fluid element is passing through the restriction between particles, and the rest phase as the period when the fluid element is in the void space. If values are assigned to the probabilities of motion or rest, consideration of the geometry of the fluid elements' motions will lead to

$$p(X, t) dX dt = e^{-X-t} dX dt \quad (87)$$

as the probability density for any "jump" of the element (see Cairns (C1) for details). Consideration of a large number of "jumps" then yields

$$p_{\text{tot}} = e^{-X'-t'} I_0(2\sqrt{X't'}) \quad (88)$$

as the probability of finding all particles at relative position X' and at relative time t' that entered at time $t' = 0$. In other words, Eq. (88) gives the impulse response or **C** curve for the system. The relationship between the relative position, X' , and physical position, X , depends on the length of each step. Similarly, there is a relation between t' and t . Thus by comparing Eq. (88) with the solution of the axial-dispersed plug-flow model at very large X and t , it is found that

$$X' = \frac{Xu}{D_L} \quad \text{and} \quad t' = \frac{u^2 t}{D_L} \quad (89)$$

Thus Eq. (88) can be used to find the dispersion coefficient, and was used by Cairns and Prausnitz (C5) with a step input which corresponds to the time integral of Eq. (88). It would seem that the use of this model would involve problems similar to those for the ordinary dispersion models.

Giddings and Eyring (G2), Giddings (G1), and Klinkenberg (K10) have also proposed a model based on similar "rest-phase"—"motion phase" considerations. However, they used different assignments of the probabilities.

4. Turner's Structures

Turner (T14) has proposed two detailed models of packed beds which try to closely approximate the true physical picture. The first model considers channels of equal diameter and length but with stagnant pockets of various lengths opening into the channels. There is no flow into or out of these pockets, and all mass transfer occurs only by molecular diffusion. The second model considers a collection of channels of various lengths and diameters. We will briefly discuss each of these models, which are probably more representative of consolidated porous materials than packed unconsolidated beds.

a. Model I. It is assumed that the dispersion in the channel may be represented by an axial-dispersed plug-flow model,

$$D_L \frac{\partial^2 C}{\partial X^2} - u \frac{\partial C}{\partial X} - \frac{\partial C}{\partial t} - \sum_r \beta_r \frac{\partial q_r}{\partial t} = 0 \quad (90)$$

where D_L is the axial dispersion coefficient in the channel, β_r is the volume of stagnant pocket of length l_r per unit channel volume, and q_r

is the average concentration in the r th pocket. Turner originally took D_L to be the same as that for flow in a tube with no pockets, such as we have previously discussed. However, Aris (A10) showed that D_L is influenced by the pockets, and so this modified value should be used. In the pockets, ordinary molecular diffusion equation was assumed:

$$\mathfrak{D} \frac{\partial^2 C_r}{\partial X_r^2} = \frac{\partial C_r}{\partial t} \quad (91)$$

where C_r is the concentration in the r th pocket. The solution of Eq. (91) is used to find $\partial q_r / \partial t$, which is needed to solve Eq. (90).

For a periodic sinusoidal input of tracer, Turner (T14) showed how to find the values of l_r and β_r from the experimental data taken at different frequencies, ω . Aris (A9) generalized the model by taking $\beta(l)$ to be a continuous distribution of pocket volume rather than a set of discrete values, β_r . The problem of finding $\beta(l)$ then becomes one of solving the integral equation,

$$\mu(\omega') = \int_0^\infty \beta(l) \eta(\omega', l) dl \quad (92)$$

where

$$\begin{aligned} \omega' &= (\omega/2\mathfrak{D})^{1/2} \\ \mu(\omega') &= \text{function determined from amplitude ratio} \\ &\quad \text{and phase lag of experimental data.} \\ \eta(\omega', l) &= \frac{1}{2\omega' l} \frac{\sinh 2\omega' l - \sin 2\omega' l}{\cosh 2\omega' l + \cos 2\omega' l} \end{aligned}$$

Aris presented a graphical method for the solution of Eq. (92). If the integral were approximated by a sum, the equations used by Turner would be generated.

In a later paper, Turner (T15) used experimental data from apparatus with known β in order to see how the method would work. He found approximate agreement between the experimental and known β 's; quite accurate data would be needed to obtain good estimates of β .

b. Model II. It was again assumed that the dispersion in any one channel could be represented by the axial-dispersed plug-flow model, Eq. (90) with $\beta_r = 0$, since there were no pockets. He defined ϵ_{qr} as that part of the void fraction contributed by the channel of length l_r and radius r_q . Then, by a procedure similar to that used for Model I, a set of equations was developed for a sinusoidal input of tracer. For the measurement at the frequency ω_j ,

$$\mu_j = \sum_r \sum_q \epsilon_{qr} \eta_{qrj} \quad (93)$$

where

μ_j = function determined from amplitude ratio
and phase angle of experimental data

$$\eta_{qrj} = \left(\frac{r_g}{l_r}\right)^2 \exp \left[\frac{M l_r^2}{r_q^4} (1 - \sqrt{1 + \sqrt{1 + N_j^2 r_q^4 / M^4}}) \right] \\ \times \cos \left[\frac{M l_r^2}{r_q^4} \sqrt{\frac{\sqrt{1 + N_j^2 r_q^4 / M^4} - 1}{2}} \right]$$

$$M = 192 \mathfrak{D} \mu / p$$

$$N_j = 3072 \mathfrak{D} \mu^2 \omega_j / p$$

μ = viscosity of fluid

p = pressure drop

From Eqs. (93) the values of ϵ_{qr} could be found, similarly to solving the integral equation in Model I. Aris (A9) has also generalized this discrete model with circular channels to a continuous model with channels of any shape. Unfortunately, the equations for the continuous case can not easily be solved.

Even though the use of Turner's structures to represent packed beds may be too complex, the overall concept of utilizing frequency-response experiments to construct detailed models is very interesting and might find use for other situations.

5. Concentration Fluctuations

In order to get a more detailed picture of the processes occurring in flowing systems, several investigators have directly measured concentration fluctuations. The basic ideas were introduced by Taylor (T1) in a classic paper, and are discussed in detail in books on turbulence such as those by Hinze (H9) and Pai (P1).

The elements of Taylor's treatment are as follows. Consider a particle of fluid with turbulent velocity u in a homogeneous turbulent field. The distance that the fluid particle travels in time t is,

$$X(t) = \int_0^t u(t') dt' \quad (94)$$

Since the motion is supposed to be random, the value of $X(t)$ could be positive or negative with equal probability, and so the average for a large number of particles would be zero,

$$\overline{X}(t) = 0$$

However, the quantity, $\overline{X^2}$, which measures the spreading of the particles will not be zero:

$$\overline{X^2}(t) = \int_0^t dt_1 \int_0^t \overline{u(t_1)u(t_2)} dt_2 \quad (95)$$

If we introduce a Lagrangian correlation coefficient

$$R(s) = \frac{\overline{u(t)u(t+s)}}{\overline{u^2}} \quad (96)$$

Equation (95) becomes

$$\overline{X^2}(t) = \overline{u^2} \int_0^t dt_1 \int_0^t R(t_2 - t_1) dt_2 \quad (97a)$$

Kampé de Fériet (K1) showed that this can be changed to the form,

$$\overline{X^2}(t) = 2\overline{u^2} \int_0^t (t-s)R(s) ds \quad (97b)$$

For very short times, $R(s) \rightarrow 1$, and

$$\begin{aligned} \overline{X^2}(t) &= 2\overline{u^2} \int_0^t (t-s) ds \\ &= \overline{u^2} t^2 \end{aligned} \quad (98)$$

The dispersion is thus proportional to the square of the time. For very long times, $t \gg s$,

$$\begin{aligned} X^2(t) &\simeq 2\overline{u^2} t \int_0^\infty R(s) ds - 2\overline{u^2} \int_0^\infty sR(s) ds \\ &= 2\overline{u^2} \tau t + \text{constant} \end{aligned}$$

where the Lagrangian integral time scale is

$$\tau = \int_0^\infty R(s) ds \quad (99)$$

For long times, we see that the dispersion is proportional to the first power of time. The dispersion coefficient can be defined in a way similar to the Einstein equation for molecular diffusion,

$$\begin{aligned} D &= \frac{1}{2} \frac{d\overline{X^2}}{dt} \\ &= \overline{u^2} t \quad \text{short time} \end{aligned} \quad (100)$$

$$= \overline{u^2} \tau \quad \text{long time} \quad (101)$$

Thus, the dispersion coefficient can be taken as a constant only for long times. This, of course, would mean that the dispersion-type models would only be valid for long diffusion times.

Unfortunately the correlation coefficient $R(s)$ can not be predicted at the present time, although empirical relationships have been used. This means that Eq. (98) is limited to use for the short and long diffusion

times already discussed, and it is not very useful for the intermediate (and interesting) time ranges. Thus, other methods are necessary for determining the dispersion coefficients.

Direct measurement of concentration fluctuations for liquid flow in packed and fluidized beds have been made by Hanratty *et al.* (H4), Prausnitz and Wilhelm (P12), Cairns (C1), and Cairns and Prausnitz (C4). Detailed descriptions of electrical conductivity probes used for measurement of these fluctuations have been given by Prausnitz and Wilhelm (P11) and Lamb *et al.* (L1).

A concentration-fluctuation correlation coefficient, similar to that proposed by Danckwerts (D3, D5), may be defined,

$$R_C = \frac{\overline{C_1' C_2'}}{\sqrt{(\overline{C_1'})^2} \sqrt{(\overline{C_2'})^2}} \quad (102)$$

where C_1' , C_2' are the concentration fluctuations at points 1 and 2.

This correlation coefficient has properties similar to the one defined by Eq. (96). In particular, a scale of concentration fluctuation may be defined as

$$\lambda = \int_0^\infty |R_C| d\rho \quad (103)$$

where ρ is the distance between points 1 and 2. This scale is used as a measure of the order of magnitude of the size of a particle of fluid that has a uniform concentration. In other words, fluid particles of this size are approximately homogeneous in character. A length scale of radial turbulent diffusion may be defined by

$$D_R = \Lambda_R \sqrt{u^2} \quad (104)$$

In terms of the Lagrangian integral time scale, Eq. (99), we find

$$\Lambda_R = \tau \sqrt{u^2} \quad (105)$$

These various scales, along with the intensity, or strength, of the concentration fluctuations,

$$\sqrt{(\overline{C'})^2} / \bar{C} \quad (106)$$

can be used as a means of characterizing the mixing.

The detailed fluctuation data for packed beds can be found in Prausnitz and Wilhelm (P12). They found that the fluctuation intensity was directly proportional to the radial position in the bed except at the center and near the tube wall. The magnitude of the intensity was of the order of 8%. The radial scale, Λ_R , was found to be about one fourth of a particle diameter. An estimate was made for an axial scale, Λ_L , and it was found that approximately,

$$\Lambda_L \simeq 7\Lambda_R \quad (107)$$

It was also found that for fully developed turbulent flow the above values were essentially independent of the Reynolds number.

The mixing in fluidized beds is somewhat more complicated, as might be expected. The over-all results found by the previously mentioned authors are summarized by Cairns and Prausnitz (C4):

- “(1) The mixing properties in a fluidized bed are a strong function of the fraction voids. Minimum values of radial Peclet numbers (ud_p/D_R) are observed at $\epsilon = 0.7$, corresponding to a transition in the type of particle circulation in the bed.
- (2) The packing particle density and fraction voids strongly affect the radial scale of turbulence (Λ_R); larger scales are found for beds containing denser particles at a given fraction voids. The scale of turbulence has a maximum value at $\epsilon = 0.7$.
- (3) The root-mean-square value of the radial velocity fluctuation $[(C')^2]^{1/2}/C$ varies only slightly with fraction voids and appears to be independent of particle density.
- (4) The scale of concentration fluctuation (λ) is affected by the fraction voids in the same manner as the scale of turbulence, but it is not greatly influenced by the particle density. The scales of concentration fluctuation show that there are isoconcentration eddies several times the size of a packing particle.”

The above concentration fluctuation information should aid in the fundamental description of mixing in packed beds and fluidized beds. Exactly how this information should be used in designing such systems must be the subject of further research.

III. Tanks-in-Series or Mixing-Cell Models

A. INTRODUCTION

In the preceding section we discussed the dispersion model which can account for small deviations from plug flow. It happens that a series of perfectly mixed tanks (backmix flow) will give tracer response curves that are somewhat similar in shape to those found from the dispersion model. Thus, either type of model could be used to correlate experimental tracer data.

A perfectly mixed tank can also be used, of course, to represent a real stirred tank. Since the patterns of flow in many real stirred tanks are rather complicated, more complex models are often required. This whole topic will be discussed in Section IV on combined models. Thus we will only discuss here the use of a series of perfectly mixed tanks to

represent other types of flow systems, in particular those which deviate only slightly from plug flow.

B. MATHEMATICAL DESCRIPTION

First we must derive the equations for the perfectly stirred tanks. In these ideal tanks, it is assumed that the entire contents have the same composition as the outlet stream. Thus the C curve, or the response to a pulse input, can be found quite easily by a material balance.

(material in) = (material out) + (accumulation of material in tank)

$$C^0 V \delta(t) = vC + V \frac{dC}{dt} \quad (108)$$

where C^0 is the initial concentration of the pulse of tracer in the perfectly mixed stirred tank. For a j -tank system, to be considered next, C^0 is the average concentration of tracer if evenly distributed in the j -tank system. In dimensionless form, Eq. (108) becomes

$$\delta(\theta) = c + \frac{dc}{d\theta} \quad (109)$$

where

$$\theta = \frac{t}{\bar{t}} = \frac{tv}{V} \quad (2)$$

and

$$c = C/C^0$$

Equation (109) can easily be solved using Laplace transforms with the result,

$$c = C = e^{-\theta} \quad (110)$$

1. One-Dimensional Array

The preceding results can easily be generalized to j perfectly mixed tanks in series. This has been discussed by many authors: Ham and Coe (H2), MacMullin and Weber (M2, M3), Mason and Piret (M5), Kandiner (K2), Katz (K3) and Young (Y3). Other authors have dealt with stirred tanks specifically for use as chemical reactors, and these will be discussed later. The material balance around the i th tank then becomes

$$vC_{i-1} = vC_i + V_i \frac{dC_i}{dt} \quad (111)$$

where V_i is the volume of the i th tank. For simplicity, we will only deal with the case where all the tanks have the same volume, V_i . The more general case of unequal-sized tanks is discussed, for example, by Mason and Piret (M5).

The **C** curve, or pulse response, may be found by solving the set of Eqs. (111) for $i = 1, 2, 3, \dots, j$ with the condition that the input to the first tank, $i = 1$, is a delta function of tracer. In other words the conditions on Eq. (111) are

$$C_{i \neq 0}(0) = 0 \quad \text{and} \quad C_{i=0} = C^0 \frac{V}{v} \delta(t)$$

where V = total volume of the j -tank system. Equations (111) can again be solved by the Laplace transform, as follows:

$$pV_i \bar{C}_i + v \bar{C}_i = v \bar{C}_{i-1}$$

where \bar{C}_i is the transform of C_i . Then,

$$\begin{aligned} \bar{C}_j &= \frac{\bar{C}_{j-1}}{p \frac{V_i}{v} + 1} \\ &= \frac{\bar{C}_{j-2}}{\left(p \frac{V_i}{v} + 1\right)^2} \\ &= \frac{\bar{C}_0}{\left(p \frac{V_i}{v} + 1\right)^j} \\ &= \frac{C^0(V/v)}{\left(p \frac{V_i}{v} + 1\right)^j} \end{aligned} \quad (112)$$

The inverse transform of Eq. (112) is

$$C_j = \frac{C^0}{(j-1)!} \frac{V}{V_i} \left(\frac{tv}{V_i}\right)^{j-1} e^{-tv/V_i} \quad (113)$$

The total volume of the system is

$$V = jV_i$$

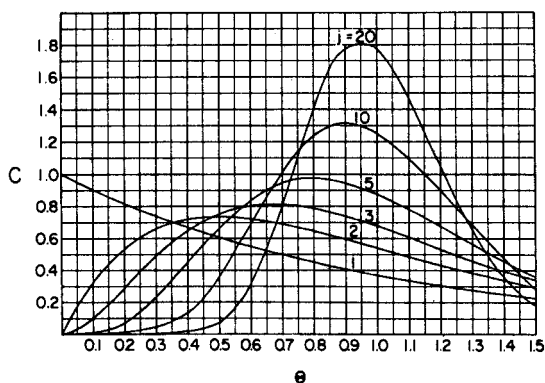
so that

$$\bar{t} = \frac{V}{v} = j \frac{V_i}{v}$$

Thus Eq. (113) may be written in dimensionless form

$$c_j = \frac{j^j}{(j-1)!} \theta^{j-1} e^{-j\theta} \quad (114)$$

Equation (114) is the **C** curve for a series of j stirred tanks, and is shown in Fig. 18. It has roughly the same shape as the **C** curve of the dispersion model. This relationship will be further considered later.

FIG. 18. **C** curve for tanks in series model.

As was done with the dispersion models, the mean and the variance can be found either directly from Eq. (114) or from the Laplace transform, Eq. (112). The results are,

$$\mu_1 = 1 \quad (115)$$

$$\sigma^2 = \frac{1}{j} \quad (116)$$

Thus, similarly to the dispersion model, the experimental **C** curve data could be used to determine a variance, σ^2 , and then Eq. (116) used to find j .

If a perfect delta function input is not possible, a method can again be devised utilizing two measurement points to find the parameter, j , of this model. Consider the experimental set up of Fig. 19. The concentra-

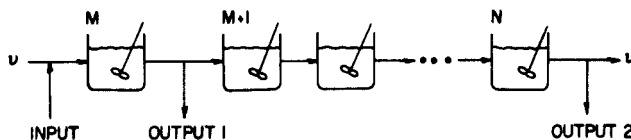


FIG. 19. Determination of tanks-in-series model parameter by two-measurement method.

tion of tracer is measured both entering the $(M + 1)$ th tank (or leaving the M th tank) and leaving the N th tank, and let j now be the number of tanks in the experimental region which is between these two measurement points, or $j = N - M$. The injection is upstream of both tanks. Now Eq. (111) can be used for any tank i between these measurement points giving,

$$V_i \frac{dC_i}{dt} + vC_i = vC_{i-1} \quad (117)$$

with boundary conditions

$$C_{i>M}(0) = 0 \quad \text{and} \quad C_i(t)|_{i=M} = C_M(t)$$

The algebraic manipulations will be easier to follow if Eq. (117) is changed to dimensionless form. Define,

$$\begin{aligned} V &= \text{volume of } j\text{-tank experimental section} \\ &= V_{M+1} + V_{M+2} + \cdots + V_N \\ &= jV_i \end{aligned}$$

$$\theta = \frac{t}{\bar{t}} = \frac{tv}{V}$$

$$\bar{t} = \frac{V}{v} = \text{mean residence time in the } j\text{-tank experimental section}$$

$$c = \frac{C}{C^0}$$

C^0 = average concentration of all entering tracer if evenly distributed in the j -tank experimental section

Then Eq. (117) becomes for the N th tank

$$\frac{1}{j} \frac{dc_N}{d\theta} + c_N = c_{N-1} \quad (118)$$

Solving Eq. (118) by Laplace transforms,

$$\begin{aligned} \bar{c}_N &= \frac{\bar{c}_{N-1}}{\left(\frac{p}{j} + 1\right)} \\ &= \frac{\bar{c}_{N-2}}{\left(\frac{p}{j} + 1\right)^2} \\ &= \frac{\bar{c}_M}{\left(\frac{p}{j} + 1\right)^j} \end{aligned} \quad (119)$$

Now if Eq. (119) is manipulated in exactly the same way as that used for the dispersion model by Aris (A8), Bischoff (B11), and Bischoff and Levenspiel (B14) (Section II,2,c), the following relationships are found:

$$\Delta\mu_1 = \mu_{1N} - \mu_{1M} = 1 \quad (120)$$

$$\Delta\sigma^2 = \sigma_N^2 - \sigma_M^2 = \frac{1}{N - M} = \frac{1}{j} \quad (121)$$

Thus if an imperfect delta function is injected into a system and the mean and variance measured at two measurement locations, the tanks-in-series model can also be used to interpret the results.

There would seem to be little reason for using the tanks-in-series model for flow in empty tubes, since little correspondence exists between the physical picture and the model. However, Coste *et al.* (C22) found recently that a system with mass and heat dispersion combined with chemical reaction was easier to handle with this model than with the dispersion model. On the other hand, Carberry and Wendel (C8) have solved a similar problem with the dispersion-model by a finite-difference technique different from the one used by Coste *et al.*, and found no difficulties. Thus the question of which model is best computationally is still not answered.

The use of the tanks-in-series model for packed beds can be more strongly justified. The fluid can be visualized as moving from one void space to another through the restrictions between particles. If the fluid in each void space were perfectly mixed, the mixing could be represented by a series of stirred tanks each with a size the order of magnitude of the particle. This has been discussed in detail by Aris and Amundson (A14). The fluid in the void spaces is not perfectly mixed, and so an "efficiency" of mixing in the void spaces has to be introduced (C6). This means that the analogy is somewhat spoiled and the model loses some of its attractiveness. In laminar flow the tanks-in-series model may be still less applicable.

2. Three-Dimensional Array

We have discussed the tanks-in-series model in the sense that the composition in the system was constant over a cross-section. Recently Deans and Lapidus (D12) devised a three-dimensional array of stirred tanks, called a finite-stage model, that was able to take radial as well as axial mixing into account. Because of the symmetry, only a two-dimensional array is needed if the stirred tanks are chosen of different sizes across the radius and are properly weighted. By a geometrical argument, Deans and Lapidus arrived at the following equation for the (i, j) tank:

$$\frac{dC_{i,j}}{dt} + C_{i,j} = \varphi_{i-1,j} \quad (122)$$

where

$$\varphi_{i-1,j} = \frac{(j - \frac{3}{4})C_{i-1,j-1/2} + (j - \frac{1}{4})C_{i-1,j+1/2}}{(2j - 1)}$$

with boundary conditions,

$$\begin{aligned} C_{i,j} &= C_0 && \text{(initial condition)} \\ C_{0,j} &= C' && \text{(inlet to bed)} \end{aligned}$$

By choosing the stirred-tank size about the same as a particle in the packed bed, Eq. (122) will reproduce experimental mixing data. This is similar, of course, to what was found for the one-dimensional case previously discussed.

The reason for constructing this rather complex model was that even though the mathematical equations may be easily set up using the dispersion model, the numerical solutions are quite involved and time consuming. Deans and Lapidus were actually concerned with the more complicated case of mass and heat dispersion with chemical reactions. For this case, the dispersion model yields a set of coupled nonlinear partial differential equations whose solution is quite formidable. The finite-stage model yields a set of differential-double-difference equations. These are ordinary differential equations, which are easier to solve than the partial differential equations of the dispersion model. The stirred-tank equations are of an initial-value type rather than the boundary-value type given by the dispersion model, and this fact also simplifies the numerical work.

Thus, it would seem that calculations using the finite-stage model might be easier than with the dispersion model. However, it has been found by Schechter and Wissler (S5) that the set of difference equations used in the finite-stage model are equivalent to one of the sets of possible difference equations that could be used to solve numerically the partial differential equations of the dispersion model. Looking at the finite-stage model equations from the numerical-analysis point of view, it is seen that the finite-difference mesh size is dictated by the particle size and the experimental value of the dispersion coefficient that is to be simulated. This lack of flexibility could conceivably cause inaccuracies in the calculated results. A further problem when the finite-stage model is used for simultaneous mass and heat dispersion is that the magnitudes of the two types of dispersion must be taken to be equal, since they are both fixed by the same mesh size.

Thus, we conclude that the computational effort required will be approximately the same for either model. On the one hand the finite-stage model is somewhat inflexible as indicated above, but on the other hand it might be superior to the dispersion model in systems with large particles where the continuum approach of the dispersion model would probably not be appropriate. On the whole, more work is needed to determine the practicality of the various computation methods.

C. COMPARISON WITH DISPERSION MODEL

Since both the tanks-in-series model and the dispersion model give about the same shape of **C** curve, the question arises as to how similar

are the predictions of the two models. There are several methods to compare the two. One method uses variances. Kramers and Alberda (K14) used the variance for the doubly infinite dispersion model, which from Section II, C, 2,b is,

$$\sigma^2 \simeq 2 \left(\frac{D_L}{uL} \right) \quad (123)$$

Using this with Eq. (116) gives

$$\frac{1}{j} = 2 \left(\frac{D_L}{uL} \right) \quad (124)$$

Unfortunately, Eq. (124) does not extrapolate to $j = 1$ as $D_L \rightarrow \infty$. Therefore, Kramers and Alberda suggested using

$$\frac{1}{j-1} = 2 \left(\frac{D_L}{uL} \right) \quad (125)$$

This expression extrapolates correctly, and is approximately the same as Eq. (124) for large j , say $j > 10$.

Levenspiel (L13a) later showed that the reason for the incorrect extrapolation of Eq. (124) was that the doubly infinite vessel was not the proper one to use for the comparison. Instead, the closed vessel (plug flow into and out of the vessel) must be used. The expression for the variance can be found from van der Laan (V4), and when combined with Eq. (116) gives

$$\frac{1}{j} = 2 \left(\frac{D_L}{uL} \right) - 2 \left(\frac{D_L}{uL} \right) [1 - e^{-uL/D_L}] \quad (126)$$

Equation (126) does extrapolate properly to $j = 1$ for $D_L \rightarrow \infty$. For small D_L/uL (large j) it approaches Eq. (124).

We also notice, from either Eq. (124) or Eq. (126), that $j \rightarrow \infty$ as $D_L \rightarrow 0$. This is the basis for the statement that an infinite number of stirred tanks in series is the equivalent to plug flow.

Trambouze (T10) suggests two alternate methods of comparison. By matching the **C** curve maxima for these two models, he showed that

$$\frac{D_L}{uL} = \frac{(2j-1)^2}{2j(j-1)(4j-1)} \quad (127)$$

and by matching the **C** curves at $\theta = 1$ he obtained

$$\left[\left(\frac{uL}{D_L} \right)^2 + 2 \left(\frac{uL}{D_L} \right) - \frac{3}{4} \right] = \frac{2j}{(1 + 1/2j)^2} \quad (128)$$

Both equations extrapolate properly for $D_L/uL \rightarrow 0$, but only Eq. (127) gives $j = 1$ for $D_L/uL = \infty$. Equation (127) also reduces to Eq. (124) for small D_L/uL (large j).

From the above it is seen that there is no unique way of matching the two models. This conclusion is strengthened when chemical reactions are considered because the comparisons for each reaction type and degree of conversion are different, and none of them is the same as the comparison obtained from matching tracer curves. An illustration of the different methods of comparison is given in Fig. 30.

As a means of choosing between models it has been suggested that some of the higher moments of the *C* curve could be used. The skewedness, or third moment, of either the dispersion or tanks-in-series model is uniquely determined by the value of the dispersion coefficient or the number of tanks. Thus, the parameter is determined from the second moment and then used to calculate the third moment. This is compared with the third moment computed from the experimental data; whichever model has the closest third moment would be chosen. Unfortunately, this method has two drawbacks that severely limit its usefulness. One is that experimental data is not good enough to give meaningful third moments. The other is that the third moments as calculated from the different models have almost the same values, as was shown by van Deemter (V2).

As mentioned when discussing the three-dimensional finite-stage model, by a proper choice of the stage size, experimental dispersion data may be simulated as discussed previously for packed beds. Aris and Amundson (A14) originally showed that by taking the size of the individual stirred tanks equal to one particle diameter, the value $D_L/ud_p = 0.5$ can be reproduced. Inspection of Fig. 8 shows this to be a rough estimate of the value found from experiment. Deans and Lapidus (D12) found that for the same size of stirred tanks, the value $D_R/ud_p = 1/8$ can be reproduced. Inspection of Fig. 11 shows that this also is a reasonable estimate of the experimental data. By using a finite-stage size other than exactly one particle diameter, other values of the dispersion groups may be generated.

In conclusion then, it would seem that for small deviations from plug flow, both the dispersion and the tanks-in-series models will give satisfactory results. Up to the present, which one is used may be largely a matter of personal preference.

IV. Combined Models

A. INTRODUCTION

When the gross flow pattern of fluid deviates greatly from plug flow because of channeling or recirculation of fluid, eddies in odd corners, etc., then the dispersion model or the tanks-in-series model can not satisfactorily characterize flow in the vessel. This type of flow can be found,

for example, in industrial stirred-tank reactors, shell-and-tube heat exchangers, and in fluidized beds. In these situations it is probably most fruitful to view the real vessel to consist of interconnected flow regions with various modes of flow between and around these regions. Models such as these can be called *combined* or *mixed models*.

The following kinds of regions are used in the construction of combined models:

- Plug flow regions,*
- Backmix flow regions,*
- Dispersed plug-flow regions,*
- Deadwater regions.*

The last-mentioned region accounts for the portion of fluid in the vessel which is relatively slow moving and, for practical purposes, stagnant. As we shall see, there are two ways to deal with deadwater regions: to assume their contents to be completely stagnant or to view a slow interchange of their contents with the fluid passing through the vessel. In the first approach the treatment is quite simple; the second approach more closely approximates real situations but requires quite involved analyses.

In addition to these regimes, combined models may use the following kinds of flow:

- Bypass flow*, where a portion of the fluid bypasses the vessel or a particular flow region,

- Recycle flow*, where a portion of the fluid leaving the vessel or leaving a flow region is recirculated and returned to mix with fresh fluid,

- Cross flow*, where interchange, but no net flow, of fluid occurs between different flow regions.

With these as the components of combined models the problem then is to find the volumes of the various regions and the rate of each type of flow occurring such that the response curves of the model match as closely as possible the response curves for the real vessel.

B. DEFINITION OF DEADWATER REGIONS

1. *Completely Stagnant*

In attempting to represent flow in a real vessel by combined models containing completely stagnant fluid, we meet with difficulties. For example the existence of completely stagnant fluid cannot be reconciled with the assumption of steady flow through the vessel. Again, with this definition the mean age of the vessel contents would not be useful in matching models because even if a deadwater region consisted of only

one molecule, the calculated mean age of the vessel would still be infinite.

The following definition of deadwater regions by Levenspiel (L12) overcomes these difficulties while still maintaining a concept of these regions which is useful in matching models with real situations.

"In a vessel the deadwater regions are the relatively slow moving portions of the fluid which we chose to consider to be completely stagnant. Deadwater regions contribute to the vessel volume; however we ignore these regions in determining the various age distributions."

The cutoff point in residence time between what we chose to consider as active and as stagnant fluid depends on the accuracy of predictions of vessel performance. In most cases material which stays in a vessel twice the mean residence time can, with negligible error, be taken as stagnant.

2. *Slow Cross Flow*

Instead of considering fluid in deadwater regions to be completely stagnant, an alternate view considers that there is a slow interchange or cross flow between the fluid in these regions and the active fluid passing through the vessel. With this approach Adler and Hovorka (A2) treated the combined model shown in Fig. 20. This consists of j identical units

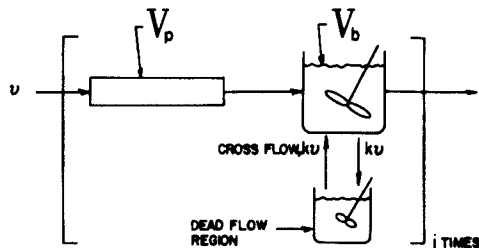


FIG. 20. Combined model used by Adler and Hovorka (A2).

in series, each of which contains a plug flow, a backmix and a deadwater region. The deadwater region is viewed to be in backmix flow and to be interchanging fluid slowly with the active backmix flow region. This model has four parameters; the cross flow rate, the number of units in series, and two parameters for the ratio of sizes of the three types of regions. The procedure developed for determining the model's parameters is as follows:

- (1) From the experimental **C** curve find when tracer just appears (where the **C** curve just rises from zero) and also locate the maximum of this curve.

- (2) Specially prepared charts for different integral j then give sets

of parameter values, one for each j , consistent with the above **C** curve findings.

(3) The tracer curves for these different j are then matched with the experimental **C** curve to select the curve of best fit with its corresponding set of parameters.

This fitting procedure is designed to match closely the critical part (the early section) of the tracer curve, hence the predictions of this model should correspond to actual performance. This model is quite flexible in that it is capable of fitting extremely skewed age distributions. Its disadvantage when compared with the simpler combined models employing completely stagnant regions is that the third step of the matching procedure necessitates the use of computers.

In a model for the structure of packed beds, Turner (T14, T15) and Aris (A9, A10) have also used stagnant pockets with crossflow by only molecular diffusion.

C. MATCHING COMBINED MODELS TO EXPERIMENT

The following suggestions may be helpful in searching for and devising flow models to fit given experimental response curves. This section has particular application to models which employ the simple stagnant-fluid definition of deadwater regions. The matching procedure for the particular model of Adler and Hovorka has already been outlined.

1. *Existence of Deadwater Regions.*

Select a reasonable cutoff point, say $\theta = 2$, then find the mean of the **C** curve up to that point. If no deadwater regions are present, then

$$\bar{\theta}_C = \frac{\text{measured } \bar{t}_C}{V/v} \simeq 1$$

If deadwater regions are present, then

$$\bar{\theta}_C < 1$$

The fraction of vessel consisting of deadwater regions is given by the deviation of $\bar{\theta}_C$ from unity. Hence with V_d as the volume of deadwater region, and with v_d/v as the fraction of active fluid as given by the area of the **C** curve up to the cutoff point,

$$\bar{\theta}_C = \frac{\bar{t}_C}{\bar{t}} = \frac{V_d/v_d}{V/v} \quad \text{or} \quad \frac{V_d}{v} = 1 - \bar{\theta}_C \frac{v_d}{v} \quad (129)$$

Danckwerts (D9) discusses this type of method for finding the location of stagnant regions in systems. Alternatively the area under the **I** curve will give the dead volume. Figure 21 summarizes these results.

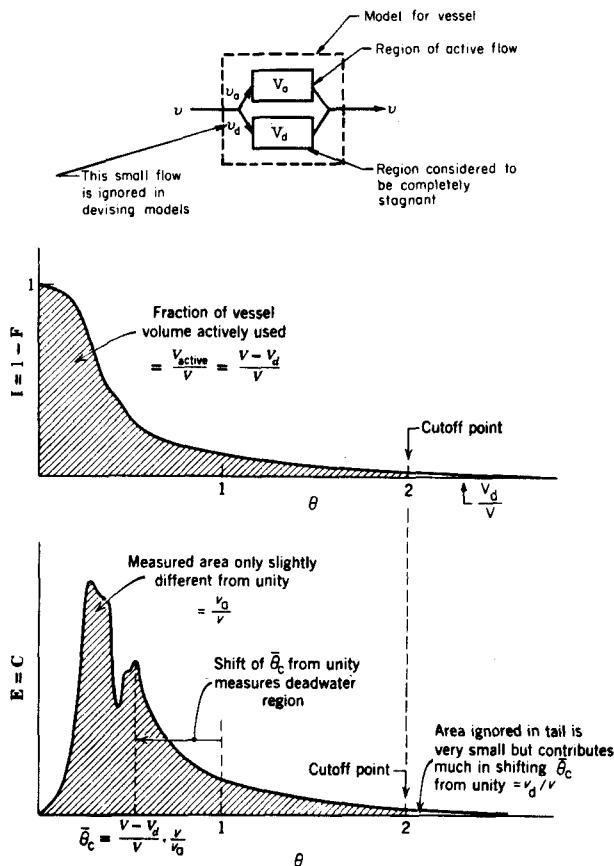


FIG. 21. Particular features of age distribution curves for combined models which include deadwater regions. Adapted from (L13).

2. Existence of Bypass Flow

In bypass flow we may look at the incoming fluid as splitting into two parallel streams, the fraction passing through the vessel being v_1 , the fraction bypassing it instantaneously being v_2 . Figure 22 shows characteristics of typical response curves when bypass flow occurs. From the rapid initial drop in the I curve, the shift in mean value for the main portion of the E curve, or from the area of the main portion of the E curve the magnitude of such short-circuiting can be estimated. Probably the role of bypass flow can be evaluated more easily from F or I curves than from the C or E curves.

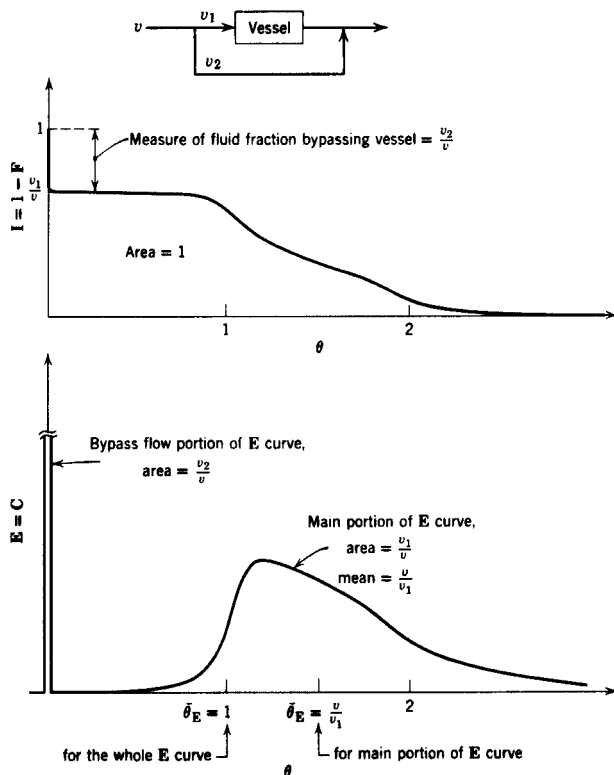


FIG. 22. Particular features of age distribution curves for models which include bypassing of fluid (L13).

3. Regions in Series

For flow regions 1, 2, . . . connected in series the mean age of vessel contents is

$$\bar{t}_I = \bar{t}_{I,1} \frac{V_1}{V} + (\bar{t}_{E,1} + \bar{t}_{I,2}) \frac{V_2}{V} + (\bar{t}_{E,1} + \bar{t}_{E,2} + \bar{t}_{I,3}) \frac{V_3}{V} + \dots \quad (130)$$

while the mean age of fluid in the exit stream is

$$\bar{t}_E = \bar{t}_{E,1} + \bar{t}_{E,2} + \dots \quad (131)$$

Here V_1, V_2, \dots refer only to the active volumes,

V refers to the total vessel volume including deadwater regions

$\bar{t}_1, \bar{t}_2, \dots$ refer to the separately measured mean time for the flow regions 1, 2, . . .

4. Regions in Parallel

For flow regions 1, 2, . . . connected in parallel the mean age of vessel contents is

$$\bar{t}_I = \bar{t}_{I,1} \frac{v_1}{v} + \bar{t}_{I,2} \frac{v_2}{v} + \dots \quad (132)$$

while the mean age of fluid in the exit stream is

$$\bar{t}_E = \frac{V_1 + V_2 + \dots}{v} \quad (133)$$

5. Number of Parameters in a Model

The number of parameters used in a model is an indication of its flexibility in fitting a wide variety of situations, and in addition suggests, to some extent, the complexity of the accompanying mathematics. With more and more parameters, the models are able to fit a wider variety of conditions. However, we must balance this gain against the unwieldiness of the accompanying mathematics as well as the possibility that such a model may have very little correspondence with fact. The latter is a serious objection because an unrealistic many-parameter model may closely fit all present data "after the fact," but may be quite unreliable for prediction in new untried situations. Hence, in fitting a real situation, we should aim for the simplest model which fits the facts and whose various regions are suggested by the real vessel. This way the parameters of the model have physical meaning and may be predicted by independent methods. This question is of especial concern in fitting models to fluidized beds.

The tanks-in-series and dispersion models are one-parameter models. In general, the number of parameters in a combined model is

$$\begin{aligned} \left(\begin{array}{c} \text{number of} \\ \text{parameters} \end{array} \right) &= \sum \left(\begin{array}{c} \text{flow regions in} \\ \text{excess of one} \end{array} \right) + \sum \left(\begin{array}{c} \text{flow paths in} \\ \text{excess of one} \end{array} \right) \\ &\quad + \sum \left(\begin{array}{c} \text{zones of} \\ \text{cross flow} \end{array} \right) + \sum \left(\begin{array}{c} \text{flow regions} \\ \text{with dispersion} \end{array} \right) \\ &\quad - \sum \left(\begin{array}{c} \text{arbitrary restrictions on} \\ \text{flow and volume ratios} \end{array} \right) \quad (134) \end{aligned}$$

Using the "completely stagnant" interpretation of deadwater regions, Fig. 23 illustrates some simple combined models and their tracer-response curves. In these models V_b , V_p , and V_d stand for the volume of backmix, plug flow, and deadwater regions. If V is the volume of vessel we then have

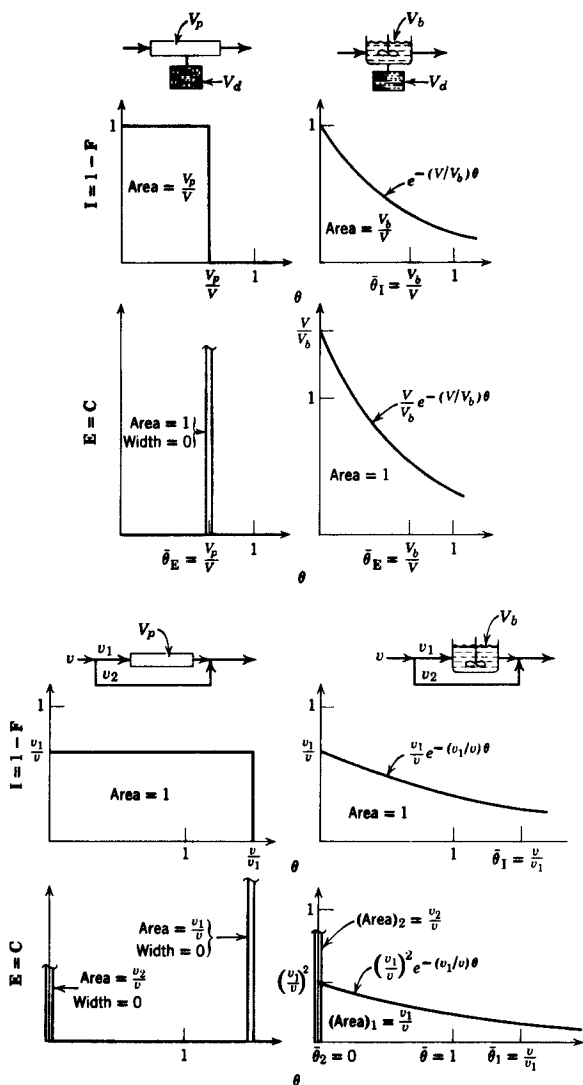


FIG. 23. Simple combined models and their corresponding age distribution functions (L13). (Continued on pp. 166 and 167.)

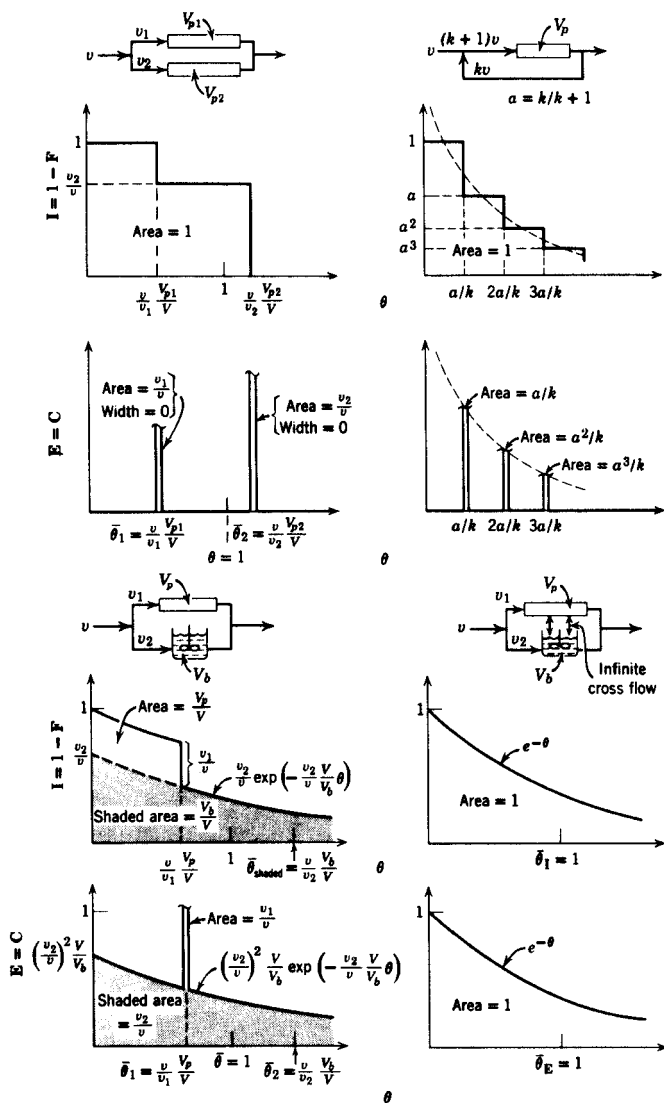


FIG. 23 (Continued).

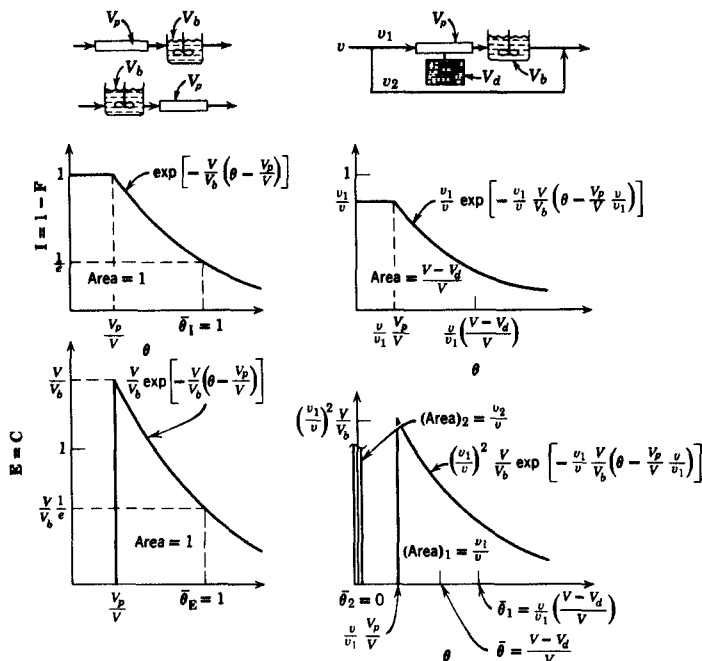


FIG. 23 (Continued).

$$V = \Sigma V_b + \Sigma V_p + \Sigma V_d \quad (135)$$

The volumetric flow rates of streams in parallel are designated by v_1 , $v_2 \dots$. If v is the flow rate of fluid to the vessel, we then have

$$v = v_1 + v_2 + \dots \quad (136)$$

Varying the relative sizes of the flow regions as well as the flow rate of parallel streams allows great flexibility in matching the response curves of these models to that for the real vessel. Model F of this Figure has also been extended to j such units in series by Brothman *et al.* (B22).

The following brief discussion shows how combined models are being used to characterize flow in two broad classes of process equipment, stirred tanks and fluidized beds. Other types of mixed models have also been devised for various purposes; by Bartok *et al.* (B3), Cholette and Cloutier (C16), Handlos *et al.* (H3), Pansing (P3), and Singer *et al.* (S17). Eguchi (E2) presents and discusses some of the models used to date.

D. APPLICATION TO REAL STIRRED TANKS

When the time required for an element of entering fluid to achieve homogeneity with the rest of the vessel contents is small with respect

to the mean residence time of fluid in the vessel, then the fluid in this vessel may be considered to be in backmix flow.

Stead *et al.* (S23) and Johnson and Edwards (J3) showed that homogeneity can be achieved in as short a time as 0.1 sec., with sufficient agitation in a laboratory sized stirred tank. The relation between this time and the intensity of agitation was studied by MacDonald and Piret (M1). Eldridge and Piret (E5) then used kinetic experiments to show that a series of up to five laboratory-sized stirred tanks with sufficient agitation acted as perfect backmix reactors.

Aiba (A3), Fox and Gex (F8), Kramers, Baars and Knoll (K15), Metzner and Taylor (M10), Norwood and Metzner (N3), Van de Vusse (V5) and Wood *et al.* (W12) have studied flow patterns and mixing times. In addition, Brothman *et al.* (B22), Gutoff (G9), Sinclair (S16) and Weber (W3) analyzed flow in a stirred tank in terms of the recycle flow model of Fig. 23F. This model corresponds to the draft-tube reactor, and with sufficiently large recycle rate the performance prediction of this model approximates backmix flow.

A study aimed at devising a model for the experimentally found deviations from backmix flow of fluids through vessels was made by Cholette and Cloutier (C16). Using various low agitation rates, these investigators explored the nonideal flow of fluid in a 30-in.-i.d. 30-in.-high stirred tank. Matching **F** curves, they found that their data were best described by a combination of a backmix and a deadwater region with a portion of the fluid shortcircuiting the vessel. The internal age-distribution function for this model is

$$\mathbf{I} = 1 - \mathbf{F} = \frac{v_1}{v} \exp \left[-\frac{v_1}{v} \frac{V}{V_b} \theta \right] \quad (137)$$

or

$$\mathbf{I}(t) = \frac{V_b}{V} \frac{1}{\bar{t}_a} e^{-t/\bar{t}_a} \quad (138)$$

and the exit age-distribution function is

$$\mathbf{E} = \mathbf{C} = \left(\frac{v_1}{v} \right)^2 \frac{V}{V_b} \exp \left[-\frac{v_1}{v} \frac{V}{V_b} \theta \right] + \frac{v_2}{v} \delta(\theta) \quad (139)$$

or

$$\mathbf{E}(t) = \frac{v_1}{v} \frac{1}{\bar{t}_a} e^{-t/\bar{t}_a} + \frac{v_2}{v} \delta(t) \quad (140)$$

The first term of Eq. (140) represents flow through the active portion of the vessel with a mean residence time of $\bar{t}_a = V_b/v_1$. The second term of Eq. (140) represents the fluid which is bypassing the vessel. This model

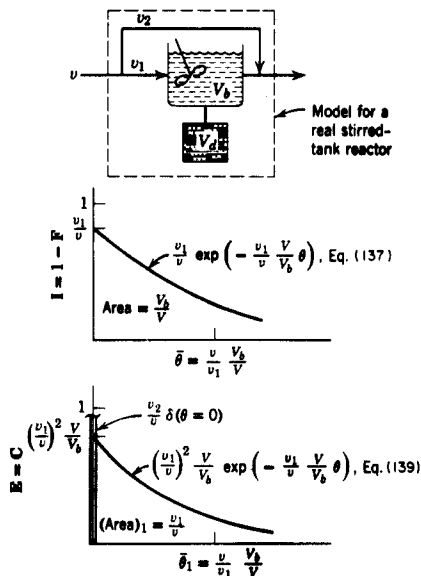


FIG. 24. Combined model of Cholette and Cloutier for real stirred tanks (C16, L13).

and its tracer-response curves are shown in Fig. 24. In this study it was also found, as expected, that the experimental conditions influenced the parameters of the model.

In a follow-up study Cloutier and Cholette (C19) examined in detail the influence of feed inlet location, impeller size, and impeller speed on the parameters of the model. Their results, shown in Fig. 25, indicate that:

- (1) If the agitator speed falls below some critical value then the active volume V_b/V drops to and remains at some constant value.
- (2) At a given feed rate this critical agitator speed is a function of

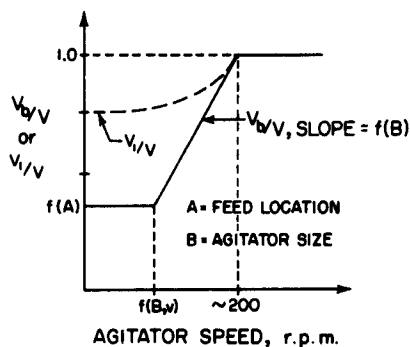


FIG. 25. Effect of intensity of agitation on the parameters of the model for real stirred tanks (C19).

impeller size, suggesting that the energy input into the fluid could determine when the deadwater region reaches a maximum.

(3) The minimum active volume depends on feed location but not on impeller size. This suggests that the maximum size of deadwater region depends on the geometry of the vessel.

(4) Above the critical agitator speed, the active volume rises linearly to unity with r.p.m. This rate of rise is a function of impeller blade size (hence energy input) but is independent of feed location (or vessel geometry).

(5) Although a smooth line can be drawn through the values of v_1/v , it is difficult to correlate this factor with the experimental conditions. Results indicate that while the onset of bypassing and deadwater may be concurrent they need not be so.

E. APPLICATION TO FLUIDIZED BEDS

Numerous investigators have studied mixing of fluids in fluidized beds. Danckwerts *et al.* (D10), Gilliland and Mason (G4, G5), Gilliland *et al.* (G6), and Huntley *et al.* (H16) have given data on the distribution of residence times. Others have used the dispersion model to characterize flow in fluidized beds: Askins *et al.* (A17), Brötz (B23), Cairns and Prausnitz (C3), Gilliland and Mason (G4), Handlos *et al.* (H3), Hanratty *et al.* (H4), Muchi *et al.* (M13), Reman (R2), Trawinski (T13), Wicke and Trawinski (W9), Wakao *et al.* (W1), and Yagi and Miyauchi (Y1). The inability of this approach to yield broad predictive correlations, particularly with solid-catalyzed gas-phase reactions, seems to show that this one-parameter model can not satisfactorily explain fluidized-bed behavior. A different approach was needed, the basis for which was found in the observation that gas-solid fluidized beds seemed to consist of dense regions through which pass bubbles of gas.

A number of models all having a dense or emulsion phase and a lean or bubble phase have been proposed. These are all special cases of the

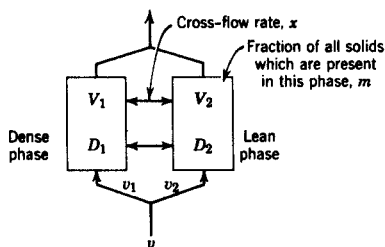


FIG. 26. General two-region model of a fluidized bed. Fluid is in dispersed plug flow in both regions. The six parameters of this model are m , x , V_1 , v_1 , D_1 , and D_2 (L13).

general two-region, six-parameter model shown in Fig. 26. This general model has not yet been used, for two reasons: the difficulty in interpreting experimental data so as to evaluate the model parameters, and the fact that probably fewer parameters could equally well represent reality. Many different sets of restrictions have been proposed to reduce the general model to more tractable form with fewer parameters. The restrictions used are of the following kind:

- (1) Fix the dispersion coefficients of the dispersed plug flow model, $D_L = D_1$ or D_2 , at infinity or zero to obtain backmix or plug flow in the individual regions.
- (2) Assume that no solids are present in the lean phase.
- (3) Assume that there is no net gas flow upward through the dense phase.
- (4) Assume that the volume of dense phase, the fraction solids in it, and the gas flow through it remain the same at all gas velocities, in which case, the lean phase alone expands and contracts to account for the variation in total volume of fluidized bed with change in gas flow rate. The dense-phase characteristics are given by the conditions at incipient fluidization.

Table IV shows the restrictions which must be placed on this general model to obtain each of the special cases studied. Also shown are the number of parameters for each of the models. What is now needed is an evaluation of these models: to find those models which fit the fluidized bed in its wide range of behavior, and then to select from these the simplest model of good fit. Practically every one of these models is flexible enough to correlate the data of any single investigation; consequently a proper evaluation would require testing every model under the extremely wide variety of operating conditions of different investigators.

Other aspects of the behavior of fluidized beds can be found in books by Leva (L9) and Zenz and Othmer (Z1), and in the literature from which these books have drawn.

V. Applications of Nonideal Patterns of Flow to Chemical Reactions

Conversion in a reactor with nonideal flow can be determined either directly from tracer information or by use of flow models. Let us consider each of these two approaches, both for reactions with rate linear in concentration (the most important example of this case being the first-order reaction) and then for other types of reactions where information in addition to age distributions is needed.

TABLE IV
MODELS FOR FLUIDIZED BEDS^a

Model	Restrictions on general model		Model parameters for		
	Dense phase	Lean phase	Homogeneous reactions	Heterogeneous reactions	Reference
M1	$D_1 = 0$ (plug flow) v_1, V_1 fixed ^b	$D_2 = 0$ (plug flow) no solids, $m = 0$	x	x	Shen and Johnstone (S12) Gomezplata and Shuster (G7)
M2	$D_1 = \infty$ (backmix) v_1, V_1 fixed ^b	$D_2 = 0$ (plug flow) no solids, $m = 0$	x	x	Shen and Johnstone (S12)
M3	$D_1 = 0$ (plug flow) v_1, V_1 fixed ^b	$D_2 = 0$ (plug flow)	m, x	m, x	Mathis and Watson (M7)
M4	$D_1 = 0$ (plug flow) $v_1 = 0$	$D_2 = 0$ (plug flow)	V_1, m, x	m, x	Lewis <i>et al.</i> (L17)
M5	$D_1 = \infty$ (backmix) $v_1 = 0$	$D_2 = 0$ (plug flow)	V_1, m, x	m, x	Lewis <i>et al.</i> (L17)
M6		$D_2 = 0$ (plug flow) no solids, $m = 0$	V_1, v_1, x, D_1	v_1, x, D_1	May (M8)
M7		no solids, $m = 0$ no cross flow, $x = 0$	V_1, v_1, D_1, D_2	v_1, D_1, D_2	van Deemter (V1)
M8	$D_1 = 0$ (plug flow)	$D_2 = 0$ (plug flow)	V_1, v_1, m, x	V_1, m, x	Lanneau (L2)

x = cross-flow rate.

m = fraction of all solids present in lean phase.

^a From Levenspiel, O., "Chemical Reaction Engineering," John Wiley, New York, 1962.

^b As given by conditions of incipient fluidization.

Note: $V = V_1 + V_2$ and $v = v_1 + v_2$ are known and are not parameters of the models.

A. DIRECT USE OF AGE DISTRIBUTION INFORMATION

1. *General*

The distribution of residence times gives information on how long various elements of fluid spend in the reactor, but not on the detailed exchange of matter within and between the elements. For a reaction with rate linear in concentration, the extent of reaction can be predicted solely from knowledge of the length of time each molecule has spent in the reactor. The exact nature of the surrounding molecules is of no importance. Thus the distribution of residence times yields sufficient information for the prediction of the average concentration in the reactor effluent.

For all other types of nonlinear reactions, however, the extent of the reaction depends not only on the length of time spent in the reactor but also on what other molecules were "seen" during the passage through the reactor. In this case then, the distribution of residence times is not sufficient, and detailed information on the degree of mixing would be required to predict the average concentration in the reactor effluent.

If it is assumed that each element of fluid passes through the reactor with no intermixing with adjacent elements (termed segregated flow), the distribution of residence times can be used to determine the conversion. Thus

$$\left(\begin{array}{l} \text{mean concentration} \\ \text{of reactant leaving} \\ \text{the reactor} \\ \text{unreacted} \end{array} \right) = \sum_{\substack{\text{all} \\ \text{elements} \\ \text{of exit} \\ \text{stream}}} \left(\begin{array}{l} \text{concentration} \\ \text{of reactant} \\ \text{remaining in} \\ \text{an element of} \\ \text{age between} \\ t \text{ and } t + dt \end{array} \right) \left(\begin{array}{l} \text{fraction of} \\ \text{exit stream} \\ \text{which consists} \\ \text{of elements of} \\ \text{age between} \\ t \text{ and } t + dt \end{array} \right)$$

or

$$C = \int_0^{\infty} C_{\text{element}} \mathbf{E}(t) dt \quad (141)$$

Equation (141) predicts the conversion for what can be termed a "macro-fluid" in which aggregates of molecules move about in "insulated" packets. (In plug flow, this model will always apply.) The other extreme, which can be called a "microfluid," is a fluid in which mixing occurs on the molecular scale. A real fluid lies somewhere between these two extremes, and in normal cases, much closer to the microfluid extreme. The effects of this mixing on reactions has been studied by Danckwerts (D7, D8), Greenhalgh *et al.* (G8), Metzner and Pigford (M9), Gilliland and Mason (G5), Gilliland *et al.* (G6), Sherwood (S13), and Zwietering (Z2). Further papers in this field were included in two Symposia on "Chemical

Reaction Engineering," published in *Chem. Eng. Sci.* **8**, (1958) and **14**, (1961). We will discuss these effects for each type of reaction.

2. Linear Rate Equations

As was discussed previously, the exact state of mixing has no effect for reactions with rate linear in concentration. For such reactions Eq. (141) may always be used to predict the conversions. Thus, we have

$$-r_c = -\frac{dC_{\text{element}}}{dt} = k_1(C_{\text{element}} - k_2) \quad (142)$$

From a physical standpoint, C can never be negative; thus, we must restrict $k_2 \geq 0$ for the following treatment. This restriction eliminates zero-order reactions, whose conversions do depend on the state of mixing.

With $C_{\text{element}} = C_0$ at $t = 0$, integration gives

$$C_{\text{element}} = (C_0 - k_2)e^{-k_1 t} + k_2 \quad (143)$$

Substituting into Eq. (141) yields

$$C = \int_0^\infty [(C_0 - k_2)e^{-k_1 t} + k_2] \mathbf{E}(t) dt \quad (144)$$

We consider now the special forms of Eq. (144) for a first-order reaction (i.e., $k_2 = 0$) occurring in various types of flow. In plug flow

$$\mathbf{E}(t) = \delta(t - \bar{t}) \quad (145)$$

Hence, as expected from the usual methods of kinetics,

$$\frac{C}{C_0} = \int_0^\infty e^{-k_1 t} \delta(t - \bar{t}) dt = e^{-k_1 \bar{t}} \quad (146)$$

For backmix flow, in a single backmix reactor,

$$\mathbf{E}(t) = \frac{e^{-t/\bar{t}}}{\bar{t}} \quad (147)$$

hence,

$$\frac{C}{C_0} = \int_0^\infty e^{-k_1 t} \frac{e^{-t/\bar{t}}}{\bar{t}} dt = \frac{1}{1 + k_1 \bar{t}} \quad (148)$$

Again this is the expected result from the methods of kinetics.

For a series of equal-sized backmix reactors the exit age distribution function is

$$\mathbf{E}(t) = \frac{1}{(j-1)!} \left(\frac{t}{\bar{t}_i} \right)^{j-1} \frac{e^{-t/\bar{t}_i}}{\bar{t}_i} \quad (149)$$

hence Eq. (141) becomes

$$\frac{C}{C_0} = \int_0^\infty e^{-kt} \cdot \frac{1}{(j-1)!} \left(\frac{t}{\bar{t}_i}\right)^{j-1} \frac{e^{-t/\bar{t}_i}}{\bar{t}_i} dt = \frac{1}{(1 + k\bar{t}_i)^j} \quad (150)$$

For a series of unequal-sized backmix reactors with mean residence times $\bar{t}_1, \bar{t}_2, \dots, \bar{t}_i, \dots, \bar{t}_k$ we have

$$\mathbf{E}(t) = \sum_{i=1}^j \frac{1}{\prod_{l=1, l \neq i}^j \left(1 - \frac{\bar{t}_i}{\bar{t}_l}\right)} \cdot \frac{e^{-t/\bar{t}_i}}{\bar{t}_i} \quad (151)$$

hence Eq. (141) becomes

$$\frac{C}{C_0} = \frac{1}{(1 + k\bar{t}_1)(1 + k\bar{t}_2) \cdots (1 + k\bar{t}_j)} \quad (152)$$

For flow with arbitrary exit age distribution $\mathbf{E}(t)$ Eq. (144) must be solved directly. A convenient graphical method for doing this has been devised by Schoenemann (S9) who then discusses the application of this method to some industrial reactors. The direct use of Eq. (144) is also illustrated by Levenspiel (L13), Sherwood (S13) and Petersen's (P5) treatment of catalyst-activity levels in regenerator-reactor systems.

3. Nonlinear Rate Equations

For reactions with rates that are linear in concentration, conversions cannot be calculated from tracer information alone, since a given tracer curve can represent a range of flow patterns with earlier or later mixing

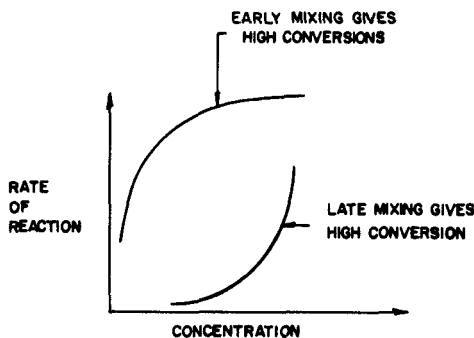


FIG. 27. Characteristic curvature of the rate-concentration curves for reactions which favor either early or late mixing of fluid.

of fluid. Thus a specific tracer response curve can be consistent with a range of possible conversions. As shown in Fig. 27 the curvature of the rate-concentration curve will tell whether early or late mixing will favor high conversions.

a. Conversion for Late Mixing. Since Eq. (141) assumes the latest possible mixing, thus no intermixing of fluid elements, and this in turn implies that the concentration of reactants remain as high as possible, it yields the upper bound to conversion for reactions with order greater than unity, but yields the lower bound for reaction orders smaller than unity.

b. Conversion for Early Mixing. Zwietering (Z2) has given a treatment that shows how to calculate the conversion for the earliest possible mixing consistent with a given age distribution. It is based on a quantity, J , called the degree of segregation, introduced by Danckwerts (D8):

$$J = \frac{\text{variance of ages between points}}{\text{variance of ages of all molecules in system}}$$

$$= \frac{1/V \int_V (\alpha_p - \bar{\alpha})^2 dV}{\int_0^\infty (\alpha - \bar{\alpha})^2 \mathbf{I}(\alpha) d\alpha} \quad (153)$$

where,

α = age of a molecule in the system

$\bar{\alpha}$ = mean age of molecules

$$= \int_0^\infty \alpha \mathbf{I}(\alpha) d\alpha \quad (154)$$

α_p = mean age within a point P

$$= \int_0^\infty \alpha' \mathbf{I}_p(\alpha') d\alpha' \quad (155)$$

$\mathbf{I}_p(\alpha')$ = age distribution within a point P

and the volume integral represents the sum over all points. The term "point" is taken to mean a region small compared to the scale of segregation but large enough to contain many molecules (D8).

Danckwerts (D8) discussed the case of a perfect mixer. For the completely segregated case, all molecules within a point have the same age, α , and so

$$\mathbf{I}_p(\alpha') = \delta(\alpha' - \alpha)$$

and

$$\alpha_p = \int_0^\infty \alpha' \delta(\alpha' - \alpha) d\alpha' = \alpha \quad (156)$$

Also, the distribution of points can be found from the $\mathbf{I}(\alpha)$ curve, and so,

$$J = \frac{1/V \int_V (\alpha - \bar{\alpha})^2 dV}{\int_0^\infty (\alpha - \bar{\alpha})^2 \mathbf{I}(\alpha) d\alpha} = \frac{\int_0^\infty (\alpha - \bar{\alpha})^2 \mathbf{I}(\alpha) d\alpha}{\int_0^\infty (\alpha - \bar{\alpha})^2 \mathbf{I}(\alpha) d\alpha} = 1 \quad (157)$$

For mixing uniform on a molecular scale, the distribution of ages within any point is the same as that in the entire system, and so

$$I_p(\alpha') = I(\alpha') \quad (158)$$

and,

$$\alpha_p = \int_0^\infty \alpha' I(\alpha') d\alpha' = \bar{\alpha} \quad (159)$$

Thus,

$$J = \frac{1/V \int_V (\bar{\alpha} - \bar{\alpha}) dV}{\int_0^\infty (\alpha - \bar{\alpha})^2 I(\alpha) d\alpha} = 0 \quad (160)$$

In summary, for a backmix reactor, J is unity for perfect segregation and zero for perfect molecular mixing.

Zwietering (Z2) generalized this treatment to an arbitrary age distribution. The argument for perfect segregation is still valid for this case, and so the upper limit of J is again unity. The lower limit is not zero, however, because there must be a difference in ages at various points in the system. The state of "maximum mixedness," or earliest possible mixing, is arrived at by a rather lengthy argument involving the definition of the life expectation in the vessel, λ , of a molecule,

$$\begin{aligned} \left(\begin{array}{c} \text{residence time} \\ \text{of a molecule} \end{array} \right) &= (\text{age of a molecule}) + (\text{life expectation of a molecule}) \\ t &= \alpha + \lambda \end{aligned} \quad (161)$$

Life-expectation distribution functions are derived, and the final result for earliest mixing, assuming no radial variations, is,

$$\frac{1}{V} \int_V (\alpha_p - \bar{\alpha})^2 dV = \int_0^\infty \left[\frac{1}{I(\lambda_p)} \int_{\lambda_p}^\infty I(s) ds - \bar{\alpha} \right]^2 I(\lambda_p) d\lambda_p \quad (162)$$

Thus knowledge of the $I(t)$ curve will permit calculation of the lower bound of J . Unfortunately there is yet no way to determine the variance between points for the general case, and so all that we can do is calculate the two extremes.

For a chemical reactor operating with earliest possible mixing, Zwietering gives an equation for the calculation of conversion,

$$\frac{dC}{d\lambda} = -r_c(C) + \frac{E(\lambda)}{tI(\lambda)} (C - C_0) \quad (163)$$

The reactor outlet conversion is found from $C(0)$. The conversion for segregated flow is, of course, found from Eq. (141), discussed previously. With these equations, the limits between which the conversion must lie

for any real reactor can be predicted. More work is needed, however, before any closer predictions within the two extremes may be made.

B. STIRRED TANK REACTORS

1. *Ideal Stirred Tanks*

For one perfect stirred tank, the formulation used in Section III,B is used, modified by adding a term for the chemical reaction,

$$C_0v = C_1v + V \frac{dC_1}{dt} - Vr_c(C_1) \quad (164)$$

The steady state solutions of these equations are well known and will not be considered here. Extensions to steady state flow in a chain of stirred tanks also have been extensively treated in the literature: Denbigh (D16, D17), Devyatov and Bogatchev (D18), Eldridge and Piret (E5), Fan (F3), Jenney (J2), Kirillov (K6, K7), Kirillov and Smirnova (K8), Leclerc (L6), Lessells (L8), MacMullin and Weber (M2, M3), Stead *et al.* (S23), and Weber (W3).

Numerous short cut procedures for solving graphically the design equations for n th order reactions are available in the literature; for example see Fan (F3), Hofmann (H10), Jenney (J2), Lessells (L8), Levenspiel (L13) and MacMullin and Weber (M2, M3). For more complex reaction types, Eldridge and Piret (E5) have given a catalog of solutions. Bilous and Piret (B8), Jones (J4), Jungers *et al.* (J5), Levenspiel (L13), and Trambouze and Piret (T12) have discussed general design methods.

The solutions of the nonsteady-state expression, Eq. (164), both for single tanks and chains of tanks have been made by Acton and Lapidus (A1), Mason and Piret (M5, M6), and Standart (S22). Aris and Amundson (A15, A16), Bilous and Amundson (B7), Bilous *et al.* (B9), and Gilles and Hofmann (G3) have studied the stability, control, and response of a stirred tank reactor.

Nagata, *et al.* (N1, N2), Kawamura *et al.* (K4), and Yagi and Miyauchi (Y2) have studied the characteristics of various impeller agitated multistaged vessels. Such vessels were assumed to be a succession of plug-flow and backmix units, whose relative sizes were a function of the impeller speed. The parameter of the model, the fraction of total volume in a plug-flow, could also be related to a dispersion coefficient. Verification of the model was then obtained with kinetic experiments.

Aris (A13), Cholette and Blanchet (C15), Cholette *et al.* (C17), and Trambouze and Piret (T12) have discussed using combinations of backmix and plug-flow reactors.

2. Nonideal Stirred Tanks

The conversion in a real, hence, nonideal, stirred tank reactor can be calculated for the model proposed by Cholette and Cloutier (see Section IV,D). The exit stream consists of reacted fluid from the active backmix region combined with unreacted bypassing fluid. By material balance, then,

$$\left(\begin{array}{c} \text{total exit} \\ \text{stream} \end{array} \right) = \left(\begin{array}{c} \text{fluid from the} \\ \text{backmix region} \end{array} \right) + \left(\begin{array}{c} \text{unreacted} \\ \text{by-passing} \\ \text{fluid} \end{array} \right)$$

$$(v_1 + v_2)C = v_1 C_{BM} + v_2 C_0$$

or

$$\frac{C}{C_0} = \frac{v_1}{v} \frac{C_{BM}}{C_0} + \frac{v_2}{v} \quad (163)$$

where C_{BM}/C_0 is found from the design equation for backmix flow, or,

$$\bar{t}_a = \frac{V_b}{v_1} = \frac{C_0 - C_{BM}}{(-r_c)} \quad (164)$$

For first order reactions, $-r_c = k_1 C_{BM}$; thus, combining,

$$\frac{C}{C_0} = \frac{v_1}{v} \frac{1}{1 + k_1 \bar{t}_a} + \frac{v_2}{v} \quad (165)$$

while for second order reactions,

$$\frac{C}{C_0} = \frac{v_1}{v} \frac{-1 + \sqrt{1 + 4k_1 C_0 \bar{t}_a}}{2k_1 C_0 \bar{t}_a} + \frac{v_2}{v} \quad (166)$$

C. TUBULAR AND PACKED BED REACTORS

Both the dispersion and tanks in series models can be used to represent the non-ideal flow behavior of fluids in packed bed and tubular reactors. As mentioned in the previous sections dealing with these models, they are both good for the slight deviations from plug flow encountered in the above systems.

General discussions of several aspects concerning the treatment of chemical reactions with diffusion are given by Damköhler (D2), Horn and Küchler (H12), Prager (P7), Schoenemann and Hofmann (S10), and Trambouze (T11). Corrsin (C21) has discussed the effects of turbulence on chemical reactions from the fundamental point of view of turbulence theory. We will first discuss the application of each type of model to chemical reactors. Then a short comparison will be made between the different approaches.

1. Dispersion Model

a. Axial-Dispersed Plug-Flow Model. The mathematical description of the process is provided by Eq. (I-5) of Table I. For steady flow the equation reduces to

$$u \frac{\partial C}{\partial X} = D_L \frac{\partial^2 C}{\partial X^2} + r_c \quad (167)$$

For a reaction of order n , Eq. (167) becomes,

$$u \frac{\partial C}{\partial X} = D_L \frac{\partial^2 C}{\partial X^2} - k_1 C^n \quad (168)$$

The proper boundary conditions to use with Eq. (167) have been extensively discussed. Wehner and Wilhelm (W4) gave a general treatment and used the conditions already discussed in Section II,C,2,b, Eq. (26). This involved using three sections with different dispersion characteristics in each: the fore section, $X \leq 0$, the reaction section, $0 \leq X \leq L$, and the after section, $X \geq L$. Similar boundary conditions for the special case of no dispersion in the fore and after sections have been discussed by Damköhler (D1), Hulburt (H14), Danckwerts (D4), Pearson (P4), and Yagi and Miyauchi (Y1). For this case,

$$C_0 = C(0^+) - \frac{D_L}{u} \frac{dC(0^+)}{dX} \quad (169)$$

and

$$\frac{dC(L^-)}{dX} = 0 \quad (170)$$

where C_0 = concentration of unreacted feed. Wehner and Wilhelm solved Eq. (168) with the general boundary conditions for a first-order reaction, $n = 1$, and obtained the following result for $X = L$,

$$\frac{C}{C_0} = \frac{4a \exp \left[\frac{1}{2} \frac{uL}{D_L} \right]}{(1+a)^2 \exp \left[\frac{a}{2} \frac{uL}{D_L} \right] - (1-a)^2 \exp \left[-\frac{a}{2} \frac{uL}{D_L} \right]} \quad (171)$$

where

$$a = \sqrt{1 + 4k_1 \bar{t} \frac{D_L}{uL}}$$

Equation (171) turned out to be the same result that had been obtained using the simpler boundary conditions assuming no diffusion in the fore and after sections. In other words, the solution of Eq. (168) with the general boundary conditions gives the same result as with the simpler boundary conditions. Wehner and Wilhelm used their analytical solutions for a first order reaction to show that this indeed was true; Eqs. (169)

and (170) are valid even *with* diffusion in the fore and after sections. Bischoff (B12) later showed that this is so for any order of reaction. Förster and Geib (F6) derived Eq. (171) by using what we now call the distribution of residence times for a finite vessel with axial dispersion.

Figure 28 is a graphical representation of Eq. (171). The ratio of reactor volume actually needed with dispersion to the plug-flow value is

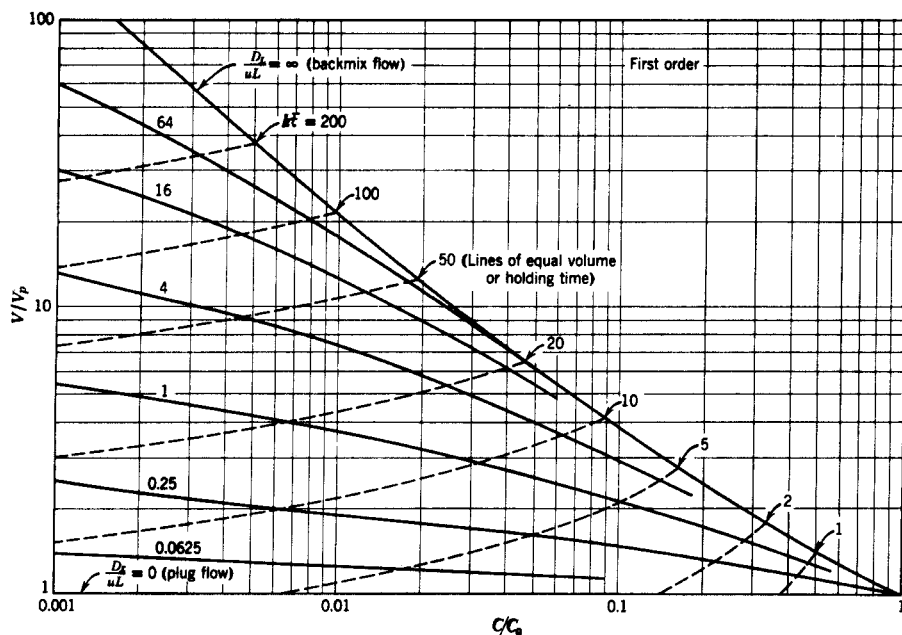


FIG. 28. Comparison of performance of reactors for the plug flow and dispersed plug flow models. Reaction is of first order, $aA \rightarrow \text{products}$, and constant density, occurring in a closed vessel (L14, L15).

plotted against the fraction of reactant remaining at the outlet with the dispersion group, D_L/uL , as a parameter. It is seen that for large values of the group D_L/uL and for high conversions (low fraction of reactant remaining), a significantly larger reactor would be needed than predicted using the plug flow analysis. However, the dispersion model might not be valid for large D_L/uL , and so in practice, only the lower section of the chart could be relied upon. For small D_L/uL , Eq. (171) gives approximately, for equal conversions in the two reactors,

$$\frac{V}{V_p} = \frac{L}{L_p} = 1 + (k_1 \bar{t}) \left(\frac{D_L}{uL} \right) \quad (172a)$$

and for equal sizes,

$$\frac{C}{C_p} = 1 + (k_1 \bar{t})^2 \left(\frac{D_L}{uL} \right) \quad (172b)$$

Carberry (C7) and Epstein (E6) discussed the magnitudes of the corrections necessary for dispersion in packed beds. It was found that for many practical cases of interest, the axial mixing effect was very small.

Levenspiel and Bischoff (L14, L15) later extended the above treatment to second order reactions, and presented a chart similar to Fig. 28. Fan and Bailie (F4) presented results for reactions of order $n = 1/4, 1/2, 2, 3$. They gave the complete set of concentration profiles throughout the reactor section.

All of the preceding work was for simple, or one step, reactions. The more interesting case of multiple reactions has been studied by de Maria *et al.* (D15) and by Tichacek (T7). de Maria *et al.* considered the catalytic oxidation of naphthalene.⁴ They found that the consideration of the dispersion effects enabled them to obtain a better design. Tichacek considered the selectivity for several different types of reactions. Naturally, the results were rather complicated, and the statement of general conclusions is rather difficult. For small values of the reactor dispersion group, $D_L/uL < \sim 0.05$, it was found that the fractional decrease in the maximum amount of intermediate formed is closely approximated by the value of D_L/uL itself. For other ranges of the parameters, we refer to the original work (T7).

Coste *et al.* (C22) considered simultaneous mass and heat dispersion in a tubular reactor. As discussed previously (Section III,b) they found that the numerical computations caused some trouble, although Carberry (C8) used a finite difference scheme that seemed to avoid the difficulties. Hovorka and Kendall (H13) discussed reactions in a baffled vessel.

One final point that should be mentioned is that for nonlinear reaction rates, where the distribution of residence times is not sufficient information to predict conversions, the validity of the preceding theoretical calculations is questionable. However, in view of the fact that the dispersion model should only be relied upon for slight deviations from plug flow (small D_L/uL), this problem might not arise since the nonlinear effects in this range would not be too important. However, not enough experimental work has been done as of yet to determine whether or not the above predicted results can actually be measured in a real reactor. These experiments should be performed so that the necessity (or neglect) of taking dispersion effects into account in reactor design can be determined.

b. Dispersed Plug-Flow Model. For this model, Eq. (I-4) of Table I is used. For steady flow, the equation reduces to,

$$u \frac{\partial C}{\partial X} = D_L \frac{\partial^2 C}{\partial X^2} + \frac{D_R}{R} \frac{\partial}{\partial R} R \frac{\partial C}{\partial R} + r_c \quad (173)$$

⁴ Their work was actually for a fluidized bed, but since they used the dispersion model, it is discussed here.

The solution of Eq. (173) poses a rather formidable task in general. Thus the dispersed plug-flow model has not been as extensively studied as the axial-dispersed plug-flow model. Actually, if there are no initial radial gradients in C , the radial terms will be identically zero, and Eq. (173) will reduce to the simpler Eq. (167). Thus for a simple isothermal reactor, the dispersed plug flow model is not useful. Its greatest use is for either nonisothermal reactions with radial temperature gradients or tube wall catalysed reactions. Of course, if the reactants were not introduced uniformly across a plane the model could be used, but this would not be a common practice. Paneth and Herzfeld (P2) have used this model for a first order wall catalysed reaction. The boundary conditions used were the same as those discussed for tracer measurements for radial dispersion coefficients in Section II,C,3,b, except that at the wall,

$$-D_R \frac{\partial C(R_0)}{\partial R} = k_1 C(R_0)$$

The solution is

$$\frac{C}{C_0} = \sum_{n=1}^{\infty} \frac{2J_1(b_n)}{b_n[J_0^2(b_n) + J_1^2(b_n)]} J_0\left(b_n \frac{R}{R_0}\right) e^{-\gamma_n x} \quad (174a)$$

where

$$\gamma_n = -\frac{u}{2D_R} + \sqrt{\left(\frac{u}{2D_R}\right)^2 + \left(\frac{b_n}{R_0}\right)^2} \quad (174b)$$

$$b_n J_1(b_n) = \frac{k_1 R_0}{D_R} J_0(b_n) \quad (174c)$$

The principal use of Eq. (173) is in conjunction with a similar heat dispersion equation. Unfortunately, a system of coupled nonlinear partial differential equations then has to be solved, which is very difficult even with the aid of computers. In the oxidation of sulfur dioxide, Hall and Smith (H1) found relatively good agreement between theory and experiment near the center of the reactor. Their calculations were based on the heat-dispersion equation, and they did not take detailed mass dispersion into account. Baron (B2) later solved the mass and heat dispersion equations simultaneously by a novel graphical method, and found better agreement between his calculations and the data of Hall and Smith.

Kjaer (K9) gives a very comprehensive study of concentration and temperature profiles in fixed-bed catalytic reactors. Both theoretical and experimental work is reported for a phthallic anhydride reactor and various types of ammonia converters. Fair agreement was obtained, but due to the lack of sufficiently accurate thermodynamic and kinetic data, definite conclusions as to the suitability of the dispersed plug flow model could not be reached. However, the results seemed to indicate that the

model did provide a basis for the successful prediction of reactor performance.

Amundson (A5) discussed the analytical solution of the heat dispersion equations for a packed bed chemical reactor. The form of the differential equations is, of course, similar to the mass dispersion equations for certain cases. A wealth of analytical methods and results are presented for various types of boundary conditions.

c. General Dispersion Model. The general dispersion model has been used only for fully developed laminar flow in empty tubes: Chambré (C12, C13), Cleland and Wilhelm (C18), Damköhler (D2), Krongelb and Strandberg (K16), Lauwerier (L5), Schechter and Wissler (S4), Walker (W2), and Wissler and Schechter (W11). Most of the work has been concerned with the computations involved in solving Eq. (I-2) of Table I with $u(R) = 2u(R_0^2 - R^2)$. A solution has usually been obtained by using the separation-of-variables technique to reduce the partial differential equation to a Sturm-Liouville problem. The Sturm-Liouville eigenfunctions were then computed by a series expansion or other numerical method. In order to use this method, the equation must be linear, and so first-order reactions were considered. Schechter and Wissler (S4) considered a more complicated case of a first-order photochemical reaction with a position-variable photon intensity.

Cleland and Wilhelm (C18) used a finite-difference technique which could be used for nonlinear reactions, but they limited their study to a first-order reaction. Experiments were also performed to test the results of the theory. In a small reaction tube, the two checked quite well. In a large tube there were differences which were explained by consideration of natural convection effects which were due to the fact that completely isothermal conditions were not maintained. This seems to be the only experimental data in the literature to date, and shows another area in which more work is needed. The preceding discussion considered only isothermal conditions except for Chambré (C12) who presented a general method for nonisothermal reactors.

2. Tanks-in-Series Model

As discussed in Section III, for small deviations from plug flow such as those occurring in tubular and packed-bed reactors, a model consisting of a series of tanks can be used to represent the fluid mixing. The conversion predicted by the model can be found from the equations discussed in the section on conversion in ideal stirred tanks. Figure 29 shows the ratio of reactor volume needed with j stirred tanks to the volume needed

with plug flow versus the fraction of reactant remaining at the vessel outlet for a first order reaction. It is seen that the graph is quite similar to the one for the dispersion model, Fig. 28.

The discussion in Section III,C showed that there was no unique way to compare the stirred tank and dispersion models based on the tracer curves. Each different basis of comparison gave different results. The two models have been compared for chemical reactions by van Krevelen (V6), Trambouze (T10), and Levenspiel (L13a). Levenspiel used Figs. 28 and 29 to determine the correspondence of the models. His results are shown in Fig. 30. The various criteria give results that differ increasingly with rise in reaction order, conversion, and degree of mixing.

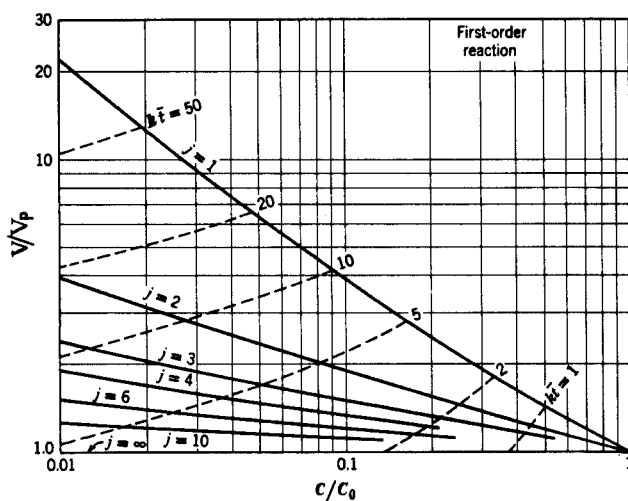


FIG. 29. Comparison of performance of reactors for the plug flow and tanks in series models. Reaction is of first order, $aA \rightarrow$ products, and constant density, occurring in a closed vessel (L13).

Thus it seems that the type of comparison that should be made depends on the purpose of the model. For design of mixing vessels the tracer curves should be matched, and for reactor design conversions should be matched. Unfortunately, this means that a general approach is not possible for all cases. However, the various criteria of correspondence approach each other with approach to plug flow ($j \rightarrow \infty$ or $D_L/uL \rightarrow 0$), and so for many practical cases of interest a comparison is possible. Thus, for small deviations from plug flow, either the dispersion model or stirred tanks model may be satisfactorily used depending on one's personal preference.

Deans and Lapidus (D12) have also extended their finite-stage model

to chemical reactions. As was discussed in Section III,B,2, the reason for devising this model was to avoid, if possible, the mathematical complexity of solving the coupled partial differential equations. However, since Schechter and Wissler (S5) showed (see Section III,B,2) that the

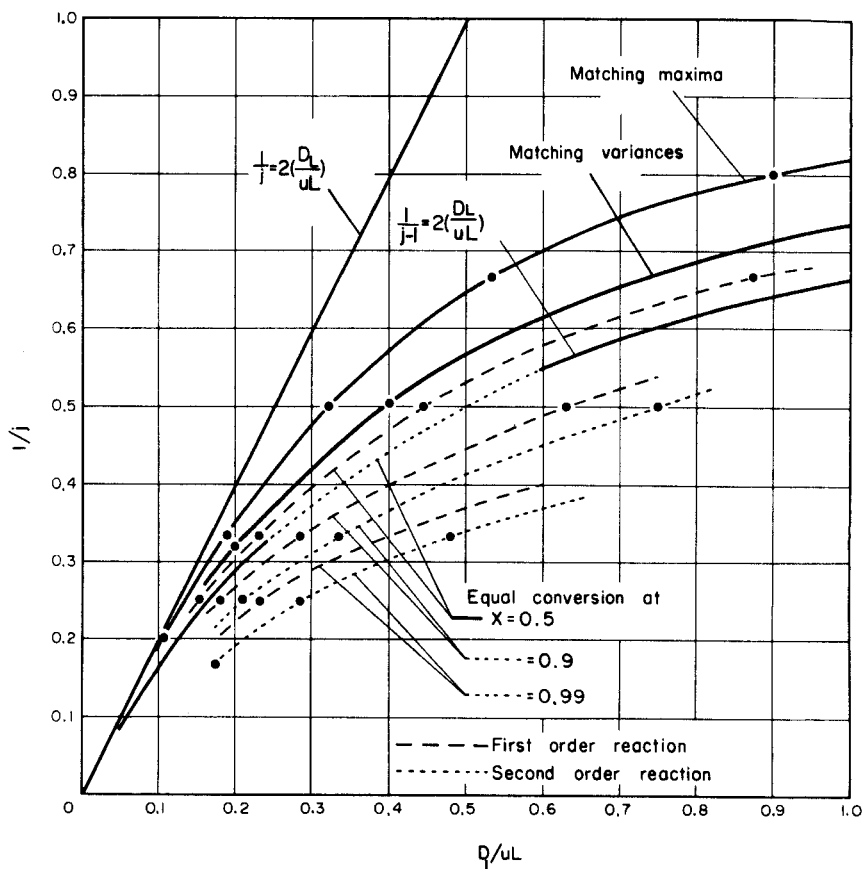


FIG. 30. Ways of comparing the dispersed plug flow and tanks in series models (L13a).

finite stage equations were one of a family of difference-equation representations of the partial differential equations, there may not be any actual computational advantages. Again, all that can be said is that more work is required in this area.

D. FLUIDIZED BED REACTORS

If the dispersion model is chosen to represent fluidized-bed behavior, then the expressions found for packed-bed reactors and tubular reactors

are applicable. These have been presented by Blickle and Kaldi (B18), de Maria *et al.* (D15), Gilliland and Mason (G5), and Wicke (W8). On the other hand, if the two-region flow models of Table IV are used, the conversion must be determined for the specific model being used. Each of the references given in Section IV,E should be consulted for details. Different types of expressions will be obtained for homogeneous and solid-catalyzed reactions, since in the catalytic case reaction does not occur where solid is absent. Thus, for homogeneous systems, the volume-ratio of phases is a parameter of the model, but in catalytic systems it is not. This fact is shown in the number of parameters tabulated for each of the models listed in Table IV and is further discussed in (L13).

Due to lack of applications, conversion expressions for these two-region models have not been developed for homogeneous systems. For heterogeneous systems, which are outside the scope of this article, the appropriate expressions can be found in the works of the individual investigators.

VI. Other Applications

A. INTERMIXING OF FLUIDS FLOWING SUCCESSIVELY IN PIPELINES

A pipeline may be used to transport a variety of fluids, and in switching from one fluid to another a region of intermixing (or zone of contamination) forms between the leading and following fluid. For proper design and operation of a pipeline so as to minimize contamination, it is necessary to be able to predict the extent of such intermixing. This was done by Levenspiel (L11) using the dispersed plug-flow model. For the general findings and design charts see (L11).

B. BRIEF SUMMARY OF APPLICATIONS TO MULTIPHASE FLOW AND OTHER HETEROGENEOUS PROCESSES

For two phase systems, deviations of flow patterns from ideality can be more serious than for single phase systems, and thus errors in design can be much greater. Recently, much work has been done in this area, but the treatment is necessarily more cumbersome and difficult. It is not within the scope of this article to deal with these cases. The following references are presented simply to indicate the type of work being done during the last few years.

- Acrivos, A., On the combined effect of longitudinal diffusion and external mass transfer resistance in fixed bed operations. *Chem. Eng. Sci.* **13**, 1 (1960).
Asbjornson, O. A., The distribution of residence times in a falling water film. *Chem. Eng. Sci.* **14**, 211 (1961).
Bradshaw, R. D., and Bennett, C. O., Fluid-particle mass transfer in a packed bed. *A.I.Ch.E. Journal* **7**, 48 (1961).

- de Maria, F., and White, R. R., Transient response study of gas flowing through irrigated packing. *A.I.Ch.E. Journal* **6**, 473 (1960).
- Foss, A. S., Gerster, J. A., and Pigford, R. L., Effect of liquid mixing on the performance of bubble trays. *A.I.Ch.E. Journal* **4**, 231 (1958).
- Gilbert, T. J., Liquid mixing on bubble-cap and sieve plates. *Chem. Eng. Sci.* **10**, 243 (1959).
- Gray, R. I., and Prados, J. W., The dynamics of a packed gas absorber by frequency response analysis. *A.I.Ch.E. Journal* **9**, 211 (1963).
- Houston, R. H., Univ. California Radiation Lab. Rept. 3817 (1958). "A Theory for Industrial Gas-Liquid Chromatographic Columns."
- Hennico, A., Jacques, G. L., and Vermeulen, T., Longitudinal dispersion in packed extraction columns. Univ. California Radiation Lab. Rept. 10696 (1963).
- Kada, H., and Hanratty, T. J., Effect of solids on turbulence in a fluid. *A.I.Ch.E. Journal* **6**, 624 (1960).
- Kasten, P. R., and Amundson, N. R., An elementary theory of adsorption in fluidized beds. *Ind. Eng. Chem.* **42**, 1341 (1950).
- Lapidus, L., Flow distribution and diffusion in fixed-bed two-phase reactors. *Ind. Eng. Chem.* **49**, 1000 (1957).
- Mar, B. W., and Babb, A. L., Longitudinal mixing in a pulsed sieve-plate extraction column. *Ind. Eng. Chem.* **51**, 1011 (1959).
- Miyauchi, T., and Vermeulen, T., Longitudinal dispersion in two-phase continuous-flow operations. *Ind. Eng. Chem. Fundamentals* **2**, 113 (1963).
- Miyauchi, T., Influence of longitudinal dispersion on tray efficiency. *Chem. Eng. (Tokyo)* **24**, 443 (1960).
- Oliver, E. D., Liquid mixing on bubble trays—a correction. *A.I.Ch.E. Journal* **5**, 564 (1959).
- Oliver, E. D., and Watson, C. C., Correlation of bubble cap fractionating-column plate efficiencies. *A.I.Ch.E. Journal* **2**, 18 (1956).
- Otake, T., and Kunugita, E., Mixing characteristics of irrigated packed towers. *Chem. Eng. (Tokyo)* **22**, 144 (1958).
- Schiesser, W. E., and Lapidus, L., Further studies of fluid flow and mass transfer in trickle beds. *A.I.Ch.E. Journal* **7**, 163 (1961).
- Seimes, W., and Weiss, W., Flüssigkeitsdurchmischung in engen Blasensäulen. *Chem. Ing. Tech.* **29**, 727 (1957).
- Sleicher, C. A., Axial mixing and extraction efficiency. *A.I.Ch.E. Journal* **5**, 145 (1959).
- Sleicher, C. A., Entrainment and extraction efficiency of mixer settlers. *A.I.Ch.E. Journal* **6**, 529 (1960).
- Van Deemter, J. J., Zuiderweg, F. J., and Klinkenberg, A., Longitudinal diffusion and resistance to mass transfer as causes of nonideality in chromatography. *Chem. Eng. Sci.* **5**, 271 (1956).
- van de Vusse, J. G., Residence times and distribution of residence times in dispersed flow systems. *Chem. Eng. Sci.* **10**, 229 (1959).
- Vermeulen, T., Separation by adsorption methods. *Advances Chem. Eng.* **2**, 147 (1958).
- Dunn, W. E., Vermeulen, T., Wilke, C. R., and Word, T. T., Longitudinal dispersion in packed gas absorption columns. Univ. California Radiation Lab. Rept. 10394 (1963).
- Weber, H., Dissertation, Tech. Hochschule, Darmstadt, Germany, 1960; quoted in Hofmann, Reference (H11).

VII. Recent References

A list of recent work not included in the preceding discussion is presented here. The pertinent section in this article is indicated after the reference.

- Bailey, H. R., and Gogarty, W. B., Numerical and experimental results on the dispersion of a solute in a fluid in laminar flow through a tube. *Proc. Roy. Soc. A* **269**, 352 (1962). (II,C,2,h; II,D,2; II,D,3)
- Biggs, R. D., Mixing in continuous-flow stirred tanks. Paper presented at A.I.Ch.E. Meeting, Los Angeles, February, 1962. (IV,D)
- Carter, D., and Bir, W. G., Axial mixing in a tubular high pressure reactor. *Chem. Eng. Progr.* **58**, 40 (March, 1962). (II,C,2,h)
- Curl, R. L., Dispersed phase mixing-theory and effects in simple reactors. *A.I.Ch.E. Journal* **9**, 175 (1963). (IV,D; V,B,2)
- De Baun, R. M., and Katz, S., Approximations to residence time distribution in mixing systems and some applications thereof. *Chem. Eng. Sci.* **16**, 97 (1961). (I; IV)
- Farrell, M. A., and Leonard, E. F., Dispersion in laminar flow by simultaneous convection and diffusion. *A.I.Ch.E. Journal* **9**, 190 (1963). (II,D)
- Froment, G. F., Design of fixed-bed catalytic reactors based on effective transport models. *Chem. Eng. Sci.* **17**, 849 (1962). (VC)
- Glaser, M. B., and Litt, M., A physical model for mixed phase flow through beds of porous catalyst. *A.I.Ch.E. Journal* **9**, 103 (1963). (II,E)
- Glaser, M. B., and Lichtenstein, I., Interrelation of packing and mixed phase flow parameters with liquid residence time distribution. *A.I.Ch.E. Journal* **9**, 30 (1963). (II,E)
- Gottschlich, C. F., Axial dispersion in packed beds. *A.I.Ch.E. Journal* **9**, 88 (1963). (II,C,2,h; II,E)
- Leonard, E. F., and Ruszkay, R. J., Frequency, transient and moment methods in process analysis. Paper presented at A.I.Ch.E. Meeting, New York, December, 1961. (I)
- Miller, R. S., Ralph, J. L., Curl, R. L., and Towell, G. D., Dispersed phase mixing-measurements in organic dispersed systems. *A.I.Ch.E. Journal* **9**, 196 (1963). (IV,D)
- Muchi, I., Mamuro, T., and Sasaki, K., Studies on the mixing of fluid in a fluidized bed. *Chem. Eng. (Tokyo)* **25**, 747 (1961). (IV,E)
- Rosenweig, R. E., Hottel, H. C., and Williams, G. C., Smoke-scattered light measurement of turbulent concentration fluctuation. *Chem. Eng. Sci.* **15**, 111 (1961). (II)
- Schügerl, K., Merz, M., and Fetting, F., Rheologische Eigenschaften von gasdurchströmten Fließbettsystemen. *Chem. Eng. Sci.* **15**, 1 (1961). (IV,E)
- Stoyanovskii, I. M., Investigation of the longitudinal transfer of iodine in various solvents during the motion of a liquid stream through a granular glass bed. *J. Appl. Chem. USSR (Engl. Transl.)* **34**, 1863 (1961). (II,C,2,h)
- Yablonskii, V. S., Asaturyan, A. Sh., and Khizgilov, I. Kh., Turbulent diffusion in pipes. *Intern. Chem. Eng.* **2**, 3 (1962). (II,C,2,h)
- Zelmer, R. G., Residence times in continuous multistage reactors. *Chem. Eng. Progr.* **58**, 37 (March 1962). (V)

Nomenclature

a	$= \mathbf{P}/\mathbf{P}_a$	D_R	Radial dispersion coefficient, dispersed plug flow model
a_i	Roots of $J_1(a_i) = 0$	D_{Rm}	Mean value of $D_R(R)$
b	$= \mathbf{P}/\mathbf{P}_b$	D'_{Rm}	Radial dispersion coefficient, uniform dispersion model
\mathbf{C}	Dimensionless response curve to a pulse input, defined in Section I	$D_R(r)$	$= D_R(R)$ Radial dispersion coefficient, general dispersion model in cylindrical coordinates
C	Concentration	\mathfrak{D}	Molecular diffusivity
C_0	Initial concentration of tracer or reactant entering the vessel or reactor	\mathbf{E}	Exit age distribution function, defined in Section I
C^0	Average concentration of tracer in system	E	Radius of injector tube
C_{ave}	Integral average tracer concentration in vessel during steady state injection (dispersion model)	e	$= E/R_0$. Dimensionless radius of injector tube
C'_{ave}	Mean concentration of pulse of tracer if uniformly distributed in experimental section of vessel of length L	\mathbf{F}	Dimensionless response to step input, defined in Section I
c	$= C/C^0$. Dimensionless concentration $= C/C_{ave}$. Dimensionless concentration	$f_1(R)$	$= [u(R) - u]/u$. Measure of variation of $u(R)$ from its mean value
c'	$= C/C'_{ave}$. Dimensionless concentration	$f_2(R)$	$= D_R(R)/D_{Rm}$. Measure of variation of $D_R(R)$ from its mean value
d_e	Effective diameter, defined by Eq. (50)	$f_3(R)$	$= D_L(R)/D_{Lm}$. Measure of variation of $D_L(R)$ from its mean value
d_p	Particle diameter	f_L	$= (\mathbf{P} - \mathbf{P}_\infty)/\mathbf{P} $
d_t	Tube diameter	f_R	$= (c - c_\infty/c) $
\mathbf{D}	Dispersion coefficient	h	Defined by Eq. (73)
D_L	Axial dispersion coefficient, dispersed plug flow model	\mathbf{I}	Internal age distribution function, defined in Section I
D'_L	Axial dispersion coefficient, axial-dispersed plug, flow model shown equal to D_L in Eq. (72)	I	Injection rate of tracer
D_{Lm}	Mean value of $D_L(R)$	j	Number of ideal stirred tanks in series
D_{Lm}'	Axial dispersion coefficient, uniform dispersion model	J_0, J_1	Bessel functions
$D_L(r)$	$= D_L(R)$ Axial dispersion coefficient, general dispersion model in cylindrical coordinates	k	Moment order, see Eq. (65)
		k_1, k_2	Reaction rate constants
		L	$= X_m - X_0$. Distance between measurement

	points, or length of experimental section	$\theta = ut/L = t/\bar{t}$. Dimensionless time
M_k	k th moment of tracer distribution averaged over the cross section of tube, defined by Equation (65)	\mathbf{u} Velocity vector
N_t	Defined by Equations (56) and (57)	u Mean velocity in axial direction
O	The order symbol	$u(R)$ Velocity as a function of radial position
p	Laplace transform variable	u_0 Mean velocity in a packed bed based on empty tube
\mathbf{P}	$= uL/D_L'$. Dimensionless parameter	$U(t)$ Unit step function
P_L	$= uR_0/D_L$. Dimensionless parameter	v Volumetric flow rate
P_L'	$= uR_0/D_L'$. Dimensionless parameter	V Volume of vessel
P_{Lm}	$= uR_0/D_{Lm}$. Dimensionless parameter	V_b Volume of backmix flow region
P_R	$= uR_0/D_R$. Dimensionless parameter	V_d Volume of deadwater region
P_{Rm}	$= uR_0/D_{Rm}$. Dimensionless parameter	V_p Volume of plug flow region
\mathbf{q}	$= \sqrt{(1/4) + (p/\mathbf{P})}$	X Axial position measured from start of test section
q	$= \sqrt{(1/4) + (a_i^2/P_L P_R)}$	$x = X/R_0$. Dimensionless axial variable
R	Radial position	$\mathbf{x} = X/L$. Dimensionless axial variable
R_0	$= d_t/2$. Tube radius	$\delta(t)$ Dirac delta function, see reference (S20)
r	$= R/R_0$. Dimensionless radial position	ϵ Fraction voids in packed bed
r_c	Rates of chemical reaction, (moles/time-volume)	λ_1 Eigenvalue in Eq. (67c), (68c), and (69c)
$R(s)$	Lagrangian correlation coefficient	μ_1 Mean of tracer curve at measurement point (dimensionless)
N_{Re}	Reynolds number	$\Delta\mu_1 = \mu_{1m} - \mu_{10}$ Difference in means of the tracer curves at the two measurement points X_m and X_0
s	Time difference used in correlation coefficient	ν Kinematic viscosity of fluid
S	Source term, defined by Eq. (12)	σ^2 Variance of tracer curve at the measurement point (dimensionless)
S_c	Schmidt number	$\Delta\sigma^2 = \sigma_m^2 - \sigma_0^2$ Difference in variance of the tracer curve at the two measurement points X_0 and X_m
t	time	
\bar{t}	$= V/v$. Mean residence time of fluid in the system	
θ'	$= ut/R_0$. Dimensionless time	

ϕ	Tortuosity factor	measurement point or to the second of two measurement points;
	SUBSCRIPT	applies to X , x , and \mathbf{x}
a	Refers to entrance or upstream section	0 Refers to the injection point or the first of two measurement points;
b	Refers to exit or downstream section.	applies to X , x , and \mathbf{x}
e	Refers to end of test section; applies to X , x and \mathbf{x}	∞ Refers to the doubly infinite tube, the open vessel
m	Refers to the single	

TEXT REFERENCES

- A1. Acton, F. S., and Lapidus, L., *Ind. Eng. Chem.* **47**, 706 (1955).
A2. Adler, R. J., and Hovorka, R. B., "A Finite-Stage Model for Highly Asymmetric Residence-Time Distributions," Preprint 3, Second Joint Automatic Control Conference, Denver, Colorado, June, 1961.
A3. Aiba, S., *A.I.Ch.E. Journal* **4**, 485 (1958).
A3a. Allen, C. M., and Taylor, E. A., *Trans. Am. Soc. Mech. Eng.* **45**, 285 (1923).
A4. Ampilogov, I. E., Kharin, A. N., and Kurochkina, I. S., *Zh. Fiz. Khim.* **32**, 141 (1958).
A5. Amundson, N. R., *Ind. Eng. Chem.* **48**, 26 (1956).
A6. Aris, R., *Proc. Roy. Soc.* **A235**, 67 (1956).
A7. Aris, R., *Proc. Roy. Soc.* **A245**, 268 (1958).
A8. Aris, R., *Chem. Eng. Sci.* **9**, 266 (1959).
A9. Aris, R., *Chem. Eng. Sci.* **10**, 80 (1959).
A10. Aris, R., *Chem. Eng. Sci.* **11**, 194 (1959).
A11. Aris, R., *Proc. Roy. Soc.* **A252**, 538 (1959).
A12. Aris, R., *Proc. Roy. Soc.* **A259**, 370 (1960).
A13. Aris, R., *Can. J. Chem. Eng.* **40**, 87 (1962).
A14. Aris, R., and Amundson, N. R., *A.I.Ch.E. Journal* **3**, 380 (1957).
A15. Aris, R., and Amundson, N. R., *Chem. Eng. Sci.* **7**, 121 (1958).
A16. Aris, R., and Amundson, N. R., *Chem. Eng. Sci.* **9**, 250 (1958).
A17. Askins, J. W., Hinds, G. P., and Kunreuther, F., *Chem. Eng. Progr.* **47**, 401 (1951).
B1. Baldwin, L. V., and Walsh, T. J., *A.I.Ch.E. Journal* **7**, 53 (1961).
B2. Baron, T., *Chem. Eng. Progr.* **48**, 118 (1952).
B3. Bartok, W., Heath, C. E., and Weiss, M. A., *A.I.Ch.E. Journal* **6**, 685 (1960).
B4. Batchelor, G. K., and Townsend, A. A., in "Surveys in Mechanics" (G. K. Batchelor and R. M. Davies, eds.), p. 352. Cambridge Univ. Press, London and New York, 1965.
B5. Beran, M. J., *J. Chem. Phys.* **27**, 270 (1957).
B6. Bernard, R. A., and Wilhelm, R. H., *Chem. Eng. Progr.* **46**, 233 (1950).
B7. Bilous, O., and Amundson, N. R., *A.I.Ch.E. Journal* **1**, 513 (1955).
B8. Bilous, O., and Piret, E. L., *A.I.Ch.E. Journal* **1**, 480 (1955).
B9. Bilous, O., Block, H. D., and Piret, E. L., *A.I.Ch.E. Journal* **3**, 248 (1957).
B10. Bird, R. B., Stewart, W. E., and Lightfoot, E. N., "Transport Phenomena." Wiley, New York, 1959.
B11. Bischoff, K. B., *Chem. Eng. Sci.* **12**, 69 (1960).

- B12. Bischoff, K. B., *Chem. Eng. Sci.* **16**, 131 (1961).
B13. Bischoff, K. B., Ph.D. Dissertation, Illinois Inst. Technol., Chicago, 1961.
B14. Bischoff, K. B., and Levenspiel, O., *Chem. Eng. Sci.* **17**, 245, 257 (1962).
B15. Blackwell, R. J., An investigation of miscible displacement processes in capillaries. Paper presented at local section A.I.Ch.E. Meeting, Galveston, Texas, October, 1957.
B16. Blackwell, R. J., Laboratory studies of microscopic dispersion phenomena. Paper presented at A.I.Ch.E.—Soc. Petrol. Eng. Symp., San Francisco, California, Dec. 6, 1959.
B17. Blackwell, R. J., Rayne, J. R., and Terry, W. M., *J. Petrol. Technol.* **11**, 1 (1959).
B18. Blickle, T., and Kaldi, P., *Chem. Tech. (Berlin)* **11**, 181 (1959).
B19. Bournia, A., Coull, J., and Houghton, G., *Proc. Roy. Soc.* **A261**, 227 (1961).
B20. Bosworth, R. C. L., *Phil. Mag.* **39**, 847 (1948).
B21. Bosworth, R. C. L., *Phil. Mag.* **40**, 314 (1949).
B22. Brothman, A., Weber, A. P., and Barish, E. Z., *Chem. Met. Eng.* **50**, 111 (July, 1954); **50**, 107 (August, 1943); **50**, 113 (September, 1943).
B23. Brötz, W., *Chem.-Ing.-Tech.* **28**, 165 (1956).
- C1. Cairns, E. J., Ph.D. Dissertation, Univ. of California, Berkeley, 1959.
C2. Cairns, E. J., and Prausnitz, J. M., *Ind. Eng. Chem.* **51**, 1441 (1959).
C3. Cairns, E. J., and Prausnitz, J. M., *A.I.Ch.E. Journal* **6**, 400 (1960).
C4. Cairns, E. J., and Prausnitz, J. M., *A.I.Ch.E. Journal* **6**, 554 (1960).
C5. Cairns, E. J., and Prausnitz, J. M., *Chem. Eng. Sci.* **12**, 20 (1960).
C6. Carberry, J. J., *A.I.Ch.E. Journal* **4**, 13M (1958).
C7. Carberry, J. J., *Can. J. Chem. Eng.* **36**, 207 (1958).
C8. Carberry, J. J., and Wendel, M. M., *A.I.Ch.E. Journal* **9**, 129 (1963).
C9. Carberry, J. J., and Bretton, R. H., *A.I.Ch.E. Journal* **4**, 367 (1958).
C10. Carman, P. C., "Flow of Gases Through Porous Media." Academic Press, New York, 1956.
C11. Carrier, G. F., *Quart. Appl. Math.* **14**, 108 (1956).
C12. Chambré, P., *Appl. Sci. Res.* **A9**, 157 (1960).
C13. Chambré, P., *J. Chem. Phys.* **32**, 24 (1960).
C14. Chandrasekhar, S., *Rev. Mod. Phys.* **15**, 1 (1943).
C15. Cholette, A., and Blanchet, J., *Can. J. Chem. Eng.* **39**, 192 (1961).
C16. Cholette, A., and Cloutier, L., *Can. J. Chem. Eng.* **37**, 105 (1959).
C17. Cholette, A., Blanchet, J., and Cloutier, L., *Can. J. Chem. Eng.* **38**, 1 (1960).
C18. Cleland, F. A., and Wilhelm, R. H., *A.I.Ch.E. Journal* **2**, 489 (1956).
C19. Cloutier, L., and Cholette, A., private communication (1962).
C20. Converse, A. O., *A.I.Ch.E. Journal* **6**, 334 (1960).
C21. Corrsin, S., *Phys. Fluids* **1**, 42 (1958).
C22. Coste, J., Rudd, D., and Amundson, N. R., *Can. J. Chem. Eng.* **39**, 149 (1961).
C23. Croockewit, P., Honig, C. E., and Kramers, H., *Chem. Eng. Sci.* **4**, 111 (1955).
- D1. Damköhler, G., *Z. Elektrochem.* **43**, 1 (1937).
D2. Damköhler, G., in "Der Chemie-Ingenieur" Eucken, A. and Jakob, M., eds., Vol. III, Part I. Akad. Verlagsges., Leipzig, 1937.
D3. Danckwerts, P. V., *Appl. Sci. Res.* **A3**, 279 (1952).
D4. Danckwerts, P. V., *Chem. Eng. Sci.* **2**, 1 (1953).
D5. Danckwerts, P. V., *Research* **6**, 355 (1953).

- D6. Danckwerts, P. V., *Ind. Chemist* **3**, 102 (1954).
D7. Danckwerts, P. V., *Chem. Eng. Sci.* **7**, 116 (1957).
D8. Danckwerts, P. V., *Chem. Eng. Sci.* **8**, 93 (1958).
D9. Danckwerts, P. V., *Chem. Eng. Sci.* **9**, 78 (1958).
D10. Danckwerts, P. V., Jenkins, J. W., and Place, G., *Chem. Eng. Sci.* **3**, 26 (1954).
D11. Davidson, J. F., Farquharson, D. C., Picken, J. Q., and Taylor, D. C., *Chem. Eng. Sci.* **4**, 201 (1955).
D12. Deans, H. A., and Lapidus, L., *A.I.Ch.E. Journal* **6**, 656 (1960).
D13. Deissler, P. F., and Wilhelm, R. H., *Ind. Eng. Chem.* **45**, 1219 (1953).
D14. de Josselin de Jong, G., *Trans. Am. Geophys. Union* **39**, 67 (1958).
D15. de Maria, F., Longfield, J. E., and Butler, G., *Ind. Eng. Chem.* **53**, 259 (1961).
D16. Denbigh, K. G., *Trans. Faraday Soc.* **40**, 352 (1944).
D17. Denbigh, K. G., *Trans. Faraday Soc.* **43**, 648 (1947).
D18. Devyatov, B. H., and Bogatchev, A. N., *Zh. Prikl. Khim.* **24**, 1156 (1951).
D19. Dhanak, A. M., *A.I.Ch.E. Journal* **4**, 190 (1958).
D20. Dorweiler, V. P., and Fahien, R. W., *A.I.Ch.E. Journal* **5**, 134 (1959).
- E1. Ebach, E. A., and White, R. R., *A.I.Ch.E. Journal* **4**, 161 (1958).
E2. Eguchi, W., *Kagaku Soshi* **2**, 43 (1960).
E3. Einstein, H. A., Dissertation, Eidg. tech. Hochschule, Zürich, Switzerland, 1937.
E4. Elder, J. W., *J. Fluid Mech.* **5**, 544 (1959).
E5. Eldridge, J. W., and Piret, E. L., *Chem. Eng. Progr.* **46**, 290 (1950).
E6. Epstein, N., *Can. J. Chem. Eng.* **36**, 210 (1958).
E7. Evans, R. B., Watson, G. M., and Mason, E. A., *J. Chem. Phys.* **35**, 2076 (1961).
- F1. Fahien, R. W., Ph.D. Dissertation, Purdue University, Lafayette, Indiana, 1954.
F2. Fahien, R. W., and Smith, J. M., *A.I.Ch.E. Journal* **1**, 28 (1955).
F3. Fan, L., *Ind. Eng. Chem.* **52**, 921 (1960).
F4. Fan, L., and Bailie, R. C., *Chem. Eng. Sci.* **13**, 63 (1960).
F5. Flint, D. L., Kada, H., and Hanratty, T. J., *A.I.Ch.E. Journal* **6**, 325 (1960).
F6. Förster, T., and Geib, K. H., *Ann. Physik* [5] **20**, 250 (1934).
F7. Fowler, F. C., and Brown, G. G., *Trans. Am. Inst. Chem. Eng.* **39**, 491 (1943).
F8. Fox, E. A., and Gex, V. E., *A.I.Ch.E. Journal* **2**, 539 (1956).
F9. Froment, G. F., *Belg. Chem. Ind.* **24**, 619 (1959).
- G1. Giddings, J. C., *J. Chem. Phys.* **26**, 169 (1957).
G2. Giddings, J. C., and Eyring, H., *J. Chem. Phys.* **59**, 416 (1955).
G3. Gilles, E. D., and Hofmann, H., *Chem. Eng. Sci.* **15**, 328 (1961).
G4. Gilliland, E. R., and Mason, E. A., *Ind. Eng. Chem.* **41**, 1191 (1949).
G5. Gilliland, E. R., and Mason, E. A., *Ind. Eng. Chem.* **44**, 218 (1952).
G6. Gilliland, E. R., Mason, E. A., and Oliver, R. C., *Ind. Eng. Chem.* **45**, 1177 (1953).
G7. Gomezplata, A., and Shuster, W. W., *A.I.Ch.E. Journal* **6**, 454 (1960).
G8. Greenhalgh, R. E., Johnson, R. L., and Nott, H. D., *Chem. Eng. Progr.* **55**, 44 (February, 1959).
G9. Gutoff, E. B., *A.I.Ch.E. Journal* **6**, 347 (1960).

- H1. Hall, R. E., and Smith, J. M., *Chem. Eng. Progr.* **45**, 459 (1949).
H2. Ham, A., and Coe, H. S., *Chem. Met. Eng.* **19**, 663 (1918).
H3. Handlos, A. E., Kunstman, R. W., and Schissler, D. O., *Ind. Eng. Chem.* **49**, 25 (1957).
H4. Hanratty, T. J., Latinen, G. A., and Wilhelm, R. H., *A.I.Ch.E. Journal* **2**, 372 (1956).
H5. Harai, E., *Chem. Eng. (Tokyo)* **18**, 528 (1954).
H6. Hartman, M. E., Wevers, C. J. H., and Kramers, H., *Chem. Eng. Sci.* **9**, 80 (1958).
H7. Hawthorn, R. D., *A.I.Ch.E. Journal* **6**, 443 (1960).
H8. Hiby, J. W., and Schümmer, P., *Chem. Eng. Sci.* **13**, 69 (1960).
H9. Hinze, J. O., "Turbulence." McGraw-Hill, New York, 1959.
H10. Hofmann, H., quoted in Schoenemann, K., *Chem. Eng. Sci.* **8**, 161 (1958).
H11. Hofmann, H., *Chem. Eng. Sci.* **14**, 193 (1961).
H12. Horn, F., and Kuchler, L., *Chem.-Ing.-Tech.* **31**, 1 (1959).
H13. Hovorka, R. B., and Kendall, H. B., *Chem. Eng. Progr.* **56**, 58 (August, 1960).
H14. Hulburt, H., *Ind. Eng. Chem.* **36**, 1012 (1944).
H15. Hull, D. E., and Kent, J. W., *Ind. Eng. Chem.* **44**, 2745 (1952).
H16. Huntley, A. R., Glass, W., and Heigl, J. J., *Ind. Eng. Chem.* **53**, 381 (1961).
H17. Hyman, D., and Corson, W. B., *Ind. Eng. Chem. Process Design Develop.* **1**, 92 (1962).

J1. Jacques, G. L., and Vermeulen, T., *Univ. California Radiation Lab. Rept.* 8029 (1957).
J2. Jenney, T. M., *Chem. Eng.* **62**, 198 (December, 1955).
J3. Johnson, J. P., and Edwards, L. J., *Trans. Faraday Soc.* **45**, 286 (1949).
J4. Jones, R. W., *Chem. Eng. Progr.* **47**, 46 (1951).
J5. Jungers, J. C., Balaceanu, J. C., Coussemant, F., Eschard, F., Giraud, A., Hellin, M., Leprince, P., and Limido, G. E., "Cinétique chimique appliquée." Technip, Paris, 1958.

K1. Kampé de Fériet, J., *Ann. Soc. Sci. Bruxelles Ser. I.*, **59**, 145 (1939).
K2. Kandiner, H. J., *Chem. Eng. Progr.* **44**, 383 (1948).
K3. Katz, S., *Chem. Eng. Sci.* **9**, 61 (1958).
K4. Kawamura, S., Suzuki, E., and Saito, Y., *Chem. Eng. (Tokyo)* **21**, 91 (1957).
K4a. Keyes, J. J., *A.I.Ch.E. Journal* **1**, 305 (1955).
K5. King, G. W., *Ind. Eng. Chem.* **43**, 2475 (1951).
K6. Kirillov, N. I., *Zh. Priklad. Khim.* **13**, 978 (1940).
K7. Kirillov, N. I., *Zh. Priklad. Khim.* **18**, 381 (1945).
K8. Kirillov, N. I., and Smirnova, V. P., *J. Appl. Chem. USSR (Engl. Transl.)* **18**, 381 (1945); *Zh. Priklad. Khim.* **18**, 393 (1945).
K9. Kjaer, J., "Measurement and Calculation of Temperature and Conversion in Fixed-Bed Catalytic Converters." Gjellerups Forlag, Copenhagen, 1958.
K10. Klinkenberg, A., *J. Phys. Chem.* **59**, 1184 (1955).
K11. Klinkenberg, A., and Sjenitzer, F., *Chem. Eng. Sci.* **5**, 258 (1956).
K12. Klinkenberg, A., Krajenbrink, H. J., and Lauwerier, H. A., *Ind. Eng. Chem.* **45**, 1202 (1953).
K13. Kohl, J., and Newacheck, R. L., *Petrol. Engr.* **26**, D13 (1954).
K14. Kramers, H., and Alberda, G., *Chem. Eng. Sci.* **2**, 173 (1953).

- K15. Kramers, H., Baars, G. M., and Knoll, W. H., *Chem. Eng. Sci.* **2**, 35 (1953).
K16. Krongelb, S., and Strandberg, M. W. P., *J. Chem. Phys.* **31**, 1196 (1959).
- L1. Lamb, D. E., Manning, F. S., and Wilhelm, R. H., *A.I.Ch.E. Journal* **6**, 682 (1960).
L2. Lanneau, K. P., *Trans. Inst. Chem. Engrs. (London)* **38**, 125 (1960).
L3. Lapidus, L., and Amundson, N. R., *J. Phys. Chem.* **56**, 984 (1952).
L4. Latinen, G. A., Ph.D. Dissertation, Princeton Univ., Princeton, New Jersey, 1957.
L5. Lauwerier, H. A., *Appl. Sci. Res.* **A8**, 366 (1959).
L6. Leclerc, V. R., *Chem. Eng. Sci.* **2**, 213 (1953).
L7. Lee, J. C., *Chem. Eng. Sci.* **12**, 191 (1960).
L8. Lessells, G. A., *Chem. Eng.* **64**, 251 (August, 1957).
L9. Leva, M., "Fluidization." McGraw-Hill, New York, 1959.
L10. Levenspiel, O., *Ind. Eng. Chem.* **50**, 343 (1958).
L11. Levenspiel, O., *Petrol. Refiner* **37**, 191 (1958).
L12. Levenspiel O., *Can. J. Chem. Eng.* **40**, 135 (1962).
L13. Levenspiel, O., "Chemical Reaction Engineering." Wiley, New York, 1962.
L13a. Levenspiel, O., *Chem. Eng. Sci.* **17**, 575 (1962).
L14. Levenspiel, O., and Bischoff, K. B., *Ind. Eng. Chem.* **51**, 1431 (1959).
L15. Levenspiel, O., and Bischoff, K. B., *Ind. Eng. Chem.* **53**, 314 (1961).
L16. Levenspiel, O., and Smith, W. K., *Chem. Eng. Sci.* **6**, 227 (1957).
L17. Lewis, W. K., Gilliland, E. R., and Glass, W., *A.I.Ch.E. Journal* **5**, 419 (1959).
L18. Liles, A. W., and Geankoplis, C. J., *A.I.Ch.E. Journal* **6**, 591 (1960).
L19. Longwell, J. P., and Weiss, M. A., *Ind. Eng. Chem.* **45**, 667 (1953).
L20. Lynn, S., Corcoran, W. H., and Sage, B. H., *A.I.Ch.E. Journal* **3**, 11 (1957).
- M1. MacDonald, R. W., and Piret, E. L., *Chem. Eng. Progr.* **47**, 363 (1951).
M2. MacMullin, R. B., and Weber, M., *Trans. Am. Inst. Chem. Engrs.* **31**, 409 (1935).
M3. MacMullin, R. B., and Weber, M., *Chem. Met. Eng.* **42**, 254 (1935).
M4. McHenry, K. W., and Wilhelm, R. H., *A.I.Ch.E. Journal* **3**, 83 (1957).
M5. Mason, D., and Piret, E. L., *Ind. Eng. Chem.* **42**, 817 (1950).
M6. Mason, D., and Piret, E. L., *Ind. Eng. Chem.* **43**, 1210 (1951).
M7. Mathis, J. F., and Watson, C. C., *A.I.Ch.E. Journal* **2**, 518 (1956).
M8. May, W. G., *Chem. Eng. Progr.* **55**, 49 (1959).
M9. Metzner, A. B., and Pigford, R. L., in "Scale-Up in Practice" (R. Fleming, ed.), p. 16. Reinhold, New York, 1958.
M10. Metzner, A. B., and Taylor, J. S., *A.I.Ch.E. Journal* **6**, 109 (1960).
M11. Mickelson, W. R., *Natl. Advisory Comm. Aeron. Tech. Note* 3570 (1955).
M12. Mott, R. A., in "Some Aspects of Fluid Flow." (H. R. Lang, ed.) Arnold, London, 1951.
M13. Muchi, I., Mamuro, T., and Sasaki, K., *Chem. Eng. (Tokyo)* **25**, 747 (1961).
- N1. Nagata, S., Eguchi, W., Inamura, T., Tanigawa, K., and Tanaka, T., *Chem. Eng. (Tokyo)* **17**, 387 (1953).
N2. Nagata, S., Eguchi, W., Kasai, H., and Morino, I., *Chem. Eng. (Tokyo)* **21**, 784 (1957).
N3. Norwood, K. W., and Metzner, A. B., *A.I.Ch.E. Journal* **6**, 432 (1960).

- O1. Opfell, J. B., and Sage, B. H., *Advan. Chem. Eng.* **1**, 241 (1956).
- P1. Pai, S., "Viscous Flow Theory," Vol. II. Van Nostrand, Princeton, New Jersey, 1957.
- P2. Paneth, F., and Herzfeld, K. F., *Z. Elektrochem.* **37**, 577 (1931).
- P3. Pansing, W. F., *A.I.Ch.E. Journal* **2**, 71 (1956).
- P4. Pearson, J. R. A., *Chem. Eng. Sci.* **10**, 281 (1959).
- P5. Petersen, E. E., *A.I.Ch.E. Journal* **6**, 488 (1960).
- P6. Plautz, D. A., and Johnstone, H. F., *A.I.Ch.E. Journal* **1**, 193 (1955).
- P7. Prager, S., *Chem. Eng. Progr. Symp. Ser.* **25**, 55, 11 (1959).
- P8. Prager, S., *J. Chem. Phys.* **33**, 122 (1960).
- P9. Prausnitz, J. M., Ph.D. Dissertation, Princeton University, Princeton, New Jersey, 1955.
- P10. Prausnitz, J. M., *A.I.Ch.E. Journal* **4**, 14M (1958).
- P11. Prausnitz, J. M., and Wilhelm, R. H., *Rev. Sci. Instr.* **27**, 941 (1956).
- P12. Prausnitz, J. M., and Wilhelm, R. H., *Ind. Eng. Chem.* **49**, 979 (1957).
- R1. Ranz, W. E., *Chem. Eng. Progr.* **48**, 247 (1952).
- R2. Reman, G. H., *Chem. Ind. (London)* p. 46 (1955).
- R3. Roberts, P. H., *J. Fluid Mech.* **11**, 257 (1960).
- R4. Robinson, W. G., Univ. California Radiation Lab. Rept. 9193 (1960).
- R5. Rosen, J. B., and Winsche, W. E., *J. Chem. Phys.* **18**, 1587 (1950).
- S1. Saffman, P. G., *J. Fluid Mech.* **6**, 321 (1959).
- S2. Saffman, P. G., *Chem. Eng. Sci.* **11**, 125 (1959).
- S3. Saffman, P. G., *J. Fluid Mech.* **7**, 194 (1960).
- S4. Schechter, R. S., and Wissler, E. H., *Appl. Sci. Res.* **A9**, 334 (1960).
- S5. Schechter, R. S., and Wissler, E. H., private communication (1961).
- S6. Scheidegger, A. E., "The Physics of Flow Through Porous Media." Macmillan, New York, 1960.
- S7. Scheidegger, A. E., *Can. J. Phys.* **39**, 1573 (1961).
- S8. Schlinger, W. G., and Sage, B. H., *Ind. Eng. Chem.* **45**, 657 (1953).
- S9. Schoenemann, K., *Dechema. Monograph* **21**, 203 (1952).
- S10. Schoenemann, K., and Hofmann, H., *Chem.-Ing.-Tech.* **29**, 665 (1957).
- S11. Schwartz, C. E., and Smith, J. M., *Ind. Eng. Chem.* **45**, 1209 (1953).
- S12. Shen, C. Y., and Johnstone, H. F., *A.I.Ch.E. Journal* **1**, 349 (1955).
- S13. Sherwood, T. K., *Chem. Eng. Progr.* **51**, 303 (1955).
- S14. Sherwood, T. K., and Woertz, B. B., *Ind. Eng. Chem.* **31**, 1034 (1939).
- S15. Shipley, J. R., *Pipe Line News* **23**, 31 (December, 1951).
- S16. Sinclair, G. G., *A.I.Ch.E. Journal* **7**, 709 (1961).
- S17. Singer, E., Todd, D. B., and Guinn, V. P., *Ind. Eng. Chem.* **49**, 11 (1957).
- S18. Sjenitzer, F., *Petrol. Engr.* **30**, D31 (1958).
- S19. Smith, S. S., and Schultz, R. K., *Petrol. Engr.* **19**, 94 (1948); **20**, 330 (1948).
- S20. Sneddon, I. N., "Fourier Transforms." McGraw-Hill, New York, 1951.
- S21. Spaulding, D. B., *Chem. Eng. Sci.* **9**, 74 (1958).
- S22. Standart, G. L., *Ind. Eng. Chem.* **48**, 1228 (1956).
- S23. Stead, B., Page, F. M., and Denbigh, K. G., *Discussions Faraday Soc.* **2**, 263 (1947).
- S24. Strang, D. A., and Geankoplis, C. J., *Ind. Eng. Chem.* **50**, 1305 (1958).

- T1. Taylor, G. I., *Proc. London Math. Soc.* **20**, 196 (1921).
T2. Taylor, G. I., *Proc. Roy. Soc.* **A219**, 186 (1953).
T3. Taylor, G. I., *Appl. Mech. Rev.* **6**, 265 (1953).
T4. Taylor, G. I., *Proc. Roy. Soc.* **A223**, 446 (1954).
T5. Taylor, G. I., *Proc. Roy. Soc.* **A225**, 473 (1954).
T6. Taylor, G. I., *Proc. Phys. Soc. (London)* **B67**, 857 (1954).
T7. Tichacek, L. J., Selectivity in experimental reactors. Paper presented at A.I.Ch.E. Meeting, San Francisco, California, 1959.
T8. Tichacek, L. J., Barkelew, C. H., and Baron, T., *A.I.Ch.E. Journal* **3**, 439 (1957).
T9. Towle, W. L., and Sherwood, T. K., *Ind. Eng. Chem.* **31**, 457 (1939).
T10. Trambouze, P. J., *Rev. Inst. Franc. Petrole Ann. Combust. Liquides* **15**, 1948 (1960).
T11. Trambouze, P. J., *Genie Chim.* **84**, 189 (1960).
T12. Trambouze, P. J., and Piret, E. L., *A.I.Ch.E. Journal* **5**, 384 (1959).
T13. Trawinski, H., *Chem.-Ing.-Tech.* **23**, 416 (1951).
T14. Turner, G. A., *Chem. Eng. Sci.* **1**, 156 (1958).
T15. Turner, G. A., *Chem. Eng. Sci.* **10**, 14 (1959).

V1. Van Deemter, J. J., *Chem. Eng. Sci.* **13**, 143 (1961).
V2. Van Deemter, J. J., *Chem. Eng. Sci.* **13**, 190 (1961).
V3. Van Deemter, J. J., Broeder, J. J., and Lauwerier, H. A., *Appl. Sci. Res.* **A5**, 374 (1956).
V4. Van der Laan, E. T., *Chem. Eng. Sci.* **7**, 187 (1958).
V5. Van de Vusse, J. G., *Chem. Eng. Sci.* **4**, 178, 209 (1955).
V6. Van Krevelen, D. W., *Chem.-Ing.-Tech.* **30**, 553 (1958).
V7. Von Rosenberg, D. V., *A.I.Ch.E. Journal* **2**, 55 (1956).

W1. Wakao, N., Oshima, T., and Yagi, S., *Chem. Eng. (Tokyo)* **22**, 786 (1958).
W2. Walker, R. E., *Phys. Fluids* **4**, 1211 (1961).
W3. Weber, A. P., *Chem. Eng. Progr.* **49**, 26 (1953).
W4. Wehner, J. F., and Wilhelm, R. H., *Chem. Eng. Sci.* **6**, 89 (1956).
W5. Westhaver, J. W., *Ind. Eng. Chem.* **34**, 126 (1942).
W6. Westhaver, J. W., *Ind. Eng. Chem.* **39**, 706 (1947).
W7. Westhaver, J. W., *J. Res. Natl. Bur. Std.* **38**, 169 (1947).
W8. Wicke, E., *Chem. Eng. Sci.* **6**, 160 (1957).
W9. Wicke, E., and Trawinski, H., *Chem.-Ing.-Tech.* **25**, 114 (1953).
W10. Wilhelm, R. H., *Chem. Eng. Progr.* **49**, 150 (1953).
W11. Wissler, E. H., and Schechter, R. S., *Appl. Sci. Res.* **A10**, 198 (1961).
W12. Wood, J. C., Whittemore, E. R., and Badger, W. L., *Chem. Met. Eng.* **27**, 1176 (1922).

Y1. Yagi, S., and Miyauchi, T., *Chem. Eng. (Tokyo)* **17**, 382 (1953).
Y2. Yagi, S., and Miyauchi, T., *Chem. Eng. (Tokyo)* **19**, 507 (1955).
Y3. Young, E. F., *Chem. Eng.* **64**, 241 (1957).

Z1. Zenz, F. A., and Othmer, D. F., "Fluidization and Fluid Particle Systems." Reinhold, New York, 1960.
Z2. Zwietering, T. N., *Chem. Eng. Sci.* **11**, 1 (1959).

PROPERTIES OF COCURRENT GAS-LIQUID FLOW

Donald S. Scott

Department of Chemical Engineering
University of British Columbia
Vancouver, British Columbia, Canada

I. Introduction to Two-Phase Gas-Liquid Flow Processes	200
A. Importance and Scope of Cocurrent Two-Phase Flow Applications ...	200
B. Characteristics of Two-Phase Flow	201
C. Variables Governing Two-Phase Transport Processes	202
D. Present Status of Investigations	203
II. Descriptions of Two-Phase Gas-Liquid Cocurrent Flow	204
A. Introduction	204
B. Flow Patterns in Horizontal Tubes	207
C. Flow Patterns in Vertical Tubes	210
D. Flow Regimes in Two-Phase Flow	213
III. Pressure Drop and Holdup	214
A. General	214
B. Momentum and Energy Balances	214
C. Physical Significance of Balances in Two-Phase Flow	217
IV. Correlating Methods for Two-Phase Pressure Drops and Void Fractions	220
A. Introduction	220
B. Lockhart-Martinelli and Martinelli-Nelson Correlations	220
C. Chenoweth and Martin Correlation	225
D. "Friction-Factor" Methods	226
E. Other Correlation Models	228
V. Mechanics of Specific Flow Patterns	233
A. Slug Flow	233
B. Bubble Flow	241
C. Annular (Climbing-Film) and Dispersed Flow	246
D. Stratified and Wave Flow	252
VI. Heat Transfer to Two-Phase Mixtures	254
A. Description of Boiling in Tubes	254
B. Correlations of Forced Convection Heat-Transfer Coefficients for Two-Phase Flow	259
C. Burn-out in Film Flow	263
VII. Mass Transfer in Cocurrent Gas-Liquid Flow	265
A. General	265
B. Vertical Flow	266
C. Horizontal Flow	267
VIII. Miscellaneous Considerations	270
A. Flow of Two Liquid Phases and a Gas Phase	270
B. Flow in Inclined Tubes	271
C. Two-Phase Flow in Long Pipelines	271
Nomenclature	272
References	273

I. Introduction to Two-Phase Gas-Liquid Flow Processes

A. IMPORTANCE AND SCOPE OF COCURRENT TWO-PHASE FLOW APPLICATIONS

The problems of two-phase gas-liquid flow in pipe lines have become of greater concern to engineers in recent years. This type of flow is encountered in an increasing number of important situations, and a clear understanding of the rates of transfer of momentum, heat, and material will be required for logical and careful design and operation of a very wide variety of chemical engineering equipment and processes.

In the production and transport of crude petroleum and petroleum products, two-phase flow is finding increasing use. Apart from the obvious economies in pipe line construction, it is possible in oil field practice by using two-phase flow to centralize gas processing, crude oil, or condensate stabilization facilities, thus giving improved economics. Two-phase flow is also encountered extensively in the operation of heat-transfer equipment, such as steam generators, refrigeration equipment, evaporators, and partial condensers. Heat removal from nuclear reactors is an important recent application of two-phase heat transfer. The use of cocurrent gas-liquid contacting in chemical reactors is entirely practical when pure gas is used as a reactant, or when an irreversible chemical reaction is occurring in the liquid phase. A growing number of such potential applications can be found in the organic and metallurgical processing industries.

In many of these operations the engineer is concerned primarily with prediction of pressure losses. However, the heat transfer rate through the tube wall into the gas or the liquid phase is also of major concern in heat-exchange equipment. In the design of chemical reactors for heterogeneous gas-liquid systems, it is necessary to be able to predict not only pressure drops and rates of heat transfer into or out of the channel, but also the rates of mass transfer from the gas into the liquid phase.

Although all the information necessary to accomplish the above purposes is far from being readily available, it will be shown in the succeeding sections that a reasonable beginning has been made in the understanding, and therefore in the correlating, of transport processes in two-phase gas-liquid flow.

Two-phase flow systems may be classified initially by composition, as containing a single component (a pure liquid and its vapor), or two or more components with any one component present in both phases or only essentially in one or the other phase. Systems may further be described as involving transfer of mass between phases, or otherwise; and as isothermal, or adiabatic, or as having some intermediate temperature behavior.

B. CHARACTERISTICS OF TWO-PHASE FLOW

An outstanding feature of two-phase cocurrent flow is the variety of possible flow patterns, ranging all the way from a small quantity of gas dispersed as bubbles in a continuous liquid medium, to the opposite extreme of a small amount of liquid dispersed as droplets in a continuous gas stream. The importance of these flow patterns can be shown when one plots the rate of a transport process as a function of a flow rate of one phase while the flow rate of the second phase is maintained constant. The flux will be found not merely to increase or decrease in a smooth fashion, but rather to show in different flow ranges minima or maxima demonstrating the presence of fundamentally different transfer processes. A comprehensive understanding of the flow processes is necessary before the nature of the flow pattern can be predicted for any given set of flow conditions.

The apparent visual changes in flow pattern may not always coincide with an observed change in transport behavior. In addition, unstable regions of transition exist between one flow pattern and the next, making precise definition of these patterns based on visual appearance alone extremely difficult. At identical values of the flow variables, it is sometimes possible to have two distinctly different flow patterns depending on such factors as the inlet arrangement. Presumably one of these configurations is unstable, but its transition to the more stable pattern may not be observable within the limited scale of an experimental apparatus. Further, the pattern must vary not only with flow rates and fluid properties, but must depend also on the flow geometry as given by the pipe diameter and inclination.

A well-known fact regarding two-phase cocurrent flow is that the gas and liquid velocities are rarely equal, although this may be assumed as an approximation in certain cases. If the gas and liquid velocities are not equal, and it has been shown that they can differ widely, then the volume fraction of a component flowing in the pipe will not be the same as the volume fraction of that component in the feed at the inlet. Thus the volume fraction is an unknown, which must depend on the same variables that govern flow pattern. A knowledge of this fraction of pipe volume filled by each fluid is necessary in many instances, e.g., in estimating steam quality, in neutron-capture calculations, or in determining an average fluid density.

When one refers to the *in situ* gas-volume fraction, R_G , the term "void fraction" is commonly used. The "holdup ratio," (H_R), is a related quantity, and is defined as the ratio of the gas-liquid volume ratio in the feed to the gas-liquid volume ratio in the flow section. Analogous to these

terms is the use of "slip velocity" (V_s') which is the difference in the actual average lineal velocities of the gas and the liquid phases.

These quantities may all be related by the following expressions,

$$\text{Void Fraction} = R_G = 1 - R_L = \frac{1}{\frac{H_R Q_L}{Q_G} + 1} = \frac{1}{\frac{H_R G_L \rho_G}{G_G \rho_L} + 1} \quad (1)$$

$$\begin{aligned} \text{Slip velocity} = V_s' &= V_G' - V_L' = \frac{V_G}{R_G} - \frac{V_L}{1 - R_G} \\ &= \frac{G_G}{\rho_G R_G} - \frac{G_L}{\rho_L (1 - R_G)} = \frac{H_R V_L}{(1 - R_G)} - 1 \end{aligned} \quad (2)$$

The flow behavior which is observed is generally of a highly mixed character, that is, in only a few cases could it be called reasonably homogeneous. Bubbles, plugs, or slugs of gas or of liquid are usually found in the various flow patterns. Therefore, although it may be necessary and convenient to treat two-phase flow as a continuum having average properties, such an approach can only be considered a rather arbitrary approximation.

When two-phase flow is compared to the single-phase case for the same flow rate of an individual phase, it is an experimental fact that the frictional pressure drop will always be higher for two-phase flow. This higher pressure drop may be caused by the increased velocity of the phases due to the reduction in cross-sectional area available for flow, and also to interactions occurring at the extended gas-liquid interface which exists in most of the possible flow patterns. It is equally true that the heat flux will always be higher for two-phase flow than for the same situation in single-phase flow with the same liquid flow rate. On the other hand, mass transfer will depend upon both the extent of the gas-liquid interface and the relative velocity between the two flowing phases.

C. VARIABLES GOVERNING TWO-PHASE TRANSPORT PROCESSES

The independent variables involved in the simultaneous flow of gas and liquid phases are the viscosities, densities, and mass flows of the individual phases and the interfacial tension between the two phases. To these variables the channel diameter and shape must be added, and the inclination; for horizontal flow the acceleration of gravity must be considered, and in vertical flow the elevation will be a factor. Finally, tube roughness may be an important variable.

When heat transfer is to be considered, one must add to the above variables the thermal properties of each phase, such as thermal conductivity and specific heat, and the temperature profiles of the system. When

mass transfer is taking place, additional factors will be the diffusion coefficient in each phase of each component to be transferred, the concentration of each component in each phase, and equilibrium relationships between phases for each component. This very large number of factors makes it clear that a universal or general correlation for any transport process would be very complex. However, the possibility exists that certain of the variables given are of little significance, at least over limited ranges which may be of definite practical importance; this appears to be the case with respect to gas-phase viscosity and to surface tension in momentum transfer. There is not yet a sufficiently good theoretical understanding to allow confident prediction of the variables that will be most significant in any given set of circumstances.

D. PRESENT STATUS OF INVESTIGATIONS

In the years since 1940, a voluminous literature has appeared on the subject of two-phase cocurrent gas-liquid flow. Most of the work reported has been done in restricted ranges of gas or liquid flow rates, fluid properties, and pipe diameter, and has usually been specific to horizontal or vertical pipe lines. The studies have in most instances been isothermal when two components were being considered; nonisothermal cases were almost entirely single-component two-phase situations. Reports of investigations of two-phase two-component cocurrent flow where one component is being transferred across the interphase boundary are nearly nonexistent.

The primary purpose of most of the investigations was to arrive at workable correlations for the calculation of pressure drops, or for estimating heat fluxes. In some instances, flow patterns and their dependence on system variables have been investigated, usually visually; in other cases, little attention has been paid to this aspect. Many of the correlations or relationships proposed are specifically limited to specific flow patterns. In the main, the interpretation of results has been from a macroscopic viewpoint, and has involved varying degrees of empiricism. Since 1955, however, an increasing effort has been made to gain a basic understanding of the mechanics of various two-phase flow patterns, and to apply this information to develop sound transport equations.

Govier and Omer, in a recent article in the *Canadian Journal of Chemical Engineering*, have summarized the present (G4) state of knowledge concerning the calculation of pressure drop and other quantities in two-phase flow: "The principal flow patterns are understood in a qualitative way and the effect on flow pattern of the major variables, mainly the lineal or mass velocities of the phases, is recognized. In nearly all cases the real significance of the viscosities of the phases, the possible separate roles of the densities of the phases, and the influence of the diameter of the pipe is not known.

"Extensive experimental data confirm the fact that the pressure drop for a two-phase system is influenced by the flow pattern, and indicate the need either for separate pressure drop correlations for each flow pattern, or for the incorporation into a master pressure drop correlation of these variables which in fact define the flow pattern.

"A large number of correlations are available for the prediction of the pressure drop attending two-phase flow in terms of the major variables affecting it. Each of these has its own shortcomings, being restricted to certain flow patterns, to gases of specified densities, to certain ranges of liquid flow rates, to certain diameters of pipe, or the like. There is as yet no generally satisfactory universal correlation.

"Only a limited number of attempts have been made to correlate the liquid hold-up or the equivalent in the pipe. Again it seems clear that the liquid hold-up will be significantly influenced by the flow pattern, and that either separate correlations will be required for each flow pattern, or a master correlation incorporating those variables which influence flow pattern will need to be developed. With one or two exceptions the few existing correlations suffer from the same kind of disadvantage as those for the prediction of pressure drop."

In the following sections, major emphasis has been placed on recent literature, appearing in the years 1955-62. The term "literature" means those technical journals in which research or experimental conclusions are commonly published; much excellent data, and many useful correlations and observations, are available only in theses, or in institutional, industrial, or government reports. Although reports of this type which contain unique results are included in the present discussion, a deliberate attempt has been made to give priority in discussion to those articles which have been most widely circulated and are therefore most readily available.

Three major reviews exist which give detailed coverage of the literature available up to about 1955. In particular, the review by Gresham *et al.* (G7) may be consulted for empirical correlations limited to specific flow patterns, and the papers by Isbin *et al.* (I1) and by Bennett (B9) are particularly valuable for aspects of two-phase flow related to steam-water systems. Bennett has also given useful tabulations of available correlations (up to 1957) for the estimation of two-phase pressure drops.

II. Descriptions of Two-Phase Gas-Liquid Cocurrent Flow

A. INTRODUCTION

It is necessary to distinguish at the outset between a physical or visual description of the state of flow in two-phase mixtures, and a phenomenological one. A large variety of flow patterns which differ in visual appearance are possible; however, a change in the appearance does not necessarily mean that a significant change has also occurred in the basic mechanism whereby momentum, heat, or material is being transferred. For example, various flow patterns involving gas dispersed in a continu-

REFERENCE	PRESSURE		DROP		REGIME		IV	
	I		II		III			
GOSLINE '936	— GAS — DISPERSED	— GAS — 	PISTON	LIQUID	SLUG	— — 	ANNULAR	— — LIQUID DISPERSED
CROMER and HUNTINGTON 1940	— BUBBLE — 	PISTON	and SLUG	— — 	FROTH	— — 	ANNULAR	— —
MARTINELLI et al 1944	LIQUID VISCIOUS — GAS VISCIOUS		LIQUID VISCIOUS — GAS TURBULENT		LIQUID	TURBULENT — GAS	TURBULENT	— —
BERGELIN 1949	— BUBBLE — 		SLUGGING				ANNULAR	— —
RADFORD 1949	— SLUGGING —			MIXED FROTHY		WALL FILM		— — MIST
DUNN 1952	— SLUG —			FROTH		ANNULAR	FILM	— — MIST
CALVERT and WILLIAMS 1955	— AERATED — 	PISTON		CHURN		WAVE ENTRAINMENT	ANNULAR	— — DROP ENTRAINMENT
GALEGAR et al 1956	— AERATED — 	SLUG		TURBULENT		SEMI-ANNULAR	ANNULAR	— —
GOVIER et al 1957	— BUBBLE — 	SLUG		FROTH		RIPPLE	FILM	— — MIST

Fig. 1. Examples of flow pattern terminology for vertical cocurrent flow [after Govier *et al.* (G6)].

ous liquid phase (or vice versa) might well be supposed to have much in common from a phenomenological viewpoint, however much they may differ in appearance. The large number of correlations which have been proposed by various workers have been based on one or the other of these classifications.

A reasonable organization of flow types on the basis of the mechanism of transport requires detailed theoretical analysis and extensive data. Perhaps for this reason, the majority of investigators with less comprehensive data have adhered to a classification based on visual observation of flow patterns. In the following sections both types of flow description will be used, and defined, with "pattern" referring to visual observations, and "type" or "regime" being applied to flow behavior which can be described by more quantitative expressions.

The problem of two-phase-flow classification is complicated by the inevitable differences due to individual interpretations of visual observations, and also by differences in terminology. Fig. 1, taken from the work of Govier *et al.* (G6), shows the variation in terminology used for vertical gas-liquid flow patterns. It includes a classification of flow regimes proposed by Govier *et al.* based on pressure-drop behavior rather than visual observations, as illustrated in Fig. 2. In the definitions adopted by the writer, which follow, an attempt has been made to select the most

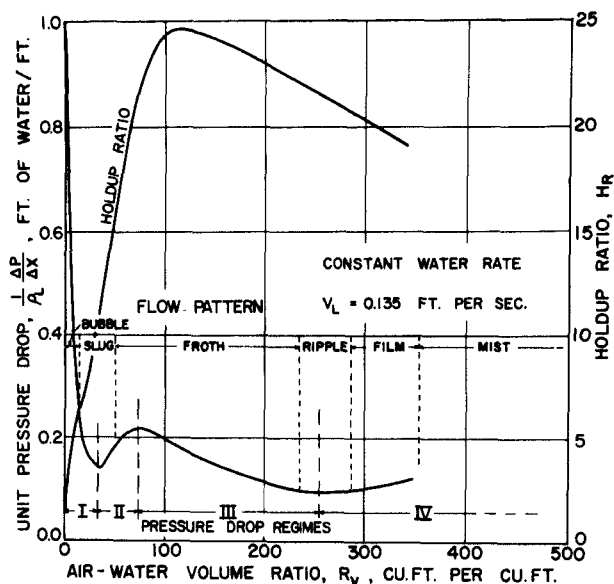


FIG. 2. Typical pressure drops, flow patterns, and flow regimes in vertical cocurrent air-water flow [after Govier *et al.* (G6)].

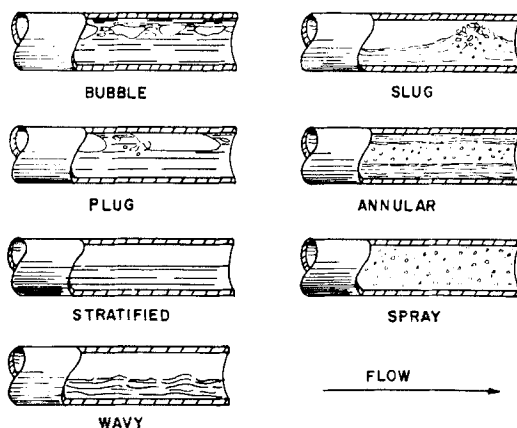


FIG. 3. Flow patterns in horizontal flow.

easily definable flow patterns, and to use the most widely preferred terminology.

B. FLOW PATTERNS IN HORIZONTAL TUBES

1. Visual Appearance

The classification made by Alves (A1) for two-phase flow in horizontal tubes appears to describe adequately the majority of flow patterns for this case. The following patterns are clearly observable, and are shown sketched in Fig. 3.

(a) *Bubble flow.* Discrete gas bubbles move along the upper surface of the pipe at approximately the same velocity as the liquid. At high liquid rates, bubbles may be dispersed throughout the liquid, a pattern often referred to as *froth flow*.

(b) *Plug flow.* The gas bubbles tend to coalesce as gas flow rate increases, to form gas plugs which may fill a large part of the cross-sectional area of smaller tubes.

(c) *Stratified flow.* Complete stratification of gas and liquid, with the gas occupying a constant fraction of the cross-sectional area in the upper portion of pipe, over a smooth liquid-gas interface. It occurs at lower liquid rates than bubble or plug flow, and more readily in larger tubes.

(d) *Wavy flow.* Increasing gas rate produces waves of increasing amplitude at the stratified gas-liquid interface, because of the higher gas velocity.

(e) *Slug flow.* Wave amplitudes increase to seal the tube, and the liquid wave is picked up by the rapidly moving gas to form a frothy slug which passes through the pipe at a much greater velocity than the average

liquid velocity. Slug flow is also formed from plug flow as the gas flow rate is increased at constant liquid rate.

(f) *Annular flow*. Gravitational forces become less important than interphase forces, and the liquid is mainly carried as a thin film along the tube wall. The gas moves at a high velocity in the core of the tube and carries with it some of the liquid as a spray. *Film flow* is a name also applied to this pattern.

(g) *Mist or spray flow*. More and more liquid is carried in the gaseous core at the expense of the annular film, until nearly all of the liquid is entrained in the gas. This pattern has also been called *dispersed flow* or *fog flow*.

At a constant low liquid-flow rate with steadily increasing gas flow, the patterns observed will tend to be stratified, wavy, annular and mist flow. At a somewhat higher liquid rate, stratified, plug, slug, annular, and mist flow occur; while at high liquid flows the patterns follow the order bubble, plug, slug, annular, and mist, as gas flow increases.

2. Prediction of Flow Patterns

A number of attempts have been made to prepare charts which would allow prediction of the state of flow from a knowledge of flow variables. Such charts usually take the form of a set of curves outlining regions in which various flow patterns might be expected to occur. Kosterin (K3) Hoogendoorn (H6, H7) and Hughes *et al.* (H10) used the volumetric fraction of the gas fed as ordinate and the mixture velocity as abscissa. Bergelin and Gazley (B12) Johnson and Abou-Sabe (J2) and Govier and Omer (G4) defined the flow patterns by plotting liquid superficial mass-velocity against gas superficial mass-velocity. Alves (A1) plotted superficial gas and liquid velocities. Baker (B2) used the data of Kosterin (K2), Bergelin (B12), and Alves (A1) and plotted gas mass-velocity against the liquid-to-gas mass-velocity ratio of the feed. Correction factors for fluids of differing densities, viscosities, and surface tensions were introduced in an empirical way. Flow-pattern diagrams of the types used by Baker and others serve a very useful purpose, in allowing designers to predict the nature of the flow pattern that might be expected in a given case, and thus to select the most suitable correlation for calculation of transport fluxes. The boundaries on these charts represent transition zones, often rather broad, between the clearly observable flow patterns.

Tube diameter is clearly an important factor, as one can easily appreciate by considering wave flow in a small-diameter pipe where this pattern can hardly exist, and the same situation in a large-diameter pipe where conditions must approach those of a free liquid surface. Since the

existing correlations are not entirely dimensionless, it may prove possible to introduce this term explicitly. Apparently, the only investigation of flow patterns which has considered to some extent the effect of all variables is that of Hoogendoorn (H6) and Hoogendoorn and Buitelaar (H7). In this work, it was stated that all gas-oil mixture patterns could be represented approximately by a single chart for tube sizes greater than about 1-in. in inside diameter. This same chart could also be used for gas-water mixtures by enlarging the wave pattern area. Additional charts were given for the flow of Freon 11 vapor and liquid, and also for Freon-water flow (H7).

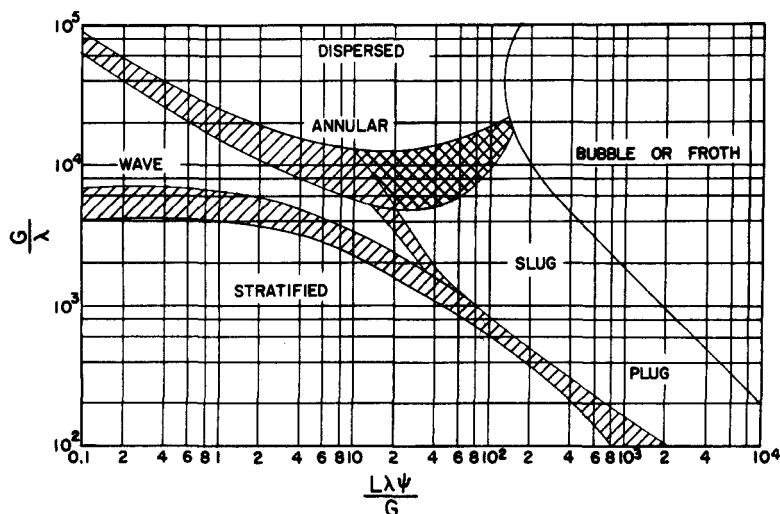


FIG. 4. Suggested flow pattern map for horizontal cocurrent flow (modified from that of Baker).

The shape of the areas on the charts presented by Hoogendoorn is not particularly convenient, as fairly extensive and important ranges of flow behavior tend to be squeezed together in a small area of the plot. Plots given on a weight basis seem to yield a more equable arrangement of flow areas than do those on a volume basis. In Fig. 4, the type of chart given by Baker is reproduced, incorporating modifications to improve somewhat the agreement with the recent data of Hoogendoorn (H6) and of Govier and Omer (G4). The wave-flow area may be somewhat less extensive than shown when oils are the flowing liquids, and somewhat greater than shown for water. For pipes having a diameter less than one inch, the extent of the areas shown will tend to change rapidly as diameters decrease.

The empirical correction factors

$$\lambda = \left(\frac{\rho_G}{0.075} \right) \left(\frac{\rho_L}{62.3} \right)^{0.5}$$

(for variations in densities) and

$$\psi = \left(\frac{73}{\sigma} \right) \left[\mu_L \left(\frac{62.3}{\rho_L} \right)^2 \right]^{1/3}$$

(for surface tension and liquid viscosity) have not been completely verified and may not in fact be the correct parameters. For example, work by Kosterin and Rubinovitch (K4) and others indicates that the flow pattern shows very little dependence on surface tension unless emulsification results. Qualitative agreement with the flow-pattern areas on this chart has been shown by Wickes and Dukler (W2) and Davis and David (D2) for annular and mist flow, by Kordyban (K1) for slug flow, and by Reid *et al.* (R1) for larger pipe diameters. Hoopes (H8) has used this type of chart for downward flow in an annulus. Isbin and co-workers (I7) have shown revisions to the Baker plot to give better agreement of the flow patterns in froth, annular, or mist flow, with their results for steam-water mixtures over wide ranges of temperature and pressure.

On recalculation, the data of Govier and Omer (G4) for air-water flow, and of Hoogendoorn (H6) for air-water and air-oil, give reasonable agreement with the Baker plot, except for transitions from slug to annular, and of wave to annular flow. This transition to annular or film flow seems to be the least reproducible one, among various workers. Some evidence indicates that centrifugal effects, for example those due to return bends, may have a large influence. In a transition region, Hoogendoorn has produced either slug or wave flow in an oil-air mixture at identical conditions by variation of inlet conditions only. The two patterns differ by nearly 100% in pressure drop.

In summary, the plot suggested by Baker (Fig. 4) appears to predict approximately the probable flow pattern, for horizontal flow in tubes. Additional investigation is still needed, to give more universally applicable flow-pattern charts.

C. FLOW PATTERNS IN VERTICAL TUBES

1. Visual Appearance

The terminology used by various authors for visual description of upward vertical two-phase gas-liquid flow has already been given in Fig. 1. Typical pressure drop and hold-up ratio curves are shown in Fig. 2. Inasmuch as the liquid feed rate is constant in Fig. 2, the pressure-drop

behavior is characteristic of that observed as the gas flow rate is increased.

Visual definitions of flow patterns in vertical flow appear to cause more difficulty than do those in horizontal flow. As the gas rate increases at a constant liquid rate, a dispersed type of flow will be reached at lower gas velocities in a vertical tube than in a horizontal one because of the influence of gravity in causing back flow of liquid. Also, vertical flow patterns tend toward radial symmetry, which is not the case in horizontal flow. A classification of vertical flow patterns based largely on air-water mixtures is given below. Surprisingly little work has been carried out for the vertical upward flow of components other than these, or steam-water mixtures.

If the liquid flow rate is not too high, the following flow patterns can be described: These patterns are shown sketched in Fig. 5.

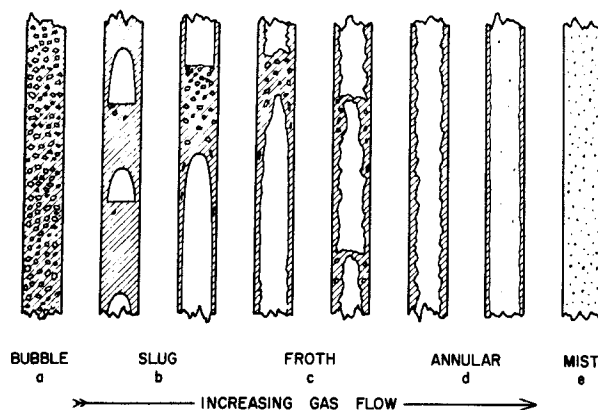


Fig. 5. Flow patterns in vertical flow [after Nicklin and Davidson (N3)].

(a) *Bubble flow*. Gas is dispersed in the upward flowing liquid in the form of individual bubbles of various sizes. As gas flow increases, the bubbles increase steadily in numbers and size.

(b) *Slug (or plug) flow*. The gas bubbles coalesce to form larger bullet shaped slugs having a parabolic outline at the head. These slugs increase in length and diameter, and their upward velocity increases as the gas rate increases. The slugs are separated by liquid plugs which contain gas bubble inclusions. As the gas slug moves along the tube, liquid flows down through the thin liquid annulus surrounding it into the bubble-filled liquid plug beneath.

(c) *Froth flow*. When back flow of the liquid around the slugs nearly stops, the slug becomes unstable, and gas slugs seem to merge with the liquid into a patternless turbulent mixture having the general nature of

a coarse emulsion. The elements of this structure are in a continual process of collapse and reformation.

(d) *Annular (or climbing film) flow*. The gas travels up the core of the tube at a high velocity and the liquid forms an annular film around the tube walls. Initially, this film may be fairly thick, and have long waves on which are superimposed a pattern of fine capillary waves. As gas flow rate increases, the film becomes thinner and the amount of the liquid entrained as droplets in the central gaseous core increases.

(e) *Mist (spray, fog, fully dispersed) flow*. At very high gas rates the amount of liquid entrainment increases until apparently all the liquid is carried up the tube as a mist or fog. Although a thin liquid film may exist on the wall, its presence is not obvious in this region.

The transition from froth to annular flow, in particular, seems to cover a fairly wide range of flow conditions, and to lack reproducibility.

2. Prediction of Flow Patterns

Apparently no attempts have been made to prepare a complete chart for the prediction of flow patterns in vertical flow, analogous to Fig. 4. Kozlov (K5) has stated, on the basis of his experiments with air and water in a 1-in. diameter tube, that the flow pattern can be defined by plotting the volumetric gas fraction fed and the average Froude number, V_M^2/gD . He gives equations for the boundary lines between types of flow (assumed to be straight lines on a log-log plot of the type suggested).

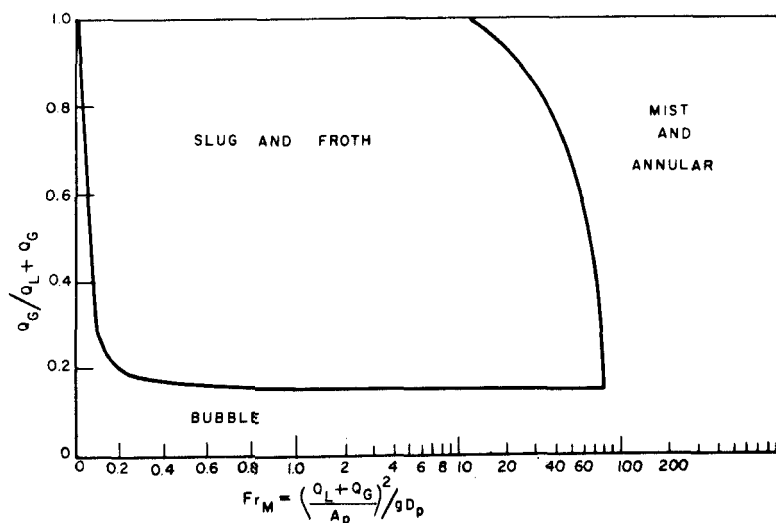


FIG. 5a. Flow pattern map for vertical air-water flow [as proposed by Griffiths and Wallis (G8)].

Griffith and Wallis (G8) have presented a map of the flow patterns using the coordinates proposed by Kozlov (see Fig. 5a). All possible flow patterns are lumped into three areas classed as bubble, slug, and annular-mist. Most of the data used by Griffith and Wallis were in the slug and froth flow regions, and the boundary lines proposed in their map do not agree with those suggested by Kozlov. Apparently the pattern transition point obtained between bubble and slug flow is highly dependent on the method of introducing gas and liquid, and the distance from the entrance. In Griffith and Wallis' experiments it was found that up to 300 diameters might be required to stabilize a slug flow pattern. On the basis of this result, some of the lack of agreement among other experimenters becomes understandable.

D. FLOW REGIMES IN TWO-PHASE FLOW

Govier *et al.* (G5, G6, B14) have correlated flow patterns in terms of the location of the two minima and the maximum observed in the pressure drop vs. gas-liquid volumetric feed ratio (R_v) curves (cf. Fig. 2). Gas-liquid ratios, gas flow, liquid flow, pipe diameter and gas-phase density were investigated for the air-water system in isothermal flow. From the correlations presented (as V_L against a function, $R_v \rho_G^{1/3} D^n$, when n varies in every case) it is possible to predict the flow patterns varying from bubble to annular flow. Mist flow was not investigated in this work.

Some detailed analyses of the mechanics of vertical slug flow (N4, G8) and vertical annular flow (A2, C1, C6, L1) have appeared in recent years, and give a clearer picture of the microscopic behavior in these patterns. In general, this type of analysis is yielding better results with many vertical flow patterns because of their radial symmetry, than with horizontal flow patterns.

Perhaps the simplest classification of flow regimes is on the basis of the superficial Reynolds number of each phase. Such a Reynolds number is expressed on the basis of the tube diameter (or an apparent hydraulic radius for noncircular channels), the gas or liquid superficial mass-velocity, and the gas or liquid viscosity. At least four types of flow are then possible, namely liquid in apparent viscous or turbulent flow combined with gas in apparent viscous or turbulent flow. The critical Reynolds number would seem to be a rather uncertain quantity with this definition. In usage, a value of 2000 has been suggested (L6) and widely adopted for this purpose. Other workers (N4, S5) have found that superficial liquid Reynolds numbers of 8000 are required to give turbulent behavior in horizontal or vertical bubble, plug, slug or froth flow. Therefore, although this classification based on superficial Reynolds number is widely used

because of its simplicity, it appears to be arbitrary and not enlightening.

III. Pressure Drop and Holdup

A. GENERAL

Two approaches may be noted to the problem of predicting pressure drop and holdup in two-phase gas-liquid flow. Correlations could be sought by the general means used so successfully for single-phase flow, in the hope that equally widely applicable relationships in terms of dimensionless groups or other parameters might result. Such correlations based on analogy have been applied very extensively, in numerous forms such as the Lockhart and Martinelli method, the homogeneous flow method, and various so-called "friction factor" methods. Alternatively, one may consider the detailed hydrodynamics of individual flow patterns, or groups of related patterns; such a mechanistic approach will usually be more difficult to apply quantitatively.

In the following sections, only the most useful of the "empirical" correlations will be reviewed. For fuller compilations of empirical relationships, reference should be made to the reviews of Isbin, Moen and Mosher (I1), Bennett (B9), or Gresham *et al.* (G7). Additional correlations based on operating large-diameter pipe lines have been given by Baker (B2, B3, B4). References to more recent relationships will be found in succeeding sections, and more detailed discussions of the mechanics of various flow patterns are given in Sections IV and V.

B. MOMENTUM AND ENERGY BALANCES

Differential momentum, mechanical-energy, or total-energy balances can be written for each phase in a two-phase flowing mixture for certain flow patterns, e.g., annular, in which each phase is continuous. For flow patterns where this is not the case, e.g., plug flow, the equivalent expressions can usually be written with sufficient accuracy as macroscopic balances. These equations can be formulated in a perfectly general way, or with various limitations imposed on them. Most investigations of two-phase flow are carried out with definite limits on the system, and therefore the balances will be given for the commonest conditions encountered experimentally.

For single-phase flow the momentum balance can be written to give the static pressure drop as the resultant of acceleration, hydrostatic, and wall-friction pressure-drop terms.

$$-dP = dP_a + dP_z - dP_w \quad (3)$$

For one-dimensional steady-state flow, neglecting density changes, the above equation can be expressed as

$$\frac{d(WV)}{g_c} + \frac{g}{g_c} A dz + AdP = AdP_w \quad (4)$$

where the term $AdP_w = \tau_w C_w dz$, where τ_w is the wall shearing stress, and C_w is the wetted-wall perimeter. This equation in turn can be expressed as the well-known mechanical-energy balance per unit time, by taking the product with the mean velocity.

In two-phase flow, most investigations are carried out in one dimension in the steady state with constant flow rates. The system may or may not be isothermal, and heat and mass may be transferred either from liquid to gas, or vice versa. The assumption is commonly made that the pressure is constant at a given cross section of the pipe. Momentum and energy balances can then be written separately for each phase, and with the constraint that the static pressure drop, dP , is identical for both phases over the same increment of flow length dz , these balances can be added to give over-all expressions. However, it will be seen that the resulting over-all balances do not have the simple relationships to each other that exist for single-phase flow.

Writing a momentum balance for the gas phase in a two-phase mixture and assuming no mass transfer [see Lamb and White (L3)], we have

$$\begin{aligned} \frac{d(W_G V_G')}{g_c} + \frac{g}{g_c} A_G \rho_G dz + A_G dP &= (\tau_{LG} C_{LG} + \tau_{WG} C_{WG}) dz \\ &= \tau_{LG} C_{LG} dz + A_G dP_{WG} \end{aligned} \quad (5)$$

where the "frictional" pressure term now includes the effect of both interfacial and wall shearing stresses (τ_{LG} and τ_{WG}), but neglects surface tension effects.

For the same case, a mechanical energy balance gives the equation

$$\frac{d(W_G V_G'^2)}{2g_c} + \frac{g}{g_c} A_G V_G' \rho_G dz + A_G V_G' dP = \tau_{LG} C_{LG} V_{ig}' dz - dE_G \quad (6)$$

The first term on the right expresses the energy transferred from liquid to gas (V_{ig}' being the actual relative velocity at the gas-liquid interface), and the second term the energy dissipated in wall friction.

If similar equations are written for the liquid phase, we have for the momentum balance,

$$\frac{d(W_L V_L')}{g_c} + \frac{g}{g_c} A_L \rho_L dz + A_L dP = (\tau_{GL} C_{GL} + \tau_{WL} C_{WL}) dz \quad (7)$$

$$= \tau_{GL} C_{GL} dz + A_L dP_{WL}$$

and for the mechanical-energy balance,

$$\frac{d(W_L V_L'^2)}{2g_c} + \frac{g}{g_c} A_L V_L' \rho_L dz + A_L V_L' dP = \tau_{GL} C_{GL} V_{iL}' dz - dE_L \quad (8)$$

If the equality of dP over the length dz is assumed, and the two momentum equations added, recognizing that $\tau_{GL} C_{GL} = -\tau_{LG} C_{LG}$, then

$$\begin{aligned} \frac{d(W_L V_L')}{g_c} + \frac{d(W_G V_G')}{g_c} + A dP + (\rho_L A_L + \rho_G A_G) \frac{g}{g_c} dz \\ = (\tau_{WG} C_{WG} + \tau_{WL} C_{WL}) dz \\ = (A_L dP_{WL} + A_G dP_{WG}) \end{aligned} \quad (9)$$

Similarly, if Eqs. (6) and (8), are added, using the fact that $V_{iL}' = V_{iG}'$, an over-all mechanical-energy balance results,

$$\begin{aligned} \frac{d(W_G V_G'^2)}{2g_c} + \frac{d(W_L V_L'^2)}{2g_c} + (A_L V_L' + A_G V_G') dP \\ + (\rho_L A_L V_L' + \rho_G A_G V_G') \frac{g}{g_c} dz = -dE_G - dE_L = -dE_{GL} \end{aligned} \quad (10)$$

For the common case when acceleration effects are negligible in Eq. (9), and kinetic-energy terms can be neglected in Eq. (10), the above equations can be simplified,

$$\begin{aligned} A dP + \frac{g}{g_c} (\rho_L A_L + \rho_G A_G) dz = dF_{GL} \\ = (A_L dP_{WL} + A_G dP_{WG}) \end{aligned} \quad (11)$$

and

$$(A_L V_L' + A_G V_G') dP + (W_L + W_G) \frac{g}{g_c} dz = -dE_{GL} \quad (12)$$

For two-phase flow, it is apparent that the over-all momentum equation and the over-all mechanical energy balance are not readily transformed one into the other, because of the necessity for weighting the momentum terms by their respective velocities in order to form the correct energy quantity. Either one could be legitimately used as a basis for correlations of two-phase pressure drops, but if friction factors are formulated by analogy to single-phase flow by writing expressions for either dF_{GL} or dE_{GL} equivalent to an over-all Fanning equation, then these friction factors will have quite a different significance depending on their definition.

If mass transfer occurs between phases, the appropriate momentum or energy terms must be introduced into the balances written for each

phase. Equations showing mass transfer have been given by Levy (L4). When the separate balances are added, however, Equation (9) and (10) will result, because all terms representing transfer of momentum or energy between phases will cancel out. For example, momentum balances with mass transfer of dW_L from liquid to gas will have the following forms, for the gas and liquid phases respectively,

$$\frac{1}{g_c} d(W_G V_G') + V_L' dW_L + \frac{g}{g_c} A_{GPG} dz + A_G dP = dF_{iG} \quad (13)$$

$$\frac{1}{g_c} d(W_L V_L') - V_L' dW_L + \frac{g}{g_c} A_{LPL} dz + A_L dP = dF_{iL} \quad (14)$$

On addition, the above equations yield Eq. (9).

The total energy balance can be derived in the same fashion, by writing the energy balance for each phase, and then adding the equations together. For a system as before, with constant mass-flow rates and no mass transfer between phases, but with heat transfer possible between phases, the total energy balance over a differential length of pipe has the form for the gas phase (see Vohr, V5),

$$\frac{W_G}{\rho_G} dP + \frac{W_G V_G' dV_G'}{g_c} + W_G g dz + W_G dU_G + dW_{GL} + dq_{GL} = 0 \quad (15)$$

where dW_{GL} and dq_{GL} represent the work done by the gas on the liquid, and the heat transferred from the gas to the liquid respectively. The quantity dU_G is the thermodynamic internal energy expressed as energy per unit mass of fluid.

Similarly for the liquid phase, the total energy balance is

$$\frac{W_L dP}{\rho_L} + \frac{W_L V_L' dV_L'}{g_c} + W_L \frac{g}{g_c} dz + W_L dU_L + dW_{LG} + dq_{LG} = 0 \quad (16)$$

Adding the above two equations, and using the fact that $dW_{GL} = -dW_{LG}$ and $dq_{GL} = -dq_{LG}$, then

$$\left(\frac{W_G}{\rho_G} + \frac{W_L}{\rho_L} \right) dP + \frac{W_G V_G' dV_G'}{g_c} + \frac{W_L V_L' dV_L'}{g_c} + (W_G + W_L) \frac{g}{g_c} dz + W_G dU_G + W_L dU_L = 0 \quad (17)$$

A great deal of use has been made of the overall momentum, mechanical-energy, and total-energy balances in various forms. Some of these applications are mentioned in the succeeding sections.

C. PHYSICAL SIGNIFICANCE OF BALANCES IN TWO-PHASE FLOW

Because of the complexity of two-phase gas-liquid flow a qualitative picture of the different ways in which the equations just given specify

the various irreversibilities of the system as a whole would be very useful. Such a comparison has been given recently by Nicklin (N2), and his approach is described briefly below based on the general problem of cocurrent gas-liquid flow in a vertical pipe.

If the volume change of the gas is neglected, and hence accelerative effects are also neglected, then for single-phase fluid flow, Equation (3) becomes

$$-dP = \frac{g}{g_c} \rho dz - dP_i = dP_z - dP_w \quad (18)$$

and from the energy balance

$$-dP = \frac{g}{g_c} \frac{V \rho dz}{V} - \frac{V dP_F}{V} = dP_R - dP_i \quad (19)$$

If the obvious equalities in the single-phase flow equations above are given separate designations, then these quantities can be compared to their counterparts when two-phase flow equations are written in the same form. Therefore, in Eq. (18), and (19), we define the following terms:

- $-dP$ = static head pressure drop
- dP_z = pressure drop due to the weight of the contents of a tube
- dP_w = pressure drop due to wall friction
- dP_i = pressure drop due to irreversible energy losses
- dP_R = pressure drop due to reversible work done in lifting a liquid

Obviously for single phase flow $dP_i = dP_w$ and $dP_z = dP_R$.

Considering the case of two-phase flow, with constant mass rates, no mass transfer and negligible accelerative effects, the total energy balance of Equation (17) can be rewritten, where $W_G/\rho_G = Q_G$ and $W_L/\rho_L = Q_L$, to yield

$$dP + \frac{g}{g_c} \left(\frac{W_G}{Q_G + Q_L} \right) dz + \frac{g}{g_c} \left(\frac{W_L}{Q_G + Q_L} \right) dz + H_L dz + H_G dz = 0 \quad (20)$$

The quantities H_L and H_G are the time rates of heat generation per unit length of tube in the liquid phase and gas phase respectively. No attempt is made to separate the cause of these effects, or to attribute them to one phase or the other.

Rewriting the previous equation in the same form as that of Eq. (19), by analogy, we obtain

$$-dP = dP_{RL} + dP_{RG} + dP_{iL} + dP_{iG} = dP_R + dP_i \quad (21)$$

Again dP_R represents useful work done, and dP_i represents irreversible degradation of energy.

The momentum balance gives another way of defining the pressure drops; Eq. (11) for two phases can be rewritten to give

$$-dP = \frac{g}{g_c} \frac{A_L}{A} \rho_L dz + \frac{g}{g_c} A_G \rho_G dz + dP_W = dP_s + dP_W \quad (22)$$

Comparing Eq. (21) and (22), the division of pressure drops is not equivalent in the two, unless

$$\frac{A_G}{A} = \frac{Q_G}{Q_G + Q_L} = R_G$$

Because of slip, R_G is always less than $Q_G/(Q_G + Q_L)$, and so in two-phase flow the irreversible pressure drop, dP_i , must always be greater than the pressure drop due to wall shear alone, dP_W . It follows that the hydrostatic component dP_s must exceed the reversible pressure drop dP_R .

If now these facts are used to divide the energy loss due to irreversibilities into two parts, one part can be specified as being due to wall friction, and the other part due to relative motion between the phases. Defining this energy loss due to "slip" as $(Q_G + Q_L)dP_s$, we have

$$(Q_G + Q_L)dP_s = (Q_G + Q_L)(dP_i - dP_W) \quad (23)$$

where

$$dP_i = dP_s + dP_W, \text{ and, from Eq. (21),} \quad (24)$$

$$-dP = dP_R + dP_s + dP_W$$

These different interpretations of the momentum or energy balances are shown pictorially in Fig. 6. Defining a pressure drop due to interaction of the two phases affords a link between these subdivisions. In Fig. 6, the interesting fact is shown that the total pressure drop may be less than the weight of the contents of the tube because of a negative

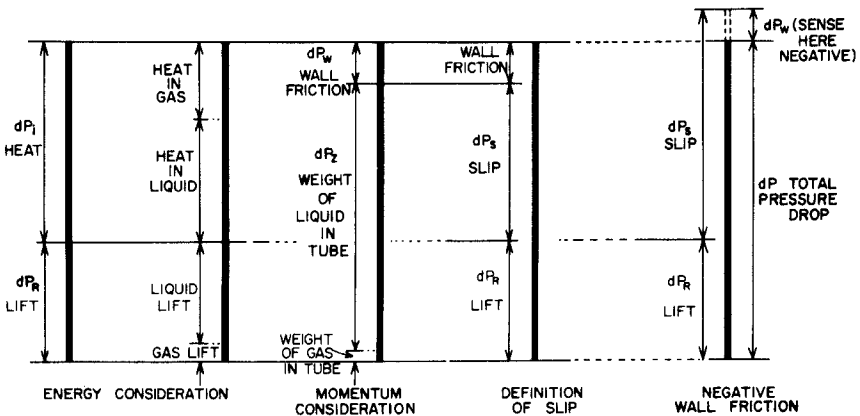


FIG. 6. Representation of pressure drops in vertical cocurrent flow [after Nicklin (N2)].

wall friction resulting from local downflows of liquid which give a "negative" shear at the wall.

From the above equations it is also apparent that in horizontal two-phase flow, all irreversibilities appear as wall friction, provided gas-liquid interfacial tension effects are neglected.

IV. Correlating Methods for Two-Phase Pressure Drops and Void Fractions

A. INTRODUCTION

A variety of methods has been presented in the literature, for correlation of pressure-drops, or of *in situ* volume fractions for specified conditions of system geometry, operating conditions, or phase properties; but no completely generalized correlation yet exists. Only those methods which have been most widely used are discussed in the following section. For more complete listings, reference to recent reviews should be made (B9, G7).

B. LOCKHART-MARTINELLI AND MARTINELLI-NELSON CORRELATIONS

1. Lockhart-Martinelli Correlation

This derivation is based on certain limiting assumptions, although the resulting correlations have been applied to all regions of two-phase flow both by the originators and by many other investigators. Briefly, the original assumptions were:

(a) The static pressure drop for the gas phase is equal to that of the liquid phase, regardless of flow pattern.

(b) The volume occupied by the gas plus that occupied by liquid at any instant equals the pipe volume.

(c) Momentum and hydrostatic-pressure drops are neglected or are calculated separately. The extension of the Lockhart-Martinelli approach which includes momentum and hydrostatic-pressure losses is commonly called the Martinelli-Nelson method.

(d) Four types of flow were specified consisting of the four combinations possible with either phase being considered in turbulent or viscous flow. Boelter, Martinelli, *et al.* (B13, M3, M4) originally introduced correlations for turbulent-turbulent, and viscous-turbulent flow. (In the Lockhart-Martinelli nomenclature, the flow designation is for liquid and gas, in that order; turbulent or laminar flow is arbitrarily defined as greater than a superficial Reynolds number of 2000 or less than a value of 1000.) Martinelli *et al.* (M3) extended this work to viscous-viscous flow. A final correlation for all four combinations, as well as for void-fractions, was presented by Lockhart and Martinelli (L6).

The correlation is presented as a plot of an empirical function, φ , against a parameter X , with one curve representing each of the four flow regimes. The correlating quantities are defined as

$$\varphi_G^2 = \frac{(\Delta P/\Delta Z)_{TP}}{(\Delta P/\Delta Z)_G} \quad \text{or} \quad \varphi_L^2 = \frac{(\Delta P/\Delta Z)_{TP}}{(\Delta P/\Delta Z)_L} \quad (25)$$

and

$$X^2 = \frac{(\Delta P/\Delta Z)_L}{(\Delta P/\Delta Z)_G} \quad (26)$$

In the above terms, the quantities $(\Delta P/\Delta Z)_L$ or $(\Delta P/\Delta Z)_G$ are calculated from conventional single-phase correlations on the basis that the liquid or gas is flowing in the pipe alone at the same individual mass-flow rate as in the two-phase case. Lockhart and Martinelli (L6) have given the appropriate expressions for X^2 , and the relationships between φ_G , φ_L , R_G , and R_L for the various flow regimes. The relationships are shown graphically in Fig. 7.

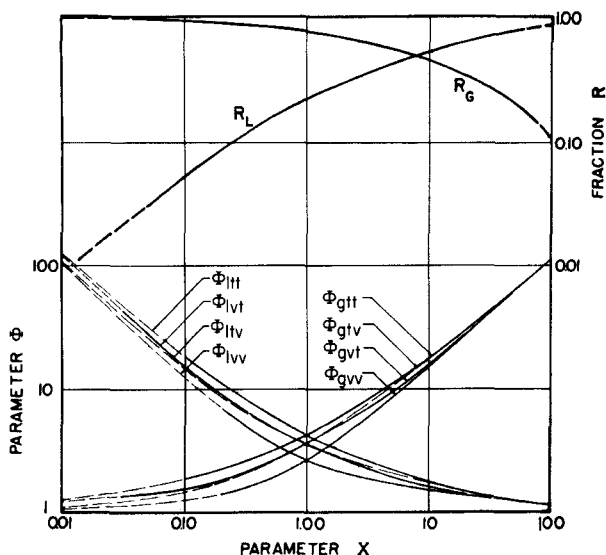


FIG. 7. Pressure drop correlation of Lockhart and Martinelli for frictional pressure losses in horizontal cocurrent flow.

2. Martinelli-Nelson Correlation

These empirical correlations were originally based mainly on data obtained for isothermal horizontal flow at pressures close to atmospheric (to 50 psi), normal temperatures, and pipe diameters to one inch using air and eight different liquids. In order to apply these equations to single-component two-phase flow with mass transfer between phases, Martinelli

and Nelson (M2) devised an empirical procedure applicable for steam-water mixtures in turbulent flow. The parameters φ^2 and X^2 were taken to be point values rather than incremental, with the assumption that the steam quality x is zero at the inlet and varies linearly with tube length, and the Lockhart-Martinelli correlation was then integrated with pressure level as a parameter. The resulting values did not agree with experiments at intermediate pressures, or with requirements at the critical point, so corrections were applied to the calculations. In effect, an empirical pressure dependence was enforced on the factor φ^2 . Similarly, given values for R_G or R_L as a function of X^2 at atmospheric pressure and at critical conditions ($R_G = R_L$), values for other pressures were arbitrarily interpolated. The resulting sets of curves given by Martinelli and Nelson (M2) allow calculation of frictional pressure-drops in the steam-water system.

The momentum pressure-drop can often be neglected, particularly when no mass transfer occurs in a system. Three equations, all approximate, are given below for calculation of these acceleration pressure losses, ΔP_a , between two sections, 1 and 2, using the mean velocities of gas and liquid,

$$\Delta P_a = \frac{G_M^2}{g_c} \left[\frac{x_2^2}{\rho_{G_2} R_{G_2}} - \frac{x_1^2}{\rho_{G_1} R_{G_1}} + \frac{(1-x_2)^2}{\rho_L(1-R_{G_2})} - \frac{(1-x_1)^2}{\rho_L(1-R_{G_1})} \right] \quad (27)$$

For an inlet quality, $x_1 = 0$, (Martinelli-Nelson form)

$$\Delta P_a = \frac{G_M^2}{g_c} \left[\frac{x_2^2}{R_{G_2} \rho_{G_2}} + \frac{(1-x_2)^2}{(1-R_{G_2}) \rho_L} - \frac{1}{\rho_L} \right] = \frac{r_2 G_M^2}{g_c} \quad (28)$$

For an assumption of "non-slip" or homogeneous flow,

$$\Delta P_a = \frac{G_M^2}{g_c} \left[\frac{x_2}{\rho_{G_2}} - \frac{x_1}{\rho_{G_1}} + \frac{x_1}{\rho_L} - \frac{x_2}{\rho_L} \right] \quad (29)$$

Graphs giving the quantity, r_2 , as a function of quality and pressure have been given by Martinelli and Nelson, based on their empirical correlations.

For no mass transfer between phases, the acceleration loss is approximately,

$$\Delta P_a = G_L^2 \left[\frac{1}{\rho_L R_{L_2}} - \frac{1}{\rho_L R_{L_1}} \right] + G_G^2 \left[\frac{1}{\rho_{G_2} R_{G_2}} - \frac{1}{\rho_{G_1} R_{G_1}} \right] \quad (30)$$

3. Comparisons with Experiment

Since 1949 the correlations of Lockhart and Martinelli, and of Martinelli and Nelson, have been used or checked by many investigators of two-phase flow phenomena. The assumptions made in the derivations of these correlations would seem to rule out certain flow patterns, e.g.,

stratified, wave, slug, and mist flow; nevertheless this method has been tested for all flow patterns in both horizontal and vertical flow, for isothermal and non-isothermal systems, and at a wide variety of temperatures and pressures, and for a number of different fluids. Although widely used, these relationships have also been frequently criticized on both theoretical and practical grounds. For earlier work (prior to 1957) reference should be made to the reviews mentioned already (B9, G7, I1).

The original correlation showed a scatter of nearly $\pm 50\%$ in predicting two-phase pressure drops, and, in addition, a decided dependence on liquid rate (which the correlation averaged out). Much of this scatter seemed to be a systematic drift depending on total mass flow rate. This dependence on mass flow was pointed out by Gazley and Bergelin (L6) and by Isbin *et al.* (I2). In the following summary, "satisfactory predictions" can be taken to mean prediction of pressure drops no worse than the above, and, in some cases, considerably better.

(a) For horizontal small-diameter pipes, up to 5-in., better results are obtained for turbulent-turbulent flows than for the other three regimes, where the correlation tends to give pressure drops that are too high. For the turbulent-viscous, and viscous-turbulent regimes, agreement is generally satisfactory for values of $X > 1.0$; see Govier and Omer (G4), and Alves (A1).

(b) Predicted pressure drops are high by 50% or more for horizontal turbulent-turbulent flow in large-diameter pipes, 6-in. and larger, at either high or low pressures. See Baker (B2, B3); Reid *et al.* (R1); and Hoogendoorn (H6).

(c) At pressures considerably in excess of atmospheric, the predicted pressure-drops are high, with the error greater than at normal pressures; see Hoogendoorn (H6), Isbin *et al.* (I7), and Chenoweth and Martin (C3).

(d) For vertical flow, when applied for prediction of frictional pressure-drop in turbulent-turbulent flow, values are obtained which are too low for $X < 10$, but are satisfactory for $X > 10$ for air-water flow in small diameter tubes; see Davis (D1), and Collier and Hewitt (C6). The fact that the calculation of the hydrostatic component of the pressure drop depends on a knowledge of the gas or liquid volume-fraction in the tube should be noted in connection with vertical flow. For all but the annular flow-pattern, this is the major term. An experimental knowledge of the void-fraction was required to test this correlation, because until recently no accurate prediction method was available for vertical flow. The possible error in calculating the frictional part of the observed pressure drop therefore can become quite large for all but the annular or

spray flow-regions. The behavior of the air-water system in vertical flow in terms of the Lockhart-Martinelli parameters has been shown recently by Hughmark and Pressburg (H12).

(e) In small horizontal tubes carrying gaseous Freon 11 (trichloromonofluoromethane) with water, or with liquid Freon 11, in turbulent-turbulent flow, the Lockhart-Martinelli curve gives values at least 40% too high; see Hoogendoorn and Buitelaar (H7), and Hatch and Jacobs (H3).

(f) For any flow, the correlation does not account for the effect of pipe-wall roughness. However, the normal roughness variation does not cause an error in predicting pressure drops as great as that arising from other sources, according to Chisholm and Laird (C4), and Hoogendoorn (H6).

(g) A dependence of the two-phase pressure-drop on liquid or total mass-flow rate, which is not allowed for in these correlations, has been shown by several investigators. In general, the variation of the pressure drop with G_M is nearly as great as its dependence on X . The Lockhart-Martinelli curve roughly averages this variation.

(h) The Martinelli-Nelson method of predicting pressure drops becomes increasingly less accurate as pressure increases, and as quality decreases. For steam-water flows in horizontal tubes, an extensive comparison with experiment has been carried out by Isbin and coworkers (I2, I5, I7). Their data covered wide ranges of pressure, quality, and flow rates, with most of the results lying in the annular or dispersed flow-pattern region. On the basis of this work, it was concluded by Isbin *et al.* that when accelerative effects became important, neither the Martinelli-Nelson method nor other proposed correlations was adequate.

It should be remembered that these correlations as originally devised by Lockhart and Martinelli were based almost entirely on experimental data obtained for situations in which accelerative effects were minor quantities. The Lockhart-Martinelli correlation thus implies the assumption that the static pressure-drop is equal to the frictional pressure-drop, and that these are equal in each phase. The Martinelli-Nelson approach supposes that the sum of the frictional and accelerational pressure-drops equals the static pressure-drop (hydrostatic head being allowed for) and that the static pressure-drop is the same in both phases. When acceleration pressure losses become important (e.g., as critical flow is approached), they are likely to be significantly different in the gas and liquid phases, and hence the frictional pressure losses will not be the same in each phase. In these circumstances, the correlation must begin to show deviations from experiment.

(i) Void fractions as predicted by the Lockhart-Martinelli or Marti-

nelli-Nelson correlations are applicable for horizontal flow only, and show large potential percentage errors at low values of R_g . Improved expressions are available to aid in estimating void-fractions over wide ranges of conditions for both horizontal and vertical two-phase flow. (I4, I5, N4, S5). At present it would appear necessary to use the Lockhart or Martinelli relationship only for horizontal flow with superficial liquid Reynolds numbers below 8000, or for void fractions exceeding 0.80; for these conditions, it gives a useful approximation.

(j) These correlations have been reported to be applicable for predicting pressure drops over certain ranges (usually annular and mist patterns or the turbulent-turbulent region), with varying degrees of success for the following flow cases: upward flow in tubes and annuli [Collier and Hewitt (C6)], horizontal flow in rectangular channels [Davis and David (D2)], upward flow in rectangular channels [Sher and Green (S7)], downward flow in annuli [Hoopes (H8)], and downward flow in tubes [Wright (W3)]. It has been suggested also that, when acceleration effects are significant, better correlation is obtained if the total two-phase pressure drop (i.e. friction plus acceleration losses) is used rather than just the frictional component [Schrock and Grossman (S2)].

In summary, the calculation of pressure drops by the Lockhart-Martinelli method appears to be reasonably useful only for the turbulent-turbulent regions. Although it can be applied to all flow patterns, accuracy of prediction will be poor for other cases. Perhaps it is best considered as a partial correlation which requires modification in individual cases to achieve good accuracy. Certainly there seems to be no clear reason why there should be a simple general relationship between the two-phase frictional pressure-drop and fictitious single-phase drops. As already pointed out, at the same value of X in the same system, it is possible to have two different flow patterns with two-phase pressure-drops which differ by over 100%. The Lockhart-Martinelli correlation is a rather gross smoothing of the actual relationships.

C. CHENOWETH-AND-MARTIN CORRELATION

This correlation (C3) is intended to apply for turbulent-turbulent horizontal flow in pipes, and was developed to give better pressure-drop prediction for higher pressures and larger-diameter pipes. On an entirely empirical basis, the quantity $\Delta P_{TP}/\Delta P_L^*$ is given as a function of liquid volume-fraction of the feed, with a quantity $\psi_G^* \rho_L / \psi_L^* \rho_G$ as a parameter. For this correlation ΔP_L^* is evaluated as the pressure-drop based on the total mass-flow using the liquid-phase properties. The parameter $\psi_G^* \rho_L / \psi_L^* \rho_G$ is defined as

$$\frac{\psi_G^* \rho_L}{\psi_L^* \rho_G} = \frac{\Delta P_G^*}{\Delta P_L^*} = \frac{[f_G^* Z/D + \Sigma K] \rho_L}{[f_L^* Z/D + \Sigma K] \rho_G} \quad (31)$$

where the f^* are evaluated at the total mass flow from a Moody chart, and the term ΣK is an allowance for valves and fittings.

The originators claimed an agreement with the experimental pressure drops of $\pm 35\%$ for this correlation. Only a few additional evaluations have been made of this relationship. For air-water in vertical annular flow, Collier and Hewitt (C6) found that the frictional drop was predicted as well by this relationship as by the Lockhart-Martinelli one. For annular and mist flow, however, Govier and Aziz (G3) found only a poor agreement for low liquid volume-fractions. Isbin *et al.* (I7), for steam-water flows at pressures from 400–1000 psia, concluded that errors of over 100% occurred over much of the liquid volume-fraction range, predictions being low at low volume-fractions, and high at high fractions. In general, when used for conditions removed from those on which it is based, this correlation gives results somewhat worse than the Lockhart-Martinelli methods.

Recently, Hughmark (H13) has proposed a correlation which has essentially the same basis as that of Chenoweth and Martin. Hughmark plots the ratio of the friction factors for two-phase flow and the flow of a fictitious single phase fluid (see discussion of friction factor methods following) against the liquid volume fraction fed, but uses a slightly different parameter, that is $(R_{eTPM}) (P_G/P_L) (0.085/D)$ as a third quantity. This choice of parameters amounts to using a fluid viscosity weighted for the quantities of the two fluids, rather than a ratio of viscosities as in Chenoweth and Martin's work, and introducing a diameter ratio, inasmuch as Hughmark's work was based on 1 in. pipe. The correlation is claimed to be generally applicable for horizontal flow, but it is interesting to note that, of the comparisons made by Hughmark with other common two-phase pressure drop equations, the closest agreement is with the Chenoweth-Martin equation, and, on the average, the improvement shown by Hughmark's modification is slight.

D. "FRICTION-FACTOR" METHODS

By analogy to single-phase flow, the two-phase frictional pressure-drop can be expressed by the conventional Fanning equation, and thereby a "friction factor" is defined. These friction factors may be based on liquid properties, gas properties, or on a fictitious single fluid of mean properties obtained by some averaging procedure. Typical definitions, such as those shown in equation (32), have been given and discussed recently by Govier and Omer (G4):

$$\left(\frac{\Delta P}{\Delta Z}\right)_{TP} = \frac{2f_{TFL}G_L^2}{g_c D \rho_L} = \frac{2f_{TPG}G_G^2}{g_c D \rho_G} = \frac{2f_{TPM}G_M^2}{g_c D \rho_M} \quad (32)$$

Obviously, correlations of one of these friction factors with an analogous Reynolds number, or with two-phase pressure-drop, throws little light on the other variables concerned, and these quantities will appear as parameters in any proposed relationship. However, Govier and Omer point out that plots of such a form do give a systematic spread of data above the single phase lines and allow easy comparison of trends.

The definition of friction factor using mean fluid properties has been most widely used because it reduces to the correct single-phase value for both pure liquid and pure gas flow. This technique is very similar to the so-called "homogeneous" model, because it has a clear physical significance only if the gas and liquid have equal velocities, i.e., without slip. Variations of this approach have also been used, particularly the plotting of a ratio of a two-phase friction factor to a single-phase factor against other variables. This approach is then very similar to the Lockhart-Martinelli method, since it can be seen that (G4)

$$\phi_G^2 = \frac{f_{TPG}}{f_G}; \quad \phi_L^2 = \frac{f_{TPL}}{f_L}; \quad X^2 = \left(\frac{G_L}{G_G}\right)^2 \left(\frac{f_L}{f_G}\right) \left(\frac{\rho_G}{\rho_L}\right) \quad (33)$$

where f_G and f_L are the friction factors obtained from a conventional correlation for the gas or liquid flowing alone.

The basic assumptions implied in the "homogeneous" model, which is most frequently applied to single-component two-phase flow at high velocities (with annular and mist flow-patterns) are that (a) the velocities of the two phases are equal; (b) if vaporization or condensation occurs, physical equilibrium is approached at all points; and (c) a single-phase friction factor can be applied to the mixture if the Reynolds number is properly defined. The first assumption is true only if the bulk of the liquid is present as a dispersed spray. The second assumption (which is also implied in the Lockhart-Martinelli and Chenoweth-Martin models) seems to be reasonably justified from the very limited evidence available.

This model has met with some success, particularly at high flow rates and high qualities in small tubes. Isbin *et al.* (I7) show that it can give reasonable predictions for dispersed flow if the momentum pressure-drops are small. When momentum pressure losses are significant, Isbin *et al.* (I4) point out that the homogeneous model can predict such high momentum losses that the frictional pressure loss becomes negative. Charts presented by Hoopes (H8) also show clearly that the error in evaluation of momentum or kinetic-energy terms caused by the "no-slip" assumption can be very large.

As a correlating procedure, the friction-factor approach has been used

very widely, because it permits application of the mechanical-energy and total-energy balances in their familiar single-phase forms. The resulting equations may then be applied to cases involving mass transfer, with or without simultaneous heat transfer, by stepwise integration along a pipe; or, if appropriate assumptions are made, analytical integration may sometimes be possible. Isbin *et al.* (I1, I7) and Hoopes (H8) have given methods and appropriate forms of the equations for carrying out the calculation procedures.

The partial success of homogeneous models for predicting pressure drops and void fractions in dispersed flow (the only pattern for which the "no-slip" assumption may be justified) has led to some overstatement of the range of value; e.g., see Owens (O1). However, this simple model has often given good correlations, though the choice of correlating parameters varies widely and the resultant expressions are entirely empirical. In general, "friction-factor" methods do not require the assumptions made in the special case of the homogeneous model, and can be applied equally well to vertical or horizontal flow; such methods of "correlation by analogy" give good results, although they shed very little light on the fundamental behavior of two-phase systems.

E. OTHER CORRELATION MODELS

1. Momentum-Exchange Model

Levy (L4) has recently proposed that if the frictional plus hydrostatic head losses in the gas phase equalled the sum of the same losses in the liquid phase, then one could assume that momentum was exchanged between the phases rapidly enough to maintain this equilibrium. This condition then requires that any changes in quality, void fraction, or density of the phases results in such a momentum exchange. By writing a mechanical-energy balance for each phase, and then subtracting one from the other the necessary relationship between x , R_G , and ρ_L/ρ_G can be established so that the model will be satisfied. This relationship, including mass transfer between phases, is

$$\frac{(1-x)^2}{(1-R_G)} + \frac{x^2}{R_G} \frac{\rho_L}{\rho_G} - \frac{1}{2} \frac{(1-x)^2}{(1-R_G)^2} = 0 \quad (34)$$

Equation (34) gives reasonable agreement with experiment, in horizontal tubes, only for high void volumes. In vertical tubes with heat transfer, agreement is generally better at low void volumes and low pressures. This correlation was improved by adding an empirical factor to allow for a momentum difference between phases at high heat fluxes. Pressure drops were calculated by using an approximate relation between R_G and ϕ_L ,

$$\varphi_L^2 = \frac{1}{(1 - R_G)^2} \quad (35)$$

This equation can be derived by supposing that the wall is in contact with liquid only, and that shearing forces are equal at the gas-liquid interface. Experimental pressure drops were predicted to +50% to -30% on the average, although larger individual variations existed. An attempt was made by Marchaterre (M1) to refine this method by expressing the mechanical-energy balance in terms of φ_L .

2. Modified Lockhart-Martinelli Methods

Davis (D1) has suggested that the introduction of the Froude number into the Lockhart-Martinelli parameter, X , gives a description of gravitational and inertial forces so that this model can be applied to vertical flow. The revised parameter, X , is defined empirically for turbulent-turbulent flow as,

$$X = 0.19 \left(\frac{W_L}{W_G} \right)^{0.9} \left(\frac{\rho_G}{\rho_L} \right)^{0.5} \left(\frac{\mu_L}{\mu_G} \right)^{0.1} \left(\frac{V_M^2}{Dg} \right)^{0.185} \quad (36)$$

this relation being based largely on low-pressure data from Govier *et al.* (G6) for air-water, and from Isbin *et al.* (I3) for steam-water. Comparison with other sets of data give an agreement of $\pm 20\%$ for liquid Reynolds numbers above 8000, or, above 6000 if the Froude number exceeds 100.

It should be noted that the frictional drop was calculated by subtracting the hydrostatic head and acceleration losses from the measured total pressure-drop; where void data were lacking, a homogeneous flow model was assumed. This modification of X by use of the Froude number appears very similar to the technique used by Kosterin (K2, K3) for horizontal pipes, in which the equivalent of φ_L^2 was plotted against volume-fraction of gas flowing, with mixture Froude number as the correlating parameter.

3. Slip-Velocity Methods

The slip velocity itself (i.e., $V_G' - V_L'$) has been used as a correlating parameter as well as the slip-velocity ratio, V_G'/V_L' . Lottes and Flinn (L7) used the latter to form a graphical correlation to allow determination of the quality in boiling steam-water flow in vertical rectangular ducts. Hughmark and Pressburg (H12) have correlated vertical two-phase pressure drops with the slip velocity in a plot of $(\Delta P_{TP} - \Delta P_L)/\Delta Z$ against V_s' , obtaining a family of curves having as a parameter $\psi = 1/\mu_L^{0.147} \sigma^{0.194} G_M^{0.07}$. The quantity ψ was determined by a statistical correlation of numerous data obtained by these workers as well as by others.

The use of a slip-velocity in any relationship depends on the ability

to make a reasonably close estimate of the void fraction [see Eq. (2)]. Hence, pressure drop correlations of this type are often accompanied by suitable void fraction correlations (e.g., for that developed by Hughmark and Pressburg see Section IV, E, 5).

4. Pipe Roughness as a Variable

Another modification of the Lockhart-Martinelli approach has been proposed by Chisholm and Laird (C4) to account for the effect of pipe roughness. For the turbulent-turbulent region, it is suggested that the Lockhart-Martinelli correlations, which were presented graphically, can be represented by the equation

$$\phi_{LTT}^2 = 1 + \frac{21}{X} + \frac{1}{X^2} \quad (37)$$

If $X > 0.4$, the last term is negligible. On the basis that the exponents on the flow terms in the definition of X vary as a function of pipe roughness, it was found that plots of $(\phi_{LTT}^2 - 1)$ against C/X^m gave straight lines, where $m = 1.0$ for smooth tubes, and 0.80 for the roughest tube; 1-in.-diameter horizontal tubes with roughness ratios e/D to 0.068 were used with air-water flow. The quantity C was found to be a function of liquid flow rate, and of tube roughness.

An interesting comparison can be made of this work and that of Hoogendoorn (H6). The latter work covered plug, slug, and froth flow-patterns for air and various liquids (about the same flow-pattern range covered by Chisholm and Laird), pipe diameters from about 1 in. to 5½ in., roughness ratios to 0.030, liquid-to-gas viscosity ratios from 60 to 1500 and a gas-density variation of about 100% (ρ_G/ρ_L from 0.0016 to 0.0030). For turbulent-turbulent flow, Hoogendoorn gives the correlation,

$$\frac{\Delta P_{TP}}{\Delta P_L^*} = \left[1 + 230 \left(\frac{G_G}{G_M} \right)^{0.84} \right] \left[0.00138 \frac{\rho_L}{\rho_G} \right]^\alpha \quad (38)$$

where ΔP_L^* is the pressure drop for the total mass flow calculated as liquid, and α is a function of (G_G/G_M) and varies from about 0.90 to 1.0. This correlation applies for $(G_G/G_M < 0.05)$, that is for $G_M \approx G_L$. If this factor is now taken into account, $\Delta P_L^* \approx \Delta P_L$; the right-hand side of the above equation is very nearly equal to $1 + 21/X$, and therefore these correlations are basically identical. Roughness was accounted for by Hoogendoorn by evaluating ΔP_L^* at the appropriate roughness factor from a Moody chart, while Chisholm and Laird have done the equivalent by giving C as a function of superficial liquid Reynolds number, and of the ratio of smooth- and rough-pipe friction factors.

Chisholm and Laird also measured and correlated the *in situ* volume-fraction of liquid with an equation of the general form,

$$\frac{1}{R_L^n} = 1 + \frac{21}{X} + \frac{1}{X^2} \quad (39)$$

For smooth tubes, a correlation also existed between $1/R_L$ and φ_{LTT}^2 , but for rough tubes the liquid flow rate was a parameter, especially for $X < 3.5$. In general, it would appear that the parameter X correlates the void fraction over wide ranges better than it can correlate the quantity φ_{LTT} , although the roughness ratio remains a separate parameter. An effect of roughness on the flow pattern is indicated, and this would also explain to some extent the observed effects of pipe roughness on pressure-drop.

5. Miscellaneous Void-Fraction Correlations

Hughmark and Pressburg (H12) have correlated statistically their void data and others for vertical flow, using a modified Lockhart-Martinelli parameter, X , given as

$$X = \left(\frac{W_L}{W_G} \right)^{0.9} \frac{\mu_L^{0.19} \sigma^{0.205} \rho_G^{0.70}}{G_M^{0.435} \rho_L^{0.72}} \quad (40)$$

An average deviation for the prediction of R_G of ± 0.038 was claimed for air and for a variety of fluids in vertical pipes from 0.4 to 2.34 in. diameter.

A summary of data on void-fraction investigations, and tests of various correlations for the steam-water system have been given by Isbin *et al.* (I5). These workers conclude that the variety of flow conditions possible make a single general correlation of void data unlikely; in any case, insufficient data are presently available.

In a later publication (I4) Isbin *et al.* show the effect of using different void-fraction correlations for the calculation of acceleration effects in horizontal steam-water flow when critical velocities are approached. In this work, additional void-fraction correlations are given: The Fauske model (for annular flow when velocities are very high) results in

$$R_G = \frac{1}{\left(\frac{1-x}{x} \right) \left(\frac{\rho_G}{\rho_L} \right)^{1/2} + 1} \quad (41)$$

The Modified Armand equation, for void fractions > 0.8 , is

$$R_G = (0.833 + 0.167x) \frac{Q_G}{Q_G + Q_L} \quad (42)$$

It has been shown by Scott (S5) that the theoretical equation proposed by Nicklin, Wilkes, and Davidson (which is identical with Armand's (A7) empirical equation for steam-water flow) is applicable to horizontal

flow for the conditions of their derivation, i.e., for superficial liquid Reynolds numbers exceeding 8000, excluding wave and stratified flow-patterns, with void fractions up to 0.8. The Nicklin equation for horizontal flow is

$$R_G = 0.833 \frac{Q_G}{Q_G + Q_L} \quad (43)$$

The corresponding equation for vertical flow, again for liquid Reynolds number above 8000 and for void fractions to 0.80, was given by Nicklin *et al.* (see Section V, A), and was shown to agree with experiment:

$$R_G = \frac{Q_G}{1.2(Q_G + Q_L) + 0.35A(gD)^{1/2}} \quad (44)$$

where A is the cross-sectional area of the pipe.

A similar equation to that of Eq. (43) was proposed by Bankoff (B6) on the basis of a bubble-flow model for vertical flow. His derivations are discussed in the following section (Section V, B). Finally, it should be mentioned that the "momentum exchange" model of Levy (L4), and the "slip-ratio" model of Lottes and Flinn (L7) are more readily applied for the determination of void fractions than for pressure drops. In general, these methods seem to give rather poorer accuracy than those already discussed.

Many of the void-fraction correlations which have been prepared for both vertical and horizontal flow of steam-water mixtures have recently been tested by Haywood *et al.* (H4) against their extensive experimental data for 1-in. and 1½-in. tubes. Additional valuable evaluation is given by others in the published discussion of this paper.

Petrick and Swanson (P1) have measured the effect of sudden contractions and expansions on void fractions found in vertical air-water flow, for pressures from 150 psi to 600 psi. As might be expected, a change does occur in the void fraction due to the difference in relative gas-liquid velocities in the two sections. In an unstable zone extending for several diameters from the point of change of the cross section, the voidage may vary abnormally, particularly for an expansion, due to the jetting action of the fluid. Petrick and Swanson give a semitheoretical equation for estimating the downstream value of R_G at atmospheric pressure from a knowledge of the pressure ratio and area ratio, and the upstream void fraction.

Liquid metals represent a special case in the estimation of two phase void fractions. Because of the great differences in vapor and liquid density, very low qualities correspond to high void fractions, and for the same reason very large slip velocity ratios occur. In a recent paper, Smith *et al.* (S13) review previous measurements of void fractions in

vertical channels made on liquid metals (mainly by Soviet workers), and suggest a void fraction correlation in which a slip velocity ratio, V_s' , is plotted against a "relative flow area" with an inlet velocity ratio as a parameter. The relative flow area is defined as the ratio of the actual area of flow to the flow area giving a Froude number of unity at the same total mass rate. Basically, this variable is proportional to the total mean liquid velocity. The results of Smith *et al.*, as well as those of others, are presented as a graphical correlation in terms of these quantities.

V. Mechanics of Specific Flow Patterns

A number of definite flow patterns have been investigated in varying detail, with those occurring in vertical flow receiving the most attention because of the radial symmetry existing in this case. In the following sections, brief reviews are given of some of the more significant work reported up to 1962.

A. SLUG FLOW

1. Vertical Tubes

Careful theoretical analyses of fully developed (i.e., ideal) slug flow in vertical pipes have been made along related lines by Griffith and Wallis (G8), and by Nicklin *et al.* (N4). The latter approach appears to be more fundamental, and is therefore reviewed here. In fully developed slug flow, the slugs of gas bear a resemblance to so-called "Dumitrescu" or "G. I. Taylor" bubbles. These bubbles are described as "wakeless" bubbles, and are best pictured as resulting when a narrow tube full of liquid and sealed at the top is allowed to empty from the bottom. Both theory and experiment show that in a stationary liquid, the rising velocity of such bubbles relative to the tube wall is given by

$$V_B = 0.35(gD)^{1/2} \quad (45)$$

It was shown by Nicklin *et al.* that long slugs (those several diameters in length) rise relative to the liquid ahead of them at exactly this velocity. If the liquid has a net flow ahead of the nose of the slug, then the slug velocity in space is given by Eq. (45), plus a component which must be added to account for the net liquid velocity. Downward liquid flow is more complicated than upward, because the slug shape becomes distorted in an effort to avoid the fastest downflowing liquid at the tube center. When a slug expands due to a change in hydrostatic head, the slug velocity is increased by an amount dependent on the velocity of the displaced liquid, and on the absolute pressure of the system. Usually the

velocity of bubble rise is not a function of slug length, thus there is no effect of wake on this velocity.

For turbulent upward liquid flow, it was found experimentally that the slug velocity is given for superficial liquid Reynolds numbers over 8000 by

$$V_s = 1.2V_L + 0.35(gD)^{1/2} \quad (46)$$

That is, the component of the slug velocity due to liquid upflow is very nearly the same as the maximum liquid velocity at the tube center for turbulent flow.

By continuity, it can be shown that the average superficial liquid velocity, V_L , is given by

$$\frac{Q_G + Q_L}{A} = V_L \quad (47)$$

In addition, the velocity rise of the slugs must also equal the true average gas velocity, that is,

$$V_{G'} = V_s = \frac{Q_G}{R_G A} \quad (48)$$

Incorporating these latter two expressions in Eq. (46), the gas volume-fraction in slug flow can be obtained.

$$R_G = \frac{1}{1.2 \left(1 + \frac{Q_L}{Q_G} \right) + \frac{0.35A(gD)^{1/2}}{Q_G}} \quad (44)$$

This equation reproduces the work of several investigators over wide ranges of air and water flow rates and for pipe diameters to $2\frac{1}{2}$ in., up to the point where annular flow begins. For comparison, Griffith and Wallis present a similar development using in place of Eq. (46) the expression

$$V_s = V_L + 0.35C_2(gD)^{1/2} \quad (49)$$

where C_2 was correlated empirically. Nicklin *et al.* also point out that if the buoyancy term in the denominator of equation (44) is omitted, then an equation which might apply to horizontal bubble flow results.

Moissis and Griffith (M5) measured velocity profiles in a tube in the wake of a slug, and found that all disturbances died away within about 5 tube diameters. Therefore, as long as slugs are separated by about this distance, they will not tend to coalesce, or to be distorted by the presence of other slugs preceding them up the tube. Further, if the expansion of the slug is not large, they will rise with a constant velocity, and remain a constant distance apart.

The calculation of pressure drop in vertical slug flow requires an understanding of the distribution of shear stress and pressure around a

single slug rising in still liquid, and an extension of this analysis to a moving liquid. Except at very high flow rates, frictional effects are small relative to the pressure drop due to the weight of liquid in the tube. Therefore, pressure drops can be obtained to a close approximation for most conditions by a calculation of the average density of the fluid mixture, that is,

$$\rho_{av.} = \rho_L(1 - R_G) + \rho_G R_G \quad (50)$$

At high flow rates, and for other transport processes, however, it is useful to have some information on the fluid mechanics of the system. Therefore, a semi-empirical description of this aspect of slug flow is given below, as developed by Nicklin *et al.* (N4) as an extension of the work of Laird and Chisholm (L2).

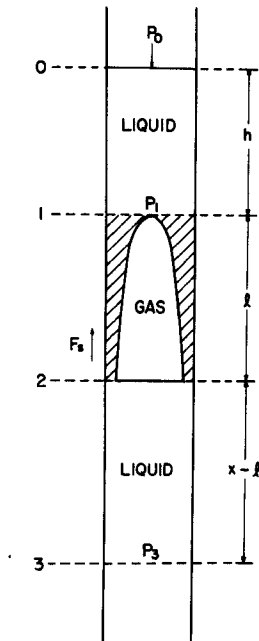


FIG. 8. Sketch of a rising slug in vertical flow.

Referring to Fig. 8, from a force balance between sections 0 and 3, Laird and Chisholm derived Equation (51) for a single slug rising in still liquid,

$$P_3 = P_0 + g\rho_L(h + \lambda + x - l) - F_s \quad (51)$$

Here λ is the height of tube required to hold the volume of liquid sur-

rounding the slug, l is the slug length, and F_s are the shearing forces between the tube walls and liquid, which must act upwards to balance the downward motion of the liquid around the slug. F_s is usually determined experimentally by measuring the change in P_3 when the slug breaks the surface.

At the stagnation point at the nose of the slug, the pressure is P_1 (also the pressure inside the bubble); applying Bernoulli's equation between sections 0 and 1, we obtain

$$P_1 = \rho_L g h + \frac{\rho_L V_s^2}{2} + P_0 \quad (52)$$

A quantity P_R is defined as the pressure recovery in the wake due to the change in momentum of liquid between sections 2 and 3. This pressure recovery can be calculated from a momentum balance if the liquid velocity at section 2 is known. Applying Bernoulli's equation again at sections 1 and 3, remembering that the pressure around the slug must be constant, we have

$$P_3 = P_1 + \rho_L g(x - l) + P_R \quad (53)$$

Combining Eq. (51), (52), and (53) gives

$$F_s = \rho_L g \lambda - P_R - \frac{1}{2} \rho_L V_s^2 \quad (54)$$

By generating single slugs, and measuring liquid levels in the tube during and after the passage of a slug, Nicklin *et al.* determined the quantity λ experimentally to be 10.2% of the slug length for long slugs. Tests on long, true Dumitrescu bubbles gave a value of 10.4%.

The liquid at the nose region of a slug can be assumed to accelerate freely under gravity; near the tail of the slug a region of constant liquid thickness exists where gravity is just balanced by wall shear forces.

At the nose, viscous forces can be neglected, and therefore the velocity in the liquid film can be calculated from Bernoulli's theorem. Nicklin *et al.* show that for these assumptions

$$\lambda = 0.495(Dl)^{1/2} \quad (55)$$

For small values of l , that is, 6 in. or less, the above equation agrees well with experiment. Therefore, λ can be estimated for both long and short bubbles. From a knowledge of λ and slug length, the velocity of the liquid entering the wake can be found, and P_R can then be calculated as mentioned above. Given these experimental results, F_s can then be determined from Eq. (54). The equivalence of the experimental value and the value of F_s obtained indirectly has been shown by Nicklin *et al.* The film thickness for a slug rising with a velocity of 0.566 ft./sec. in a 1.02-in. Perspex

tube was found to be 0.0262 in., for the region of constant thickness where the liquid is no longer accelerating. This value is somewhat less than that predicted by Dukler and Bergelin (D5).

When liquid and gas are flowing concurrently in fully developed vertical slug flow, the liquid moves upward with a velocity given by $(Q_G + Q_L)/A$. The wall friction acts in a positive sense, and can be calculated from single phase flow data. In the region around the slug, shearing forces at the wall act upward, as already mentioned, so that the friction acts in a negative sense, and if interfacial shear stresses are small, just supports the liquid in the film. This liquid weight can therefore make no contribution to the total pressure drop.

The resultant frictional pressure drop could be negative, so that the total pressure drop might be less than the weight of the liquid in the tube. The exact frictional drop is not easy to calculate because of the difficulty of determining the thickness of the liquid film around the slug, where the behavior approximates that of a wetted wall column being operated at very high liquid rates.

One additional conclusion arises from the work of Nicklin, Wilkes, and Davidson. Eq. (44) and (48), when $Q_L = 0$, transform to:

$$V_s = 1.2 \frac{Q_G}{A} + 0.35(gD)^{1/2} \quad (56)$$

Thus, even with zero liquid flow, a bubble or slug rises at a rate greater than its basic rising velocity, given by $0.35 (gD)^{1/2}$. It can be concluded, therefore, that continuously generated bubbles or slugs rising through stagnant liquid rise faster than single bubbles or groups of bubbles which are not being continuously generated. An extra increment proportional to the superficial gas velocity must be added to the basic rising velocity. At high gas rates, this increment may be the major factor in determining bubble velocity.

2. Horizontal Slug Flow

A flow model for horizontal slug flow of steam-water mixtures has been proposed by Kordyban (K1). This model supposes that the liquid flow is divided into two flow fractions, one of which flows along a sector of the tube bottom at one velocity (channel flow), while the remainder flows in the rest of the tube cross-section in the form of ideal flat discs (slug flow). The assumptions made are: (a) the vapor to liquid weight ratio flowing is small, and therefore the friction loss due to vapor flow can be neglected; (b) the liquid is turbulent in both the channel flow and slug flow; (c) the liquid in channel flow is negligibly influenced by shear

forces at its free surface; (d) for the liquid in slug flow, the shear stress at the interface equals the shear at the tube walls; and (e) no mass transfer occurs.

The Bernoulli equation can now be written for the liquid in channel flow in the bottom part of the tube, and for the liquid in slug flow in the upper part. The acceleration terms are then neglected, and the friction factors for each type of liquid flow found from the Blasius equation and from true Reynolds numbers. The resulting equations cannot be readily evaluated because of the two hydraulic-radius terms involved in the two types of flow, and an unknown fraction defining the relative mass of liquid in each part of the tube.

If it is assumed that most of the liquid flows in the form of slugs, then only one of the mechanical energy balances needs to be considered, and the cross-sectional area for slug flow becomes approximately the same as the tube area. The resulting expression is,

$$\Delta P_{TP} = \Delta P_L \left(1 + \frac{Q_G}{Q_L} \right)^{0.75} \quad (57)$$

where ΔP_L is the pressure drop for the liquid flowing alone in the tube.

In the region of slug flow, Chenoweth and Martin's correlation of superficial liquid volume fraction against a pressure-drop ratio can be represented by an expression

$$\frac{\Delta P_{TP}}{\Delta P_L^*} = \left(1 + \frac{Q_G}{Q_L} \right)^{0.86} \quad (58)$$

The similarity of this equation and that of Kordyban is obvious. However, as Kordyban points out, the assumption that all the liquid flows in the slugs is not a particularly good one, and agreement of Eq. (57) or (58) with slug-flow data for steam-water in small tubes (0.420 in. or less) at lower pressures is not too good ($\pm 70 - 100\%$). Comparison of Eq. (57) with the data of Reid *et al.* (R1) for slug flow in large diameter pipes gave considerably better agreement.

3. Unstable Slug Flow (Froth, Turbulent, Semi-Annular) in Vertical Tubes

The region in which vertical slug flow begins to show serious instabilities, with the slugs collapsing, or coalescing, has been described in various terms by different workers. It can certainly be specified as a transition region between two more definite patterns, slug and annular flow. There have been two recent attempts to analyze this unstable region, one by Moissis and Griffith (M5) and the second by Nicklin and Davidson (N3), from quite different viewpoints.

Moissis and Griffith suppose that as short gas bubbles rise through the tube, they tend to be unstable because of the short separation distances between them and hence of the consequent wake effects. They assume that coalescence of these bubbles will occur eventually to produce larger slugs, with a sufficient separation distance to give fully developed slug flow. For this reason, the unstable region was given the name "developing" slug flow, and assumed to be an entrance effect which could persist for long distances. This viewpoint is questionable in light of the fact that many investigators have found this froth or turbulent flow region to be quite constant in appearance, and to show little evidence at steady flow conditions that the nature of the flow pattern varied progressively along the tube.

It is not clear from Moissis and Griffith's work exactly how they produced the so-called "developing" slug flows they studied. In fact, the conditions studied by Moissis and Griffith appear to be those of coalescence of large bubbles, in what is really an artificially produced bubble flow. On the other hand, the work of Nicklin and Davidson seems to have been concerned with the instability developing from true slug flow as the gas flow rate increases. Further evidence in support of these conclusions lies in the fact that Moissis and Griffith in 1-in. pipe used a maximum superficial gas velocity of about 0.8 ft./sec. at zero liquid flow to produce their unstable conditions, and were apparently able to produce unstable regimes at even lower flow rates, whereas, Nicklin and Davidson found that for zero liquid flow in a 1-in. pipe, the change in flow pattern began between 5 and 6 ft./sec. superficial gas velocity. It would appear that the "developing" slug-flow results presented by Moissis and Griffith pertain to a transient region preceding the establishment of fully developed slug flow, which usually tends to disappear in about 20 diameters.

As mentioned in the previous section, the existence of a liquid film of uniform thickness around the base of a slug was pointed out by Nicklin, Wilkes, and Davidson (N4). In an extension of this work, Nicklin and Davidson (N3) have carried the analogy between this situation and a wetted-wall column to the instability point known to occur in wetted-wall columns at high gas-flow rates.

Considering a section of a vertical pipe through the base of a gas slug where the liquid film thickness is constant, and calling the gas volume fraction at this point R_g' and the true point gas flow Q_g' , we find from Eq. (46) that

$$Q_g' = R_g'AV_s = R_g'A[1.2(Q_g + Q_L)/A + 0.35(gD)^{1/2}] \quad (59)$$

If bubble expansion is neglected between the entrance and the section under consideration, and if Q_L' is the true liquid flow in the film

$$Q_L' = Q_G' - Q_G - Q_L \quad (60)$$

Finally, the forces around a slug must be in balance, and therefore, in theory, a third equation can be written allowing Q_G' , Q_L' , and R_G' to be determined. In practice, the liquid film is not sufficiently stable to allow calculation of the forces; thus, mutually compatible values must be found experimentally. This was done by Nicklin and Davidson in a wetted-wall column; they found that R_G' was independent of the gas velocity, Q_G'/A , and a function only of Q_L'/A . In addition, the flooding point was determined for both long and short columns. By combining Eq. (59) and (60), mutually compatible values of Q_G' , Q_L' , and R_G' were found, and these were solved graphically with the R_G' vs. Q_L'/A plot to give a real solution. From flooding results, this solution could then show what conditions were within the stable region, and at what point flooding would begin for given gas and liquid flow rates. The point of instability in a slug-flow pattern was determined by Nicklin and Davidson for no liquid flow in a one-inch tube, and was found to lie between $Q_G/A = 5$ and $Q_G/A = 6$ ft./sec., whereas flooding results predicted instability at $Q_G/A = 5.5$ ft./sec.

When flooding occurs, liquid is prevented from running down the column around the slug, and therefore the slug following must also collapse because of insufficient liquid. Hence, a process of continuous collapse and reforming of bubbles begins. At higher gas flows, a more vigorous action would be expected. The flooding action should result in a sudden increase in pressure drop, just as it does in a wetted-wall column; reference to Fig. 2 shows that this does in fact occur.

At low liquid rates, the onset of instability occurs at a constant value of the total superficial velocity, and is predictable from holdup and flooding data for wetted wall columns. As liquid flow rates increase, Nicklin and Davidson predict that unstable flow begins at lower values of the gas flow rate. For high liquid flow rates, however, the slug length becomes important, and the unstable flow will begin at higher values of gas flow rate. Therefore, a definite liquid flow rate exists at which an unstable flow pattern appears with a minimum gas flow rate.

Recently Bashforth *et al.* (B15) have made a study of the special region in which the transition from countercurrent to cocurrent liquid flow occurs with vertical upward gas flow. At this point, the liquid film is suspended, and the net liquid flow rate is zero corresponding to the limiting flooding case for wetted wall columns.

By assuming a parabolic velocity gradient in the film, these authors have derived an equation relating the hold up of liquid in the tube to the change in pressure drop due to a change in film length. Hence, this holdup could be predicted, and these predictions compared favorably

to that measured at various film lengths. In addition, the liquid-gas interfacial shear was calculated, and a friction factor for skin drag was shown to be a linear function of the superficial gas Reynolds number. The liquid holdup was also found to vary linearly with this Reynolds number.

From the relative magnitudes of liquid-wall and liquid-gas shearing forces, it was concluded that the circulation of liquid in the film must be such that two-thirds of the film is supported in upward motion by the gas flow, and one third is supported through downward motion by the wall of the tube. Hence, the net force on the tube wall is downwards against the air flow.

For air and water, in a one inch tube, the superficial gas velocity limits for the film suspension region were about 31 ft./sec. to 41 ft./sec. (see Fig. 10 also). The value of 31 ft./sec. agrees with the value to be expected for the critical gas flooding velocity at zero liquid flow from an extrapolation of the results of Nicklin and Davidson. Hence, the approach of the latter workers in their analysis of unstable slug flow would seem to be valid for net liquid flows down to zero.

B. BUBBLE FLOW

1. *Vertical Tubes*

Many of the considerations discussed in the previous section can be applied to vertical bubble flow. Two cases are of interest; first, one in which there is no downward or upward liquid flow ($Q_L = 0$), for example, on a distillation tray. With a shallow liquid layer there will be no liquid velocity profile, and hence bubble-rise velocities for uniformly sized bubbles will be the same at each cross-section. It can be shown (see Nicklin, N2) that if the rising velocity of a swarm of bubbles not continuously generated in a still liquid is V_0 , then the rising velocity relative to the tube of a swarm of continuously generated bubbles will be, for $Q_L = 0$,

$$V_B = \frac{Q_G}{K_G A} = V_0 + \frac{Q_G}{A} \quad (61)$$

Second, when a liquid is flowing in a long tube, a liquid velocity profile will develop, and bubbles near the center of the tube will rise more rapidly than those near the wall. In slug flow, all slugs rise with nearly the maximum velocity, but in dispersed bubble flow, the variations in speed tend to cancel and give a component to the bubble velocity due to the average liquid velocity. As before, from continuity, this mean liquid velocity at any cross section must be $(Q_G + Q_L)A$, so that the bubble rise velocity is

$$V_B = \frac{Q_G}{R_G A} = V_0 + \frac{(Q_G + Q_L)}{A} \quad (62)$$

The relative velocity between rising bubbles and liquid is also a matter of interest in transport processes. For bubbles in still liquid, this is given by Nicklin (N2) and by Wallis (W1) as

$$V_R = V_0 + \frac{Q_G}{A} = \frac{V_0}{(1 - R_G)} \quad (63)$$

In the case of a flowing liquid and continuously generated bubbles, the relative velocity is

$$V_R = V_B - V_L' = \frac{Q_G}{R_G A} - \frac{Q_L}{(1 - R_G)A} = \frac{V_0}{(1 - R_G)} \quad (64)$$

where V_L' is the true velocity of the liquid relative to the tube. Hence, for a given system and a given value of R_G , the relative velocity of the phases is a constant of the system, independent of the liquid flow rate, or whether the bubbles are generated continuously or not.

In bubble flow, the pressure-drop is almost entirely due to the weight of the fluid, and thus pressure-drops can be approximated very closely from a knowledge of the *in situ* volume-fractions as given by Eq. (62).

2. Horizontal or Vertical Tubes

Another analysis of two-phase bubble flow has been given by Bankoff (B6). Further discussion of this approach can be found in the articles by Zuber (Z2) and Hughmark (H11). Bankoff proposes, for the particular problem of bubble flow, a model which substitutes a single-phase fluid having a variable radial density; this model might be used for either vertical or horizontal tubes. The radial density occurs because of the observed fact that the bubble population is greater in the center of the tube. Further assumptions are that the bubble everywhere moves with the liquid velocity, but because of the nonuniform radial distribution, the mean bubble velocity is greater than the mean liquid velocity. The above assumption also means that buoyancy components of the bubble velocity are neglected (about 0.83 ft./sec. for air in still water). Power function distributions for velocity and gas volume-fraction in the radial (y) direction are assumed, viz.,

$$V_L^* = \frac{1}{\left(\frac{y}{r}\right)^m} = \frac{V_L''}{V_L''} \quad (65)$$

$$R_G^* = \frac{R_G'}{R_G''} = \frac{1}{\left(\frac{y}{r}\right)^n} \quad (66)$$

where V_L'' or R_G' are the point values, and V_L' or R_G' are the respective values at the tube centerline.

If now the definitions of the average gas volume-fraction and of the mass-flow rates, W_L and W_G , are written, and Eq. (65) and (66) are substituted in them together with the definition of the quality, $x = W_G/(W_L + W_G)$, then integration gives

$$\frac{1}{x} = 1 - \frac{\rho_L}{\rho_G} \left(1 - \frac{K}{R_G} \right) \quad (67)$$

where K is a "flow factor" defined by

$$K = \frac{2(m + n + mn)(m + n + 2mn)}{(n + 1)(2n + 1)(m + 1)(2m + 1)} \quad (68)$$

Further, one can define a "slip-velocity ratio," to show the difference between the mean true bubble velocity and the mean true liquid velocity:

$$\psi = \frac{V_G'}{V_L'} = \frac{1 - R_G}{K - R_G} \quad (69)$$

from which it can be shown that

$$R_G = \frac{K(V_G + V_L)}{V_G} = \frac{K(Q_G + Q_L)}{Q_G} \quad (70)$$

According to Bankoff, bubble flow occurs at gas volume-fractions to 0.8, and for qualities above about 0.6. He showed that, over this range, Eq. (70) with a value of $K = 0.89$ gave good results in comparison both with experimental data and with the Martinelli-Nelson correlation; the fit given by Eq. (70) was somewhat better than that given by the momentum theory of Levy (L4). This agreement was also true for pressure-drops, when the wall shear stress was calculated as for a single-phase fluid having the mixture properties.

Zuber showed that Eq. (70) corresponded to the result obtained experimentally by Armand (A7), with $K = 0.833$, and that it could correlate gas void-fractions as a function of quality for values of R_G to 0.8 for vertical flow.

It is interesting to compare the assumptions made by Bankoff to the restrictions operating in the investigation by Nicklin, Wilkes, and Davidson for slug flow. In their work the velocity component of the slugs due to liquid flow approached the maximum liquid velocity at the tube center-line. If this is also true of the bubbles of Bankoff's model and the bubble rise velocity due to buoyancy is ignored, then the velocity of the bubbles as given by Nicklin *et al.* would be,

$$V_B = 1.2 \frac{(Q_G + Q_L)}{A} = \frac{Q_G}{R_G A} \quad (71)$$

so that

$$R_G = \frac{0.83 Q_G}{(Q_G + Q_L)} = \frac{0.83 V_G}{(V_G + V_L)} \quad (72)$$

a result practically identical to that of Bankoff. It may be concluded that the variable-density assumptions made by Bankoff effectively approximate slug flow in vertical pipes; the success of his equation is largely due to the fact that over fairly wide ranges this serves as a reasonable model for vertical bubble flow. The slug and bubble models will give similar results as long as they are compared at sufficiently high liquid flow rates so that buoyancy differences can be neglected. Also, if the gas velocity component due to buoyancy is entirely neglected, then the horizontal and vertical models become identical.

Hughmark (H11) has extended this approach to obtain an empirical correlation covering wide ranges of data for the air-water systems in vertical flow. Basically the correlation consists of using Eq. (70) with a variable value of the coefficient K . This coefficient was expressed by Hughmark as a function of the mixture Reynolds number, Froude number, and liquid volume-fraction. Hughmark's approach gives

$$K = f(Z), \quad (73)$$

where

$$Z = \frac{(Re_M)^{1/6} (Fr_M)^{1/8}}{(R_{Ls})^{1/4}}$$

with the Reynolds and Froude numbers superficial values for the mixture. The quantity K was then found empirically from air-water data in vertical flow. An analysis of the terms involved in Eq. (73) indicates that the only strong effect not given in Eq. (70) is a variation in Z with $1/D^{0.75}$.

Correlation of R_G according to Eq. (73) is claimed for air-water and steam-water in vertical tubes, and for air with various liquids in horizontal tubes. Any fundamental significance of Hughmark's dimensionless groups, with their small exponents, is not readily evident. No apparent reason exists why the coefficient K should have a value differing from 0.83, even though pressure, temperature, or fluid properties might vary, as long as the assumptions corresponding to a slug type of flow are met. The use of a variable coefficient in Eq. (70) may simply reflect the deviation of the system from slug-flow behavior.

Zuber (Z2) has reported that Russian workers have used a similar but simpler approach to correlate their void-fraction data successfully for steam-water mixtures. The "modified Armand equation" described in

Section 1V, D, also belongs in this category. While the equations of Nicklin *et al.* for void fractions are firmly based on theory for slug or bubble flow, the extension of these equations to other flow patterns, or to void-fractions above 0.8, is empirical.

A knowledge of the mechanics of vertical cocurrent bubble, slug, and froth flow is important for an understanding of the performance of gas-lift pumps. These devices will not be discussed here, but reference may be made to a recent article by Nicklin (N1).

3. Horizontal Bubble Flow

An investigation has been reported by Wallis (W1) in which finely dispersed bubbles could be injected into liquid in horizontal flow through porous walls, either to give a constant quality, i.e., at only one point, or continuously along the tube length to give a simulation of forced-convection boiling. The latter experimental analogy is open to question, inasmuch as there is a large amount of evidence that nucleation is suppressed at high liquid velocities. However, the correlations presented by Wallis apply only to bubble flow and, presumably, therefore, to relatively low velocities and qualities. If this is true, the model may apply in some ranges of forced-convection boiling.

Wallis points out that, from continuity considerations and bubble dynamics, the cocurrent flow of uniformly dispersed bubbles as a discontinuous phase in a liquid can always be made to occur in any system and for any void volume. (This is not true for countercurrent flow.) Coalescence of bubbles may occur, of course, and if this coalescence is sufficiently rapid, a developing type of flow is observed, usually from bubble to slug flow. Because of this behavior, the particular flow pattern observed in bubble flow is quite dependent on the previous history of the two-phase mixture. This would be true for both horizontal and vertical flow.

Wallis states that if bubbles were uniformly dispersed, and nonrigid, then their effect at a constant total mass-flow rate would be simply to increase the stream velocity, and at a constant friction factor, the pressure-drop would be,

$$\Delta P_{TP} = \Delta P_L \left(1 + \frac{Q_G}{Q_L} \right) \quad (74)$$

where ΔP_L is calculated as liquid at the total mass flow. This equation appears to be actually a close approximation, good for low gas densities or low qualities.

The above equation was found to be inadequate; and hence Wallis suggests the following dimensional empirical form for horizontal bubble flow,

$$\frac{\Delta P_{TP}}{\Delta P_L} = 1 + 300 \left(\frac{Q_G}{Q_L} \right) G_M^{-1/3} \quad (75)$$

where G_M is expressed in lb. mass/(hr.) (sq. ft.). For the air-water mixtures used, this correlation is equivalent to those of Hoogendoorn (H6) or Laird and Chisholm (L2), except that a specific term is included to allow for the fact that the Lockhart-Martinelli parameter X_{tt} is also a function of G_M (see Section IV,E,4.)

Experiments carried out with accelerating horizontal bubble flow, that is, with variable quality, were correlated by similar but separate equations for $\frac{3}{8}$ -in., $\frac{5}{8}$ -in., and $\frac{7}{8}$ -in. diameter pipe. For the $\frac{7}{8}$ -in. pipe,

$$\frac{\Delta P_{TP}}{\Delta P_L} = 1 + \left(490 \frac{u_G}{V_L} \right)^{0.82} \quad (76)$$

where u_G is the gas velocity *normal* to the pipe wall. The numerical constants differ for each pipe size. The equations correlate total pressure-drop, that is, the sum of frictional and acceleration losses.

C. ANNULAR (CLIMBING-FILM) AND DISPERSED FLOW

These two flow-patterns should be considered together, because of the experimental evidence that liquid entrainment in the form of droplets is probably always present to some degree in annular flow, and because the transition from one flow-pattern to the other is very gradual.

This flow-pattern is of great importance in heat transfer processes. Consideration is being given to cooling nuclear reactors by use of this type of two-phase flow. It occurs in the commonly used long-tube evaporator, in thermosiphon reboilers, and probably to a considerable degree in water-tube boilers as well. Because of these potential and current uses, a great many experimental and theoretical studies of this flow pattern are under way. The relatively few investigations carried out prior to 1958 have been reviewed by Bennett (B9). A recent, comprehensive review of this work has been given by Lacey *et al.* (L1), who list 57 references mostly referring to work recently completed or still in progress.

Superficially it would seem that the symmetry presented by upward annular liquid flow in tubes should offer a good opportunity for a rigorous analysis of the fluid mechanics. Indeed, a fair success has resulted from efforts in this direction, but many difficulties still remain. In the following section, a largely qualitative description of methods of analyzing annular and spray flow will be given. Discussion referring specifically to heat transfer will be given in Section VI.

In upward or climbing-film flow, waves or ripples are *always* present. At low gas rates and low liquid rates, films are thin, wave amplitude and entrainment may be relatively small, and straightforward hydrodynamic

analysis ignoring these factors may give reasonable prediction of behavior. At higher gas flow rates, entrainment increases, and a high-velocity "ring" wave of large amplitude appears. If the amount of liquid entrainment becomes appreciable, then prediction of film thickness or pressure-drops will depend on a knowledge of the relative distribution of the liquid mass-flow between the two phases, which has not yet been given much experimental attention. Moreover, the mass-fraction of liquid entrained may increase along the pipe. Anderson and Mantzouranis (A3) have found that entrainment increases exponentially with velocity; hence, since the gas velocity itself increases continuously due to pressure drop, entrainment equilibrium is apparently never reached. Further, the method of adding the liquid feed will affect this situation markedly, and it may require a thousand diameters (L1) to approach spray equilibrium. *Therefore, at higher flow rates, experimental results may only be comparable for identical entrance arrangements, and theoretical analyses based on steady-state models may never be duplicated in practice.*

Pressure drops for these higher flow rates are very much larger than would be anticipated from a smooth-liquid-surface model, even if the fluid properties are modified to allow for the appreciable entrained-liquid content. A large additional dissipation of energy must occur because of (1) the behavior of the wavy film as a rough wall, (2) wave generation, and (3) liquid interchange between the film and the gas.

Entrainment behavior may be summarized from the work of Wicks and Dukler (W2) and Collier and Hewitt (C6) in the following way, based on jet- or shock-type injection of liquid. Very little entrainment occurs until a certain pressure-drop is reached which, in general, is about twice the pressure drop which would have occurred if the gas had been flowing alone in the tube. At constant liquid rate and increasing gas rate, the film thickness decreases, and at the highest gas rates approaches a reasonably constant value. When the liquid rate is also high, the entrained liquid approaches 90% of the total. Presumably, at this point, the liquid film owes its existence to a process of continuous deposition and removal of liquid droplets. At constant gas rate, liquid-film thickness increases with increasing liquid feed rate, until at fairly high gas rates it becomes nearly independent of liquid rate; the entrainment increases steadily as liquid flow rate increases. Pressure drops increase steadily with increasing gas rates, but at constant gas rate they tend to be much less dependent on liquid rate.

For the relatively simple case where entrainment need not be considered, Calvert and Williams (C1), Anderson and Mantzouranis (A2, A3), and Collier and Hewitt (C6) have attempted analyses of the mechanics of upward film flow. Calvert and Williams made use of the

Prandtl-Nikuradse treatment and considered the liquid film to involve a laminar and a turbulent layer. Anderson and Mantzouranis' work is an extension of the equations presented by Dukler and Bergelin (D5), and makes use of the von Karman universal velocity profile. In general, if any two of pressure drop, liquid flow rate, or film thickness are known, the third quantity can be calculated.

Collier and Hewitt have compared results from the two approaches of Calvert and Williams, and Anderson and Mantzouranis, and give the following summary:

(1) For very low values of τ_w , the wall shear force, the Anderson and Mantzouranis analysis predicts film flow rates from film thickness and pressure drop which are very much lower than are the actual values (down to about one-third). In this region, the Calvert and Williams theory predicts film flow rates quite close to the measured values.

(2) For high values of τ_w , both theories predict much higher film flow rates than those observed (in the worst case by a factor of 4).

Film thickness is predicted more closely from film flow rate and pressure drop, than is film flow rate from film thickness and pressure drop. This improvement results from the fact that the film flow rate is approximately proportional to the square of the thickness.

(3) For most of the results, the values of y_i+ (dimensionless distance parameter), at the gas/liquid interface correspond to the buffer region

$$(5 < y_i+ < 30)$$

(4) The Anderson and Mantzouranis analysis always predicts lower values for film flow rate than the Calvert and Williams theory. This difference is accentuated at low values of τ_w and reached about 300%. For high values of τ_w the difference is only about 10%.

More recently Hewitt (H5) has adapted a downward-film-flow analysis by Dukler (D4) based upon the Deissler velocity profile, to upward film flow; this approach, also requiring numerical solution, is claimed to give better correlation of film thickness with theory, over wider ranges than previous data, and for different types of liquid injections. The Deissler velocity profile was developed specifically to describe the velocity variation in the zone close to a solid wall, and, might be expected to give the best description of film flow. However, when gross wave motion or significant entrainment occurs, this correlation also shows deviations from experiment.

The effect of the method of liquid injection is worth noting. In general, the higher the entrance shock when the two phases are mixed, the greater the amount of entrainment will be. Injection methods giving smooth annular films with a minimum of entrainment give higher pressure-drops (C6, W2). For example, pressure-drop decreases in the following order for different injection methods: porous walls > annular slots or rings

> radial jets > tees or ells. Entrainment decreases in the reverse direction, suggesting that less energy is required to transport liquid as droplets than is required to move it as a wavy climbing film.

Entrainment studies have been relatively few, as pointed out earlier. Anderson and Mantzouranis (A3) used the results of measurements of entrainment (which was small in their work) to correct their calculated liquid film thickness, and thus obtained somewhat better agreement with experimental values. Wicks and Dukler (W2) measured entrainment in horizontal flow, and obtained a correlation for the amount of entrainment in terms of the Lockhart and Martinelli parameter, X . The entrainment parameter, R , of Wicks and Dukler is given by

$$R = \frac{(Q_L/Q_G)We_c E}{(dP/dL)_G} \quad (77)$$

where (dP/dL) has the usual significance, E is the mass of liquid entrained per unit time, and We_c is the "critical" Weber number:

$$We_c = \rho_G \frac{(V'_{G_0} - V'_{L_0})^2 d_c}{\sigma_L g_c} \quad (78)$$

Here V'_{G_0} and V'_{L_0} are the true velocities at the entrance, of gas and liquid, respectively, and d_c is the critical droplet diameter. The value of the We_c depends on the degree of shock at the entrance section; e.g., for smooth liquid injection, 22 was used, and for tee entrances, 13 to 16. Collier and Hewitt (C6) also measured entrainment in air-water mixtures, and have extended the same correlation to much wider ranges, using $We_c = 13$ in the case of jet injection with the results shown in Fig. 9. Anderson *et al.* (A5), during mass-transfer studies in a water-air-ammonia system, found en-

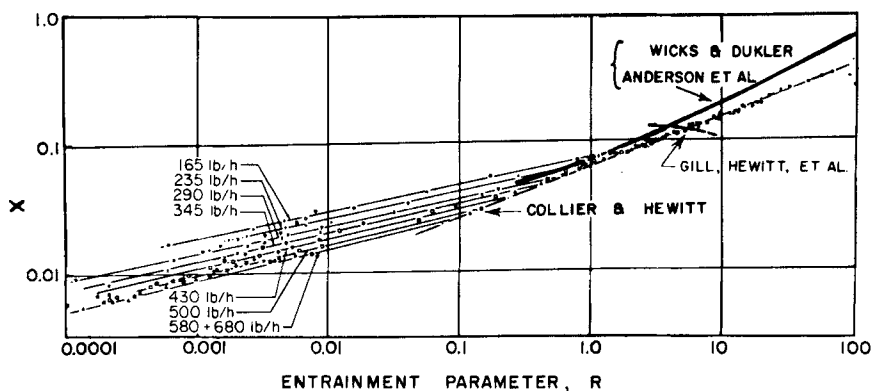


Fig. 9. Entrainment Correlation of Wicks and Dukler [after Collier and Hewitt (C6)].

trainment values that were in complete agreement with the Wicks and Dukler correlation.

In a recent publication, Gill *et al.* (G12) present results of new studies of film thickness and entrainment for upward annular flow of air and water at constant rates in a long, 1 $\frac{1}{4}$ -in. pipe. A porous inlet section for liquid was used, so that all entrainment arose from the annular film itself. These authors conclude that entrainment increases steadily along a tube, and arises from the continuous presence of film surface waves, so that a very long tube might be required to reach equilibrium (which might never occur if surface waves never disappeared).

Inasmuch as the amount of entrainment varies continuously along the tube length, it is apparent that the Wicks and Dukler correlation cannot be completely general, as it does not contain any allowance for this effect. Gill *et al.* found from their results (also shown in Fig. 9), that this correlation gives an entrainment value corresponding to a position about 6–8 ft. along a pipe, for air and water. Depending on the point in the pipe and the degree of entrance shock, the predicted and measured values can vary by $\pm 50\%$. However, for a given distance from the entrance, the type of correlation shown in Fig. 9 can be obtained for a given gas-liquid system. No data appear to be available for systems other than air and water.

Gill *et al.* also measured both entrained liquid flow rates and gas velocity profiles across the core as a function of pipe length. The local mass velocity of entrained liquid varies as might be expected for smooth liquid injection. Close to the injection point the entrained water flow decreased from the wall toward the center, but at a position remote from the entrance the reverse was true and the liquid mass velocity in the gaseous core was greatest at the center. At intermediate positions, a reasonably uniform liquid flux existed across a diameter, as reported by others (A3, W2). Measurements of the gas velocity profile gave a fairly sharply peaked parabolic form, which was shown to follow the form of the classical velocity deficiency law for very rough surfaces, but with a new numerical coefficient. The combination of increased liquid mass velocity near the tube center and a peaked velocity profile resulted in a very uniform volumetric fraction of liquid existing in the core at any radial position.

An interesting study of entrainment from horizontal liquid films has also been carried out by Van Rossum (V1). On the basis of a liquid film in laminar flow with a flat and smooth surface, he found that the mean actual film thickness was about 0.6 times the theoretical one. The critical Weber number corresponding to the onset of atomization was determined for five different liquids, with Weber number defined as

$$We = \frac{\rho_G V_R^2 y_i}{\sigma_L} \quad (79)$$

where V_R is the relative velocity between gas and liquid, and y_i is the liquid-film thickness. For velocities above 82 ft./sec., and viscosities above about 4 cp, the critical Weber number was constant at about 17. For less viscous materials, the critical Weber number decreased, as surface tension increased and as viscosity decreased, from 17 to about 3. For all liquids, there is a velocity below which no entrainment will occur, regardless of film depth, and roughly this velocity in meters/sec. is given by,

$$V_{\min.} = \sigma_L/4 \quad (80)$$

with σ_L in dynes/cm. In summary, the present correlations for entrainment are useful, but its basic mechanics is just beginning to be understood, and further testing will be needed to determine the ranges over which the correlations apply.

A recent publication by Zhivaikin (Z1) has reviewed Soviet work on film thickness and entrainment from films, and has presented correlations both for the thickness and for critical entrainment velocities. The relationships, given in terms of dimensionless quantities for downward cocurrent flow, upward cocurrent flow, and gas-liquid counterflow, follow. For laminar flow of *liquid alone vertically downward* along a pipe wall, the Nusselt equation was found to apply,

$$b = \left(\frac{3\mu}{g\rho} \right)_L^{1/3} \Gamma^{1/3} \text{ cms.} \quad (81)$$

where Γ is the liquid flow in cm.³/(sec.) (cm. of film width), and μ , ρ , g , are expressed in c.g.s. units.

For the turbulent region,

$$b = 0.317 \left(\frac{\mu}{\rho g^4} \right)_L^{1/12} \Gamma^{7/12} \quad (82)$$

The transition region falls at liquid-phase Reynolds numbers ($4\Gamma\rho/\mu$) between = 1800 and 4000. *For downward cocurrent flow*, in the region of no entrainment ($V_G < 4$ meters/sec.),

$$b = [1 - 0.022(V_G - 4)] \left(\frac{3\mu}{\rho g} \right)^{1/3} \Gamma^{1/3} \quad (83)$$

The critical gas velocity, V_{GCR} , at the start of entrainment is expressed by three separate equations, for low, medium and high Reynolds numbers.

For $Re < 0.85\rho_L^2/\mu_L^2$,

$$V_{GCR} = \frac{10.3\sigma}{\mu_L^{0.25}\rho_L^{0.75}\Gamma^{0.75}} \text{ meters/sec.} \quad (84)$$

For $0.85\rho_L^2/\mu_L^2 < Re < 28.8\rho_L/\mu_L$

$$V_{GCR} = \frac{70.8\sigma\mu_L^{0.25}}{\rho_L^{1.25}\Gamma^{0.25}} \quad (85)$$

For $Re > 28.8\rho_L/\mu_L$

$$V_{GCR} = \frac{43.2\mu_L^{0.25}\sigma}{\rho_L^{1.25}} \quad (86)$$

For velocities in excess of the critical velocity, that is, when entrainment occurs,

$$b = [1 - 0.022(V_G - 4)] \left(\frac{3\mu_L}{\rho_L g} \right)^{1/3} \Gamma^{1/3} + 255 \left(\frac{3\mu_L}{\rho_L g} \right)^{1/3} \left(\frac{\Gamma - \Gamma_{CR}}{V_G^{1/8}} \right)^{1/3} \quad (87)$$

For upward film flow of gas and liquid,

$$\Gamma_{CR} = \frac{656\mu_L^{0.8}\sigma^{0.2}}{\rho_L V_{GCR}^{0.2}} \quad (88)$$

Zhivaikin obtains a correlation for the film-thickness data of several workers for upward cocurrent flow by plotting $bV_G^{3/4}$ against Γ (with b in cm. and V_G in meters/sec.). Two lines result, one for the region showing no entrainment, and one for the entrainment region with Γ_{CR} about $0.575 \text{ cm.}^2/\text{sec.}$ and affected only slightly by gas velocity. The two lines are:

For no entrainment,

$$b = 3.36 \left(\frac{\Gamma\mu_L}{\rho_L} \right)^{1/2} \left(\frac{1}{V_G^{3/4}} \right) \quad (89)$$

For the entrainment region,

$$b = 5.65 \left(\frac{\Gamma\mu_L^3}{\rho_L^3} \right)^{2/9} \left(\frac{1}{V_G^{3/4}} \right) \quad (90)$$

All of these results are expressed graphically in Fig. 10. The equations apply to systems using air and water (or water plus glycerol) over a range of liquid viscosities. The effect of gas density and viscosity are not mentioned by Zhivaikin. The applicability of Equation (81) through (90) to other systems is therefore not known.

D. STRATIFIED AND WAVE FLOW

This flow-pattern occurs only in horizontal flow, in larger pipes and channels, at low liquid rates. Few studies have been made of this type of flow in confined channels, as distinct from wave studies on a more extended liquid surface. The initial work was by Bergelin and Gazley

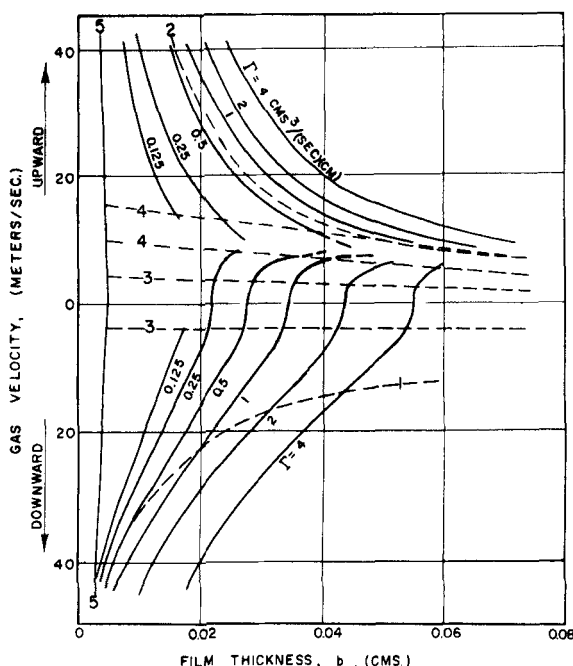


FIG. 10. Correlation of film thickness with gas and liquid flow rates for air-water system in vertical flow, according to Zhivaikin (Z1). 1, 2: limits for onset of entrainment in downward and upward flow, respectively. 3, 3: limits for small effect of gas velocity on liquid flow (smooth wetted wall operation). 4, 4: region of film suspension. 5: limit for existence of film flow.

(B12), and by Gazley (G1), using air-water. It was shown that when a gas-liquid interface is smooth, energy transfer from gas to liquid is entirely dissipated in surface friction, but when a liquid surface is hydrodynamically rough, energy transfer from gas to liquid may amount to twice that to be expected on the basis of interfacial friction (G1). Presumably this excess energy is dissipated in the formation and maintenance of surface waves.

The first paper by Bergelin and Gazley (B12) analyzed the principal characteristics of stratified flow. An hydraulic gradient exists in the channel, which is a function of the ratio, W_L/W_G , but this gradient may be positive (the liquid becoming deeper downstream), negative, or zero. If the gradient is negative, the liquid receives less energy from the gas than it loses due to wall friction. At a given point in a channel, average liquid depth always increases with an increase in liquid flow rate, and decreases with increasing gas flow rate.

The transition from laminar to turbulent liquid flow was reported to

occur at a true liquid Reynolds number (using the hydraulic radius) between 7000 and 8000. In stratified flow, if an appreciable hydraulic gradient exists, the void-fraction varies along the pipe. Although data were presented for midpoint void-fractions by Bergelin and Gazley, these were not correlated, except roughly by the Lockhart-Martinelli curves.

For a relatively thin liquid film flowing cocurrently with gas on a fairly wide surface of uniform depth, three types of waves have been described by Hanratty and Engen (H1). These wave forms are classified as "two-dimensional," "squall," and "roll" waves. The first of these seems to correspond to situations described as "ripple" or "capillary" waves by other workers. The "squall" surface has also been called "pebbled," and seems to correspond to the "hydrodynamically rough" surface described by Gazley (G1). The "roll" or "cresting" waves may, in fact, take the form of slug flow when generated in tubes, as suggested by Hanratty and Hershman (H2).

Stratified or wave flow in horizontal pipes has unique features not reproduced in uniformly thick liquid layers. Liquid-film thickness is not uniform because of the pipe curvature, and wall drag effects are very appreciable. Hanratty and Hershman point out that at high gas rates, where wave-annular flow occurs, gravity should have a stabilizing influence on waves on the bottom of a horizontal tube, little effect at the mid-point, and a destabilizing influence at the top. Surface tension should affect wave form only slightly at the bottom, but should act as a restoring force at the top. The waves observed in stratified pipe flow are generally not the same in form as those reported on flat liquid surfaces; however, for both cases, a hydrodynamically rough surface in air-water seems to appear at a gas velocity between 10 and 15 ft./sec. Entrance effects, vibration, and similar factors affect the point at which the first small ripples appear, but apparently not the point where a rough surface forms.

Up to the present time, work has been done which allows prediction of the onset of large waves (H2), and of formation of other types of waves (V1, H1), but only on flat uniform liquid surfaces. The extent to which these results can be applied to pipe line flow is uncertain. Apparently, Gazley's papers are still the only basic reports of stratified and wave flow in horizontal pipe; incidentally they also show a parallel between liquid instability in pipe flow as evidenced by wave formation, and that evidenced in packed towers by flooding.

VI. Heat Transfer to Two-Phase Mixtures

A. DESCRIPTION OF BOILING IN TUBES

Although equipment such as long-tube evaporators, thermosiphon reboilers, and tubular steam generators has been used for many years, rela-

tively little analysis of the vaporization or heating process has been made. The boiling of liquids in vertical tubes is the most important application of two-phase heat transfer, and will now be considered.

A common situation will be assumed in which a tube, long relative to its diameter, is fed at the bottom with an approximately saturated liquid. The temperature of the heating surface is not so high that so-called "film

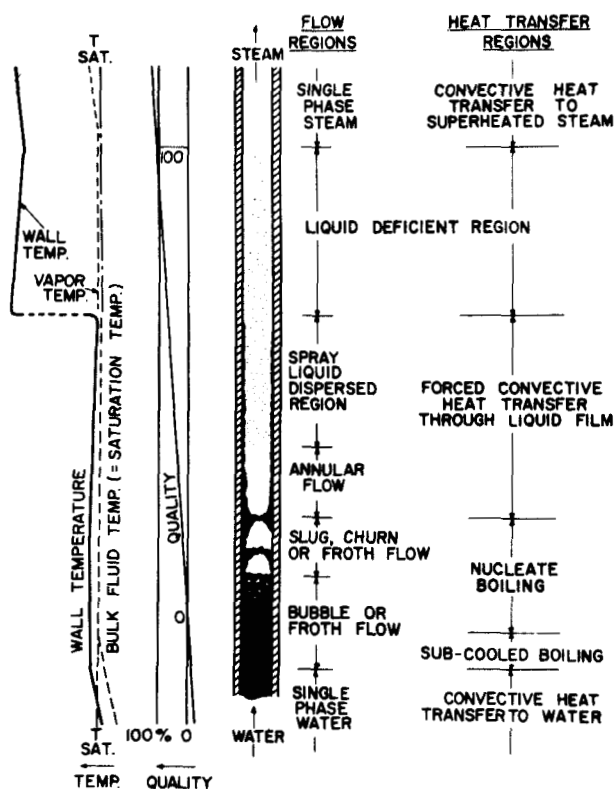


FIG. 11. Single component vertical upward flow behavior in boiling [after Lacey *et al.* (L1)].

boiling" can occur, and the pressure is low enough (less than $\frac{1}{3}$ of critical pressure) so that upon vaporization appreciable volume changes occur. As the tube length increases, the flow-patterns observed will then pass successively through those described for vertical flow in Section II,C. This behavior is shown schematically in Fig. 11, together with the quality and temperature variations along the tube.

Although there are several flow-patterns, hydrodynamically quite different, only three heat-transfer regions really need to be defined. At the

bottom of the tube, where there is little vapor phase, nucleate boiling will occur. As the quantity of vapor increases, and therefore the fluid velocity, nucleation is suppressed by the fluid turbulence, and the hydraulic behavior of the system gives rise to a forced-convection region of heat transfer. Because of the high heat-transfer coefficients for these two types of behavior, the wall temperature will remain relatively constant. As the quantity of vapor increases and that of the liquid decreases, annular flow occurs, and finally a point is reached at which a sharp rise in wall temperature is found, together with a corresponding drop in heat transfer coefficient. On the assumption that disruption of the liquid film has now occurred at this point, the ensuing region is known as "liquid-deficient." Beyond this region, the liquid film disappears entirely, and "dry-wall" conditions are attained. The point in the liquid-deficient region at which a rise in wall temperature is observed is usually referred to as a "burn-out" position, and the corresponding maximum heat flux as the "burn-out flux."

In many applications of two-phase boiling heat transfer, the coefficients are so high that their precise evaluation is not a significant factor, in comparison to the importance of other thermal resistances of the system. However, there are many other instances where fairly exact prediction would be valuable. In all cases of two-phase boiling, if it is carried to high qualities, the prediction of burn-out is important because of the radical change in heat transfer behavior occurring at this point, whether or not this is accompanied by physical damage to the channel walls.

The general aspects of nucleate boiling will not be discussed here. Perhaps the most important consideration is that it should be possible to specify the factors governing the transition from nucleate boiling to the forced-convection regions. In nucleate boiling, the heat flux increases with the temperature differential approximately as $(\Delta T)^4$, as does the heat-transfer coefficient. However, in the forced-convection region, the temperature differential remains relatively constant although the heat flux (or the heat-transfer coefficient) increases with increasing quality or mass flow. Quality and mass-flow changes, except at very low heat fluxes, have little effect on nucleate-boiling coefficients.

The transition from nucleate boiling to forced-convection heat transfer is gradual. As fluid velocity increases, nucleation becomes more difficult, and therefore this boiling mechanism makes up a decreasing part of the total heat transfer. The transition will occur at higher velocities as pressure increases, and because the velocity at a constant quality decreases with pressure, a higher quality will also be required to suppress nucleation.

Bennett *et al.* (B11) have represented this behavior graphically as shown in Fig. 12. The following explanation of the boiling phenomena in two-phase flow is taken from their paper:

In order to explain the reasons for the changes of heat transfer mechanism between the regions, the following tentative and somewhat qualitative picture is suggested. Figure 12 shows the observed relationship between the heat flux and surface temperature difference for nucleate boiling at atmospheric pressure (line AB). Also shown are the lines for water in forced convection at various velocities and extrapolated to meet the boiling curve. The transition between the forced convective process and the boiling process is not sharp and the lines curve at the ends to blend smoothly with the boiling curve.

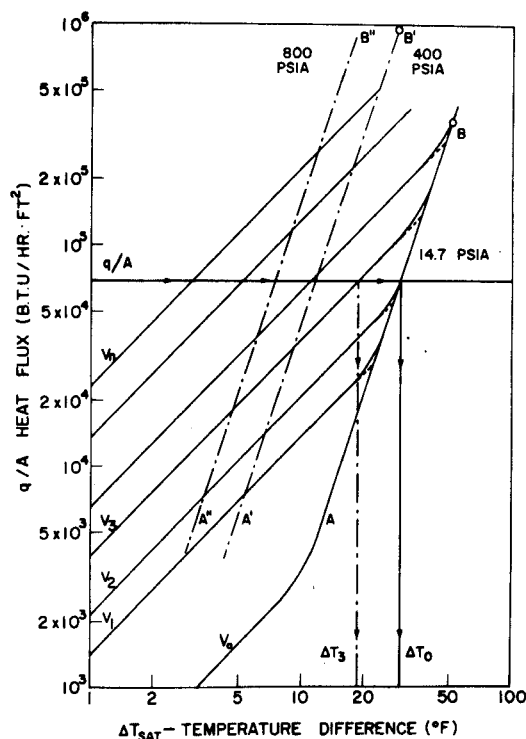


FIG. 12. Representation of conditions for nucleate and forced convection boiling in vertical flow [after Bennett *et al.* (B11)].

Consider a tube heated uniformly at a heat flux q/A fed with saturated water at the base at a velocity V_0 . For this velocity and heat flux, nucleate boiling will take place, and a temperature difference ΔT_0 will be established. At some distance up the tube vaporization will occur and increase the volumetric flow of material and hence the velocity to, say, V_1 . The line for forced convective heat transfer meets the boiling curve below the heat flux of q/A and so nucleate boiling will still be the mode of heat transfer and the temperature difference ΔT_0 , and hence the heat transfer

coefficient remains constant. This effect of constant heat transfer coefficient as the quality rises from zero has been experimentally observed and coefficients in the nucleate boiling region are solely functions of heat flux.

Further up the tube, the vaporization increases the velocity further to, say, V_s . The forced convective line meets the boiling curve at the heat flux q/A . This point may be considered the point of suppression of nucleate boiling observed by a number of workers investigating boiling in tubes. The velocity V_s will correspond to a fixed degree of vaporization which, for the 0.623 in O. D. heater, corresponded to between 7% and 15% steam quality. Still further up the tube where the velocity is still greater, e.g., V_s , the heat flux line now crosses the corresponding forced convective line to give a temperature difference ΔT_s lower than ΔT_0 . Forced convection is now the main process of heat transmission and any increase in velocity yields a corresponding decrease in temperature difference or increase in heat transfer coefficient. This process will continue until the transition to the "liquid deficient" regime, where the thin statistical liquid film no longer totally wets the heating surfaces. Heat transfer is no longer to a highly conducting thin film of water but to a poorly conducting gas (i.e., steam), so that the heat transfer coefficient drops precipitously. This transition is clearly not related to any so-called critical temperature difference phenomena as is the transition from nucleate boiling to film boiling.

Referring to Fig. 12, it is clear that not all the three regions need necessarily be present when a liquid is boiled in a tube. For instance, the exit velocity of the two-phase mixture may never exceed that required for two-phase forced convection to take place, or the heat flux may be such that with an inlet velocity V_s , nucleate boiling cannot occur and only forced convective heat transfer takes place.

The above explanation represents the picture qualitatively and if this is so, then certain predictions may be made regarding the effects of such variables as pressure and geometry. Many workers have investigated heat transfer in the nucleate boiling region and a number of generalized correlations including the effects of liquid properties; pressure, etc., have been proposed. These indicate that, with an increase in pressure, the line AB in Fig. 12 moves to the left, i.e., to A'B' or A''B'', so that a somewhat higher velocity would be required for the suppression of nucleate boiling.

For the forced convective region, only limited data are available on the effects of the different variables involved, since the existence of this region has only been recognized recently. As previously mentioned, the velocity required for the suppression of nucleate boiling increases with pressure; further, an increase in pressure reduced the specific volume of the vapour and hence the linear velocity of the two phase mixture at a given quality will be reduced. Thus higher velocities and steam qualities would be required for the forced convective region to be entered at the same heat flux. The effect of diameter is, as far as can be seen from the work of previous experiments and from these experiments, that to be expected with convective heat transfer, namely, that the coefficient is proportional to the diameter or the equivalent diameter to the power -0.2 .

Very little quantitative measurement has been made in the liquid deficient region. The critical steam quality is known to be a function of heat flux and flow rate together with pressure and also geometry. The effect of pressure would be to markedly increase the lower limit for the values of the coefficients to be found in this region.

One additional feature of upward vertical flow with heat transfer needs to be mentioned. If subcooled liquid is present, local boiling may occur, that is, vapor bubbles may be formed at the wall which will col-

lapse upon moving into the bulk liquid. Hence the void fraction may not be zero, even though the quality (by energy balance) is zero. Sher and Green (S7), and Hubers (H9) have discussed the uncertainty of void measurements at low qualities.

B. CORRELATIONS OF FORCED-CONVECTION HEAT-TRANSFER COEFFICIENTS FOR TWO-PHASE FLOW

1. Use of the Lockhart-Martinelli Parameters for Heat Transfer

In order to achieve a meaningful correlation of heat transfer coefficients for two-phase flow, it is necessary to measure local heat fluxes and temperature differences. Relatively few studies have been made in this category. Dengler and Addoms (D3), Guerrieri and Talty (G11), Bennett *et al.* (B11), and Schrock and Grossman (S4) measured such coefficients for the boiling of liquids in vertical tubes or in a vertical annulus. Groothuis and Hendal (G10) extended the earlier work of Stemerding and Verschoor (S12) on heat transfer to nonboiling two-phase mixtures in horizontal tubes. Johnson (J1) and Johnson and Abou-Sabe (J2), have also reported data for the heating of air-oil and air-water mixtures in horizontal pipes. Davis and David (D2) have measured coefficients for water boiling in horizontal rectangular channels.

In the forced-convection region, Dengler and Addoms and also Guerrieri and Talty correlate their results by analogy to the Lockhart and Martinelli approach, and show that the following equations can be used:

$$\frac{h_{TP}}{h_{L_1}} = 3.5 \left(\frac{1}{X_{tt}} \right)^{0.5} \quad (\text{Dengler and Addoms}) \quad (91)$$

$$\frac{h_{TP}}{h_{L_1}} = 3.4 \left(\frac{1}{X_{tt}} \right)^{0.45} \quad (\text{Guerrieri and Talty}) \quad (92)$$

where X_{tt} is the Lockhart-Martinelli parameter for turbulent-turbulent flow, h_{TP} is the heat transfer coefficient for two-phase flow, and h_{L_1} is the coefficient calculated from a Dittus-Boelter equation for the total flow, and h_{L_2} that for the liquid flowing alone; that is,

$$h_{L_1} = 0.023 \left(\frac{k_L}{D} \right) \left(\frac{DG_M}{\mu_L} \right)^{0.8} \left(\frac{C_{pL}\mu_L}{k_L} \right)^{0.4} \quad (93)$$

or

$$h_{L_1} = 0.023 \left(\frac{k_L}{D} \right) \left(\frac{DG_M(1-x)}{\mu_L} \right)^{0.8} \left(\frac{C_{pL}\mu_L}{k_L} \right)^{0.4} \quad (94)$$

Only the Reynolds number differs in these two expressions.

Bennett *et al.* (B11) used the same method of correlation, but allowed

for a slight dependence on total heat flux with a relationship not entirely dimensionless:

$$\frac{h_{TP}}{h_{Ls}} = 0.64 \left(\frac{q}{A} \right)^{0.11} \left(\frac{1}{X_{tt}} \right)^{0.74} \quad (95)$$

Departure of results from these correlations in all cases signified an appreciable contribution by nucleate boiling to the heat transfer.

Schrock and Grossman (S3, S4) also obtained a similar correlation for boiling in very small tubes ($\frac{1}{8}$ -in. diameter),

$$\frac{h_B}{h_{Ls}} = 2.5 \left(\frac{1}{X_{tt}} \right)^{0.75} \quad (96)$$

However, an effect of total heat flux was also noted by these latter authors, who ascribed this variation to a contribution due to nucleate boiling, and therefore proposed the following over-all equation (S4),

$$\frac{(Nu)_B}{(Re)_L^{0.8} (Pr)_L^{1/3}} = 170 \left[\left(\frac{q}{G_M h_{fg}} \right) + 1.5 \times 10^{-4} \left(\frac{1}{X_{tt}} \right)^{0.67} \right] \quad (97)$$

where $(Nu)_B$ is the Nusselt number for boiling $= h_B D / k_L$, the quantity $q / G_M h_{fg}$ is called the boiling number B_0 , and the Reynolds number is based on the liquid mass-velocity. The quantity q is the total heat flux, and h_{fg} the enthalpy of vaporization.

Wright (W3) has recently measured local boiling coefficients in vertical downflow systems, which have the advantage of being free of hydrostatic-head effects. His results were correlated reasonably well by equations of the type of (91) or (92),

$$\frac{h_{TP}}{h_{Ls}} = 2.72 \left(\frac{1}{X_{tt}} \right)^{0.581} \quad (98)$$

Better correlation over wide ranges was obtained by the use of the correlation of Schrock and Grossman given in Eq. (97), with a numerical coefficient of 320 rather than 170. Wright also gives modified empirical correlations for downflow, based on his experimental findings, that correspond to the general relationship:

$$h_{TP} \propto G_M^{0.6} q^{0.3} x^{0.4} \quad (99)$$

2. Dimensionless Group Correlations

In addition to correlations of the above type, that is, where the ratio of a two-phase heat-transfer coefficient is compared to a fictitious single-phase coefficient, relationships in terms of dimensionless groups have also been presented. In general, these are of the form,

$$\begin{aligned}(Nu)_{TP} &= a(Re)_L^b(Pr)_L^c \\ &= \left(\frac{h_{TP} D_e}{k_L} \right)\end{aligned}\quad (100)$$

where $(Nu)_{TP}$ refers to the Nusselt number for two-phase convective heat transfer. This type of equation, which has been found to apply successfully for forced-convection single-phase flow, can be justified for mixed flow on the basis that the controlling heat-transfer mechanism in the two-phase case is the same—that is, forced convection transfer from the wall to the liquid, in this case usually present as a film. However, the Reynolds number must now be correctly specified. It may be calculated from a knowledge of slip ratio, or of void-volume in the channel. Alternately, a homogeneous model may be assumed, which may well be satisfactory at lower pressures and higher qualities, e.g. above 10%, as the bulk of the liquid will be in spray form.

For water boiling in a horizontal rectangular channel at high qualities (above 30%) and low pressures (below 150 psia), Davis and David (D2) found that a model based either on the slip ratio or on the homogeneous model gave nearly equally good correlations for the forced-convection region of two-phase flow. For the slip-ratio model, they gave

$$\frac{h_{TP} D}{k_L} = 0.060 \left(\frac{\rho_L}{\rho_G} \right)^{0.28} \left(\frac{DxG_M}{\mu_L} \right)^{0.87} \left(\frac{C_p \mu}{k} \right)_L^{0.4} \quad (101)$$

For the homogeneous model,

$$\frac{h_{TP} D}{k_L} = 0.033 \left(\frac{DG_M}{\mu_{TP}} \right)^{0.87} \left(\frac{C_p \mu}{k} \right)_L^{0.4} \quad (102)$$

where μ_{TP} was defined as for the homogeneous model, and D was taken as the hydraulic radius of the channel, that is, as for single-phase flow. Both equations fit the data to within $\pm 15\%$. Equation (102) was shown by Davis and David to be practically the same as that obtained by Groothuis and Hendal (G10) for heat transfer to boiling air-water mixtures in vertical tubes,

$$\frac{h_{TP} D}{k_L} = 0.029 \left(\frac{DG_M}{\mu_{TP}} \right)^{0.87} \left(\frac{C_p \mu}{k} \right)_L^{1/3} \left(\frac{\mu_b}{\mu_w} \right)^{0.14} \quad (103)$$

which is a modification of the Sieder-Tate equation for single-phase forced-convection transfer.

3. Discussion of Correlating Methods

The procedure of taking a ratio of two coefficients, as done in equations (91) and (92), using a Dittus-Boelter equation for the hypothetical liquid-only case, leads to the relation:

$$\begin{aligned} \frac{h_{TP}}{h_L} &= \frac{h_{TP}}{0.023 \left(\frac{k_L}{D} \right) (Re)_L^{0.8} (Pr)_L^{1/3}} = \frac{(Nu)_{TP}}{0.023 (Re)_L^{0.8} (Pr)_L^{1/3}} \\ &= f \left(\frac{1}{X_{tt}} \right) = f \left[\left(\frac{\mu_G}{\mu_L} \right)^{0.1} \left(\frac{\rho_L}{\rho_G} \right)^{0.5} \left(\frac{x}{1-x} \right)^{0.9} \right] \end{aligned} \quad (104)$$

From the above relationships, the strong similarity between all the preceding correlations is evident. For example, Eq. (101) may be rewritten, by substituting $xG_M = xG_L/(1-x)$,

$$\frac{(Nu)_{TP}}{(Pr)_L^{1/3} (Re)_L^{0.87}} = 0.060 \left(\frac{\rho_L}{\rho_G} \right)^{0.28} \left(\frac{x}{1-x} \right)^{0.87} \quad (105)$$

If the viscosity dependence, which is small, is neglected, then the obvious parallel with Eq. (91) or (92) is readily apparent.

The physical meaning of these correlations for the forced convection region, and the observed occurrence of some nucleate boiling contribution at high heat fluxes has been discussed clearly by Schrock and Grossman (S4), in presenting their more general correlation, given in Eq. (97). The following explanations are offered by Schrock and Grossman:

At sufficiently low values of the boiling number the local heat transfer coefficient is a function of X_{tt} alone, while for large values of the boiling number the heat transfer becomes independent of X_{tt} and depends solely on B_0 over a wide range of exit qualities. This dependence may be explained by assuming that in the former case one has a two-phase flow established in an annular pattern with the liquid flowing on the wall while the vapor flows in the core. This occurs at very low quality at low and moderate pressures for water because of the large difference between vapor and liquid densities. If the thickness of the liquid layer is small enough so that the liquid can sustain the necessary temperature difference to transmit the heat without nucleation occurring, then there is evaporation at the interface but no boiling *per se*. It is this case where X_{tt} is a sufficient parameter for correlating the heat transfer coefficients.

Without nucleate boiling in the liquid annulus, the heat transfer coefficient is determined by the thermal resistance of the liquid layer which may contain laminar and turbulent zones, or may be entirely laminar. The wall temperature then depends on the temperature at the liquid-vapor interface, which is close to saturation temperature, and the thermal resistance of the liquid layer. Recalling that the physical interpretation of X_{tt} ² is the ratio of pressure gradients of the liquid and the vapor, each flowing alone at the same rate in the same pipe, we see then that a correlation in terms of X_{tt} alone is essentially a heat-momentum analogy. The heat-transfer coefficient ratio expresses the reduction in thermal resistance which is brought about by the vapor forcing the liquid to flow in a thin annular layer on the wall of the tube. The pressure gradient ratio mentioned above characterizes the relative velocity and temperature profiles.

A direct numerical relationship between heat and momentum fluxes, as for the simple Reynolds' analogy for a single phase, is not obtained in this case because of a basic and significant difference in heat transfer coefficient definitions. For single-phase flow in pipes, the mixed mean or integrated average temperature is used in

defining temperature difference, while in the boiling case the bulk fluid temperature is taken arbitrarily as the saturation temperature at the local value of the pressure. A similar problem would arise in defining a friction coefficient for the vaporization case, although here there is no convenient analog to saturation temperature.

It is interesting to note that the heat transfer coefficients due to this forced convection effect, when it suppresses nucleation, may be higher than the coefficients for nucleate boiling with the same heat flux and no forced convection effect.

Consider now increasing the heat flux after the condition described above is established. The temperature drop through the liquid layer will increase, thus increasing the wall temperature. Eventually the liquid superheat at the wall will be so large that nucleation will occur. When it does, it augments the forced convection effect. Now the heat transfer coefficient is higher than for cases where the heat flux is the same, but where the higher mass flux suppresses the nucleation.

For sufficiently large heat flux to mass flow ratios, the nucleation mechanism predominates and the heat transfer becomes independent of the two-phase flow characteristics of the system. Thus at large values of the boiling number, the heat transfer coefficients are virtually independent of the Lockhart-Martinelli parameter, X_{tt} .

C. BURN-OUT IN FILM FLOW

The problem of burn-out prediction is a difficult one, and one on which a great deal of experimental work is being carried out, particularly in connection with nuclear-reactor development. Much of the earlier literature is rather confused, due to the fact that the mechanics of the burn-out were not carefully defined. Silvestri (S8) has discussed the definitions applicable to burn-out heat flux. It appears possible to define two distinctly different kinds of burn-out, one due to a transition from nucleate to film boiling, and one occurring at the liquid deficient point of the forced-convection region. The present discussion treats only the latter type of burn-out fluxes. The burn-out point in this instance is usually determined by the sudden rise in wall temperature and the corresponding drop in heat flux and heat-transfer coefficient which occur at high qualities.

The assumption commonly made in the forced-convection boiling region is that heat is transferred to the liquid, and from the liquid to the vapor, with a close approach to thermodynamic equilibrium being maintained at all times. Nearly all the evidence for steam-water systems not too close to critical conditions suggests that over most of the quality range, where fluid velocities are reasonably high, little heat transfer by boiling occurs, although there are indications that nucleation might not be entirely suppressed. At qualities over 10% the flow is annular-mist, and the presence or absence of a liquid film may depend upon re-entrainment of spray, or upon droplet diffusion to the wall, much more than upon the mechanics of film flow.

An excellent review of the burn-out phenomena in climbing-film flow has been given by Lacey *et al.* (L1). According to these authors, when

the liquid deficient region is first entered, a moderately high heat-transfer coefficient is still obtained, and this behavior might be ascribed to droplet impingement on the wall. At higher temperatures, the droplets would bounce from the wall (the Leidenfrost point), and only normal convective heat transfer would occur. Goldmann, Fristenberg, and Lombardi have developed this model (G2). Nevertheless, it suffers from a lack of knowledge of expressions for the rates of droplet diffusion. Further, the burn-out flux at constant burn-out enthalpy is found experimentally to decrease as the mass-flow rate increases, while the droplet diffusion model predicts the reverse.

The decrease in film burn-out heat flux with increasing mass velocity of flow at constant quality has been explained by Lacey *et al.* in the following way. At constant quality, increasing total mass flow rate means increasing mass flow of vapor as well as liquid. It has been shown that above certain vapor rates increased liquid rates do not mean thicker liquid layers, because the increased flow is carried as entrained spray in the vapor. In fact, the higher vapor velocity, combined with a heat flux, might be expected to lead to easy disruption of the film with consequent "burn-out," which seems to be what actually occurs at a constant steam mass velocity over very wide ranges of conditions—that is, the critical burn-out steam quality is inversely proportional to the total mass flow rate.

Isbin *et al.* (16) have proposed a model which attempts to include both droplet diffusion and liquid flow along the wall. Empirical functions for droplet diffusion and re-entrainment were determined from a limited amount of data, and equal velocities for the two phases were assumed. The resulting correlation (based on material and energy balances for the liquid which were integrated numerically) predicted burn-out heat fluxes closely for narrow rectangular channels, small-diameter tubes, and also for uneven heat fluxes, all at pressures of 2000 psia. The assumptions made in this derivation would tend to give better results at high pressures. The method appears to predict correctly the observed reduction in burn-out heat flux with increasing flow rates.

Another possible approach to burn-out prediction is to study film breakdown due to hydrodynamic effects. Presumably, if thin spots occur in a film for any reason, the film becomes hotter, the surface tension is reduced, and increased vaporization tends to cause a break in the liquid layer. Although studies of surface tension and wetting angle in thin-film flow have been made, no successful correlation of burn-out in these terms has yet been offered.

Finally, it has been suggested that oscillations in the flowing film may

contribute to the occurrence of burn-out. The "upstream" history of the film is thus important, as is the conduit geometry.

Lacey *et al.* (L1) summarize the present state of knowledge of film breakdown in the following paragraph:

In film breakdown at burn-out, nucleation may be a factor together with loss by entrainment and evaporation (in excess of spray deposition), and instabilities associated with surface tension. There is evidence for the existence of a critical vapor mass velocity, independent of pressure, above which the film is easily disrupted by heat flux; it is also clear that upstream conditions, including the inlet arrangements, must strongly influence the film breakdown at the exit.

Specific studies of liquid-deficient burn-out have been reported for various situations. For internally heated annuli with upward flow, Lacey *et al.* (L1) have shown that burn-out occurs at a constant steam flow rate over most of the range of total mass-flow rates used. Burn-out in long tubes sealed at the bottom but connected to a liquid reservoir on the top (in simulation of accidental heater-tube blockage) has been studied by Griffith *et al.* (G9), who concluded that the burn-out heat flux can be predicted from the critical flooding velocity. For vertical upflow Bell (B8) has presented an empirical five-constant correlation for burn-out flux, based on high-pressure data for the high-quality region. Viskata (V4) gives burn-out fluxes for swirling flow, and states that they are higher for this type of flow. Although he does not state the cause of swirling-flow burn-out, it is probably film-boiling; this latter conclusion also seems to apply to data of Sonneman (S10).

Levy *et al.* (L5) have studied the effect of eccentricity on the burn-out flux in upward vertical annular flow. Eccentricity does not affect the burn-out flux until the annular separation is about 20% or less of its concentric value. Burn-out fluxes for great eccentricities are increased about 30%, which is ascribed to poor fluid mixing; pressure-drop at the same conditions is reduced. The small effect of moderate eccentricity in downward annular flow of steam-water mixtures was also reported earlier by Stein *et al.* (S11) in their study of pressure-drop and critical flow.

VII. Mass Transfer in Cocurrent Gas-Liquid Flow

A. GENERAL

In the case of single-component two-phase flow, such as in vaporizing water, physical equilibrium is commonly assumed and seems to yield reasonable results, even though it might seem that supersaturation could occur. The rate of mass transfer between phases, therefore, is not a limiting process for single component flow.

For mass transfer in two-component cocurrent two-phase flow, very little work seems to have been carried on in systems analogous to those for which pressure-drops have been measured, that is, in tubes, pipes, or rectangular channels. Only two publications dealing with vertical flow (V2, V3), and two concerned with horizontal flow (A5, S6), have appeared.

In carrying out heterogeneous gas-liquid reactions, there are many cases in which it is immaterial whether the gas and liquid flow are cocurrent or countercurrent. If a pure gas is being used, or if the chemical reaction proceeding behaves irreversibly, nothing is lost by cocurrent operation. Intuitively, one would suppose that certain of the two-phase flow patterns might give high rates of gas absorption. Hence the use of "pipe line" reactors could easily supplant packed-tower or agitated-tank operations if design criteria were available.

B. VERTICAL FLOW

The use of the gas-lift pump as a chemical reactor has been studied by Varlamov *et al.* (V2, V3) who used a variety of designs, including two with 2 and 7 vertical passes in series. According to this work, the conditions giving minimum pressure-drop correspond to a maximum value of the overall gas-absorption coefficient. This overall coefficient applies specifically to the chemically reacting system studied by Varlamov and his coworkers, (solution of nitrogen oxides in 2.5 *N* sodium hydroxide), and is based on the wetted surface area of the tube. Also, it would appear that the effective lift in this work must have been essentially zero. Rectangular channels were also used; this change of shape made little difference in the results, although somewhat higher pressure drops and absorption coefficients resulted. According to Varlamov, the gas-absorption coefficients obtained exceed those for comparable packed-tower operations by a factor of 100.

Investigations have been undertaken by Baird and Davidson (B1), and by Beek and van Heuven (B7) on absorption from rising gas bubbles. In the former work, the bubbles were large (0.8–4.2 cm.), rising in still water, and in the latter case, bubbles were formed in narrow gas lift tubes (0.48 and 0.238 cm.). For the large free bubbles, absorption rates for carbon dioxide in water were 50% greater than predicted for absorption from the upper surface of a spherical cap bubble. The additional absorption was credited to rippling on the rear surface of the bubble. The addition of surface-active agents which suppressed this rippling resulted in absorption rates approximately as predicted. Large bubbles (over 2.5 cm. diameter) absorbed at an unsteady rate, due apparently to increasing saturation of the liquid carried up behind the bubble.

In the narrow tubes used by Beek and van Heuven, the bubbles assumed the shape of Dumitrescu (or Taylor) bubbles. Using the hydrodynamics of bubble rise and the penetration theory of absorption, an expression was developed for the total absorption rate from one bubble. The liquid surface velocity was assumed to be that of free fall, and the bubble surface area was approximated by a spherical section and a hyperbola of revolution. Values calculated from this model were 30% above the measured absorption rates. Further experiments indicated that velocities are reduced at the rear of the bubble, and are certainly much less than free fall velocities. A reduction in surface tension was also indicated by extreme curvature at the rear of the bubble.

C. HORIZONTAL FLOW

Mass transfer controlled by diffusion in the gas phase (ammonia in water) has been studied by Anderson *et al.* (A5) for horizontal annular flow. In spite of the obvious analogy of this case with countercurrent wetted-wall towers, gas velocities in the cocurrent case exceed these used in any reported wetted-wall-tower investigations. In cocurrent annular flow, smooth liquid films free of ripples are not attainable, and entrainment and deposition of liquid droplets presents an additional transfer mechanism. By measuring solute concentrations of liquid in the film and in entrained drops, as well as flow rates, and by assuming absorption equilibrium between droplets and gas, Anderson *et al.* were able to separate the two contributing mechanisms of transfer. The agreement of their entrainment values (based on the assumption of transfer equilibrium in the droplets) with those of Wicks and Dukler (W2) was taken as supporting evidence for this supposition.

Results of experiments in annular flow showed that the over-all mass-transfer coefficient, K_G , based on the tube surface area and the liquid-film compositions, was a function of both gas and liquid superficial Reynolds number, but depended much more strongly on that of the liquid. When plotted as j_D factors, that is,

$$j_D = \frac{K_G p_{BM} M_G}{G_G} (Sc)_G^{2/3} \quad (106)$$

against the gas Reynolds numbers, nearly parallel straight lines were obtained with liquid Reynolds numbers as parameters, and these lines in turn were parallel to the Reynolds analogy for mass transfer,

$$j_D' = \frac{f}{2} = 0.0395(Re)_G^{-1/4} \quad (107)$$

It was shown by Anderson *et al.* that the increase in mass transfer,

over that expected if transfer were from gas to liquid film only, was entirely a function of the amount of exchange of liquid between film and droplets. The percentage interchange of liquid was found to be nearly constant at from 3% to 5% per foot of contactor for Re_G from 30,000 to 150,000, and for Re_L from 2750 to 12,000. For liquid Reynolds numbers below 2750, entrainment becomes much less significant, and interchange decreases. Hence the amount of transfer occurring in this type of annular flow can be correlated by the same relationships as those used for wetted-wall towers, but with an additional contribution directly proportional to the liquid Reynolds number provided it is greater than 2750.

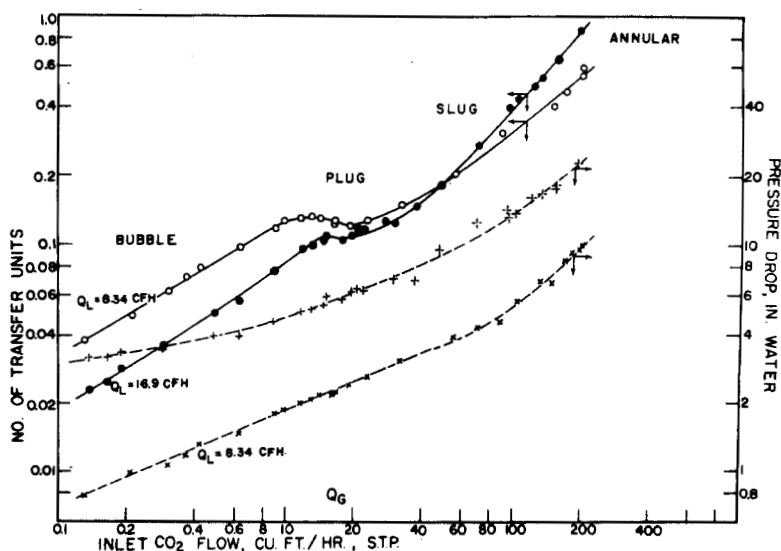


FIG. 13. Typical result for absorption of pure carbon dioxide in water in horizontal cocurrent flow for two liquid rates. Tubing: 0.0575 ft. inside diameter; 7.7 ft. long test section; 15°C.; outlet pressure 1 atm. abs.

Results for the absorption of pure carbon dioxide in water for a variety of flow patterns in horizontal tubes with diameters up to 1 in. have been reported by Scott and Hayduk (S6). In this case there is only a liquid-phase resistance to mass transfer. Typical absorption data are shown in Fig. 13, in terms of the number of transfer units in a test section 7.7 ft. long, as a function of the gas volumetric feed rate. These data apply to a smooth tube 1.75 cm. inside diameter, for two liquid rates, and for bubble, plug, slug, and annular flow regions. Pressure-drops over the same test section are also shown. In the slug and annular regions the length of a transfer unit was found to depend only slightly on the liquid

rate, to vary almost inversely as the gas rate, and to be a moderate function of tube diameter. An empirical correlation based on these facts is shown in Fig. 14, and covers three tube diameters, gas superficial Reynolds numbers from 100 to 15,000, and liquid Reynolds numbers from about 500 to 10,000.

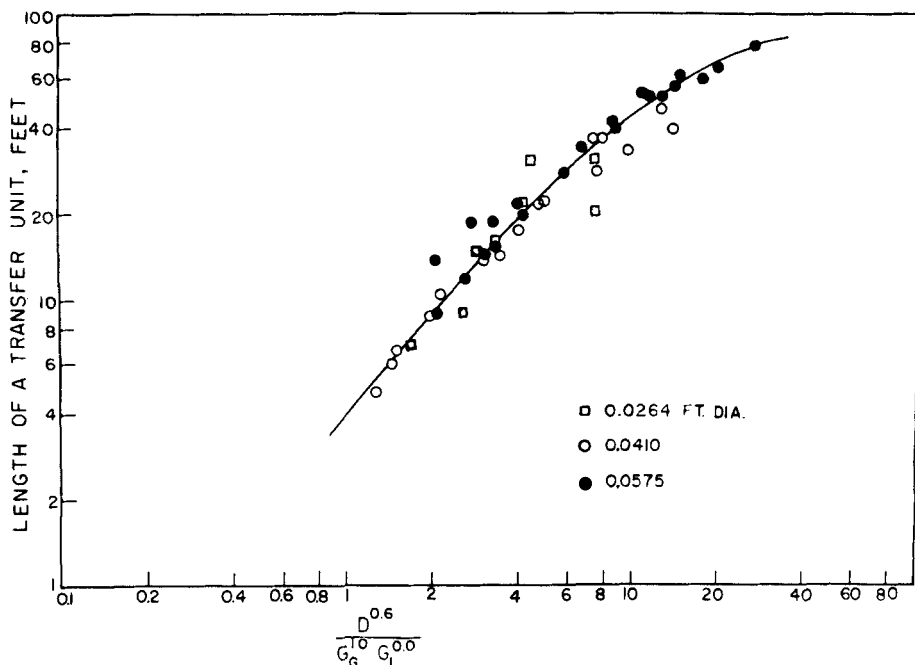


FIG. 14. Partial correlation of absorption results for the liquid phase controlling, slug, and annular flow, for CO_2 in water.

A qualitative explanation of these observations was given by Scott and Hayduk, based on the following assumptions:

- (1) Transfer coefficients for the liquid phase can be described by the kind of dimensionless relationship commonly obtained from wetted-wall tower experiments.
- (2) Void-fractions in slug and annular flow can be estimated from the Lockhart-Martinelli correlations.
- (3) The amount of interfacial transfer area created by the action of the flowing gas on the liquid is proportional to some fraction of the power transferred from the gas per unit volume of liquid.

On the basis of these assumptions and the experimental evidence given in Fig. 14, an approximate relationship was derived,

$$LTU \propto \frac{D^{0.8}}{G_L^{0.1} G_G^{0.8}} \left(\frac{\mu_L}{\mu_G} \right)^{0.1} \rho_G^{0.42} \frac{\sigma_{LG}}{\mathfrak{D}^{0.5}} \quad (108)$$

Additional work under way in the author's laboratory will be directed toward further examining the effects of variables other than gas or liquid flow rates and tube diameter on the rate of absorption in horizontal slug or annular flow.

Again referring to Fig. 13, the same general trend is apparent in both the pressure-drop and number-of-transfer-unit curves. This suggests that another empirical correlating procedure could be arrived at; for example, an approximate relationship exists between the length of a transfer unit (LTU) and the Lockhart-Martinelli parameters, X .

VIII. Miscellaneous Considerations

A. FLOW OF TWO LIQUID PHASES AND A GAS PHASE

One relatively recent investigation of multiphase flow has been carried out in pipelines. Sobocinski and Huntington (S9) used air, water, and gas-oil having a viscosity of 3.38 cp and a surface tension of 23.5 dynes/cm. (both measured at 100°F.). Stratified, wave, and annular flow-patterns were observed in horizontal 3-in.-inside-diameter plastic pipe. The feed ratio of gas-oil to water was kept constant, a constant total liquid mass velocity was used, and the gas mass-velocity was varied. Under these conditions at low gas velocities [below 2000 lb./(hr.) (sq. ft.)] stratified flow occurred; gentle ripples were visible on the oil-air surface, but the oil-water interface was smooth. The oil layer moved at 1.5 times the velocity of the aqueous layer. As the gas mass-velocity increased to 3000-4000, deep waves appeared on the oil surface, and smaller ones occurred at the oil-water interface. The oil layer moved 2.27 times as fast as the water; the relative velocity was a maximum in this region, accompanied necessarily by a maximum for the in-place ratio of water to oil. Further increases in gas velocity caused wave motion on both liquid surfaces, and emulsification began. At high gas velocities, complete emulsification occurred when the flow became semiannular or annular, both liquid phases moving with equal velocity. Pressure-drop in pipes carrying two liquid phases is always higher than that occurring if only one liquid phase is flowing at the same total mass-velocity. The pressure-drop becomes a maximum at the point where oil emulsion dispersed in water changes to a water dispersion in oil. In Sobocinski and Huntington's work this occurred at a liquid-feed mass-ratio of water:oil of 4.0, and at this point the pressure drop was 3 to 5 times as great as that expected for flow of gas and one liquid phase.

Pressure-drop data obtained in these tests were correlated empirically by defining a friction-factor based on gas-phase properties and superficial gas-flow rates. This friction-factor was plotted against the group $G_L \mu_L / G_G \mu_G$ with the water-oil feed mass-ratio as a parameter.

B. FLOW IN INCLINED TUBES

In the original work on two-phase pressure-drops at the University of California (B13), tests were made in tubes inclined at 1:6, as well as in horizontal tubes. In general, these data for small inclinations also fitted the correlations proposed finally by Lockhart and Martinelli for horizontal tubes.

Kosterin (K3) investigated the effect of tube inclination on flow patterns for air-water systems. As tube inclination increases, the flow patterns become more dispersed; tube slope is an important variable at the lower liquid or gas rates. At high gas rates, when annular or dispersed flow normally occurs in horizontal tubes, tube inclination has little effect on flow-pattern.

Pressure pulsations for incremental flow-patterns are of the least amplitude in horizontal tubes, and increase steadily with tube inclination to become a maximum in vertical tubes. Apparently no correlations for pressure-drops which allow specifically for the effect of tube inclination have yet been developed.

C. TWO-PHASE FLOW IN LONG PIPELINES

Baker (B3, B4) has discussed design considerations and operating experiences with two-phase pipeline flows. Flanigan (F1) has outlined a procedure for obtaining test data from operating multiphase-flow pipelines.

In a recent article (B5), Baker reviews two-phase flow in long pipelines, and presents individual empirical equations for estimating pressure-drop for the major flow patterns. These equations are based on actual operating experience with large diameter pipelines, and should be used only for their valid range of variables as given by Baker. In general, the correlations are based on those of Lockhart and Martinelli with the parameter X modified as required to give a fit to experimental data.

The effect of hills is interesting, in that no credit can be taken for the downhill side of the pipeline. The sum of all the uphill elevations appears as a pressure loss in actual operating practice. Baker includes an "elevation correction factor" which attempts to allow for the fact that the fluid-mixture density in the inclined uphill portion of the line is not accurately known. The gas mass-velocity seems to be the major variable affecting this correction factor, although liquid mass-velocity, phase properties,

and tube inclination have some effect. A correlation due to Flanigan (F1) is recommended for estimating this elevation correction factor, F_E . Hence, the elevation pressure drop, ΔP_{TPZ} , is given by

$$\Delta P_{TPZ} = \frac{\rho_L F_E g}{144gc} \Sigma h_i \quad (109)$$

where h_i is the height of each hill. Apparently, froth flow is an exception, and behaves like single-phase flow with respect to elevation pressure-drops.

As a consequence of this type of behavior by two-phase flow in long pipelines, it might be expected that such lines in hilly country would show very high pressure-drops, and the elevation pressure-drop would be the major factor. This appears to be the situation in actual practice.

ACKNOWLEDGMENT

The writer wishes to express his thanks to those authors and publishers who have kindly allowed him to use direct quotations, or to reproduce figures exactly as they have appeared elsewhere, or in a somewhat modified form.

Nomenclature

In the text, the force-mass-length-time system of units has been used, with exceptions noted. Primed symbols refer to actual average values, as distinct from superficial or apparent values. A double prime indicates a point value.

A	Area	k	Thermal conductivity
b	Film thickness	K	Mass transfer coefficient
B_0	Boiling number, dimensionless, defined in text	l	Length of tube
C	Wetted perimeter	M	Molecular weight
\mathcal{D}	Diffusion coefficient	Nu	Nusselt number
D	Diameter	P	Pressure
E_G, E_L	Energy dissipated by gas or liquid in wall friction	ΔP	Pressure differential
E	Mass of liquid entrained by gas per unit time	Pr	Prandtl number
f	Friction factor	q	Rate of heat transfer
F	Force, or momentum per unit time	Q	Volumetric rate of flow
Fr	Froude number	r	Radius
g	Acceleration of gravity	Re	Reynolds Number
g_c	Conversion factor	R	Volume fraction
G	Mass velocity, mass per unit area per unit time	R_v	Volumetric gas-liquid feed ratio
h	Heat transfer coefficient	Sc	Schmidt number
h_{fg}	Enthalpy of vaporization	u	Velocity in a direction normal to the flow velocity
H_R	Holdup ratio	U	Thermodynamic internal energy
j_D	j factor for mass transfer	V	Velocity in the direction of flow
		W	Mass rate of flow
		We	Weber number
		x	Quality, mass percent vapor
		X	Dimensionless Lockhart-

Martinelli parameter	τ Shearing stress
y Film thickness	φ Lockhart-Martinelli dimensionless parameter
y^+ Dimensionless distance parameter	ψ Correlating parameter, various definitions (given in text)
Z Length of tube	λ Tube length, or density correction term
α Constant	σ Gas-liquid interfacial tension
Γ Volumetric film flow rate per unit width of film	μ Viscosity
ρ Mass density	

SUBSCRIPTS

a Acceleration	WL Wall-liquid
b Bulk	i Irreversible
B Boiling (heat transfer) or bubble (velocities)	M Gas-liquid mixture property
C Critical	o Entrance condition
G Gas phase	R Reversible or relative (velocities)
L Liquid phase	S Slip (velocity) or slug (velocity)
iG Interface-gas	TP Two-phase
iL Interface-liquid	W Wall
LG or GL Gas-liquid	Z Elevation or hydrostatic
WG Wall-gas	

REFERENCES

- A1. Alves, G. E., *Chem Eng. Progr.* **50**, 449 (1954).
- A2. Anderson, G. H., and Mantzouranis, B. G., *Chem. Eng. Sci.* **12**, 109 (1960).
- A3. Anderson, G. H., and Mantzouranis, B. G., *Chem. Eng. Sci.* **12**, 233 (1960).
- A4. Anderson, G. H., Haselden, G. C., and Mantzouranis, B. G., *Chem. Eng. Sci.* **16**, 222 (1961).
- A5. Anderson, J. D., Bollinger, R. E., and Lamb, D. E., "Mass Transfer in Two Phase Annular Horizontal Flow." Presented at A.I.Ch.E. Natl. Meeting, Los Angeles, February, 1962.
- A6. Anderson, R. P., Bryant, L. T., Carter, J. C., and Marchaterre, J. F., presented at A.I.Ch.E.-ASME, 5th Natl. Heat Transfer Conf., Houston, Texas, August, 1962.
- A7. Armand, A. A., *Vse. Teplitekhn. Inst. Isv.* **No. 1**, 16-23 (January, 1946).
- B1. Baird, M. H. I., and Davidson, J. F., *Chem. Eng. Sci.* **17**, 87 (1962).
- B2. Baker, O., *Oil Gas J.* July 26 (1954).
- B3. Baker, O., "Some Design Suggestions for Multiphase Flow in Pipelines." Presented before Am. Gas Assoc., New York, May 8, 1958. (Available from AGA.)
- B4. Baker, O., *Pipeline Eng.* **H-67**, February, 1960.
- B5. Baker, O., *Can. Oil Gas Ind.* **14**, No. 3, 43 (1961).
- B6. Bankoff, S. G., *Trans. ASME (Am. Soc. Mech. Eng.) Ser. C* **82**, 265 (1960).
- B7. Beek, W. J., and van Heuven, J. W., *Chem. Eng. Sci.* **18**, 377 (1963).
- B8. Bell, D. W., *Nucl. Sci. Eng.* **7**, 245 (1960).
- B9. Bennett, J. A. R., AERE Rept. CE/R 2497 (H. M. Stationery Office, London), 1958.
- B10. Bennett, J. A. R., and Thornton, J. D., *Trans. Inst. Chem. Engrs. (London)* **39**, 101 (1961).

- B11. Bennett, J. A. R., Collier, J. G., Pratt, H. R. C., and Thornton, J. D., *Trans. Inst. Chem. Engrs. (London)* **39**, 113 (1961).
- B12. Bergelin, O. P., and Gazley, C., *Proc. Heat Transfer Fluid Mech. Inst., Am. Soc. Mech. Eng.* 1949.
- B13. Boelter, L. M. K., and Kepner, R. H., *Ind. Eng. Chem.* **31**, 426 (1939).
- B14. Brown, R. A. S., Sullivan, G. A., and Govier, G. W., *Can. J. Chem. Eng.* **38**, 62 (1960).
- B15. Bashforth, E. Q., Fraser, J. B. P., Hutchison, H. P., and Nedderman, R. M., *Chem. Eng. Sci.* **18**, 41 (1963).
- C1. Calvert, S., and Williams, B., *A.I.Ch.E. Journal* **1**, 78 (1955).
- C2. Carter, C. O., and Huntington, R. L., *Can. J. Chem. Eng.* **39**, 248 (1961).
- C3. Chenoweth, J. M., and Martin, M. W., *Petrol. Refiner* No. 10, **34**, 151 (1955).
- C4. Chisholm, D., and Laird, D. K., *Trans. ASME (Am. Soc. Mech. Eng.)* **80**, 276 (1958).
- C5. Collier, J. G., AERE Rept. CE/R 3808. H. M. Stationery Office, London, 1962.
- C6. Collier, J. G., and Hewitt, G. F., *Trans. Inst. Chem. Engrs. (London)* **39**, 127 (1961).
- C7. Cromer, S., and Huntington, R. L., *Trans. AIME* **136**, 79 (1940).
- D1. Davis, W. J., "Effect of the Froude Number in Estimating Vertical Two-Phase Gas-Liquid Friction Losses." Presented at A.I.Ch.E. Nat. Meeting, Los Angeles, February, 1962.
- D2. Davis, E. J., and David, M. M., *Can. J. Chem. Eng.* **39**, 99 (1961).
- D3. Dengler, C. E., and Addoms, J. N., *Chem. Eng. Progr. Symp. Ser. No. 18*, 52, (1956).
- D4. Dukler, A. E., *Chem. Eng. Progr. Symp. Ser. No. 30*, **56**, 1 (1960).
- D5. Dukler, A. E., and Bergelin, O. P., *Chem. Eng. Progr.* **48**, 557 (1952).
- F1. Flanagan, O., *Oil Gas J.* March 10, 1958.
- F2. Foltz, H. L., and Murray, R. G., *Chem. Eng. Progr. Symp. Ser. No. 30*, **56**, 83 (1960).
- G1. Gazley, C., *Proc. Heat Transfer Fluid Mech. Inst. ASME (Am. Soc. Mech. Eng.)* 1949.
- G2. Goldmann, K., Fristenberg, H., and Lombardi, C., *Trans. ASME (Am. Soc. Mech. Eng.) Ser. C83*, 158 (1961).
- G3. Govier, G. W., and Aziz, K., *Can. J. Chem. Eng.* **40**, 51 (1962).
- G4. Govier, G. W., and Omer, M. M., *Can. J. Chem. Eng.* **40**, 93 (1962).
- G5. Govier, G. W., and Short, W. L., *Can. J. Chem. Eng.* **36**, 195 (1958).
- G6. Govier, G. W., Radford, B. A., and Dunn, J. S. C., *Can. J. Chem. Eng.* **35**, 58 (1957).
- G7. Gresham, W. A., Jr., Foster, P. A., Jr., and Kyle, R. J., WADC-TR-55-422 (June, 1955).
- G8. Griffith, P., and Wallis, G. B., *Trans. ASME (Am. Soc. Mech. Eng.) Ser. C83*, 307 (1961).
- G9. Griffith, P. Schumann, W. A., and Neustal, A. D., in "Symposium on Two Phase Flow." Paper No. 5. Inst. Mech. Engrs., London, February, 1962.
- G10. Groothuis, H., and Hendl, W. P., *Chem. Eng. Sci.* **11**, 212 (1959).
- G11. Guerrieri, S. A., and Talty, R. D., *Chem. Eng. Progr. Symp. Ser. No. 18*, 52, 69 (1956).
- G12. Gill, L. E., Hewitt, G. F., Hitchon, J. W., and Lacey, P. M. C., *Chem. Eng. Sci.* **18**, 525 (1963).

- H1. Hanratty, T. J., and Engen, J. M., *A.I.Ch.E. Journal* **3**, 299 (1957).
- H2. Hanratty, T. J., and Hershman, A., *A.I.Ch.E. Journal* **7**, 488 (1961).
- H3. Hatch, M. R., and Jacobs, R. B., *A.I.Ch.E. Journal* **8**, 18 (1962).
- H4. Haywood, R. W., Knights, G. A., Middleton, G. E., and Thom, J. R. S., *Proc. Inst. Mech. Engrs. (London)* **175**, 669 (1961).
- H5. Hewitt, G. F., AERE—R 3680 (H. M. Stationery Office, London), 1961.
- H6. Hoogendoorn, C. J., *Chem. Eng. Sci.* **9**, 205 (1959).
- H7. Hoogendoorn, C. J., and Buitelaar, A. A., *Chem. Eng. Sci.* **16**, 208 (1961).
- H8. Hoopes, J. W., Jr., *A.I.Ch.E. Journal* **3**, 268 (1957).
- H9. Hubers, C., *Nucl. Sci. Eng.* **13**, 54 (1962).
- H10. Hughes, R. R., Evans, H. D., and Sternling, C. V., *Chem. Eng. Progr.* **49**, 78 (1953).
- H11. Hughmark, G. A., "Holdup in Gas-Liquid Flow." Presented at A.I.Ch.E. Annual Meeting, Los Angeles, February, 1962.
- H12. Hughmark, G. A., and Pressburg, B. S., *A.I.Ch.E. Journal* **7**, 677 (1961).
- H13. Hughmark, G. A., "Pressure Drop in Horizontal and Vertical Upward Isothermal Gas-Liquid Flow." Presented at 55th Annual Meeting, A.I.Ch.E., Chicago, December 2-6, 1962.
- I1. Isbin, H. S., Moen, R. H., and Mosher, D. R., AECU-2994, University of Minnesota, Minneapolis, 1954.
- I2. Isbin, H. S., Moy, J. E., and Da Cruz, A. J. R., *A.I.Ch.E. Journal* **3**, 361 (1957).
- I3. Isbin, H. S., Sher, N. C., and Eddy, K. C., *A.I.Ch. E. Journal* **3**, 136 (1957).
- I4. Isbin, H. S., Fauske, H., Grace, T., and Garcia, J., in "Symposium on Two-Phase Fluid Flow." Paper No. 10. Inst. Mech. Engrs., London, February, 1962.
- I5. Isbin, H. S., Rodriguez, H. A., Larson, H. C., and Pattie, B. D., *A.I.Ch.E. Journal* **5**, 427 (1959).
- I6. Isbin, H. S., Vanderwater, R., Fauske, H., and Singh, S., *Trans. ASME (Am. Soc. Mech. Eng.) Ser. C83*, 149 (1961).
- I7. Isbin, H. S., Moen, R. H., Wickey, R. O., Mosher, D. R., and Larson, H. C., *Chem. Eng. Progr. Symp. Ser. No. 23*, **55**, 75 (1959).
- J1. Johnson, H. A., *Trans. ASME (Am. Soc. Mech. Eng.)* **77**, 1257 (1955).
- J2. Johnson, H. A., and Abou-Sabe, A. H., *Trans. ASME (Am. Soc. Mech. Eng.)* **74**, 997 (1952).
- K1. Kordyban, E. S., *Trans. ASME (Am. Soc. Mech. Eng.) Ser. D83*, 613 (1961).
- K2. Kosterin, S. I., *Izv. Akad. Nauk SSSR, Otd. Tekh. Nauk* **No. 11/12**, 37 (1943).
- K3. Kosterin, S. I., *Izv. Akad. Nauk SSSR, Otd. Tekh. Nauk* **No. 12**, 1824 (1949).
- K4. Kosterin, S. I., and Rubinovitch, M. N., *Izv. Akad. Nauk SSSR, Otd. Tekh. Nauk* **No. 7**, 1085 (1949).
- K5. Koslov, B. K., *J. Tech. Phys.* **24**, 2285 (1954).
- L1. Lacey, P. M. C., Hewitt, G. F., and Collier, J. G., in "Symposium on Two Phase Flow." Paper No. 1. Inst. Mech. Engrs., London, February, 1962.
- L2. Laird, A. D. K., and Chisholm, D., *Ind. Eng. Chem.* **48**, 1361 (1956).
- L3. Lamb, D. E., and White, J. L., *A.I.Ch.E. Journal* **8**, 281 (1962).
- L4. Levy, S., *Trans. A.S.M.E. (Am. Soc. Mech. Eng.) Ser. C82*, 113 (1960).
- L5. Levy, S., Polomik, E. E., Swan, C. L., and McKinney, A. W., *Intern. J. Heat Mass Transfer* **5**, 595 (1962).
- L6. Lockhart, R. W., and Martinelli, R. C., *Chem. Eng. Progr.* **45**, 39 (1949).
- L7. Lottes, P. A., and Flinn, W. S., *Nucl. Sci. Eng.* **I**, 461 (1956).
- L8. Lunde, K. E., *Chem. Eng. Progr. Symp. Ser. No. 32*, **57**, 104 (1961).

- M1. Marchaterre, J. F., *Trans. ASME (Am. Soc. Mech. Eng.) Ser. C83*, 503 (1961).
- M2. Martinelli, R. C., and Nelson, D. B., *Trans. ASME (Am. Soc. Mech. Eng.)* **70**, 695 (1948).
- M3. Martinelli, R. C., Putnam, J. A., and Lockhart, R. W., *Trans. A.I.Ch.E.* **42**, 681 (1946).
- M4. Martinelli, R. C., Boelter, L. M. K., Taylor, T. H. M., Thomsen, E. G., and Morrin, E. H., *Trans. ASME (Am. Soc. Mech. Eng.)* **66**, 139 (1944).
- M5. Moissis, R., and Griffith, P., *Trans. ASME (Am. Soc. Mech. Eng.) Ser. C84*, 29 (1962).
- N1. Nicklin, D. J., *Trans. Inst. Chem. Engrs. (London)* **41**, 29 (1963).
- N2. Nicklin, D. J., *Chem. Eng. Sci.* **17**, 693 (1962).
- N3. Nicklin, D. J., and Davidson, J. F., "Symposium on Two-Phase Flow." Paper No. 4. Inst. Mech. Engrs., London, February 1962.
- N4. Nicklin, D. J., Wilkes, J. O., and Davidson, J. F., *Trans. Inst. Chem. Engrs.* **40**, 61 (1962).
- O1. Owens, W. L., Jr., *Proc. Intern. Heat Transfer Conf., 1961*, Part II, p. 363. (Am. Soc. Mech. Engrs., New York, 1961.)
- P1. Petrick, M., and Swanson, B. S., *A.I.Ch.E. Journal* **5**, 440 (1959).
- R1. Reid, R. C., Reynolds, A. B., Diglis, A. J., Spiewak, I., and Klipstein, D. H., *A.I.Ch.E. Journal* **3**, 321 (1957).
- R2. Richardson, J. F., and Higson, D. J., *Trans. Inst. Chem. Engrs. (London)* **40**, 169 (1962).
- S1. Schrock, V. E., and Grossman, L. M., *Univ. Calif. (Berkeley) Inst. Eng. Res. No. 1*, September, 1957.
- S2. Schrock, V. E., and Grossman, L. M., *Nucl. Sci. Eng.* **3**, 245 (1959).
- S3. Schrock, V. E., and Grossman, L. M., *Univ. Calif. Berkeley Inst. Eng. Res. No. 2* (November, 1959).
- S4. Schrock, V. E., and Grossman, L. M., *Nucl. Sci. Eng.* **12**, 474 (1962).
- S5. Scott, D. S., *Can. J. Chem. Eng.* **40**, 224 (1962).
- S6. Scott, D. S., and Hayduk, W., *Can. J. Chem. Eng.* In press.
- S7. Sher, N. C., and Green, S. J., *Chem. Eng. Progr. Symp. Ser. No. 23*, **55**, 61 (1959).
- S8. Silvestri, N., *Proc. Intern. Heat Transfer. Conf. 1961*, Part II, p. 341. (Am. Soc. Mech. Engrs., New York, 1961.)
- S9. Sobocinski, D. P., and Huntington, R. L., *Trans. ASME (Am. Soc. Mech. Eng.)* **80**, 252 (1958).
- S10. Sonneman, G., *Nucl. Sci. Eng.* **5**, 242 (1959).
- S11. Stein, R. P., Hoopes, J. W., Markels, M., Selke, W. A., Bendler, A. J., and Bonilla, C. F., *Chem. Eng. Progr. Symp. Ser.* **11**, 115 (1954).
- S12. Stemerding, S., and Verschoor, H., *Proc. Gen. Discussions on Heat Transfer, London, September 1951*. (Inst. Mech. Engrs., London; Am. Soc. Mech. Engrs., New York.)
- S13. Smith, C. R., Tang, Y. S. and Walker, C. L., "Slip Velocity in Two-Phase Metallic Fluids" Presented at 55th Annual Meeting, A.I.Ch.E., Chicago, December 2-6, 1962.
- T1. Teletov, S. G., *Dokl. Akad. Nauk SSSR* **51**, 579 (1946).
- V1. Van Rossum, J. J., *Chem. Eng. Sci.* **11**, 35 (1959).
- V2. Varlamov, M. L., Manakin, G. A., and Staroselski, Ya. I., *J. Appl. Chem. USSR* **32**, 2504 (1959).

- V3. Varlamov, M. L., Manakin, G. A., and Staroselski, Ya. I., *J. Appl. Chem. USSR* **32**, 2511 (1959).
- V4. Viskata, R., *Nucl. Sci. Eng.* **10**, 202 (1961).
- V5. Vohr, J., *A.I.Ch.E. Journal* **8**, 280 (1962).
- W1. Wallis, G. B., *Proc. Intern. Heat Transfer Conf., 1961*, Part II, p. 319. (Am. Soc. Mech. Engrs., New York, 1961).
- W2. Wicks, M., and Dukler, A. E., *A.I.Ch.E. Journal* **6**, 463 (1960).
- W3. Wright, R. M., "Downflow Forced Convection Boiling of Water in Uniformly Heated Tubes," Lawrence Radiation Lab., Univ. of California, Berkeley, August, 1961. Rept. UCRL-9744.
- Z1. Zhivaikin, L. Ya., *Intern. Chem. Eng.* **2**, 337 (1962).
- Z2. Zuber, N., *Trans. ASME (Am. Soc. Mech. Eng.) Ser. C* **82**, 255 (1960).

This Page Intentionally Left Blank

A GENERAL PROGRAM FOR COMPUTING MULTISTAGE VAPOR-LIQUID PROCESSES

D. N. Hanson and G. F. Somerville*

Department of Chemical Engineering
University of California, Berkeley, California

I. Introduction	279
II. Calculation Methods	281
A. Problem Description and Variables	281
B. Stage-by-Stage Solutions	285
C. Iteration Solutions	287
D. Relaxation Solutions	288
E. Nomenclature	291
III. Description of the Program	291
A. Problem Formulation	291
B. Basic Program	297
C. Subroutine INPUT	304
D. Subroutine OUTPUT	305
E. Subroutine REBOIL	305
F. Subroutine CONDEN	306
G. Subroutine INVEN	306
H. Subroutines, BUBPT, DEWPPT, ISOVFL, ISOTFL	307
I. Examples	308
J. Program Nomenclature	310
IV. Program GENVL	317
References	356

I. Introduction

Multistage separation operations have received the attention of chemical engineers for many years now, and their importance in chemical processing is apparent from the tremendous number of papers written on the subject. The ability to achieve rational design of distillation columns contributed greatly to the early success of the petroleum industry, and, in turn, the continued emphasis placed on study of the separation operations has aimed mainly at improving or simplifying the design methods used by the petroleum industry.

The first realistic and practical method of solving separation problems was the stage-by-stage analysis shown by Sorel in 1893 (S3). The only

* Present address: California Research Corporation, Richmond, California.

assumption made by Sorel was that equilibrium was established between the exit phases from each stage, an assumption which is unfortunately still a part of almost every calculation procedure today. Heat balance was included in vapor-liquid processes, and the method was capable of providing much accurate and detailed information about separation processes. As later elaborated by many people, this basic method of calculating from stage to stage has become the standard tool of chemical engineers for design of multistage systems.

The stage-by-stage procedure has defects. It is difficult to use with many processes, and more important, in the period before computers came into general use, it was extremely laborious and time-consuming.

Because of the tedious nature of stage-by-stage calculations, much effort was spent to devise "short-cut" methods, correlations, and analytical methods which determined whole sections of a column of stages in one calculation. These methods have much utility, in that they are in most cases fast and simple, and are accurate enough for many purposes. However, again, they have many defects. They are available only for a few simple multistage processes, notably, distillation, absorption, and stripping. The analytical methods involve severely restrictive assumptions whose effect is impossible to determine. The correlations are trustworthy only over the range of systems which were used to obtain the correlation. In general, the engineer who uses such simplified calculational means is left with considerable doubt about his results.

The advent of high-speed digital computers has again changed the picture during the last few years. Without question, the great majority of problems on stagewise operations will be solved on computers in the future. Stage-by-stage calculations are no longer tedious and expensive. Performed on the computer, they are often less costly than the engineer's time to obtain much less accurate answers. In addition, a whole new group of methods identifiable as "iteration methods" has been highly developed and widely used on the computer. Despite the fact that they were introduced in 1933, the iteration methods were so prohibitively time-consuming that before computers became available, they were essentially not used at all.

Programs are presently available which can be used to obtain rapid and cheap solutions to many problems. There is still a considerable art in the use of the programs, however, and techniques have not been well-established for the computation of unusual processes or unusual systems. Frequently, existing programs for stage-by-stage calculation or iteration calculation cannot be applied to a process without extensive and knowledgeable modification. Further, too often, the programs fail to yield a solution when applied to unusual cases, since the techniques used to

obtain convergence are inadequate. Under such circumstances, computer calculation can be exceedingly costly. The computation time to discover that the technique will not yield an answer is costly, and the time to develop a new technique is even more so.

In this article, the authors present still another method of solution, a "relaxation" method, which can be used for any multistage separation process, and which is conceptually extremely simple. The relaxation method is most useful for certain processes, just as the stage-by-stage and iteration methods are most useful for certain other processes, and for certain types of problems on those processes. In order to clarify the usefulness of each method, a general classification of problems on separation processes is briefly discussed; but, since space will not permit showing each method in detail, only the relaxation method is given along with a highly flexible program which allows calculation of vapor-liquid processes of great complexity. It is hoped that the program will provide the readers who do not specialize in multistage calculation with an effective means of solving essentially all vapor-liquid problems without modification of the program, or with only slight and simple modification. For those well-acquainted with other methods, it should yield solutions of problems that cannot be solved by other methods. Moreover, it is hoped that this presentation will stimulate additional work on the development of techniques on relaxation solutions that will result in even faster solution of problems.

II. Calculation Methods

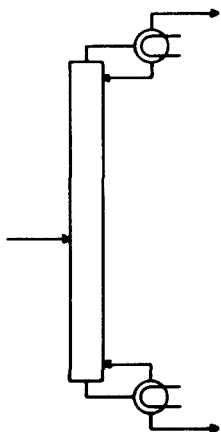
A. PROBLEM DESCRIPTION AND VARIABLES

The description of any operation or design problem in a multistage separation process requires assigning numerical values to, or "setting," a certain number of independent variables. The number of variables to be set depends on the process, and is usually determined easily by the method the authors have called the description rule (H1). Alternatively the number of variables to be set may be determined by writing all of the independent equations which define the process, then counting the number of variables and the number of equations. In order to solve the equations, a sufficient number of independent variables must be set so that the number of dependent variables remaining equals the number of equations.

As an illustration of this method of determining variables, consider a distillation column with a partial condenser. The complete set of equations for this column is shown in Table I. The equations are self-explanatory, but a few points about them should be noted. First, even if written

TABLE I
EQUATIONS FOR DISTILLATION COLUMN WITH PARTIAL CONDENSER

	Component material balance around each stage (xR)	Energy balance around each stage
Condenser	$V_t y_t - r x_r = D y_D$ $V_{t-1} y_{t-1} - L_t x_t = V_t y_t - r x_r$ $V_{t-2} y_{t-2} - L_{t-1} x_{t-1} = V_{t-1} y_{t-1} - L_t x_t$ \vdots \vdots \vdots	$V_t H_t - r h_r = D H_D + Q_c$ $V_{t-1} H_{t-1} - L_t h_t = V_t H_t - r h_r$ $V_{t-2} H_{t-2} - L_{t-1} h_{t-1} = V_{t-1} H_{t-1} - L_t h_t$ \vdots \vdots \vdots
Feed Stage	$V_f y_f - L_{f+1} x_{f+1} = V_{f+1} y_{f+1} - L_{f+2} x_{f+2}$ $V_{f-1} y_{f-1} - L_f x_f + F x_F = V_f y_f - L_{f+1} x_{f+1}$ $V_{f-2} y_{f-2} - L_{f-1} x_{f-1} = V_{f-1} y_{f-1} - L_f x_f$ \vdots \vdots \vdots	$V_f H_f - L_{f+1} h_{f+1} = V_{f+1} H_{f+1} - L_{f+2} h_{f+2}$ $V_{f-1} H_{f-1} - L_f h_f + F h_F = V_f H_f - L_{f+1} h_{f+1}$ $V_{f-2} H_{f-2} - L_{f-1} h_{f-1} = V_{f-1} H_{f-1} - L_f h_f$ \vdots \vdots \vdots
Reboiler	$V_R y_R - L_1 x_1 = V_1 y_1 - L_2 x_2$ $-b x_b = V_R y_R - L_1 x_1$	$V_R H_R - L_1 h_1 = V_1 H_1 - L_2 h_2$ $Q_R - b h_b = V_R H_R - L_1 h_1$



Component equilibrium relations (xR)	Defining equations for component equilibrium relations (xR)	Defining equations for molal enthalpy			
$y_D = K_c x_r$	$K_c = \phi(T_c, P)$	$H_D = \phi(T_c, y_D)$	$h_r = \phi(T_c, x_r)$	$\Sigma y_D = 1$	$\Sigma x_r = 1$
$y_t = K_t x_t$	$K_t = \phi(T_t, P)$	$H_t = \phi(T_t, y_t)$	$h_t = \phi(T_t, x_t)$	$\Sigma y_t = 1$	$\Sigma x_t = 1$
$y_{t-1} = K_{t-1} x_{t-1}$	$K_{t-1} = \phi(T_{t-1}, P)$	$H_{t-1} = \phi(T_{t-1}, y_{t-1})$	$h_{t-1} = \phi(T_{t-1}, x_{t-1})$	$\Sigma y_{t-1} = 1$	$\Sigma x_{t-1} = 1$
.
.
$y_{f+1} = K_{f+1} x_{f+1}$	$K_{f+1} = \phi(T_{f+1}, P)$	$H_{f+1} = \phi(T_{f+1}, y_{f+1})$	$h_{f+1} = \phi(T_{f+1}, x_{f+1})$	$\Sigma y_{f+1} = 1$	$\Sigma x_{f+1} = 1$
$y_f = K_f x_f$	$K_f = \phi(T_f, P)$	$H_f = \phi(T_f, y_f)$	$h_f = \phi(T_f, x_f)$	$\Sigma y_f = 1$	$\Sigma x_f = 1$
$y_{f-1} = K_{f-1} x_{f-1}$	$K_{f-1} = \phi(T_{f-1}, P)$	$H_{f-1} = \phi(T_{f-1}, y_{f-1})$	$h_{f-1} = \phi(T_{f-1}, x_{f-1})$	$\Sigma y_{f-1} = 1$	$\Sigma x_{f-1} = 1$
.
.
$y_1 = K_1 x_1$	$K_1 = \phi(T_1, P)$	$H_1 = \phi(T_1, y_1)$	$h_1 = \phi(T_1, x_1)$	$\Sigma y_1 = 1$	$\Sigma x_1 = 1$
$y_R = K_R x_b$	$K_R = \phi(T_R, P)$	$H_R = \phi(T_R, y_R)$	$h_b = \phi(T_R, x_b)$	$\Sigma y_R = 1$	$\Sigma x_b = 1$
					$\Sigma x_F = 1$

in other ways, they would consist basically of a mass balance for each component around each stage, an energy balance around each stage, and a relation between the concentrations of each component in the phases leaving a stage. In the equations shown, this last set of relations has been taken to be thermodynamic equilibrium. Second, the relations defining the equilibrium constants (K 's) could have included composition, and the enthalpy relations could have included pressure; but since no new variables would have been introduced, the results would be the same. Third, the pressure has been assumed constant for all stages. The pressure in each stage could have been made a function of the pressure at one point in the column; an additional set of equations would be necessary to define these pressures, but no new variables except the pressures would be introduced, and again the results would be unchanged.

The number of equations can now be counted. If R components exist in the feed, n stages are above the feed stage, and m stages are below the feed stage, the number of equations is:

$$[R(n + m + 3)] + [n + m + 3] + [R(n + m + 3)] + [R(n + m + 3)] \\ + [n + m + 3] + [n + m + 3] + [n + m + 3] \\ + [n + m + 4] = [(3R + 5)(n + m + 3)] + 1$$

Similarly, the number of variables is:

$$[R(2)(n + m + 3) + R + 2(n + m + 3) + 1] + [2(n + m + 3) + 3] \\ + [R(n + m + 3)] + [n + m + 4] \\ = [(3R + 5)(n + m + 3)] + R + 5$$

For the column shown in Table I, then, $R + 4$ variables must be assigned values in the set of equations in order to describe a meaningful problem. Actually, in writing the set of equations, two other variables, n and m , must also be assigned values; so that, in defining problems for this column, $R + 6$ variables must be set.

The variables that are to be set must of course be independent. The first one set is naturally independent, but all other variables that are assigned values could be dependent on those previously set. Thus, care must be exercised in choosing the variables to be set; fortunately, in most problems which can be solved directly, it is relatively easy to determine which variables are independent.

The result just obtained by writing the equations defining the process and counting both equations and variables could have been obtained much more easily by means of the description rule. The description rule states that the number of independent variables is equal to the number of variables that can be arbitrarily set in construction or through operation. For the same example, n and m can be arbitrarily set in construc-

tion, i.e., one can build as many stages above the feed and below the feed as desired. In operation, one can feed as much, F_{x_F} , as he desires of any component (R variables). The total molal enthalpy of the feed, h_F , can be arbitrarily set; the column can operate at an arbitrary pressure, P ; and the reboiler and condenser loads, Q_R and Q_C , can be arbitrarily adjusted. Listing these variables, one has

$$n; m; R \text{ values of } F_{x_F}; h_F; P; Q_R; Q_C.$$

Counting them, one obtains $R + 6$, the same result as before.

Thus the description rule simplifies the counting of the *number* of independent variables to be set for any process. However, few problems of interest are described by the list obtained through counting with the rule, and it is usually necessary to replace these independent variables with others of more interest. Again, it is necessary that the variables introduced as replacements be independent, and that the variables be set within their allowable limits. Although independent variables may always be arbitrarily set, there will usually be limits within which they must be set. These limits are often difficult to determine, and the list of problems which can be directly solved is severely restricted because of this. For example, no one would define a problem by replacing n , m , Q_R , Q_C in the above list with four consecutive stage temperatures in the column, even though the temperatures are independent. Such a problem would be prohibitively difficult to solve directly because the allowable limits on the temperatures would be too small.

Counting variables is of obvious importance in setting up problems, but it is relatively simple. Ensuring that the variables of interest are independent may be difficult for complicated processes, and determining the allowable limits of these variables can be extremely difficult.

Fortunately, in almost all problems of interest, certain variables are always set. To enumerate, in vapor-liquid processes, usually all feeds to a column and their enthalpies are set. Also, the column pressure is set. Setting these variables reduces the number left to be set to a relatively small number, small enough to be manageable.

B. STAGE-BY-STAGE SOLUTIONS

As the name implies, stage-by-stage calculations are useful for calculating from a composition and set of flows in one stage to the composition and flows in an adjoining stage. By successive repetition of the procedure it is possible to calculate from one end of a column of stages to the other end.

From the nature of the calculations, the problems which can be solved straightforwardly by this method are those in which a partial separation

of a mixture is part of the list of variables set. As the majority of design problems in separation processes are of this type, this method is ideally suited to design.

As an example, consider the distillation column of Table I with a feed of six components, A, B, C, D, E, F . If one sets the amounts of each of these in the feed, along with the enthalpy of the feed and the column pressure, then four variables remain to be set. In the present problem, one might choose to set the fraction of component C recovered in the top product and the fraction of D recovered in the bottom product. The third variable set would probably be the reflux. The fourth variable, the arbitrary location of the feed stage, would be set during the calculation.

The list of these four variables would be

$$(\textit{C})_d$$

$$(\textit{D})_b$$

$$r$$

Feed stage location

Thus the number of stages, the answer sought, becomes a dependent variable. Other problems, unless very similar to that above, would be difficult to solve and would best be done by a parametric solution, plotting answers to the problem above, to obtain the particular solution of interest.

The general method of stage-by-stage calculation for multicomponent systems was first shown by Lewis and Matheson (L1) and by Underwood (U1) in 1932. The method of Lewis and Matheson was further improved by Robinson and Gilliland (R1), but substantially unchanged. In its most basic form, the concept of the method is simple. Consider the example cited above. If the amounts of each component in both of the products could be exactly calculated, it would only be necessary to start at one end and calculate until a stage was reached at which the composition matched that of the other product.

However, the products cannot be calculated exactly and the procedure outlined is difficult to accomplish. Instead, calculations are made from both ends of the column to a match on an internal stage, perhaps first neglecting certain components, and later correcting the calculation by adding those components. The method has been well described by Robinson and Gilliland, and is certainly useful for simple distillation columns. Greenstadt *et al.* (G1) have shown its application to computers.

Extension of the method to more complicated columns presents more problems; if more than one column and/or feed is present, the calculation becomes formidable.

C. ITERATION SOLUTIONS

Iteration methods are best-suited for solution of almost the reverse problem for which stage-by-stage methods can be used. Consider again the column of Table I with the feed variables and column pressure fixed. Four variables remain to be set, and these must inevitably be the number of stages in both sections of the column, the total amount of either top or bottom product, and the reflux (or some other flow). Thus the list of set variables is

$$\begin{array}{c} n \\ m \\ d \\ r \end{array}$$

Here the answers sought are the fractionation of each component which will be obtained under the set conditions. Solution of other problems must again be done parametrically.

Iteration solutions were first proposed by Thiele and Geddes (T1) in 1933. In this method, all temperatures and flows must be estimated before the solution can begin. The solution is broken into three parts: first, solution of the mass-balance equations under the estimated flows and temperatures; second, correction of the temperatures; and third, correction of the flows. Assuming values for all temperatures and flows reduces the set of mass-balance equations shown in Table I to a linear set of equations which can be solved for the compositions at each point. Because the starting assumptions are completely arbitrary, the compositions will undoubtedly be wrong (the liquid and vapor mole-fractions will not sum to unity), and better values of temperature and flows must then be obtained for use in the next iteration.

Either the temperatures or flows could be adjusted first. The common choice is to correct the temperature. Correction of temperatures is usually done through either bubble-point or dew-point determinations on the calculated stage compositions. After correcting the stage temperatures, the liquid and vapor enthalpies may be obtained from the calculated compositions, and the flows corrected by solution of the now linear heat balance equations of Table I.

Many recent workers have contributed to the development of iteration solutions, especially in the method of solving the mass balance equations. Amundson and Pontinen (A1) have proposed a general method of solution through matrices. Edmister (E1) has solved the equations through development of a series expression relating the amount of a component at a stage to the amount in a product. Matching relations at

the junctures of sections of the column then allow calculation of the products. Thiele and Geddes used essentially the same technique. Smith (S1, S2) and Hanson *et al.* (H1) have solved the equations by a method which assumes the amount of a component in a product and calculates to the other end of the column, tracking the error made at each stage. After the end of the column is reached, the initial error made in the assumed amount can be calculated and precise corrections applied at each stage. Lyster *et al.* (L2) and Holland (H2) have developed correction methods to improve the calculated product compositions for complicated columns, and have worked extensively on convergence techniques.

The solution of the mass balances and the temperature correction has been heavily studied, and is now quite rapid. In distillation columns, the correction of flows through solution of the stage heat-balances is also simple and well developed. Even for complicated columns, distillation processes are readily solved by the present iteration methods, convergence often being reached after only a few iterations.

Many vapor-liquid multistage processes besides distillation are in common use, however, for which the iteration solutions are not so reliable. Reboiled absorption is a familiar example of an intractable process. Here the difficulty lies completely in the heat balance, the mass balance still being readily solved for any process. Also, in certain processes, the number of variables to be set will not permit setting the total amount of product; for these processes, the simple heat balance can predict flow changes in the wrong direction. An ordinary stream stripper shows this effect. Since the top and bottom products cannot be set if all feeds are set, they must be guessed initially and corrected through use of the overall heat balance around the column. If the initial flows are assumed such that the calculated temperature rises down the stripper, the bottom product will be too high in enthalpy, and more enthalpy will be leaving the column than entering. As the heat balance predicts new product amounts, it will lower the amount of high-enthalpy product, thus decreasing the bottom product and predicting new product flows in the wrong direction.

Iteration methods thus are very useful for problems on many processes, but their failure to converge in problems on other processes can result in considerable waste of computer time.

D. RELAXATION SOLUTIONS

Relaxation solutions are conceptually the most simple methods of solution for any multistage separation process. They were first proposed by Rose *et al.* (R2) in 1958 and Duffin (D1) in 1959. Both authors in

effect proposed that the unsteady-state equations be solved for each stage in turn, through sufficient time that the steady state is approached as closely as desired. Both authors also considered only the mass-balance solution, fixing all flows in the column by postulating that the necessary amount of heating or cooling be done at each stage to hold the set flows. Extension of the relaxation method to include heat balance was proposed by Hanson *et al.* (H1).

The relaxation method is restricted to the direct solution of the same type of problem as the iteration methods; other problems must again be solved parametrically. The relaxation method possesses one distinct advantage and one distinct disadvantage in comparison to the iteration solution. The disadvantage is one shared by all relaxation methods; convergence is slow, because of asymptotic approach to the steady-state conditions. However, the development of more rapid computers is fast reducing the cost of even the slow solutions. Also, it has been observed that processes such as absorption and stripping, which do not possess large internal recycles, solve rapidly. Reboiled absorbers and refluxed strippers are slower, and distillation columns can be quite slow. Fortunately, the majority of processes which solve slowly are usually readily attacked by the iteration methods.

The advantage of the relaxation method over the iteration methods is simply that, in the experience of the authors, any process can be solved. Processes for which the iteration methods will not converge, inevitably converge by the relaxation method. Because of the surety of solution the authors wish to stress the relaxation method in this article and have presented a general program on vapor-liquid processes for the use of engineers who need solutions to separation process problems.

Although simple, the conceptual base of the method should be discussed. Consider a stage P somewhere in a column of stages. In general, for a vapor-liquid process, a vapor stream would enter the stage from stage $P - 1$ and a liquid would enter from stage $P + 1$. The differential equation for the mass balance on component i would be

$$A \frac{d(y_i)_P}{d\theta} + a \frac{d(x_i)_P}{d\theta} = L_{P+1}(x_i)_{P+1} + V_{P-1}(y_i)_{P-1} - L_P(x_i)_P - V_P(y_i)_P$$

where L and V are liquid and vapor flow rates, x and y are mole fractions in liquid and vapor, A and a are the stage holdups of vapor and liquid, and θ is the time. If a knowledge of the time behavior of the stage or column were desired, a set of these equations for all components and all stages along with a set of equations for energy balance would have to be solved.

However, if only the steady-state result is desired, the holdups on the

stages may be assumed to be zero for calculational purposes, and the equation written above simplifies to

$$L_P(x_i)_P + V_P(y_i)_P = L_{P+1}(x_i)_{P+1} + V_{P-1}(y_i)_{P-1}$$

If it is further assumed that the exit streams are in thermodynamic equilibrium this equation reduces to the familiar flash equation,

$$L_P(x_i)_P = \frac{L_{P+1}(x_i)_{P+1} + V_{P-1}(y_i)_{P-1}}{[V_P(K_i)_P/L_P] + 1}$$

Any other streams could enter and would join the entering vapor and liquid streams from the adjoining stages to constitute a "feed" to the stage. Also the flows leaving the stage could be split into side streams plus flows to the adjoining stages without changing the basic equations.

Thus a very simple concept is apparent; it is only necessary to answer the question, "if a known feed is brought into the stage, what will be the resulting streams leaving the stage?" For a vapor-liquid process consisting of stages in which equilibrium is reached, the question can be answered by an isenthalpic flash of the total feed to the stage. A new estimate of exit flows, compositions, and temperature for the stage will result. The new flows from this stage can be used in calculating the feed to the adjoining stages, and isenthalpic flash calculations on these stages will yield new flows which are feeds to other stages, etc. The stages can be considered in any order; the authors have found no particular benefit in any specific order of consideration of the stages. Complicated connections between stages and columns pose no problem since the calculation concerns itself with only one stage at a time. Furthermore, it is not necessary to converge the isenthalpic flash calculation, itself a trial and error calculation, on any given stage. Partial calculation of the flash and prediction suffice.

In a process such as liquid-liquid extraction the enthalpy balance is usually unimportant, and the temperature can be assumed constant through the column of stages. Here the question is simply how do the components of the input feed streams distribute. Any other process, such as washing, isotope separation, etc. for which the enthalpy balance is unimportant, requires only the answer to the same simple question.

The relaxation method is certainly slower than the other methods of calculation. However, because of its simple nature, any process can be calculated and the complexities of the process cease to be a major concern. If future attention were directed toward performing an exact calculation of the individual stage, these more exact calculations could replace the flash calculations of the theoretical stages, and the calculated process would then fit much more closely the actual process operation.

Nomenclature

<i>A</i>	Holdup of vapor in a stage (moles)	<i>P</i>	Column pressure
<i>a</i>	Holdup of liquid in a stage (moles)	<i>Q</i>	Heat duty in a reboiler or condenser (B.t.u./hr.)
<i>b</i>	Bottom product (moles/hr.)	<i>R</i>	Number of components fed
<i>D</i>	Vapor top product (moles/hr.)	<i>r</i>	Reflux (moles/hr.)
<i>F</i>	Total feed (moles/hr.)	<i>T</i>	Temperature
<i>H</i>	Molal enthalpy of a vapor (B.t.u./mole)	<i>V</i>	Vapor flow from a stage (moles/hr.)
<i>h</i>	Molal enthalpy of a liquid (B.t.u./mole)	<i>x</i>	mole fraction of a component in a liquid
<i>K</i>	Component equilibrium constant, $= y/x$	<i>y</i>	mole fraction of a component in a vapor
<i>L</i>	Liquid flow from a stage (moles/hr.)	ϕ	Function
<i>m</i>	Number of stages between reboiler and feed stage	θ	Time
<i>n</i>	Number of stages between feed stage and condenser	(/i) _b	Recovery fraction of a component in the bottom product, $= b(x_i)_b/F(x_i)_F$
		(/i) _a	Recovery fraction of a component in the top product, $= d(x_i)_d/F(x_i)_F$

Subscripts

<i>b</i>	Bottom product	<i>p</i>	Stage or plate in general
<i>c</i>	Condenser	<i>R</i>	Reboiler
<i>D</i>	Vapor top product	<i>r</i>	Reflux
<i>d</i>	Liquid top product	<i>t</i>	Top stage or plate in column
<i>F</i>	Feed	1, 2, 3 . . .	Plate number in column, numbering up
<i>f</i>	Feed stage		
<i>i</i>	Component in general		

III. Description of the Program

A. PROBLEM FORMULATION

A general program for vapor-liquid processes has been written and is presented as Program GENVL. The program is written in Fortran language, for any number of components up to 20, for any number of columns up to 5, and for any number of stages in a column up to 40. These ranges can of course be altered by simply changing the DIMENSION statement.

An external feed of any amount, of one or more components, can be fed to any stage in the system of columns. This stage may be a plate, a reboiler, or a condenser. All external feed compositions, flows, and enthalpies are independent variables that are set in the problem description. A side stream of either vapor or liquid (or both) may be withdrawn from any stage except a reboiler or condenser, and either removed as product or sent to any stage of any column. The flow of each side stream

of this type is treated as an independent variable (its total amount is set). The flows leaving the end stages of the columns would normally be the products from the system of columns. However, in the program, each of them may alternatively be sent to any stage of another column; these flows may or may not be independent variables whose amounts are fixed.

Provision has been made for intercoolers between any two stages in a column. Each intercooler introduces another degree of freedom into the equations; and requires that an independent variable be set. In the program this independent variable has been taken to be the temperature to which the stream is cooled. The intercoolers could obviously also function as interheaters, but the program will calculate such heaters as if no vaporization occurs in the heating; this is correct if the pressure in the heater is high enough to prevent vaporization. Provision also exists for introducing or removing a specified amount of heat on any stage—a feed of zero mass and a positive or negative enthalpy equal to the desired heating or cooling load is introduced into the stage concerned.

1. *End Stage Flows*

Each reboiler or condenser introduces a degree of freedom and requires setting an independent variable. In the program, this variable may be either the liquid flow or the vapor flow from a reboiler, or either the reflux or product amount from any type of condenser. Again, the “product” may not be a product, but can be sent to another column.

Three types of condensers are provided for: a partial condenser in which the two streams produced are reflux and a vapor product, both saturated; a total condenser in which the two streams are reflux and liquid product, both at their bubble point; and a two-product condenser in which reflux is produced, along with both a vapor and a liquid product, if both are possible. The two-product condenser introduces one additional degree of freedom over the other types of condenser. The temperature of a two-product condenser can be arbitrarily set, thus controlling the ratio between vapor and liquid in the product. There is no lower limit on specification of this temperature, since at a low enough value the product (as well as the reflux) will simply be entirely subcooled liquid. However, there may be an upper limit on the temperature; if reflux amount has been chosen as the independent variable to be set, the highest temperature permissible will be the dew point of the product, the product being now completely vapor. If the condenser temperature has been specified above this limit, the program will correct it downward to the highest permissible value. A temperature specification intermediate between the dew point and bubble point of the product will produce two products, one

vapor and one liquid. In the program, the total of these products may be set, if desired, rather than the reflux. Again, either or both of the products can be sent to other columns rather than being removed as product.

It might be well at this point to summarize briefly the variables which must be set in order to define problems to be solved by Program GENVL. Other problems can be solved parametrically or by rewriting the program to accommodate them.

The variables set are :

- (1) Amount of each component in each feed.
- (2) Enthalpy of each feed.
- (3) Number of stages in each column (includes reboiler and condenser, if used).
- (4) Pressure of each column (set through constants in equilibrium expression for each component).
- (5) Amount of each side stream.
- (6) Destination (stage and column) for each side stream that is not a product removed from the system of columns.
- (7) Temperature to which liquid is cooled in each intercooler.
- (8) Destination (stage and column) for each flow from an end stage if the flow is not a product removed from the system of columns.
- (9) Reboiler vapor *or* liquid flow from each reboiler.
- (10) Reflux *or* vapor flow from each partial condenser; reflux *or* liquid "product" flow from each total condenser; temperature and reflux *or* total "product" flow from each two-product condenser.

This list of variables completely describes any problem in the system of interlinked columns which can be solved by Program GENVL. Following the description rule, (3), (6), and (8) are set by construction, the others by operation.

2. Independence of Variables

The only *choices* of independent variables allowed by the program come from the degree of freedom introduced by the reboiler, (9), and one of the degrees of freedom introduced by the condenser, (10). Again it should be emphasized that the variables set in these two instances must be independent. For example, if the column system consists of the single column of Table I and one sets the liquid bottom product from the reboiler, the vapor top product is no longer an independent variable and hence cannot be set under (10). Instead the reflux must be set as the last independent variable.

Whether or not a variable is independent may be more difficult to determine in other cases. For example, a distillation column with a side stripper is shown in Fig. 1. The side stripper in Fig. 1(a) has a reboiler and that in Figure 1(b) is stripped with steam. Under the program, the liquid side stream which feeds the side stripper must be set. Also, in the column arrangement of Fig. 1(b) the amount and enthalpy of the steam fed must be set, since it constitutes an external feed. For illustration, we assume that the bottom product from the reboiler of the main column has

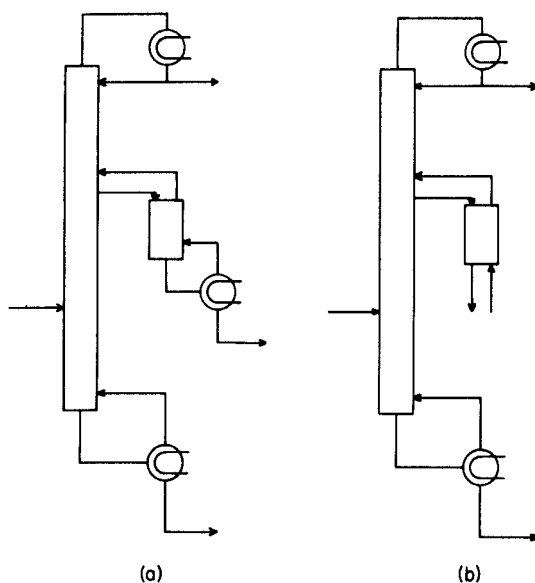


FIG. 1. Process arrangements for illustration of dependence of variables.

been set in both cases. In the column system of Fig. 1(a), it might appear that either the bottom product from the side stripper or the top product from the main column is independent, but not both. However, while the bottom product from the side stripper can be independent, the top product from the main column cannot. In the column system of Fig. 1(b), neither the bottom product from the side stripper nor the top product from the main column is independent. If doubt exists as to whether or not the flow leaving an end stage is independent (whether it is actually a product or goes to another point in the system of columns is immaterial), the safest procedure is simply to use reboiler vapor and reflux as the set variables, since they are of necessity independent.

3. Variable Limits

In the discussion of the description rule, it was also pointed out that limits exist on the possible values of independent variables. These limits, for a particular variable, depend on the values assigned to all variables previously set; as stated, determination of the limits is often prohibitively difficult. Taking the variables in order, there are obviously no limits on the amounts of components in the feed streams, or essentially on the enthalpy of the feeds. Again there are no limits on the number of stages in the columns, or on the linkages between columns in terms of the stage and column from which the streams come or to which they go. However, limits are possible on the amounts of side streams and of streams emanating from end stages of columns. A few illustrations will show the way in which the limits occur.

For the first of these illustrations, Fig. 2(a) shows a reboiled absorber.

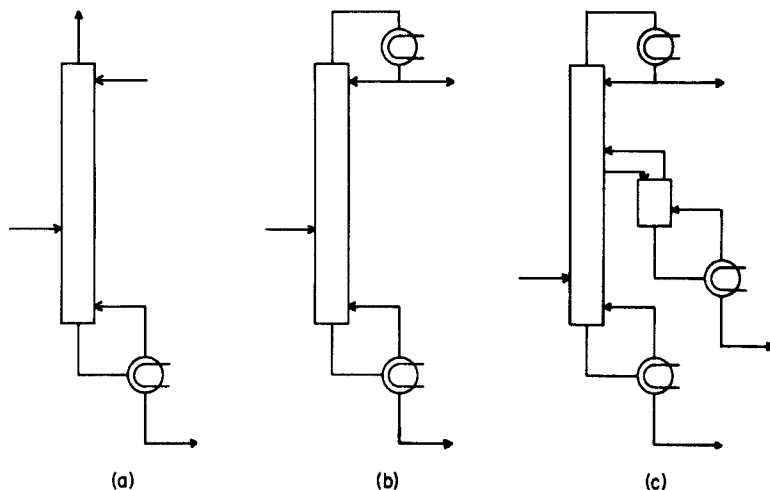


FIG. 2. Process arrangements for illustration of limits on variables.

One degree of freedom is provided by the reboiler; a choice of setting either the bottom product or the reboiler vapor is thus provided. If the bottom product is chosen, the lower limit would be zero and the upper limit generally something less than the total of the two feeds, since the center feed would normally be vapor, and the absorptive capacity of the lean oil feed for this vapor would not usually be high enough to absorb it all, even if the reboiler vapor shrank to zero. This limit would be relatively easy to determine by calculating this same case as a simple absorber, i.e., without the stripping section.

Figure 2(b) shows a simple distillation column with two degrees of freedom provided by the reboiler and condenser. For example, for liquid feed, the top product might be set at an intermediate value between zero and the amount of feed; although no upper limit would exist on reboiler vapor, a lower limit would exist corresponding to zero reflux. It would be quite easy to set the reboiler vapor below this limit, unless a calculation had been made to determine what the limit was. Such a calculation would not be too difficult in this case.

Figure 2(c) shows a distillation column with four degrees of freedom provided by the two reboilers, the condenser, and the liquid side stream from the main column. Many possibilities of limits exist, depending on what variables have been set first. One example might be taken in which the liquid side stream was set last. The limits on the amount of this stream would then be, as a lower limit, the amount of bottom product (or reboiler vapor) in the side stripper; and, as an upper limit, the total amount of liquid flow off the stage from which the stream was drawn. (The latter of these limits would not be easy to determine.)

Any problem involving variables that are set outside the allowable limits cannot be solved. If the solution of such a problem is attempted, much computer time can be wasted, since the fact that the problem is impossible may be difficult to recognize. Also, to determine the allowable limits on variables in complex processes is essentially impossible.

4. Problem Alteration by the Program

Program GENVL has been designed to circumvent these difficulties. If during the solution of the problem, the program finds the problem specifications impossible, it will reset to the nearest possible problem for solution. This procedure is also time-consuming, but after solution the limit which has been exceeded is clearly indicated. Thus, in the example on Fig. 2(a), the amount of bottom product would be reset to as much product as could be produced, and the reboiler vapor would be set to zero. The stripping section of the column would operate essentially as a pipe for the transport of liquid and would be calculated as such. In the example on Fig. 2(b), the amount of top product would be reset downward to that which could be made at the stipulated reboiler vapor, while the reflux would be cut to zero. In the example on Fig. 2(c), the amount of the liquid side stream would be set to all liquid available, producing a zero liquid flow in the main column between that point and the feed plate. If this amount were not sufficient to produce the specified bottom product, say, of the side stripper, this product would be reduced to that available and the reboiler vapor in the side stripper would be reset to zero.

Thus, Program GENVL has been designed to insure, in every way possible, the obtaining of a solution. All problems which have been attempted to date have been solved, although several have been solved to only a low degree of accuracy because of time limitations. One problem has been solved to an accuracy of 1 part in 100,000 in the total mass balance close to the maximum accuracy allowed by the significant figures carried in the computer. Many problems have been solved to an accuracy of 1 part in 1000 in the total mass balance, and this accuracy appears to be reasonable in terms of time consumption.

B. BASIC PROGRAM

The basic program performs the function of using the existing estimates of component flows and stream enthalpy values to predict a new stage temperature and the flows of components from the stage. This is accomplished partly by calculation in the basic program and partly by calling for calculation in various subroutines.

At the beginning of the basic program, the arbitrarily chosen functions for calculation of component equilibrium constants and component enthalpies are shown:

$$K = \exp [A/(T + 460) + B + C(T + 460)]$$
$$H = YT + Z$$

where A, B, C, Y, and Z are component-dependent constants to be supplied as data to the program. Both of these functions are independent of composition, but any other functions could have been used. If it is desired to add activity coefficients and/or heats of mixing, the program could easily be changed to include them.

1. Stage Sequencing

The first step in the basic program is to call subroutine INPUT which reads in the program specifications. Next, the iteration counter, ITERAT, and a calculational variable, KINVEN, are set to zero. The amount of each component entering the system of columns is summed up in SUMFD(I) where the subscript (I) refers to component. Subscript (J) refers to stage, and subscript (K) refers to column. Also the total feed of all components is summed in TOTFD.

At statement 3 the calculation of the stages begins. After every iteration, the program returns to 3 to start the next iteration. A calculational variable, KALTER, is set to zero, to be reset to 1 later in the iteration if the program changes the original problem specification in order to obtain a workable problem. The program then calculates each column in turn, performing all calculations through statement 140. For the particu-

lar column being calculated, the number of stages, including a possible reboiler and condenser, is set up as the index JT . The stage index, J , is set to 1, and a calculational variable $JDELTA$ is set to +1. The program has been written to calculate the stages in the following order: starting at stage 1, up through stage JT , reversing direction and recalculating stage $JT-1$, recalculating down through stage 1. This order is completely arbitrary and could be changed at will. However, calculating in this way, $2(JT)-1$ stage calculations will be made for the column in an iteration, and hence a dummy counter, $KTIMES$, is set to this number to be used in the next loop. The loop starting at statement 4 calculates through statement 114 $KTIMES$ number of times, thus twice for all stages in the column except the top stage.

2. Stage Feeds

For any one stage, the first step is to determine the total amount of each component entering from all possible sources, and the total energy entering the stage. The total amount of each component entering is summed up in a variable called $FLFEED$, flash feed, since this is in essence the feed to a flash calculation to be performed on the stage. The total enthalpy input is summed in QIN . The program first sets $FLFEED$ at any external feed of component I to the stage and QIN at the enthalpy of the external feed to the stage, plus any load associated with an intercooler immediately above the stage. The possibility of one or more streams entering the stage from another column or from another stage in the same column is examined next. Statement 6 examines the array $KSVFRO$ at the position J, K where J is the number of the stage being calculated and K is the column number in which the stage exists. If this number is zero, no side vapor stream comes into the stage from any point in the column system. If the number is positive, a vapor side stream does come in. The calculation then branches to statement 7 where the stage and column from which the stream is coming are set up as the variables JV and KV . The amount of the side vapor flow from JV and KV is examined; if it is zero due to a reset from the original specifications on the amount of the stream, the program branches to statement 10; but if the side stream is positive the program branches to statement 8, where the amount of each component in the sidestream is added to $FLFEED$ and the enthalpy is added to QIN .

All other possibilities of streams entering the stage are examined in the same way. At statement 10 possible liquid side streams entering the stage are examined. At statement 14 the possibility of a vapor flow coming from an end stage (either a condenser or an ordinary stage) is considered. At statement 18 the possibility of a liquid stream coming

from an end stage is considered. The liquid stream could come from either a reboiler or an ordinary stage, if the end stage from which the stream comes is at the bottom of a column, or it could come from a condenser. *JV* is examined to see if it is unity. If so, unless the column from which the liquid stream comes consists of only a condenser, the liquid flow comes from the bottom of the column and is labeled as *QUID*. If the stage number is greater than unity, the stream must come from a condenser, and is *QUITOP* for the column from which it comes.

2. *Necessity of Flash Calculation*

After all possible feeds to the stage have been determined, the calculation goes to statement 26 where a variable *KEXTFD* is set to zero. The program then determines whether a flash calculation should be done on the stage. If an external feed (from outside or through a stream coming from another point) enters the stage, or if there is heating or cooling on the stage, or if both a liquid and a vapor stream enter from adjoining stages, a flash calculation should be done. If, on the other hand, no streams come from outside and no heating or cooling takes place, and no liquid stream enters from the stage above, but a vapor stream enters from the stage below, then nothing will happen to the vapor stream in the stage being considered, and the stage will simply act as a pipe for transit of the vapor. This possibility, and the reverse possibility, are allowed for.

In the next statement below statement 26, *QIN* is examined. If it is not zero, the stage is being heated or cooled or an external feed is entering. If so, *KEXTFD* is set to 1. If *QIN* is zero, *KEXTFD* is left at zero. Next the number of the stage is examined to see if the stage is the lowest stage in the column, namely stage 1. If it is, no vapor can come from the next lower stage. If not, the program branches to statement 31 and the vapor coming from the next lower stage is examined. If the vapor flow is not zero, all of the component flows in the vapor are added to the feed to the stage, the enthalpy is added to *QIN*, and the variable *KVIN* is set to 1, indicating that a vapor flow enters the stage from the stage immediately below.

The liquid flow from the stage immediately above is treated in the same way, except that the calculation is slightly different if the stage above is a condenser. At statement 40, the entire feed of components to the stage is added up in *FLFEES* and the data necessary to calculate an isenthalpic flash on the stage is complete.

3. *Reboilers and Condensers*

At the statement immediately above statement 42, and at statement 44, the index of the stage being calculated is examined to determine

whether the stage is the bottom or top stage in the column. If it is either of these, either JRETYP or JCOTYP for the column is examined to determine whether the stage is an ordinary stage or a reboiler or condenser. If the stage is either a reboiler or a condenser, the calculation of the stage is done in the appropriate subroutine, REBOIL or CONDEN. If the stage is an ordinary one, the program goes to statement 47 to calculate the isenthalpic flash on the stage.

At statement 47 the program sets a variable, KTRANS, to be used in determining how the flash of the stage will be calculated. Next the total amount of material fed to the stage is examined. If it is zero, all flows out of the stage and their enthalpies are set to zero and the stage is not calculated further. If material is entering the stage, there is still the possibility that only one stream enters, either liquid or vapor from an adjoining stage. This possibility is checked at statement 50. If vapor comes from the stage below $KVIN = 1$; if not, $KVIN = 0$. If liquid comes from the stage above, $KLIN = 1$; if not, $KLIN = 0$. If an external feed from any source enters the stage or if the stage is heated or cooled, $KEXTFD = 1$; if not, $KEXTFD = 0$. The stage will act as a pipe only if either $KVIN$ or $KLIN = 1$ and all others are zero. The program then determines which stream is being transported through the stage and sets the stage conditions and flows to simply pass the flow through.

4. Flash Calculation

If the stage does not act as a pipe, the program transfers to statement 56. The program from this point to statement 65 sets up initial estimates of the vapor and liquid flow rates from the stage, using the existing values of the flows. Since the total input to the stage will change from iteration to iteration, the flows leaving this stage cannot be the same. If values exist for exit flows of both liquid and vapor, the program estimates new flows in the same proportion as the old flows (statements 63 and 64). If one or both phase flows are zero, the program estimates new flows respectively either by using a small percentage of the feed for the missing flow or by dividing the input in two.

The program then predicts a new set of conditions and exit flows for the stage by one of two methods, one starting at statement 65, the other starting at statement 75. The choice of methods is controlled by KMODE, as described later. In the first method, the existing temperature of the stage is accepted, and a complete isothermal flash is calculated on the total input of material to the stage at the stage temperature. The amount of each component in the resulting vapor and liquid phases is then known. The temperature is next set either 1° higher or lower, the direc-

tion being chosen to increase the smaller phase, and the flash calculation is repeated. A complete knowledge of two isothermal flashes is then obtained. In the second method, the relative flows of vapor and liquid are accepted, and a flash calculation is done at the estimated flows to determine the amounts of the individual components in the flows together with the temperature. Again, a second flash calculation is done with the smaller flow increased by 1% of the total input, and two complete flash calculations have been obtained.

In either procedure, the enthalpy of the streams resulting from the first flash is calculated as $QOUT$. At statement 80, the enthalpy of the streams resulting from the second flash is calculated as $TOTH$. In addition the enthalpy of the streams of the first flash at the temperature of the second flash is calculated as $SENSH$. The temperature of the first flash is called T , the temperature of the second flash is called T_1 . In the same way the vapor phases resulting from the two flashes are FLV and FLV_1 . In the ordinary case FLV_1 would not equal FLV , nor would T_1 equal T . These differences are then used to predict temperature and flow amounts at the solution to the isenthalpic flash. $TOTCP$ is the amount of energy which must be added to the system to raise the temperature by $1^\circ F$. and is calculated by $(TOTH - QOUT)/(T_1 - T)$. Similarly the amount of energy added to produce one more mole of vapor (and hence one less mole of liquid) is $TOTMCP = (TOTH - QOUT)/(FLV_1 - FLV)$. $SENSCP$ is the amount of sensible heat which would have to be added to raise the temperature $1^\circ F$. if no vaporization or condensation occurred in changing from T to T_1 .

The predicted change in temperature, $DELT$, to be added to T is then $(QIN - QOUT)/TOTCP$, and the predicted vapor change, $DELVS$, to be added to FLV , is $(QIN - QOUT)/TOTMCP$. These corrections, since they are linear, only solve the isenthalpic flash approximately. As convergence is approached, however, the amount of correction to T and FLV becomes smaller and smaller, and linear corrections suffice. The isenthalpic flash could of course be solved as exactly as one desired, but the authors have found the partial solution and linear extrapolation used here to be quite satisfactory for the purposes of this program.

In the program section from the statement just below 81 to statement 85, precaution is taken against those systems in which $T_1 = T$ and $FLV_1 = FLV$. Both circumstances can occur because of the way in which the program is written, but the normal case, starting at statement 85, will show changes in both temperature and vapor amount.

The amount of each component in the predicted flows of vapor and liquid is obtained by a separate prediction for each component in the loop ending at statement 97. If the amount of any component in either

phase is less than 1×10^{-20} , its amount in the phase is arbitrarily set at 1×10^{-20} . The summations of the amounts of the components in the two phases, SUMVY and SUMLX, are then obtained; if either of these is less than 1×10^{-6} of the total input to the stage, that phase is set to zero. Enthalpies of the phases are also determined.

5. Determination of Flash Type

Lastly, at statement 103, the result of the calculation is used to determine which method of flash calculation should be used on the stage in the next iteration. If the input to the stage is essentially pure component, a very inaccurate calculation would result from arbitrarily moving from τ to $\tau + 1.0$ in the two flash calculations. Similarly, if very little change in vaporization will occur on moving the temperature, the calculation of the temperature shift by moving FLV by 1% may yield a very inaccurate extrapolation. In short, a system in which changes in sensible heat predominate when heat is added should be calculated by movement of temperature, while a system in which changes in latent heat predominate should be calculated by movement of the phase amounts. At statement 103, if the sensible heat capacity is more than half of the total heat capacity of the system, KMODE for the stage is set at 1, and if less than half, KMODE is set at 2. When the stage is next calculated, KMODE will direct the calculation to the better path.

The predictions of the flash calculation show only the total amounts of vapor and liquid resulting. If a side vapor or side liquid flow has been specified from the stage it must be subtracted from the total phase, the remainder constituting the flow to the adjoining stage. This is done between statements 106 and 111. If it is found, for example, the predicted amount of liquid is less than the set amount of side liquid flow, all of the predicted liquid phase will be used as side flow and the flow of liquid to the stage below will be set at zero. The vapor is treated in the same way, but in either case the program notes that the problem has been altered.

At statement 111, the number of the stage being calculated is examined. If the stage is the top stage, the program goes through statement 112 at which JDELTA is changed from +1 to -1. When JDELTA is added to J, the next lower stage is next calculated, and in this way the order of treatment of stages is made to go from the bottom to the top stage and back to the bottom.

The next section, statements 115 through 140, is used to calculate the heat unbalance on each stage, the input of energy minus the output of energy. If the stage is a reboiler or condenser, the unbalance is of course

zero and the reboiler or condenser load is calculated instead. Intercooler loads are also calculated.

The program repeats the entire calculation through statement 140 for each column in turn and then proceeds to the next section in which the calculated amounts of each component in all products leaving the system of columns are summed in PRDSUM. Each side flow or flow from an end stage is examined to determine whether it goes to some other point in the column systems; if not, it is a product. The over-all unbalance for each component is calculated as CUNBAL, equal to the total input of the component to the column system minus the total output.

6. Accuracy Check

In the section titled OUTPUT, the iteration counter is raised by unity and a variable, PRSERR, is generated to indicate the extent of error in the over-all mass balance. PRSERR is taken as the sum of the absolute values of the component unbalances, since the simple sum of component unbalances would often give a falsely low answer for the error due to cancellation of plus and minus terms. Provision is made to print the value of PRSERR along with the iteration number by depressing sense-switch 1. By this means the calculation can be followed quite well, and this feature has proved quite useful to the authors. At statement 169 PRSERR is checked against the acceptable limit of accuracy of the calculation, PRDERR, which is read into the computer in the input data. If PRSERR is below the limit, the program will write a complete output of answers and return to statement 1 which calls the input subroutine and starts the calculation of a new problem.

However, if the accuracy of the calculation is not good enough the program will examine sense switch 5 and sense switch 6. If 5 is depressed, a complete output will be written; if 6 is depressed, a short output will be written. In either case, the program then goes on to statement 175. The last section of the basic program is used to call a subroutine for the correction of the column inventory of components which are not in balance. The program examines sense switch 2; if it is depressed, the program will call the subroutine, but only under the conditions that the energy balance is reasonably correct, i.e., if the sum of the absolute values of all stage unbalances is less than 1% of the heat loads in the reboilers and condensers of the columns). If the subroutine is called, a variable, KINVEN, is set to 1; if not, the variable is set to 0. KINVEN is used in the on-line printing of results to show whether or not the subroutine was used. The program then returns to statement 3 to perform the next iteration.

C. SUBROUTINE INPUT

The first step in the basic program is to call subroutine INPUT. The subroutine serves two purposes; to bring in the data defining the problem, and to set up the conditions under which the first iteration will be calculated.

The reading in of data requires only a little explanation. The first two data cards have been specified as cards on which any statement can be typed in columns 2 through 72. The statements typed in these columns are read into FORMATS 1000 and 1001 and immediately written out to serve as a label or identification of the problem. Column 1 of the cards can be used to control the spacing of the identification, as suggested by the 1 and 0 of the formats shown.

Next, the number of components, number of columns, and all physical data are read, followed by the two preset error-limits used by the program. PRDERR is the highest acceptable sum of component unbalances, and is expressed in moles. BDFERR is the accuracy to which bubble-points, dew-points, and flashes are calculated, expressed as a fractional error. The authors have found a tight limit on this error is beneficial, and have commonly used 1×10^{-6} .

The external feeds to the columns are read; first the stage and column to which the feed goes, then the amount of each component in the feed, and last the total enthalpy of the feed.

Next, side streams are read as shown in the program, and possible linkages through streams from end stages being sent to other points are read. The liquid stream from the bottom of a column, for example, will be considered a product leaving the system of columns unless it is specified as going to some other point. Since such a stream could be a dependent variable with its amount unknown, it cannot be sent back to the same column.

Any intercoolers are specified by reading the numbers of the stage and column to which the cooled flow goes and by reading the temperature to which the flow will be cooled. The flow is always taken to be the liquid flow from the stage above, QUID in the program nomenclature.

Any reboilers are specified next. If a reboiler exists, either the vapor flow or liquid flow leaving it, respectively FIXRV or FIXBL, must be specified. Both are read in from the input card, but only the one which corresponds to JRETP will be used, so that the other can simply be read in as zero.

Any condensers are specified in the same way. Here several choices of variables can be made for each condenser. Again only the one or two numbers corresponding to JCOTYP need be punched; the others can simply

be zero, but the numbers needed must be in the field on the card which corresponds to their position in the list of statement 33.

The last data required are an estimate of top and bottom temperatures for each column.

The program then writes out the input data to provide a record of the constants used and specifications made, zeroes certain variables used, and sets up a maximum temperature 300° higher than the highest estimated end temperature and a minimum temperature 200° lower than the lowest estimated end temperature. In calculation, the program will not predict temperatures outside this range.

D. SUBROUTINE OUTPUT

The output subroutine is used to write out either the final converged results of the calculation or, if desired, the results at the end of any iteration. A complete set of results is written when the problem is converged, including compositions of both phases on every stage. The short output, which can be obtained by depressing sense switch 6, omits these compositions, but writes all other pertinent data. It might be noted that the output subroutine will report that the originally specified problem has been altered if any of the flows specified in the problem description have been changed from their set values during the last iteration.

E. SUBROUTINE REBOIL

Any reboiler is calculated in the subroutine written specifically for this purpose. The subroutine first checks the variable *FLFEES* which is the total mass input to the reboiler. If *FLFEES* is zero, the exit streams from the reboiler are set to zero, it is noted that the problem has been altered, and the calculation returns to the basic program.

If *FLFEES* is not zero, the value of *JRETYP* is examined to find which of either the reboiler vapor or bottom liquid has been set in the problem description. If reboiler vapor has been set, the program examines *FLFEES* to see if it is less than the fixed amount of reboiler vapor, *FIXRV*. If so, all of *FLFEES* is taken as reboiler vapor, the bottom liquid is set at zero, *KALTER* is set to 1, the temperature is determined by a dewpoint calculation on the reboiler vapor, and the calculation returns to the basic program. On the other hand, if *FLFEES* is more than large enough to supply *FIXRV*, the remainder is taken as bottom liquid and the temperature and compositions are obtained by calculation of a flash for which the total vapor and total liquid are known (*ISOVFL*). If the bottom liquid is specified, exactly the same procedure is followed except that in the case of a mass input less than the specified bottom liquid, *FIXBL*, all of the input

is taken as this liquid, reboiler vapor is set to zero, and the temperature is determined by a bubble point calculation.

F. SUBROUTINE CONDEN

Subroutine CONDEN is used to calculate all condensers. It operates in very much the same fashion as subroutine REBOIL, except that more possibilities occur. If reflux has been fixed, the amount of FLFEES is examined to see if it is larger than FIXRE. If not the product is set to zero and temperature is determined by bubble point. If the condenser is a two product condenser with a set temperature, TCSET, this temperature is accepted if it is below the bubble point, indicating subcooled reflux. If FLFEES is large enough, the remainder after subtraction of FIXRE is taken as the appropriate product, and temperature is determined either by ISOVFL or BUBPT for the cases of partial and total condenser respectively. For two-product condensers, the division of the total product at TCSET must be determined and calculation transfers to statement 21.

If the end (or "product") flow has been specified, the calculation, at either statement 14 or statement 18, is simply the reverse of the calculation for fixed reflux. Again, for two-product condensers, the calculation transfers to statement 21.

Two-product condensers must be considered differently from the other condensers, since the temperature has been specified and will determine the relative amounts of vapor and liquid product along with their compositions. This analysis is performed from statement 21 through statement 53. The temperature specification may be such that it will produce superheated vapor product or subcooled liquid product, or any material in between. Superheated vapor product, however, is outside the realm of possibility if reflux is to be made; the program has been written to lower the condenser temperature arbitrarily to the dew point of the product, if this circumstance occurs. The analysis of a two-product condenser is additionally complicated by the fact that a flash of the total mass input at TCSET may produce less liquid than the amount fixed as reflux. If so, the program arbitrarily changes the condenser temperature to yield an amount of liquid equal to the fixed reflux, assigning the remaining product as vapor. Neither of these temperature changes is reported as an alteration of the problem specifications.

G. SUBROUTINE INVEN

The relaxation calculation, as mentioned previously, converges quite slowly after the component unbalances in the individual stages have become small. Other circumstances can also cause the calculation to proceed slowly. For example, if the internal flows of material (reflux and reboiler

vapor) are high compared to the product amounts, the initial iterations can build up high inventories of a component in the column which are reduced only slowly to the steady-state amounts if the amounts of the component in the products are small. Subroutine `INVEN` is designed to speed up the depletion of such inventories, by calculating through the column several times in an approximate and rapid fashion before returning to the next iteration.

Each component is calculated in turn. It is assumed that the relative split of the component on a stage is correct as reported from the iteration just calculated. A simple mass balance then gives new estimates for the amount of the component in the phases without any calculation of a flash. If the component is in exact balance at all points, no change will be made in its flow amount at any point by this procedure. However, if there is an unbalance at any point, this unbalance will be lessened and propagated outward.

The program calculates each component completely through the system of columns five times before returning to the basic program. The five is arbitrary, but there is not sufficient evidence to justify any particular figure. The subroutine has proved to be of great value in some cases, but also may have been harmful in others. Whether or not it is of benefit in a particular case can best be determined by following the calculation on the on-line printer. By depressing sense switch 2 the subroutine can be called. After a few iterations, if it appears to be aiding the calculation, its use can be continued; if not, it can be removed by raising the sense switch. In any event, there is no question that the use of the subroutine changes the pattern of the calculation, and its sporadic use may be of value if the convergence is slow.

H. SUBROUTINES `BUBPT`, `DEWPT`, `ISOVFL`, `ISOTFL`

These subroutines are used to calculate respectively, the bubble temperature of a liquid composition, dew temperature of a vapor composition, equilibrium temperature and composition of the phases produced by the flash of a particular stream at known values of total vapor and liquid, and the composition and amount of the phases produced by the flash of a particular stream at a known temperature. All are done at the column pressure which applies.

The first three subroutines, `BUBPT`, `DEWPT`, and `ISOVFL`, are very similar in form. Using an estimated temperature, $\Sigma(Kx)$, $\Sigma(y/K)$, or $\Sigma(Vy/V_{\text{assumed}})$ together with $\Sigma(Lx/L_{\text{assumed}})$ is calculated. This (or these) summation must be within `BDFERR` of unity; if not, the temperature is moved by `TINT` (10° originally) in the correct direction until the summation crosses unity. The correct temperature is then estimated by inter-

polation, TINT is reduced by a factor of 10 and the process repeated. In the subroutine ISOVFL, the slope given by the smaller of the two flows is used for the interpolation.

Subroutine ISOTFL calculates in similar fashion, except that the smaller phase is changed by a fraction of itself, the fraction being 10% at the start and diminishing by a factor of 10 each time the calculation crosses the correct solution. A flash calculation at a set temperature can result in all vapor or all liquid, if the temperature is above the dew point or below the bubble point of the feed; this possibility is provided for by setting the small phase to zero if it falls below one millionth of the feed.

I. EXAMPLES

Many problems of varying size and complexity have been solved with Program GENVL. The most difficult problem solved (with a slightly altered program to allow for the large number of components) was a crude distillation unit containing four side strippers. The total number of stages was 57 and the number of components considered was 76. Sixteen solutions under varying conditions were obtained on an IBM 7094 computer with an average solution time of 20 min., successive solutions being derived from the data of the previous solution.

To illustrate the use of the program, two short examples are shown below.

1. *Example 1. Reboiled Absorber*

The column is a nine-stage reboiled absorber, fed with a vapor of seven components, the feed entering stage 3 of the column. The feed consists of:

Component	Moles
1	245.5
2	31.6
3	221.8
4	131.4
5	7.5
6	2.1
7	7.4
	647.3

A lean oil (pure component 7) is fed to the top stage in the amount of 1055 moles.

The feed enthalpy is 3,606,728 B.t.u. The lean oil is almost at a temperature of 0°F and its enthalpy is 5,330,915 B.t.u.

An intercooler is to be placed between stages 4 and 5 and will cool the liquid flow back to 2°F.

The equilibrium-constant coefficients at the column pressure are

Component	A	B	C
1	0	5.0	0
2	-226.106	1.11346	0.002865
3	-2782.98	7.7319	-0.003341
4	-1995.21	4.60582	-0.000686
5	-4289.97	9.47394	-0.004080
6	-6017.13	13.1817	-0.007132
7	-5930.29	6.38204	-0.000142

and the enthalpy coefficients (with liquid enthalpy equal to $KT + L$ and vapor enthalpy $UT + W$) are:

Component	K	L	U	W
1	6.80	1310	6.80	1360
2	15.20	2990	9.00	4600
3	16.80	3250	13.50	7020
4	17.30	3330	16.50	7870
5	23.00	4330	22.60	9360
6	30.70	5740	30.20	12500
7	36.40	4980	23.90	18660

The total feed to the column is approximately 2000 moles. The calculation will be done to an accuracy of 2 moles. $BDFERR = 1 \times 10^{-6}$ will be used.

The separation desired is between components 2 and 3. The total feed of component 3 and heavier components is 1425.2 moles. On this basis the bottom product was set at 1420 moles for the calculation. The top temperature was estimated to be 50°F. and the bottom temperature 225°F.

The results of the computer calculation are shown in the next two pages. (The program was altered to produce only a short output, omitting the mole fractions.) It is apparent that the number of iterations to the converged solution, 80, is large. The time of solution on an IBM 704 computer was 10.3 min., which when roughly translated into operation on a more modern machine at prevailing industrial rates costs about

\$13.00. Actually, the example represents a problem which was particularly difficult by other methods probably due to the rapid changes in temperature near the feed plate, but which was solved with no difficulty on the present program.

2. Example 1A.

As a further example, the same problem was solved with the reboiler vapor set instead of the bottom product. The reboiler vapor chosen was that calculated in Example 1, hence the two calculations should yield identical results. The pages which follow show that the same results were obtained within the error of the calculation. Also they show that Example 1A converged in 22 iterations as compared to 80 for Example 1. Since the time per iteration is the same, the cost of solving with a set reboiler vapor is obviously much less, not just in this case but for many systems. If a flow such as reflux or reboiler vapor is not set, the program uses many iterations to finally adjust the internal flows, since the energy-unbalance driving-forces become much smaller near convergence. From the design standpoint, it is usually more desirable to set products and leave the reflux or reboiler vapor unset; nevertheless, if many cases are to be run to provide a parametric solution to a problem, it is advantageous to set the reboiler vapor or reflux in the various runs.

3. Example 2. Distillation Column with Side Stripper

Example 2 shows a distillation column of 13 stages with a side stripper of 5 stages. The side stripper receives liquid from stage 9 of the main column and returns vapor from its top stage to stage 10 of the main column.

The feed, introduced into stage 6 of the main column, is 1635.3 moles. The reboiler vapor of the main column is fixed at 1200 moles; the reflux is also fixed at 2500 moles. The liquid side stream is set at 1210 moles, and the bottom product from the side stripper is fixed at 945 moles in order to recover component 3 in fairly pure form in the side stripper.

The input data and results of the computation are shown in the following sheets. The calculation required 22 iterations to converge to an accuracy of 0.5%, and took 4.5 min. on an IBM 704.

J. PROGRAM NOMENCLATURE

$A(I, K)$	= component dependent constant appearing in the equilibrium relation (EQUILKF).
$B(I, K)$	= component dependent constant appearing in the equilibrium relation (EQUILKF).
BDFERR	= limit of accuracy on bubble point calculation, ΣKx must be within BDFERR of unity; on dew point calculation, $\Sigma y/K$ must

- be within BDFERR of unity; on isothermal flash calculation, $\Sigma(Vy)_{calc}/V_{assumed}$ must be within BDFERR of unity; on set V flash calculation, $\Sigma(Vy)_{calc}/V$ must be within BDFERR of unity.
- BOTT = initial estimate of bottom stage temperature ($^{\circ}\text{F}$).
- BUBPT = subroutine for calculation of bubble point. Calculates equilibrium temperature and vapor (VAPY) for a liquid composition given by QUIDX.
- c(I, K) = component dependent constant appearing in the equilibrium relation (EQUILKF).
- CHECK = code number to determine length of output printout.
- CIN = summation of feed streams to a stage (moles).
- CONDEN = subroutine for calculation of condenser.
- CONDLB(K) = condenser heat load for column K (B.t.u.).
- COOLD(J, K) = intercooler heat load for stage J of column K (B.t.u.).
- COOLH = enthalpy of liquid leaving intercooler at TCOOL(J, K) (B.t.u.).
- CUNBAL(I) = mass unbalance of individual components over entire system; that is, the difference between the amount of I entering the system and the amount leaving the system (moles).
- DELL = predicted change in amount of a component in the liquid from a flash calculation (moles of I).
- DELT = predicted temperature change of stage ($^{\circ}\text{F}$).
- DELV = predicted change in amount of a component in the vapor from a flash calculation (moles of I).
- DELVS = predicted increase in vapor flow from a flash calculation (moles).
- DEWPPT = subroutine for calculation of dew point. Calculates equilibrium temperature and liquid composition (QUIDX) for a vapor composition given by VAPY.
- DUTY = set intercooler load (B.t.u.).
- ENTHK(I) = component dependent constants for enthalpy of liquids appearing in the relation THALPF.
- ENTHL(I) = component dependent constants for enthalpy of vapors appearing in the relation THALPF.
- ENTHU(I) = component dependent constants for enthalpy of vapors appearing in the relation THALPF.
- ENTHW(I) = value of the equilibrium constant of component I.
- EQK(I) = equilibrium function defined by the equation
- (A, B, C, K, T)
- $$\exp \left[\frac{A(I, K)}{TEMP(J, K) + 460.0} + B(I, K) + C(I, K)(TEMP(J, K) + 460.0) \right]$$
- EXTFD = array for external feed flow of any component I to any stage J of a column K (moles of component I).
- EXTFDH = array for enthalpy of total external feed to each stage J of column K (B.t.u.).
- (J, K)
- FD(J) = summation of feed streams to stage J (moles).
- FIXBL(K) = fixed liquid flow from reboiler of column K (moles).
- FIXRE(K) = fixed liquid reflux for column K (moles).
- FIXRV(K) = fixed reboiler vapor of column K (moles).
- FIXSL(J, K) = fixed amount of liquid arbitrarily withdrawn from a side stage J of column K (moles).
- FIXSV(J, K) = fixed amount of vapor arbitrarily withdrawn from a side stage J of column K (moles).
- FIXTL(K) = fixed nonreflux liquid from condenser of column K (moles).

FIXTV(K)	= fixed vapor flow from condenser of column K (moles).
FIXTVL(K)	= fixed sum of nonreflux liquid and vapor from condenser of column K (moles).
FLINT	= factor used to alter vapor and liquid streams in ISOTFL.
FLL	= assumed total liquid flow in iterative flash calculation of a stage (moles).
FLLIS	= general calculational variable for sum of individual component amounts in liquid (moles).
FLLISO	= old value of calculated total liquid flow from a stage used to predict movement of liquid (moles).
FLO	= old value of assumed total vapor flow in iterative flash calculation of a stage (moles).
FLLI	= assumed total liquid flow in iterative flash calculation at conditions slightly altered from FLL (moles).
FLLIQ(I)	= calculational vector used for the liquid amount of individual components resulting when FLFEED(I) is flashed one step in an iterative flash calculation (moles of I).
FLLIQ(I)	= predicted value of component I in liquid from a flash calculation (moles of I).
FLV	= assumed total vapor flow in iterative flash calculation of a stage (moles).
FLVAS	= general calculational variable for sum of individual component amounts in vapor (moles).
FLVASO	= old value of calculated total vapor flow from a stage used to predict movement of vapor (moles).
FLVO	= old value of assumed total liquid flow in iterative flash calculation of a stage (moles).
FLVI	= assumed total vapor flow in iterative flash calculation at conditions slightly altered from FLV (moles).
FLVAP(I)	= calculational vector used for the liquid amounts of individual components resulting when FLFEED(I) is flashed one step in an iterative flash calculation (moles of I).
FLVAP(I)	= predicted value of component I in vapor from a flash calculation (moles of I).
FLFEED(I)	= vector set aside for amounts of individual component feeds to a flash process (moles of I).
FLFEES	= sum of individual amounts of components to a flash calculation (Σ FLFEED(I)).
GENLX (I, J, K)	= amount of component I in liquid on any stage J of column K (moles).
GENLXN	= predicted value of component liquid amount of any stage (moles).
GENVY (I, J, K)	= amount of component I in vapor on any stage J of any column K (moles).
GENVYN	= predicted value of component vapor amount on any stage (moles).
HL	= enthalpy of component I in liquid on any stage (B.t.u.).
HV	= enthalpy of component I in vapor on any stage (B.t.u.).
I	= component index.
INPUT	= subroutine for reading all problem input into arrays.
INVEN	= subroutine that may be used to correct the component mass balance.

ISOTFL	= subroutine to determine the liquid and vapor amounts of an isothermal flash calculation.
ISOVFL	= subroutine for calculating the flash temperature when the vapor and liquid amounts are known.
ITERAT	= counter used by program to tally the iterations.
J	= stage index.
JCOOL(J, K)	= array set aside for indicating if there is an intercooler at stage J of any column K.
JCOTYP(K)	= vector set aside for indicating type of condenser, if any, used with a column K.
JDELTA	= code number for indicating whether calculation is proceeding up or down a column.
JELFRO(J, K)	= array set aside for storing JFROM value of a liquid stream leaving the end stage of any column. It is stored in the array at a point corresponding to where the flow is to go; that is, at the (JTO, KTO) array position.
JELTO (J, K)	= array set aside for storing JTO value of liquid stream leaving the end stage of any column. It is stored in the array at a point corresponding to where the flow is from; that is, at the (JFROM, KFROM) array position.
JEVfro(J, K)	= array set aside for storing JFROM value of a vapor stream leaving the end stage of any column. It is stored in the array at a point corresponding to where the flow is to go; that is at the (JTO, KTO) array position.
JEVTO(J, K)	= array set aside for storing JTO value of vapor stream leaving the end stage of any column. It is stored in the array at a point corresponding to where the flow is from; that is, at the (JFROM, KFROM) array position.
JFROM	= number specifying which stage of a column an interconnecting stream is from.
JRETP(K)	= vector set aside for indicating type of reboiler, if any, used with a column K.
JSLFRO(J, K)	= array set aside for storing JFROM value of SLFLO at a point in the array corresponding to where SLFLO is to go; that is, at the (JTO, KTO) array position.
JSLTO(J, K)	= array set aside for storing JTO value of SLFLO at a point in the array corresponding to where SLFLO is from; that is, at the (JFROM, KFROM) array position.
JSTAGE	= counter set to current value of stage number.
JSVFRO(J, K)	= array set aside for storing JFROM value of SVFLO at a point in the array corresponding to where SVFLO is to go; that is, at the (JTO, KTO) array position.
JSVTO(J, K)	= array set aside for storing JTO value of SVFLO at a point in the array corresponding to where SVFLO is from; that is, at the (JFROM, KFROM) array position.
JT	= index set to number of stages in column K, i.e., set to NSTGS(K).
JTO	= number specifying which stage of a column an interconnecting stream is to go to.
JV	= calculation stage index set to the number stored in JSVFRO, JSLFRO, JEVFRO, JELFRO, at the J. position in the array. J then gives the

	stage to which the flow comes and JV gives the stage from which the flow comes.
K	= column index.
KALTER	= code number used to note whether the problem set can be solved.
KCOUNT	= variable counter used during calculation up and down a column.
KELFRO (J, K)	= array set aside for storing KFROM value of a liquid stream leaving the end stage of any column. It is stored in the array at a point corresponding to where the flow is to go; that is, at the (JTO, KTO) array position.
KELTO (J, K)	= array set aside for storing KTO value of a liquid stream leaving the end stage of any column. It is stored in the array at a point corresponding to where the flow is from; that is, at the (JFROM, KFROM) array position.
KEVFRO (J, K)	= array set aside for storing KFROM value of a vapor stream leaving the end stage of a column. It is stored in the array at a point corresponding to where it is to go; that is, at the (JTO, KTO) position.
KEVTO(J, K)	= array set aside for storing KTO value of vapor stream leaving the end stage of any column. It is stored in the array at a point corresponding to where the flow is from; that is, at the (JFROM, KFROM) array position.
KEXTFD	= code number used to note if there is any feed stream to a column.
KFROM	= number specifying which column an interconnecting stream is from.
KINVEN	= code number used to note whether INVEN has been used.
KLIN	= code number used to indicate presence of liquid stream entering a stage.
KMODE (J, K)	= array used in determining how flash calculation will be done.
KSLFRO (J, K)	= array set aside for storing KFROM value of SLFLO at a point in the array corresponding to where SLFLO is to go; that is, at the (JTO, KTO) array position.
KSLTO (J, K)	= array set aside for storing KTO value of SLFLO at a point in the array corresponding to where SLFLO is from; that is, at the (JFROM, KFROM) array position.
KSVFRO (J, K)	= array set aside for storing KFROM value of SVFLO at a point in the array corresponding to where SVFLO is to go; that is, at the (JTO, KTO) array position.
KSVTO (J, K)	= array set aside for storing KTO value of SVFLO at a point in the array corresponding to where SVFLO is from; that is, at the (JFROM, KFROM) array position.
KTIMES	= fixed number used during calculation of a column.
KTO	= number specifying which column an interconnecting stream is to go to.
KTRANS	= general code number used in calculation.
KV	= calculation column index used with JV.
KVIN	= code number used to indicate presence of vapor stream entering a stage.
NCOLS	= number of columns in the system.
NCOMPS	= number of components fed to the system.

NCOOLS	= total number of intercoolers in system of columns.
NFEEDS	= total number of feed streams entering the system of columns.
NLFLOS	= total number of fixed side liquid streams leaving the system and/or interconnecting any stage in any column with any other stage in any column.
NQUIDS	= total number of liquid streams interconnecting the end stage of a column with any stage of any column.
NSTGS(K)	= vector for storing number of stages in each of K columns. Includes a stage for reboiler and/or condenser if either is used.
NTIMES	= variable counter used during calculation up and down a column.
NVAPOS	= total number of vapor streams interconnecting the end stage of any column with any other stage in any column.
NVFLOS	= total number of fixed side vapor streams leaving the system and/or interconnecting any stage in any column with any other stage in any column.
OUTPUT	= subroutine for printing solution to problem.
PRDERR	= limit below which PRSERR must be in order for mass balance to be satisfied.
PRDSUM(I)	= the sum of the amounts of component I in all product streams leaving the system of columns.
PRSERR	= sum of absolute values of individual component unbalances; i.e. $\sum CUNBAL(I) $ (moles)
QIN	= total enthalpy input to any stage (B.t.u.).
QOUT	= total enthalpy leaving any stage (B.t.u.).
QUID (J, K)	= array set aside for variable liquid flow from stage J of column K (moles).
QUIDX(I)	= calculation vector used for liquids.
QUIDXs	= sum of calculated liquid mole fractions for a given feed and set temperature.
QUIMOH (J, K)	= molal enthalpy of liquid from stage J of column K (B.t.u./lb. mole).
QUNBAL (J, K)	= energy unbalance at stage P of column K, input-output (B.t.u.).
QUITOP(K)	= vector set aside for liquid top product amount from the condenser of a column K (moles).
REBLD(K)	= reboiler heat load for column K (B.t.u.).
REBOIL	= subroutine for calculation of reboiler.
RFSUM(I)	= sum of recovery fractions of component I in all product streams leaving the system of columns.
SENSCP	= combined heat capacity of vapor and liquid at any stage temperature (B.t.u./lb. mole °F.).
SENSH	= combined enthalpy of vapor and liquid streams at a temperature above assumed stage temperature (B.t.u.).
SLFLO (J, K)	= fixed amount of vapor withdrawn from stage J of column K as a product or for interconnecting stream.
SLOPE	= slope used in predicting new values in BUBPT, DEWPT, ISOVFL, ISOTFL.
SUMFB(I)	= vector for amounts of all external feeds of component I to the system of columns (moles of I).
SUMLD	= sum of condenser and reboiler loads for entire system of columns (B.t.u.).

SUMLX	= counter for summing liquid flows.
SUMVY	= counter for summing vapor flows.
SUMX	= counter used in summation of y/K during DEWPT.
SUMXO	= old value of summation of y/K (SUMX) during DEWPT.
SUMY	= counter used in summation of Kx during BUBPT.
SUMYO	= old value of summation of Kx , (SUMY) used in prediction.
SVFLO (J, K)	= fixed amount of vapor withdrawn from stage J of column K as a product or interconnecting stream.
T	= assumed value of stage temperature ($^{\circ}\text{F}$).
T1	= adjusted value of temperature used for prediction of new value ($^{\circ}\text{F}$).
TCOOL (J, K)	= array for storing exit intercooler temperature for any stage J of any column K ($^{\circ}\text{F}$).
TCSET(K)	= vector set aside for set value of condenser temperature of any two-product condenser used with column K ($^{\circ}\text{F}$).
TEMP(J, K)	= array for storing temperature at stage J of column K ($^{\circ}\text{F}$).
TINT	= interval of temperature change in prediction of new temperature value. Used in BUBPT, DEWPT, ISOVFL.
TMAX	= upper limit of temperature for system ($^{\circ}\text{F}$).
TMIN	= lower limit of temperature for system ($^{\circ}\text{F}$).
TO	= old value of temperature used in predicting new values of temperature in BUBPT, DEWPT, ISOVFL.
TOPT	= initial estimate of top stage temperature ($^{\circ}\text{F}$).
TOTCP	= heat capacity of combined vapor and liquid flows, including latent heat effects (B.t.u./mole $^{\circ}\text{F}$).
TOTFD	= summation of external feeds to a stage (moles).
TOTH	= summation of outlet vapor and liquid enthalpies for flash calculation of temperature T1 (B.t.u.).
TOTMCP	= heat absorbed per mole through vaporization of liquid on any stage (B.t.u./mole).
TUNBAL	= sum of absolute value of stage unbalances for any column K, i.e., $\sum QUNBAL(J, K) $.
VAPMOH (J, K)	= molal enthalpy of vapor from stage J of column K (B.t.u./lb.-mole).
VAPOR (J, K)	= array set aside for variable vapor flow from stage J of column K (moles).
VAPY(I)	= calculational vector used for vapors.
VAPYS	= sum of calculated vapor mole fractions for a given feed and set temperature.

IV. Program GENVL

```

C GENERAL PROGRAM FOR VAPOR LIQUID EQUILIBRIUM STAGE PROCESSES
C
C PROGRAM GENVL      BASIC PROGRAM
C
C
  DIMENSION A(20,5),B(20,5),C(20,5),NSTGS(5),ENTHK(20),ENTHL(20),
  1ENTHU(20),ENTHW(20),EXTFD(20,40,5),EXTFDH(40,5),SVFLO(40,5),
  2SLFLO(40,5),JSVFRD(40,5),KSVFRD(40,5),JSVTO(40,5),KSVTO(40,5),
  3JSLFRD(40,5),KSLFRD(40,5),JSLTO(40,5),KSLTO(40,5),JEVFRD(40,5),
  4KEVFRD(40,5),JEVTO(40,5),KEVTO(40,5),JELFRD(40,5),KELFRD(40,5),
  5JELTO(40,5),KELTO(40,5),JRETY(5),JCOTYP(5),JCOCL(40,5),
  6TCOOL(40,5),TEMP(40,5),VAPOR(40,5),QUID(40,5),QUITOP(5),TCSET(5),
  7FIXRV(5),FIXBL(5),FIXRE(5),FIXTV(5),FIXTL(5),FIXTVL(5),
  8FIXSV(40,5),FIXSL(40,5),QUIMOH(40,5),VAPMCH(40,5),GLNLX(20,40,5),
  9GENVY(20,40,5),KMODE(40,5),FLFCD(20),FLVAP(20),FLLIQ(20)
  DIMENSION SUMFD(20),FLVAP1(20),FLLIQ1(20),QUNBAL(40,5),
  1COOLLD(40,5),REBLD(5),CONOLD(5),PRDSUM(20),RFSUM(20),CUNBAL(20),
  2QUIDX(20),VAPY(20),EQK(20),FD(40)
  COMMON A,B,C,NSTGS,ENTHK,ENTHL,ENTHU,ENTHW,EXTFD,EXTFDH,SVFLO,
  1SLFLO,JSVFRD,KSVFRD,JSVTO,KSVTO,JSLFRD,KSLFRD,JSLTO,KSLTO,
  2JEVFRD,KEVFRD,JEVTO,KEVTO,JELFRD,KELFRD,JELTO,KELTO,JRETY,
  3JCOTYP,JCCOL,TCOOL,TEMP,VAPOR,QUID,QUITOP,TCSET,FIXRV,
  4FIXBL,FIXRE,FIXTV,FIXTL,FIXTVL,FIXSV,FIXSL,QUIMOH,VAPMCH,GENLX,
  5GENVY,KMODE,FLFCD,SUMFD,CUNBAL,COOLLD,REBLD,CONOLD,PRDSUM,RFSUM,
  6CUNBAL,QUIDX,VAPY,ECK,FC,NCCMPS,K,BDFERR,FLFEES,KALILR,NCCLS,
  7PDERR,ITERAT,CHECK,PRSERR,IMAX,TMIN
  EQUILKF(A,B,C,T)=EXP(F/(T+460.0))+B+C*(T+460.0)
  THALPF(Y,Z,I)=Y+I+Z
1 CALL INPUT
  ITERAT=0
  KINVEN=0
  TOTFD=0.0
  DO 2 I=1,NCCMPS
    SUMFD(I)=0.0
  DO 2 K=1,NCCLS
    JT=NSTGS(K)
    DO 2 J=1,JT
      SUMFD(I)=SUMFD(I)+EXTFD(I,J,K)
2 TOTFD=TOTFD+EXTFD(I,J,K)
3 KALTER=0
  DO 140 K=1,NCCLS
    JT=NSTGS(K)
    J=1
    JOELTA=1
    KTIMES=2*JT-1
4 DO 114 KCOUNT=1,KTIMES
C
C DETERMINATION OF COMPONENT FEEDS AND ENTHALPIES TO THE STAGE
C
  DO 5 I=1,NCCMPS
5 FLFEED(I)=EXTFD(I,J,K)
  QIN=EXTFDH(J,K)-COOLLD(J,K)
6 IF (KSVFRD(J,K)) 10,10,7
7 JV=JSVFRD(J,K)
  KV=KSVFRD(J,K)
  IF (SVFLO(JV,KV)) 10,10,8
8 DO 9 I=1,NCCMPS
9 FLFEED(I)=FLFEED(I)+GENVY(I,JV,KV)*SVFLO(JV,KV)/(SVFLO(JV,KV)+
  1VAPOR(JV,KV))
  QIN=QIN+SVFLO(JV,KV)*VAPMCH(JV,KV)
10 IF (KSLFRD(J,K)) 14,14,11

```

```

11 JV=JSLFRO(J,K)
   KV=KSLFRO(J,K)
   IF (SLFLO(JV,KV)) 14,14,12
12 DO 13 I=1,NCOMPS
13 FLFEED(I)=FLFEED(I)+GENLX(I,JV,KV)*SLFLO(JV,KV)/(SLFLO(JV,KV)+
   IQUID(JV,KV))
   QIN=QIN+SLFLO(JV,KV)*QUIMCH(JV,KV)
14 IF (KEVFR(J,K)) 18,18,15
15 JV=JEVFR(J,K)
   KV=KEVFR(J,K)
   IF (VAPOR(JV,KV)) 18,18,16
16 DO 17 I=1,NCOMPS
17 FLFEED(I)=FLFEED(I)+GENVY(I,JV,KV)*VAPOR(JV,KV)/(VAPOR(JV,KV)+
   ISVFLO(JV,KV))
   QIN=QIN+VAPOR(JV,KV)*VAPMCH(JV,KV)
18 IF (KELFR(J,K)) 26,26,19
19 JV=JELFR(J,K)
   KV=KELFR(J,K)
   IF (JV-1) 20,20,23
20 IF (QUID(JV,KV)) 26,26,21
21 DO 22 I=1,NCOMPS
22 FLFEED(I)=FLFEED(I)+GENLX(I,JV,KV)*QUID(JV,KV)/(QUID(JV,KV)+
   ISLFLO(JV,KV))
   QIN=QIN+QUID(JV,KV)*QUIMQH(JV,KV)
   GO TO 26
23 IF (QUITOP(KV)) 26,26,24
24 DO 25 I=1,NCOMPS
25 FLFEED(I)=FLFEED(I)+GENLX(I,JV,KV)*QUITOP(KV)/(QUITOP(KV)+
   IQUID(JV,KV))
   QIN=QIN+QUITOP(KV)*QUIMCH(JV,KV)
26 KEXTD=0
   IF (QIN) 29,27,29
27 DO 28 I=1,NCOMPS
   IF (FLFEED(I)) 29,28,29
28 CONTINUE
   GO TO 30
29 KEXTFC=1
30 KVIN=0
   KLIN=0
   IF (J-1) 31,34,31
31 IF (VAPOR(J-1,K)) 34,34,32
32 DO 33 I=1,NCOMPS
33 FLFEED(I)=FLFEED(I)+GENVY(I,J-1,K)*VAPOR(J-1,K)/(VAPOR(J-1,K)+
   ISVFLO(J-1,K))
   QIN=QIN+VAPOR(J-1,K)*VAPMCH(J-1,K)
   KVIN=1
34 IF (J-JT) 35,40,35
35 IF (QUID(J+1,K)) 40,40,36
36 DO 39 I=1,NCOMPS
   IF (J-(JT-1)) 37,38,37
37 FLFEED(I)=FLFEED(I)+GENLX(I,J+1,K)*QUID(J+1,K)/(QUID(J+1,K)+
   ISLFLO(J+1,K))
   GO TO 39
38 FLFEED(I)=FLFEED(I)+GENLX(I,J+1,K)*QUID(J+1,K)/(QUID(J+1,K)+
   IQUITOP(K)+SLFLO(J+1,K))
39 CONTINUE
   QIN=QIN+QUID(J+1,K)*QUIMQH(J+1,K)
   KLIN=1
40 FLFEES=0.0
   DO 41 I=1,NCOMPS
41 FLFEES=FLFEES+FLFEED(I)

```

C

```

C  CALCULATION OF REBCILER
C
    IF (J-1) 42,42,44
    42 IF (JREIYP(K)) 47,47,43
    43 CALL REBOIL
    GO TO 111
C
C  CALCULATION OF CONDENSER
C
    44 IF (J-J1) 47,45,45
    45 IF (JCOTYP(K)) 47,47,46
    46 CALL CONDEN
    GO TO 111
C
C  CALCULATION OF COMPONENT FLOWS FROM TYPICAL STAGE
C
    47 KTRANS=KMODE(J,K)
    IF (FLFEES) 46,48,50
    48 SUMVY=0.0
    SUMLX=0.0
    VAPMOH(J,K)=0.0
    QUIMOH(J,K)=0.0
    DO 49 I=1,NCOMPS
    GENVY(I,J,K)=0.0
    49 GENLX(I,J,K)=0.0
    GO TO 106
    50 IF (2*KEXTFC+KVIN+KLIN-2) 51,56,56
    51 IF (KVIN-KLIN) 54,48,52
    52 SUMVY=FLFEES
    SUMLX=0.0
    VAPMOH(J,K)=VAPMOH(J-1,K)
    QUIMOH(J,K)=0.0
    TEMP(J,K)=TEMP(J-1,K)
    DO 53 I=1,NCOMPS
    GENVY(I,J,K)=FLFEED(I)
    53 GENLX(I,J,K)=0.0
    GO TO 106
    54 SUMLX=FLFEES
    SUMVY=0.0
    QUIMOH(J,K)=QUIMOH(J+1,K)
    VAPMOH(J,K)=0.0
    TEMP(J,K)=TEMP(J+1,K)
    DO 55 I=1,NCOMPS
    GENLX(I,J,K)=FLFEED(I)
    55 GENVY(I,J,K)=0.0
    GO TO 106
    56 IF (VAPOR(J,K)+SVFLC(J,K)-1.0E-4*FLFEES) 57,57,59
    57 IF (KVIN) 62,62,58
    58 VAPOR(J,K)=VAPOX(J-1,K)+1.0E-4*FLFEES
    KMODE(J,K)=2
    KTRANS=2
    59 IF (QUID(J,K)+SLFLO(J,K)-1.0E-4*FLFEES) 60,60,63
    60 IF (KLIN) 62,62,61
    61 QUID(J,K)=QUID(J+1,K)+1.0E-4*FLFEES
    KMODE(J,K)=2
    KTRANS=2
    GO TO 63
    62 FLV=.5*FLFEES
    FLL=FLFEES-FLV
    KMODE(J,K)=2
    KTRANS=2
    GO TO (65,75),KTRANS

```

```

63 FLV=FLFEES/((QUID(J,K)+SLFLC(J,K))/(VAPOR(J,K)+SVFLU(J,K))+1.0)
64 FLL=FLFEES/((VAPOR(J,K)+SVFLO(J,K))/(QUID(J,K)+SLFLC(J,K))+1.0)
   GO TO (65,75),KIRANS
65 T=TEMP(J,K)
   CALL ISOTFL (FLVAP,FLLIQ,FLV,FLL,T)
   IF (FLV-1.0E-4*FLFEES) 66,66,67
66 FLV=1.0E-4*FLFEES
   FLL=FLFEES-FLV
   KMODE(J,K)=2
   KTRANS=2
   GO TO (65,75),KTRANS
67 IF (FLL-1.0E-4*FLFEES) 68,68,69
68 FLL=1.0E-4*FLFEES
   FLV=FLFEES-FLL
   KMODE(J,K)=2
   KTRANS=2
   GO TO (65,75),KTRANS
69 QOUT=0.0
   DO 70 I=1,NCOMPS
70 QOUT=QOUT+FLVAP(I)*THALPF(ENTHU(I),ENTHW(I),T)+FLLIQ(I)*THALPF(
   I,ENTHK(I),ENTHL(I),T)
   IF (FLV-FLL) 71,71,72
71 T1=T+1.0
   GO TO 73
72 T1=T-1.0
73 FLV1=FLV
   FLL1=FLL
74 CALL ISOTFL (FLVAP1,FLLIQ1,FLV1,FLL1,T1)
   GO TO 80
75 T=TEMP(J,K)
   CALL ISOVFL (FLVAP,FLLIQ,FLV,FLL,T)
   QOUT=0.0
   DO 76 I=1,NCOMPS
76 QOUT=QOUT+FLVAP(I)*THALPF(ENTHU(I),ENTHW(I),T)+FLLIQ(I)*THALPF(
   I,ENTHK(I),ENTHL(I),T)
   IF (FLL-FLV) 77,77,78
77 FLL1=FLL+.01*FLFEES
   FLV1=FLFEES-FLL1
   GO TO 79
78 FLV1=FLV+.01*FLFEES
   FLL1=FLFEES-FLV1
79 T1=T
   CALL ISOVFL (FLVAP1,FLLIQ1,FLV1,FLL1,T1)
80 TOTM=0.0
   SENS=0.0
   DO 81 I=1,NCOMPS
   HV=THALPF(ENTHU(I),ENTHW(I),T1)
   HL=THALPF(ENTHK(I),ENTHL(I),T1)
   TOTM=TOTM+HV*FLVAP1(I)+HL*FLLIQ1(I)
81 SENS=SENS+HV*FLVAP(I)+HL*FLLIQ(I)
   IF (T1-T) 83,82,83
82 TOTCP=1.0E20
   SENS=0.0
   TOTMCP=(TOTM-QOUT)/(FLV1-FLV)
   DELT=0.0
   DELVS=(QIN-QOUT)/TOTMCP
   GO TO 86
83 IF (FLV1-FLV) 85,84,85
84 TOTMCP=1.0E20
   TOTCP=(TOTM-QOUT)/(T1-T)
   SENS=SENS-QOUT/(T1-T)
   DELVS=0.0

```

```

      DELT=(QIN-QOUT)/TOTCP
      GO TO 86
85  TOTMCP=(TOTH-QOUT)/(FLV1-FLV)
      TOTCP=(TOTH-QOUT)/(T1-T)
      SENSCP=(SENSH-QOUT)/(T1-T)
      DELVS=(QIN-QOUT)/TOTMCP
      DELT=(QIN-QOUT)/TOTCP
86  TEMP(J,K)=T+DELT
      SUMVY=0.0
      SUMLX=0.0
      VAPMOH(J,K)=0.0
      QUIMOH(J,K)=0.0
      DO 97 I=1,NCOMPS
      GO TO (87,86),KTRANS
87  DELV=DELT/(T1-T)*(FLVAP1(I)-FLVAP(I))
      DELL=DELT/(T1-T)*(FLLIQ1(I)-FLLIQ(I))
      GO TO 89
88  DELV=DELVS/(FLV1-FLV)*(FLVAP1(I)-FLVAP(I))
      DELL=DELVS/(FLV1-FLV)*(FLLIQ1(I)-FLLIQ(I))
89  IF (FLVAP(I)+DELV-1.0E-20) 90,90,91
90  GENVY(I,J,K)=1.0E-20
      GENLX(I,J,K)=FLFEED(I)
      GO TO 95
91  GENVY(I,J,K)=FLVAP(I)+DELV
92  IF (FLLIQ(I)+DELL-1.0E-20) 93,93,94
93  GENLX(I,J,K)=1.0E-20
      GENVY(I,J,K)=FLFEED(I)
      GO TO 95
94  GENLX(I,J,K)=FLLIQ(I)+DELL
95  VAPMOH(J,K)=VAPMOH(J,K)+GENVY(I,J,K)*THALPF(ENTHU(I),ENTHW(I),
      ITEMP(J,K))
      QUIMOH(J,K)=QUIMOH(J,K)+GENLX(I,J,K)*THALPF(ENTHK(I),ENTHL(I),
      ITEMP(J,K))
      SUMVY=SUMVY+GENVY(I,J,K)
97  SUMLX=SUMLX+GENLX(I,J,K)
      VAPMOH(J,K)=VAPMOH(J,K)/SUMVY
      QUIMOH(J,K)=QUIMOH(J,K)/SUMLX
      IF (SUMVY-1.0E-6*FLFEES) 98,98,100
98  SUMVY=0.0
      SUMLX=FLFEES
      VAPMOH(J,K)=0.0
      QUIMOH(J,K)=0.0
      DO 99 I=1,NCOMPS
      GENVY(I,J,K)=0.0
      GENLX(I,J,K)=FLFEED(I)
99  QUIMOH(J,K)=QUIMOH(J,K)+FLFEED(I)*THALPF(ENTHK(I),ENTHL(I),
      ITEMP(J,K))/FLFEES
      GO TO 103
100 IF (SUMLX-1.0E-6*FLFEES) 101,101,103
101 SUMLX=0.0
      SUMVY=FLFEES
      QUIMOH(J,K)=0.0
      VAPMOH(J,K)=0.0
      DO 102 I=1,NCOMPS
      GENLX(I,J,K)=0.0
      GENVY(I,J,K)=FLFEED(I)
102 VAPMOH(J,K)=VAPMOH(J,K)+FLFEED(I)*THALPF(ENTHU(I),ENTHW(I),
      ITEMP(J,K))/FLFEES
103 IF (SENSCP/TOTCP-.5) 104,104,105
104 KMODE(J,K)=2
      GO TO 106
105 KMODE(J,K)=1

```



```

106 SVFLU(J,K)=FIXSV(J,K)
    SLFLO(J,K)=FIXSL(J,K)
    VAPOR(J,K)=SUMVY-SVFLC(J,K)
    QUID(J,K)=SMLX-SLFLC(J,K)
    IF (VAPOR(J,K)) 107,108,108
107 VAPOR(J,K)=0.0
    SVFLU(J,K)=SUMVY
    KALTER=1
108 IF (QUID(J,K)) 109,111,111
109 QUID(J,K)=0.0
    SLFLO(J,K)=SMLX
    KALTER=1
111 IF (J-J1) 113,112,112
112 JDELTA=-1
113 J=J+JDELTA
114 CONTINUE
C
C  CALCULATION OF HEAT UNBALANCES
C
115 DO 136 J=1,JT
    IF (J-1) 116,116,117
116 QUNBAL(1,K)=EXTFDH(1,K)+QUID(2,K)*QUIMOH(2,K)
    GO TO 120
117 IF (J-JT) 119,118,118
118 QUNBAL(JT,K)=EXTFDH(JT,K)+VAPCR(JT-1,K)*VAPMOH(JT-1,K)
    GO TO 120
119 QUNBAL(J,K)=EXTFDH(J,K)+VAPCR(J-1,K)*VAPMOH(J-1,K)+QUID(J+1,K)*
    QUIMOH(J+1,K)
120 QUNBAL(J,K)=QUNBAL(J,K)-(VAPOR(J,K)+SVFLU(J,K))*VAPMOH(J,K)-
    1*(QUID(J,K)+SLFLO(J,K))*QUIMOH(J,K)
    IF (KSVFRO(J,K)) 122,122,121
121 JV=JSVFRO(J,K)
    KV=KSVFRO(J,K)
    QUNBAL(J,K)=QUNBAL(J,K)+SVFLU(JV,KV)*VAPMOH(JV,KV)
122 IF (KEVFRO(J,K)) 124,124,123
123 JV=KEVFRO(J,K)
    KV=KEVFRO(J,K)
    QUNBAL(J,K)=QUNBAL(J,K)+VAPCR(JV,KV)*VAPMOH(JV,KV)
124 IF (KSLFRO(J,K)) 126,126,125
125 JV=JSLFRO(J,K)
    KV=KSLFRO(J,K)
    QUNBAL(J,K)=QUNBAL(J,K)+SLFLO(JV,KV)*QUIMOH(JV,KV)
126 IF (KELFRO(J,K)) 130,130,127
127 JV=JELFRO(J,K)
    KV=KELFRO(J,K)
    IF (JV-1) 128,128,129
128 QUNBAL(J,K)=QUNBAL(J,K)+QUID(JV,KV)*QUIMOH(JV,KV)
    GO TO 130
129 QUNBAL(J,K)=QUNBAL(J,K)+QUITOP(KV)*QUIMOH(JV,KV)
130 IF (JCOOL(J,K)) 136,136,131
131 COOLH=0.0
    DO 132 I=1,NCOMPS
132 COOLH=COOLH+THALPF(ENTHK(I),ENTHL(I),TCOOL(J,K))*GENLX(I,J+1,K)
    IF (QUID(J+1,K)) 133,133,134
133 COOLH=0.0
    GO TO 135
134 COOLH=CCOOLH=QUID(J+1,K)/(QUID(J+1,K)+SLFLO(J+1,K))
135 COOLLD(J,K)=QUID(J+1,K)*QUIMOH(J+1,K)-CCOOLH
    QUNBAL(J,K)=QUNBAL(J,K)-CCOOLLD(J,K)
136 CONTINUE
    IF (JRETP(K)) 138,138,137
137 REBLD(K)=-QUNBAL(1,K)

```

```

      QUNBAL(I,K)=0.0
138 IF (JCOTYP(K)) 140,140,139
139 CONDL(K)=QUNBAL(JT,K)-QUITOP(K)*QUIMOH(JT,K)
      QUNBAL(JT,K)=0.0
140 CONTINUE
C
C  CALCULATION OF COMPONENT RECOVERY FRACTIONS AND PRODUCTS
C
      DO 141 I=1,NCOMPS
141  PROSUM(I)=0.0
      DO 161 K=1,NCOLS
      JT=NSTGS(K)
      DO 149 J=1,JT
      IF (SVFLO(J,K)) 145,145,142
142 IF (KSVTO(J,K)) 143,143,145
143 DO 144 I=1,NCOMPS
144  PRDSUM(I)=PRDSUM(I)+GENVY(I,J,K)*SVFLO(J,K)/(SVFLO(J,K)+
      1VAPOR(J,K))
145 IF (SLFLO(J,K)) 149,149,146
146 IF (KSLTO(J,K)) 147,147,149
147 DO 148 I=1,NCOMPS
148  PRDSUM(I)=PRDSUM(I)+GENLX(I,J,K)*SLFLO(J,K)/(SLFLO(J,K)+QUID(I,K))
149 CONTINUE
      IF (KELTO(I,K)) 150,150,153
150 IF (QUID(I,K)) 153,153,151
151 DO 152 I=1,NCOMPS
152  PROSUM(I)=PRDSUM(I)+GENLX(I,I,K)*QUID(I,K)/(QUID(I,K)+SLFLO(I,K))
153 IF (KEVTO(JT,K)) 154,154,157
154 IF (VAPOR(JT,K)) 157,157,155
155 DO 156 I=1,NCOMPS
156  PRDSUM(I)=PRDSUM(I)+GENVY(I,JT,K)*VAPOR(JT,K)/(VAPOR(JT,K)+
      1SVFLO(JT,K))
157 IF (KELTO(JT,K)) 158,158,161
158 IF (QUITOP(K)) 161,161,159
159 DO 160 I=1,NCOMPS
160  PRDSUM(I)=PRDSUM(I)+GENLX(I,JT,K)*QUITOP(K)/(QUITOP(K)+QUID(JT,K))
161 CONTINUE
      DO 162 I=1,NCOMPS
      RFSUM(I)=PRDSUM(I)/SUMFD(I)
162 CUNBAL(I)=SUMFD(I)-PRDSUM(I)
C
C  OUTPUT
C
      ITERAT=ITERAT+1
      PRSERR=0.0
      DO 163 I=1,NCOMPS
163  PRSERR=PRSERR+ABSF(CUNBAL(I))
      IF (SENSE SWITCH 1) 166,169
164 FORMAT (15,E20.8)
165 FORMAT (15,E20.8,9H      (1))
166 IF (KINVEN) 167,167,168
167 PRINT 164,ITERAT,PRSERR
      GO TO 169
168 PRINT 165,ITERAT,PRSERR
169 IF (PRSERR-PRGERR) 170,170,171
170 CHECK=1.0
      CALL OUTPUT
      GO TO 1
171 IF (SENSE SWITCH 5) 172,173
172 CHECK=1.0
      CALL OUTPUT
      GO TO 175

```

```

173 IF (SENSE SWITCH 6) 174,175
174 CHECK=0.0
    CALL OUTPUT
C
C CORRECTION OF INVENTORY OF UNBALANCED COMPONENTS
C
175 TUNBAL=0.0
    IF (SENSE SWITCH 2) 176,181
176 SUMLD=0.0
    DO 178 K=1,NCGLS
        JT=NSTGS(K)
        DO 177 J=1,JT
177 TUNBAL=TUNBAL+ANSF(CUNBAL(J,K))
178 SUMLD=SUMLD+CONCLD(K)+REBLD(K)
        IF (SUMLD) 181,181,179
179 IF (TUNBAL/SUMLD-.01) 180,180,181
180 CALL INVEN
    KINVLN=1
    GO TO 3
181 KINVEN=0
    GO TO 3
END

```

```

C PROGRAM GENVL      SUBROUTINE FOR INPUT
C
C      SUBROUTINE INPUT
        DIMENSION A(20,5),B(20,5),C(20,5),NSTGS(5),ENTHK(20),ENTHL(20),
        1ENTHU(20),ENTHW(20),EXTFD(20,40,5),EXTFDH(40,5),SVFLC(40,5),
        2SLFLU(40,5),JSVFRU(40,5),KSVFRU(40,5),JSVTO(40,5),KSVTO(40,5),
        3JSLFRU(40,5),KSLFRU(40,5),JSLTO(40,5),KSLTO(40,5),JEVFRU(40,5),
        4KEVFRU(40,5),JEVTO(40,5),KEVTC(40,5),JELFRU(40,5),KELFRU(40,5),
        5JELTO(40,5),KELTO(40,5),JREIYP(5),JCEIYP(5),JCOUL(40,5),
        6TCOOL(40,5),TLMF(40,5),VAPUR(40,5),QUID(40,5),QUITCP(5),TCSET(5),
        7FIXRV(5),FIXBL(5),FIXRE(5),FIXTV(5),FIXTL(5),FIXTVL(5),
        8FIXSV(40,5),FIXSL(40,5),QUIMOH(40,5),VAPMOH(40,5),GLNLX(20,40,5),
        9GENVY(20,40,5),KMODE(40,5),FLFEE(20),FLVAP(20),FLLIC(20),
        DIMENSION SUMFD(20),FLVAP1(20),FLLIC1(20),QUNBAL(40,5),
        1COOLLD(40,5),REBLD(5),CCNCLC(5),PRODSUM(20),RFSUM(20),CUNBAL(20),
        2QUIDX(20),VAPY(20),EQK(20),FD(40)
        COMMON A,B,C,NSTGS,ENTHK,ENTHL,ENTHU,ENTHW,EXTFD,EXTFDH,SVFLU,
        1SLFLU,JSVFRU,KSVFRU,JSVTO,KSVTO,JSLFRU,KSLFRU,JSLTO,KSLTO,
        2JEVFRU,KEVFRU,JEVTO,KEVTO,JELFRU,KELFRU,JELTO,KELTO,JREIYP,
        3JCOTYP,JCOUL,TCOOL,TLMF,VAPUR,QUID,QUITCP,TCSET,FIXRV,
        4FIXBL,FIXRE,FIXIV,FIXTL,FIXIVL,FIXSV,FIXSL,QUIMOH,VAPMOH,GENLX,
        5GENVY,KMODE,FLFEE,SUMFD,CUNBAL,COOLLD,REBLD,CONDLD,PRODSUM,RFSUM,
        6CUNBAL,QUID,VAPY,ECK,FC,NCUMPS,K,BDFERR,FLFEES,KALIER,NCOLS,
        7PRDERR,ITERAT,CHECK,PRSENR,TMAX,TMIN
1000 FORMAT (72H1
1      )
      READ INPUT TAPE 5,1000
      WRITE OUTPUT TAPE 6,1000
      PRINT 1000
1001 FORMAT (72HC
1      )
      READ INPUT TAPE 5,1001
      WRITE OUTPUT TAPE 6,1001
      PRINT 1001
1 FORMAT (5I3)
      READ INPUT TAPE 5,1,NCUMPS,NCCLS
      READ INPUT TAPE 5,1,(NSTGS(K),K=1,NCCLS)
2 FORMAT (9F8.0)
      DO 3 K=1,NCCLS
        READ INPUT TAPE 5,2,(A(I,K),I=1,NCUMPS)
        READ INPUT TAPE 5,2,(B(I,K),I=1,NCUMPS)
3      READ INPUT TAPE 5,2,(C(I,K),I=1,NCUMPS)
        READ INPUT TAPE 5,2,(ENTHK(I),I=1,NCUMPS)
        READ INPUT TAPE 5,2,(ENTHL(I),I=1,NCUMPS)
        READ INPUT TAPE 5,2,(ENTHU(I),I=1,NCUMPS)
        READ INPUT TAPE 5,2,(ENTHW(I),I=1,NCUMPS)
        READ INPUT TAPE 5,2,PRDERR,BDFERR
C
C SPECIFY FEEDS      NFEEDS IS THE TOTAL NUMBER OF EXTERNAL FEED STREAMS,
C A PARTICULAR FEED ENTERING STAGE J OF COLUMN K
C
4 DO 5 K=1,NCCLS
  JT=NSTGS(K)
  DO 5 J=1,JT
    EXTFDH(J,K)=0.0
    DO 5 I=1,NCUMPS
5    EXTFD(I,J,K)=0.0
    READ INPUT TAPE 5,1,NFEEDS
    DO 6 JV=1,NFEEDS
      READ INPUT TAPE 5,1,J,K

```

```

      READ INPUT TAPE 5,2,(EXTFD(I,J,K),I=1,NCOMPS)
      6 READ INPUT TAPE 5,2,EXTFDH(J,K)
C
C SPECIFY FIXED SIDE STREAMS LEAVING ANY STAGE NOT A REBOILER OR
C CONDENSER IN ANY COLUMN AND EITHER LEAVING AS PRODUCTS OR ENTERING
C ANY OTHER STAGE IN ANY COLUMN  NVFLOS IS THE TOTAL NUMBER OF FIXED
C SIDE VAPOR STREAMS, NLFLOS IS THE TOTAL NUMBER OF FIXED SIDE LIQUID
C STREAMS, A PARTICULAR SIDE STREAM OF AMOUNT FIXSV OR FIXSL LEAVING
C STAGE JFROM OF COLUMN KFROM AND ENTERING STAGE JTO OF COLUMN KTO
C IF THE STREAM LEAVES AS PRODUCT, JTO AND KTO ARE ZERO
C
      7 DO 8 K=1,NCCLS
        JT=NSTGS(K)
        DO 8 J=1,JT
          FIXSV(J,K)=0.0
          FIXSL(J,K)=0.0
          JSVFRD(J,K)=0
          KSVFRD(J,K)=0
          JSVTO(J,K)=0
          KSVTO(J,K)=0
          JSLFRD(J,K)=0
          KSLFRD(J,K)=0
          JSLTO(J,K)=0
        8 KSLTO(J,K)=0
        READ INPUT TAPE 5,1,NVFLOS,NLFLOS
        IF (NVFLOS) 13,13,9
      9 DO 12 JV=1,NVFLOS
        READ INPUT TAPE 5,1,JFRDM,KFRDM,JTO,KTO
        READ INPUT TAPE 5,2,FXSV(JFRDM,KFRDM)
        IF (JTO) 11,11,10
      10 JSVFRD(JTO,KTO)=JFRDM
        KSVFRD(JTO,KTO)=KFRDM
      11 JSVTO(JFROM,KFROM)=JTO
      12 KSVTO(JFROM,KFROM)=KTO
      13 IF (NLFLOS) 18,18,14
      14 DO 17 JV=1,NLFLOS
        READ INPUT TAPE 5,1,JFRDM,KFRDM,JTO,KTO
        READ INPUT TAPE 5,2,FXSL(JFRDM,KFROM)
        IF (JTO) 16,16,15
      15 JSLFRD(JTO,KTO)=JFRDM
        KSLFRD(JTO,KTO)=KFRDM
      16 JSLTO(JFROM,KFROM)=JTO
      17 KSLTO(JFROM,KFROM)=KTO
C
C SPECIFY STREAMS LEAVING ANY END STAGE IN ANY COLUMN AND ENTERING ANY
C STAGE IN ANY OTHER COLUMN  NVAPLS IS THE TOTAL NUMBER OF END VAPOR
C STREAMS LINKING COLUMNS, NQLIDS IS THE TOTAL NUMBER OF END LIQUID
C STREAMS LINKING COLUMNS, A PARTICULAR STREAM LEAVING STAGE JFROM OF
C COLUMN KFROM AND ENTERING STAGE JTO OF COLUMN KTO  VAPOR STREAMS
C WILL BE VAPOR(JT,K) FROM EITHER AN ORDINARY STAGE OR A CONDENSER
C LIQUID STREAMS WILL BE QUID(I,K) FROM AN ORDINARY STAGE OR A REBOILER
C OR QUITOP(K) FROM A CONDENSER
C
      18 DO 19 K=1,NCOLS
        JT=NSTGS(K)
        DO 19 J=1,JT
          JEVFRD(J,K)=0
          KEVFRD(J,K)=0
          JEVTO(J,K)=0
          KEVTO(J,K)=0
          JELFRD(J,K)=0
          KELFRD(J,K)=0

```

```

      JELTO(J,K)=0
19  KELTO(J,K)=0
      READ INPUT TAPE 5,1,NVAPOS,NQUIDS
      IF (NVAPOS) 23,23,20
20  DO 22 JV=1,NVAPUS
21  READ INPUT TAPE 5,1,JFRCM,KFRCM,JTO,KTO
      JEVFC(JTO,KTO)=JFRCM
      KEVFC(JTO,KTO)=KFRCM
      JEVTO(JFROM,KFROM)=JTC
22  KEVTO(JFROM,KFROM)=KTC
23  IF (NQUIDS) 27,27,24
24  DO 26 JV=1,NQUIDS
25  READ INPUT TAPE 5,1,JFRCM,KFRCM,JTO,KTO
      JELFC(JTO,KTO)=JFRCM
      KELFC(JTO,KTO)=KFRCM
      JELTO(JFROM,KFROM)=JTC
26  KELTO(JFROM,KFROM)=KTC
C
C SPECIFY INTERCOOLERS  NCOOLS IS THE TOTAL NUMBER OF STREAMS TO BE
C COOLED, A PARTICULAR LIQUID FLOW LEAVING STAGE J+1 TO BE COOLED TO
C TCOOL(J,K) BEFORE ENTERING STAGE J OF COLUMN K
C
27  DO 28 K=1,NCOLS
      JT=NSTGS(K)
      DO 28 J=1,JT
28  JCOOL(J,K)=0
      READ INPUT TAPE 5,1,NCOOLS
      IF (NCOOLS) 31,31,29
29  DO 30 JV=1,NCOOLS
      READ INPUT TAPE 5,1,J,K
      JCOOL(J,K)=1
      READ INPUT TAPE 5,2,TCOOL(J,K)
30  CONTINUE
C
C SPECIFY REBOILER TYPE AND FIXED FLOWS AT BOTTOM OF COLUMN K FOR ALL
C COLUMNS  JRETYP(K)=0 INDICATES NO REBOILER  JRETYP(K)=1 INDICATES
C PARTIAL REBOILER, VAPOR FLOW FROM REBOILER WILL BE HELD CONSTANT AT
C FIXRV(K)  JRETYP(K)=2 INDICATES PARTIAL REBOILER, LIQUID FLOW FROM
C REBOILER WILL BE HELD CONSTANT AT FIXBL(K)  ONLY VALUES OF FLOWS
C READ WHICH CORRESPOND TO JRETYP(K) WILL BE USED BY THE PROGRAM
C
31  DO 32 K=1,NCOLS
      READ INPUT TAPE 5,1,JRETYP(K)
32  READ INPUT TAPE 5,2,FIXRV(K),FIXBL(K)
C
C SPECIFY CONDENSER TYPE AT TOP OF COLUMN K FOR ALL COLUMNS
C JCOTYP(K)=0 INDICATES NO CONDENSER  JCOTYP(K)=1 INDICATES PARTIAL
C CONDENSER, REFLUX WILL BE HELD CONSTANT AT FIXRE(K)  JCOTYP(K)=2
C INDICATES PARTIAL CONDENSER, VAPOR FLOW WILL BE HELD CONSTANT AT
C FIXTV(K)  JCOTYP(K)=3 INDICATES TOTAL CONDENSER, SATURATED REFLUX
C WILL BE HELD CONSTANT AT FIXRE(K)  JCOTYP(K)=4 INDICATES TOTAL
C CONDENSER, NON-REFLUX SATURATED LIQUID FLOW WILL BE HELD CONSTANT AT
C FIXTL(K)  JCOTYP(K)=5 INDICATES TWO PRODUCT CONDENSER, REFLUX WILL
C BE HELD CONSTANT AT FIXRE(K)  JCOTYP(K)=6 INDICATES TWO PRODUCT
C CONDENSER, SUM OF VAPOR AND NON-REFLUX LIQUID FLOWS WILL BE HELD
C CONSTANT AT FIXTVL(K)  TEMPERATURE OF TWO PRODUCT CONDENSERS WILL
C BE HELD CONSTANT AT TCSET(K) IF POSSIBLE  ONLY VALUES OF FLOWS READ
C WHICH CORRESPOND TO JCOTYP(K) WILL BE USED BY THE PROGRAM
C
      DO 33 K=1,NCOLS
      READ INPUT TAPE 5,1,JCOTYP(K)
33  READ INPUT TAPE 5,2,FIXRE(K),FIXTV(K),FIXTL(K),FIXTVL(K),TCSET(K)

```

```

C
C INITIAL ESTIMATES OF TEMPERATURES
C
      DO 34 K=1,NCOLS
      JT=NSTGS(K)
      READ INPUT TAPE 5,2,TCPI,BOTT
      TINT=(TOPI-BOTT)/FLGATF(JT-1)
      TEMP(1,K)=BCTT
      DO 34 J=2,JT
      TEMP(J,K)=TEMP(J-1,K)+TINT
34 CONTINUE

C
C PRINT INPUT DATA
C
37 FORMAT (11HCINPUT DATA)
      WRITE OUTPUT TAPE 6,37
38 FORMAT (37HCNO. OF COMPONENTS          NO. OF COLUMNS/110,120)
      WRITE OUTPUT TAPE 6,38,NCOMPS,NCOLS
39 FORMAT (63HC*****
1 COLUMN 11,56H *****
2****)
40 FORMAT (20HCNUMBER OF STAGES = 12)
41 FORMAT (18HCEXTERNAL FEED OF E15.8,16H MOLES TO STAGE 12,11H OF CO
11 COLUMN 11)
42 FORMAT (20H COMPONENT AMOUNTS/(5E20.8))
43 FORMAT (22H ENTHALPY OF FEED = E15.8)
44 FORMAT (12HCNO REBOILER)
45 FORMAT (34HCOREBOILER, FIXED REBOILER VAPOR = E15.8)
46 FORMAT (31HCOREBOILER, FIXED LIQUID FLOW = E15.8)
47 FORMAT (13HCNO CONDENSER)
48 FORMAT (35HCPARTIAL CONDENSER, FIXED REFLUX = E15.8)
49 FORMAT (39HCPARTIAL CONDENSER, FIXED VAPOR FLOW = E15.8)
50 FORMAT (43HCOTAL CONDENSER, FIXED SATURATED REFLUX = E15.8)
51 FORMAT (49HCOTAL CONDENSER, FIXED NON-REFLUX LIQUID FLOW = E15.8)
52 FORMAT (39HCOTWO PRODUCT CONDENSER, FIXED REFLUX = E15.8,22H CO
INDENSER TEMP = E15.8,12H IF POSSIBLE)
53 FORMAT (74HCOTWO PRODUCT CONDENSER, FIXED COMBINED VAPOR AND NON-RE
IFLUX LIQUID FLOW = E15.8/22H CONDENSER TEMP = E15.8,12H IF POS
SSIBLE)
      DO 104 K=1,NCOLS
      JT=NSTGS(K)
      WRITE OUTPUT TAPE 6,39,K
      WRITE OUTPUT TAPE 6,40,ASTGS(K)
      DO 56 J=1,J1
      TOTFD=0.0
      DO 54 I=1,NCOMPS
54 TOTFD=TOTFD+EXTFD(I,J,K)
      IF (TOTFD) 55,56,55
55 WRITE OUTPUT TAPE 6,41,TOTFD,J,K
      WRITE OUTPUT TAPE 6,42,(EXTFD(I,J,K),I=1,NCOMPS)
      WRITE OUTPUT TAPE 6,43,EXTFDH(J,K)
56 CONTINUE
      IF (JRE(TYP(K)) 58,58,57
57 KTRANS=JRE(TYP(K)
      GO TO (59,60),KTRANS
58 WRITE OUTPUT TAPE 6,44
      GO TO 61
59 WRITE OUTPUT TAPE 6,45,FXRV(K)
      GO TO 61
60 WRITE OUTPUT TAPE 6,46,FXBL(K)
61 IF (JCOTYP(K)) 63,63,62
62 KTRANS=JCOTYP(K)

```

```

      GO TO (64,65,66,67,68,69),KTRANS
63  WRITE OUTPUT TAPE 6,47
      GO TO 70
64  WRITE OUTPUT TAPE 6,48,FXRX(K)
      GO TO 70
65  WRITE OUTPUT TAPE 6,49,FXTV(K)
      GO TO 70
66  WRITE OUTPUT TAPE 6,50,FXRX(K)
      GO TO 70
67  WRITE OUTPUT TAPE 6,51,FXTL(K)
      GO TO 70
68  WRITE OUTPUT TAPE 6,52,FXRX(K),TCSET(K)
      GO TO 70
69  WRITE OUTPUT TAPE 6,53,FXTVL(K),TCSET(K)
70  CONTINUE
71  FORMAT (29HFIXED SIDE VAPOR PRODUCT OF E15.8,18H MOLES FROM STAGE
1  12,11H OF COLUMN 11)
72  FORMAT (30HFIXED SIDE LIQUID PRODUCT OF E15.8,18H MOLES FROM STAG
1E 12,11H OF COLUMN 11)
73  FORMAT (28HFIXED SIDE VAPOR STREAM OF E15.8,18H MOLES FROM STAGE
1  12,11H OF COLUMN 11,10H TO STAG 12,11H OF COLUMN 11)
74  FORMAT (29HFIXED SIDE LIQUID STREAM OF E15.8,18H MOLES FROM STAGE
1  12,11H OF COLUMN 11,10H TO STAGE 12,11H OF COLUMN 11)
75  FORMAT (45HINTERCONNECTING VAPOR STREAM FROM END STAGE 12,11H OF
1  COLUMN 11,10H TO STAGE 12,11H OF COLUMN 11)
76  FORMAT (46HINTERCONNECTING LIQUID STREAM FROM END STAGE 12,11H OF
1  COLUMN 11,10H TO STAGE 12,11H OF COLUMN 11)
      DO 84 J=1,JT
      IF (FIXSV(J,K)) 80,80,77
77  IF (JSVTO(J,K)) 78,78,79
78  WRITE OUTPUT TAPE 6,71,FXSV(J,K),J,K
      GO TO 80
79  WRITE OUTPUT TAPE 6,73,FXSV(J,K),J,K,JSVTO(J,K),KSVTO(J,K)
80  IF (FIXSL(J,K)) 84,84,81
81  IF (JSLTO(J,K)) 82,82,83
82  WRITE OUTPUT TAPE 6,72,FXSL(J,K),J,K
      GO TO 84
83  WRITE OUTPUT TAPE 6,74,FXSL(J,K),J,K,JSLTO(J,K),KSLTO(J,K)
84  CONTINUE
      DO 88 J=1,JT
      IF (KEVTO(J,K)) 85,86,85
85  WRITE OUTPUT TAPE 6,75,J,K,JEVTO(J,K),KEVTO(J,K)
86  IF (KELTO(J,K)) 87,88,87
87  WRITE OUTPUT TAPE 6,76,J,K,JELTO(J,K),KELTO(J,K)
88  CONTINUE
89  FORMAT (32HHEATER SUPPLYING HEAT TO STAGE 12,19H      HEATER LOAD
1= E15.8)
90  FORMAT (33HCooler REMOVING HEAT FROM STAGE 12,19H      COOLER LOAD
1 = E15.8)
91  FORMAT (27HINTERCOOLER BETWEEN STAGE 12,11H AND STAGE 12,30H COOL
1  ING LIQUID FLOW TO STAGE 12,19H TO TEMPERATURE OF E15.8)
      DO 96 J=1,J1
      IF (EXTFQH(J,K)) 92,96,92
92  DO 93 I=1,NCOMPS
      IF (EXTFO(I,J,K)) 96,93,96
93  CONTINUE
      IF (EXTFQH(J,K)) 94,94,95
94  DUTY=-EXTFQH(J,K)
      WRITE OUTPUT TAPE 6,90,J,DUTY
      GO TO 96
95  WRITE OUTPUT TAPE 6,89,J,EXTFQH(J,K)
96  CONTINUE

```



```

      DO 98 J=1,JT
      IF (JCOOL(J,K)) 98,98,97
97  JV=J+1
      WRITE OUTPUT TAPE 6,91,J,JV,J,TCOOL(J,K)
98  CONTINUE
99  FORMAT (82HCEQUILIBRIUM CONSTANTS A      EQUILIBRIUM CONSTANTS B
      1      EQUILIBRIUM CONSTANTS C/(E19.8,2E29.8))
100 WRITE OUTPUT TAPE 6,99,(A(I,K),B(I,K),C(I,K),I=1,NCCMPS)
101 FORMAT (13HTEMPERATURES/(5E20.8))
102 FORMAT (E57.8)
      WRITE OUTPUT TAPE 6,101,(TEMP(J,K),J=1,JT)
104 CONTINUE
105 FORMAT (120HO*****
      1 ALL COLUMNS *****
      2)
106 FORMAT (99HCENTHALPY CONSTANTS K      ENTHALPY CONSTANTS L      EN
      1THALPY CONSTANTS U      ENTHALPY CONSTANTS W/(E18.8,3E26.8))
107 FORMAT (52HUPRODUCT ERRCR LIMIT      BUBBLE DEW FLASH ERRCR LIMIT/(E
      117.8,E28.8))
      WRITE OUTPUT TAPE 6,105
      WRITE OUTPUT TAPE 6,106,(ENTHK(I),ENTHL(I),ENTHU(I),ENTHW(I),I=1,
      1NCCMPS)
      WRITE OUTPUT TAPE 6,107,PRDERR,BDFERR
C
C SET UP INITIAL CONDITIONS
C
      DO 109 K=1,NCOLS
      JT=NSTGS(K)
      QUITCP(K)=0.0
      REBLD(K)=0.0
      CONDLK(K)=0.0
      DO 109 J=1,JT
      VAPOR(J,K)=0.0
      QUID(J,K)=0.0
      SVFLO(J,K)=0.0
      SLFLO(J,K)=0.0
      COOLLD(J,K)=0.0
      VAPMCH(J,K)=0.0
      QUIMCH(J,K)=0.0
      KMODE(J,K)=2
      DO 108 I=1,NCCMPS
      GENVY(I,J,K)=0.0
108  GENLX(I,J,K)=0.0
109  CONTINUE
      JT=NSTGS(1)
      TMAX=TEMP(1,1)
      TMIN=TEMP(JT,1)
      DO 117 K=1,NCOLS
      JT=NSTGS(K)
      IF (TEMP(1,K)-TMAX) 111,111,110
110  TMAX=TEMP(1,K)
111  IF (TEMP(JT,K)-TMAX) 113,113,112
112  TMAX=TEMP(JT,K)
113  IF (TEMP(1,K)-TMIN) 114,115,115
114  TMIN=TEMP(1,K)
115  IF (TEMP(JT,K)-TMIN) 116,117,117
116  TMIN=TEMP(JT,K)
117  CONTINUE
      TMAX=TMAX+300.0
      TMIN=TMIN-200.0
      RETURN
      END

```

C PROGRAM GENVL SUBROUTINE FOR OUTPUT

C

```

      SUBROUTINE OUTPUT
      DIMENSION A(20,5),B(20,5),C(20,5),NSTGS(5),ENTHK(20),ENTHL(20),
      1ENTHU(20),ENTHM(20),EXTFD(20,40,5),EXTFCH(40,5),SVFLC(40,5),
      2SLFLO(40,5),JSVFRD(40,5),KSVFRO(40,5),JSVTD(40,5),KSVTD(40,5),
      3JSLFRO(40,5),KSLFRO(40,5),JSLTD(40,5),KSLTD(40,5),JEVFRD(40,5),
      4KEVFRD(40,5),JEVTC(40,5),KEVTC(40,5),JELFRO(40,5),KELFRO(40,5),
      5JELTD(40,5),KELTD(40,5),JREIYP(5),JCCIYP(5),JCCOL(40,5),
      6TCCOL(40,5),TEMP(40,5),VAPOR(40,5),QUID(40,5),QUITOP(5),TCSET(5),
      7FIXRV(5),FIXBL(5),FIXRE(5),FIXTV(5),FIXTL(5),FIXTVL(5),
      8FIXSV(40,5),FIXSL(40,5),QUIMCH(40,5),VAPMCH(40,5),GENLX(20,40,5),
      9GENVY(20,40,5),KMODE(40,5),FLFELD(20),FLVAP(20),FLLIQ(20)
      DIMENSION SUMFD(20),FLVAP1(20),FLLIQ1(20),QUNBAL(40,5),
      1COOLLD(40,5),REBLD(5),CCNOLD(5),PRDSUM(20),RFSUM(20),CUNBAL(20),
      2QUIDX(20),VAPY(20),EQK(20),FD(40)
      COMMON A,B,C,NSTGS,ENTHK,ENTHL,ENTHU,ENTHM,EXTFD,EXTFCH,SVFLC,
      1SLFLO,JSVFRD,KSVFRO,JSVTD,KSVTD,JSLFRO,KSLFRO,JSLTD,KSLTD,
      2JEVFRD,KEVFRD,JEVTD,KEVTD,JELFRO,KELFRO,JELTD,KELTD,JREIYP,
      3JCCIYP,JCCOL,TCCOL,TEMP,VAPOR,QUID,QUITOP,TCSET,FIXRV,
      4FIXBL,FIXRE,FIXTV,FIXTL,FIXTVL,FIXSV,FIXSL,QUIMCH,VAPMCH,GENLX,
      5GENVY,KMODE,FLFELD,SUMFD,CUNBAL,COOLLD,REBLD,CCNOLD,PRDSUM,RFSUM,
      6CUNBAL,QUIDX,VAPY,EQK,FD,NCCMPS,K,BDFERR,FLFEES,KALTER,NCOLS,
      7PRDERN,ITERAT,CHECK,PRSEERR,TMAX,TMIN
      1 FORMAT (17H11 ITERATION NO. = I3)
      WRITE OUTPUT TAPE 6,1,ITERAT
      2 FORMAT (47H0 SPECIFIED PROBLEM ALTERED TO OBTAIN A SOLUTION)
      IF (KALTER) 4,4,3
      3 WRITE OUTPUT TAPE 6,2
      4 DO 113 K=1,NCOLS
      JT=NSTGS(K)
      5 FORMAT (63H0 *****
      1 COLUMN I1,56H *****
      2****)
      WRITE OUTPUT TAPE 6,5,K
      IF (CHECK) 33,33,7
      6 FORMAT (63H0 LIQUID AND VAPOR MOLE FRACTIONS LISTED AS COMPONENTS P
      1ER STAGE)
      7 WRITE OUTPUT TAPE 6,6
      8 FORMAT (19H0 STAGE NO. = 12/7H LIQUID/(5E20.8))
      9 FORMAT (6H VAPOR/(5E20.8))
      DO 24 J=1,J1
      IF (VAPOR(J,K)+SVFLC(J,K)) 10,10,12
      10 DO 11 I=1,NCMPS
      11 VAPY(I)=0.0
      GO TO 14
      12 DO 13 I=1,NCMPS
      13 VAPY(I)=GENVY(I,J,K)/(VAPOR(J,K)+SVFLC(J,K))
      14 IF (J-JT) 15,20,20
      15 IF (QUID(J,K)+SLFLO(J,K)) 16,16,18
      16 DO 17 I=1,NCMPS
      17 QUIDX(I)=0.0
      GO TO 23
      18 DO 19 I=1,NCMPS
      19 QUIDX(I)=GENLX(I,J,K)/(QUID(J,K)+SLFLO(J,K))
      GO TO 23
      20 IF (QUID(J,K)+QUITOP(K)+SLFLO(J,K)) 16,16,21
      21 DO 22 I=1,NCMPS
      22 QUIDX(I)=GENLX(I,J,K)/(QUID(J,K)+QUITOP(K)+SLFLO(J,K))
      23 WRITE OUTPUT TAPE 6,8,J,(QUIDX(I),I=1,NCMPS)

```

```

      WRITE OUTPUT TAPE 6,9,{VAPY(I),I=1,NCOMPS}
24 CONTINUE
25 FORMAT (59HGVAPOR AND LIQUID PRODUCT AMOUNTS AND INTERCONNECTING F
  LLOWS)
26 FORMAT (34H LIQUID SIDE PRODUCT FROM STAGE 12,5H OF E15.8,7H M
  MOLES)
27 FORMAT (33H VAPOR SIDE PRODUCT FROM STAGE 12,5H OF E15.8,7H M
  MOLES)
28 FORMAT (21H BOTTOM PRODUCT OF E15.8,7H MOLES)
29 FORMAT (25H LIQUID TOP PRODUCT OF E15.8,7H MOLES)
30 FORMAT (24H VAPOR TOP PRODUCT OF E15.8,7H MOLES)
31 FORMAT (23H COMPONENT AMOUNTS/(5E20.8))
32 FORMAT (34H COMPONENT RECOVERY FRACTIONS/(5E20.8))
33 WRITE OUTPUT TAPE 6,25
34 IF (KELTO(I,K)) 35,35,38
35 WRITE OUTPUT TAPE 6,28,QUID(I,K)
  IF (QUID(I,K)) 38,38,36
36 DO 37 I=1,NCOMPS
  QUIDX(I)=GENX(I,1,K)*QUID(I,K)/(QUID(I,K)+SLFLO(I,K))
37 VAPY(I)=QUICX(I)/SUMFD(I)
  WRITE OUTPUT TAPE 6,31,(QUIDX(I),I=1,NCOMPS)
  WRITE OUTPUT TAPE 6,32,(VAPY(I),I=1,NCOMPS)
38 DO 49 J=1,JT
39 IF (FIXSL(J,K)) 44,44,4C
40 IF (KSLTO(J,K)) 41,41,44
41 WRITE OUTPUT TAPE 6,26,J,SLFLC(J,K)
  IF (SLFLO(J,K)) 44,44,42
42 DO 43 I=1,NCOMPS
  QUIDX(I)=GENX(I,J,K)*SLFLO(J,K)/(SLFLO(J,K)+QUID(J,K))
43 VAPY(I)=QUICX(I)/SUMFD(I)
  WRITE OUTPUT TAPE 6,31,(QUIDX(I),I=1,NCOMPS)
  WRITE OUTPUT TAPE 6,32,(VAPY(I),I=1,NCOMPS)
44 IF (FIXSV(J,K)) 49,49,45
45 IF (KSVTO(J,K)) 46,46,49
46 WRITE OUTPUT TAPE 6,27,J,SVFLC(J,K)
  IF (SVFLO(J,K)) 49,49,47
47 DO 48 I=1,NCOMPS
  QUIDX(I)=GENVY(I,J,K)*SVFLO(J,K)/(SVFLO(J,K)+VAPOR(J,K))
48 VAPY(I)=QUICX(I)/SUMFD(I)
  WRITE OUTPUT TAPE 6,31,(QUIDX(I),I=1,NCOMPS)
  WRITE OUTPUT TAPE 6,32,(VAPY(I),I=1,NCOMPS)
49 CONTINUE
  IF (JCOTYP(K)-2) 55,55,50
50 IF (KELTO(J,K)) 51,51,54
51 WRITE OUTPUT TAPE 6,29,QUITOP(K)
  IF (QUITOP(K)) 54,54,52
52 DO 53 I=1,NCOMPS
  QUIDX(I)=GENX(I,JT,K)*QUITOP(K)/(QUITOP(K)+QUID(JT,K))
53 VAPY(I)=QUICX(I)/SUMFD(I)
  WRITE OUTPUT TAPE 6,31,(QUIDX(I),I=1,NCOMPS)
  WRITE OUTPUT TAPE 6,32,(VAPY(I),I=1,NCOMPS)
54 IF (JCOTYP(K)-4) 59,59,55
55 IF (KEVTO(JT,K)) 56,56,59
56 WRITE OUTPUT TAPE 6,30,VAPOR(JT,K)
  IF (VAPOR(JT,K)) 59,59,57
57 DO 58 I=1,NCOMPS
  QUIDX(I)=GENVY(I,JT,K)*VAPOR(JT,K)/(VAPOR(JT,K)+SVFLO(JT,K))
58 VAPY(I)=QUICX(I)/SUMFD(I)
  WRITE OUTPUT TAPE 6,31,(QUIDX(I),I=1,NCOMPS)
  WRITE OUTPUT TAPE 6,32,(VAPY(I),I=1,NCOMPS)
59 CONTINUE
60 FORMAT (23H SIDE LIQUID FLOW OF E15.8,19H MOLES FROM STAGE 12,1

```

```

11H TO STAGE 12,12H OF COLUMN 11)
61 FORMAT (22H0 SIDE VAPOR FLOW OF E15.8,19H MOLES FROM STAGE 12,11
1H TO STAGE 12,12H OF COLUMN 11)
62 FORMAT (18H0 LIQUID FLOW OF E15.8,19H MOLES FROM STAGE 12,11H T
10 STAGE 12,12H OF COLUMN 11)
63 FORMAT (18H0 LIQUID FLOW OF E15.8,31H MOLES FROM REBOILER TO STA
1GE 12,12H OF COLUMN 11)
64 FORMAT (18H0 LIQUID FLOW OF E15.8,32H MOLES FROM CONDENSER TO ST
1AGE 12,12H OF COLUMN 11)
65 FORMAT (17H0 VAPOR FLOW OF E15.8,19H MOLES FROM STAGE 12,11H TO
1 STAGE 12,12H OF COLUMN 11)
66 FORMAT (17H0 VAPOR FLOW OF E15.8,32H MOLES FROM CONDENSER TO STA
1GE 12,12H OF COLUMN 11)
J=1
IF (KELTO(1,K)) 73,73,67
67 IF (JRETP(K)) 68,68,69
68 WRITE OUTPUT TAPE 6,62,QUID(1,K),J,JELTO(1,K),KELTO(1,K)
GO TO 70
69 WRITE OUTPUT TAPE 6,63,QUID(1,K),JELTO(1,K),KELTO(1,K)
70 IF (QUID(1,K)) 73,73,71
71 DO 72 I=1,NCOMPS
72 QUIDX(I)=GENLX(1,1,K)*QUID(1,K)/(QUID(1,K)+SLFLO(1,K))
WRITE OUTPUT TAPE 6,31,(QUIDX(I),I=1,NCOMPS)
73 DO 83 J=1,JT
IF (FIXSL(J,K)) 78,78,74
74 IF (KSLTO(J,K)) 78,78,75
75 WRITE OUTPUT TAPE 6,60,SLFLO(J,K),J,JSLTO(J,K),KSLTO(J,K)
IF (SLFLO(J,K)) 78,78,76
76 DO 77 I=1,NCOMPS
77 QUIDX(I)=GENLX(1,J,K)*SLFLO(J,K)/(SLFLO(J,K)+QUID(J,K))
WRITE OUTPUT TAPE 6,31,(QUIDX(I),I=1,NCOMPS)
78 IF (FIXSV(J,K)) 83,83,79
79 IF (KSVTO(J,K)) 83,83,80
80 WRITE OUTPUT TAPE 6,61,SVFLO(J,K),J,JSVTO(J,K),KSVTO(J,K)
IF (SVFLO(J,K)) 83,83,81
81 DO 82 I=1,NCOMPS
82 QUIDX(I)=GENVY(1,J,K)*SVFLO(J,K)/(SVFLO(J,K)+VAPOR(J,K))
WRITE OUTPUT TAPE 6,31,(QUIDX(I),I=1,NCOMPS)
83 CONTINUE
IF (JCOTYP(K)-2) 89,89,84
84 IF (KELTO(JT,K)) 88,88,85
85 WRITE OUTPUT TAPE 6,64,QUITCP(K),JELTO(JT,K),KELTO(JT,K)
IF (QUITCP(K)) 88,88,86
86 DO 87 I=1,NCOMPS
87 QUIDX(I)=GENLX(1,JT,K)*QUITCP(K)/(QUITCP(K)+QUID(JT,K))
WRITE OUTPUT TAPE 6,31,(QUIDX(I),I=1,NCOMPS)
88 IF (JCOTYP(K)-4) 96,96,89
89 IF (KEVTO(JT,K)) 96,96,90
90 IF (JCOTYP(K)) 96,91,92
91 WRITE OUTPUT TAPE 6,65,VAPOR(JT,K),JT,JEVTO(JT,K),KEVTO(JT,K)
GO TO 93
92 WRITE OUTPUT TAPE 6,66,VAPOR(JT,K),JLVTO(JT,K),KEVTC(JT,K)
93 IF (VAPOR(JT,K)) 96,96,94
94 DO 95 I=1,NCOMPS
95 QUIDX(I)=GENVY(1,JT,K)*VAPOR(JT,K)/(VAPOR(JT,K)+SVFLO(JT,K))
WRITE OUTPUT TAPE 6,31,(QUIDX(I),I=1,NCOMPS)
96 CONTINUE
97 FORMAT (16H0STAGE VARIABLES/11H0STAGE TEMPERATURE VAPO
1R FLOW LIQUID FLOW VAP MOL ENTH LIQ MOL ENTH
2 HEAT UNBALANCE/(14,6E19.8))
WRITE OUTPUT TAPE 6,97,(J,TEMP(J,K),VAPOR(J,K),QUID(J,K),
1VAPMOH(J,K),QUIMOH(J,K),QUNBAL(J,K),J=1,JT)

```

```

98 FORMAT (E61.8)
   IF (JCOIYP(K)-3) 102,99,99
99 WRITE OUTPUT TAPE 6,98,CUITCP(K)
100 FORMAT (17HC(BUILLER LOAD = E15.8)
101 FORMAT (18HC(CONDENSER LCAC = E15.8)
102 IF (JREIYP(K)) 104,104,103
103 WRITE OUTPUT TAPE 6,100,REBLD(K)
104 IF (JCOIYP(K)) 108,108,105
105 WRITE OUTPUT TAPE 6,101,CCNOLD(K)
106 FORMAT (27HC(INTERCOOLER BETWEEN STAGE 12,11H AND STAGE 12,30H COOL
      1ING LIQUID FLOW TO STAGE 12,19H TO TEMPERATURE CF E15.8)
107 FORMAT (20HC(INTERCOOLER LCAC = E15.8)
108 DO 110 J=1,J1
   IF (JCOOL(J,K)) 110,110,109
109 JV=J+1
   WRITE OUTPUT TAPE 6,106,J,JV,J,TCOOL(J,K)
   WRITE OUTPUT TAPE 6,107,CCOLLD(J,K)
110 CONTINUE
111 FORMAT (31HC(TOTAL COLUMN HEAT UNBALANCE = E15.8)
      TUNBAL=0.0
      DO 112 J=1,J1
112 TUNBAL=TUNBAL+QUNBAL(J,K)
   WRITE OUTPUT TAPE 6,111,TUNBAL
113 CONTINUE
114 FORMAT (120H0*****
1)*****
2)
115 FORMAT (51HC(TOTAL PRODUCT MASS BALANCES AND RECOVERY FRACTIONS)
116 FORMAT (46H(RECOVERY FRACTION SUMMATIONS FOR EACH COMPONENT/(5E20.
      18))
117 FORMAT (91H(EXCESS MOLES OF EACH COMPONENT ENTERING THE SYSTEM IN
      1FEEDS OVER MOLES LEAVING IN PRODUCTS/(5E20.8))
   WRITE OUTPUT TAPE 6,114
   WRITE OUTPUT TAPE 6,115
   WRITE OUTPUT TAPE 6,116,(RFSUM(I),I=1,NCOMPS)
   WRITE OUTPUT TAPE 6,117,(CUNBAL(I),I=1,NCOMPS)
118 FORMAT (77H(TOTAL MASS UNBALANCE (SUM OF ABSOLUTE VALUES OF COMP
      1ONENT UNBALANCES) = E15.8)
   WRITE OUTPUT TAPE 6,118,PRSEKK
   RETURN
END

```

C PROGRAM GENVL SUBROUTINE FOR CALCULATION OF REBOILER
C
C

```

SUBROUTINE REBCIL
  DIMENSION A(20,5),B(20,5),C(20,5),NSTGS(5),ENTHK(20),ENTHL(20),
  1ENTHU(20),ENTHW(20),EXTFD(20,40,5),EXTFCH(40,5),SVFLC(40,5),
  2SLFLO(40,5),JSVFRD(40,5),KSVFRD(40,5),JSVTO(40,5),KSVTO(40,5),
  3JSLFRD(40,5),KSLFRD(40,5),JSLTO(40,5),KSLTO(40,5),JLVFRC(40,5),
  4KEVFRD(40,5),JEVTO(40,5),KEVTC(40,5),JELFRD(40,5),KELFRC(40,5),
  5JELTC(40,5),KELTO(40,5),JREIYP(5),JCOIYP(5),JCOCL(40,5),
  6TCOOL(40,5),TEMP(40,5),VAPOR(40,5),QUID(40,5),QUITOP(5),TCSET(5),
  7FIXRV(5),FIXBL(5),FIXRE(5),FIXTV(5),FIXTL(5),FIXTVL(5),
  8FIXSV(40,5),FIXSL(40,5),QUIMOH(40,5),VAPMCH(40,5),GENLX(20,40,5),
  9GENVY(20,40,5),KMODE(40,5),FLFEED(20),FLVAP(20),FLLIQ(20)
  DIMENSION SUMFD(20),FLVAPL(20),FLLIQ1(20),QUNBAL(40,5),
  1COOLLD(40,5),REBLD(5),CENDLG(5),PROSUM(20),RFSUM(20),CUNBAL(20),
  2QUIDX(20),VAPY(20),EQK(20),FD(40)
  COMMON A,B,C,NSTGS,ENTHK,ENTHL,ENTHU,ENTHW,EXTFD,EXTFCH,SVFLO,
  1SLFLO,JSVFRD,KSVFRD,JSVTO,KSVTO,JSLFRD,KSLFRD,JSLTO,KSLTO,
  2JEVFRD,KEVFRD,JLVTO,KEVTO,JELFRD,KELFRD,JELTC,KELTC,JREIYP,
  3JCOIYP,JCOOL,TCOOL,TEMP,VAPOR,QUID,QUITOP,TCSET,FIXRV,
  4FIXBL,FIXRE,FIXTV,FIXTL,FIXTVL,FIXSV,FIXSL,QUIMOH,VAPMCH,GENLX,
  5GENVY,KMODE,FLFEED,SUMFD,CUNBAL,COOLLD,REBLD,CENDLG,PROSUM,RFSUM,
  6CUNBAL,QUIDX,VAPY,ECK,FD,NCCMPS,K,BDFERR,FLFEES,KALTER,NCOLS,
  7PDERR,ITLRAI,CHECK,PRSENR,IMAX,IMIN
  THALP(Y,Z,1)=Y+T+Z
  IF (FLFEES) 1,1,3
1  QUID(1,K)=0.0
  VAPOR(1,K)=C.0
  DO 2 I=1,NCCMPS
    GENVY(I,1,K)=0.0
2  GENLX(I,1,K)=0.0
  KALTER=1
  GO TO 14
3  KTRANS=JREIYP(K)
  GO TO (4,8),KTRANS
4  IF (FLFEES-FIXRV(K)) 5,5,7
5  VAPOR(1,K)=FLFEES
  QUID(1,K)=0.0
  DO 6 I=1,NCCMPS
    GENVY(I,1,K)=FLFEED(I)
    GENLX(I,1,K)=0.0
6  VAPY(I)=FLFEED(I)/FLFEES
  CALL CENPT (TEMP(1,K))
  KALTER=1
  GO TO 14
7  VAPOR(1,K)=FIXRV(K)
  QUID(1,K)=FLFEES-FIXRV(K)
  GO TO 12
8  IF (FLFEES-FIXBL(K)) 9,9,11
9  QUID(1,K)=FLFEES
  VAPOR(1,K)=C.0
  DO 10 I=1,NCCMPS
    GENVY(I,1,K)=0.0
    GENLX(I,1,K)=FLFEED(I)
10 QUIDX(I)=FLFEED(I)/FLFEES
  CALL CENPT (TEMP(1,K))
  KALTER=1
  GO TO 14
11 QUID(1,K)=FIXBL(K)
  VAPOR(1,K)=FLFEES-FIXBL(K)

```

```

12 FLV=VAPCR(1,K)
   FLL=QUID(1,K)
   CALL ISOVFL (FLVAP,FLLIC,FLV,FLL,TEMP(1,K))
   DO 13 I=1,NCOMPS
      GENVY(I,1,K)=FLVAP(I)
13  GENLX(I,1,K)=FLLIC(I)
14  VAPMOH(1,K)=0.0
      QUIMOH(1,K)=0.0
      DO 15 I=1,NCOMPS
         VAPMOH(1,K)=VAPMOH(1,K)+GENVY(I,1,K)*THALPF(ENTHU(I),ENTHW(I),
            1TEMP(1,K))
15  QUIMOH(1,K)=QUIMOH(1,K)+GENLX(I,1,K)*THALPF(ENTHX(I),ENTHL(I),
            1TEMP(1,K))
      IF (VAPUR(1,K)) 17,17,16
16  VAPMOH(1,K)=VAPMOH(1,K)/VAPCR(1,K)
17  IF (QUID(1,K)) 19,19,18
18  QUIMOH(1,K)=QUIMOH(1,K)/QUID(1,K)
19  CONTINUE
   RETURN
   END

```

```

C PROGRAM GENVL      SUBROUTINE FOR CALCULATION OF CONDENSER
C
C
      SUBROUTINE CONDNL
      DIMENSION A(20,5),R(20,5),C(20,5),NSTGS(5),ENTHK(20),ENTHL(20),
      1ENTHU(20),ENTHW(20),EXTFD(20,40,5),EXTFDH(40,5),SVFLG(40,5),
      2SLFLG(40,5),JSVFRD(40,5),KSVFRD(40,5),JSVTD(40,5),KSVTD(40,5),
      3JSLFRD(40,5),KSLFRD(40,5),JSLTD(40,5),KSLTD(40,5),JEVFRD(40,5),
      4KEVFRD(40,5),JEVTD(40,5),KEVTD(40,5),JELFRD(40,5),KELFRD(40,5),
      5JELTD(40,5),KELTD(40,5),JRETYP(5),JCOTYP(5),JCOCL(40,5),
      6TCOOL(40,5),TEMP(40,5),VAPOR(40,5),QUID(40,5),QUITOP(5),TCSET(5),
      7FIXRV(5),FIXBL(5),FIXRE(5),FIXTV(5),FIXTL(5),FIXTVL(5),
      8FIXSV(40,5),FIXSL(40,5),QUIMOH(40,5),VAPMCH(40,5),GENLX(20,40,5),
      9GENVY(20,40,5),KMODE(40,5),FLFELD(20),FLVAP(20),FLLIQ(20)
      DIMENSION SUMFD(20),FLVAPL(20),FLLIQL(20),QUNBAL(40,5),
      1COOLLD(40,5),REHLD(5),CONDLD(5),PRDSUM(20),RFSUM(20),CUNBAL(20),
      2QUIDX(20),VAPY(20),EQK(20),FD(40)
      COMMON A,B,C,NSIGS,ENTHK,ENTHL,ENTHU,ENTHW,EXTFD,EXTFDH,SVFLO,
      1SLFLO,JSVFRD,KSVFRD,JSVTD,KSVTD,JSLFRD,KSLFRD,JSLTD,KSLTD,
      2JEVFRD,KEVFRD,JEVTD,KEVTD,JELFRD,KELFRD,JELTD,KELTD,JRETYP,
      3JCOTYP,JCOOL,TCOOL,TEMP,VAPOR,QUID,QUITOP,TCSET,FIXRV,
      4FIXBL,FIXRE,FIXTV,FIXTL,FIXTVL,FIXSV,FIXSL,QUIMOH,VAPMCH,GENLX,
      5GENVY,KMODE,FLFELD,SUMFD,CUNBAL,COOLLD,REHLD,CONDLD,PRDSUM,RFSUM,
      6CUNBAL,QUIDX,VAPY,EQK,FD,NCUMPS,K,BDERR,FLFEES,KALIER,NCCLS,
      7PRDEHR,ITERAT,CHECK,PRSERH,IMAX,TMIN
      EQUILKF(A,B,C,T)=EXP(A/(T+460.0))+B+C*(T+460.0)
      THALPF(Y,Z,T)=Y*T+Z
      JT=NSTGS(K)
      IF (FLFLES) 1,1,3
1  QUID(JT,K)=0.0
      VAPOR(JT,K)=0.0
      QUITOP(K)=0.0
      DO 2 I=1,NCUMPS
      GENVY(I,JT,K)=0.0
2  GENLX(I,JT,K)=0.0
      KALIER=1
      GO TO 60
3  KTRANS=JCOTYP(K)
      GO TO (4,14,4,18,4,21),KTRANS
C
C
C FIXED REFLUX
C
      4 IF (FLFEES-FIXRE(K)) 5,5,10
      5 QUID(JT,K)=FLFEES
      VAPOR(JT,K)=0.0
      QUITOP(K)=0.0
      DO 6 I=1,NCUMPS
      GENVY(I,JT,K)=0.0
      GENLX(I,JT,K)=FLFELD(I)
      6 QUIDX(I)=FLFELD(I)/FLFEES
      CALL BUBPT (TEMP(JT,K))
      GO TO (9,60,9,60,7,60),KTRANS
      7 IF (TEMP(JT,K)-TCSET(K)) 9,9,8
      8 TEMP(JT,K)=TCSET(K)
      9 KALIER=1
      GO TO 60
10 QUID(JT,K)=FIXRE(K)
      GO TO (11,60,12,60,21,60),KTRANS
11 VAPOR(JT,K)=FLFEES-QUID(JT,K)
      GO TO 58
12 QUITOP(K)=FLFEES-QUID(JT,K)

```



```

13 GO TO 54
C
C FIXED END FLOWS
C
C PARTIAL CONDENSER
14 IF (FLFEES-FIXTV(K)) 15,15,17
15 VAPOR(JT,K)=FLFLES
16 QUID(JT,K)=0.0
   KALTER=1
   GO TO 56
17 VAPOR(JT,K)=FIXTV(K)
   QUID(JT,K)=FLFEES-VAPOR(JT,K)
   GO TO 58
C TOTAL CONDENSER
18 IF (FLFEES-FIXTL(K)) 19,19,20
19 QUITOP(K)=FLFEES
   QUID(JT,K)=0.0
   KALTER=1
   GO TO 54
20 QUITOP(K)=FIXTL(K)
   QUID(JT,K)=FLFEES-QUITOP(K)
   GO TO 54
C
C TWO PRODUCT CONDENSER
C
21 TEMP(JT,K)=TCSET(K)
   VAPYS=0.0
   QUIDXS=0.0
   DO 22 I=1,NCOMPS
     EQK=EQUILKF(A(I,K),B(I,K),C(I,K),TCSLT(K))
     VAPYS=VAPYS+FLFEED(I)/FLFEES*EQK
22 QUIDXS=QUIDXS+FLFEED(I)/FLFEES/EQK
   IF (VAPYS-1.0) 23,23,30
23 VAPOR(JI,K)=0.0
   GO TO (60,60,60,60,27,24),KTRANS
24 IF (FLFEES-FIXTVL(K)) 25,25,26
25 QUITOP(K)=FLFEES
   QUID(JT,K)=0.0
   GO TO 28
26 QUITOP(K)=FIXTVL(K)
   QUID(JT,K)=FLFEES-QUITOP(K)
   GO TO 28
27 QUID(JT,K)=FIXRE(K)
   QUITOP(K)=FLFEES-QUID(JT,K)
28 DO 29 I=1,NCOMPS
   GENVY(I,JT,K)=0.0
29 GENLX(I,JT,K)=FLFEED(I)
   GO TO 60
30 IF (QUIDXS-1.0) 31,31,36
31 QUITOP(K)=0.0
   GO TO (60,60,60,60,32,33),KTRANS
32 QUID(JT,K)=FIXRE(K)
   VAPOR(JT,K)=FLFEES-QUID(JT,K)
   GO TO 58
33 IF (FLFEES-FIXTVL(K)) 34,34,35
34 QUID(JT,K)=0.0
   VAPOR(JT,K)=FLFLES
   KALTER=1
   GO TO 56
35 VAPOR(JT,K)=FIXTVL(K)
   QUID(JT,K)=FLFEES-VAPOR(JT,K)
   GO TO 58

```

```

36 IF (QUID(JT,K)+QUITOP(K)) 37,37,38
37 FLL=1.0E-4*FLFEES
   FLV=FLFEES-FLL
   GO TO 43
38 IF (VAPOR(JT,K)) 39,39,40
39 FLV=1.0E-4*FLFEES
   FLL=FLFEES-FLV
   GO TO 43
40 IF ((QUID(JT,K)+QUITOP(K))-VAPOR(JT,K)) 41,41,42
41 FLL=FLFEES/(VAPOR(JT,K)/(QUID(JT,K)+QUITOP(K))+1.0)
   FLV=FLFEES-FLL
   GO TO 43
42 FLV=FLFEES/((QUID(JT,K)+QUITOP(K))/VAPOR(JT,K)+1.0)
   FLL=FLFEES-FLV
43 CALL ISCTFL (FLVAP,FLLIQ,FLV,FLL,TEMP(JT,K))
   GO TO (60,60,60,60,44,47),KTRANS
44 IF (FLL-FIXRE(K)) 45,45,46
45 QUITOP(K)=0.0
   QUID(JT,K)=FIXRL(K)
   VAPOR(JT,K)=FLFEES-QUID(JT,K)
   GO TO 53
46 QUID(JT,K)=FIXRE(K)
   QUITOP(K)=FLL-QUID(JT,K)
   VAPOR(JT,K)=FLV
   GO TO 52
47 IF (FLFEES-FIXTVL(K)) 48,48,49
48 QUID(JT,K)=0.0
   VAPOR(JT,K)=FLV
   QUITOP(K)=FLL
   KALTER=1
   GO TO 52
49 IF (FLV-FIXTVL(K)) 51,51,50
50 QUITOP(K)=0.0
   VAPOR(JT,K)=FIXTVL(K)
   QUID(JT,K)=FLFEES-VAPOR(JT,K)
   GO TO 58
51 VAPOR(JT,K)=FLV
   QUITOP(K)=FIXTVL(K)-VAPOR(JT,K)
   QUID(JT,K)=FLFEES-FIXTVL(K)
52 DO 53 I=1,NCOMPS
   GENLX(I,JT,K)=FLLIQ(I)
53 GENVY(I,JT,K)=FLVAP(I)
   GO TO 60

C
C CALCULATION OF CONDENSER TEMPERATURE
C
C BUBBLE POINT
54 DO 55 I=1,NCOMPS
   GENLX(I,JT,K)=FLFEED(I)
   GENVY(I,JT,K)=0.0
55 QUIDX(I)=FLFEED(I)/FLFEES
   CALL RUBPT (TEMP(JT,K))
   GO TO 63
C DEW POINT
56 DO 57 I=1,NCOMPS
   GENLX(I,JT,K)=0.0
   GENVY(I,JT,K)=FLFEED(I)
57 VAPY(I)=FLFEED(I)/FLFEES
   CALL DEWPT (TEMP(JT,K))
   GO TO 60
C FLASH
58 FLV=VAPOR(JT,K)

```

```

      FLL=QUID(JT,K)+QUITCP(K)
      CALL ISUVFL (FLVAP,FLLIC,FLV,FLL,TEMP(JT,K))
      DO 59 I=1,NCOMPS
        GENLX(I,JT,K)=FLLIQ(I)
59     GENVY(I,JT,K)=FLVAP(I)
60     VAPMCH(JT,K)=0.0
        QUIMOH(JT,K)=0.0
        DO 61 I=1,NCOMPS
          VAPMOH(JT,K)=VAPMOH(JT,K)+GENVY(I,JT,K)*THALPF(LNTHU(I),ENTHW(I),
            ITEMP(JT,K))
61     QUIMOH(JT,K)=QUIMCH(JT,K)+GENLX(I,JT,K)*THALPF(LNTHK(I),LNTFL(I),
            ITEMP(JT,K))
          IF (VAPUR(JI,K)) 63,63,62
62     VAPMCH(JT,K)=VAPMOH(JT,K)/VAPCR(JI,K)
63     IF (QUID(JT,K)+QUITCP(K)) 65,65,64
64     QUIMCH(JT,K)=QUIMOH(JT,K)/(QUID(JT,K)+QUITCP(K))
65     CONTINUE
      RETURN
      END

```

C PROGRAM GENVL SUBROUTINE FOR CORRECTION OF INVENTORY OF COMPONENTS
C
C

```

SUBROUTINE INVEN
  DIMENSION A(20,5),B(20,5),C(20,5),NSTGS(5),ENTHK(20),ENTHL(20),
  1ENTHU(20),ENTHW(20),EXTFD(20,40,5),EXTFDH(40,5),SVFLC(40,5),
  2SLFLO(40,5),JSVFRD(40,5),KSVFRD(40,5),JSVTO(40,5),KSVTO(40,5),
  3JSLFRD(40,5),KSLFRD(40,5),JSLTD(40,5),KSLTD(40,5),JEVFRD(40,5),
  4KEVFRD(40,5),JEVTO(40,5),KEVTO(40,5),JELFRD(40,5),KELFRD(40,5),
  5JELTD(40,5),KELTD(40,5),JRETY(5),JCOITY(5),JCOUL(40,5),
  6TCOOL(40,5),TEMP(40,5),VAPOR(40,5),QUID(40,5),QUITOP(5),TCSET(5),
  7FIXRV(5),FIXBL(5),FIXRE(5),FIXTV(5),FIXTL(5),FIXTVL(5),
  8FIXSV(40,5),FIXSL(40,5),QUIMOH(40,5),VAPMOH(40,5),GENLX(20,40,5),
  9GENVY(20,40,5),KMODE(40,5),FLFEE(20),FLVAP(20),FLLIQ(20)
  DIMENSION SUMFD(20),FLVAP1(20),FLLIQ1(20),QUNBAL(40,5),
  1COOLLD(40,5),REBLD(5),CCNDLD(5),PRODSUM(20),RFSUM(20),CUNBAL(20),
  2QUIDX(20),VAPY(20),EQK(20),FD(40)
  COMMON A,B,C,NSTGS,ENTHK,ENTHL,ENTHU,ENTHW,EXTFD,EXTFDH,SVFLC,
  1SLFLO,JSVFRD,KSVFRD,JSVTO,KSVTO,JSLFRD,KSLFRD,JSLTD,KSLTD,
  2JEVFRD,KEVFRD,JEVTO,KEVTO,JELFRD,KELFRD,JELTD,KELTD,JRETY,
  3JCOITY,JCOUL,TCOOL,TEMP,VAPOR,QUID,QUITOP,TCSET,FIXRV,
  4FIXBL,FIXRE,FIXTV,FIXTL,FIXTVL,FIXSV,FIXSL,QUIMOH,VAPMOH,GENLX,
  5GENVY,KMODE,FLFEE,SUMFD,QUNBAL,COOLLD,REBLD,CCNDLD,PRODSUM,RFSUM,
  6CUNBAL,QUIDX,VAPY,ECK,FD,NCCMPS,K,BDFERR,FLFEES,KALTER,NCOLS,
  7PRDERR,ITERAT,CHECK,PRSEERR,TMAX,TMIN
  DO 30 I=1,NCOMPS
1 DO 29 K=1,NCOLS
    JT=NSTGS(K)
    DO 16 J=1,JT
      FD(J)=EXTFD(I,J,K)
      IF (KSVFRD(J,K)) 4,4,2
2    JV=JSVFRD(J,K)
      KV=KSVFRD(J,K)
      IF (SVFLC(JV,KV)) 4,4,3
3    FD(J)=FD(J)+GENVY(I,JV,KV)*SVFLC(JV,KV)/(SVFLC(JV,KV)+
      1VAPOR(JV,KV))
4    IF (KSLFRD(J,K)) 7,7,5
5    JV=JSLFRD(J,K)
      KV=KSLFRD(J,K)
      IF (SLFLO(JV,KV)) 7,7,6
6    FD(J)=FD(J)+GENLX(I,JV,KV)*SLFLO(JV,KV)/(SLFLO(JV,KV)+
      1LIQID(JV,KV))
7    IF (KEVFRD(J,K)) 10,10,8
8    JV=JEVFRD(J,K)
      KV=KEVFRD(J,K)
      IF (VAPOR(JV,KV)) 10,10,9
9    FD(J)=FD(J)+GENVY(I,JV,KV)*VAPOR(JV,KV)/(VAPOR(JV,KV)+
      1SVFLC(JV,KV))
10   IF (KELFRD(J,K)) 16,16,11
11   JV=JELFRD(J,K)
      KV=KELFRD(J,K)
      IF (JV=1) 12,12,14
12   IF (QUID(JV,KV)) 16,16,13
13   FD(J)=FD(J)+GENLX(I,JV,KV)*QUID(JV,KV)/(QUID(JV,KV)+SLFLO(JV,KV))
      GO TO 16
14   IF (QUITOP(KV)) 16,16,15
15   FD(J)=FD(J)+GENLX(I,JV,KV)*QUITOP(KV)/(QUITOP(KV)+QUID(JV,KV))
16 CONTINUE
    DO 29 NTIMES=1,5
      J=1
      JDELTA=1

```

```

      KTIMES=2*JT-1
      DO 29 KCOUNT=1,KTIMES
      CIN=FD(J)
      IF (J-1) 17,19,17
17  IF (VAPOR(J-1,K)) 19,19,18
18  CIN=CIN+GENVY(I,J-1,K)*VAPOR(J-1,K)/(VAPOR(J-1,K)+SVFLO(J-1,K))
19  IF (J-JT) 20,24,20
20  IF (QUID(J+1,K)) 24,24,21
21  IF (J-(JT-1)) 23,22,23
22  CIN=CIN+GENLX(I,J+1,K)*QUID(J+1,K)/(QUID(J+1,K)+QUITOP(K)+
      ISLFLO(J+1,K))
      GO TO 24
23  CIN=CIN+GENLX(I,J+1,K)*QUID(J+1,K)/(QUID(J+1,K)+SLFLC(J+1,K))
24  IF (GENLX(I,J,K)+GENVY(I,J,K)) 26,26,25
25  GENLXN=CIN*GENLX(I,J,K)/(GENLX(I,J,K)+GENVY(I,J,K))
      GENVYN=CIN*GENVY(I,J,K)/(GENLX(I,J,K)+GENVY(I,J,K))
      GENLX(I,J,K)=GENLXN+1.0E-20
      GENVY(I,J,K)=GENVYN+1.0E-20
26  IF (J-JT) 28,27,28
27  JDELTA=-1
28  J=J+JDELTA
29  CONTINUE
30  CONTINUE
      RETURN
      END

```

```

C PROGRAM GENVL      SUBROUTINE FOR BUBBLE POINT CALCULATION
C
C
      SUBROUTINE BUOPI (I)
      DIMENSION A(20,5),H(20,5),C(20,5),NSTGS(5),ENTHK(20),ENTHL(20),
      1ENTHU(20),ENTHW(20),EXTFCH(20,40,5),LXTFCH(40,5),SVFLC(40,5),
      2SLFLO(40,5),JSVFRD(40,5),KSVFRD(40,5),JSVTD(40,5),KSVTD(40,5),
      3JSLFRD(40,5),KSLFRD(40,5),JSLTD(40,5),KSLTD(40,5),JEVFRD(40,5),
      4KEVFRD(40,5),JEVTD(40,5),KEVTD(40,5),JELFRD(40,5),KELFRD(40,5),
      5JELTD(40,5),KELTD(40,5),JRETYD(5),JRETYD(5),JCCUTD(40,5),
      6TCDL(40,5),TEMP(40,5),VAPOR(40,5),QUID(40,5),QUITOP(5),TCSET(5),
      7FIXRV(5),FIXRL(5),FIXRE(5),FIXTV(5),FIXTL(5),FIXTVL(5),
      8FIXSV(40,5),FIXSL(40,5),QUIMCH(40,5),VAPMCH(40,5),GENLX(20,40,5),
      9GENVY(20,40,5),KMODE(40,5),FLFELD(20),FLVAP(20),FLLI(20)
      DIMENSION SUMFD(20),FLVAP1(20),FLLI1(20),QUNBAL(40,5),
      1COOLLD(40,5),REBLD(5),CCNCLC(5),PKDSUM(20),RFSUM(20),CUNBAL(20),
      2QUIDX(20),VAPY(20),LOK(20),FD(40)
      COMMON A,H,C,NSTGS,ENTHK,ENTHL,ENTHU,ENTHW,EXTFCH,EXTFCH,SVFLC,
      1SLFLO,JSVFRD,KSVFRD,JSVTD,KSVTD,JSLFRD,KSLFRD,JSLTD,KSLTD,
      2JEVFRD,KEVFRD,JEVTD,KEVTD,JELFRD,KELFRD,JELTD,KELTD,JRETYD,
      3JCCUTD,JCCUTD,TCDL,TEMP,VAPOR,QUID,QUITOP,TCSET,FIXRV,
      4FIXRL,FIXRE,FIXTV,FIXTL,FIXSV,FIXSL,QUIMCH,VAPMCH,GENLX,
      5GENVY,KMODE,FLFELD,SUMFD,CUNBAL,COOLLD,REBLD,CCNCLD,PKDSUM,RFSUM,
      6CUNBAL,QUIDX,VAPY,ECK,FC,NCCMPS,K,BDFERR,FLFEES,KALIR,ACOLS,
      7PRDERR,ITERAT,CHECK,PRSERK,TMAX,TMIN
      EQUILKF(A,B,C,T)=EXP(A/(T+460.0))+B+C*(T+460.0)
      KTIMES=1
      TINT=10.0
      1 SUMY=C.0
      DO 2 I=1,NCCMPS
      2 SUMY=SUMY+QUIDX(I)*EQUILKF(A(I,K),B(I,K),C(I,K),T)
      IF (ABS(SUMY-1.0)-BDFERR) 9,9,3
      3 KTIMES=KTIMES+1
      IF (KTIMES) 7,4,4
      4 SUMY0=SUMY
      TC=T
      IF (SUMY-1.0) 5,5,6
      5 T=T+TINT
      IF (T-TMAX) 1,10,10
      6 T=T-TINT
      IF (T-TMIN) 11,11,1
      7 IF ((SUMY0-1.0)*(SUMY-1.0)) 8,4,4
      8 SLOPE=(SUMY-SUMY0)/(T-TC)
      SUMY0=SUMY
      TC=T
      T=((1.0-SUMY)/SLOPE)+T
      TINT=TINT/10.0
      GO TO 1
      9 RETURN
      10 T=TMAX
      RETURN
      11 T=TMIN
      RETURN
      END

```

```

C PROGRAM GENVL      SUBROUTINE FOR DEW POINT CALCULATION
C
C
      SUBROUTINE DEWPT (T)
      DIMENSION A(20,5),B(20,5),C(20,5),NSTGS(5),ENTHK(20),ENTHL(20),
      1ENTHU(20),ENTHW(20),EXTFD(20,40,5),EXTFDH(40,5),SVFLO(40,5),
      2SLFLO(40,5),JSVFRO(40,5),KSVFRO(40,5),JSVTO(40,5),KSVTO(40,5),
      3JSLFRO(40,5),KSLFRO(40,5),JSLTO(40,5),KSLTO(40,5),JEVFRC(40,5),
      4KEVFRO(40,5),JEVTO(40,5),KEVTO(40,5),JELFRO(40,5),KELFRO(40,5),
      5JELTO(40,5),KELTO(40,5),JRETYP(5),JCOTYP(5),JCOOL(40,5),
      6TCOOL(40,5),TEMP(40,5),VAPOR(40,5),QUID(40,5),QUITOP(5),TCSET(5),
      7FIXRV(5),FIXBL(5),FIXRE(5),FIXTV(5),FIXTL(5),FIXTVL(5),
      8FIXSV(40,5),FIXSL(40,5),QUIMOH(40,5),VAPMOH(40,5),GENLX(20,40,5),
      9GENVY(20,40,5),KMODE(40,5),FLFEED(20),FLVAP(20),FLLIQ(20)
      DIMENSION SUMFD(20),FLVAP1(20),FLLIQ1(20),QUNBAL(40,5),
      1COOLLD(40,5),REBLD(5),CCNDLD(5),PRDSUM(20),RFSUM(20),CUNBAL(20),
      2QUIDX(20),VAPY(20),EQK(20),FD(40)
      COMMON A,B,C,NSTGS,ENTHK,ENTHL,ENTHU,ENTHW,EXTFD,EXTFDH,SVFLO,
      1SLFLO,JSVFRO,KSVFRO,JSVTO,KSVTO,JSLFRO,KSLFRO,JSLTO,KSLTO,
      2JEVFRO,KEVFRO,JEVTO,KEVTO,JELFRO,KELFRO,JELTO,KELTO,JRETYP,
      3JCOTYP,JCOOL,TCOOL,TEMP,VAPOR,QUID,QUITOP,TCSET,FIXRV,
      4FIXBL,FIXRE,FIXTV,FIXTL,FIXTVL,FIXSV,FIXSL,QUIMOH,VAPMOH,GENLX,
      5GENVY,KMODE,FLFEED,SUMFD,QUNBAL,COOLLD,REBLD,CONDLD,PRDSUM,RFSUM,
      6CUNBAL,QUIDX,VAPY,EQK,FD,NCOMPS,K,BDFERR,FLFEES,KALTER,NCOLS,
      7PRDERR,ITERAT,CHECK,PRSERK,TMAX,TMIN
      EQUIPKF(A,B,C,T)=EXP(A/(T+460.0)+B+C*(T+460.0))
      KTIMES=1
      TINT=10.0
      1 SUMX=0.0
      DO 2 I=1,NCOMPS
      2 SUMX=SUMX+VAPY(I)/EQUIPKF(A(I,K),B(I,K),C(I,K),T)
      IF (ABSF(SUMX-1.0)-BDFERR) 9,9,3
      3 KTIMES=KTIMES-1
      IF (KTIMES) 7,4,4
      4 SUMXD=SUMX
      TO=T
      IF (SUMX-1.0) 5,5,6
      5 T=T-TINT
      IF (T-TMIN) 10,10,1
      6 T=T+TINT
      IF (T-TMAX) 11,11,11
      7 IF ((SUMXD-1.0)*(SUMX-1.0)) 8,4,4
      8 SLOPE=(SUMX-SUMXD)/(T-TC)
      SUMXD=SUMX
      TO=T
      T=((1.0-SUMX)/SLOPE)+T
      TINT=TINT/10.0
      GO TO 1
      9 RETURN
      10 T=TMIN
      RETURN
      11 T=TMAX
      RETURN
      END

```

C PROGRAM GENVL SUBROUTINE FOR FLASH TEMPERATURE CALCULATION
C
C

```

SUBROUTINE ISOVFL (FLVAP,FLLIQ,FLV,FLL,T)
  DIMENSION A(20,5),B(20,5),C(20,5),NSTGS(5),ENTHK(20),ENTHL(20),
  1ENTHU(20),ENTHW(20),EXTFD(20,40,5),EXTFDH(40,5),SVFLO(40,5),
  2SLFLO(40,5),JSVFRO(40,5),KSVFRO(40,5),JSVTO(40,5),KSVTO(40,5),
  3JSLFRO(40,5),KSLFRO(40,5),JSLTO(40,5),KSLTO(40,5),JEVFRC(40,5),
  4KEVFRO(40,5),JEVTO(40,5),KEVTO(40,5),JELFRO(40,5),KELFRO(40,5),
  5JELTO(40,5),KELTO(40,5),JRETYP(5),JCOTYP(5),JCOOL(40,5),
  6TCOOL(40,5),TEMP(40,5),VAPOR(40,5),QUID(40,5),QUITOP(5),TCSET(5),
  7FIXRV(5),FIXBL(5),FIXRE(5),FIXTV(5),FIXTL(5),FIXTVL(5),
  8FIXSV(40,5),FIXSL(40,5),QUIMOH(40,5),VAPMOH(40,5),GENLX(20,40,5),
  9GENVY(20,40,5),KMODE(40,5),FLFEED(20),FLVAP(20),FLLIQ(20)
  DIMENSION SUMFD(20),FLVAP1(20),FLLIQ1(20),QUNBAL(40,5),
  1COOLLD(40,5),REBLD(5),CONDLD(5),PRDSUM(20),RFSUM(20),CUNBAL(20),
  2QUIDX(20),VAPY(20),EQK(20),FD(40)
  COMMON A,B,C,NSTGS,ENTHK,ENTHL,ENTHU,ENTHW,EXTFD,EXTFDH,SVFLO,
  1SLFLO,JSVFRO,KSVFRO,JSVTO,KSVTO,JSLFRO,KSLFRO,JSLTO,KSLTO,
  2JEVFRO,KEVFRO,JEVTO,KEVTO,JELFRO,KELFRO,JELTO,KELTO,JRETYP,
  3JCOTYP,JCOOL,TCOOL,TEMP,VAPOR,QUID,QUITOP,TCSET,FIXRV,
  4FIXBL,FIXRE,FIXTV,FIXTL,FIXSV,FIXSL,QUIMOH,VAPMOH,GENLX,
  5GENVY,KMODE,FLFEED,SUMFC,QUNBAL,COOLLD,REBLD,CONDLD,PRDSUM,RFSUM,
  6CUNBAL,QUIDX,VAPY,EQK,FD,NCOMPS,K,BDFERR,FLFEES,KALTER,NCOLS,
  7PRDERR,ITERAT,CHECK,PRSEERR,TMAX,TMIN
  EQUILKF(A,B,C,T)=EXP(A/(T+460.0))+B+C*(T+460.0)
  KTIMES=1
  TINT=10.0
1  FLVAS=0.0
  FLLIS=0.0
  DO 2 I=1,NCOMPS
    EQK=EQUILKF(A(I,K),B(I,K),C(I,K),T)
    FLVAP(I)=FLFEED(I)/(FLL/FLV/EQK+1.0)
    FLLIQ(I)=FLFEED(I)/(FLV*EQK/FLL+1.0)
    FLVAS=FLVAS+FLVAP(I)
2  FLLIS=FLLIS+FLLIQ(I)
  IF (ABSF(FLVAS/FLV-1.0)-BDFERR) 3,3,4
3  IF (ABSF(FLLIS/FLL-1.0)-BDFERR) 15,15,4
4  KTIMES=KTIMES-1
  IF (KTIMES) 10,5,5
5  FLVASO=FLVAS
  FLLISO=FLLIS
  TO=T
  IF (FLV-FLL) 6,6,7
6  IF (FLVAS/FLV-1.0) 8,8,9
7  IF (FLLIS/FLL-1.0) 9,9,8
8  T=T+TINT
  IF (T-TMAX) 1,1,16
9  T=T-TINT
  IF (T-TMIN) 17,1,1
10 IF (FLV-FLL) 11,11,13
11 IF ((FLVASO/FLV-1.0)*(FLVAS/FLV-1.0)) 12,5,5
12 SLOPE=(FLVAS/FLV-FLVASO/FLV)/(T-TO)
  FLVASO=FLVAS
  FLLISO=FLLIS
  TO=T
  T=((1.0-FLVAS/FLV)/SLOPE)+T
  TINT=TINT/10.0
  GO TO 1
13 IF ((FLLISO/FLL-1.0)*(FLLIS/FLL-1.0)) 14,5,5
14 SLOPE=(FLLIS/FLL-FLLISO/FLL)/(T-TO)

```



```

      FLVASO=FLVAS
      FLLISO=FLLIS
      TO=T
      T=((1.0-FLLIS/FLL)/SLOPE)+T
      TINT=TINT/10.0
      GO TO 1
15  RETURN
16  T=TMAX
      GO TO 18
17  T=TMIN
18  FLVAS=0.0
      FLLIS=0.0
      DO 19 I=1,NCOMPS
        EQK=EQUILKF(A(I,K),B(I,K),C(I,K),T)
        FLVAP(I)=FLFEED(I)/(FLL/FLV/EQK+1.0)
        FLLIQ(I)=FLFEED(I)/(FLV*EQK/FLL+1.0)
        FLVAS=FLVAS+FLVAP(I)
19  FLLIS=FLLIS+FLLIQ(I)
      FLV=FLVAS
      FLL=FLLIS
      RETURN
      END

```

```

C PROGRAM GENVL      SUBROUTINE FOR ISOTHERMAL FLASH CALCULATION
C
C
      SUBROUTINE ISOTFL (FLVAP,FLLIQ,FLV,FLL,T)
      DIMENSION A(20,5),B(20,5),C(20,5),NSTGS(5),ENTHK(20),ENTHL(20),
      1ENTHU(20),ENTHW(20),EXTFD(20,40,5),EXTFDH(40,5),SVFLO(40,5),
      2SLFLO(40,5),JSVFRO(40,5),KSVFRO(40,5),JSVTO(40,5),KSVTO(40,5),
      3JSLFRO(40,5),KSLFRO(40,5),JSLTO(40,5),KSLTO(40,5),JEVFRO(40,5),
      4KEVFRO(40,5),JEVTO(40,5),KEVTO(40,5),JELFRO(40,5),KELFRO(40,5),
      5JELTO(40,5),KELTO(40,5),JRETY(5),JCOTYP(5),JCOOL(40,5),
      6TCOOL(40,5),TEMP(40,5),VAPOR(40,5),QUID(40,5),QUITOP(5),TCSET(5),
      7FIXRV(5),FIXBL(5),FIXRE(5),FIXTV(5),FIXTL(5),FIXTVL(5),
      8FIXSV(40,5),FIXSL(40,5),QUIMOH(40,5),VAPMOH(40,5),GENLX(20,40,5),
      9GENVY(20,40,5),KMODE(40,5),FLFEED(20),FLVAP(20),FLLIQ(20)
      DIMENSION SUMFD(20),FLVAP1(20),FLLIQ1(20),QUNBAL(40,5),
      1COOLLD(40,5),REBLD(5),CONDLD(5),PRDSUM(20),RFSUM(20),CUNBAL(20),
      2QUIDX(20),VAPY(20),EQK(20),FD(40)
      COMMON A,B,C,NSTGS,ENTHK,ENTHL,ENTHU,ENTHW,EXTFD,EXTFDH,SVFLO,
      1SLFLO,JSVFRO,KSVFRO,JSVTO,KSVTO,JSLFRO,KSLFRO,JSLTO,KSLTO,
      2JEVFRO,KEVFRO,JEVTO,KEVTO,JELFRO,KELFRO,JELTO,KELTO,JRETY,
      3JCOTYP,JCOOL,TCOOL,TEMP,VAPOR,QUID,QUITOP,TCSET,FIXRV,
      4FIXBL,FIXRE,FIXTV,FIXTL,FIXSV,FIXSL,QUIMOH,VAPMOH,GENLX,
      5GENVY,KMODE,FLFEED,SUMFD,QUNBAL,COOLLD,REBLD,CONDLD,PRDSUM,RFSUM,
      6CUNBAL,QUIDX,VAPY,EQK,FD,NCOMPS,K,BDFERR,FLFEES,KALTER,NCOLS,
      7PRDERR,ITERAT,CHECK,PRSEERR,TMAX,TMIN
      EQUILKF(A,B,C,T)=EXPFA/(T+460.0)+B+C*(T+460.0)
      KTIMES=1
      FLINT=.1
      DO 1 I=1,NCOMPS
      1 EQK(I)=EQUILKF(A(I,K),B(I,K),C(I,K),T)
      2 FLVAS=0.0
      FLLIS=0.0
      DO 4 I=1,NCOMPS
      FLVAP(I)=FLFEED(I)/(FLL/FLV/EQK(I)+1.0)
      FLLIQ(I)=FLFEED(I)/(FLV*EQK(I)/FLL+1.0)
      FLVAS=FLVAS+FLVAP(I)
      4 FLLIS=FLLIS+FLLIQ(I)
      IF (ABSF(FLVAS/FLV-1.0)-BDFERR) 5,5,6
      5 IF (ABSF(FLLIS/FLL-1.0)-BDFERR) 23,23,6
      6 IF (FLVAS/FLFEES-1.0E-6) 24,24,7
      7 IF (FLLIS/FLFEES-1.0E-6) 26,26,8
      8 KTIMES=KTIMES-1
      IF (KTIMES) 18,9,9
      9 FLVASO=FLVAS
      FLLISO=FLLIS
      FLVO=FLV
      FLLD=FLL
      IF (FLV-FLL) 10,10,14
      10 IF (FLVAS-FLV) 11,12,12
      11 FLV=FLV*(1.0-FLINT)
      GO TO 13
      12 FLV=FLV*(1.0+FLINT)
      13 FLL=FLFEES-FLV
      GO TO 2
      14 IF (FLLIS-FLL) 15,16,16
      15 FLL=FLL*(1.0-FLINT)
      GO TO 17
      16 FLL=FLL*(1.0+FLINT)
      17 FLV=FLFEES-FLL
      GO TO 2
      18 IF (FLV-FLL) 19,19,21

```

```

19 IF ((FLVASO-FLVO)*(FLVAS-FLV)) 20,9,9
20 SLOPE=(FLVAS/FLV-FLVASO/FLVO)/(FLV-FLVO)
   FLVASO=FLVAS
   FLLISO=FLLIS
   FLVO=FLV
   FLLO=FLL
   FLV=((1.0-FLVAS/FLV)/SLOPE)+FLV
   FLL=FLFEES-FLV
   FLINT=FLINT/10.0
   GO TO 2
21 IF ((FLLISO-FLLU)*(FLLIS-FLL)) 22,9,9
22 SLOPE=(FLLIS/FLL-FLLISO/FLLU)/(FLL-FLLU)
   FLLISO=FLLIS
   FLVASO=FLVAS
   FLLO=FLL
   FLVO=FLV
   FLL=((1.0-FLLIS/FLL)/SLOPE)+FLL
   FLV=FLFEES-FLL
   FLINT=FLINT/10.0
   GO TO 2
23 RETURN
24 DO 25 I=1,NCOMPS
   FLVAP(I)=0.0
25 FLLIQ(I)=FLFEED(I)
   FLV=0.0
   FLL=FLFEES
   RETURN
26 DO 27 I=1,NCOMPS
   FLLIQ(I)=0.0
27 FLVAP(I)=FLFEED(I)
   FLL=0.0
   FLV=FLFEES
   RETURN
END

```

EXAMPLE 1 REBOILED ABSORBER (7 COMPONENTS - 9 STAGES)
 BOTTOM PRODUCT SET INTERCOOLER ABOVE FEED PLATE

INPUT DATA

NO. OF COMPONENTS 7 NO. OF COLUMNS 1

***** COLUMN 1 *****

NUMBER OF STAGES = 9

EXTERNAL FEED OF 0.64729998E 03 MOLES TO STAGE 3 OF COLUMN 1

COMPONENT AMOUNTS

0.24550000E 03 0.31599999E 02 0.22179999E 03 0.13140000E 03 0.75000000E 01
 0.20999999E 01 0.73999999E 01
 ENTHALPY OF FEED = 0.36067279E 07

EXTERNAL FEED OF 0.10550000E 04 MOLES TO STAGE 9 OF COLUMN 1

COMPONENT AMOUNTS

-0. -0. -0. -0. -0.
 -0. 0.10550000E 04
 ENTHALPY OF FEED = 0.53309149E 07

REBOILER, FIXED LIQUID FLOW = 0.14200000E 04

NO CONDENSER

INTERCOOLER BETWEEN STAGE 4 AND STAGE 5 COOLING LIQUID FLOW TO STAGE 4 TO TEMPERATURE OF 0.20000000E 01

EQUILIBRIUM CONSTANTS A

-0.
 -0.22610600E 03
 -0.27829800E 04
 -0.19952100E 04
 -0.42899700E 04
 -0.60171299E 04
 -0.59302899E 04

EQUILIBRIUM CONSTANTS B

0.50000000E 01
 0.11134600E 01
 0.77318999E 01
 0.46058199E 01
 0.94739398E 01
 0.13181700E 02
 0.63820399E 01

EQUILIBRIUM CONSTANTS C

-0.
 0.28649999E-02
 -0.33409999E-02
 -0.68600000E-03
 -0.40799999E-02
 -0.71220000E-02
 -0.14200000E-03

TEMPERATURES

0.22499999E 03 0.20312500E 03 0.18125000E 03 0.15937500E 03 0.13750000E 03
 0.11562499E 03 0.93750000E 02 0.71875000E 02 0.50000000E 02

***** ALL COLUMNS *****

ENTHALPY CONSTANTS K

0.67999999E 01
 0.15200000E 02
 0.16800000E 02
 0.17299999E 02
 0.23000000E 02
 0.30700000E 02
 0.36399999E 02

ENTHALPY CONSTANTS L

0.13100000E 04
 0.29899999E 04
 0.32500000E 04
 0.33300000E 04
 0.43300000E 04
 0.57399999E 04
 0.49800000E 04

ENTHALPY CONSTANTS U

0.67999999E 01
 0.90000000E 01
 0.13500000E 02
 0.16500000E 02
 0.22600000E 02
 0.30199999E 02
 0.23899999E 02

ENTHALPY CONSTANTS W

0.13600000E 04
 0.45999999E 04
 0.70200000E 04
 0.78699999E 04
 0.93600000E 04
 0.12500000E 03
 0.18660000E 03

PRODUCT ERROR LIMIT

0.20000000E 01

BUBBLE DEW FLASH ERROR LIMIT

0.99999999E-06

ITERATION NO. = 80

***** COLUMN 1 *****
VAPOR AND LIQUID PRODUCT AMOUNTS AND INTERCONNECTING FLOWS

BOTTOM PRODUCT OF 0.14200000E 04 MOLES					
COMPONENT AMOUNTS					
0.12847170E-02	0.51427767E 00	0.21751072E 03	0.13058984E 03	0.74867361E 01	
0.20979225E 01	0.10617995E 04				
COMPONENT RECOVERY FRACTIONS					
0.52330633E-05	0.16274609E-01	0.98066148E 00	0.99383446E 00	0.99823148E 00	
0.99901071E 00	0.99943475E 00				
VAPOR TOP PRODUCT OF 0.28031856E 03 MOLES					
COMPONENT AMOUNTS					
0.24546584E 03	0.31070086E 02	0.29914765E 01	0.36706624E-00	0.42377779E-06	
0.94971218E-11	0.42409919E-00				
COMPONENT RECOVERY FRACTIONS					
0.99986084E 00	0.98323057E 00	0.13487270E-01	0.27935026E-02	0.56503705E-07	
0.45224389E-11	0.39918975E-03				

STAGE VARIABLES

STAGE	TEMPERATURE	VAPOR FLOW	LIQUID FLOW	VAP MOL ENTH	LIQ MOL ENTH	HEAT UNBALANCE
1	0.22331616E 03	0.63440771E 03	0.14200000E 04	0.11482784E 05	0.11606853E 05	0.
2	0.89738540E 02	0.50123933E 03	0.20544077E 04	0.85517238E 04	0.66681604E 04	0.24349750E 05
3	0.48761774E 02	0.10327732E 04	0.19239867E 04	0.63513061E 04	0.55756069E 04	-0.29623750E 04
4	0.32829596E 02	0.73153252E 03	0.18073594E 04	0.54444105E 04	0.51945792E 04	-0.44146875E 04
5	0.44966235E 02	0.56703161E 03	0.15056229E 04	0.48746716E 04	0.58331919E 04	0.61003750E 04
6	0.32306398E 02	0.43137398E 03	0.13413865E 04	0.37754188E 04	0.56434273E 04	0.50043750E 04
7	0.17378777E 02	0.35320637E 03	0.12059206E 04	0.27915682E 04	0.53399421E 04	0.24708749E 04
8	0.82386826E 01	0.31502271E 03	0.11278766E 04	0.22099546E 04	0.51418741E 04	0.61650000E 03
9	0.41170742E 01	0.28031856E 03	0.10877099E 04	0.18436698E 04	0.50565770E 04	0.83937500E 02

REBOILER LOAD = 0.10067378E 08

INTERCOOLER BETWEEN STAGE 4 AND STAGE 5 COOLING LIQUID FLOW TO STAGE 4 TO TEMPERATURE OF 0.20000000E 01

INTERCOOLER LOAD = 0.19752259E 07

TOTAL COLUMN HEAT UNBALANCE = 0.31248750E 05

TOTAL PRODUCT MASS BALANCES AND RECOVERY FRACTIONS

RECOVERY FRACTION SUMMATIONS FOR EACH COMPONENT			
0.99986607E 00	0.99950517E 00	0.99414875E 00	0.99662795E 00
0.99901071E 00	0.99983393E 00		0.99823154E 00
EXCESS MOLES OF EACH COMPONENT ENTERING THE SYSTEM IN FEEDS OVER MOLES LEAVING IN PRODUCTS			
0.32878876E-01	0.15636444E-01	0.12978058E 01	0.44308662E-00
0.20774901E-02	0.17642212E-00		0.13263464E-01
TOTAL MASS UNBALANCE (SUM OF ABSOLUTE VALUES OF COMPONENT UNBALANCES) = 0.19811708E 01			

EXAMPLE 1A REBOILED ABSORBER (7 COMPONENTS - 9 STAGES)
 REBOILER VAPOR SET INTERCOOLER ABOVE FEED PLATE

INPUT DATA

NO. OF COMPONENTS 7 NO. OF COLUMNS 1

***** COLUMN 1 *****

NUMBER OF STAGES = 9

EXTERNAL FEED OF 0.64729998E 03 MOLES TO STAGE 3 OF COLUMN 1
 COMPONENT AMOUNTS
 0.24550000E 03 0.31599999E 02 0.22179999E 03 0.13140000E 03 0.75000000E 01
 0.20999999E 01 0.73999999E 01
 ENTHALPY OF FEED = 0.36067279E 07

EXTERNAL FEED OF 0.10550000E 04 MOLES TO STAGE 9 OF COLUMN 1
 COMPONENT AMOUNTS
 -0. -0. -0. -0. -0.
 -0. 0.10550000E 04
 ENTHALPY OF FEED = 0.53309149E 07

REBOILER, FIXED REBOILER VAPOR = 0.63440770E 03

NO CONDENSER

INTERCOOLER BETWEEN STAGE 4 AND STAGE 5 COOLING LIQUID FLOW TO STAGE 4 TO TEMPERATURE OF 0.20000000E 01

EQUILIBRIUM CONSTANTS A EQUILIBRIUM CONSTANTS B EQUILIBRIUM CONSTANTS C

-0. 0.50000000E 01 -0.
 -0.22610600E 03 0.11134600E 01 0.28649999E-02
 -0.27829800E 04 0.77318999E 01 -0.33409999E-02
 -0.19952100E 04 0.46058199E 01 -0.68600000E-03
 -0.42899700E 04 0.94739398E 01 -0.40799999E-02
 -0.60171299E 04 0.13181700E 02 -0.71320000E-02
 -0.59302899E 04 0.63820399E 01 -0.14200000E-03

TEMPERATURES
 0.22499999E 03 0.19812500E 03 0.17124999E 03 0.14437500E 03 0.11750000E 03
 0.90625000E 02 0.63750000E 02 0.36875000E 02 0.09999999E 02

***** ALL COLUMNS *****

ENTHALPY CONSTANTS K ENTHALPY CONSTANTS L ENTHALPY CONSTANTS U ENTHALPY CONSTANTS W

0.67999999E 01 0.13100000E 04 0.67999999E 01 0.13600000E 04
 0.15200000E 02 0.29899999E 04 0.90000000E 01 0.45999999E 04
 0.16800000E 02 0.32500000E 04 0.13500000E 02 0.70200000E 04
 0.17299999E 02 0.33300000E 04 0.16500000E 02 0.78699999E 04
 0.23000000E 02 0.43300000E 04 0.22400000E 02 0.93600000E 04
 0.30700000E 02 0.57399999E 04 0.30199999E 02 0.12500000E 05
 0.36399999E 02 0.44980000E 04 0.23899999E 02 0.18660000E 05

PRODUCT ERROR LIMIT 0.20000000E 01 BUBBLE DEW FLASH ERROR LIMIT 0.99999999E-06

ITERATION NO. = 22

***** COLUMN 1 *****

VAPOR AND LIQUID PRODUCT AMOUNTS AND INTERCONNECTING FLOWS

BOTTOM PRODUCT OF 0.14215221E 04 MOLES

COMPONENT AMOUNTS

0.12728422E-02 0.51080858E 00 0.21771807E 03 0.13135239E 03 0.75225109E 01

0.21025914E 01 0.10623144E 04

COMPONENT RECOVERY FRACTIONS

0.51848936E-05 0.16164828E-01 0.98159638E 00 0.99963773E 00 0.10030014E 01

0.10012340E 01 0.99991951E 00

VAPOR TOP PRODUCT OF 0.28054288E 03 MOLES

COMPONENT AMOUNTS

0.24549218E 03 0.31164028E 02 0.30807643E 01 0.38107616E-00 0.45293911E-06

0.10363089E-10 0.42483938E-00

COMPONENT RECOVERY FRACTIONS

0.49996813E 00 0.98620344E 00 0.13889830E-01 0.29001229E-02 0.60391881E-07

0.49348043E-11 0.39988647E-03

STAGE VARIABLES

STAGE	TEMPERATURE	VAPOR FLOW	LIQUID FLOW	VAP. MOL ENTH	LIQ. MOL ENTH	HEAT UNBALANCE
1	0.22294358E 03	0.63440770E 03	0.14215221E 04	0.11473969E 05	0.11592564E 05	0.
2	0.89724497E 02	0.50530794E 03	0.20559299E 04	0.85535868E 04	0.66669865E 04	-0.10387000E 05
3	0.48772026E 02	0.10377322E 04	0.19268301E 04	0.63599119E 04	0.55736573E 04	-0.18418749E 04
4	0.32883620E 02	0.73531319E 03	0.18118002E 04	0.54576842E 04	0.51929630E 04	-0.23796874E 04
5	0.45480654E 02	0.57177944E 03	0.15092070E 04	0.49060863E 04	0.58448264E 04	0.54350000E 03
6	0.32929513E 02	0.43471207E 03	0.13457421E 04	0.38111437E 04	0.56576134E 04	0.21628749E 04
7	0.17795375E 02	0.35476288E 03	0.12089275E 04	0.28143570E 04	0.53497027E 04	0.15082499E 04
8	0.84111117E 01	0.31563499E 03	0.11291541E 04	0.22196526E 04	0.51459672E 04	0.51875000E 03
9	0.41641755E 01	0.28054288E 03	0.10900842E 04	0.18469136E 04	0.50576640E 04	0.96937500E 02

REBOILER LOAD = 0.10051404E 08

INTERCOOLER BETWEEN STAGE 4 AND STAGE 5 COOLING LIQUID FLOW TO STAGE 4 TO TEMPERATURE OF 0.20000000E 01

INTERCOOLER LOAD = 0.20015999E 07

TOTAL COLUMN HEAT UNBALANCE = -0.97782499E 04

TOTAL PRODUCT MASS BALANCES AND RECOVERY FRACTIONS

RECOVERY FRACTION SUMMATIONS FOR EACH COMPONENT

0.99997732E 00 0.10023683E 01 0.99548620E 00 0.10025378E 01 0.10030015E 01

0.10012340E 01 0.10003193E 01

EXCESS MOLES OF EACH COMPONENT ENTERING THE SYSTEM IN FEEDS OVER MOLES LEAVING IN PRODUCTS

0.65498352E-02 -0.74837208E-01 0.10011596E 01 -0.33347321E-00 -0.22511303E-01

-0.25914609E-02 -0.33932495E-00

TOTAL MASS UNBALANCE (SUM OF ABSOLUTE VALUES OF COMPONENT UNBALANCES) = 0.17804476E 01

EXAMPLE 2 DISTILLATION COLUMN WITH SIDE STRIPPER (5 COMPONENTS -
13 STAGES AND 5 STAGES) REFLUX AND STRIPPER PRODUCT SET

INPUT DATA

NO. OF COMPONENTS 5 NO. OF COLUMNS 2

***** COLUMN 1 *****

NUMBER OF STAGES = 13

EXTERNAL FEED OF 0.16352999E 04 MOLES TO STAGE 6 OF COLUMN 1

COMPONENT AMOUNTS

0.14200000E 02 0.27119999E 03 0.94679999E 03 0.25830000E 03 0.14479999E 03
ENTHALPY OF FEED = 0.36340000E 08

REBOILER, FIXED REBOILER VAPOR = 0.12000000E 04

PARTIAL CONDENSER, FIXED REFLUX = 0.25000000E 04

FIXED SIDE LIQUID STREAM OF 0.12100000E 04 MOLES FROM STAGE 9 OF COLUMN 1 TO STAGE 5 OF COLUMN 2

EQUILIBRIUM CONSTANTS A EQUILIBRIUM CONSTANTS B EQUILIBRIUM CONSTANTS C

-0.68535999E 04 0.15499999E 02 -0.54880000E-02
-0.67535000E 04 0.13890000E 02 -0.43284999E-02
-0.73860999E 04 0.11089999E 02 -0.19069999E-02
-0.10974800E 05 0.10800000E 02 -0.68499999E-03
-0.12060200E 05 0.98399999E 01 -0.23199999E-03

TEMPERATURES

0.59999999E 03 0.56500000E 03 0.52999999E 03 0.49500000E 03 0.45999999E 03
0.42500000E 03 0.38999999E 03 0.35500000E 03 0.31999999E 03 0.28500000E 03
0.25000000E 03 0.21500000E 03 0.18000000E 03

***** COLUMN 2 *****

NUMBER OF STAGES = 5

REBOILER, FIXED LIQUID FLOW = 0.94499999E 03

NO CONDENSER

INTERCONNECTING VAPOR STREAM FROM END STAGE 5 OF COLUMN 2 TO STAGE 10 OF COLUMN 1

EQUILIBRIUM CONSTANTS A EQUILIBRIUM CONSTANTS B EQUILIBRIUM CONSTANTS C

-0.68535999E 04 0.15499999E 02 -0.54880000E-02
-0.67535000E 04 0.13890000E 02 -0.43284999E-02
-0.73860999E 04 0.11089999E 02 -0.19069999E-02
-0.10974800E 05 0.10800000E 02 -0.68499999E-03
-0.12060200E 05 0.98399999E 01 -0.23199999E-03

TEMPERATURES

0.40499999E 03 0.38999999E 03 0.37500000E 03 0.36000000E 03 0.34500000E 03

***** ALL COLUMNS *****

ENTHALPY CONSTANTS K ENTHALPY CONSTANTS L ENTHALPY CONSTANTS U ENTHALPY CONSTANTS W

0.45259999E 02 -0.39080000E 04 0.34069999E 02 0.58580000E 04
0.54780000E 02 -0.49500000E 04 0.42629999E 02 0.65239999E 04
0.72549999E 02 -0.65260000E 04 0.57799999E 02 0.11172000E 05
0.14719000E 03 -0.13603000E 05 0.12185000E 03 0.20993000E 05
0.20517000E 03 -0.19101000E 05 0.17581999E 03 0.24511000E 05

PRODUCT ERROR LIMIT
0.80000000E 01

BUBBLE DEW FLASH ERROR LIMIT
0.99999999E-06

ITERATION NO. = 22

***** COLUMN 1 *****

VAPOR AND LIQUID PRODUCT AMOUNTS AND INTERCONNECTING FLOWS

BOTTOM PRODUCT OF 0.40806741E 03 MOLES

COMPONENT AMOUNTS	0.23976675E-03	0.53277725E 01	0.25796781E 03	0.14477155E 03
0.72784330E-06				
COMPONENT RECOVERY FRACTIONS				
0.51256470E-07	0.88409570E-06	0.56271362E-02	0.99871397E 00	0.99980357E 00

VAPOR TOP PRODUCT OF 0.28289108E 03 MOLES

COMPONENT AMOUNTS	0.26514885E 03	0.29947919E 01	0.64033674E-15	0.11301813E-22
0.14747446E 02				
COMPONENT RECOVERY FRACTIONS				
0.10385525E 01	0.97768751E 00	0.31630670E-02	0.24790427E-17	0.78051198E-25

SIDE LIQUID FLOW OF 0.12100000E 04 MOLES FROM STAGE 9 TO STAGE 5 OF COLUMN 2

COMPONENT AMOUNTS	0.37101807E 02	0.11719964E 04	0.36346019E-02	0.44777169E-05
0.89806247E 00				

STAGE VARIABLES

STAGE	TEMPERATURE	VAPOR FLOW	LIQUID FLOW	VAP MOL ENTH	LIQ MOL ENTH	HEAT UNBALANCE
1	0.65426882E 03	0.12000000E 04	0.40806741E 03	0.97707521E 05	0.93661217E 05	0.
2	0.54708186E 03	0.95306121E 03	0.16080674E 04	0.58893517E 05	0.67773326E 05	0.12995999E 05
3	0.38596197E 03	0.15000437E 04	0.13611286E 04	0.34467977E 05	0.35174616E 05	-0.12577000E 05
4	0.33228021E 03	0.17942639E 04	0.19075555E 04	0.30473727E 05	0.22772047E 05	-0.14892000E 05
5	0.32449218E 03	0.17268858E 04	0.22011002E 04	0.29738995E 05	0.21079681E 05	-0.31690000E 04
6	0.31438836E 03	0.20167211E 04	0.21335466E 04	0.27974720E 05	0.20188574E 05	-0.22615000E 04
7	0.29607704E 03	0.21743074E 04	0.78796405E 03	0.26960980E 05	0.14965606E 05	-0.30989999E 04
8	0.29528861E 03	0.21729320E 04	0.94540089E 03	0.26894591E 05	0.14801671E 05	-0.96850000E 03
9	0.29320453E 03	0.21140827E 04	0.94399432E 03	0.26563940E 05	0.14630602E 05	-0.12672500E 04
10	0.28477720E 03	0.21972281E 04	0.20951114E 04	0.25277333E 05	0.13952105E 05	-0.65441874E 04
11	0.25036707E 03	0.21585907E 04	0.19131483E 04	0.20860287E 05	0.11202516E 05	-0.11085000E 05
12	0.18154863E 03	0.27834901E 04	0.18743356E 04	0.14924171E 05	0.58205923E 04	0.36532500E 04
13	0.14284064E 03	0.28289108E 03	0.25000000E 04	0.12586980E 05	0.29703437E 04	0.

REBOILER LOAD = 0.46485036E 08

CONDENSER LOAD = 0.30554680E 08

TOTAL COLUMN HEAT UNBALANCE = -0.39214187E 05

***** COLUMN 2 *****

VAPOR AND LIQUID PRODUCT AMOUNTS AND INTERCONNECTING FLOWS

BOTTOM PRODUCT OF 0.94499999E 03 MOLES

COMPONENT AMOUNTS

0.60219639E-02 0.28103220E 01 0.94218002E 03 0.36229840E-02 0.44758786E-05

COMPONENT RECOVERY FRACTIONS

0.42408196E-03 0.10362544E-01 0.99512043E 00 0.14024264E-04 0.30910743E-07

VAPOR FLOW OF 0.26496548E 03 MOLES FROM STAGE 5 TO STAGE 10 OF COLUMN 1

COMPONENT AMOUNTS

0.89181279E 00 0.34273197E 02 0.22980046E 03 0.11478066E-04 0.18155316E-08

STAGE VARIABLES

STAGE	TEMPERATURE	VAPOR FLOW	LIQUID FLOW	VAP MOL ENTH	LIQ MOL ENTH	HEAT UNBALANCE
1	0.30588578E 03	0.31462017E 03	0.94499999E 03	0.286911774E 05	0.15654559E 05	0.
2	0.30427870E 03	0.30439479E 03	0.12596202E 04	0.28411440E 05	0.15524354E 05	0.18442500E 04
3	0.30211191E 03	0.29208098E 03	0.12494582E 04	0.28038908E 05	0.15348986E 05	-0.66000000E 02
4	0.29941484E 03	0.27853895E 03	0.12371426E 04	0.27583475E 05	0.15130986E 05	-0.34249999E 03
5	0.29635713E 03	0.26496548E 03	0.12235915E 04	0.27077147E 05	0.14884286E 05	-0.69599999E 03

REBOILER LOAD = 0.42657795E 07

TOTAL COLUMN HEAT UNBALANCE = 0.73975000E 03

TOTAL PRODUCT MASS BALANCES AND RECOVERY FRACTIONS

RECOVERY FRACTION SUMMATIONS FOR EACH COMPONENT

0.10389767E 01 0.98805092E 00 0.10039106E 01 0.99872798E 00 0.99980360E 00

EXCESS MOLES OF EACH COMPONENT ENTERING THE SYSTEM IN FEEDS OVER MOLES LEAVING IN PRODUCTS

-0.55346906E 00 0.32405891E 01 -0.37025909E 01 0.32855988E-00 0.28438548E-01

TOTAL MASS UNBALANCE (SUM OF ABSOLUTE VALUES OF COMPONENT UNBALANCES) = 0.78536475E 01

REFERENCES

- A1. Amundson, N. R. and Pontinen, A. J., *Ind. Eng. Chem.* **50**, 730 (1958).
D1. Duffin, J. H., "Solution of Multistage Separation Problems by Using Digital Computers." Ph.D. Thesis, University of California, Berkeley, 1959.
E1. Edmister, W. C., *A.I.Ch.E. Journal* **3**, 165 (1957).
G1. Greenstadt, J., Brady, Y., and Morse, B., *Ind. Eng. Chem.* **50**, 1644 (1958).
H1. Hanson, D. N., Duffin, J. H., and Somerville, G. F., "Computation of Multistage Separation Processes," Reinhold, New York, 1962.
H2. Holland, C. D., "Multicomponent Distillation," Prentice-Hall, Englewood Cliffs, New Jersey, 1963.
L1. Lewis, W. K. and Matheson, G. L., *Ind. Eng. Chem.* **24**, 494 (1932).
L2. Lyster, W. N., Sullivan, S. L., Jr., Billingsley, D. S., and Holland, C. D., *Pet. Ref.*, **38**, No. 6, 221 (1959), *Pet. Ref.*, **38**, No. 7, 151 (1959). *Pet. Ref.* **38**, No. 10, 139 (1959).
R1. Robinson, C. S., and Gilliland, E. R., "Elements of Fractional Distillation," 4th Ed. McGraw-Hill, New York, 1950.
R2. Rose, A., Sweeney, R. F., and Schrodtt, V. N., *Ind. Eng. Chem.* **50**, 737 (1958).
S1. Smith, B. D., and Brinkley, W. K., *A.I.Ch.E. Journal* **6**, 451 (1960).
S2. Smith, B. D., "Design of Equilibrium Stage Processes." McGraw-Hill, New York, 1963.
S3. Sorel, "La rectification de l'alcool." Paris, 1893.
T1. Thiele, E. W., and Geddes, R. L., *Ind. Eng. Chem.* **24**, 289 (1933).
U1. Underwood, A. J. V., *Trans. Inst. Chem. Engr. (London)* **10**, 112 (1932).

AUTHOR INDEX

Numbers in parentheses are reference numbers, and are inserted to enable the reader to locate a reference when the authors' names are not cited in the text. Numbers in *italic* indicate the page on which the full reference is cited.

A

- Abou-Sabe, A. H., 208, 259, *275*
 Acton, F. S., 178, *192*
 Adams, H., 57 (B1), *92*
 Addoms, J. M., 259, *274*
 Adler, R. J., 160, *192*
 Aiba, S., 168, *192*
 Alberda, G., 120, 123, 157, *195*
 Alexander, A. E., 15, *47*
 Allen, C. M., 124, *192*
 Alves, G. E., 207, 208, 213 (A2), 223, *273*
 Amberkar, S., 59 (K2), 65, *92, 93*
 Ampilogov, I. E., 123, *192*
 Amundson, N. R., 118, 155, 158, 178, 182, 184, *192, 193, 196, 287, 356*
 Anderès, G., *49*
 Anderson, G. H., 213 (A2), 247, 249, 250 (A3), *273*
 Anderson, J. D., 249, 266 (A5), 267, *273*
 Anderson, R. P., *273*
 Andreas, J. M., 57 (A2), 58, *92*
 Andrew, S. P. S., 44 (95), *49*
 Aris, R., 111, 115, 116 (A8), 117, 135, 136, 137 (A6), 138, 139, 146, 147, 154, 155, 158, 161, 178, *192*
 Armand, A. A., 231, 243, *273*
 Askins, J. W., 170, *192*
 Aziz, K., 226, *274*

B

- Baars, G. M., 168, *196*
 Baba, A., 34 (61), *48*
 Badger, W. L., 168, *198*
 Baillie, R. C., 182, *194*
 Baird, M. H. I., 35 (67a), 41 (67a), *48, 266, 273*
 Baker, O., 208, 214, 223, 271 (B3, B4, B5), *273*
 Balaceanu, J. C., 178, *195*
- Baldwin, L. V., 132, *192*
 Banchero, J. T., 36 (75), 39 (77E), *48, 61* (E1), 62 (E1), 74 (E1), 75, 80 (E1), 82 (E1), 83, *93*
 Bankoff, S. G., 232, 242, *273*
 Barish, E. Z., 167, 168, *193*
 Barkelew, C. H., 135, 139, *198*
 Barker, P. E., 46 (100), *49*
 Baron, T., 135, 139, 143, 183, *192, 198*
 Bartok, W., 167, *192*
 Bashforth E. Q., 240, *274*
 Bashforth, F., 57 (B1), *92*
 Batchelor, G. K., 107 (B4), *192*
 Beek, W. J., 266, *273*
 Bell, D. W., 265, *273*
 Bendler, A. J., 265, *276*
 Bendre, A. R., 65, *92*
 Bennett, J. A. R., 204, 214, 220 (B9), 223 (B9), 246, 257, 259, *273, 274*
 Bennett, R. J., 44 (94), 45 (94), 45 (94), *49*
 Beran, M. J., 143, *192*
 Bergelin, O. P., 208, 237, 248, 253, *274*
 Bernard, R. A., 129 (B6), 132, *192*
 Billingsly, D. S., 288 (L2), *356*
 Bilous, O., 178, *192*
 Bircumshaw, I., 86 (H5), *93*
 Bird, R. B., 59 (B3, B4), 78 (B4), *92, 122* (B10), *192*
 Bischoff, K. B., 106, 115, 116 (B11, B14), 117, 118, 123 (B13), 123, 124, 126, 129 (B14), 131 (B13), 132 (B14), 135, 136, 139, 140 (B14), 141 (B14), 154, 181, 182, *192, 193*
 Blackwell, R. J., 123, 125, 130, 139, 140, *193*
 Blanchet, J., 178, *193*
 Blank, M., 13 (20), 14 (22), *47*
 Blickle, T., 187, *193*
 Bliss, H., *49*

Block, H. D., 178, 192
 Blokker, P. C., 24 (40), 26 (44), 27 (44),
 31 (44), 32 (44), 47
 Boelter, L. M. K., 220 (B13), 271 (B13),
 274, 276
 Bogatchev, A. N., 178, 194
 Bogusz, E., 61 (W1), 65 (W1), 94
 Bollinger, R. E., 249, 266 (A5), 267, 273
 Bond, W. N., 55 (B5), 92
 Bonilla, C. F., 265, 276
 Bosworth, R. C. L., 193
 Bournia, A., 125, 139, 193
 Boussinesq, J., 61, 75, 92
 Bowman, C. W., 68 (B7), 92
 Boye-Christensen, G., 32 (58), 35 (58), 38
 (77a), 39 (77a), 48
 Bradley, R. S., 5 (6), 46
 Brady, Y., 286, 356
 Braida, L., 57 (J1), 61 (J1), 65, 93
 Brenner, H., 66, 92
 Bretton, R. H., 123, 193
 Brink, J. C., 34 (62), 48
 Brinkley, W. K., 288, 356
 Brinsmade, D. S., 49
 Broeder, J. J., 139, 198
 Brötz, W., 170, 193
 Brookes, F. R., 5 (6), 46
 Brooks, L. H., 23 (40), 24 (40), 47
 Brothman, A., 167, 168, 193
 Brown, F. E., 55 (H6), 93
 Brown, G. G., 62 (B9), 92, 124, 194
 Brown, R. A. S., 213 (B14), 274
 Bryant, L. T., 273
 Buitelaar, A. A., 208, 209, 224, 275
 Burtis, T. A., 89 (B10), 92
 Butler, G., 182, 187, 194
 Byrne, B. J., 66, 93

C

Cairns, E. J., 122, 123, 124 (C5), 144, 145,
 149, 150, 170, 193
 Calderbank, P. H., 34 (61), 35 (63), 48,
 65, 92
 Calvert, S., 213 (C1), 247, 274
 Carberry, J. J., 123, 155, 182, 193
 Carman, P. C., 123, 193
 Carrier, G. F., 134, 193
 Carter, C. O., 274
 Carter, J. C., 273

Chambré, P., 184, 193
 Chandrasekhar, S., 143 (C14), 193
 Charles, G. E., 86 (C2), 87, 93
 Chenoweth, J. M., 223, 225 (C3), 274
 Chisholm, D., 224, 230, 235, 246, 274, 276
 Cholette, A., 167, 168, 169, 178, 193
 Chu, J. C., 44 (88), 49
 Church, J. M., 57, 90, 94
 Cleland, F. A., 184, 193
 Cloutier, L., 167, 168, 169, 178, 193
 Coe, H. S., 151, 195
 Collier, J. G., 213 (L1, C6), 223, 225, 226,
 246, 247, 248 (C6), 249, 257, 259, 263,
 265, 274, 275
 Contractor, R. M., 44 (93), 46 (100), 49
 Converse, A. O., 139, 193
 Conway, J. B., 35 (68), 48
 Corcoran, W. H., 133, 139, 196
 Cornish, A. R. H., 63, 92
 Corrsin, S., 179, 193
 Corson, W. B., 119, 195
 Coste, J., 155, 182, 193
 Coull, J., 125, 139, 193
 Coussemant, F., 178, 195
 Crank, J., 20 (35), 47
 Cromer, S., 274
 Croockewit, P., 125, 193
 Cullen, E. J., 18 (31), 19 (33, 34), 47

D

Da Cruz, A. J. R., 223, 224 (I2), 275
 Damköhler, G., 179, 180, 184, 193
 Danckwerts, P. V., 10, 17 (17), 45 (99), 46
 (100), 46, 49, 102, 123, 149, 161, 170, 173,
 176, 180, 193, 194
 David, M. M., 210, 225, 259, 261, 274
 Davidson, J. F., 18 (32), 19 (33, 34), 47,
 124, 194, 211, 213 (N4), 225 (N4), 233,
 235, 238, 239 (N3, N4), 266, 273, 276
 Davidson, J. H., 35 (67a), 41 (67a), 48
 Davies, J. T., 1 (1), 4 (1), 5 (1), 7 (1),
 11 (24), 12 (24), 13 (24), 14 (1), 15
 (24), 16, 17 (28), 18 (1, 30), 21 (37),
 22 (1), 23 (37), 24 (37), 26 (50), 27 (50),
 28, 29 (50), 30 (1), 31 (50), 32 (50), 33
 (37, 50), 36 (1), 37 (24), 38 (24), 40 (1,
 24), 41 (1, 24, 30), 43 (1), 44 (89), 45
 (97, 98), 46, 47, 49, 77 (D2), 78 (D2),
 83 (D1, D2), 93
 Davis, E. J., 210, 225, 259, 261, 274

Davis, W. J., 223, 229, 274
 Deans, H. A., 155, 158, 185, 194
 Deissler, P. F., 120, 194
 de Josselin de Jong, G., 143, 144, 194
 de Maria, F., 182, 187, 194
 Denbigh, K. G., 168, 178, 194, 197
 Dengler, C. E., 259, 274
 Devyatov, B. H., 178, 194
 Dhanak, A. M., 132, 194
 Diglis, A. J., 210, 223, 238, 276
 Dorweiler, V. P., 129 (D20), 132, 134, 139, 194
 Downing, A. L., 15 (25), 47
 Dressler, R. G., 3 (4), 4 (4), 46
 Drickamer, H. G., 6 (9), 21 (9), 23 (42, 43), 25 (42, 43), 32 (42), 46, 47
 Duffin, J. H., 281 (H1), 288 (H1, D1), 289, 356
 Dukler, A. E., 210, 237, 247, 248, 249, 250 (W2), 267, 274, 277
 Dunn, J. S. C., 205 (G6), 206, 213, 229, 274

E

Ebach, E. A., 120, 121, 123, 124 (E1), 194
 Eddy, K. C., 229, 275
 Edmister, W. C., 287, 356
 Edwards, L. J., 168, 195
 Eguchi, W., 167, 178, 194, 196
 Einstein, H. A., 144, 194
 Eisner, H. S., 5 (6), 46
 Elder, J. W., 135, 194
 Eldridge, J. W., 168, 178, 194
 Elgin, J. C., 65, 94
 Ellis, S. R. M., 44 (93, 94), 45 (94, 96), 45 (94), 46 (100, 103), 49
 Elzinga, E. R., 36 (75), 39 (77E), 48, 61 (E1), 62 (E1), 74 (E1), 75, 80 (E1), 82 (E1), 83, 93
 Engen, J. M., 254, 275
 Epstein, N., 182, 194
 Eschard, F., 178, 195
 Evans, H. D., 208, 275
 Evans, J. E., 35 (68), 48
 Evans, R. B., 143, 194
 Eyring, H., 145, 194

F

Fahien, R. W., 129 (F2, D20), 132, 134, 139, 194

Fan, L., 178, 182, 194
 Fararoui, A., 65 (F1), 72 (F1), 73 (F1), 74 (F1), 93
 Farley, R. W., 84, 94
 Farquharson, D. C., 124, 194
 Fauske, H., 225 (I4), 227, 231, 275
 Fedosov, A. I., 35 (66), 39 (77C), 48
 Flanigan, H. L., 271, 272, 274
 Flinn, W. S., 229, 232, 276
 Flint, D. L., 132, 194
 Fodiman, N. M., 89 (V2), 94
 Förster, T., 181, 194
 Foltz, H. L., 274
 Foord, A., 36 (76), 48
 Foster, P. A., Jr., 204, 214, 220 (G7), 223 (G7), 274
 Fowler, F. C., 124, 194
 Fox, E. A., 168, 194
 Frank, O., 49
 Franke, M., 42 (79), 48
 Fraser, J. B. P., 240, 274
 Fristenberg, H., 264, 274
 Froment, G. F., 124, 189, 194
 Frossling, N., 35 (64), 48
 Frumkin, A., 37 (70), 39 (70), 48
 Fujinawa, K., 36 (74), 48

G

Garcia, J., 225 (I4), 227, 231, 275
 Garner, F. H., 33 (59, 60), 34 (60), 35 (67, 71), 36 (72, 76), 41 (72), 42 (71), 48, 58, 63 (G2), 69 (G2, G6), 71, 72 (G7), 73 (G7), 78 (G3), 79 (G7), 80, 93
 Gayler, R., 42 (84), 49
 Gazley, C., 208, 253 (B12, G1), 274, 274
 Geankoplis, C. J., 123, 196, 197
 Geddes, R. L., 287, 356
 Geib, K. H., 181, 194
 Gex, V. E., 168, 194
 Giddings, J. C., 145, 194
 Gill, L. E., 250, 274
 Gilles, E. D., 178, 194
 Gilliland, E. R., 65, 68 (H11), 74, 93, 170, 173, 187, 194, 196, 286, 356
 Girard, O., 178, 195
 Glass, W., 170, 195, 196
 Goldmann, K., 264, 274
 Gomezplata, A., 194
 Gorodetskaya, A. V., 35 (65), 40 (65), 48
 Govier, G. W., 203, 205 (G6), 206, 208,

209, 210, 213 (G5, G6, B14), 223, 226,
227 (G4), 229, 274
Grace, T., 225 (I4), 227, 231, 275
Grassman, P., 49
Graumann, R. E., 59 (K2), 69 (K2), 71
(K2), 93
Green, H., 86 (G8), 93
Green, H. L., 5, 46
Green, S. J., 225, 259, 276
Greenhalgh, R. E., 173, 194
Greenstadt, J., 286, 356
Gresham, W. A., Jr., 204, 214, 220 (G7),
223 (G7), 274
Griffith, P., 212, 213, 233, 234, 238, 265,
274, 276
Griffith, R. M., 39, 40 (77F), 48
Grimley, S. S., 65, 93
Groothius, H., 7, 34 (61), 42 (85), 43 (85),
46, 48, 49, 86 (G10), 87, 93, 259, 261, 274
Grossmann, L. M., 225, 259, 260 (S3, S4),
262, 276
Grundy, F., 3 (4), 4 (4), 46
Guerrieri, S. A., 259, 274
Guinn, V. P., 167, 197
Gutoff, E. B., 168, 194

H

Haberman, W. L., 65, 66, 68 (H2), 69
(H2), 74, 78 (H2), 80 (H1), 93
Hadamard, J. S., 60 (H3), 93
Hahn, H. T., 23 (41), 25 (41), 47
Hale, A. R., 33 (60), 34 (60), 36 (72), 41
(72), 48, 58, 93
Hall, R. E., 183, 195
Ham, A., 151, 195
Hammerton, D., 35 (67), 48
Handlos, A. E., 167, 170, 195
Hanratty, T. J., 132, 149, 170, 194, 195,
254 (H1, H2), 275
Hanson, D., 19 (34), 47
Hanson, D. N., 281 (H1), 288, 289, 356
Happel, J., 66, 93
Harai, E., 195
Hardy, W. B., 86 (H5), 93
Harkins, W. D., 55 (H6), 93
Harmathy, T. Z., 61 (H7), 71 (H7), 93
Harmens, A., 44 (90), 49
Hartman, M. E., 132, 195
Harvey, G. A., 14 (21), 47
Haselden, G. C., 273
Hatch, M. R., 224, 275
Hatta, S., 34 (61), 48
Hauser, E. A., 57 (A2), 58, 92
Hawke, J. G., 15, 47
Hawthorn, R. D., 135, 195
Haycock, P. J., 63 (G2), 69 (G2, G6), 71,
93
Haydon, D. A., 8 (12), 22 (12), 46
Hayduk, W., 266 (S6), 268, 276
Haywood, R. W., 232, 275
Hayworth, C. B., 55 (H8), 57, 93
Heath, C. E., 167, 192
Heigl, J. J., 170, 195
Hellin, M., 178, 195
Hendal, W. P., 259, 261, 274
Hershman, A., 254, 275
Herzfeld, K. F., 183, 197
Hewitt, G. F., 213 (L1, C6), 223, 225, 226,
246, 247, 248, 249, 250, 263, 265, 274, 275
Hiby, J. W., 107 (H8), 130, 195
Higbie, R., 9, 46
Higson, D. J., 276
Hinds, G. P., 170, 192
Hinze, J. O., 107, 132 (H9), 133, 142, 143
(H9), 147, 195
Hitchon, J. W., 250, 274
Hixson, A. N., 61 (K1), 73 (K1), 93
Hofmann, H., 124, 178, 179, 194, 195, 197
Holland, C. D., 288 (L2), 356
Holm, A., 32 (57), 35 (57), 48
Honig, C. E., 125, 193
Hoogendoorn, C. J., 208, 209, 210, 223,
224, 230, 246, 275
Hoopes, J. W., Jr., 210, 225, 227, 228, 265,
275, 276
Horn, F., 179, 195
Horton, T. J., 59 (K2), 69 (K2), 70 (H9),
71, 80 (H9), 84 (H9), 93
Houghton, G., 125, 139, 193
Hovorka, R. B., 160, 182, 192, 195
Hu, S., 61 (H10), 62 (H10), 64, 73 (H10),
93
Hubers, C., 259, 275
Hughes, R. R., 65, 68 (H11), 74, 93, 208,
275
Hughmark, G. A., 224, 226, 229, 231, 242,
244, 275
Hulburt, H., 180, 195
Hull, D. E., 124, 195

Hunter, T. G., 42 (80), 48
 Huntington, R. L., 270, 274, 276
 Huntley, A. R., 170, 195
 Hutchinson, M. H., 16 (26), 26 (46), 47
 Hutchison, H. P., 240, 274
 Hyman, D., 119, 195

I

Inamura, T., 178, 196
 Isbin, H. S., 204, 210, 214, 223 (I1, I2, I7),
 224 (I1, I5, I7), 225 (I4, I5), 226, 227
 (I4, I7), 228 (I1, I7), 229, 231 (I4, I5),
 264, 275

J

Jacobs, R. B., 224, 275
 Jacques, G. L., 123, 124, 132, 144, 195
 Jeannin, P. J., 29 (56), 48
 Jenkins, J. W., 170, 194
 Jenney, T. M., 178, 195
 Johanson, A. G., 3 (4), 4 (4), 46
 Johnson, A. I., 57 (J1, P1), 58, 61 (J1),
 65, 68 (B7), 90, 92, 93, 94
 Johnson, H. A., 208, 259, (J1, J2), 275
 Johnson, H. F., 54 (N1), 56, 94
 Johnson, J. P., 168, 195
 Johnson, M., 61 (W1), 65 (W1), 94
 Johnson, R. L., 173, 194
 Johnstone, H. F., 132, 197
 Jones, R. W., 178, 195
 Jordan, G. V., 89 (J2), 93
 Jungers, J. C., 178, 195

K

Kada, H., 132, 194
 Kafarov, V. V., 11, 46
 Kaldi, P., 187, 193
 Kal'yanova, R. M., 89 (V2), 94
 Kampé de Fériet, J., 148, 195
 Kandiner, H. J., 151, 195
 Kasai, H., 178, 196
 Katz, S., 151, 195
 Kawamura, S., 178, 195
 Keey, R. B., 78 (G3), 93
 Keith, F. W., 61 (K1), 73 (K1), 93
 Kendall, H. B., 182, 195
 Kendrick, P., 33 (59), 48
 Kent, J. W., 124, 195
 Kepner, R. H., 220 (B13), 271 (B13), 274

Keyes, J. J., 132, 195
 Kharin, A. N., 123, 192
 Kilner, A. A., 16, 17 (28), 47
 King, G. W., 143 (K5), 195
 Kintner, R. C., 59 (K2), 61 (H10, S12,
 W1), 62 (H10), 64, 65 (F1, M3, W1),
 67 (S12), 69 (K2), 71 (K2), 72 (F1), 73
 (H10, F1, K5, M3, S12), 74 (F1, M3),
 93, 94
 Kirillov, N. I., 178, 195
 Kirkbride, C. G., 92
 Kishinevskii, M. K., 9 (14), 16, 34 (61),
 42 (83), 46, 47, 48, 49
 Kjaer, J., 183, 195
 Klee, A. J., 61 (K3), 64, 73 (K3), 93
 Klinkenberg, A., 123, 145, 195
 Klipstein, D. H., 210, 223, 276
 Knights, G. A., 232, 275
 Knoll, W. H., 168, 196
 Kohl, J., 124, 195
 Korchinski, I. J. O., 65, 92
 Kordyban, E. S., 210, 237, 275
 Koslov, B. K., 212, 275
 Kosterin, S. I., 208, 210, 229, 271, 275
 Krajenbrink, H. J., 195
 Kramers, H., 7, 17, 18 (29), 19 (33), 34
 (61), 46, 47, 48, 120, 123, 125, 132, 157,
 168, 195
 Krisna, P. M., 61 (K4, K5), 62 (K5), 64
 (K5), 65 (K5), 83 (K5), 93
 Krongelb, S., 184, 196
 Kronig, R., 34 (62), 48
 Küchler, L., 179, 195
 Kunreuther, F., 170, 192
 Kunstman, R. W., 167, 170, 195
 Kurihara, T., 36 (74), 48
 Kurochkina, I. S., 123, 192
 Kyle, R. J., 204, 214, 220 (G7), 223 (G7),
 274

L

Lacey, P. M. C., 213 (L1), 246, 247, 250,
 255, 263, 265, 274, 275
 Ladenburg, R., 66, 93
 Laird, D. K., 224, 230, 235, 246, 274, 275
 Lamb, D. E., 149, 196, 215, 249, 266 (A5),
 267, 273, 275
 Lamb, H., 56, 59 (L2), 75, 78 (L2), 93
 Lamm, O., 23 (39), 47
 Lane, J. J., 33 (60), 34 (60), 48

- Lane, W. R., 5, 46
 Langlois, G. E., 94
 Langmuir, D. B., 6, 7 (10), 46
 Langmuir, I., 6, 7 (10), 46
 Lanneau, K. P., 196
 Lapidus, L., 65, 94, 118, 155, 158, 178, 185, 192, 194
 Larson, H. C., 223, 224 (I5, I7), 225 (I5), 226, 227, 228, 231, 264, 275
 Latinen, G. A., 143, 149, 170, 195, 196
 Lauwerier, H. A., 139, 184, 195, 196, 198
 Leclerc, V. R., 178, 196
 Lee, J. C., 124, 196
 Legg, R. J., 45 (96), 49
 Leprince, P., 178, 195
 Lessells, G. A., 178, 196
 Leva, M., 171, 196
 Levenspiel, O., 97 (L13), 98 (L13), 100 (L13), 101 (L13), 102, 103 (L13), 104, 106, 110, 113, 115, 116 (B14), 117, 118, 121 (L13), 122 (L13), 123, 124, 126, 129 (B14), 132 (B14), 135, 136, 139, 140 (B14), 141 (B14), 154, 157, 160, 162, 163 (L13), 165 (L13), 169 (L13), 170 (L13), 175, 178, 181 (L14, L15), 182, 185, 186 (L13A), 187 (L11, L13), 193, 196
 Levich, V. G., 11, 12, 37 (70), 39 (70), 47, 48
 Levy, D. J., 44 (88), 49
 Levy, S., 217, 228, 232, 243, 265, 275
 Lewis, J. B., 26 (48), 27 (48), 28 (53), 29 (48), 31 (48), 47
 Lewis, W. K., 2 (2), 8, 46, 196, 286, 356
 Licht, W., 35 (68), 48, 61 (L3), 73 (L3), 74 (L3), 93
 Lightfoot, E. N., 59 (B4), 78 (B4), 122 (B10), 92, 192
 Liles, A. W., 123, 196
 Limida, M., 178, 196
 Lindland, K. P., 36 (72), 41 (72), 48, 64 (L4), 82, 93
 Linton, M., 3 (5), 15 (25), 35 (69), 37, 38 (69), 41 (69), 46, 47, 48
 Lockhart, R. W., 213 (L6), 220, 221, 223 (L6), 275, 276
 Lombardi, C., 264, 274
 Longcor, J. V. A., 35 (68), 48
 Longfield, J. E., 182, 187, 194
 Longwell, J. P., 132, 196
 Lottes, P. A., 229, 232, 276
 Lunde, K. E., 276
 Lynn, S., 17 (29), 18 (29), 19 (33), 47, 133, 139, 196
 Lyster, W. N., 288, 356
- M**
- McAvoy, R., 65, 93
 MacDonald, R. W., 168, 196
 McHenry, K. W., 120, 123, 196
 MacKay, G. D. M., 43 (87), 49
 McKinney, A. W., 265, 275
 McManamey, W. J., 27, 28 (54), 29 (54), 47, 48
 MacMullin, R. B., 151, 178, 196
 Mamuro, T., 170, 196
 Manakin, G. A., 266 (V2, V3), 277
 Manning, F. S., 149, 196
 Mansfield, W. W., 3 (3), 46
 Mantzouranis, B. G., 213 (A2), 247, 249, 250 (A3), 273
 Marchaterre, J. F., 229, 273, 276
 Marchello, J. M., 10, 46
 Markels, M., 265, 276
 Maroudas, N. G., 22 (38), 47
 Martin, M. W., 223, 225 (C3), 274
 Martin, T. W., 29 (55), 48
 Martinelli, R. C., 213 (L6), 220, 221, 222, 223 (L6), 275, 276
 Mason, D., 151, 178, 196
 Mason, E. A., 143, 170, 173, 187, 194
 Mason, S. G., 43 (87), 49, 86 (C2), 87, 93
 Matheson, G. L., 286, 356
 Mathis, J. F., 196
 May, W. G., 196
 Mayers, G. R. A., 26 (50), 27 (50), 28, 29 (50), 31 (50), 32 (50), 33 (50), 47
 Meksyn, D., 80, 93
 Metzner, A. B., 168, 173, 196
 Mhatre, M. V., 65 (M3), 73 (M3), 74 (M3), 93
 Mickelson, W. R., 132, 196
 Middleton, G. E., 232, 275
 Miyauchi, T., 114, 170, 178, 180, 198
 Miyazaki, Y., 40 (78), 41 (78), 48
 Moen, R. H., 204, 210, 214, 223 (I1, I7), 224 (I7), 226, 227, 228 (I1, I7), 275
 Moissis, R., 234, 238, 276
 Morino, I., 178, 196
 Morse, B., 286, 317
 Morrin, E. H., 276
 Morton, R. K., 65, 80 (H1), 93

Mosher, D. R., 204, 210, 214, 223 (I1),
224 (I7), 226, 227, 228 (I1, I7), 275
Mott, R. A., 122, 196
Moy, J. E., 224 (I2), 275
Muchi, I., 170, 196
Murdoch, R., 42 (82), 49
Murray, R. G., 274

N

Nagata, S., 178, 196
Nakaike, Y., 36 (74), 48
Narasimhamurty, G. S. R., 61 (K4, K5,
L3), 62 (K5), 64 (K5), 65 (K5), 73
(L3, K5), 74 (L3), 83 (K5), 93
Nash, A. W., 42 (80), 48
Nassenstein, H., 26 (47), 47
Nedderman, R. M., 240, 274
Nelson, D. B., 222, 276
Neustal, A. D., 265, 274
Newacheck, R. L., 124, 195
Nicklin, D. J., 211, 213 (N4), 218, 219,
225 (N4), 233, 235, 238, 239 (N3, N4),
241, 242, 245, 276
Norwood, K. W., 168, 196
Nott, H. D., 173, 194
Null, H. R., 54 (N1), 56, 94

O

Okazaki, S., 40 (78), 41 (78), 48
Oliver, R. C., 170, 173, 194
Omer, M. M., 203, 208, 209, 210, 223, 226,
227 (G4), 274
Opfell, J. B., 134, 197
Orell, A., 77 (O1), 94
Oshima, T., 170, 198
Othmer, D. F., 171, 198
Owens, W. L., Jr., 228, 276

P

Page, F. M., 168, 178, 197
Pai, S., 147, 197
Pamfilov, A. V., 9 (14), 46
Paneth, F., 183, 197
Panich, R. M., 89 (V2), 94
Pansing, W. F., 35 (68), 48, 167, 197
Patterson, H. S., 5, 46
Pattie, B. D., 224 (I5), 225 (I5), 231, 264,
275
Pearson, J. R. A., 180, 197
Petersen, E. E., 175, 197

Petrick, M., 232, 276
Picken, J. Q., 124, 194
Pigford, R. L., 18 (16), 42 (16), 46, 173,
196
Piret, E. L., 151, 168, 178, 192, 194, 196,
198
Place, G., 170, 194
Plautz, D. A., 132, 197
Polomik, E. E., 265, 275
Polson, A., 23 (39), 47
Pontinen, A. J., 287, 356
Poutanen, A. A., 57 (P1), 58, 90, 94
Prager, S., 143, 179, 197
Pratt, H. R. C., 36 (73), 42 (73, 82, 84),
48, 49, 257, 259, 274
Prausnitz, J. M., 122, 123, 124 (C5), 144,
145, 149, 150, 170, 193, 197
Pressburg, B. S., 224, 229, 231, 275
Putnam, J. A., 220, 221, 276

Q

Quince, B. W., 5 (6), 46
Quinn, J. A., 29 (56), 48

R

Radford, B. A., 205 (G6), 206, 213, 229,
274
Ranz, W. E., 143, 197
Ratcliff, G. A., 42, 43 (86), 49
Rayleigh, Lord 94
Rayne, J. R., 123, 140 (B17), 193
Reid, K., 42, 43 (86), 49
Reid, R. C., 210, 223, 238, 276
Reman, G. H., 170, 197
Reynolds, A. B., 210, 223, 238, 276
Richardson, J. F., 276
Rideal, E. K., 1 (1), 4 (1), 5 (1), 7 (1),
14 (1), 22 (1), 30 (1), 36 (1), 40 (1),
41 (1), 43 (1), 45 (97, 98), 46, 49, 77
(D2), 78 (D1), 83 (D2), 93
Ritchie, I. M., 44 (89), 49
Roberts, D., 19 (34), 47
Roberts, P. H., 107 (R3), 142, 197
Robinson, C. S., 286, 356
Robinson, J. W., 89 (R2), 94
Robinson, W. G., 118, 123, 197
Rodger, W. A., 94
Rodriguez, H. A., 224 (I5), 225 (I5), 231,
264, 275
Rose, A., 288, 356

Rosen, J. B., 120, 197
 Rosenberg, B., 65, 94
 Roughton, F. J. W., 13 (20), 47
 Ruban, V. L., 61 (S8), 80 (S8), 94
 Rubinovitch, M. N., 210, 275
 Rudd, D., 155, 182, 193
 Rushton, J. H., 94
 Rybczynski, W., 60, 94

S

Saffman, P. G., 143, 144, 197
 Sage, B. H., 132, 133, 134, 139, 196, 197
 Saito, S., 73, 94
 Saito, Y., 178, 195
 Sasaki, K., 170, 196
 Sasaki, T., 40 (78), 41 (78), 48
 Savic, P., 69, 94
 Sawistowski, H., 22 (38), 45 (99), 47, 49
 Sayre, R. M., 66, 68 (H2), 69 (H2), 74, 78 (H2), 93
 Schechter, R. S., 84, 94, 156, 184, 186, 197, 198
 Scheidegger, A. E., 143, 197
 Schissler, D. O., 167, 170, 195
 Sehlinger, W. G., 132, 197
 Schmidt, E., 65, 87 (S4), 94
 Schoenemann, K., 175, 179, 197
 Schrock, V. E., 225, 259, 260 (S3, S4), 262, 276
 Schrodt, V. N., 288, 356
 Schümmer, P., 107 (H8), 130, 195
 Schultz, R. K., 124, 197
 Schumann, W. A., 265, 274
 Schwartz, C. E., 134, 139, 197
 Scott, E. J., 6 (9), 21 (9), 46
 Scott, D. S., 213 (S5), 225 (S5), 231, 266 (S6), 268, 276
 Scriven, L. E., 8, 46, 77 (S10), 94
 Selke, W. A., 265, 276
 Serebryansky, V. T., 16, 47
 Sheludko, A., 94
 Shen, C. Y., 197
 Sher, N. C., 225, 229, 259, 275, 276
 Sherwood, T. K., 16 (26), 26 (49), 27 (51), 35 (68), 42 (16, 51), 46, 47, 48, 77 (S6), 94, 132, 173, 175, 197, 198
 Shinnar, R., 57, 90, 94
 Shipley, J. R., 124, 197
 Short, W. L., 213, 274
 Shuster, W. W., 194
 Siemens, W., 42 (79), 48
 Sigwart, K., 26 (47), 47
 Silvestri, N., 263, 276
 Sinclair, G. G., 168, 197
 Sinfelt, J. H., 23 (43), 25 (43), 47
 Singer, E., 167, 197
 Singh, S., 275
 Sjenitzer, F., 123, 124, 195, 197
 Sjölin, S., 25 (45), 47
 Skelland, A. H. P., 35 (71), 42 (71), 48, 69 (G6), 93
 Slack, C., 5 (6), 46
 Smirnov, N. I., 61 (S8), 80 (S8), 94
 Smirnova, V. P., 178, 195
 Smith, B. D., 288 (S1, S2), 356
 Smith, C. R., 232, 276
 Smith, J. M., 129 (F2), 132, 134, 139, 183, 194, 195, 197
 Smith, S. S., 124, 197
 Smith, W., 14 (21), 45 (99), 47
 Smith, W. K., 104, 110, 113, 196
 Sneddon, I. N., 109 (S20), 197
 Sobocinski, D. P., 270, 276
 Somerville, G. F., 281 (H1), 288, 289, 356
 Sonneman, G., 265, 276
 Sorel, 279, 356
 Southward, D. C., 44 (89), 49
 Spaulding, D. B., 104, 197
 Spells, K. E., 69, 94
 Spiewak, I., 210, 223, 238, 276
 Standart, G. L., 178, 197
 Staroselski, Ya. I., 266 (V2, V3), 277
 Stead, B., 168, 178, 197
 Stein, R. P., 265, 276
 Stermerding, S., 259, 276
 Sternling, C. V., 8, 46, 77 (S10), 94, 208, 275
 Stewart, W. E., 59 (B4), 78 (B4), 92, 122 (B10), 192
 Straatemeier, J. R., 17 (29), 18 (29), 19 (33), 47
 Strandberg, M. W. P., 184, 196
 Strang, D. A., 123, 197
 Streeter, V. L., 59 (S11), 78 (S11), 94
 Strom, J. R., 61 (S12), 67 (S12), 73 (S12), 94
 Stuke, B., 35 (65), 37 (77), 48
 Sullivan, G. A., 213 (B14), 274
 Sullivan, S. L., Jr., 288 (L2), 356

Sutherland, K. L., 3 (5), 15 (25), 35 (69),
37, 38 (69), 41 (69), 46, 47, 48
Suzuki, E., 178, 195
Swan, C. L., 265, 275
Swanson, B. S., 232, 276
Sweeney, R. F., 288, 356

T

Talty, R. D., 259, 274
Tanaka, T., 178, 196
Tang, Y. S., 232, 276
Tanigawa, K., 178, 196
Tayeban, M., 36 (76), 48, 72 (G7), 73
(G7), 79 (G7), 80, 93
Taylor, C. C., 44 (88), 49
Taylor, D. C., 124, 194
Taylor, E. A., 124, 192
Taylor, G. I., 124, 125, 135, 139, 141, 147,
198
Taylor, J. S., 168, 196
Taylor, T. H. M., 220, 276
Teletov, S. G., 276
Terjesen, S. G., 32 (57, 58), 35 (57, 58),
36 (72), 38 (77a, 77b), 39 (77a), 41
(72), 48, 61 (L4), 82, 93
Terry, W. M., 123, 140 (B17), 193
Thiele, E. W., 287, 356
Thom, J. R. S., 232, 275
Thomsen, E. G., 276
Thornton, J. D., 257, 259, 273, 274
Thorsen, G., 38 (77b), 48
Tichacek, L. J., 135, 139, 182, 198
Todd, D. B., 167, 197
Toor, H. L., 10, 46
Towle, W. L., 132, 198
Townsend, A. A., 107 (B4), 192
Trambouze, P. J., 157, 178, 179, 185, 198
Trass, O., 68 (B7), 92
Trawinski, H., 170, 198
Treybal, R. E., 55 (H8), 57, 61 (K3), 64,
73 (K3), 85, 89 (T1), 93, 94
Trice, V. G., 94
Truesdale, G. A., 15 (25), 47
Tucker, W. B., 57 (A2), 58, 92
Tung, L. H., 6 (9), 21 (9), 23 (42), 25
(42), 32 (42), 46, 47
Turner, G. A., 145, 146, 161, 198

U

Underwood, A. J. V., 286, 356

V

Van Deemter, J. J., 139, 158, 198
Van der Laan, E. T., 111, 113, 114, 116,
157, 198
Vanderwater, R., 275
Van de Vusse, J. G., 168, 198
van Heuven, J. W., 266, 273
Van Krevelen, D. W., 185, 198
Van Rossum, J. J., 250, 254 (V1), 276
Varlamov, M. L., 266 (V2, V3), 277
Venkateswarlu, D., 61 (K4, K5), 62 (K5),
64 (K5), 65 (K5), 73 (K5), 83 (K5),
93
Vermeulen, T., 123, 124, 132, 144, 94, 195
Verschoor, H., 259, 276
Vielstich, W., 18 (31), 47
Viskata, R., 265, 277
Vohr, J., 217, 277
Von Rosenberg, D. V., 123, 198
Voyutskiy, K. A., 89 (V2), 94

W

Wakad, N., 170, 198
Walker, C. L., 232, 276
Walker, R. E., 184, 198
Wallis, G. B., 212, 213, 233, 242, 245, 274,
277
Walsh, T. J., 132, 192
Ward, A. F. H., 23 (40), 24 (40), 47
Ward, D. M., 68 (B7), 92
Warshay, M., 61 (W1), 65 (W1), 94
Watson, C. C., 196
Watson, G. M., 143, 194
Weaver, R. E. C., 65, 94
Weber, A. P., 167, 168, 178, 193, 198
Weber, M., 151, 178, 196
Wehner, J. F., 113, 114 (W4), 180, 198
Wei, J. C., 27 (51), 42 (51), 47, 77 (S6),
94
Weiss, M. A., 132, 167, 192, 196
Wendel, M. M., 155, 193
West, F. B., 36 (72), 41 (72), 48
Westhaver, J. W., 135, 198
Westwater, J. W., 77 (O1), 87 (W3), 94
Wevers, C. J. H., 132, 195
White, J. L., 215, 275
White, R. R., 120, 121, 123, 124 (E1), 194
Whitman, W. G., 2 (2), 8, 46
Whittemore, E. R., 168, 198
Whytlaw-Gray, R., 5, 46

- Wicke, E., 170, 187, 198
Wickey, R. O., 210, 223, 224 (I7), 226, 227, 228, 275
Wicks, M., 210, 247, 248 (W2), 249, 250 (W2), 267, 277
Wiggill, J. B., 21 (36, 37), 23 (36, 37), 24 (36, 37), 33 (36, 37), 47
Wilhelm, R. H., 113, 114 (W4), 120, 123, 129 (B6), 132, 149, 170, 180, 184, 192, 193, 194, 195, 196, 197, 198
Wilkes, J. O., 213 (N4), 225 (N4), 233, 235, 239, 276
Williams, B., 213 (C1), 247, 274
Williams, G. C., 74, 94
Williams, G. M., 94
Winsche, W. E., 120, 197
Wissler, E. H., 156, 184, 186, 197, 198
Woertz, B. B., 132, 197
Wood, J. C., 168, 198
Wright, R. M., 225, 260, 277
- Y
- Yagi, S., 114, 170, 178, 180, 198
Young, E. F., 151, 198
- Z
- Zenz, F. A., 171, 198
Zhivaikin, L. Ya; 251, 253, 277
Zuber, N., 242, 244, 277
Zuiderweg, F. J., 42 (85), 43 (85), 44 (90), 46 (101), 49, 86 (G10), 87, 93
Zwietering, T. N., 173, 176, 177, 198

SUBJECT INDEX

A

- Absorbers, spray, 33
- Absorption
 - CO₂, 9, 14-15, 18
 - effect of surface-active agents, 17-19
 - gas into liquid solvent, 5
 - oxygen, 13-17
 - reboiled, 288
 - SO₂, 17-18
 - steady-state, oxygen into water, 15-16
- Adsorption
 - on wetted columns, 16-18
- Acceleration-pressure losses, 222
- Age-distribution
 - in backmix reactors, 174-175
 - conversion determination, 173
 - degree of segregation, 176-177
 - direct use of information, 173-174
 - exit, 100-101
 - internal function (see I curve)
 - life expectation, 177
 - linear rate equations, 174-175
 - nonlinear rate equations, 175-178
 - early mixing conversion, 176-178
 - late mixing conversion, 176
 - in segregated flow, 173
- Armand equation, modified, 231-232

B

- Beds
 - fibrous, 87-90
 - passage of an emulsion, 89-90
 - fluidized, 170-172
 - models for, 172
 - porous, 89-90
 - volume ratio of phases, 187
- Boiling phenomena,
 - forced convection, 258
 - nucleate, 257
 - in vertical tubes, 254-259

- Boundary conditions
 - in axial dispersion, 115-118, 120-128
 - in infinite pipe, 111, 118
- Boussinesq model, 61
- Bubble-flow
 - Bankoff's model, 242-245
 - gas void-fractions, 243
 - velocity of bubbles, 243-244
 - coalescence of bubbles, 245
 - flow factor, 243-244
 - horizontal, 245-246
 - pressure drop in, 242
 - two-phase gas liquid, 207, 211
 - vertical tubes, 241-242
- Bubbles
 - Dumitrescu
 - absorption from, 267
 - in vertical flow, 241-242
 - gas transfer into liquid, 34-35
 - rise velocities, 241
 - in two-phase flow, 201
 - wakeless, 233-237
 - pressure recovery in, 236
 - rising velocity, 233
- Burn-out
 - in film flow, 263-265
 - oscillations, 265
 - in forced convection region, 263
 - heat flux, decrease of, 264
 - hydrodynamic effect on, 264

C

- C curve
 - dispersion model, 118
 - maxima for comparison, 157
 - slow cross flow, 160-161
 - stirred tanks, 152-153
 - tanks-in-series, 151
- Chenoweth and Martin correlation, 225-226
 - in horizontal slug-flow, 238

- Circulation, internal, in drops
 - effect of surfactants, 83-84
 - light distortion, 69-71
 - patterns, 69-71
 - in pure systems, 63, 67
 - in ultrapure systems, 67
 - CO₂ absorption in gas-liquid systems, 9, 14-15, 18
 - effect of surface-active agents, 14
 - resistance to mass transfer, 14
 - Coalescence
 - of drops, 85-90
 - fibrous-bed phenomena, 87-90
 - partial, 87
 - rupture, 86-87
 - two-drop, 87
 - in extraction cycle, 53
 - floculation, liquid-liquid foams, 85
 - Column,
 - distillation, with partial condenser, 282-283
 - wetted wall
 - flooding, 240-241
 - gas absorption coefficient, 266, 267-288
 - Condensers
 - computer correction of temperature, 292-293
 - partial, 292
 - specification of, 304
 - total, 292
 - two-product, 292
 - calculation, 306
 - Currents, field-fluid, 84-85
- D**
- Deadwater regions
 - completely stagnant, 159-160
 - slow cross flow, 160
 - definition of, 159-161
 - determination of model parameters, 160-161
 - existence of, 160-162
 - I-curve, 161, 165-167
 - Diffusion of acetic acid into benzene, 22-23
 - Dispersion
 - axial
 - boundary conditions, 111, 115-118, 120, 128
 - experimental findings, 121-122
 - laminar flow in empty tubes, 125
 - measurement of coefficient, 109-125
 - moment order of trace distribution, 136
 - number of parameters in, 164
 - packed beds, 118, 122-124
 - turbulent flow in empty tubes, 124-125
 - radial
 - coefficient, 139-142
 - experimental findings, 131-133
 - laminar flow in empty tubes, 133
 - symmetrical pipe flow, 133
 - Dispersion coefficients
 - concentration fluctuations, 147-150
 - summary of, 150
 - correlation, 148-149
 - effect of viscosity, 135
 - general dispersion model for symmetrical pipe flow, 133-134
 - intensity, 149
 - magnitude, 142
 - measurement of, 109-134
 - axial-dispersed plug-flow model, 109-125
 - dispersed plug-flow model, 125-133
 - radial dispersion, 132-133
 - tracer injection, 109
 - random walk models, 143-144
 - mixing length theory, 144
 - radial dispersion in, 143
 - "statistical" models, 144-145
 - Taylor's treatment, 147
 - theoretical methods for predicting, 142-150
 - tracer distribution moments, summary of, 138
 - Turner's structures, 145-147
 - use of equations in interpreting experimental data, 129-131
 - mass balance, 130
 - Distillation, 44-46
 - Distribution function, internal (see I curve)
 - Drops
 - and bubbles, 33-42
 - rate of mass transfer, 41
 - rate of rise and fall, 38-42
 - velocity of fall, 39-40
 - circulation in, 36-38
 - ratio of bulk viscosities, 36-37

- falling, balance force on, 62-63
 - formation, dispersion, 54-58
 - effect of mass transfer rate, 54
 - fast formation at nozzles, 55-56
 - slow formation at nozzles, 54-55
 - turbulent dispersers, 57
 - forming, shape of, 57-59
 - other models, 58-59
 - true shape, 57-58
 - immobile interface of, 36
 - internal circulation
 - direct evidence, 68-71
 - Garner-Haycock quantitative measurements, 71
 - indirect evidence, 68
 - qualitative reports, 69-71
 - Reynolds number, 68
 - micron-size, 85
 - moving
 - shapes of, 71-74
 - spherical liquid, 61
 - surface tension forces, 61
 - velocities of, 59-67
 - of organic chemicals, 72-73
 - oscillations
 - amplitude and rupture, 75-77
 - interfacial turbulence, 77-78
 - in liquid-liquid systems, 76-77
 - random wobbling, 74-75
 - surface indentations, 75
 - single, analysis of, 53
 - in two-phase flow, 201
- E**
- E curve, 100-101
 - Einstein's equation for molecular diffusion, 148
 - Emulsification, spontaneous, 22, 77-78
 - Energy balances, 214-220
 - Nicklin approach to, 218
 - Enthalpy, 284, 287-288, 290-291, 298, 301, 304
 - Entrainment
 - behavior in annular flow, 247-252
 - parameter of, 249
 - critical velocities, 251-252
 - critical Weber number, 249, 251
 - flow types in, 251
 - horizontal liquid films, 250
 - turbulent region, 251
 - Evaporation, 3-5
 - above plane surface, 3-4
 - effect of long chain alcohol, 3
 - from drops of liquid, 4-5
 - reduction by polar oil monolayer, 3-4
 - resistance to, 3
 - Extraction
 - practical, 42-44
 - coalescence rate, 43
 - efficiency of packed columns, 42
 - variations in viscosity, 43
 - liquid, steps in mass transfer, 52-53
 - liquid-liquid, enthalpy balance, 290
- F**
- F curve
 - bypass flow, 162
 - dispersion model, 118-119
 - Fanning equation, 227
 - Films, monomolecular, 15
 - Flocculation, 85-90
 - Flow
 - annular and dispersed, 208, 211, 246-252
 - downward film flow, 248
 - effect of liquid injection, 248-249
 - entrainment behavior, 247-249
 - Fauske model, 231
 - spray equilibrium, 247
 - upward film flow, 246
 - around a rigid sphere, 78, 80
 - backmix, 168
 - degree of segregation in, 176-177
 - reactions in, 174-175
 - bubble (see Bubble-flow)
 - bubbles in two-phase, 201
 - bypass, 162-163
 - definition, 159
 - evaluation of, 162
 - characteristics, two-phase
 - holdup ratio definition, 201
 - slip and velocity definition, 202
 - void-fraction definition, 201-202
 - classification, two-phase, 200
 - composition of, 200
 - droplets in, 201
 - end stage, vapor or liquid, 292-293
 - rates, 301-302
 - film, burnout in, 263-265
 - froth, 211, 238-241
 - in long pipelines, 272

- heat generation in, 218
 - in inclined tubes, 271
 - isenthalpic flash calculations, 290
 - in long pipelines, 271-272
 - mist, 208, 211
 - momentum balance in, 215-216
 - plug-, axial dispersed
 - conversion in, 180-182
 - mathematical description, 108-109
 - tubular and packed beds, 180-182
 - plug, two-phase, 207-211
 - rates, vapor and liquid, 300-302
 - semi-annular, 238-241
 - slug (see Slug flow)
 - stratified and wave, 207, 252-254
 - energy transfer in, 253
 - use of Reynolds number in, 254
 - wave forms, 254
 - two liquid phases and a gas phase, 270-271
 - two-phase
 - processes, 200-204
 - regimes, 213-214
 - transport behavior, 201
 - transport processes, 202-203
 - turbulent, 238-241
 - wavy, 207
- Flow patterns**
- application to chemical reactions, 171-187
 - conversion in stirred tanks, 178-179
 - direct use of age information, 173-178
 - fluidized beds, 186-187
 - general dispersion, 184-186
 - multiphase, 187
 - characterizing by stimulus-response technique, 98-104
 - internal age distribution in a closed vessel, 99-100
 - mean residence time in a vessel, 99
 - pulse tracer input, 101-102
 - relationship between tracer curves, 102-104
 - residence time distribution in a closed vessel, 100-101
 - step tracer input, 101
 - in horizontal tubes, 207-210
 - types, 207-208
 - prediction of, 208-210
 - mechanics, 233-254
 - models (see Models, flow-pattern)
 - non-ideal, 96
 - tracer information, use of, 104-105
 - in vertical tubes, 210-213
 - appearance, 210
 - prediction of, 212-213
 - types, 211-212
- Fluids, intermixing in pipelines, 187**
- Foam, liquid-liquid, 85**
- Force, balance, on a falling drop, 62-63**
- Fractionation, 287**
- G**
- Gas**
- liquid, concurrent flow, 200-204
 - slugs of, 233-237
- Gas-liquid interface, 13-20**
- dynamic, 15-19
 - effect of film-covered surfaces, 14-15, 17
 - effect of surface-active agents, 14-15, 18
 - resistance to mass transfer, 14
 - static, 13-15
- H**
- Hadamard's model, 73-74**
- Hadamard-Rybczynski model, 60-61**
- Hayworth and Treybal balance, 55-57**
- Head, hydrostatic, slug velocity of, 233**
- Heat transfer**
- in annular flow, 246-252
 - boiling of liquid in vertical tubes, 254-259
 - coefficients, 256
 - nucleate boiling, 257
 - regions, 255-256
 - velocities, 258
 - coefficients for two-phase flow, 259-263
 - in homogeneous model, 261
 - in slip-ratio model, 261
 - correlating methods, 261-263
 - dependence on heat flux, 263
 - hypothetical liquid-only case, 261-262
 - dimensionless group correlation, 260-261
 - in dispersed flow, 246-252
 - local boiling, 258-259
 - Lockhart-Martinelli parameters, 259-260
 - dependence on heat flux, 260
 - two-phase mixtures, 254-265

in two-phase processes, 202
Hexadecanol, 3-4, 15, 16

I

I curve
bypass flow, 162
deadwater regions, 161, 165-167
definition, 99-100
for simple combined models, 165-167
stirred tanks, 168
Ice, soft, 14
Intercoolers, 292, 304
Iteration solutions, 287-288

J

Jet
falling vertical, 18-19
Rayleigh, 56-57

L

Langmuir's experiment, 6-7
Layers, boundary, 78-80
nonoscillating drops, 78-80
oscillating drops, 80
sphere, flow around, 78
Liquid-fields
high viscosity, 52-53
low viscosity, 63-65
Liquid, mass transfer, 52-53
Liquid-liquid systems
drop oscillations in, 75-77
dynamic, 26-33
interfacial concentrations, 21
interfacial turbulence, 22, 25
resistance to mass transfer, 20, 22-23
spontaneous emulsification, 22-23
static, 23-26
transfer coefficient, 21, 26
unstirred, 20-22
velocity versus drop size, 61-62
Litus model, 58
Lockhart-Martinelli correlation, 220-225
heat transfer in, 259-263
limiting assumption, 220
parameters, 259-260

M

Martinelli-Nelson correlation, 221-225
in bubble flow, 243
comparison with experiment, 222-225

Mass balance, 130

Mass transfer

in cocurrent gas-liquid flow, 265-271
absorption from rising bubbles, 266
in annular flow, 267-269
in horizontal flow, 267-270
in horizontal slug-flow, 269-271
coefficient, 16
dependence on Reynolds number, 16
empirical correlation for clean inter-
faces, 26-27
for gas-liquid systems, 9, 10, 16, 18
in liquid-liquid systems, 21-33
for oxygen absorption, 16
for SO₂ absorption in water, 18
for surfaces covered with monolayer,
29-33

in drops and bubbles, 33-42
effect of surface-active agents, 14
extreme turbulence, 9-11
flow over sphere, 19
between gas and liquid solvents, 5-19
and interfacial phenomena, 1-50
laminar flow, 9, 16, 18
between two liquid solvents, 20-32
theoretical values of resistance, 8-18

Metals, liquid, 232-233

Models, flow-pattern

combined, 158-171
application to fluidized beds, 170-171
application to stirred tanks, 167-170
construction of, 159
cross flow pattern, 158-159
deadwater regions, 159-171
matching models to experiments,
161-167
number of parameters, 164-167
types of flow in, 159
correlation, 229-233
dispersed plug-flow
dimensionless concentration, 126
measurement of dispersion coefficient,
125-133
moment order of tracer distribution,
136
solutions for measurement experi-
ments, 126
tracer injection, 125

dispersion

experimental verification of relation-
ship, 139-142

- limitations of theory, 141-142
 - mathematical descriptions, 107-109
 - measurement of coefficients, 109-134
 - non-ideal flow patterns, 105-150
 - relationship between, 134-142
- homogeneous, 227-228
 - acceleration pressure losses, 222
- mixed cell (see Tanks-in-series)
- plug-flow, mathematical description, 108
- slip-ratio, 261
- stirred tanks, 168-178
- symmetrical pipe flow, 107-108
- Moments, tracer distribution, 136-139
 - axial dispersed plug-flow, 136
 - dispersed plug-flow, 136
 - first moment, 137
 - general dispersion, 137
 - summary for all models, 138-139
 - ultimate values, limitation of theory, 141
 - uniform dispersion, 137
 - zereth moment, 137
- Momentum
 - exchange model, 228-229
 - pressure losses, 227
 - steady-state flow, 215
- Monolayers, effect on liquid-liquid inter-
face, 25
- N**
- Navier-Stokes equations of drop motion,
59-61, 66
- Nicklin approach, 218
- O**
- O₂ absorption in gas-liquid systems, 13-17
 - steady-state, in dynamic systems, 15
- P**
- Parameter-X, 229
- Pigford's theoretical equation, 18
- Plateau's spherules, 54-55
- Pressure
 - drop in two-phase systems, 203-204,
214-228
 - acceleration losses, 222
 - classification of flow regimes, 206
 - correlating methods, 220-223
 - defining, 219
 - diameter dependence in pipes, 223
 - friction-factor methods, 226-228
 - horizontal flow, 225
 - irreversible, 219
 - Lockhart-Martinelli correlation, 220-
225
 - mass flow rate effect on, 224
 - mean, prediction of, 223-225
 - momentum and energy balances, 214-
217
 - vertical flow, 223
 - recovery in wakeless bubbles, 236
- Program, general, for vapor-liquid proc-
esses, 291-316
 - basic, 291-303
 - accuracy check, 303
 - determination of, flash type, 302-303
 - reboilers and condensers, 299-300
 - stage feeds, 298-299
 - stage sequencing, 297
 - examples, 308-310
 - distillation column with side stripper,
310
 - reboiled absorber, bottom product
set, 308-310
 - reboiled absorber, vapor product set,
310
- nomenclature, 310-316
- problem formulation, 291-292
- subroutines, 304-308
 - BUBPT, DEWPT, ISOVFL,
ISOTFL, 307-308
 - CONDEN, 306
 - INPUT, 304-305
 - INVEN, 306-307
 - OUTPUT, 305
 - REBOIL, 305-306
- Pulse response (see C curve)
- R**
- Reactors, packed-bed
 - axial-dispersed plug-flow, 180-182
 - boundary conditions, 180
 - dispersion, 181-182
 - second order, 182
 - volume ratio, 181
 - conversion in, 179-184
 - dispersed plug-flow, 182-184
 - boundary conditions, 183
 - steady flow, 182
 - dispersion model, 184
 - tanks-in-series model, 184-186

- ratio of volume, 184-185
 - tracer curves, 185
 - Reboilers
 - calculations of, 305-306
 - specifications of, 304
 - Regions
 - backmix flow, 168
 - deadwater, 159-161
 - forced-convection, boiling, 263-264
 - liquid deficient point, 263
 - in parallel, 164
 - in series, 163
 - Relaxation solutions
 - advantages and disadvantages, 289-290
 - mass balance equations, 287-288
 - nomenclature, 291
 - subroutine INVEN, 306-307
 - unsteady-state equations, 289
 - Resistance
 - diffusional, 1-3
 - effects of surface-active agents, 2
 - mass transfer
 - in gas-liquid systems, 8-13
 - in liquid-liquid systems, 22-33
 - Reynolds numbers
 - high, 72-74
 - high viscosity fields, 73
 - low viscosity fields, 72-73
 - non-Newtonian, 73
 - prolate shape, 73-74
 - low, 71-72
 - Hadamard's development for, 68
 - use in stratified flow, 254
 - use in two-phase flow, 213
- S**
- Separation operations, multistage, 279-381
 - calculation methods, 281-291
 - iteration solutions, 287-288
 - problem description and variables, 281-285
 - relaxation solutions, 288-291
 - stage-by-stage solutions, 285-286
 - Slug-flow, 207, 211, 233-241
 - flooding action, 240-241
 - force balance, 235-236
 - frictional, 237
 - of gas, 233
 - gas volume-fraction, 234
 - horizontal, 237-238
 - unstable, 238-241
 - entrance effect, 239
 - true liquid, 239-240
 - vertical tubes, 233-237
 - downward velocity, 233
 - upward velocity, 234, 237
 - SO₂ absorption in water, 17-18
 - Sphere, solid, 19
 - interruption of the laminar flow, 19
 - Steam-water mixture, 222
 - Sternling-Scriven hydrodynamic analysis, 77
 - Stream junction, 68
 - Surface
 - active agents
 - effects on absorption, 17-19
 - film covered, 12-13
 - free clean, of a turbulent liquid, 11-12
 - hydrodynamic theory, 11
 - instability in gas-liquid systems, 6-8
 - layer immobilization, 18
 - in liquid-liquid systems, 24
 - Surfactants, effects of, 80-84
 - damping of oscillations, 82-83
 - drop soluble, 80
 - evaluation, 81-82
 - increased drag, 83
 - internal circulation, 67, 83-84
 - in ultrapure systems, 67
- T**
- Tanks-in-series, 150-158
 - boundary conditions, 154
 - C curve, 151
 - maxima, 157
 - comparison with dispersion model, 156-158
 - mathematical description, 151-156
 - one dimensional array, 151-153
 - three dimensional array, 155-156
 - number of parameters in, 164
 - perfectly mixed tank, 160
 - Tanks, stirred
 - C curve, 152-153
 - conditions, experimental, 169-170
 - conversion in ideal, 178
 - exit age-distribution, 168-169
 - homogeneity in, 168
 - internal age-distribution, 168

- multistaged, impeller-agitated, 178
 - non-ideal, 179
 - steady state in, 178
 - unsteady state in, 178
 - Tracer
 - concentration
 - characterization of data, 120
 - comparison of pulse and step methods, 119-120
 - computation errors, 120
 - experimental problems, 119
 - in dispersed plug-flow model, 125
 - distribution moments, 136-139
 - flow characterization, 104-105
 - injection methods, 109-121
 - boundary conditions, 120
 - imperfect pulse, 114-118
 - imperfect step, 119
 - perfect pulse, 110-114
 - perfect step, 118
 - periodic, 120-121
 - rate of injection, 110-111
 - in interpreting experimental data, 129-131
 - measurement of dispersion coefficient, 109-134
 - delta function in perfect pulse, 113, 115
 - Transfer between gas and liquid solvent, 5-19
 - ammonia absorption, 5
 - carbon dioxide absorption, 13-15
 - experiments on, 13-20
 - oxygen absorption, 13-17
 - resistance in pure gas or liquid, 2, 5
 - surface instability, 6-8
 - theoretical values of resistance, 8-9
 - Tubular and packed bed reactors (see Reactors)
 - Turbulence, extreme limits of, 9-13
 - in free clean surface of a liquid, 11-12
 - Turner's structures, 145-147
- V**
- Vapor-liquid processes, a general program
 - for computing, 279-317
 - calculation methods, 281-291
 - independence of variables, 295-296
 - problem alteration by program, 296-297
 - Velocity
 - bubble flow, 241
 - drop, 59-67
 - drag, 61-67
 - wall effect, 66-67
 - slip-, methods, 229-233
 - pipe roughness variable, 230-231
 - ratio, 229, 233, 243
 - slug-flow, profiles in
 - nose region, 236
 - upward, 237
 - wake region, 236-237
 - steady-state terminal, 62-63
 - Void-fraction
 - effect of concentrations and expansions, 232
 - horizontal flow, predicted in, 224-225
 - liquid metals, 232
 - steam-water system, 231
- W**
- Water, bound, 14
 - Weber number, critical, 249, 251
- X**
- X-parameter, 229